AD/A-003 251

PROCEEDINGS OF THE 23RD INTERNATIONAL WIRE AND CABLE SYMPOSIUM HELD AT ATLANTIC CITY, NEW JERSEY ON 3-5 DECEMBER 1974

ARMY ELECTRONICS COMMAND

5 DECEMBER 1974

Proceedings of the 23rd International *WIRE & CABLE* Symposium

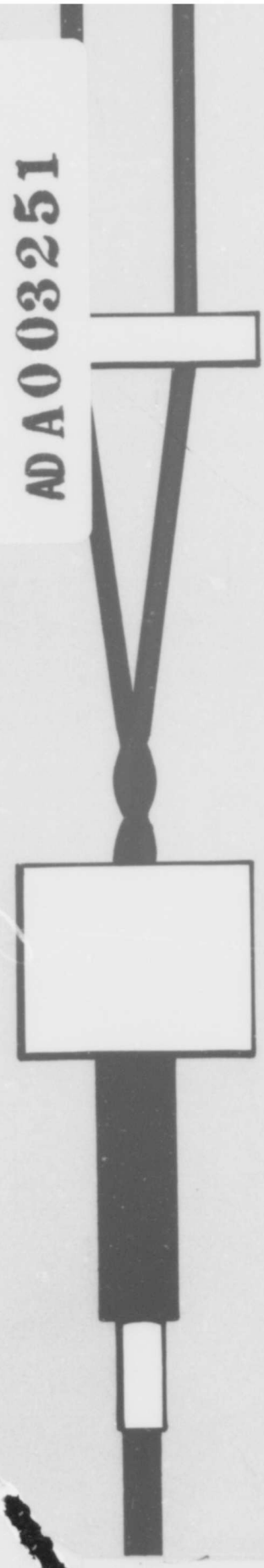

3rd, 4th & 5th of December 1974

Shelburne Hotel, Atlantic City, New Jersey

PRICES SUBJECT TO CHANGE

SPONSORED BY
THE

U.S. ARMY ELECTRONICS COMMAND

PROCEEDINGS OF 23rd INTERNATIONAL WIRE AND CABLE SYMPOSIUM

Sponsored by
U. S. Army Electronics Command

Atlantic City, N. J.
December 3, 4, and 5, 1974

23rd INTERNATIONAL WIRE AND CABLE SYMPOSIUM

SYMPOSIUM COMMITTEE

Elmer F. Godwin, Co-Chairman, USAECOM (201-535-2770)
Milton Tenzer, Co-Chairman, USAECOM (201-535-1834)
Les Dunlop, GTE Service Corp.
Marta Farago, Northern Electric
Joseph M. Flanigan, Rural Electrification Administration (REA)
Jerome Hager, Northern Petrochemical Co.
George Heller, Tensolite Co.
Irving Kolodny, General Cable Corp.
Warner T. Smith, Superior Continental Corp.
W. Robert Smith, Hercules, Inc.
Ronald Soloman, McDonnell Aircraft Co.
George H. Webster, Bell Laboratories

TECHNICAL SESSIONS

Tuesday, 3 December 1974

9:30 a.m.	Session I:	Tutorial on Effects of EMP on Cable Systems
2:15 p.m.	Session II:	Design and Manufacturing Techniques
2:15 p.m.	Session III:	Polyolefins

Wednesday, 4 December 1974

9:15 a.m.	Session IV:	Filled and Polyolefin Cable
9:15 a.m.	Session V:	Flat Cable Technology and Connections
2:15 p.m.	Session VI:	Coaxial Cables
2:15 p.m.	Session VII:	Telephone Cable Designs

Thursday, 5 December 1974

9:15 a.m.	Session VIII:	Matrix Systems and Optical Transmission Cable
9:15 a.m.	Session IX:	Cable Construction Testing and Material Conservation
2:15 p.m.	Session X:	Extrusion and Process Control
2:15 p.m.	Session XI:	Telephone Cable Applications

PROCEEDINGS

Responsibility for the contents rests upon the authors and not the Symposium Committee or its members. After the symposium all the publication rights of each paper are reserved by their authors, and requests for republication of a paper should be addressed to the appropriate author. Abstracting is permitted, and it would be appreciated if the symposium is credited when abstracts or papers are republished. Requests for individual copies of papers should be addressed to the authors. Extra copies of the Proceedings may be obtained from the Symposium Co-Chairman (Requests should include a check for $8.00 per copy, made payable to the Shelburne Hotel). Copies may also be obtained for a nominal fee from the National Technical Information Service (NTIS), Operations Division, Springfield, Virginia 22151.

Copies of papers presented in previous years may also be obtained from the National Technical Information Service. Papers from the first 20 years, with their AD numbers are cataloged in the "KWIC Index of Technical Papers, Wire and Cable Symposia (1952-1971)," December 1971.

MEMORIAM

JACK SPERGEL
1924-1974

JACK SPERGEL

Jack Spergel was born in Brooklyn, N.Y. in 1924. He attended City College of New York from 1942 to 1943, and served in the U.S. Army Air Corps from 1943 to 1945. After World War II he attended Cornell University, where he received his electrical engineering degree in 1949.

In 1949 he began working on research and development of coaxial lines, wire and cable and electrical connectors at the Electronics Technology and Devices Laboratory, U.S. Army Electronics Command, at Fort Monmouth, N.J. In 1963 he was appointed as Chief, Transmission and Electromechanical Devices Branch, and supervised the development of cable and connectors and their standardization within the Army and Defense Department. Mr. Spergel was the Army representative to the NATO Special Working Group, "Electrical Connectors and Connections," in 1967.

He was chairman of a USAMC ad hoc committee for a handbook on electrical wire and cable. He published more than 15 technical papers on connectors and cable, and wrote a chapter on coaxial transmission lines for a McGraw-Hill handbook on wire and cable.

Mr. Spergel retired from the U.S. Army Electronics Command in 1972, and joined the Communications Division of General Cable Corporation, Colonia, N.J., where he was employed until his death in May 1974.

Jack Spergel served as co-chairman of the International Wire and Cable Symposium for nine years and as a committee member for two years. His personal dedication and innovative ideas contributed in a large measure to the stature that this symposium enjoys today. In recognition thereof the award for the outstanding technical paper shall henceforth be known as the Jack Spergel Award.

He is survived by his wife, the former Helene Levine, and three children, Howard, Irene and Diane who live in West Long Branch, N.J.

MESSAGE FROM THE CO-CHAIRMEN

Welcome to the 23rd International Wire and Cable Symposium. Your co-chairmen are again pleased to report that last year's symposium (22nd) was a tremendous success, both in attendance and in the favorable responses received on the technical presentations. Attendance continued to increase, especially the international representation, with over one hundred and sixty (160) attendees, representing twenty two (22) countries other than the United States. Representatives from seven of these countries presented a total of seventeen papers, or over 40% of all the papers presented. The increase each year in international representation is indeed encouraging and again attest to the true international flavor of the symposium.

The response this year to the call for papers was greater than ever, with many excellent abstracts submitted for consideration. To provide for most of the excellent abstracts received, your committee decided to expand the program and include a tutorial session, followed by double sessions for each of the remaining morning and afternoon programs. The tutorial session on "Effects of EMP on Cable Systems," will be presented by representatives of Illinois Institute of Technology (IIT).

We were saddened by the untimely deaths this year of two of our dedicated symposium committee members, Mr. Stanley F. Luques of Brand-Rex Company and Mr. Jack Spergel of General Cable Corporation. Stan, who was serving his third year on the committee, was well-known and highly respected throughout the wire and cable community. Jack was co-chairman of the committee for 9 years during which time he initiated many new and innovative ideas for improving the technical level and content of the symposium. Both men will be long remembered by their committee colleagues and business associates for their many valuable contributions to the wire and cable industry.

Your co-chairmen once again gratefully acknowledge the unstinting efforts of our committee members and the unqualified cooperation of representatives of the many industrial organizations and government activities in attendance at these very successful symposia. The continuation of such participation will ensure comparable success in the future.

M. TENZER, Co-Chairman

E. GODWIN, Co-Chairman

HIGHLIGHTS OF THE 22nd INTERNATIONAL WIRE AND CABLE SYMPOSIUM

December 4, 5, and 6, 1973
Shelburne Hotel, Atlantic City, N. J

R. Ballard of the Rural Electrification Administration Department of Agriculture, making his keynote address at the banquet

J. D. Kirk, Alberta Government Telephones, receiving his Certificate of Appreciation for serving on the Symposium Committee for three years

L. J. Frisco, Raychem Corporation, receiving his Certificate of Appreciation for serving on the Symposium Committee for three years

J. B. Howard (left) and S. Kaufman (center), both of Bell Laboratories, accepting awards for technical papers. Mr. Howard's award was for outstanding technical paper "Stabilization Problems with Low Density Polyethylene Insulations." Mr. Kaufman's award was for outstanding presentation of his paper "Reclamation of Water-Logged Buried PIC Telephone Cable."

Dr. B. Wargotz, General Cable Corporation, discussing "Characteristics of Polyolefin Insulation for Wire and Cable" during the tutorial session on polyolefins

J. B. Howard, Bell Laboratories, discussing "Fundamentals of Stability Testing of Polyolefins" during the tutorial session on polyolefins.

Breakfast for speakers and co-authors of Sessions V and VI.

Guests and committee members at the banquet. Left to right: L. Dunlop, G. W. Heller, T. F. Scoville (honored on retirement from government service), J. D. Kirk, W. L. Doxey, and E. F. Godwin.

CANDID SCENES AT THE 22nd IWCS


QUIET PLEASE
MEETING
IN PROGRESS

AWARDS

Outstanding Technical Paper	*Best Presentation*
1968	
H. Lubars and J. A. Olszewski, General Cable Corp– "Analysis of Structural Return Loss in CATV Coaxial Cable"	N. Dean, B.I.C.C.—"The Development of Fully Filled Cables for the Distribution Network"
1969	
J. B. McCann, R. Sabia and B. Wargotz, Bell Laboratories—"Characterization of Filler and Insulation in Waterproof Cable"	J. D. Kirk, Alberta Government Telephones—"Progress and Pitfalls of Rural Buried Cable"
1970	
D. E. Setzer and A. S. Windeler, Bell Laboratories—"A Low Capacitance Cable for the T2 Digital Transmission Line"	Dr. O. Leuchs, Kabel und Metalwerke—"A New Self-Extinguishing Hydrogen Chloride Binding PVC Jacketing Compound for Cables"
1971	
R. Iyengar, R. McClean and T. McManus, Bell Northern Research—"An Advanced Multi-Unit Coaxial Cable for Tool PCM Systems"	S. Nordblad, Telefonaktiebolaget LM Ericsson—"Multi-Paired Cable of Nonlayer Design for Low Capacitance Unbalance Telecommunication Network"
	N. Kojima, Nippon Telegraph and Telephone—"New Type Paired Cable for High Speed PCM Transmission"
1972	
J. B. Howard, Bell Laboratories—"Stabilization Problems with Low Density Polyethylene Insulations"	S. Kaufman, Bell Laboratories—"Reclamation of Water-Logged Buried PIC Telephone Cable"
1973	
Dr. H. Martin, Kabelmetal—"High Power Radio Frequency Coaxial Cables, Their Design and Rating"	R. J. Oakley, Northern Electric Co., Ltd.—"A Study into Paired Cable Crosstalk."

CONTRIBUTORS

Albert Surprenet, Inc.
Jaffrey, N.H.
Allied Chemical Corp.
Morristown, N.J.
American Hoechst Corporation
Somerville, New Jersey
Amoco Chemicals Corp.
Chicago, Ill.
Amco Wire & Cable Inc.
Allendale, N.J.
AMP Incorporated
Harrisburg, Pa.
Anaconda Telecommunications
Sycamore, Illinois
Arco/Polymers, Inc.
Pittsburgh, Pa.
Arnold Field Associates
Hackensack, N.J.
Arvey Corporation
Jersey City, N.J.
Austral Standard Cables
Melbourne, Australia
Belden Corporation
Geneva, Ill.
Berk-Tek, Inc.
Reading, Pa.
Boston Insulated Wire & Cable Co.
Boston, Mass.
Boston Insulated Wire & Cable Co., Ltd.
Hamilton, Ontario, Canada
Brand Rex Company
Willimantic, Conn.
British Insulated Callendars Cables, Ltd.
Prescot, Lancashire England
Burgess Pigment Co.
Sandersville, Ga.
Burndy Corporation
Norwalk, Conn.
Cable Consultants Corporation
Larchmont, N.Y.
Cable Equipment Corp.
New York, N.Y.
Cabot Corporation
Boston, Mass.
Camden Wire & Cable Co.
Camden, N.Y.
Canada Wire & Cable Ltd., Communications Div.
Winnipeg, Manitoba, Canada
Canadian Industries, Ltd.
Montreal, P.Q., Canada
Carlew Chemicals, Ltd.
Montreal, P.Q.
R.E. Carroll, Inc.
Trenton, New Jersey
Cary Page Chemicals, Inc.
Edison, New Jersey
Cerro Wire & Cable Co.
Freehold, New Jersey
Cerro Wire & Cable Co.
Maspeth, N.Y.
Cerro Wire & Cable Co.
New Haven, Conn.
Chase & Sons, Inc.
Randolph, Mass.
Chemplast, Inc.
Wayne, N.J.
CIBA-Geigy Corporation
Ardsley, N.Y.
Cimco Wire & Cable
Allendale, N.J.
Cities Service Company
Chester, N.Y.
Collyer Insulated Wire Co.
Lincoln, R.I.
Columbia Cable & Electric Corp.
Brooklyn, N.Y.
Communications Technology Corp.
Los Angeles, Ca.
Copperweld Corporation
Pittsburgh, Pa.
Dainichi-Nippon, Ltd.
Osaka, Japan
Dart Industries, Inc.
Paramus, N.J.
Davis Standard Group
Pawcatuck, Conn.
Delco Electronics Corp.
Bristol, Pa.
Devcon Corporation
Danvers, Mass.
Diamond Shamrock Chemical Co.
Cleveland, Ohio
Dow Chemical
Midland, Michigan
Duncan M. Gillies Co., Inc.
West Boylestown, Mass.
E.I. Dupont de Nemours & Co.
Wilmington, Del.
Dupont of Canada Ltd.
Montreal, Quebec, Canada
Dussek Bros. Ltd.
Belleville, Ont. Canada
Edmands Company
Providence, R.I.
Elco Corporation
Willow Grove, Pa.
Entwistle Co.
Hudson, Mass.

Essex International, Inc.
Decatur, Ill.

Exxon Chemical Co.
Houston, Texas

Fabricon Manufacturing Ltd.
Trenton, Ontario, Canada

Firestone Tire & Rubber Co.
Pottstown, Pa.

Formulabs
Escondido, Calif.

The Fujikura Cable Works, Ltd.
Tokyo, Japan

Furukawa Electric Co., Ltd.
Tokyo, Japan

Gavitt Wire & Cable Div.
Brookfield, Mass.

Gem Gravure Co., Inc.
W. Hanover, Mass.

General Cable Corporation
Colonia, New Jersey

General Electric Co.
Waterford, N.Y.

B.F. Goodrich Chemical Co.
Cleveland, Ohio

Great American Chemical Corp.
Fitchburg, Mass.

GTE Service Corporation
Stanford, Conn.

Hardman, Inc.
Belleville, N.J.

Hepco Wire & Cable Industries
Garnerville, New York

Hercules Inc.
Crowley, Louisiana

Hercules Inc.
Wilmington, Del.

Hewlett Packard Company
Palo Alto, Calif.

Heymann Manufacturing Co.
Kenilworth, New Jersey

High Voltage Engineering Corp.
Burlington, Mass.

Hitachi Cable, Ltd.
New York, New York

Hudson Wire Co.
Ossining, New York

ICI America, Inc.
Wilmington, Del.

Independent Cable, Inc.
Hudson, Mass.

Kenrich Petrochemicals
Bayonne, New Jersey

The Kerite Company
Seymour, Conn.

Lamart Corporation
Clifton, N.J.

J. J. Lowe Associates, Inc.
Bedford Hills, N.Y.

Maillefer SA
Ecublens, Laussane, Switzerland

Minnesota Mining & Manufacturing
St. Paul, Minn.

Mobay Chemical Co.
Pittsburgh, Pa.

Monsanto
St. Louis, Missouri

Nessor Alloy Corporation
West Caldwell, N.J.

Nishi Nippon Electric Wire & Cable Co., Ltd.
Tokyo, Japan

NL Industries, Inc.
New York, N.Y.

Nonotuck Manufacturing Co.
South Hadley, Mass.

Northeast Wire Co., Inc.
Holyoke, Mass.

Northern Electric Co., Ltd.
Lachine, Quebec

Northern Petrochemical Company
Des Plaines, Ill.

Ocean Cable Co., Ltd.
Yokohama, Japan

The Okonite Company
Providence, R.I.

The Okonite Company
Ramsey, N.J.

Olen Plastics
Assonet, Mass.

Olex Cables Pty. Limited
Sunshine, Victoria, Australia

Olin Brass
East Alton, Ill.

The Pantasote Company
Passaic, N.J.

Pennwalt Corporation
Philadelphia, Penna.

Penreco Co.
Butler, Pa.

PFD Penn Color
Doylestown, Pa.

Phalo Corporation
Shrewsburg, Mass.

Phelps Dodge
Carolina, Puerto Rico

Phelps Dodge Copper Products
Elizabeth, N.J.

Phillips Cables Limited
Brockville, Canada

Phillips Petroleum Company
Bartlesville, Okla.

Pirelli USA Representative Corp.
New York, N.Y.

Plastoid Corporation
Long Island City, N.Y.

Plymouth Rubber Co.
Canton, Ma.

Plymouth Wire & Cable Co.
Worcester, Mass.

Raychem Corporation
Menlo Park, Calif.

Reichhold Chemicals, Inc.
White Plains, N.Y.

Rexene Polymers
Paramus, N.J.

The Rochester Corporation
Culpeper, Virginia

John Royle & Sons
Paterson, N.J.

Samuel Moore & Company
Aurora, Ohio

Schlichter Products Company
King of Prussia, Pa.

Shell Chemical Company
Houston, Texas

Siemens Aktiengesellschaft
Munich, Germany

Southwest Chemical & Plastics
Seabrook, Texas

Spectra-Strip, Inc.
Hamden, Conn.

Storm Products Company
Inglewood, Calif.

Sumitomo Electric Industries
Yokohama, Japan

Superior Continental Corporation
Hickory, N.C.

Syncro Machine Co.
Perth Amboy, N.J.

Taconic Plastics, Inc.
Petersburg, N.Y.

Taknor Apex Co.
Pawtucket, R.I.

Technical Coatings Co.
Nutley, N.J.

Teldor Ltd.
Kibutz, Ein-der Israel

Teledyne Thermatics
Elm City, N.C.

Telephone Cables, Ltd.
Dagenham, England

Tenneco Chemicals
Piscataway, N.J.

Tensolite Company
Tarrytown, N.Y.

Texas Instruments Inc.
Attleboro, Mass.

Times Wire & Cable Co.
Wallingford Conn.

Torpedo Wire & Strip Inc.
Pittsfield, Pa.

TRW Crescent Wire & Cable
Trenton, N.J.

UBE Industries, Ltd.
Tokyo, Japan

Union Carbide Corporation
Hackensack, New Jersey

Videx Equipment Corporation
Paterson, N.J.

Wardwell Braiding Machine Co.
Central Falls, R.I.

Ware Chemical Corp.
Bridgeport, Conn.

Weber & Scher Mfg. Co., Inc.
Newark, New Jersey

Western Electric
Kearny, N.J.

Western Electric Co.
Norcross, Georgia

Whitmor Wire & Cable Corporation
N. Hollywood, Calif.

Wilson Products Co.
Neskanic, New Jersey

Wire & Textile Machinery Corp.
Pawtucket, R.I.

Witco Chemical Corp.
New York, N.Y.

W.R. Gincor Co.-Vinyl Group
Brooklyn, N.Y.

Wyre Wynd Co.
Jewett City, Conn.

Wyrough & Loser, Inc.
Trenton, N.J.

TABLE OF CONTENTS

TECHNICAL PROGRAM

Tuesday, December 3, 1974 — 9:30 AM
Grand Ballroom — Shelburne

SESSION I: *Tutorial* — Effects of EMP on Cable Systems

Chairman: I. Kolodny, General Cable Corp.

1. AN INTRODUCTION TO EMP
2. EMP COUPLING INTO CABLES
3. TESTING TECHNIQUES FOR CABLES AND CONNECTORS
4. HARDENING TECHNIQUES.

Panel Members (All of IIT Research Institute)
Mr. I. N. Muidel
Mr. J. Bridges
Dr. W. Wells
Dr. E. Weber

Tuesday, December 3, 1974 — 2:15 PM
Grand Ballroom — Shelburne

SESSION II: — Design and Manufacturing Techniques

Chairman: George Webster, Bell Laboratories

THE MATHEMATICAL RELATIONSHIP BETWEEN THE BENDING RADIUS OF A CABLE AND THE LENGTH OF CABLE LAY, *J. C. Lilly, Plastic Wire and Cable Corp.* 1

PROGRESS IN SZ TWISTING AND STRANDING OF COMMUNICATIONS CABLES, *D. Vogelsberg, Siemens AG* 7

A RE-EXAMINATION OF STRANDING CONFIGURATIONS AND THEIR RELATIONSHIP WITH THE ELECTRICAL CONDUCTIVITY AND MASS CONCENTRICALLY-STRANDED CONDUCTORS, *J. F. McLaughlin, Raytheon Co.* 13

A MATHEMATICAL APPROACH TO TUBING EXTRUSION OF THERMOPLASTICS IN ELECTRICAL INSULATION OF WIRES AND CABLES, *Dr. R. Di Leonardo, Canada Wire and Cable Co., Ltd.* 19

METAL MICROWIRES SPUN FROM MELT COMPARED WITH THOSE COLD DRAWN, *Dr. Manfre, Technion SpA. and G. Servi, De Angeli SpA* 26

Tuesday, December 3, 1974 — 2:15 PM
Borton Hall — Dennis

SESSION III: — Polyolefins

Chairman: J. E. Hager, Northern Petrochemical

HIGH DENSITY POLYETHYLENE FOR PIC INSULATION: OXIDATIVE STABILITY, *M. G. Chan, Bell Laboratories* 34

THERMAL OXIDATIVE CRACKING OF POLYETHYLENE INSULATION ON TELEPHONE CONDUCTORS, *H. M. Gilroy, Bell Laboratories* 42

RAPID ISOTHERMAL DTA TESTING FOR CONTROL OF STABILITY IN POLYOLEFINS, *H. M. Gilroy and E. Kokta, Bell Laboratories* 46

CELLULAR INSULATION AS AN ANSWER TO MATERIAL CONSERVATION, *E. D. Metcalf, Anaconda Wire and Cable Corp.* 53

PROPERTIES OF A CELLULAR COMMUNICATIONS JACKET, *L. Bragg and I. Galperin, Continental — Hatfield* 59

RAW MATERIAL INSPECTION FOR EXPANDABLE POLYOLEFIN INSULATIONS, *D. I. Marshall, J. M. Turnipseed, Western Electric, and F. R. Wight, Bell Laboratories* ... 63

Wednesday, December 4, 1974 — 9:15 AM
Grand Ballroom — Shelburne

SESSION IV: — Filled and Polyolefin Cable

Chairman: L. R. Dunlop, GTE Systems Engineering

EFFECT OF PETROLEUM JELLY FILLER ON LOW DENSITY POLYETHYLENE TELEPHONE CABLE JACKETING, *R. Bostwick, Union Carbide Corp.* 68

SHEAR AND FLOW CHARACTERISTICS OF WATERPROOF PETROLATUM-BASED CABLE FILLER COMPOUNDS, *T. E. Luisi and J. J. Kaufman, Witco Chemical* 76

SYSTEM EVALUATION AND PROTECTION OF CONDUCTOR INSULATION IN OUTSIDE PLANT, *P. McCann and L. Ance, Rural Electrification Administration* 82

NEW MULTI-PAIR SUBMARINE CABLE, *R. Sawada, Ocean Cable Co. Ltd., and K. Suzuki, Nippon T & T Public Corp.* 91

NEW COPPER DEACTIVATOR FOR POLYOLEFIN, *T. Yoshikawa, K. Kamaguchi, H. Kishi, M. Masaki and N. Sakamoto, Ube Industries, Ltd.* 97

Wednesday, December 4, 1974 — 9:15 AM
Borton Hall — Dennis

SESSION V: — Flat Cable Technology and Connections

Chairman: G. W. Heller, Tensolite

CIRCULAR PLASTIC — A NEW GENERATION OF CONNECTORS, *P. Lannan, AMP Inc.* 105

FLAT CONDUCTOR CABLES FOR EXTREMELY HIGH TEMPERATURE APPLICATION, *W. Rigling, Martin Marietta Aerospace* 112

CONNECTOR-FLAT CABLE COMPATIBILITY, *G. C. Smith and D. A. Luzadis, Bendix Corp.* 116

NEW FLAT FLEXIBLE COAXIAL CABLE AND MASS TERMINATION TECHNIQUE FOR HIGH-SPEED DIGITAL APPLICATION, *W. Schumacher, AMP Inc.* 123

MASS WIRE INSULATION DISPLACING TERMINATION OF FLAT CABLE, *D. J. Doty and G. A. Patton, AMP Inc.* 127

Wednesday, December 4, 1974 — 2:15 PM
Grand Ballroom — Shelburne

SESSION VI: — Coaxial Cables

Chairman: M. Tenzer, US Army Electronics Command

WIDE BAND LEAKY COAXIAL CABLE FOR A 800 MHZ BAND, *T. Kishimoto, Japanese National Railways, Y. Nagai, H. Kipani and Y. Miyamoto, Sumitomo Electric Industries, Ltd.* 135

LARGE SIZE LEAKY COAXIAL CABLE FOR 400 and 800 MHZ FREQUENCY BAND, *H. Yasuhara, T. Sako, T. Naruse and T. Kato, The Fujikura Cable Works, Ltd.* 143

RELATING TRANSFER IMPEDANCE TO COAXIAL CABLE RADIATION, *K. A. Simons, Simons & Wydro Associates* 152

STRUCTURAL RETURN LOSS ASSOCIATED WITH 2.6/9.5 COAXIAL CABLE FOR 60 MHz ANALOGUE SYSTEMS AND HIGHER CAPACITY FUTURE DIGITAL SYSTEMS, *J. R. Osterfield, Pirelli General, S. Longoni and A. Manilii, Industrie Pirelli S.P.A* 161

MICROCOAXIAL CABLES IN THE PCM MEDIUM BIT RATE ITALIAN TELECOMMUNICATION NETWORK AND THEIR DEVELOPMENT, *P. Calzolari and A. Manilii, Industrie Pirelli S.P.A., G. Paladin and F. Scrofani S.I.P. — Societá Italiana per l'Esercizio Telefonico p.A.* 169

Wednesday, December 4, 1974 — 2:15 PM
Borton Hall — Dennis

SESSION VII: — Telephone Cable Design

Chairman: W. T. Smith, Superior Continental

AN APPROACH TO CROSSTALK COUPLING REDUCTION OF PAIR-TYPE CABLE, *S. Minematsu, M. Yotsuya and A. Ito, Dainichi, Nippon Cables, Ltd.* 182

INTELLIGIBLE CROSSTALK IN MODERN LOCAL AREA TELEPHONE NETWORKS, *H. W. Silcock and D. Sibbald, Standard Telecommunication Laboratories Ltd.* 194
MULTI-PAIR ALUMINUM CONDUCTOR JUNCTION CABLE, *H. Fukutomi and S. Kaibuchi, Telephone Public Corp., A. Toyokawa, The Furukawa Electric Co., Ltd., T. Higashimoto, Sumitomo Electric Industries Ltd., and H. Chiba, The Fujikura Cable Works Ltd.* 205
MATERIAL SAVINGS BY DESIGN IN EXCHANGE AND TRUNK TELEPHONE CABLE, *D. M. Mitchell and G. H. Webster, Bell Laboratories* 216
TRANSIENT SHIELDING EFFICIENCIES OF FERROMAGNETIC CABLE SHIELDS, *H. D. Campbell, Northern Electric Co., Ltd.* 226
HIGH STRENGTH, CORROSION RESISTANT CLAD METAL SHIELDING FOR TELEPHONE WIRE AND CABLE, *R. Baboian, R. Hartley and D. Hyman, Texas Instruments, Inc.* 239

Thursday, December 5, 1974 — 9:15 AM
Grand Ballroom — Shelburne

SESSION VIII: — Matrix Systems and Optical Transmission Cable

Chairman: R. Soloman, McDonnell Aircraft

A MATRIX INTERCONNECTION SYSTEM FOR AIRCRAFT WIRING, *R. A. Bradshaw, Grumman Aerospace Corp. and E. F. Godwin, U.S. Army Electronics Command* .. 252
TRANSMISSION CHARACTERISTICS OF OPTICAL FIBERS, *Dr. A. H. Cherin, Bell Laboratories* 261
TACTICAL LOW LOSS OPTICAL CABLE FOR ARMY APPLICATIONS, *Dr. R. A. Miller, Corning Glass Works and M. Pomerantz, U.S. Army Electronics Command* 266
SOME DESIGN PRINCIPLES FOR FIBER OPTICAL CABLES, *S. G. Foord, W. E. Simpson and A. Cook, Standard Telecommunication Laboratories Ltd.* 276

Thursday, December 5, 1974 — 9:15 AM
Borton Hall — Dennis

SESSION IX: — Cable Construction Testing and Material Conservation

Chairman: W. R. Smith, Hercules, Inc.

A PVC JACKETING COMPOUND WITH IMPROVED FLAME RETARDANCY AND SUPERIOR PHYSICAL PROPERTIES, *S. Kaufman, Bell Laboratories and R. S. Dedier, Emery Industries* 281
HIGH ENERGY CONDUCTOR SPLICING IN CABLE MANUFACTURE, *B. H. Cranston, D. A. Machusak and C. A. Wiechard, Western Electric* 290
THE EFFECTS OF FATIGUE DAMAGE ON THE PROPERTIES OF COPPER-CLAD STEEL CONDUCTORS, *C. A. Shumaker, Jr., Superior Continental Corp.* 297
MUTUAL CAPACITANCE CORRECTION FACTORS FOR SERIES MODE BRIDGES, *K. W. Brownell, Jr., Brand-Rex Co. and T. L. Moore, Rural Electrification Administration* 309
A COMPUTORIZED TESTING SYSTEM FOR SYMMETRICAL CABLES AND ITS POSSIBILITIES FOR STATISTICAL TESTING, *D. J. Dekker, PTT Administration of the Netherlands and H. L. Gorissen, S. Dijkhuizen and J. P. Hartwijk, NKF Kable, B.V.* . 319

Thursday, December 5, 1974 — 2:15 PM
Grand Ballroom — Shelburne

SESSION X: — Extrusion and Process Control

Chairman: M. Farago, Northern Electric

USING A LASER MICROMETER FOR PRECISION CONTROL OF WIRE DIAMETER AND POSITION ON A CV LINE, *F. M. Taylor, Autometrix* 326
THE COOLING PROCESS IN PLASTIC INSULATED WIRE, *J. C. Calhoun and W. M. Flegal, Western Electric Co* 330
GAS INJECTION EXTRUSION PROCESS FOR A FOAMED PLASTIC INSULATION, SUPPLYING A FIXED QUANTITY OF GAS, *M. Azuma, K. Orimo, K. Toyoda, T. Shimano and S. Yamamoto, The Furukawa Electric Co., Ltd.* 337

AUTOMATIC PROCESS CONTROL IN THE INSULATING OF TELEPHONE CABLES, *E. Kertscher, Maillefer, S.A.* 346
ULTRASONIC JACKET THICKNESS AND ECCENTRICITY MONITOR AND CONTROL SYSTEMS, *L. M. Boggs, A. M. Isley and J. W. Levengood, Western Electric Co.* ... 359

Thursday, December 5, 1974 — 2:15 PM
Borton Hall — Dennis

SESSION XI: — Telephone Cable Applications

Chairman: J. M. Flanigan, Rural Electrification Administration

TECHNIQUES IN MANAGING A TELEPHONE TRUNK CABLE NETWORK TO PROVIDE ECONOMICAL, DEPENDABLE SERVICE, *J. M. Robertson, Rochester Telephone Corp.* 365
SIMULTANEOUS FIELD SPLICING AND TESTING, *H. Knippelmier, Automation Products Co.* 370
AN ALL POLYETHYLENE CABLE SPLICE EMPLOYING HEAT FUSION TECHNIQUES FOR POLYETHYLENE JACKETED CABLES, *J. G. Nevison and D. T. Parr, British Insulated Callenders Cables, Ltd.* 375
POLYBUTYLENE-JACKETED AIR CORE PIC CABLE FOR USE IN STEAM EXPOSED DUCTS, *J. D. Dykes and G. F. DeVeau, Bell Laboratories* 387
RESTORATION OF WET PIC CABLE USING VAPORIZATION DRYING (ANALYSIS AND APPLICATION), *N. E. Hardwick, Bell Laboratories* 393
ECONOMICS AND PERFORMANCE CONSIDERATIONS OF TELEPHONE CABLE PLUGGING, *F. M. Farrell, III, M. Filreis, J. D. Groves and H. K. Kapell, 3M Co.* 403

THE MATHEMATICAL RELATIONSHIP BETWEEN THE BENDING RADIUS OF A CABLE AND THE LENGTH OF CABLE LAY

Joseph C. Lilly
Chief Process Engineer
Plastic Wire & Cable Corporation
A Subsidiary of Triangle Industries, Inc.
Jewett City, Connecticut 06351

ABSTRACT

A mathematical study is made of the length of a conductor in a bent cable compared to the length of the same conductor before the cable is bent. A comparison is made with graphic representations describing the effect of the cable lay, as related to the bending radius, on the change in the length of the conductor path in the cable.

SUMMARY

This study started out as an attempt to find a way to relate exactly a defined length of lay for each layer of a cable to the designed bending radius of the cable. At the time the author agreed to present the paper this seemed entirely possible and the mathematics had been worked out showing such a defined situation.

Further study then proved the original hypothesis to be incorrect. The entire problem was then reworked and the findings are published here.

This paper is a theoretical study of the relationship between two fixed cable parameters, the location of the conductor in the cable and the bending radius of the cable, and a variable parameter, the helical twist built into the cable to permit bending.

The length of the path of the conductor in the bent cable is always longer by some amount than the length of the path of the conductor in the cable prior to bending. The degree of difference in the lengths of the two paths is controlled by the pitch of the helical path of the conductor in the unbent cable. We call the pitch of the helical path the length of lay. It is the distance along the cable axis consumed during one complete twist of the conductor about the cable axis.

We learn here that we cannot design a perfect cable - one in which no stresses are imposed on the conductor by bending the cable. Because the path of the conductor in the bent cable is always increased in length compared to the path occupied in the unbent cable, a tensile force acts on the conductor tending to elongate.

The matter resolves itself into one of degree. The paper shows a solution to the degree of increased length - called the stretch - and develops an extremely interesting family of curves.

What is implied by this study is that our conventional practice of placing the shorter lay in the inner layer of a cable and the longer lay in the outer layer is not always - or not generally - the best design practice. Also, in contradiction to our conventional practice, we find here that treating the specification of lays in one layer in respect to those in other layers in linear relation is incorrect.

This paper is not intended to be a defined solution to the design problem. The author hopes this endeavor will spur other students of cable problems to examine these findings, distill and refine these ideas, and publish their own findings. Design of cables, laboratory studies, testing, and field experience are needed to resolve the design of probably the simplest of all our processes, twisting the cable.

INTRODUCTION

Continual observations of three phenomena prompted this attempt to relate the length of lay in a cable mathematically to the bending radius of the cable.

1. In cables made up with flexible stranded conductors failure occurred often in the same way. Under continual flexing conditions, one or more conductors had broken inside the insulation. Examination of these failures showed that the copper had stretched and the resulting increased length developed a kink in the conductor. Additional flexing then had severed the conductor at the kink.

2. In the same type cable flexed less severely - that is over a larger radius pulley wheel, for instance - the construction had become distorted into a corkscrewed configuration. Examination showed some conductors in the cable had become shorter than others within the same layer of the cable. The condition was obviously caused by a tensile stress acting on the conductors destroying the helical pattern in the cable.

3. Because of machine limitations, 500 MCM Class C 61 Wire Strand Copper had been put up on 24" diameter drum reels. Each layer of the strand had a lay length about 15 times the O.D. of the layer in keeping with ASTM maximum specification. As the wire paid off these reels the strands in the outer layers were "Birdcaging" to almost five inches diameter at the bottom of a 3300 foot reel length. It was quite obvious the copper strands had stretched in winding the conductor on to the reel.

During bending a tensile force had acted on the elements helically wound into these constructions. It was then reasoned that the path of the helically wound element must have been longer in the bent condition that it had been in the unbent condition.

PRELIMINARY CONSIDERATIONS

If we examine the mathematics of the unbent cable we find a simple right triangle diagram which describes the length of the helical path of the conductor.

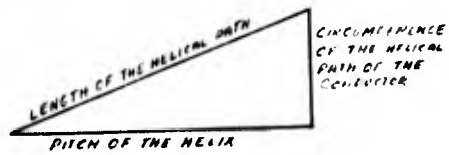

FIGURE 1

One side of this diagram is the circumference of the helical path of the conductors and the other side is the pitch length of the helical path (the length of lay). The vector sum of these two distances is the length of the helical path of the conductor for one turn of the conductor about the cable axis.

A cross section diagram of a cable layer is shown in Figure 2. All the conductors in the layer are located at a distance a from the central axis of the cable.

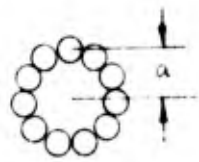

FIGURE 2

In Figure 3 we have the right triangle diagram again but this time it is labeled with mathematical dimensions.

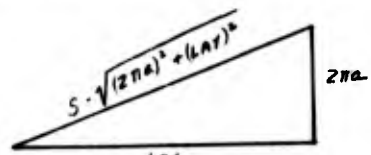

FIGURE 3

To accommodate a solution to this problem this conventional right triangle diagram must be altered into two triangles each descriptive of the conditions for one half the lay. Figure 4 shows that diagram. Note that none of the trigonometric relationships have been changed.

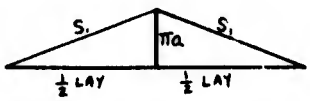

$$S_1 = \sqrt{(\pi a)^2 + \left(\frac{LAY}{2}\right)^2}\ , \quad (I)$$

FIGURE 4

Now that we have this diagram we will solve the problem comparing the length S_1 , - which is the length of the helical path of the conductor for 1/2 lay in the unbent cable - with the new length S_2 to be developed. S_2 is the length of the path of the conductor in the bent cable for the same 1/2 lay distance along the cable axis.

Half of the diagram in Figure 4 is now discarded since we have symmetry and are interested only in comparing to the length S_1 . We set the retained half of the diagram upon a circle which represents the bending radius circle of the cable measured to the central axis of the cable. See Figure 5.

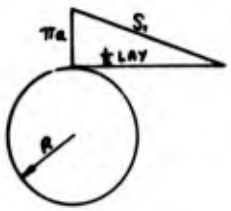

FIGURE 5

The bending radius in Figure 5 is labeled R . If we pursue a course now where the three parameters a , R and LAY are used we become involved with too many variables to effect a workable solution. At this point we recognize that for any given solution the value of a is fixed and the value of R is fixed. That is to say that the location of the conductor in the cable in respect to the central axis is fixed and the design bending radius is fixed. So we adopt a ratio:

$$N = \frac{R}{a} \qquad R = Na$$

In regard to the length of lay, we now define a value T as being the number of turns of the helical path in the circumference of the bending radius circle. Thus:

$$T = \frac{2\pi Na}{LAY}$$

$$LAY = \frac{2\pi Na}{T}$$

Recalling now the expression for S_1 , and substituting we have:

$$S_1 = \sqrt{(\pi a)^2 + \left(\frac{LAY}{2}\right)^2}\ , \quad (I)$$

$$S_1 = \sqrt{(\pi a)^2 + \left(\frac{\pi Na}{T}\right)^2} = \frac{\pi a}{T}\sqrt{(N^2+T^2)}\ , \quad (II)$$

BENDING THE CABLE

The diagram of Figure 5 is now redrawn in Figure 6 and relabeled.

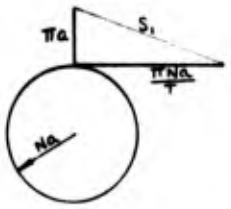

FIGURE 6

We now consider the triangle describing S_1 , as a perfectly flexible material and we bend the triangle diagram about the periphery of the bending radius circle so that the side $\frac{\pi Na}{T}$ is congruent with a portion of the circumference of the circle. The diagram in Figure 7 shows the triangle diagram in the unbent position with the length of the path of the conductor labeled S_1 , and the triangle bent about the periphery with the length of the path of the conductor labeled S_2 .

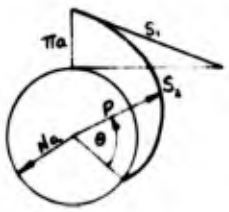

FIGURE 7

Also shown on the diagram in Figure 7 is the radius vector P of the curve developed by the hypotenuse when the triangle is bent.

The curve developed is an Archimedean spiral with the polar equation:

$$P = Na + Ta\theta = a(N + T\theta), \quad (III)$$

The geometric construction of this curve and the derivation of its equation is given in detail in Appendix A of this paper.

S_2 is a portion of the curve. S_2 is the length of arc of the curve from the point where $P = Na$, that is at $\theta = 0$, and the point where $P = Na + \pi a$ that is at $\theta = \frac{\pi}{T}$ radians. (See Appendix A).

In any basic text on integral calculus we find the length of arc of a polar curve to be:

$$S = \int_{\theta_1}^{\theta_2} \sqrt{P^2 + \left(\frac{dP}{d\theta}\right)^2}\ d\theta$$

Here:

$P = a(N + T\theta)$, (III) $\quad P^2 = a^2(N^2 + 2NT\theta + T^2\theta^2)$

$\frac{dP}{d\theta} = Ta \qquad \left(\frac{dP}{d\theta}\right)^2 = T^2a^2$

Then:

$$S_2 = a\int_0^{\frac{\pi}{T}} \sqrt{(N^2+T^2) + 2NT\theta + T^2\theta^2}\ d\theta$$

and we integrate and apply the limits and arrive at:

$$S_2 = \frac{a}{2T}\Big[\pi\sqrt{(N^2+T^2) + 2\pi N + \pi^2}$$
$$+ N\sqrt{(N^2+T^2) + 2\pi N + \pi^2}$$
$$- N\sqrt{(N^2+T^2)}$$
$$+ T^2 \ln\left(\sqrt{(N^2+T^2) + 2\pi N + \pi^2} + \pi + N\right)$$
$$- T^2 \ln\left(\sqrt{(N^2+T^2)} + N\right)\Big]$$

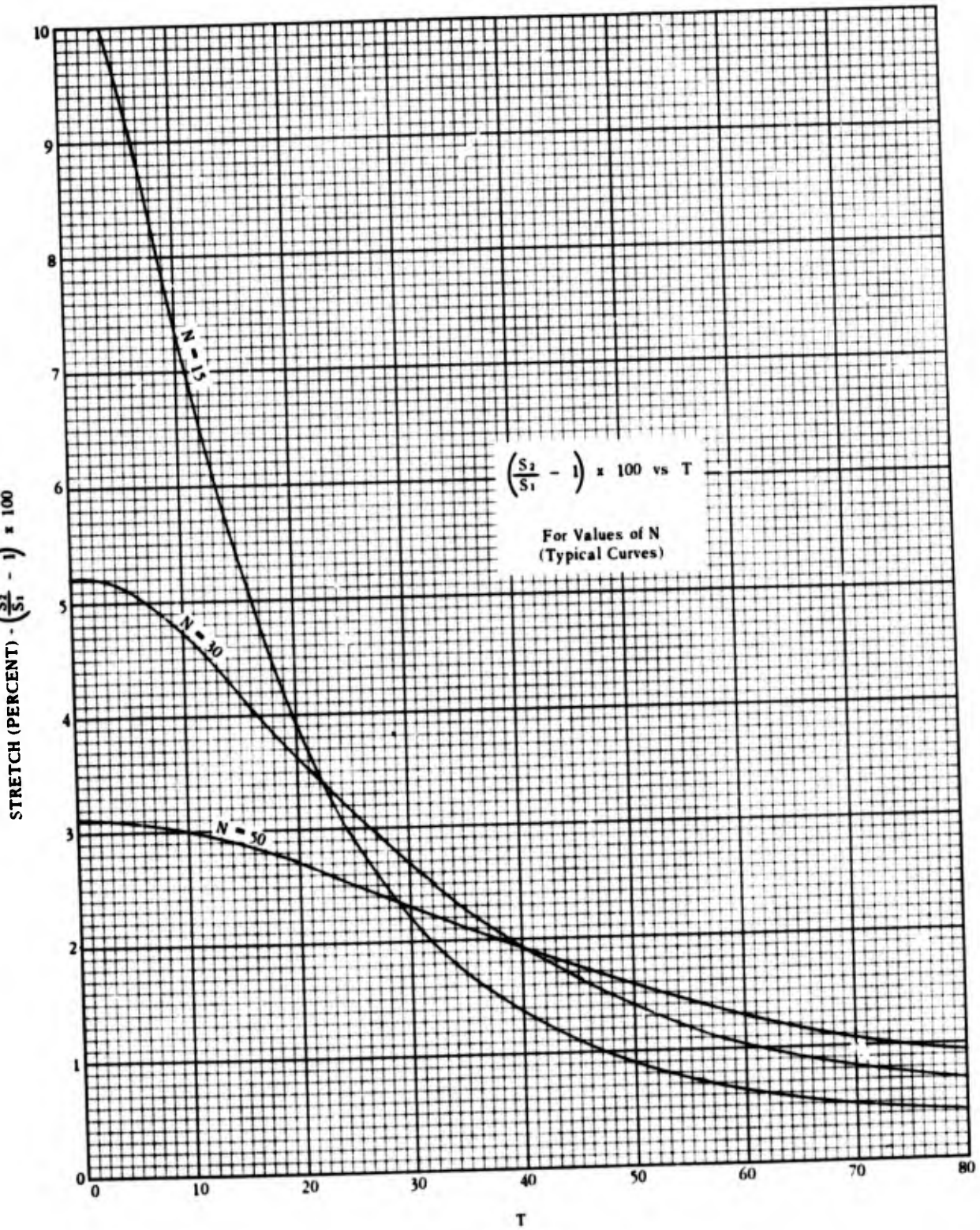
STRETCH (PERCENT) - $\left(\frac{S_2}{S_1} - 1\right) \times 100$
$\left(\frac{S_2}{S_1} - 1\right) \times 100$ vs T
For Values of N
(Typical Curves)
N = 15
N = 30
N = 50
0
1
2
3
4
5
6
7
8
9
10
0
10
20
30
40
50
60
70
80
T

FIGURE 8

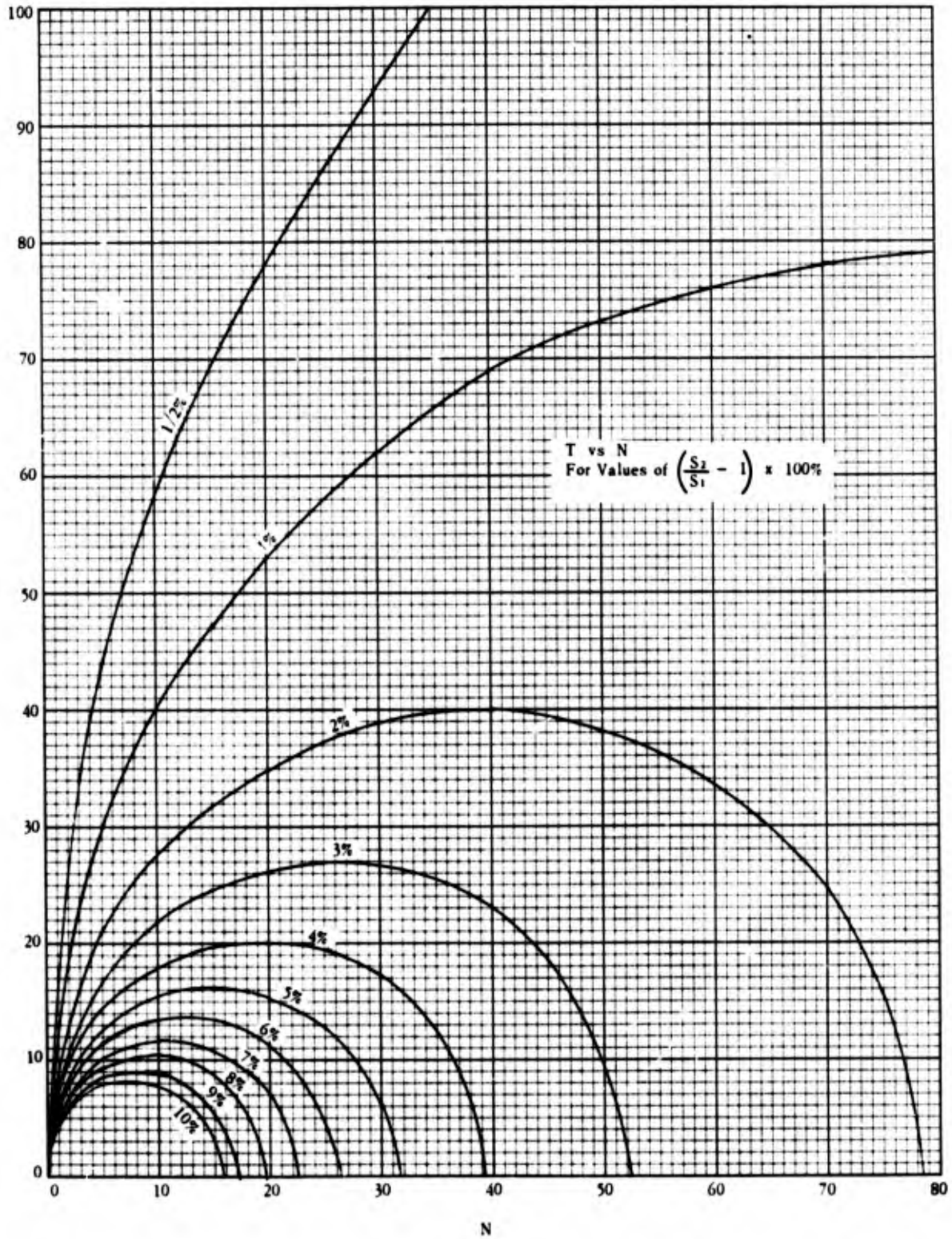
T vs N
For Values of $\left(\frac{S_2}{S_1} - 1\right) \times 100\%$
1/2%
1%
2%
3%
4%
5%
6%
7%
8%
9%
10%
0
10
20
30
40
50
60
70
80
90
100
N

FIGURE 9

Which is the length of the path of the conductor in the bent cable. We wish to compare this to the length S_1, so we recall our expression for S_1,

$$S_1 = \frac{\pi a}{T}\sqrt{(N^2+T^2)}, \quad (II)$$

Now $\left(\frac{S_2}{S_1} - 1\right) \times 100$ tells us the

percent increase of S_2 in respect to S_1, and we call this quantity the "stretch".

To simplify our writing of these equations let:

$$D = \sqrt{(N^2+T^2)+2\pi N+\pi^2}$$

$$E = \sqrt{(N^2+T^2)}$$

Then

$$\frac{S_2}{S_1} = \frac{1}{2\pi}\left[\frac{\pi D + ND - NE + T^2 \ln(D+\pi+N) - T^2 \ln(E+N)}{E}\right]$$

Values are then plotted

$$\left(\frac{S_2}{S_1} - 1\right) \times 100 \text{ vs. } T \qquad \text{for given values of } N$$

In Figure 8 typical plots of three curves are shown. Here the stretch is plotted against values of T for $N=15$, $N=30$, and $N=50$

Now from these type curves, data was picked off in order to plot T vs. N in a family of curves each of which represented a given degree of stretch. In Figure 9 such a family of curves is given where the stretch is taken as 1/2%, 1%, 2%, 3%, 4%, 5%, 6%, 7%, 8%, 9%, and 10%.

The supporting data for these curves is given in Appendix B of this paper.

CONCLUSIONS

In the design of cables which must bend and flex it seems reasonable that we should design so that the stresses imposed on the conductors by bending would be equal on all of the conductors. We should also take care that the forces on the conductors should be contained within practical design limitations.

When we examine the data developed here we find that our conventional practices in specifying lengths of lay in cables do not accomplish these requirements.

Examination of the data plotted in Figure 9 where the curves are almost half circles, shows that depending on the values of N - we might have a situation where the lays in two layers should be the same. At a different bending radius specified, N might be such that the longer lay might be required in the inner layer and the shorter lay in the outer layer. Certainly the lays would never fall in linear relation to one another. The conventional practice of calling out lays as a constant multiplier of the layer diameter is then questionable.

All the work done here is based on the position of the conductor in relation to the center axis of the cable being fixed. As long as the dimension a remains fixed the conductor will stretch to some degree when the cable is bent. This suggests that cables intended for severe or constant flexing should be made with a resilient center member which would allow the a dimension to diminish as the cable is bent and to return to proper position upon straightening the cable.

The author has one reservation about the data developed here. The curves in Figure 9 show two intercepts of the axis of abscissas, one at $N=0$ which is entirely reasonable and one at some positive value of N. If T were truly zero at some positive value of N then the lay would be infinite and zero twist would be required. The author cannot accept this as true. Rather it is believed we have here a situation which is indeterminant. Certainly more study is needed regarding the meaning of the intercept at positive values of N.

ACKNOWLEDGEMENTS

The author wishes to extend his sincere thanks to his colleague Mr. Wilbur Beckwith who tirelessly reviewed, corrected and clarified the mathematics here and offered arguments which prompted further investigation. Also appreciation is extended to all those who listened and encouraged this writing and to Mrs. Catherine DelMonte and Miss Annette Coffey who did the typewriting.

APPENDIX A

CONSTRUCTION OF THE CURVE

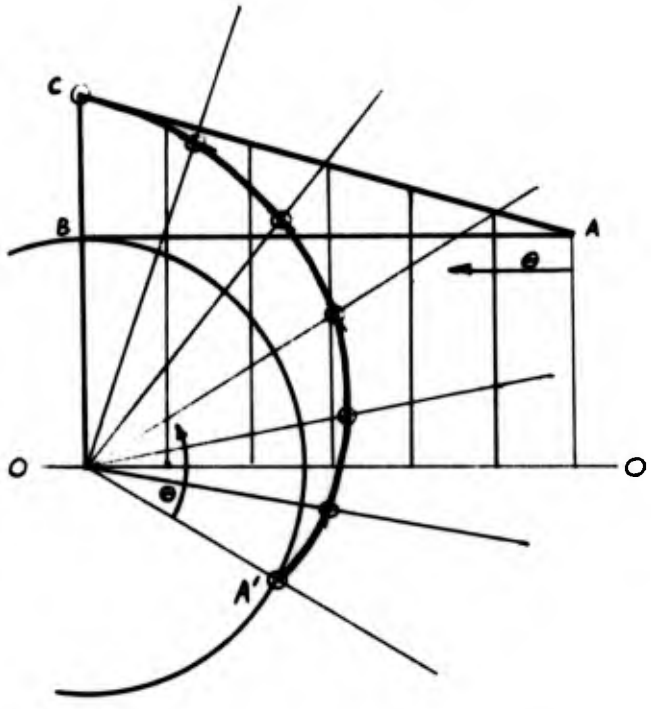

Draw a circle representing the bending radius circle. Draw a right triangle diagram ABC such that the base line of the triangle is tangent to the circle at the point B. Construct a radius line from the center of the circle to point B. Lay off the distance AB along the periphery of the circle from point B to a point designated A'. Draw a radius line from the center of the circle through A'. Construct a line parallel to AB passing through the center of the circle and label the line 00. The distance from 00 to AB is equal to the radius of the circle.

The distance AB is the same as BA' and is representative of the angle through which the arc of the curve passes. Divide AB into several equal parts (here shown six parts) and draw lines through these division points perpindicular to AB and extending from 00 to AC. These lines are equal to the radius vector to the curve at the angular divisions represented along AB. Divide the angle from A' to B into the same number of equal parts laid out along AB (here shown six parts) and extend radius lines outward beyond the periphery of the circle. Along these radius lines scale off the corresponding distance from 00 to AC to locate points on the curve. Connect the points with a smooth curve.

ARCHIMEDEAN SPIRAL

Reference: Mathematics, A Text-Book for Technical Students; Bevis, Brunel Low; Longmans, Green and Co., London, New York, Toronto, 1931.

If a radius vector rotates with uniform angular velocity and if a point moves along the radius vector with uniform velocity, then the

point describes an Archimedean spiral. For equal increments of θ there are equal increments of ρ. If successive values of θ are in arithmetical progression the corresponding values of ρ are also in arithmetical progression.

So the curve is an Archimedean spiral which in classic form has an equation

$$\rho = m\theta$$

where m is a constant, ρ is the length of the radius vector of the curve when the vector has turned through θ radians.

Our curve is removed a distance Na (the radius of the bending circle) from the center. At $\theta = 0$ radians $\rho = Na$; and when θ is at the other end of the arc $\rho = Na + \pi a$. We must then find θ when $\rho = Na + \pi a$.

The distance AB is:

$$AB = \tfrac{1}{2}\,LAY = \frac{\pi Na}{T}$$

$$AB = BA'$$

$$BA' = Na\theta$$

$$\therefore\ Na\theta = \frac{\pi Na}{T}$$

$$\theta = \frac{\pi}{T}\ RADIANS$$

So to satisfy $\rho = Na + \pi a$ at $\theta = \frac{\pi}{T}$ the curve has the equation:

$$\rho = Na + Ta\theta = a(N + T\theta),\ (III).$$

Note: The author has taken some small liberties with the Bevis reference in altering letter designations in order to avoid confusion with like letters used in solving this problem. For instance the reference text uses r as the length of the radius vector which is changed here to ρ, and the reference text letter a is changed here to m.

APPENDIX B

TABULATION OF DATA USED IN PLOTTING THE FAMILY OF CURVES IN FIGURE 9

	Values of T for Stretch Values Of:										
N	1/2%	1%	2%	3%	4%	5%	6%	7%	8%	9%	10%
5	43.2	30.0	21.0	16.8	14.4	12.6	11.3	10.2	9.3	8.6	8.0
10	58.0	40.0	27.5	21.6	17.9	15.3	13.3	11.7	10.3	9.0	7.8
15	69.0	47.0	31.9	24.5	19.7	16.2	13.4	10.9	8.6	6.2	3.2
20	78.0	53.0	34.9	26.0	20.0	15.1	11.1	7.2			
25	85.0				19.6	13.0					
30	91.4	62.0	38.9	26.6	17.1	6.4					
35	100.5				2.3						
40	108.0	69.0	40.0	23.0							
50	119.0	73.0	38.0	9.4							
60		76.0	33.8								
70		78.0	24.7								
75			15.6								
80		79.0	0								
90		78.0									

Values on N at the T = 0 Intercept:

T	1/2%	1%	2%	3%	4%	5%	6%	7%	8%	9%	10%
0	314.2	157.1	78.5	52.4	39.3	31.4	26.2	22.4	19.6	17.5	15.7

BIOGRAPHICAL SKETCH

Joseph C. Lilly began his studies in Electrical Engineering at Louisiana State University during his Army Service in World War II. He received his B.S. in E.E. from Rhode Island State College in 1949. He was employed until 1953 by the U.S. Army Signal Supply Agency as an Inspection Engineer. For the past 21 years he has been employed by the Plastic Wire and Cable Corporation in a variety of Engineering positions.

PROGRESS IN SZ TWISTING AND STRANDING OF COMMUNICATIONS CABLES

D. Vogelsberg
SIEMENS AG
Berlin, Germany

Summary

SZ twisting and stranding with"breathing" accumulators as presented during the 20th Wire and Cable Symposium has meanwhile proved an economical and operationally reliable method requiring a minimum of personnel. Universal use for conductor diameters between 0.4 and 0.8 mm is now possible with a newly developed machine being able to twist 5 star quads from 20 cores in parallel at a pull-off speed of 100 m/min and to bunch them in the same operation to form a basic unit. Owing to the good coupling quality, control measurements on the finished basic unit can be omitted.

Introduction

In cable industry like in other branches of industry it is necessary to increase the productivity of labor to be in a position to manufacture cables economically also in future despite permanently rising personnel cost. Therefore, manual routine work has to be reduced and the disengaged manpower to be employed for more qualified activities, e.g. highly productive manufacturing processes.

Let us look from this angle at the manufacture of communications cables: A great number of the twisting and stranding personnel has - out of the variety of operations required to make a communications cable - to do only a minor step, viz. to twist 2 or 4 wires with each other to form a new element - a wire pair or quad. In this connection, the personnel's duty is not to supervise a complex manufacturing process but simply to insert empty bobbins into the machine and remove full bobbins, if possible, without any interruption - an activity which, in principle, could be performed also automatically.

Since with the conventional stranding technique the whole material to be twisted and stranded has to swing around the stranding axis or to be encircled by a stranding flier, the bobbins cannot be of any size, which means that they have to be replaced most frequently. Consequently, more than half the twisting and stranding personnel has to be engaged in the pair or quad twisting process. This statement is almost independent of the working speed of the twisting and stranding machines.

SZ-Twisting and Stranding

To save personnel expenses, without using highly expensive automatic conveying and feeding equipment, it is reasonable to combine the first twisting step (the pair or quad twisting) either with the conductor insulating process or with the subsequent unit stranding process. The appropriate method here is the SZ-twisting and stranding, which means stranding with section-wise reversing direction of lay.

Since such a combination of processes has the effect that the replacement of the wire bobbins or of the pair and quad bobbins can be omitted, the productivity of the machine operators can be nearly doubled, even if, compared to the separate processes, the working speed is reduced.

The SZ-twisting and stranding method allows the use of stationary pay-off and take-up devices and thus also the use of reels of any size, which means another reserve for a productivity increase: Machinery for the combined twisting and unit stranding, where only once per shift large reels or containers have to be inserted, are, in fact, realizable today and being taken into consideration. Their operation can be organized so that, for example, during night-shift operation only a minimum of supervisory personnel is required.

Novel SZ-twisting and stranding methods for the first twisting step, i. e. for pair twisting and quadding, which had been developed by the Siemens Company, were reported in 1971[1].

SZ-Method with "Breathing" Accumulators

The SZ-method using "breathing" accumulators has meanwhile gained particular importance for local cables. The process is distinguished by two roller-type accumulators rotating with constant speed in opposite directions and altering their capacities inversely (Fig. 1)[2]. Since the sum of capacities of both "breathing" accumulators remains constant, the wires of the element to be twisted enter the first accumulator with the same constant speed with which the finished element leaves the second accumulator. Like with conventional twisting and stranding machines, deceleration and acceleration problems are, because of the uniform mode of operation, only of minor importance. Therefore, when using this method, higher pull-off speeds and thus also higher output rates than with other SZ-star quad twisting methods could be expected.

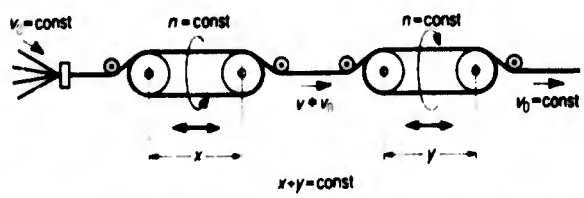

Fig. 1 SZ-twisting or stranding with two accumulators having changing capacities rotating constantly in opposite directions

Meanwhile, the SZ-method with "breathing" accumulators has been further developed, tried out in a pilot manufacture of more than 700,000 conductor-km (2.3 BCF), and introduced into normal manufacture. The process has proved suitable for the star quad twisting of plastic-insulated conductors of 0.4 to 0.6 mm (0.016 - 0.031 in) diameter and of paper-insulated conductors of 0.4 to 0.6 mm (0.016 to

0.024 in) diameter, without using an adhesive to fix the lay reversal points.

This method is, of course, also suitable for twisting wires to pairs, thereby allowing an about 40 percent higher pull-off speed at the same accumulator rotational speed, even if equal lengths of lay are assumed for pairs and star quads. This is possible by an optimized choice of the machine parameter l/l_o for the production of wire pairs, where l is the interval between lay reversal points and l_o the maximum changing rate in accumulator capacity[3].

In the following, a report is given on the experience gathered with "breathing" accumulators used for a combined quadding and bunching process. The positive results obtained in view of productivity, operational reliability, and electrical characteristics led in the Siemens Company to the decision to switch in the next years the whole plastic-insulated local cables manufacture for the German Post Office over to the combined quad twisting and basic unit stranding process.

Experience Gathered with Test Machines

Two types of test machines had been designed which, since the report given in 1971, have been further developed. According to the design of unit-stranded local cables introduced in Germany, the two machines twist 20 single wires each to 5 star quads in one single operation - with a pull-off speed of 70 m/min (230 fpm). The star quadding is performed by means of "breathing" accumulators. The intervals between the lay reversal points were reduced to about 5 m (16.4 ft).

For the basic unit stranding, two different methods are applied:

With the machine shown in Fig.2a(up to now only designed for 0.4 and 0.6 mm conductor diameter), the basic unit is also SZ-stranded by means of a "breathing" accumulator arrangement and wound onto a stationary spooler. To reduce the mechanical stress on the wires to be twisted, a rotating pull-off device is connected between the star quadding part and the basic unit SZ-stranding part[4]. SZ-stranding of the basic unit is advisable, if large unit lengths are involved and therefore very big reels with more than say 1250 mm(4.1 ft) flange diameter are to be used. The basic unit SZ-stranding makes it furthermore possible to perform the stranding process without any stops, if, for example, a double take-up stand is employed.

With the machine illustrated in Fig. 2b for 0.4 to 0.6 mm conductor diameter, the basic unit is bunched conventionally using a rotating spooler with preconnected rotating pull-off device.

It has proved that the results obtained with regard to quality and output rate are - with an appropriate machine rating and design - independent of the fact whether a machine as shown in Fig. 2a or 2b is used. The method applied for basic unit stranding has no remarkable influence on the capacitance unbalance level.

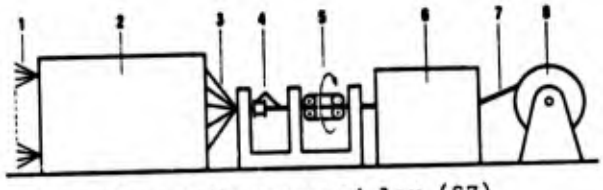

2a Stranding with reversed lay (SZ)

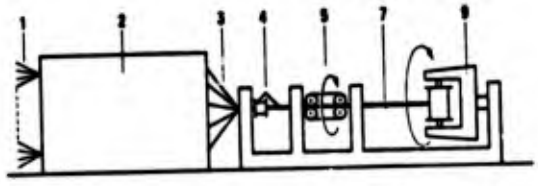

2b Stranding with constant lay (conventionally)

Fig. 2 Combined quadding and basic unit stranding machines

1 20 cores
2 SZ quadding equipment
3 5 star quads
4 central spinner
5 rotating pull-off device
6 SZ basic unit stranding equipment
7 basic unit
8 stationary take-up device
9 rotating take-up device

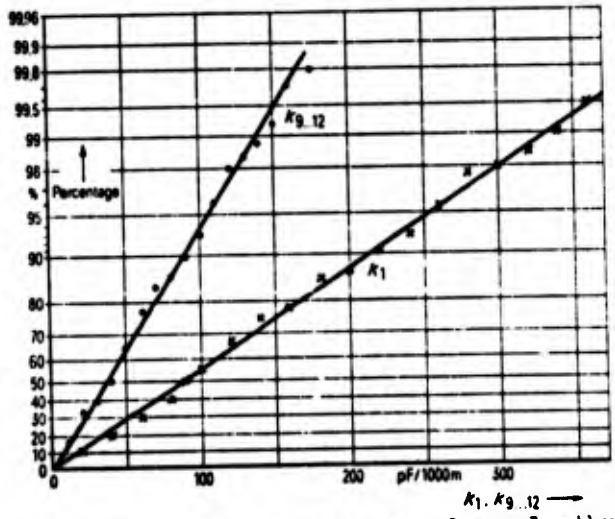

Fig. 3 Capacitance unbalances of a polyethylene-insulated local cable with SZ twisted star quads having 0.4 mm conductor diameter (0.016 in)

k_1: unbalances within a star quad (N = 200)

$k_{9...12}$: unbalances between adjacent star quads within a basic unit (N = 800)

The electrical and mechanical characteristics of the unit produced in one single operation from single plastic-insulated wires correspond to the data obtained from units produced according to the hitherto used technique, if otherwise equal prerequisites can be taken as basis.

The capacitance unbalances k_1 and k_9 to k_{12} follow most reliably a normal distribution according to Gauss (Fig. 3). The normally feared "outliers" from the normal distribution are safely avoided. Characteristic mean and maximum values for solid-PE or cellular-PE-insulated cables, referred to 300 m (984 ft), are compiled in table 1.

capacitance unbalance		mean value pF/300 m	max. value pF/300 m	number of values
within a star quad	k_1	40	200	250
between adjacent quads within a basic unit	k_9	20	110	1000
between non-adjacent quads within a basic unit	to k_{12}	13	65	1000

Table 1

To reach a satisfactory k_1-level, the wires are pulled off "overhead" by fliers provided with hysteresis brakes.

It is remarkable that the lay reversal points in the star quads themselves have no influence on the unbalances k_1 within the quads being highly sensitive to geometric disturbances, even if the distance between the reversal points is 5 m (16.4 ft). More attention has to be paid to the unbalances between adjacent quads k_9 - k_{12}, which will be treated later in a separate paragraph.

Owing to the good unbalance level obtained with the combined quadding and basic unit stranding process using "breathing" accumulators, intermediate check measurements to be conducted on the finished basic units are not necessary at all. Only where conductors of 0.4 mm (0.016 in) diameter are involved, it is useful to subject the basic units to a "ringing" test to be in a position to notice and repair conductor breaks. Next to the economical side, this is a decisive stimulus to introduce this new twisting method.

The mechanical stress on the copper conductors and the number of conductor breaks are not higher than with high-speed flier-type twisting machines. The mean resistance increase of 0.4 mm conductors - when passing the machine - comes up to about 1 to 2 percent.

One operator can service two quadding/basic unit stranding machines. The per-capita output, expressed in conductor-km or BCF, is almost double as high as with high-capacity quadding machines, since here no replacement of quad bobbins is necessary.

When twisting paper-insulated wires, the paper lapping direction (and sometimes also the paper string lapping direction) as well as the moisture of the material to be twisted have to meet certain requirements so that paper breaks are avoided. The specifications applicable to paper-insulated unit-stranded cables of the German Post Office can reliably be adhered to.

A New Quadding/Basic Unit Stranding Machine

In cooperation with the FRISCH Kabel- und Verseilmaschinenbau GmbH, Ratingen near Duesseldorf, a new universal machine for plastic-insulated and paper-insulated conductors of 0.4 to 0.8 mm (0.016 to 0.031 in) diameter has been developed. Its maximum pull-off speed is 100 m/min (328 fpm), the reversal distance in the quads is about 4 m (13.1 ft).

In 5 parallelly operating SZ-twisting devices, 5 star quads are produced simultaneously and immediately afterwards, with constant direction of lay, stranded to a basic unit (similar to Fig. 2b). Each star quad passes two roller-type accumulators arranged in series and rotating with constant speed in inverse directions, as shown in Fig. 1. By a continuous linear change of the roller distances in axial direction, the pull-off speed between the accumulators arranged in series alternates - according to the lifting tackle principle - between two different values. The interaction of constant rotational movement and periodically changing pull-off speed at the transition point between the accumulators has the effect that in each of the 5 finished star quads there is a section-wise alternating direction of lay.

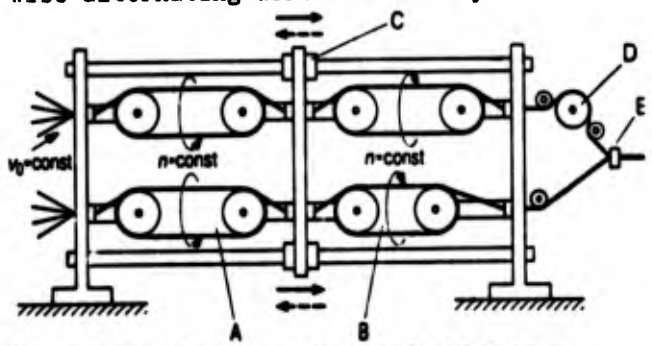

Fig. 4 Double accumulators operating in parallel with common control of the accumulator capacities

The accumulator capacity increase and decrease is performed time-synchronously for all 5 parallelly operating double accumulator arrangements by means of a middle frame C moving to and fro in axial direction, see Fig. 4. The 5 double accumulators are driven with different rotational speeds to achieve in the 5 star quads different lengths of lay and thus a good mutual decoupling. A photograph of the quadding part is shown in Fig. 5a.

The finished star quads run via guide rollers looped not more than once into the subsequent basic unit stranding closer. Rollers of different sizes (D in Fig. 4) have the effect that the lay reversal points are spatially staggered so that they are not located parallelly in the completed basic unit and undesired couplings are avoided.

The spatial staggering of the lay reversal points is also caused by different basic capacities, i.e. different axial dimensions of the back accumulators B. Here it is made use of the fact that the length shift of the

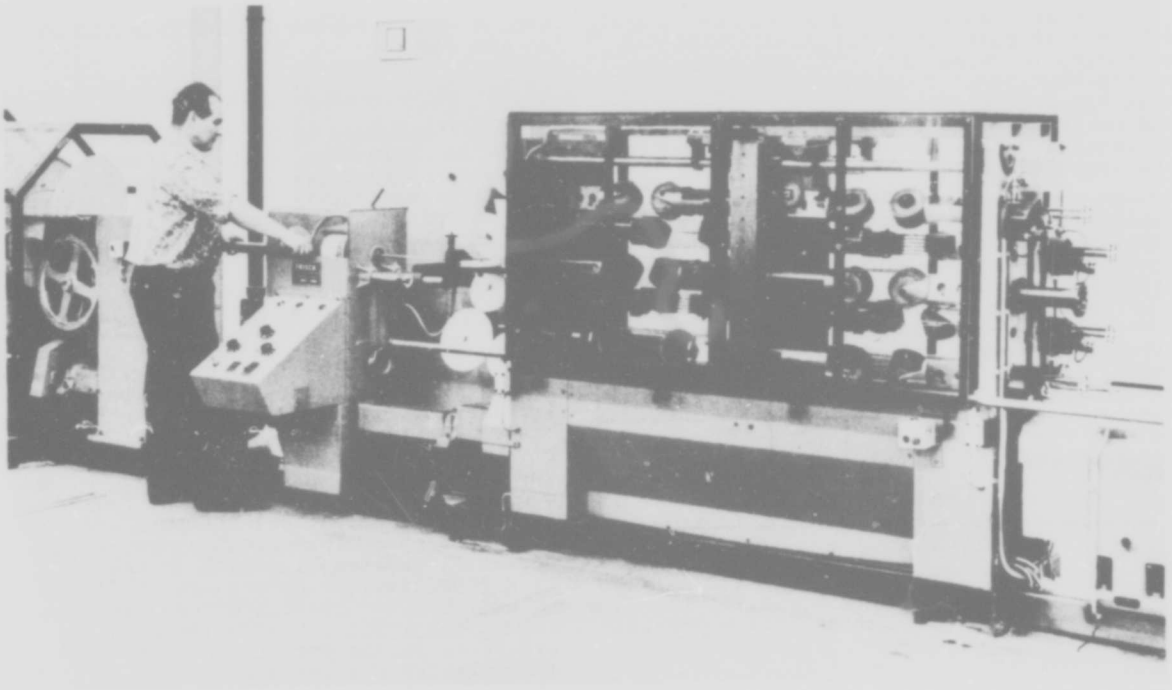

5a 5-fold star quad twisting equipment

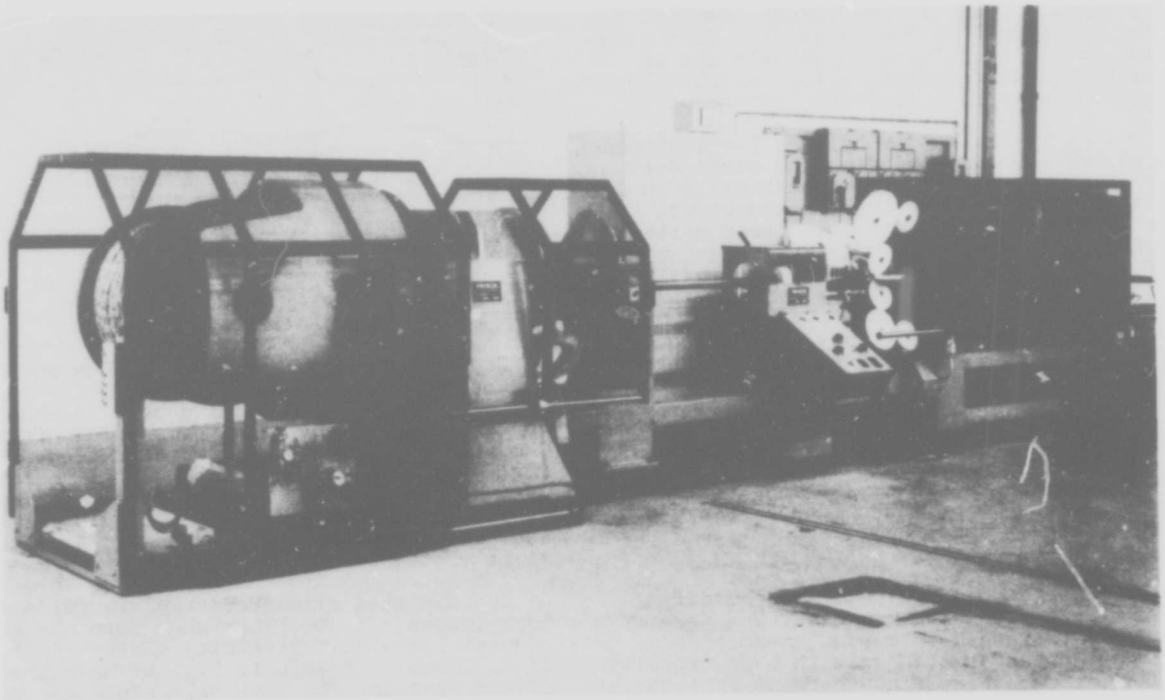

5b Basic unit stranding equipment

Fig. 5 New combined quadding and basic unit stranding machine for insulated conductors of 0.4 to 0.8 mm (0.016 to 0.031 in) diameter. Pull-off speed: 100 m/min(328 fpm).

quads in the finished unit is determined by the different path lengths between the movable frame C, on whose transverse plane the actual modulation of the stranding process takes place, and the basic unit stranding closer E.

The basic unit stranding part (Fig. 5b) corresponds to the known "Gruppenverseilmaschine" of the Frisch Company. The 5 SZ-twisted star quads are stranded conventionally by a rotor while applying a helix, and the completed unit is wound onto a reel with, say, 800 mm flange diameter.

The rotor is characterized by a cantilever eccentric pull-off capstan and a cantilever spooler[5]. The pull-off capstan of 400 mm diameter is of slightly conical shape and provided with an inclined deflector ring. Full take-up reels can be removed by a pneumatic lowering device.

The above described machine can also be designed in building-block fashion, e.g. for 10 pairs or for 7 or 14 star quads. Furthermore, the conventional basic unit stranding equipment could be replaced by a basic unit SZ-stranding part using a "breathing" double accumulator suitable for conductor diameters from 0.4 to 0.8 mm, so that, for example, a stationary spooler for very large take-up reels could be employed.

The capacitance unbalance level in plastic-insulated unit-stranded cables with 0.4 to 0.8 mm conductor diameter which were stranded with the new machine approximately correspond to that given in Fig. 3 and Table 1. The limit values of the German Post Office Specification FTZ 72 TV 1, Supplement 3, are reliably adhered to.

New Knowledge about Decoupling of SZ-Twisted Elements

Short intervals between lay reversal points of only some meters are critical mainly with regard to the couplings between adjacent twisted elements. When no special compensation measures were taken, length-proportional capacitance unbalances k_9 to k_{12} of a mean value of about 80 pF/1000 m (80 pF/3280 ft) were found between adjacent quads (curve 1 in Fig. 6).

These inadmissibly high capacitance unbalance values are only little dependent on the geometric expansion of the lay reversal points, but they are mainly due to the fact that different quads of one unit have equal constant intervals between lay reversal points. Equal constant intervals between lay reversal points for all quads of a unit are near at hand for reasons of a simple machine design.

The observed length-proportional unbalances can be explained by small remaining unbalances in each SZ-section (Fig. 7). These remaining unbalances have in each SZ-section the same amplitude and the same polarity. Therefore, the sum of unbalances increases linearly with the length.

To eliminate these unbalances which are non-existent with conventionally twisted

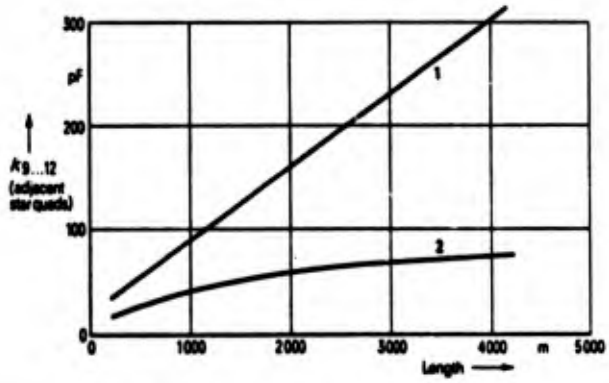

Fig. 6 Average value of capacitance unbalances $k_{9...12}$ between SZ twisted star quads as a function of cable length

1 without use of additional measures

2 with modulation of reversal distances

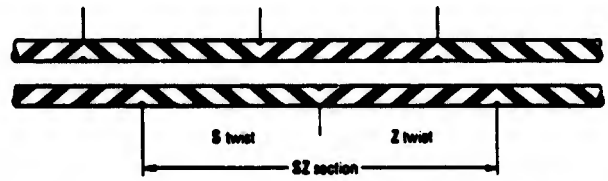

Fig. 7 Configuration of adjacent SZ star quads

quads, at first, the intervals between lay reversal points were slightly modulated. This modulation[6] was applied in same manner for all quads following either a) a random function or b) a step function. As expected, the systematic modulation according to the step function supplied the best results. At a length of 1000 m (3280 ft), the capacitance unbalances between adjacent quads were reduced by half (curve 2 in Fig. 6).

The solution with which the intervals between lay reversal points are modulated in equal steps can easily be realized when using the SZ twisting and stranding method with "breathing" accumulators, if the movement of the frame C (Fig. 4) is not reversed periodically but delayed step-wise. However, this solution, too, is not free from disadvantages: The step length of the modulation function must be adapted to the used lengths of lay of the quads.

This disadvantage is overcome by a newer and simpler method: The four wires of each quad are first guided through a lay plate 1 as usual and then through a twisting closer 2 before entering the first SZ-accumulator (Fig. 8). To compensate the capacitance unbalances k_9 to k_{12} between two quads increasing linearly with the length, the angular position of the lay plate 1 is - following a suggestion by Spatz and Dr. Gürkaynak - changed step-wise in intervals of, say, 50 m (164 ft) by turning it between 0° and 180°. In this manner, decoupling sections with same amplitude, but with opposite polarity of the undesired additional unbalances in the finished quads, are obtained. Each length

twisted in constant angular position includes a whole number of SZ-sections.

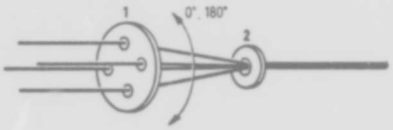

Fig. 8 Rotatable lay plate for elimination of length-proportional unbalances $k_{9...12}$ between adjacent star quads

In the SZ-machine shown in Fig. 5 five quads are twisted in parallel. To achieve here a good decoupling of all combinations k_9 to k_{12}, a turning scheme for four lay plates is used, see Fig. 9.

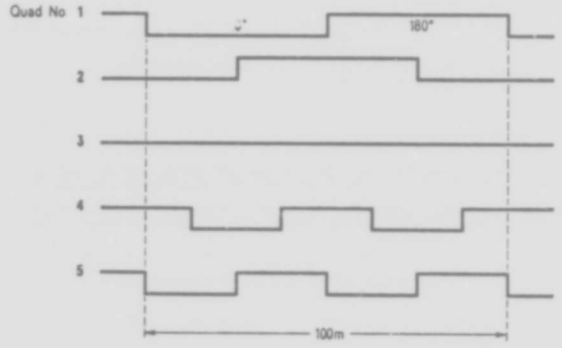

Fig. 9 Scheme for turning of rotatable lay plates (refer to Fig. 8)

This new compensation method has shown so far the best results independent of the lengths of lay of the quads and further improvements seem possible.

Limits of Economy

When the combined twisting/unit stranding in one single operation is to be more economical than the twisting and stranding in separate operations, certain prerequisites have to be fulfilled. For the combined quad twisting/basic unit stranding of local cables with 0.4 mm (0.16 in) conductor diameter as usual in Germany, the following data have been determined:

The per-shift output rate of a quad twisting/basic unit stranding machine must be at least 17.5 basic-unit-km (57,400 ft) and one operator has to service two machines. The new machine developed in cooperation with the Frisch Company allows - with 100 m/min pull-off speed - a per-shift output rate of 25 basic-unit-km (82,000 ft) thus exceeding the basic requirement by more than 40 percent.

The capital expenditure is almost the same for the combined quad twisting/basic unit stranding and for the twisting and stranding in separate operations. However, the wage-dependent costs are only half as high with the combined twisting and stranding which means a clear advantage in favour of the combined process.

When combining the basic unit/main unit stranding, comparably high cost savings cannot be achieved, since with this concept there would still be the high personnel requirement of the separate quad twisting process. Furthermore, the main unit stranding machine could not be utilized optimally. Frequent replacements of the small quad bobbins and the short unit lengths bring about undesired long downtimes, unless expensive automatic feeding devices are used: At a pull-off speed of 100 m/min, the per-shift operation of a main unit stranding machine for the different conductor sizes is by about 50 percent higher, when operating the machine with large basic unit reels instead of with small quad bobbins.

Comparable reflections apply, of course, also to the manufacture of cables made up of wire pairs.

References

1. Vogelsberg, D.: SZ Twisting and Stranding of Communications Cables Using Rotating Accumulators with Periodically Changing Capacity, International Wire and Cable Symposium 1971

2. US-Patent No. 3 481 127

3. Vogelsberg, D.: Die Verseilung von Nachrichtenkabeln mit Hilfe sich drehender Längenspeicher periodisch wechselnden Inhalts. Nachrichtentechn. Zeitschrift 23 (1970) p. 472

4. US-Patent No. 3 782 092

5. Deutsches Patent No. 1 510 088 (Frisch GmbH)

6. Deutsches Patent No. 2 213 693

D. Vogelsberg
SIEMENS AG
NK E 23
D-1000 Berlin 13
Postfach 120
Germany

Dieter Vogelsberg was born in 1930. From 1948 to 1955 study of communications engineering at Technische Universität Berlin. In 1955 he joined Siemens AG, where he has been engaged in the development of communications cables. During the last years he was responsible for communications cables research, design and measuring technique. He is currently head of a department in production engineering.

A REEXAMINATION OF STRANDING CONFIGURATIONS AND THEIR RELATIONSHIP WITH THE ELECTRICAL CONDUCTIVITY AND MASS OF CONCENTRICALLY-STRANDED CONDUCTORS

John F. McLaughlin
Raytheon Company
Sudbury Laboratory
528 Boston Post Road
Sudbury, Mass. 01776

Abstract

This paper reviews the history of conductor stranding from 1912 to 1972 and concludes that methods have not changed in these sixty (60)[1,2] years. It proposes that a reexamination of some widely accepted criteria is in order and makes some recommendations. The discussion is confined to concentric stranding of copper conductors.

Introduction

A review of accepted standards for the electrical resistance of contentrically-stranded copper conductors invariably shows the National Bureau of Standards, Handbook 100, as the root source for the data. Based on this broad acceptance, this paper will briefly review its history and, thereafter, use it as a reference point for discussion.

NBS Circular No. 31, April 1, 1912

Circular No. 31 was the original Handbook 100 and had a first edition date of April 1, 1912. The data on concentrically-stranded conductors was given in Table XII and the supportive discussion was given in Appendix IV. The Circular was published at the request of the Standards Committee of the American Institute of Electrical Engineers.

NBS Circular No. 31, January 27, 1956

This (fourth) edition provides data on concentrically-stranded conductors in Table 17 and supportive discussion in Appendix 4. The "Standard" stranding of the earlier editions is additionally classified as Class B; six additional wire sizes are given and extend the table to 5,000 MCM; the resistance change due to stranding is increased progressively from 2% to 5% for the six new wire sizes; the Committee on Wires of the American Society for Testing and Materials is named as the concurring authority.

NBS Handbook 100, February 21, 1966

Table 17 and Appendix 4 are a verbatim reprint of the 1956 version.

Nomenclature

The following terms and symbols are applicable as defined below for use with the text and the appendix.

- a = minor axis of elliptical cross-section
- b = major axis of elliptical cross-section
- c = chord length of an elliptical cross-section
- d = strand diameter
- e = major/minor axis ratio of an elliptical cross section
- h = pitch, ratio of axial length to helical diameter
- n = number of conductor strands
- n' = number of conductor strands comprising a given layer
- r = strand radius
- s = number of layers or stratums of concentric strands
- s'_k = a specific stratum or layer
- s' = number of layers or stratums within a specified diameter
- θ = pitch angle or helical angle
- ϕ = angle taken through elliptical cross-section

Stranding

Stranding is a method of physically combining a number of conductive strands into a flexible cylindrical shape for the purpose of passing current.

Foreword

NBS Handbook 100[3], from its earliest editions, established strand count for concentric stranding as a set of numbers starting with seven (7) and ending in two-hundred and seventy-one (271). It did not give any numerical criteria for lay or pitch but analyzed its impact on weight and conductor resistance.

ASTM Standard Specification B-8[4] employs the same range of strand count as in the preceding reference and in addition prescribes limits for lay as a function of flexibility. In its later editions, NBS Handbook 100 refers to the American Society of Testing and Materials as a source for this kind of data.

This section will review strand count and lay as provided in these two sources and in addition will examine their relation with strand gap, strand deformation and normal area. They will be treated initially as independent parameters but their mutual relationships will be given under the section on Normal Area Maximization.

Strand Count, n

Hexamerous Stranding. The construction most frequently used to form a concentrically-stranded conductor starts with a single conductor core and adds other layers which progressively increase in strand count by six (6), i.e., hexamerously. See Figure 1 for a typical example and equation (1) and Table 1 for strand count. It should be noted that the fundamental shape is hexagonal and not cylindrical.

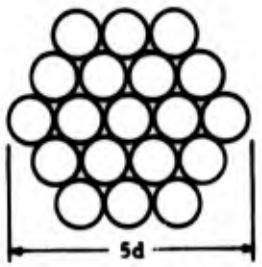

Figure 1. 19 Strand Concentric Conductor Without Lay (hexamerous)

$$n = 1 + 3s + 3s^2 \qquad (1)$$

Table 1. Hexamerous Stranding-Nine Layers

Core	Strands per layer 1	2	3	4	5	6	7	8	9	n= Total Strands
1	6									7
1	6	12								19
1	6	12	18							37
1	6	12	18	24						61
1	6	12	18	24	30					91
1	6	12	18	24	30	36				127
1	6	12	18	24	30	36	42			169
1	6	12	18	24	30	36	42	48		217
1	6	12	18	24	30	36	42	48	54	271

Polygonal Stranding. This is a construction where the strand count in any layer is determined by the perimeter of the polygon circumscribed by the pitch circle of that layer. Cable diameters are slightly less than in the hexamerous method. See Figure 2 for a typical example and equation (2) and Table 2 for strand count. It should be noted that the fundamental shape is cylindrical

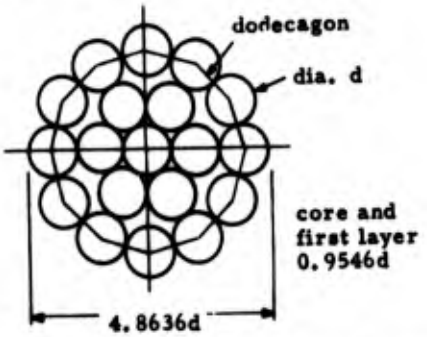

Figure 2. 19 Strand Concentric Conductor Without lay (polygonal)

$$n = 1 + \sum_{k=1}^{k=s} n'_k \qquad \left(\sin \frac{\pi}{n_k} \geq \frac{1}{2s'_k}\right) \tag{2}$$

Table 2. Polygonal Stranding-Nine Layers

Core	Strands per layer 1	2	3	4	5	6	7	8	9	n= Total Strands
1	6									7
1	6	12								19
1	6	12	18							37
1	6	12	18	25						62
1	6	12	18	25	31					93
1	6	12	18	25	31	37				130
1	6	12	18	25	31	37	43			173
1	6	12	18	25	31	37	43	50		223
1	6	12	18	25	31	37	43	50	56	279

Stranding Parameters

Lay (or pitch) and strand count are the parameters controlling the construction of stranded conduction; strand gap, strand deformation and normal area are parameters resulting from combinations of strand count and lay. Lay and pitch will be defined and subsequent paragraphs will examine the other parameters.

Lay. Lay (or lay ratio) is the ratio of the axial length of one turn of a strand and the outside diameter of the conductor. It is expressed as a numeric and may be further defined as being left or right depending upon the strand rotation around the axis of the conductor. Its usual limits are eight (8) and sixteen (16); the lower number, the tighter the lay.

Pitch, h. This term is used to give a true measure of helicality. Pitch is the ratio of the axial length of one turn of a strand and the helical or center line diameter. Pitch is also a numeric; it is always larger than the "lay" and is related to it by the following equation.

$$h = \left(\frac{2s' + 1}{2s'}\right) \text{lay ratio} \tag{3}$$

Strand Gap. When the lay of a conductor is insufficiently tight to cause all strands to bear against one another, there is an angular gap which may be equally spread between all the strands of a layer or accumulate and appear as a single gap between two adjacent strands. See Figure 3 and equation (4).

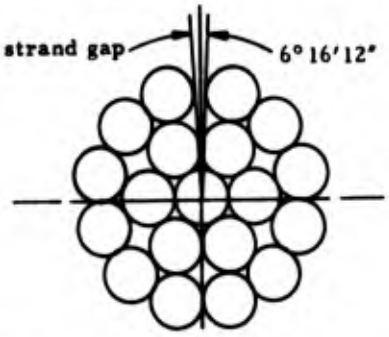

Figure 3. Strand Gap, 19 Strand Conductor Without Lay

$$\text{Strand gap} = \pi - n' \arcsin \frac{1}{2s'} \quad (h = \infty) \tag{4}$$

Strand gap can be reduced or eliminated by increasing the tightness of the lay.

Strand Deformation. Strand deformation is a metal displacement produced by the compression of adjacent strands. It is also called "cold working." It is always present in a seven-strand conductor and may be present in other strandings depending on the lay.

Figure 4 shows a cross-sectional projection of a seven-strand conductor and illustrates the apparent increase in circumferential diameter caused by twisting. Equation (5) gives the relationship. The radial diameter is not altered by twisting.

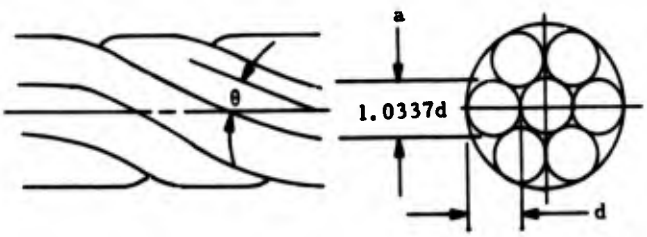

Figure 4. 7 Strand Conductor, Lay of 8

$$a = d \text{ secant } \theta \tag{5}$$

Since the strand cross-section (before deformation) was formed by the intersection of a plane and a cylinder, its shape is elliptical. The apparent diameter, a, of equation (4) is its major axis and the nominal diameter of the strand is its minor axis. Strand deformation flats or truncates this elliptical shape as the act of twisting forces the conductor into a space sufficient only for a lesser cross-section. The displaced metal appears as a distortion at the ends of the chord of contact; it may actually add to its length, but the uncertainty of its shape prevents inclusion in numerical data. The chord length will be taken as an elliptical chord. See Figure 5 and equation (6).

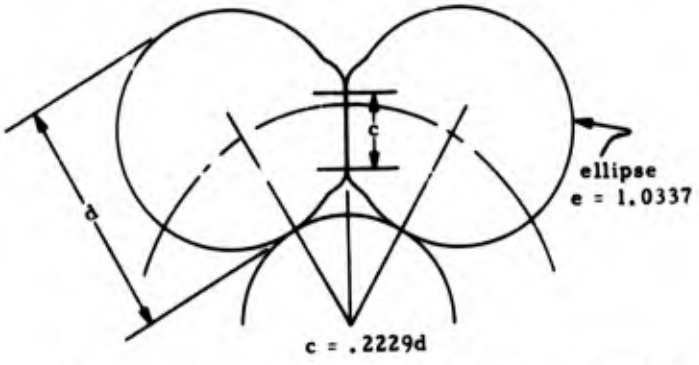

Figure 5. Chord of Contact, c, 7 Strand Conductor, Lay of 8

$$c = de \csc \frac{\pi}{n'} \frac{\sqrt{1-4s^2 + e^2 \cot^2 \frac{\pi}{n'}}}{1+e^2 \cot^2 \frac{\pi}{n'}} \quad (6)$$

Normal Area. The normal area is the total conductive area perpendicular to the axis of current flow. It is the summation of the elliptical cross-sections of the conductor strands.

Since the area of an ellipse is

$$\text{area} = \pi ab \text{ sq. mils} \quad (7)$$

the following expression develops.

$$\text{normal area per strand} = ed^2 \text{ circular mils} \quad (8)$$

and ellipticallity, e, is related to pitch by the following:

$$e = \text{secant}\left(\arctan \frac{3.14159}{h}\right) \quad (9)$$

The traditional increment of resistance and mass increase caused by stranding is given by:

$$\text{increment} = (e-1)\% \quad (10)$$

The stranding parameters which yield a 2% increment are:

$$e = 1.020 \quad (9a)$$

$$h = 15.627 \quad (9b)$$

$$\text{increment} = (1.020 - 1) = 2\% \quad (9c)$$

Normal Area Maximization. In order to provide the lowest possible current density, and therefore the highest ampacity, the normal area should be the maximum attainable within a given conductor diameter. With a fixed number of strands, maximization can occur only by increasing the lay to the maximum value allowed by wire manufacturing processes.

The maximum normal area provides circumferential contact between all strands within a given layer.

The equation which describes this maximization is

$$e = \sqrt{4s'^2 - 1} \tan \frac{\pi}{n'} \quad (11)$$

A typical arrangement is shown in Figure 6.

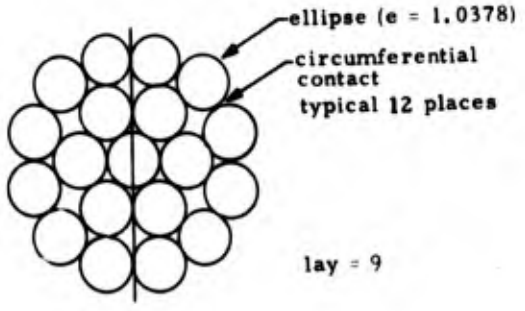

Figure 6. Normal Area Maximization, 19 Strands

Equations for pitch and lay remain unchanged.

$$h = \frac{3.14159}{\tan (\text{arcsec } e)} \quad (9)$$

$$\text{lay ratio} = \frac{2s'h}{2s' + 1} \quad (4)$$

Table 3 provides data for lay, pitch, strand count and ellipticallity for conventional concentric stranding. The number for lay provides normal area maximization and is applicable to the outermost lay of the particular conductor. For seven strand construction the lay is shown as "none"; see section on Strand Deformation for explanation.

Table 3. Normal Area Maximization

No. of Strands	e	h	Lay Ratio
7	1.0	Infinity	None
19	1.03777	11.3153	9.0522
37	1.04318	10.5720	9.0617
61	1.04494	10.3727	9.2202
91	1.04573	10.2757	9.3416
127	1.04623	10.2195	9.4334
169	1.04648	10.1801	9.5015
217	1.04659	10.1699	9.5717
271	1.04670	10.1594	9.6247

Table 4 delineates an optional stranding where additional strands have been added to loosen the lay. Conductor diameters are the same as in Table 3.

Table 4. Normal Area Maximization - Optional Stranding

No. of Strands	e	h	Lay Ratio
92	1.01180	20.4119	18.556
129	1.0717	16.8685	15.571
172	1.02274	14.6748	13.697
221	1.02522	13.9027	13.085
276	1.02770	13.2556	12.558

Conductivity

The basic concepts relating to the increment of mass and resistance increase due to stranding have not been altered since they were first published in 1912. The following is an abbreviation of what was conceived at that time.

Conductivity vs Stranding, 1912

National Bureau of Standards, Circular 31, First Edition, April 1, 1912 stated in the opening paragraph of Appendix IV "- it is proposed to show that the percent increase of resistance of a cable with all the wires perfectly insulated from one another over the resistance of the equivalent solid rod is exactly equal to the percent decrease of resistance of a cable in which each wire makes perfect contact with a neighboring wire at all points of its surface."

Figure 7 summarizes the quotation.

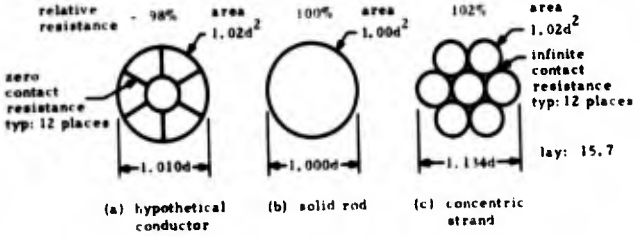

Figure 7. Traditional Concept of Resistance Increase Due to Stranding

Conductivity vs Stranding, 1966

National Bureau of Standards, Handbook 100, February 21, 1966. Verbatum the above with a limitation of 2,000,000 CM and an "allowable increase of about 1 percent for each additional million circular mils of area."

Helicality vs Resistance, 1912 and 1966

The arguments given by the National Bureau of Standards for the increase in resistance, or the lack of it, are essentially related to helicality. For example, to support Figure 7(a), their words are "the path of the current is in this case parallel to the axis of the conductor, which path has a greater cross-section than the sum of the cross-sections of each wire taken perpendicular to the axis of the wire." Similarly, to support Figure 7(c), they state "the path of the current is longer than it would be if parallel to the axis of the stranded conductor." Figure 8 details this last statement.

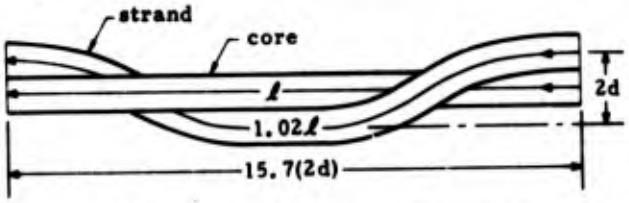

Figure 8. Traditional Concept of Longer Current Path

Electromagnetic Theory, 1934 and 1971

1934. W.V. Houston[5]: "When the current is flowing in a thin wire, the direction of the current is necessarily the direction of the wire and therefore current is usually trated as a scalar."

1971. S.R. Seshadri[6]: "Since the potential varies only along the length of the wire, it is clear that the electric field is along the length of the wire and so also is the current."

The two quotations above have been cited, not to deny that current flow in a stranded conductor may be multidirectional, but that the simultaneous use of a scalar solution and a non-axial model is questionable.

The 1974 Model - Longitudinal Current Flow

The Longitudinal Geometry. The cross-section of a stranded conductor taken through its longitudinal axis is illustrated in Figure 9.

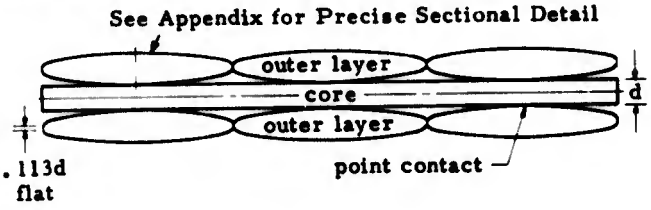

Figure 9. Longitudinal Cross-section, 7 Strands, Lay Ratio 16

The conditions for axial current flow illustrated by Figure 9 are intentionally chosen to demonstrate a concept. There is always strand deformation in a seven-strand conductor and therefore continuous strand contact along the length of the wire. The outer layer is a cylinder of conductivity surrounding the core. It should be noticed that the contact of the outer layer and the core is essentially a point contact; each strand is passing over the core at an angle of 7.5°. In practice, the contact is somewhat larger than a point but the condition is not a necessary part of construction requirements.

Figure 10 illustrates the longitudinal cross-section of a nineteen-strand conductor without strand deformation; the lay ratio is typical.

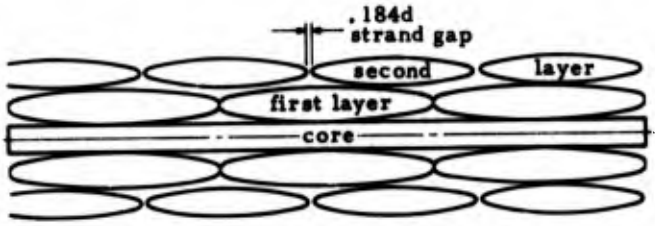

Figure 10. Longitudinal Cross-section, 19 Strand, Lay Ratio 14.4

It can be seen from viewing Figure 10 that the electrical contact of the first and second layer is longitudinally intermittent; the enclosing cylinder of conductivity, illustrated in Figure 9, is absent in the second layer because of strand gap. A nineteen strand conductor, with a lay ratio similar to that shown, appears to make inefficient use of available copper. The lay ratio which would reduce

strand gap to zero is given in Table 3 as 9.05 and is not seen in practice.

The strand gap illustrated in Figure 10 is drawn as though it were evenly divided between the twelve strands of the second layer. In practice, the gap may be concentrated between two adjacent strands and the remaining strands may be in contact or the distribution may be random.

Thermal Considerations[7]. Even though the twelve strands of a nineteen strand conductor may not efficiently add cross-section to the conductor, it can be agreed that they contribute to the ampacity rating of the conductor by providing a heat sink for the core and first layer. This contribution could increase the capability of the inner strands to pass current.

Mass

In addition to its analysis of lay-resistance relationships, NBS Handbook 100 describes an identical lay-mass equivalence as follows: "---the correction factor to obtain resistance or mass per unit length of a stranded conductor---." It continues: "This correction factor must be computed separately for each layer of strands when the lay ratio is different for different layers of the conductor." and "It should not be forgotten that usually the central wire (core) is untwisted."

It establishes a density value of: - copper density = 0.32117 lb/in^3 @ 20°C and 100% ACS. This constant is convertible to copper density = 0.003027 lbs/CM/1000 ft. When a nominal 2% increase is applied copper weight = 0.0030875 lbs/CM/1000 ft. The circular mil (CM) area is taken perpendicular to the strand axis and summed for all the strands of the conductor.

Flexibility[8] and Cylindricality

In at least two respects, stranded conductors have developed because of their rope-like applications and not because of their conductivity. To achieve flexibility, strand diameters have decreased and strand count (and number of layers) has increased. To achieve a well-defined cylindricality, the tightness of the lay has increased progressively with the number of layers. Concomittant with these increases is a resistance and mass increase. It seems fundamentally unsound but the axiom seems to be: "If you have to use more copper, you will get less conductivity."

Conclusion

Concentrically-stranded conductors have from the beginning developed around a mechanical rather than an electrical model. Their function has continued to be a carrier of current and yet no effort to give the user more ampacity for fewer dollars is apparent.

This paper raises the question of the possibility of improvement. It suggests that wire-manufacturer's publish measured resistance data as a function of strand count. This data would be helpful in analyzing conductor resistance rather than relying on a doubtful formula. This paper, in the section on Normal Area Maximization, further suggests that the contact resistance between strands is more defineable than current practice would intimate.

Acknowledgments

Messrs. Wilbur C. Beckwith and Joseph C. Lilly of the Plastic Wire and Cable Corporation have been very helpful in filling in the blanks between the theory and practice aspects of this paper.

References

1. Circular of the Bureau of Standards, No. 31, Copper Wire Tables, 1st Edition, issued April 1, 1912.
2. IPCEA Publication No. S-19-81 (Fifth Edition) Revision No. 3 - September 1973.
3. National Bureau of Standards, Handbook 100, Copper Wire Tables, issued Feb. 21, 1966.
4. ASTM Standard Specification, B8-70, for Concentric-Lay-Stranded Copper Conductors, Hard, Medium-Hard, or Soft effective April 15, 1971.
5. William V. Houston, Principles of Mathematical Physics, McGraw Hill, 1934.
6. S.R. Seshadri, Fundamentals of Transmission Lines and Electromagnetic Fields, Addition-Wesley, 1971.
7. J.H. Neher and M.H. McGrath, The Calculation of the Temperature Rise and Load Capability of Cable Systems, AIEE Transactions, pp 752-772, October 1957.
8. E.W. MacLaren, Jr. and V.L. Carney, A Theoretical Consideration of Stiffness in an Electrical Cable, Eighth Annual Wire and Cable Symposium, December 1959.

Biography

John F. McLaughlin was born on September 12, 1919 in Boston, Mass. He received the B.S. Physics and M.S. Physics degrees from Boston College, Chestnut Hill, Mass.

At present he is a senior electrical engineer in the Digital Systems and Displays Laboratory of Raytheon Company's Sudbury Facility, Sudbury, Mass. His principal assignment has been in interconnection systems. He served recently on a committee developing Divisional Standards for solderless-wrap systems.

He is a Member of I.E.E.E. and the Electronics Connector Study Group and a Registered Engineer in the Commonwealth of Massachusetts.

Appendix

Polygonal Stranding

Strand count in any layer is determined by the perimeter of the polygon circumscribed by the pitch circle of that layer. Refer to Table 2 and 62 strands with 25 strands in the 4th layer for an example.

$$\sin \frac{180}{25} = .12533 > \frac{1}{2x4} = .125 \tag{2}$$

$$\sin \frac{180}{25} > \frac{1}{2x4}$$

Conclusion: 25 strands will fit in the fourth layer.

Chord of Contact

See equation and explanation below for longitudinal cross-section.

Longitudinal Cross-Section

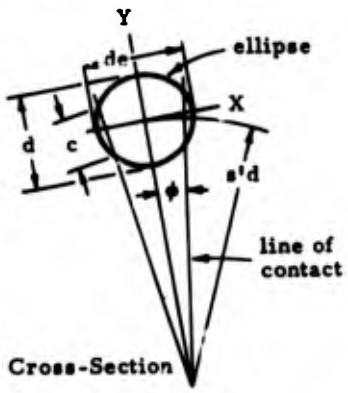

Figure 11. Axial Cross-Section

Equation of the ellipse $\frac{x^2}{\frac{de^2}{4}} + \frac{y^2}{\frac{d^2}{4}} = 1$

Equation of the line of contact $y = \cot \phi \, x - s'd$

Substitute x line in x ellipse

$\tan \phi \, (y + s'd)^2 + e^2 y^2 = \frac{de^2}{4}$

Develop the following quadratic.

$$\frac{4}{d^2}\left(\frac{1}{e^2}\tan^2\phi + 1\right) y^2 + \frac{8s'd}{de^2}\tan^2\phi \, y + \frac{4s'^2}{de^2}\tan^2\phi - 1 = 0$$

Solve and simplify. The parameter z is taken along the longitudinal axis.

$$\begin{cases} y = \dfrac{s'd \pm \operatorname{recsc}\phi \sqrt{1-4s'^2 + e^2\cot^2\phi}}{1 + e^2\cot^2\phi} & 0 < |\phi| \le \dfrac{\pi}{n'} \\ z = \dfrac{dhs'}{\pi}\phi \end{cases} \tag{12}$$

See Figure 12 below for half-section development.

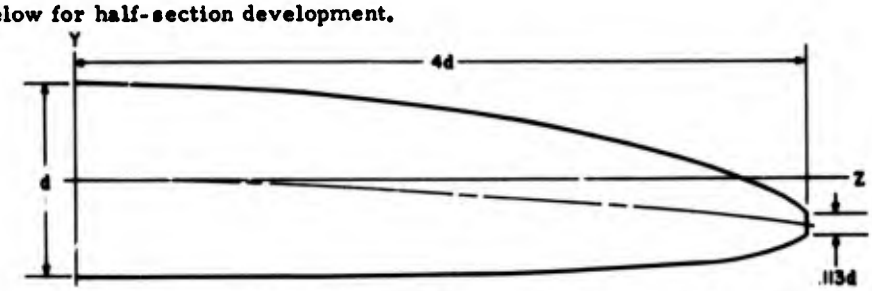

Figure 12. Longitudinal Half-Section 7 Strands, Lay Ratio 16

The chord of contact is the sum of two y intercepts when ϕ equals $\frac{\pi}{n'}$ and its equation is

$$c = de \csc \frac{\pi}{n'} \frac{\sqrt{1-4s'^2 + e^2\cot^2\frac{\pi}{n'}}}{1 + e^2\cot^2\frac{\pi}{n'}} \tag{6}$$

Tangency of the line of contact is the condition for Normal Area Maximization and is given by:

$$\sqrt{1-4s'^2 + e^2\cot^2\frac{\pi}{n'}} = 0$$

Solving for e when ϕ equals $\frac{\pi}{n'}$ gives

$$e = \sqrt{4s'^2 - 1}\tan\frac{\pi}{n'} \tag{11}$$

A MATHEMATICAL APPROACH TO TUBING EXTRUSION OF THERMOPLASTICS IN ELECTRICAL INSULATION OF WIRES AND CABLES

BY

Roberto Di Leonardo
Canada Wire and Cable Co. Ltd.
International Operations Division
Toronto, Ontario, Canada

INTRODUCTION

An approach to tubing extrusion of thermoplastics tool design is hereby treated and analytically developed. What follows is subject to the limitations resulting from the adopted assumptions.

In extrusion of thermoplastics on electric wires the tool design is to satisfy two basic requirements :-

1. Combination of tip and die dimensions which will allow to run at the desired line speed. The pressure in the head is a parameter to be accounted for within a tolerable range.

2. Shape of tip and die which will be able to impart the final properties to the product.

While the second point seems obvious, the first one is worth some discussion.

In a conventional tubing extrusion, the openings of tip and die are often calculated with a sort of step approximation, where several empirical elements are introduced. For a desired construction, a first correlation between tool size and construction of the insulated wire is obtained by defining what is called draw down ratio (D.D.R. = R),

$$R = \frac{D^2 - d^2}{c^2 - b^2} \qquad 1)$$

Where

D = Die inner diameter (inches)
d = Tip outer diameter (inches)
c = Insulated wire diameter (inches)
b = Bare wire diameter (inches)

As for the solution of # 1, which gives a measure of the amount of plastic contraction imposed during the draw down, two additional relations in the shown parameters are needed, when # 1 is considered as an equation in D and d. However, a procedure is adopted allowing a range of values for R and estimating d with respect to b, (e.g. 10 times with TEFLON F.E.P. 100) Thus, D can be empirically determined. The final combination of D and d is attained, then, with a trial-error like technique, selecting the size of the set according to some practical information as to usual range for R and rules of clearance between tip and die.

The above problem is sometimes handled by introducing different rules for # 1. Once a value for R has been picked up, D and d have to satisfy

$$D = \sqrt{R} \times c$$
$$d = \sqrt{R} \times b \qquad 2)$$

It is worth considering that # 2's are a further and tighter restriction on D and d, and, when considered as mathematical relations, they are not equivalent to # 1. In fact, they would be an imposed solution of #1 through R. It can be seen that #2's combined properly (squaring and subtracting) yield # 1. The vice versa is generally not necessary, as the solutions of # 1 are ∞^2 against the ∞1 ones of #2's.

The exposed approach, as it results, is very empirical and lacking, as to land of tip and die, angle of entrance for the melt toward the land, pressure inside the extruder head. In addition, the exposed procedure does not take into consideration the properties of the plastic being extruded. The physical characteristics of the final product are affected by processing temperatures, tip and die design, line speed and RPM set. The shear rate of the molten plastic in the annulus is also vitally affected by these factors. Without entering into details for such dependences, it may be stated that, as for extrusion process of a given construction, an over-simplification takes place and it is not unlikely that an ample manipulation of many parameters yields the desired final product, or corrects the perturbation introduced by changing tools . This paper aims to a theoretically clearer dependence of the involved parameters on one another, relating directly tool design and properties of the plastic being processed. Besides, as for extrusion optimization, considering the line speed as a dependent variable is technically questionable and mathematically undesirable. In such case, production becomes function of the design, while the vice versa should be pursued, and the number of the dependent variables to be determined is raised.

DEVELOPMENT

In order, then, to approach a design of tip and die which considers the line speed as an independent variable of the process and deals with the properties of the molten plastic being extruded, it is convenient to examine a practical case of flow characteristics of a material which is typically tube extruded, for instance Teflon FEP 100.
By looking qualitatively at its log-log plot of shear stress and shear rate, FIG. # 1, several

regions can be considered, each referring to some particular conditions of extrusion [1].

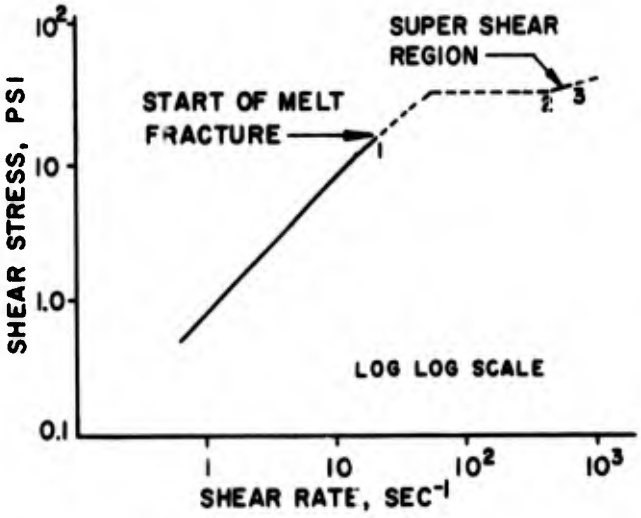

FIG. 1

Typical Characteristic for

Shear Stress vs Shear Rate (Apparent) of Teflon FEP 100. Temperature 720°F (Melt & Die). For illustrative purposes only, not for design. Shape & location of curve & points (1), (2), (3) affected by temperatures (Die & Melt) and die design. Existence, breadth & location of super shear region are influenced by temperatures and die design.

It is of interest to consider that the graph appears linear in correspondence of those regions for which the extrudate shows smoothness and good quality. A linear graph, on a log-log plot, means that the analytical dependence between the actual variables is either linear or of a power law kind. In the first case, the slope of the curve would be constant and equal to the unity; in the second case, it would be determined by the exponent appearing in the functional dependence. Really, and still qualitatively, Teflon FEP 100 is not a newtonian fluid in its molten state (slope = 1 in a log-log plot), rather its log-log plot for shear stress and rate resembles that of a pseudoplastic (slope between zero and unity).

As the design of the tools is to be related to the properties of the plastic, it is necessary to know the behavior of that in order to use the corresponding analysis.
It is assumed that Teflon FEP 100 practically behaves as an ideal fluid, i.e. a newtonian fluid, or its behavior can be treated as newtonian to a first approximation. Estimates usually made in studying FEP extrusion performances and using newtonian relations yield meaningful results.
It is to point out that the assumption is not an unreasonable extrapolation. In fact, the range of shear stress (from 10 to 30 psi) and rate (up to 20 sec - 1) corresponding to conditions of normal extrusion[2], linear region in the graph, is narrow. Moreover, it is always possible, at worst, to think of rearranging the conditions of the extrusion line around the "point" where the melt flow characteristic curve better results tangent or parallel to that of a newtonian fluid sheared in the same range.

In order to proceed further with the analytical development of the design within the adopted hypotheses, it is necessary to relate the desired flow rate of the plastic to the dimensions of the annular orifice. This is conveniently done by setting the differential conditions of dynamical equilibrium for an element of melt[3]. By developing on the basis of the pressure flow equation,

$$t = -u \frac{dv}{dr} \qquad 3)$$

with t shear stress, dv/dr shear rate and u viscosity of the plastic, and imposing the boundary conditions to the resulting linear differential equation, the flow rate equation is expressed as

$$Q = \frac{\pi P}{128uL} X \left[D^4 - d^4 - \frac{(D^2-d^2)^2}{\ln \frac{D}{d}} \right] \qquad 4)$$

where Q is the plastic flow rate, P the pressure inside the extruder head and L the die land length.

Equation # 4, although exact, is not easily handled being transcendent logarithmic of fourth degree in D and d. However, it would be solved, at worst, with a graphical solution, providing that sufficient additional relations be found among the parameters.

Instead of this cumbersome procedure, an approximate technique is used herein.

A tubing die is normally defined as an annulus, where D and d are required to satisfy

$$D \leq 3d \qquad 5)$$

Which means a linear clearance between the two circumferences of not more than d. If now, the tubing die is cut and opened up longitudinally, it will resemble a slit die, and the closer D/d is with respect to #5, the closer the analogy is. Within this approximation, the analysis may be transferred to the "new" die, if new width and length are defined. Let these be, respectively,

$$H = \frac{D - d}{2} \qquad 6)$$

$$W = \pi \frac{D + d}{2}$$

As it has been pointed out, the narrower the clearance, the more accurate the average length of the slit die. Anyway, the approximation results definitely acceptable and satisfactory in principle, as only an absolute 7% error will be made up in the melt flow, if D/d is allowed to reach a ratio of 10/1. The flow rate may be written as

$$Q = \frac{P W H^3}{12 uL} \qquad 7)$$

Equation #7 attains more interest, if the shear stress at the wall is introduced,

$$t = \frac{PH}{2L} \qquad 8)$$

With #8, the shear rate at the wall may be considered

$$g = \frac{P\,H}{2ut} \qquad 9)$$

Then #7 becomes

$$Q = \frac{g\,W\,H^2}{6} \qquad 10)$$

As it results, #10 relates Q directly to g, which gives the searched link between desired production and plastic material properties. This concept about g has a critical practical meaning, for it shows a threshold beyond which the molten plastic loses quality, degrades, fractures or anyway offers an unacceptable finish. Then, Q results determined, and so the line speed, by the threshold value of g, once the tools are thought established. As for the mentioned practical case of FEP, a typical critical value of g is 20 sec-1, in the cited normal extrusion conditions.

In order to calculate the size of tip and die, an additional relation is needed between D and d. Therefore, let the draw down of the molten plastic on to the running wire be simmetrical around the perpendicular to the front face of the die, i.e. around the running wire, FIG. #2.

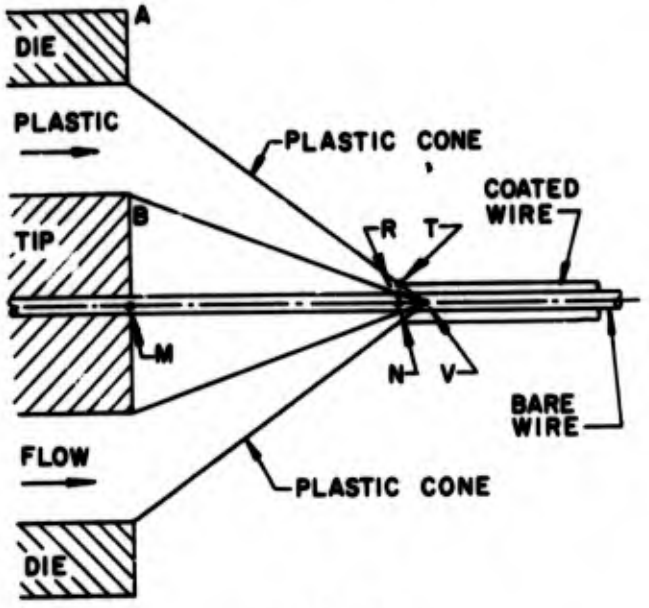

FIG. 2

Any consideration about the geometry of the draw can then be referred to any plane perpendicular to the die face and containing the wire. The cone of melt will have its vertex along the median line MV of the running wire. In practice, the wire drags the melt as soon as this touches it, but this is of little matter as the consideration is purely geometrical. Let a configuration be fixed in correspondence of a practical extrusion process, and the two sets of triangles (BMV, RNV), (AMV, TNV) considered separately.

BMV and RNV are right in M and N with one common angle. Therefore they are similar. The same is true for AMV, TNV. By geometrical similarity, for the first couple,

$$\frac{BM}{RN} = \frac{MV}{NV} \qquad 12)$$

For the same reason, with the second couple,

$$\frac{AM}{TN} = \frac{MV}{NV} \qquad 13)$$

which gives with # 12

$$TN/RN = AM/BM \qquad 14)$$

In order to use #14 practically, TR, in Figure 1 may be assumed equal to the wall thickness of the insulation. Herewith, #14 yields

$$\frac{D}{d} = \frac{c}{b} \qquad 15)$$

which when coupled with #10 is the equation solving the design problem.

Before going into calculations, it is worth making some considerations. The assumed simmetry of the drawn cone seems to be natural, providing that the flow inside the land of the die is laminar, as it must be, and tip and die result concentric. The approximation contained in #14 assumes that the shrinkage of the plastic, when this cools, affects D and d only by a small amount. In our practical case, calculations for a 26 AWG, with a final 30 mil O.D., show that the approximation is not more than 0.7%. Moreover, #15 meets the experimental indication concerning the range of variability of D/c toward d/b, or vice versa. In fact, the most convenient D/c ratio ranges

$$0.9\,\frac{d}{b} = \frac{D}{c} = 1.2\,\frac{d}{b} \qquad 16)$$

With the background of the above considerations, the tip and die dimensions can be calculated by solving together #10 and #15. The set equations may be conveniently written

$$Q = \frac{\pi}{4} K_m\, g\, \frac{(D+d)\,(D-d)^2}{12}$$

$$D = \frac{c}{b}\, d \qquad 17)$$

Where K_m is the density of the melt. The solution of the above systems offers

$$D = \sqrt[3]{\frac{4}{\pi}\,\frac{Q}{K_m g}\,\frac{12}{(c+b)\,(c-b)^2}} \times c$$

$$d = \sqrt[3]{\frac{4}{\pi}\,\frac{Q}{K_m g}\,\frac{12}{(c+b)\,(c-b)^2}} \times b \qquad 18)$$

These formulas for D and d become more expressive if the extrusion line speed is introduced. In fact, for the same Q, as in #18's, running along the line at a speed S, through the sectional area $(\pi/4)\,(c^2-b^2)$, although at a different density,

$$Q = \frac{\pi}{4} K_s (c^2 - b^2) S \qquad 19)$$

where S is in ft/min, and K_s is the density of the solid plastic. By summarizing the results,

$$D = \sqrt[3]{12 \times \frac{Ks}{K_m} \frac{S}{g} \frac{1}{c-b}} \times c$$

$$d = \sqrt[3]{12 \times \frac{Ks}{K_m} \frac{S}{g} \frac{1}{c-b}} \times b \qquad 20)$$

It is interesting, now, to go a step back and note that the introduction of relations #20's into #1 yields a useful expression for R.

$$R = \sqrt[3]{(12 \frac{Ks}{K_m} \frac{S}{g} \frac{1}{c-b})^2} \qquad 21)$$

This situation, however interesting it may appear, shows that the introduction of the parameter R is unessential, because, as already pointed out, # 15 implies # 1 (the vice versa is not unique). Therefore, the solution of the problem through # 1 and, then # 15 is a useless mathematical detour.

Thus, although the proportionality constant appearing in # 20 is just the square root of R, so that

$$D = \sqrt{R} \times c$$

$$d = \sqrt{R} \times b \qquad 22)$$

with R given in #21, it is to emphasize that this result is conceptually different from the analogous #2, as theoretically derived by adopting a different point of view for the line speed and with no introduction of empirical rules.

In order to fully design tip and die, the length of their land and the angle of entrance are to be calculated.

A simplified approach is treated here.

If #10 is considered, it appears that the same factors which contribute to specifying Q determine the P/L ratio in #9. The viscosity is considered constant. Therefore, if #9 is substituted into #10, the P/L ratio results determined, once Q is fixed. Now, as #9 determines only the ratio of P to L, these parameters may be conveniently specified by assuming P given, from which L is univocally calculated through #9. Therefore, for a certain P,

$$L = \frac{P H}{2ug} \qquad 23)$$

or through #20 and #6,

$$L = \frac{P}{4ug} \sqrt[3]{12 \frac{Ks}{K_m} \frac{S}{g} (c-b)^2} \qquad 24)$$

Actually here, P is the pressure drop through the die along L. Therefore, if the outside atmospheric pressure is taken as a reference P is the increase in pressure at the entrance of the die necessary for extruding.
As for the angle of entrance, unfortunately the above discussion does not offer any attachment to it. However, lacking this might appear, it is not unsound, as the extruder was only requested of performing at a certain rate.

The mathematical aspect of #20's can be analyzed. Relations #20's may be rearranged according to the particular parameters of interest. By considering S and c as independent variables, the corresponding analysis seems not to show particular interest, as to functional dependence. In fact, over the fields of definition S>o, c>b>o, D and d do not have any extremal points.

However, if S is considered as a parameter, the functions D(c) and d(c) show some interest. Being limited on the left by the asymptote c=b, both D(c) and d(c) go to $+\infty$ when c tends to b. On the contrary, when c tends to $+\infty$, while d(c) tends to zero, D(c) tends to $+\infty$ Therefore D(c) has a minimum. Qualitatively the plots are in FIG #3. Obviously $D(c) > d(c)$ and both D(c) and d(c) are larger than zero. If the derivative of D(c) is equated to zero, this yields the condition c = 3/2b, where D(c) has its minimum. It is recognized that the condition is consistent with #5 through #15. If #20 are inverted into S(c) functions,

$$S_D = \frac{g}{12} \frac{K_m}{K_s} \left(\frac{D}{c}\right)^3 (c-b)$$

$$S_d = \frac{g}{12} \frac{K_m}{K_s} \left(\frac{d}{b}\right)^3 (c-b) \qquad 25)$$

With D and d as parameters, $S_d(c)$ becomes a straight line, Fig #4, intersecting the absissa c line at c=b, with tangent

$$(gK_m d^3) / (12K_s b^3)$$

On the contrary $S_D(c)$, becomes a curve which is zero for c=b, becomes zero for c going to infinity and is concave downwards, as S is a physical quantity, always positive. The function $S_D(c)$ has the maximum for c=3/2b and the flex point for c=2b. This is still consistent with #5 through #15. The two curves, $S_D(c)$ and $S_d(c)$ interesect for c=bD/d, which is the condition #15.

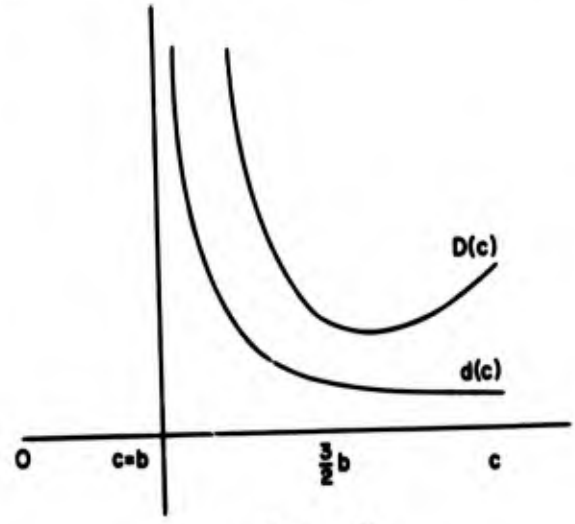

FIG. 3

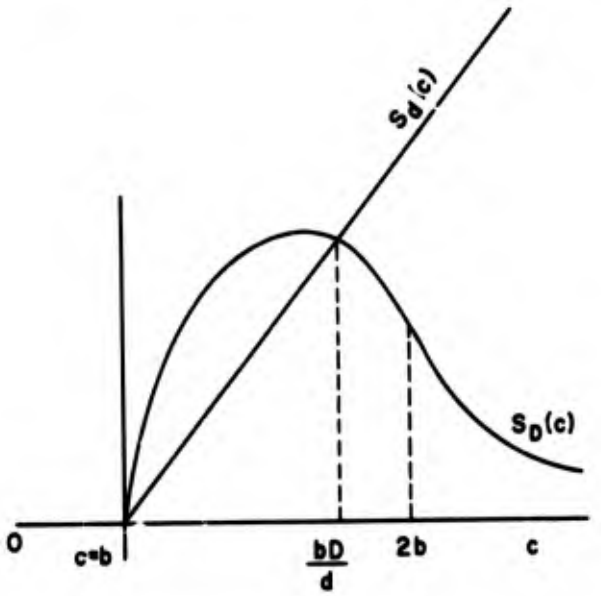

FIG. 4

In conclusion , the proportional dependence contained in #15 does not lead to contradictions. Being the speed of production a real physical quantity, it must be the same regardless of the equation that is used for its calculation. Moreover, withstanding the relation #15, if D and d are used as parameters, consistently a maximum extrusion rate corresponds to a maximum speed.

EXPERIMENTAL RESULTS.

The exposed approach has been used in tubing extrusion of thin walls of Teflon FEP 100 to insulate fine wires. The results are reported in the following tables :

TABLE I

AWG INS.(in.)	30 .005	30 .005	30 .005	30 .005
b inches	.010	.010	.010	.010
c inches	.020	.020	.020	.020
d inches	.100	.125	.150	.175
D inches	.200	.250	.300	.350
S ft/min	54	106	183	290
S_e ft/min.	52	113	180	280
$\left\lvert\frac{\Delta S}{S}\right\rvert$ %	3.7	6.6	1.6	3.4

TABLE II

AWG INS.(in.)	26 .005	26 .005	26 .005
b inches	.0159	.0159	.0159
c inches	.0259	.0259	.0259
d inches	.200	.250	.275
D inches	.326	.407	.448
S ft/min	108	210	280
S_e ft/min	115	197	280
$\left\lvert\frac{\Delta S}{S}\right\rvert$ %	6.5	6.5	0

TABLE III

AWG INS.(IN.)	24 .005	24 .005	24 .010	24 .010	24 .010
b inches	.0201	.0201	.0201	.0201	.0201
c inches	.0301	.0301	.0401	.0401	.0401
d inches	.200	.250	.200	.250	.275
D inches	.299	.374	.399	.499	.549
S ft/min	53	104	106	208	278
S_e ft/min	50	110	108	217	272
$\left\lvert\frac{\Delta S}{S}\right\rvert$ %	5.7	5.8	1.9	4.3	2.2

TABLE IV

AWG INS.(in.)	20 .010	20 .010	20 .010
b inches	.032	.032	.032
c inches	.052	.052	.052
d inches	.325	.350	.375
D inches	.528	.569	.609
S ft/min	112	142	174
Se ft/min	117	145	170
$\left\lvert\frac{\Delta S}{S}\right\rvert$ %	4.5	2.1	2.3

A conventional 1" extruder was used with L/D = 20/1. The screw was a conventional FEP screw (approximately 3/1 compression ratio, one pitch transition section, four pitches metering section, Hastelloy C). A motorized pay-off was used to minimize tensions and vibrations. The extruder had three temperature controls in the barrel, one in the adaptor, one in the crosshead, one in the die. All controls were capable of 1% of their total scale readings. From rear to front of extruder the zone temperatures respectively ranged within 580-620°F, 620-650°F, 650-680°F, 680-700°F, 680-720°F, 680-720°F.
The melt temperature reading, fixed at 720°F, was taken in the die with a common pyrometer. The wires used were all SPC wires (silver plated copper). The diameters of the insulated wires were held at ±.001" for 30 and 26 AWG, at ± .0015" - .002" for 24 and 20 AWG. The diameters were gauged in line with an electro optical monitor. All the dies used were standardized at 3/4" land length and 60° included angle of entrance. The sizes of dies in stock (.025" increments) closest to the ones calculated in the tables were used; also existing sizes of tips in stock were used for economical reasons. The aim of the experiments was to check whether, at the output imposed by the value of g (20 sec - 1), design of tip and die (#7 and #25's) the approach developed above yielded the established construction at the calculated speed. The properties of the final product would be obtained by using conventional extrusion technology.
The values of the parameters K_m and K_s used in the calculations were : K_m = .05 lbs/in^3 and K_s = .077 lbs/in^3.
The good agreement between theoretical and experimental speed values (S, S_e) does not imply that the constructions reported in the tables may not be run at higher speeds.
Despite the limitations of the exposed approach, an analytical tool is supplied which can be used to design tooling and processing of a plastic to be tube extruded. The above development, if used to calculate R in #1, yields values within the commonly used range of D.D.R's for tubing extrusion of FEP. The relation of #24 was not checked experimentally as the pressure gauge of the extruder was installed only in the front of the barrel. However, it was checked by calculating the pressures developed inside the dies specified by the calculated diameters, used land length and angle of entrance.

The results calculated through #24 are reported in Tables V - VIII.

TABLE V

AWG	30	30	30	30
INS.(in.)	.005	.005	.005	.005
S ft/min	54	106	183	290
P psi	870	696	580	497

TABLE VI

AWG	26	26	26
INS.(in.)	.005	.005	.005
S ft/min	108	210	280
P psi	690	551	503

TABLE VII

AWG	24	24	24	24	24
INS.(in.)	.005	.005	.010	.010	.010
S ft/min	53	104	106	208	278
P psi	878	702	437	351	317

TABLE VIII

AWG	20	20	20
INS.(in.)	.010	.010	.010
S ft/min	112	142	174
P psi	431	397	372

As it can be seen the yielded pressure values are in range with values of current experience (≤1000 psi). As a last consideration, it is stated that the above approach is general as its analytical development can be used for any plastic, which can be processed by tubing extrusion, once the flow characteristic curve is known. It will be then a matter of more or less involved analysis.

REFERENCES

1. - Graph Courtesy of Dr. R. Dahlen
E. I. Dupont de Nemours & Co.
Plastics Department,
Technical Services Laboratory,
Chestnut Run, Del, U.S.A.

2. - Information Bulletin X-82-d
E. I. Dupont de Nemours & Co.,
Plastics Department,
Wilmington, Del, U.S.A.

3. - E. C. Bernhardt, Processing Of
Thermoplastics Materials
Van Nostrand Reinhold Company
N.Y. N.Y.1956, U.S.A.

Pages 295 and 265-268

ACKNOWLEDGMENT

I wish to express my gratitude to Philadelphia Insulated Wire Company, Subsidiary of General Cable Corporation, Moorestown, N.J., U.S.A., for granting me permission to publish the present paper, the material for which was developed at P.I.W. while I was serving as Senior Engineer in Melt Extrusion Department.

Dr. Roberto Di Leonardo

Project Engineer in the Technical Services Department of Canada Wire andCable, Company Limited, International Operations Division, Toronto, Canada.
He graduated as a Doctor in Physics at the University of Rome in Italy in 1967.
He spent two years in Italy teaching Electrical Engineering prior to joining in 1970 Philadelphia Insulated Wire Company, Moorestown, N.J., U.S.A. as Senior Product Engineer in Melt Extrusion Department.
He joined Canada Wire International in the spring of 1973 where presently serves in the staff of the Technical Services Department.

METAL MICROWIRES SPUN FROM MELT COMPARED WITH THOSE COLD DRAWN.

G. Manfré - R & D Division - Technion SpA - Novara - Italy
G. Servi - De Angeli SpA - Desio - Milano - Italy

Summary: In order to produce metal microwires diameter less than 50 micron many approaches have been recently experimented with other than the classic cold drawn process. Among several the so named "spinning from melt" method would appear to have many advantages when the consistency of the production system is examined. Stated,simply the method and the resulting technology is to draw a filament from molten metal. The molten metal can flow out from a nozzle into controlled atmosphere or it can be drawn simultaneously with a glass capillary containing the molten metal.
The paper concerns mainly with the second spinning method with the aim to show the interdependence of process continuity with the parameters of grain size, surface texture and resultant mechanical properties.
Also reported is the effect of the process technique on the mentioned features using a variation of the drawing ratio and cooling time.
Further a comparison is made between the spun microwires with those normally obtained by the cold drawn process.
The main object of the present research and development is based upon a desire to improve the mechanical features of the spun microwires either changing some process parameter or metal composition.
At this stage the metal glass-coated microwires have applications in the electric field as mentioned in this work in addition to some suggestion for handling them in any expoitation.

INTRODUCTION

The demand for cheap production of metal fibers is rapidly increasing both in the field of composite materials and for electronic and electrical applications.
So far the cold drawn process is widely used,

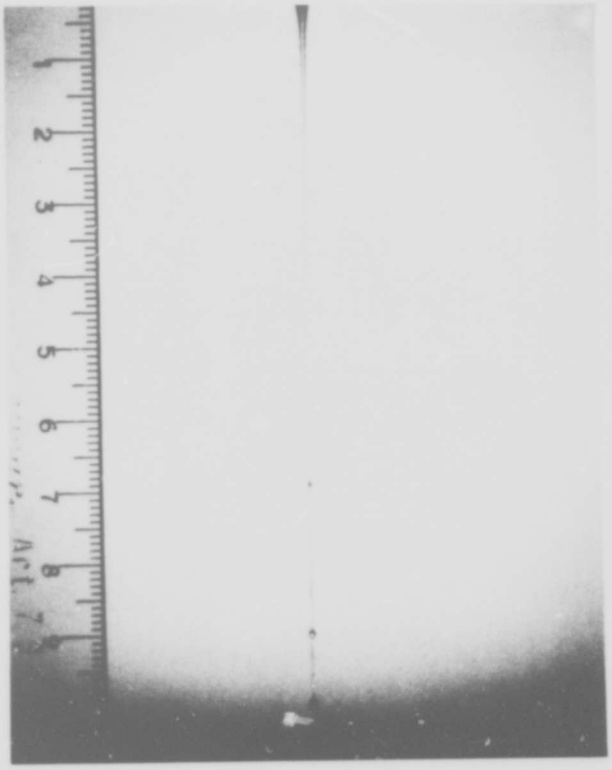

Fig. 1 : Silicon oil jet of viscosity η (poise) from a steel nozzle of 1 mm diameter; the length of the jet between the nozzle exit and the first breakage is the parameter to determine the liquid 'spinnability'

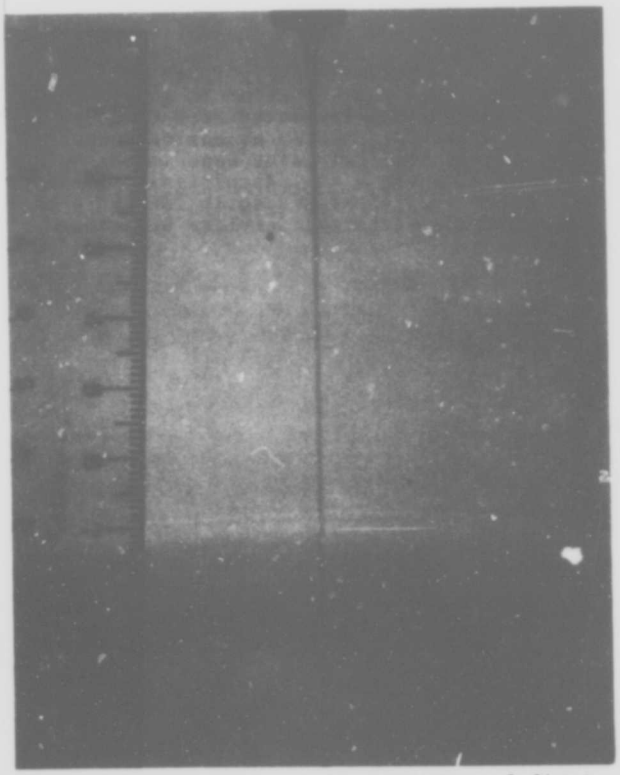

Fig.2 : Experiment similar to that of fig 1 with higher rate of flow

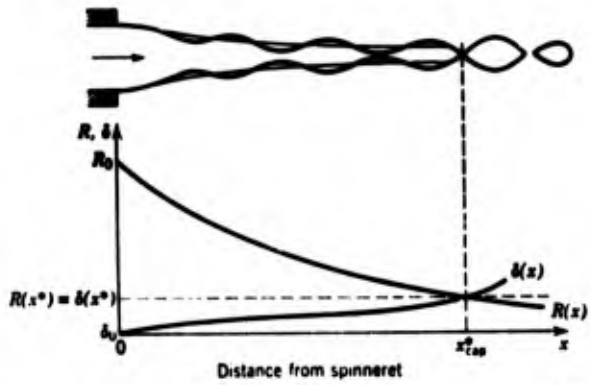

Fig. 3 : The jet breakage in metals, in stable fluidodinamic conditions, is mainly due to surface wave propagation and it occurs when the wave amplitude $\delta(x)=R(x)$ jet radius.

but the cost of fibers produced by this method increases remarkably as fibre diameter decreases. This is mainly due to the complexity of the process as the metal hardens in any passages of the die so reducing its ductility. Furtherly the cold drawing process cannot be applied to metal and alloy which does not show plastic deformation. To overcome this difficulties new production technologies have been developed in the last decade, one of them is the so called spinning process, related to the classic Taylor' method, which we have experimentally approached as following.

Spinnability of materials

In material science, spinnability is the property to make filaments or threads by drawing any materials from liquid state, included or solutions or sospensions or emulsions.
The measurement of spinnability consists to determine the length between the base of a liquid jet and the first fracture downwards of the liquid attenuation path. We made a lot of experiments on liquid jets in order to have information on spinnability or liquids, glasses and metals /1/,/2/,/3/,/4/,/5/.

Fig. 1 and Fig. 2

Fig. 1 and 2 show some experiments with a silicon oil jet flowing from a nozzle /1/.
It can be seen that for the same materials the length of the liquid thread, determining the "spinnability", depends also on the flow conditions, mainly from the rate of flow.
Usually the thread's length increases with the rate of flow at least up to a certain level, determined mainly by the elongational viscosity and surface tension of the liquid. Beyond such a level the process becomes unstable.
The rate of flow of the jet shown in Fig. 1 is lower than that of Fig. 2.
Apart the experimental conditions which involve propagation of surface liquid waves and other fluidodinamic instabilities, the spinnability can be simply a function of ratio between viscosity and surface tension:
The glasses at ordinary spinning conditions show this ratio of the order of 10, the polymers of 100, the metals of 10^{-4}.
Without entry into details the polymers and glasses can be considered spinnable, but no the metals which forms easily drops rather than threads /4/, /5/.

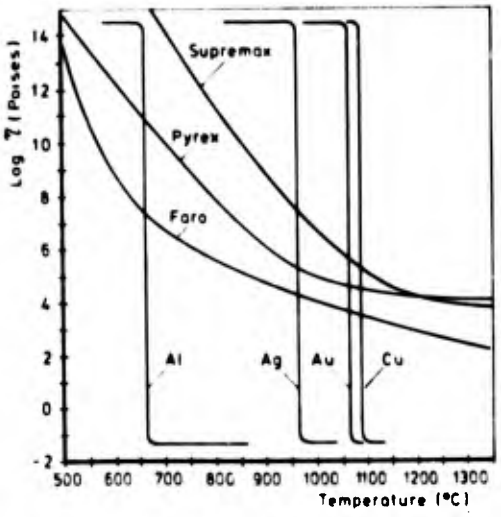

Fig. 4 : Viscosity versus temperature diagram for most common glasses and some f.c.c. metals.

Fig. 3

In fact because liquid metals show high surface tension (10^2 - 10^3 dine/cm) and low viscosity (10^{-1} - 10^{-2} poises) their rate of flow through a nozzle must be quite high (1 - 10 g/sec) in order to obtain jets.
The jets show surface waves which determine the jet's breakage when the wave amplitude of the liquid jet $\delta(x)$ is equal to the jet attenuating radius $R(x)$ as shown in fig. 3.
Liquid metals reach this condition at distance of few nozzle diameters from the exit nozzle. So to increase the spinnability ratio for metals we have to increase the viscosity or to decrease the surface tension.
We have chosen the second possibility simply melting a metal inside a capillary of glass which must have the following features in order to be drawn simultaneously with molten metal and so to obtain e metal microwires coated by glass.

Properties of glasses:

The features of glasses have to be:

1) The temperature at which the glass has a viscosity about 10^3 poises must be about the melting temperature of the testing metals.

Fig. 4

Fig. 4 shows some commercial glasses in

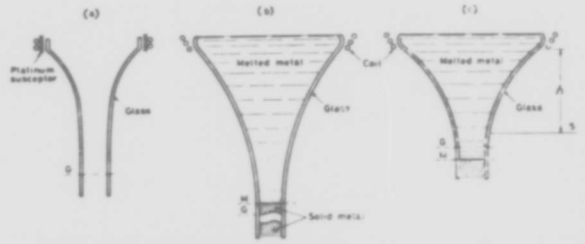

Drawing zone profiles of: (a) glass capillary; (b) glass coated microwire cooling with air; (c) as (b) cooling with a liquid. G: glass solidification point. M: metal crystallization point. h: distance between furnace and cooling device.

Fig. 5 : Drawing zone profile of: a) glass capillary; b) glass-coated microwire with no correct glass or process stable conditions; c) necessary condition for obtaining continuous coated microwires

our esperiments and also how 10^3 poises of glasses matches the melting temperature of copper, silver, gold and aluminium.

2) The chemical reaction between the metal and the glass in the drawing conditions has to occur properly. Simply it is necessary a small chemical reaction which causes some chemical bond between glass and metal at the interface.
The result is a good adhesion at the interface /6/.

3) The expansion coefficient of glass has to be the highest possible in order to match those of the tested metals.

Process conditions

The process conditions have to work in order to obtain the metal fiber continuous.
The main process phenomena are as follows:

a) the solidification point of the metal has to occur downwards the end of the glass fiber attenuation.

Fig. 5

Fig. 5 shows liquid metal breakages inside the glass capillary during the spinning in the case that the metal solidification occurs before the end of the glass capillary attenuation.

b) The atmosphere inside and outside has to avoid the bubbles formation in the drawing zone.

Fig. 6

Fig. 6 shows bubbles inside the forming glass-metal drawing zone when the outside atmosphere is not well controlled.

Heating source

The heating source can be /7/:

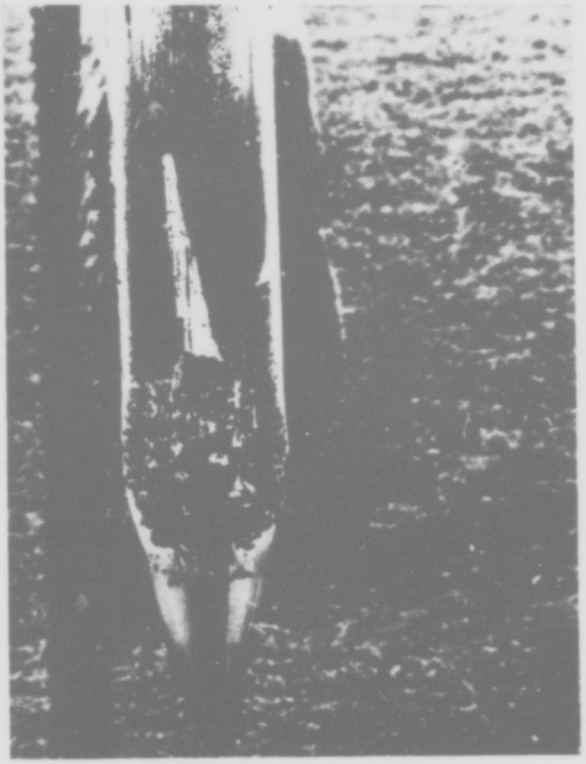

Fig. 6 : No correct surrounding atmosphere during spinning or high percentage of oxigen in copper or glass produce indesirable bubbles in the drawing zone

1) Resistor heating which softs the glass and molten the metal.
2) Induction heating which molten the metal and, by heating conduction, softs the glass.
3) Resistor and induction heating working simultaneously.

The heating source has to be optimize for copper, gold, silver and steel and other metals or alloys.
We achieved good results in copper up to 4 micron, silver up to 10 micron (0.2. micron discontinuous), gold and steel to 4 micron.
The main purpose of this paper is dedicated to a comparison between the properties of the microwire obtained by spinning and those obtained by the cold drawn method. Here we consider mainly the copper, pointing out that similar conclusions can be extrapolated to other metals /8/.

COMPARISON FOR COPPER MICROWIRES

The spun fibres compared with the draw ones show some peculiar properties in relation to:

1. Glass metal interface
2. Grain structure, their arrangement and size
3. Texture

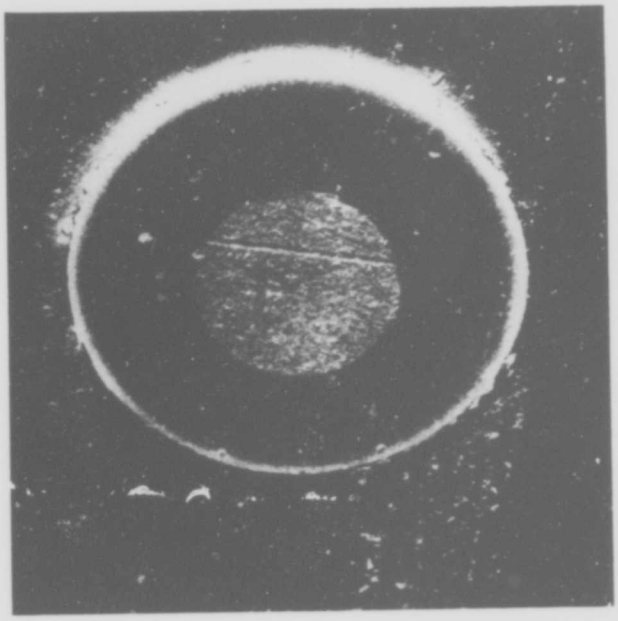

Fig. 7 : S.E.M. Micrographs of transversal section of a copper glass coated microwires (Ø = 30 microns) Magnification 1400 X. Interface looks coherent and uniform.

4.Mechanical properties

1. Glass and metal look really in close contact forming an adherent interface as shown by S.E.M. and T.E.M. micrographs in fig.7.

Fig. 7

Especially when high purity copper is used normally, O.F. copper, best adhesion is gained although any diffusion phenomena is not present (fig. 7).
Thermal differential analysis /6/ on the blend of O.F. copper and glass showed that metal does not wet the glass and that no detectable Cu_2O was diffused in the glass.
In the microwire forming process also, chemical reaction seems not to take place so that the metal glass adhesion is to be acribed to the higher shrinkage of the metal in the fibre axis direction compared with the radial shrinkage.
This produces a compressive force towards the internal capillary glass surface leading to the mentioned good adhesion in the interface. This fact lets the copper glass coated microwires to be bent up to very small bending radius (about 1 mm) without glass coating breakages.
When no O.F. copper has been tested a small chemical reaction forming CO or CO_2 has been detected in the metal glass interface. This lets to better adhesion and so to less bending radius also for thicker microwires.
Unfortunately when no O.F. is spun it is more difficult to obtain continuous microwires for the reason mentioned in the conditions process.

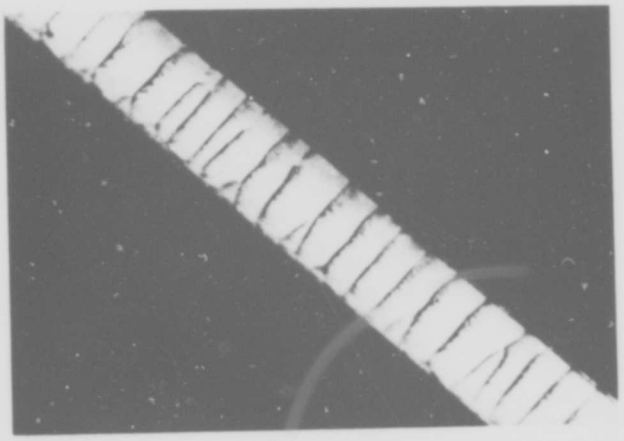

Fig. 8 : Longitudinal optical micrograph showing grain arrangement in spun copper microwires. Grain boundaries are almost perpendicular to the fiber axis.

2. Grain structure, really peculiar, of spun fibers is determined by the spinning method and their arrangement reflects the spinning conditions. Well grown grains have their boundaries nearly normal to the microwire axis and, as shown in fig. 8, are built up one upon another like bricks.

Fig. 8

The structure is sometimes interrupted by the presence of smaller grains, radially arranged near the surface of copper microwire, created by different cooling time between surface and center in the spinning process.
Grain size is bigger than those of cold drawn fibers which are randomly arranged, fig. 9, moreover.

Fig. 9

Table 1 shows some tipical results.

table 1

3. Cold drawn fiber grains arrangement led to a double texture as verified by us /2/ and shown in the literature /9/, /10/, namely /100/+ /111/ when the deformation is below 96% reduction in diameter. Copper spun microwires on the contrary present a single texture, namely /001/ and the regular stacking of grains simulates, in the respect of X - rays diffraction, a single crystal behaviour along the texture axis direction. Moreover, the misorientation angle is

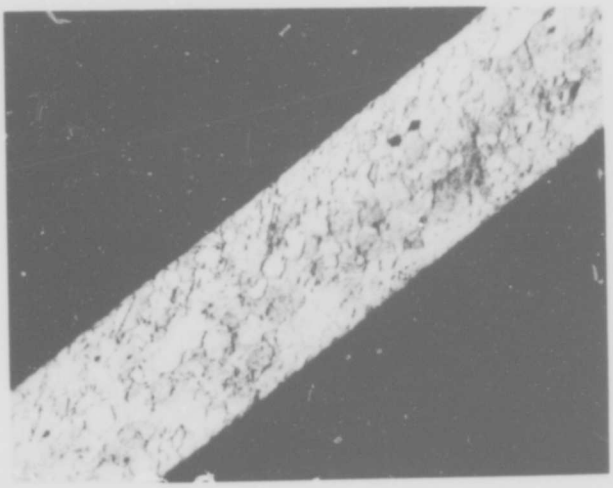

Fig. 9 : Longitudinal optical micrograph of a cold drawn copper microwire. Grains are randomly arranged. Magnification 1100 X.

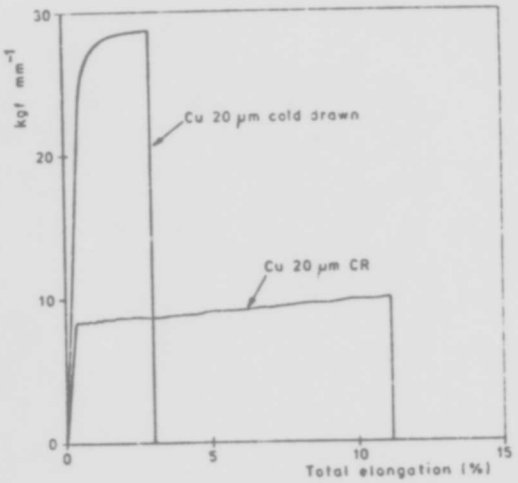

Fig.10 : Stress versus total percentage elongation diagram for cold drawn and melt spun microwires (ϕ_{Cu} = 20 microns).

relatively small when compared with that of cold drawn microwires. In fact it ranges 2°÷ 14° degrees in dependance on the diameter of the fiber compared the range of 10° - 30° degrees for the drawn microwires.

4. Mechanical properties reflect also the mentioned grain structure and texture shown in table 1 - Fig. 10 compares the elastic-plastic behaviour of spun fibers with that quasi-elastic corresponding to the cold drawn microwires.

Fig. 10

The stress-strain plot shows a very sharp transition between elastic and plastic zone and the yield point, at which plastic deformation starts, remains nearly constant with stress increasing. This feature shows the absence of a locking mechanism of dislocation, generated under the applied stress, as expected in f.c.c. metals of ordinary purity.
Consequently the total percentage of elongation is quite high, almost 15% and increases as σ_{uts} decreases.
It is worth noting that there is a relation between spinning velocity, cooling time, and mechanical characteristics of the spun fibers. Usually as the spinning velocity increases,the cooling time becomes shorter and consequently the yield point is higher and the plastic zone is reduced.
We have experimentally verified what is also reported in literature /8/ that the ultimate tensile strenght is increased by higher spinning velocity as shown in Fig 11.

Fig. 11

Note that cold drawn microwires show a shorter plastic zone and higher yield point with a total percentual elongational which does not exceed 3%.
The mechanical properties have been explained by structure investigations. In fact T.E.M. investigations on chemically thinned samples of copper fiber, have shown, as we reported before /2/, the presence of large grains with also a low dislocation density, fig. 12.

Fig. 12

Future experimental relation between structure and mechanical properties require further investigations in order to test the influence of spinning velocity and quencing time to obtain finer grained fibers which should show improved the tensile strenght of the spun metal microwires.

HANDLING AND APPLICATIONS

In spite of the mentioned weak mechanical properties of the bare copper microwire obtained from melt by a spinning process with glass, we think worth to mention the handling and the applications of the glass-coated micro wires which can be exploited as enamelled microwires up to temperature of 500°C.

Handling

One of the first question asked about handling it usually concerns stripping or baring the ends and how the wire is joined to a terminal. Since the glass is relatively brittle it may be removed by crushing with smooth jawed pliers

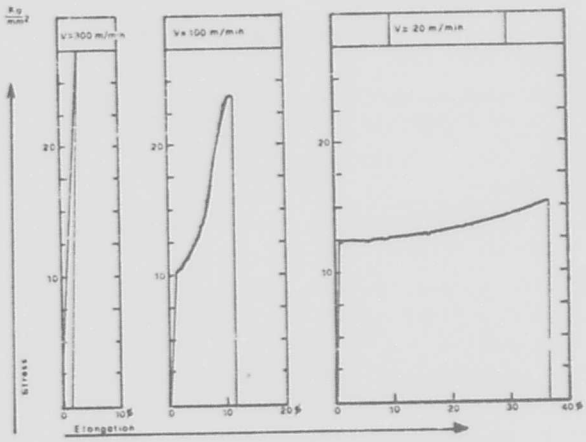

Fig.11 : Typical diagram showing the dependence of ultimate tensile stress on spinning velocity or cooling time for copper of 20 microns in diameter

Fig.12 : T.E.M. micrograph of a chemically thinned copper microwire. Small angle grain boundaries and low dislocation density are present. Magnification 220.000 X.

or with a specially built crushing machine. A second method is to etch the glass away with hydrofluoric acid but this is not a very pleasant method for general use. A third way involves the use of the glass as a flux in a brazing operation. The wire is wound round the terminal post and heat is applied from a nichrome loop or, with practice from a gas-flame. The molten glass runs and acts also as a flux for the solder during the jointing operation. In order to give added strength to the joint, soft solver and bared wire can be used. It is advisable to bury the end of the glass sheath inside the solver bead. Microwire may be wound,with care, in the same way as ordinary wire. The precaution to be taken is that, unnecessary tension has to be avoided into the wire. This means that the spool containing the wire must be mounted on needle pivots in order to reduce friction. The usual guide wheel system of pulleys must be removed and a winding machine drive must be used in which the rotation is started extremely slowly and accelerated as smoothly as possible. Because the glass covering turns ductile copper into a wire,having a brittle nature,it is essential to avoid stresses due to differential thermal expansion between the wire and any bobbin. Ceramic materials having appropriate expansion coefficient are available and it is usual to employ them wherever the temperature excursions of more than a few degrees are to be expected. With these precautions microwire is quite easily wound. Practice suggests to handle the glass covering with no bare hands if it can be avoided, and certainly the turns on a bobbin must never be touched with the fingers. In fact to scrape the turns on a bobbin of wire with a fin gernail, invariably leads to many broken turns.

Applications

The metal core diameter can be finer up to 1 micron. The covering glass thickness can be between 1,5 to more than 10 times the core diameter. So the electrical insulation can be considered up to 10 KV at 20°C and a little less at 500°C depending on the kind of glass.
A part the handling mentioned difficulties, the insulated copper microwires can be exploited as an enamelled conductor in:

- intermediate frequency transformers
- coils in pulse circuitry
- galvanometers windings
- sealed and high temperature relay coils
- miniature electric motors
- computer circuits microminiaturisation

It would appear that designer of electronic circuits and components could request the special glass-coated microwires.
Further applications have been suggested by changing the copper core with other metals or alloys as gold, silver, manganin, chromel alumel, steel. Their use could be as conductors or resistors or thermocouple working in corrosive atmosphere or other similar.
From this point of view the spinning process shows versatility to produce all the needed metal microwires included those which have not the ductility necessary to be obtained by the cold drawn process.

Table I
Typical data of tensile strenght $\sigma_{0,2\%}$ at 0,2% of elongation, ultimate tensile strenght σ_{UTS} and total elongation percentage for spun copper microwires. Grain size as a function of diameter are also shown.

Diameter ( )	Grain size d (mm)	$\sigma_{0,2\%}$ (Kgf/mm^2)	σ_{UTS} (Kgf/mm^2)	Total Elongation (%)
10	1,15	17,00	18,0	8.15
20	1,82	9,2	10,0	10,2
30	2,70	8,0	9,2	12,7
34	4,20	-	-	-
40	7,55	5,2	5,8	13,1

Note that colddrawn fibers show grain size up to 1-3 microns and their σ_{UTS} can be up to 40 Kgf/mm2 with about 3% of total elongation.

CONCLUSION

The investigation on the spinnability of liquids, glasses and metals led us to test the possibility to obtain metal microwires with the so called "melt spinning method".
The comparison of the properties of the copper microwires obtained by this technology show that new experiments must carry out to see how the spun microwires can approach the mechanical properties of the cold drawn micro wires which, at present, show a better features for the usual applications.
Meanwhile the already obtained copper microwires coated by glass have actually suggested to be used in some special electrical applications. This is mainly due to a very good insulating properties of glasses up to 500°C. The main limitations seem due to the brittleness of the covering glass which does not allow to bend the glass-coated microwires around the itself diameter as the ordinary plastic-enamelled microwires perform.
The limitations of the spinning technology on one side, its versatility to be used for many metals, included those usually no-ductile, on the other side have driven our research to go on with the spinning process for the future.

Literature references

(1) G. Manfrè, W.R. Whorlow (1967) BR .J. Applied Phys., 18, 839-43

(2) G. Manfrè, G. Servi, C. Ruffino (1974) J. of Materials Science, 9,74-80

(3) G. Manfrè, (1973) Rheological Acta, 12 349-56

(4) C.E. Anagnostopalos, (1970) Rubber J. 23-30

(5) I.G. Butler, W. Kurz, J.Gillot, B. Lux (1972) Fiber Sicence and Technology 5, 243-62

(6) G. Galante, G. Manfrè (1973) Ceramurgia 1,3-10

(7) G. Manfrè, P. Vianello (1972), Italian Patent 930,409

(8) F. Nixdorf, (1970) Proc. Roy. Soc.London 319,17-32

(9) N. Brown,(1961) Transaction AIME, 221 236-245

(10) E. Shinid, G. Wasserman (1927) Z. Phyzik, 42, 779-86

Name : Mr. Giovanni Manfrè

Address : R & D Division Director
TECHNION SPA
Via A.M. Ampère n. 28/A
20131 MILANO - ITALY
Telex 32512 TECHMIL

Biographical Sketch :
Mr. G. Manfrè, degree in Physics Mathematics on 1959 at Padova University, Italy
M. Sc. in Rheology on 1965 at Surrey University, England, has been working on glass, plastics, metals fibres rheology in several research industrial laboratories.
Many pubblications on glass spinning show his contribute to the spinning art of organic and inorganic fibres included the metal microwires.
Now he is the Director of R & D Division of TECHNION SPA working on metal drawing, including the lubricants, plastic insulation for cables, inorganic fibres for materials composites, optical fibres.

Name : Mr. Guido Servi

Address : De Angeli SPA - Desio - MILANO
Italy

Biographical Sketch :
Mr. Servi, degree in industrial chemistry, on 1967 at Bologna University, has been working in Industrial Research Laboratory in electron microscopy and X ray diffraction on semiconductors, glass and metal fibres, fiber-matrix interface in composites.
Now he is responsible of fiber, microwires and composites applied research laboratory in De Angeli SpA.

HIGH DENSITY POLYETHYLENE FOR PIC INSULATION: OXIDATIVE STABILITY

Maureen G. Chan
Bell Laboratories
Murray Hill, New Jersey 07974

Summary

The effect of replacement of low density polyethylene by a higher density resin, and of changes in the polymer's stabilization system on the oxidative stability of cable insulation was investigated. It was found that the high density resin embrittles at low levels of oxidation due to chain scission in its high molecular weight fractions. Protection of high density polyethylene against incipient oxidation is critical if long-term stability is to be achieved. Fortunately, there is a considerable increase in stability of both the high and low density resins with the modified stabilization system. This stability is enhanced further in the high density resin because of the excellent retention of stabilizers by this resin during the aging process. These factors indicate that the long-term usefulness of the new product should be very good.

Introduction

The Bell System has made two important modifications in the polyethylene resins used as primary insulation for air core, multipair cables. The low density (.92) polyethylene resins used previously as insulation have been replaced by higher density (.95) polyethylenes. In addition, the resin stabilization system has been changed from one containing a single antioxidant, 4,4'thiobis (3-methyl-6-tert.butyl phenol), to a system which utilizes both an antioxidant (A), tetrakis[methylene-3(3',5'-ditert. butyl-4'-hydroxyphenyl)propionate]methane, and a copper deactivator (B), N,N'dibenzaloxalyldihydrazide. The change from low to high density resin was made to improve physical properties of the insulation such as abrasion resistance, while the stabilization system was modified to enhance the thermo-oxidative stability of the material.

The significance of these modifications on the long-term usefulness of the insulation has been under investigation. Since oxidation has been found[1] to be one of the primary causes of deterioration in polyethylene insulations, changes in the chemical and physical properties of both the low and high density resin upon oxidation were determined. In addition, the oxidative stabilities of wire insulations produced from polyethylene resins containing the new stabilizer systems were also studied.

Experimental

Sample Preparation

Materials - Two base resins were used for the chemical and physical property studies. The low density polyethylene was an ethylene homopolymer, ASTM Type I, with a density of .92. The high density polyethylene was a copolymer of ethylene and a higher mono-olefin, ASTM Type III, with a .95 density. Melt indices of both resins were in the 0.2 to 0.3 range. Ultraviolet analysis of the two polymers showed no detectable stabilizers.

Wire insulations were manufactured from similar resins to which a nominal 0.1% each of A and B had been added. Infrared analysis of the resins before processing showed that each of the stabilizers was present at concentrations of 0.10% in the low density polyethylene and 0.12% in the high density polyethylene.

Fabrication - Films were prepared from the base resins by homogenizing pellets on a two-roll mill at 143±3°C and molding the milled material on a steam press at 165±5°C and 952 psi. Total exposure time at the elevated temperatures required for both procedures was estimated to be about ten minutes.

Wires were produced by standard Western Electric manufacturing procedures.

Oxidation - Strips (5 x 5/8 x .01") of the polymer films were suspended on glass rods and oxidized at 100°C in sealed tubes attached to mercury manometers. Oxygen-absorption levels were between 0.8 and 7 cc/gm. Control samples were heated in helium for equivalent time periods. After heating, all samples were stored in nitrogen, in the dark, until all tests were completed.

Oxygen-absorption studies on wire insulations were performed by a standard method[2] with the conductors in place. Data were obtained at four temperatures: 119±0, 139±1, 149±1, 159±1°C. Induction times, indicative of the onset of rapid oxidation, were measured by extrapolating the constant rate portion of the oxidation curve back to the baseline. Average induction times were calculated from multiple runs on each wire (2 to 4 runs at 119°C, 8 to 10 at other temperatures).

Wires were oven-aged in a Freas Model 625 circulating-air oven, at 70±1°C and a medium air-flow setting. Wires were examined after oven-aging by oxygen-absorption tests at 138±1°C. There were 2 to 4 samples of each wire examined for the reported aging periods.

Methods of Test

Dielectric Properties - The dielectric properties of the films were determined by measuring the loss angle, δ, at 30 Mhz. A high-resolution, nondestructive, air-cell method was used.[3] The dielectric loss of one area of each sample was determined with the exception of the most highly oxidized samples where several areas were examined.

Infrared Spectra - Infrared transmission spectra were obtained on a Perkin Elmer Model 621 spectrophotometer using normal instrument conditions. A single area of each sample was examined and absorbance values were normalized by dividing by film thicknesses.

Densities - Densities of three sections of each sample were determined in a density gradient column.[4]

Tensile Properties - Tensile properties were measured using microtensile specimens, (1-1/2 x 3/16 x .01").[5] Five measurements were made for each oxidation level. Crosshead speeds of .5"/ min. were used.

Molecular Weights - Molecular weights were obtained by a standard procedure[6] on a Waters Model 100 Gel Permeation Chromatograph which is equipped with four, graded porosity, Syragel^{R} columns and a refractive index detector. The unit was operated at 135°C with 1,2,4-trichlorobenzene as the eluent. A calibration standard, generated from NBS 1475 linear polyethylene, was used to compute molecular weight distributions.

Effect of Oxidation on Chemical and Physical Properties

The effect of oxidation upon the properties of low and high density polyethylene insulation was examined by studying two unstabilized polyethylenes which were similar in composition to the base resins used in the formulation of cable insulation. The polymers were allowed to absorb small quantities of oxygen, between 0.8 and 7 cc/gm, and then changes in their dielectric loss, infrared absorptions, densities, tensile properties, and molecular weights were measured. Four samples of each resin were oxidized.

Oxidation rates of two of the samples was shown in Figure 1. They are representative of all of the samples studied. While the high density polyethylene has an induction period longer than that observed for the lower density polyethylene, its rate of oxidation is considerably faster once the induction period is over.

Dielectric Properties

The dielectric loss upon oxidation increases for both polymers (Figure 2). Differences between the two materials cannot be considered significant since variations found in the multiple runs are of the same magnitude. The observed increases in dielectric loss are believed due to the accumulation of polar species, e.g., carbonyl and hydroxyl groups, in the oxidized polymers (see below).

Infrared Spectra

Both materials show changes in the hydroxyl and carbonyl regions of their infrared spectra after oxidation (Figure 3). The 3360 cm^{-1} band which is attributed[7] to bonded hydroperoxide is present in both polymers and increases with oxygen absorption. An additional band appears at 3550 cm^{-1} (free hydroperoxide)[7] in the low density resin. Complex carbonyl absorptions[8] with band heads at 1705-10 cm^{-1} also appear in each polymer. In addition, vinyl[9] and vinylidene[9] (905, 885 cm^{-1}) absorptions decrease, and both polymers show a baseline drop in the C-O (1200-1000 cm^{-1}) region.[8]

These changes are shown in Figure 4 where the normalized absorbance values of the OH, C=O, and C=C groups are plotted. These data are similar to data obtained in previous infrared studies of the oxidation of low and high density polyethylenes[10]. The results demonstrate that, while increase in carbonyl content upon oxidation is large for both polymers, it occurs to a greater extent in the high density resin. Increase in hydroperoxide content, on the other hand, is considerably more pronounced in the low density polymer. Apparently, the decomposition rate of hydroperoxides in the high density material is rapid, leading to a high concentration of carbonyl-containing products. This could be

due to the nature of the hydroperoxidic group or to the presence in the resin of materials, e.g., polymerization catalyst residues, which catalyze hydroperoxide decomposition.

Densities

The average density values measured are tabulated in Table I. All of the samples showed an increase in density upon heating, however, increases in density were far greater for samples heated in oxygen than for those heated in helium. This increase in density upon oxidation has been attributed[11] to increased chemi-crystallization of the polymer.

Tensile Properties

Data illustrating the effect of oxidation on the tensile properties of the two polymers are summarized in Table I. The elongations (Figure 5) and ultimate strengths of both resins decrease as a result of oxidation. However, the properties of the low density resin are significantly less susceptible to oxidation than are those of the high density polymer. After an absorption of 7 cc/gm of oxygen the low density samples retain moderate yield and ultimate strengths and have a measurable elongation of 62%. All of the oxidized, low density samples are pliable and show no sign of cracking when bent manually under ambient conditions. In contrast, the high density resin embrittles at very low levels of oxidation. Absorption of 0.8 cc/gm of oxygen causes the average elongation of this material to drop to less than 40%. At 1.8 cc/gm of absorbed oxygen the average elongation of the high density sample is only 5%. Yield and ultimate strengths of this material, when they still can be measured, also decrease rapidly. None of the high density samples remains pliable after oxidation. The sample that has absorbed 0.8 cc/gm of oxygen develops visible cracks, and the more highly oxidized samples fracture, upon manipulation at room temperature.

Molecular Weights

Three moments of the molecular weight distribution, $\overline{M}_n$, $\overline{M}_w$, and $\overline{M}_z$, were obtained for each sample. These average molecular weights are sensitive to different weight fractions of the polymers.[12] The number average molecular weight, $\overline{M}_n$, is influenced by changes in weight fractions of low molecular weight species and relatively insensitive to changes in high molecular weight species. In contrast, the weight and z-average molecular weights, $\overline{M}_w$ and $\overline{M}_z$, are more influenced by the presence of high molecular weight species with $\overline{M}_z$ being particularly sensitive to changes in the high molecular weight fraction.

The molecular weight averages of all the samples are summarized in Table II along with values of $\overline{M}_w/\overline{M}_n$ which are characteristic of the polydisparsity of the polymers. The molecular weight distribution of both polymers narrows with oxidation. However, comparison of the three molecular weight averages (Figure 6) shows interesting differences between the high and low density resins. The high density polymer has a sharp drop in $\overline{M}_z$, a moderate decrease in $\overline{M}_w$ and very little change in $\overline{M}_n$, upon oxidation. The low density resin, in constrast, shows a decrease in all three molecular weight averages with the decreases in $\overline{M}_z$ and $\overline{M}_w$ less pronounced than those observed for the high density polyethylene. Apparently, oxidation of the high density resin causes preferential scission of high molecular weight species possibly of the chain segments joining adjacent lamellae.[11] This immediate drop in concentration of high molecular weight species parallels, and is believed to be responsible for, the observed, rapid decrease in physical properties (Table I) of the high density polyethylene in the early stages of oxidation.

Oxidative Stability of Wire Insulation

It is clear that oxidation has a severe effect on many of the physical properties of the high density base resin. Prevention of oxidation by the addition of stabilizers to the resin thus becomes extremely important if this material is to be used for wire insulation. The Bell System currently requires the addition of two stabilizers to polyethylene cable insulation, 0.1% A and 0.1% B. Long term, low temperature, exposure tests of low density polyethylene containing these additives show[13] that they afford efficient protection to the low density resins. In order to evaluate the efficiency of these stabilizers in the high density resin, oxygen absorption and oven-aging tests were run on production wires insulated with a high density resin which contained A and B. Similar tests were run on a comparably stabilized, low density resin. Four wires were examined: white and black high density, and white and black low density, insulated samples.

Oxygen-Absorption Studies

The wires showed typical thermo-oxidative behavior. All samples had long induction periods, with little detectable oxygen absorption, followed by a period of rapid oxidation. The average induction times observed for the wire samples are shown in Figure 7. Differences among the four samples are slight. The two black samples are com-

parable in their oxidative stability. However, distinctions between the white samples are more noticeable. The high density, white material is more stable than the low density, white insulation at all test temperatures. On the basis of these data, earlier work on the low density system[14], and similar tests on laboratory samples[15], the high density insulation appears to be at least comparable to current production, low density, cable insulation.

Oven-Aging Tests

The effect of oven-aging at 70°C on the residual stability of the insulation was determined by oxygen-absorption studies at 138°C. Samples were examined before and after oven-aging for periods of up to 90 days. Per cent changes in induction times were calculated and are shown in Figure 8. It is evident from these data that the high density insulation retains its oxidative stability to a far greater degree than does the low density material.

Loss of stability in these samples upon oven-aging probably can be attributed to depletion of the resins' stabilization systems. Many antioxidants exude to the surface where they can be physically lost.[16,17] Stabilizer depletion in the wire samples was checked by infrared analysis of the two white insulations after 59 days of oven-aging. The copper deactivator, B, remained in both insulations, although it appeared slightly depleted after oven-aging. However, the antioxidant, A, while still quite evident in the aged, high density insulation, could no longer be detected in the aged, low density sample. Since B is not an antioxidant, loss of A, the phenolic antioxidant, would severely decrease the oxidative stability of the polyethylene and the observed loss of this additive would account for the severe drop in stability of the low density material after 70°C oven-aging.

Differences in stabilizer loss between the two resins is believed due to the morphology of these semicrystalline polymers. Diffusion of additives from the amorphous regions of the polymer, where physical loss can occur, is thought[18] to depend on the crystalline structure of the material. The lower density, less crystalline, resin has a structure more conducive to additive diffusion and eventual loss than does the high density polymer. Hence, the high density insulation shows a greater retention of stability during aging and should be superior to the equivalently stabilized, low density resin when in service.

Conclusions

The effect of oxidation on the electrical and physical properties of the low and high density polyethylenes presently in use in the Bell System is considerable. Polar groups are formed in the two polymers during oxidation causing an increase in the dielectric loss. This increase is approximately the same for both resins. As oxidation of both polyethylenes proceeds, significant decreases in their molecular weights occur, along with loss of mechanical strength. The effect of low levels of oxidation on mechanical degradation is much greater in the higher density material. Absorption of less than 2 cc/gm of oxygen causes severe physical degradation of the high density resin.

These results highlight the necessity of minimizing incipient oxidation of polyethylene cable insulation, particularly of the high density insulation. Fortunately, the modified stabilization system retards oxidation of the high density resin and is retained by this resin during aging. Any new stabilizer systems designed for high density polyethylene insulation must do likewise.

Acknowledgements

Many people were helpful in the design and completion of these experiments and their excellent advice is gratefully acknowledged. They include: D. R. Falcone, H. M. Gilroy, R. H. Hansen, W. L. Hawkins, J. B. Howard, G. L. Link, W. M. Martin, C. J. Motter, W. F. Moore, R. P. Wentz, and K. C. Weyts. In addition, special thanks are given to P. M. Muglia and E. P. Otocka who made the molecular weight determinations and to I. M. Plitz who oven-aged the wire samples.

References

1. See for example: W.L. Hawkins, M.G. Chan and G.L. Link, Polym. Eng. and Sci., 11, 377(1971); J.B. Howard, Proc. 21st Int. Wire and Cable Symp., 329(1972); B.B. Pusey, M.T. Chen, W.L. Roberts, Proc. 20th Int. Wire and Cable Symp. 209(1971).

2. W.L. Hawkins, R.H. Hansen, W. Matreyek, F.H. Winslow, J. Appl. Polym. Sci. I, 37(1959).

3. G.L. Link and G.E. Johnson, 1972 Annu. Rep., Conf. Elect. Insul. Dielectr. Phenom., Nat. Acad. Sci., 376(1973).

4. ASTM D1505

5. ASTM D1708

6. E.P. Otocka, R.J. Roe, M.Y. Hellman, P.M. Muglia, Macromol. 4, 507(1971).

7. J.D. Burnett, R.G.J. Miller, H.A. Willis, J. Polym. Sci., 15, 592(1955).

8. J.P. Luongo, J. Polym. Sci., 42, 139 (1960).

9. L.H. Cross, R.B. Richards, H.A. Willis, Disc. Faraday Soc., 9, 235(1950).

10. M.G. Chan and W.L. Hawkins, Polym. Eng. Sci., 7, 264(1967).

11. F.H. Winslow, M.Y. Hellman, W. Matreyek, S.M. Stills, Polym. Eng. Sci., 6, 273(1966).

12. F.W. Billmeyer, Jr., Textbook of Polym. Sci., N.Y., 1962, Chapt. 3.

13. H.M. Gilroy, Proc. 23rd Int. Wire and Cable Symp., in press.

14. J.J. Mottine and A.E. Bendix, BTL Internal Publication, Sept. 7, 1971.

15. J.W. Shea and F.C. Binkowski, BTL Internal Publication, Sept. 14, 1972.

16. H.E. Bair, Polym. Eng. Sci., 13, 435 (1973).

17. R.J. Roe, H.E. Bair, C. Gieniewski, J. Appl. Polym. Sci., 18, 843(1974).

18. P.N. Lowell and N.G. McCrum, J. Polym. Sci., A-2, 9, 1935(1971).

Maureen Chan is a Member of the Technical Staff of Bell Laboratories, Murray Hill, New Jersey in the Plastics Chemistry Research and Development Department. She received a B.S. in Chemistry from Chestnut Hill College in 1961 and an M.S. in Chemistry from Stevens Institute of Technology in 1965. She joined Bell Laboratories in 1962 and has been involved in studies on the deterioration and stabilization of polyolefins.

TABLE I

PHYSICAL PROPERTIES OF OXIDIZED POLYETHYLENES

Sample	Time at 100°C hrs.	Oxygen Absorbed cc/gm	Density[a]	Elongation[b] %	Yield[b] Strength psi	Ultimate[b] Strength psi
Low Density	0	----	.919	529	1272	2394
	47.5	-- in helium	.923	607	1448	2411
	67.4	-- "	.923	564	1425	2241
	27.3	.8	.923	501	1395	1983
	47.5	1.6	.926	314	1466	1518
	67.4	3.2	.928	144	1471	1340
	96.2	7.0	.932	62	1517	1433
High Density	0	--	.948	313	3487	2721
	29.4	-- in helium	.950	290	3690	2796
	47.5	-- "	.950	412	3672	2938
	29.5	.8	.956	36	3666	2254[c]
	31.5	1.8	.959	~5	3501	
	34.9	4.4	.963	<5	2258	
	37.0	5.9	.972	--	--	

[a] Average for three specimens

[b] Average for five specimens

[c] Single specimen

TABLE II

Molecular Weights of Oxidized Polyethylenes

Sample	Oxygen Absorption cc/gm	$\bar{M}_n \times 10^{-4}$	$\bar{M}_w \times 10^{-5}$	$\bar{M}_z \times 10^{-5}$	$\bar{M}_w / \bar{M}_n$
Low Density	-	3.20	1.44	4.60	4.5
	- in helium[a]	2.40	1.21	4.73	5.0
	- in helium[b]	3.11	1.76	8.15	5.7
	.8	1.60	1.02	4.04	6.4
	1.6	1.39	0.75	2.35	5.4
	3.2	1.70	0.58	1.54	3.4
	7.0	1.05	0.31	0.84	2.9
High Density	-	2.04	1.47	6.72	7.2
	- in helium[c]	1.75	1.29	9.30	7.4
	- in helium[a]	1.48	1.25	9.99	8.5
	.8	1.78	0.62	1.70	3.5
	1.8	1.44	0.44	1.06	3.0
	4.4	1.25	0.32	0.75	2.6
	5.9	0.98	0.23	0.50	2.3

Samples heated in helium: [a] 47.5 hours; [b] 67.4 hours; [c] 29.5 hours

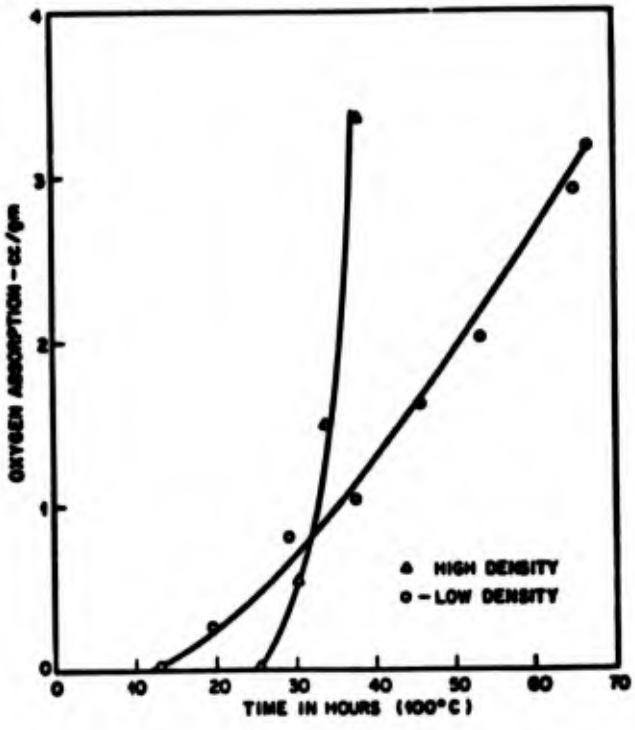

Figure 1 - Oxidation of unstabilized, polyethylene, base resins at 100°C

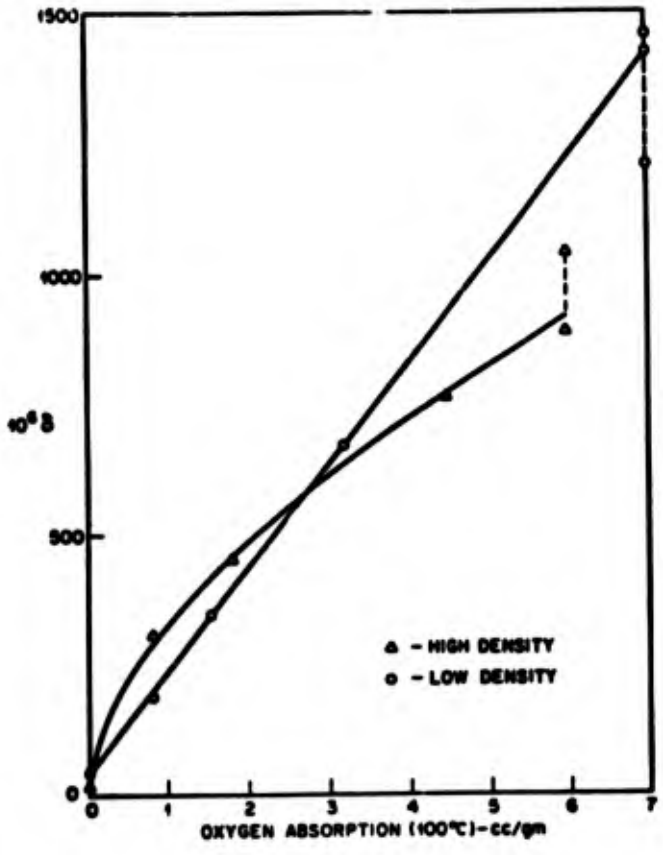

Figure 2 - Dielectric loss in oxidized polyethylenes

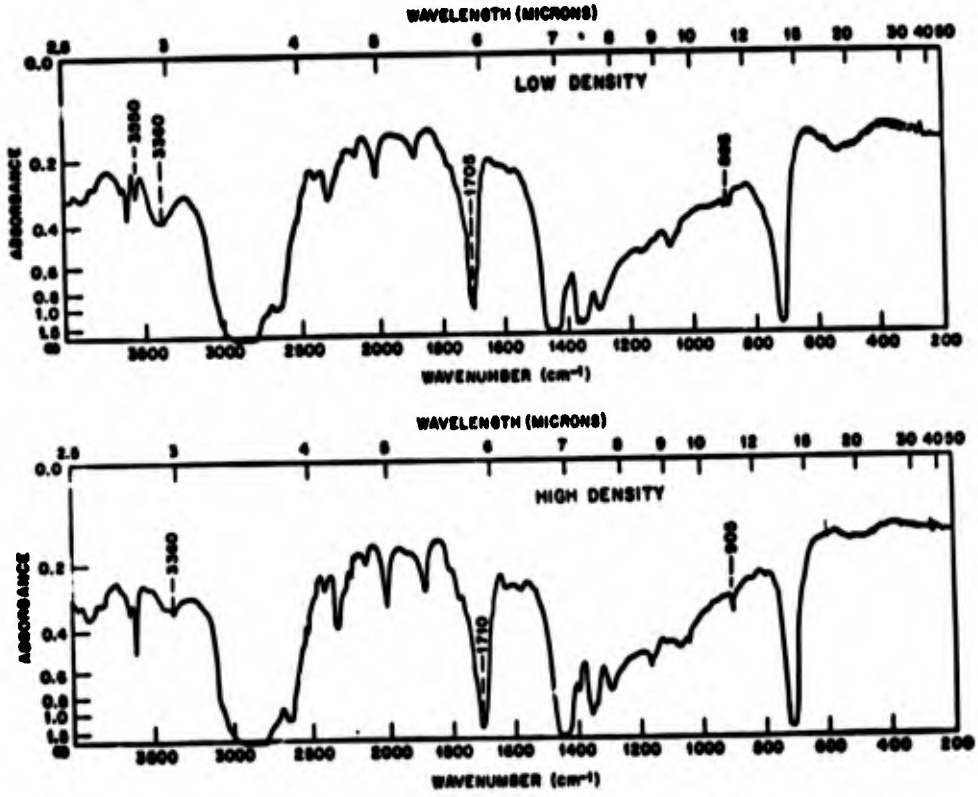

Figure 3 - Infrared spectra of oxidized polyethylenes

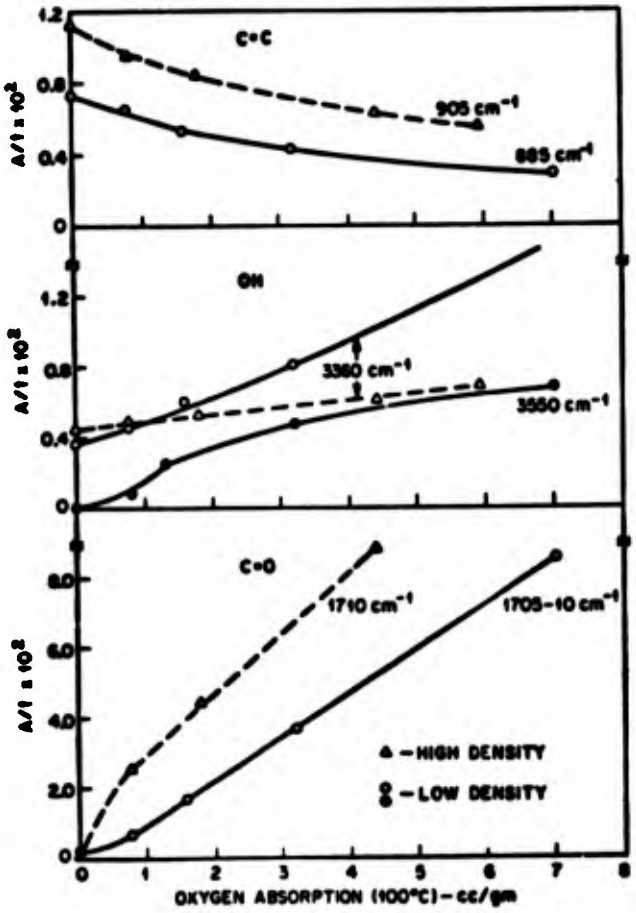

Figure 4 - Effect of oxidation on infrared absorptions

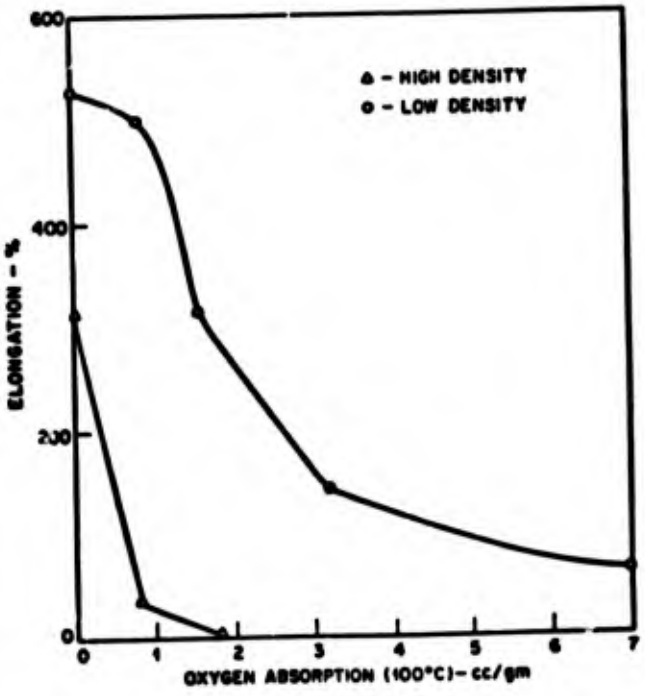

Figure 5 - Effect of oxidation on elongation

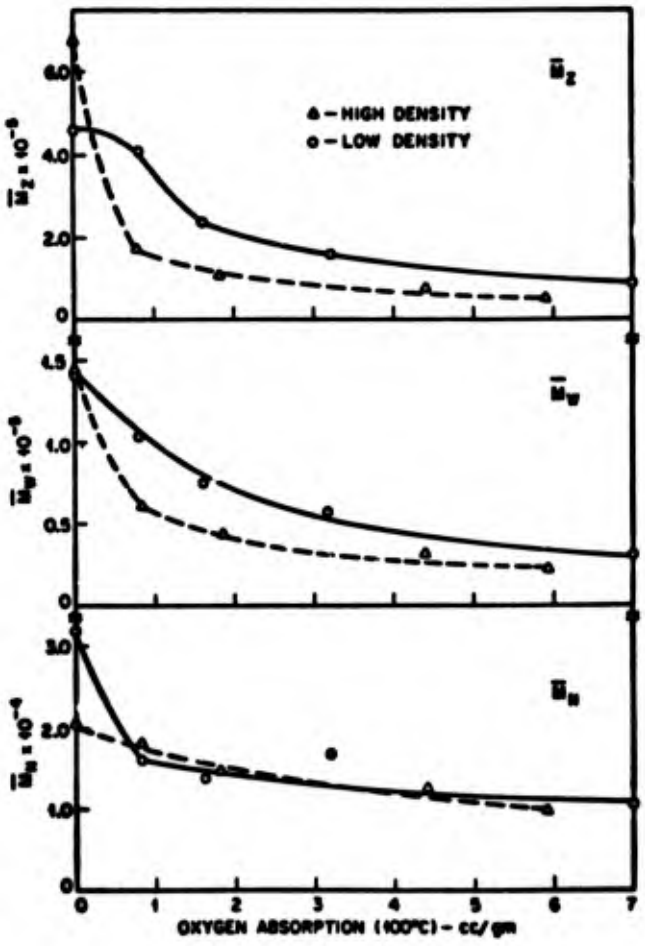

Figure 6 - Effect of oxidation on molecular weights

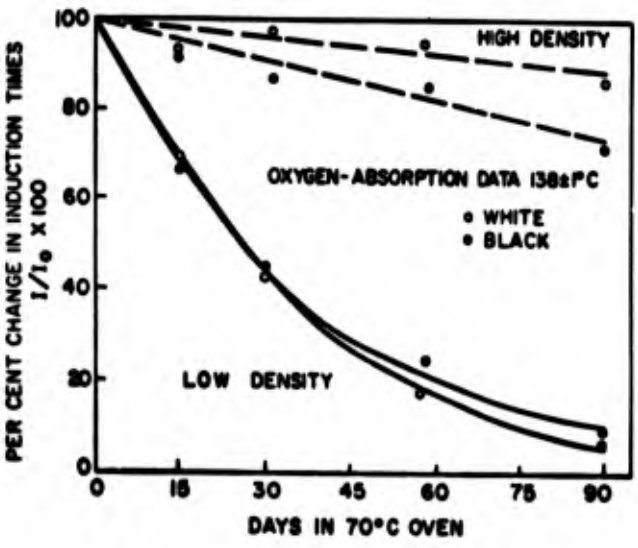

Figure 8 - Stability of polyethylene insulated wires after 70°C oven-aging

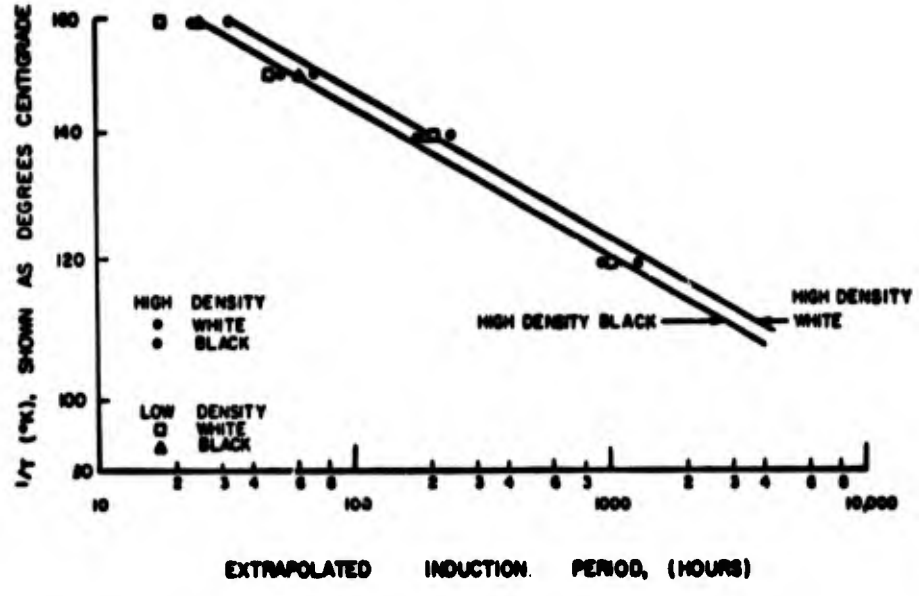

Figure 7 - Temperature effects on the oxidation of polyethylene insulated wires

THERMAL OXIDATIVE CRACKING OF POLYETHYLENE INSULATION ON TELEPHONE CONDUCTORS

H. M. Gilroy
Bell Laboratories
Murray Hill, N.J. 07974

Summary

Field failures of low-density polyethylene wire insulation, found in Bell System pedestals, have been duplicated at Bell Telephone Laboratories in the Experimental Pedestal Installation Complex. The rate of insulation failure as well as changes in cracking behavior as oxidation progresses are discussed.

Improvements obtained by means of a new stabilization system and substitution of high-density polyethylene are shown to be far superior to the stabilization system used in the past.

Introduction

Several years ago insulation failures in polyethylene insulated conductors (PIC) began to appear in Bell System field installations. Detailed discussion of these failures have been covered by J. B. Howard[1] and other field failures in low-density polyethylene (LDPE) were reported by Pusey et al.[2] These failures were mainly confined to the hotter regions in the south and only in pedestals used for above-ground terminations in buried plant.[1]

PIC samples collected from field pedestals and aerial splice cases showed that only fractional amounts of antioxidant remained in the insulation and essentially none in the samples that had failed.[1] Short term oven tests on Western Electric (WECo) production wires and experimental laboratory wires showed rapid antioxidant loss, but failure of the insulation in these short-term tests only occurred at elevated temperatures and then only on wires that were poorly stabilized.

In an effort to simulate the field conditions that have resulted in insulation failure, the Experimental Pedestal Installation Complex (EPIC) was established at Bell Labs. Standard WECo production cables with various stabilization systems were installed in actual pedestal domes maintained at a series of elevated temperatures. The wire insulation was then life tested to failure.

Apparatus

The pedestal domes used were Bell System B-type pedestals, complete with base plate. Custom-made heating mantles were used to heat the pedestal domes. Each pedestal had its own temperature controller and high temperature alarm system (Figure 1).

Cables Under Test

The cables tested were all WECo production cables, 26 gauge copper conductor, protected by several different antioxidant systems (Table 1). Testing temperatures for low-density polyethylene (LDPE) ranged from 40°C to 90°C in 10°C intervals and for high-density polyethylene (HDPE) from 40°C to 110°C.

Method of Testing

Insulation Cracking - Samples of insulated wire were periodically stressed by wrapping around a steel mandrel of the same size as the overall diameter of the insulated wire. This method was used to simulate the handling that takes place in the field when terminations are made by the installer. Samples were examined visually at 5X magnification for insulation cracking and the first appearance of cracking was recorded as the initial failure. The unstressed portion of the insulation was also examined for cracks. In each pedestal one wire of each color was twisted into a pigtail by wrapping the insulated conductor back on itself. These pigtails were also examined at selected intervals for cracking.

Residual Oxidative Stability - Insulated wire samples were removed at regular intervals for examination by Differential Thermal Analysis (DTA) to determine the rate of stability loss.[3] This loss of oxidative stability was used as a guide to determine the necessary frequency of inspection and stres ing of the insulation. All DTA measurements were made at 200°C in copper pans with the conductor in place. All testing at 200°C was carried out in pure oxygen.

Internal Reflectance Spectroscopy - The onset of oxidation was detected by internal reflectance spectroscopy on the outer surface of the wire insulation. This technique is described in detail by Harrick[4] and its application to wire insulation has been reported previously.[1]

Cracking of Low Density Polyethylene (LDPE) - Stabilization System-4,4'-thiobis(3-methyl-6-tert.butyl phenol (TMTP) - The initial insulation failures found in LDPE stabilized with TMTP are shown on an Arrhenius-type plot in Figure 2. The insulation in these cables is low-density polyethylene (LDPE) and all the tests were carried out at constant temperature. The failures were all produced after stressing the insulated conductor by wrapping around a steel mandrel 0.026 inches in diameter. All the cracked samples were devoid of antioxidant as measured by differential thermal analysis (DTA), and infrared measurements indicated that oxidation had started. None of the pigtails that were prestressed at the start of the testing program cracked prior to or at the time failures were found in the periodically stressed samples.

As can be seen from Figure 2, the curvature is in the direction of decreasing activation energy with decreasing temperature. This can possibly be attributed to a combination of causes: copper catalysis, where the catalytic effect of copper becomes more dominant at lower temperatures[5], and to morphological changes, where the rate of secondary crystallization is related to the test (annealing) temperature.

When the data in Figure 2 are extrapolated to 40°C, the temperature selected as a reasonable maximum to expect in warmer climates, the first failures could occur in as little as three years.

In all the cases of cracking of TMTP-stabilized insulation the white wires failed first, usually followed by red, and then, except for black, the other colors (Table 2) in much the same rank order of failure found in the field.[1] As failures occurred at lower temperatures (70°C, 60°C, and 50°C, the spread between the occurrence of failures in white insulation and in the other colors became more pronounced.

The samples shown in Figure 2 were maintained at constant temperature, and, as such, do not represent the real situation where pedestals heat up during the day and cool off at night. Cable samples have been placed in EPIC pedestals on temperature cycles from room temperature to 60°C and 70°C. Insulation failures in these cycling cables indicate that there is nothing unique about the failure rate or mode of cracking due to temperature cycling. The time for initial failures to occur is shown in Table 3. If we assume the same activation energy for the cyclic process as for the constant temperature process and draw companion curves to Figure 2, initial failures can be expected at 40°C in about four years. These data are in excellent agreement with field results reported previously.[1,6]

Type of Cracking Found in LDPE - The initial cracks found in LDPE stabilized with TBMA were tiny circumferential cracks, many in number, with little or no separation from the copper conductor and with very little copper exposed, often accompanied by dark exudation and discoloration of conductor and insulation. These cracks were not spontaneous but were only produced when the insulation was stressed.

After about 90 days at 90°C and about 150 days at 80°C, the character of insulation cracking changed. Cracks that developed after this period of time were, in general, more catastrophic with only one or two cracks per test section and with large portions of the insulation peeling back to expose the copper conductor but without any discoloration or exudation.

With longer times at test temperature, another change occurred in the mode of cracking. Many samples could not be made to crack even though adjacent sections had cracked in earlier tests. These samples were removed from the pedestals and exposed to boiling xylene for one hour, along with control samples of the same conductors that had not been subjected to exposure at elevated temperature. The control samples dissolved rapidly and completely, while the exposed samples that refused to crack had insoluble fractions of up to 60%, indicating a large amount of gel formation due to oxidative crosslinking.

The amount of gel found at the various test temperatures is shown in Table 4. Here it can clearly be seen that the rate of gel formation is a function of the temperature and that a maximum gel constant is rapidly reached. The change in the character of the cracking and the decrease in the rate of cracking after oxidation is assumed to be caused by the large gel fraction found in these wire insulations.

Cracking of Low-Density Polyethylene (LDPE)

Stabilization System-MBHP/DBOD - Tetrakis [methylene 3-(3,5-ditert.butyl-4-hydroxy phenol) propionate]methane and N, N'-dibenzyl oxalyl dihydrozide - Six cable samples of LDPE with MBHP/DBOD-stabilized insulation are being

tested in the BTL EPIC program. To date, failures have occurred only at 90°C and 80°C (Table 5), and the failures found are not as rapid at these temperatures as seen with the TMTP-stabilized insulation. As shown in Figure 3, the latter insulation fails within a very short time span, and with the exception of the black insulation, failures rapidly reach 100% at 90°C. In the case of the MBHP/DBOD-stabilized insulation, the failure rate is orders of magnitude slower and although the initial failures would indicate that the MBHP/DBOD system is only three times better than TMTP, the slower failure rate would indicate that the MBHP/DBOD system is considerably better, possibly ten times more permanent than TMTP in LDPE.

The failures found in the LDPE stabilized with MBHP/DBOD do not occur first in white insulation, as was the case with TMTP, but are independent of color. The failure of white insulation before pigmented insulation in TMPT-stabilized cables in field and laboratory samples has been discussed by Howard[1] and by Pusey et al.[2] The addition of the metal deactivator DBOD to the samples in this program appears to have pacified or deactivated the white pigment, preventing any deleterious effects.

Since there is, as yet, no detectable white pigment effect, it is possible that the failure rate of MBHP/DBOD insulation will not follow that of Figure 2 for TMTP but will possibly be a straight-line extrapolation. If that is the case the MBHP/DBOD system should protect LDPE for the desired 40 year life at 40°C. However, extrapolation of only a few data points over several decades can be misleading and for a firm prediction of the useful lifetime of this system, several more data points would be most desirable. Until other data is available one can justify the expected longer life of the MBHP/DBOD insulation by examining the total failures found in the EPIC pedestals. All the data is grouped together in Figure 4 giving a clearer picture of the relative failure rates of the two stabilization systems. This represents all the colors (except black) of all the cables from all the WECo plants for the entire period of EPIC testing. As can be seen from Figure 4, the MBHP/DBOD rate of failure is about ten times slower than TMTP at 90°C and 80°C, the only temperatures at which failures have been found to date in the MBHP/DBOD system, giving further credence to the superiority of this system in LDPE wire insulation.

High-Density Polyethylene Wire Insulation

Stabilization System - MBHP/DBOB - WECo production cables with high-density polyethylene (HDPE) insulation are also under test in this program. Because of the higher melting range of the HDPE the testing program was extended upward to 110°C for HDPE. Insulation cracking found to date (Table 6) shows that HDPE is inherently more resistant to oxidative cracking than LDPE and this is attributed to retention of the antioxidant system by HDPE for a longer period of time than in LDPE.

No failures have been obtained to date (2 years in test) for HDPE in EPIC pedestals at temperatures below 100°C and estimation of useful field life by straight line extrapolation indicates that service well in excess of the required 40 year life can be expected.

There is no effect of white pigment causing early failure of the insulation and this is again attributed to the presence of the metal deactivator.

Acknowledgment

The assistance of Mrs. E. Kokta, Mrs. I. M. Plitz, O. V. Colson and K. C. Weyts in the gathering of the data and the construction and maintenance of EPIC is gratefully acknowledged. Thanks also to D. W. McCall, W. L. Hawkins and J. B. Howard for their helpful guidance and suggestions.

References

1. J. B. Howard, Proc. 21th Int. Wire and Cable Symp., 329-341 (1972).

2. B. B. Pusey, M. T. Chen, and W. L. Roberts· Proc. 20th Int. Wire and Cable Symp., 209-217 (1971).

3. J. B. Howard, Soc. of Plast. Eng. 31st Tech. Con. 19, 408-412 (1973).

4. N. J. Harrick, "Internal Reflectance Spectrosography", John Wiley and Sons, Inc., New York (1965).

5. M. G. Chan and D. L. Allara, J. Coll. and Inter. Sci. 47, No. 3, 697-704 (1974).

6. G. A. Smith, Proc. 22th Int. Wire and Cable Symp., 11-22 (1973).

Harold M. Gilroy received a B.S. in Chemical Engineering from Newark College of Engineering in 1957. He is a Member of the Technical Staff of Bell Laboratories, having joined Bell Laboratories in 1960. Prior to that time he was employed by Atomics International, responsible for coolant support systems for organic reactors. At present he is engaged in the development and application of polyolefins for wire and cables.

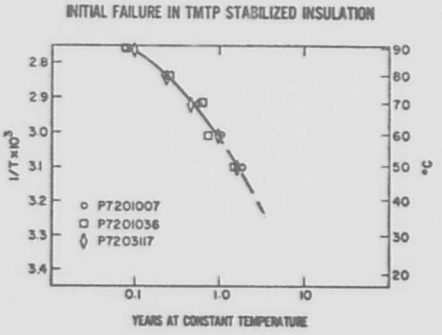

FIGURE 2

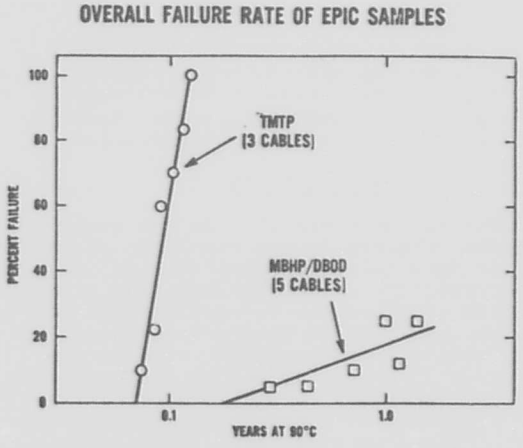

FIGURE 3

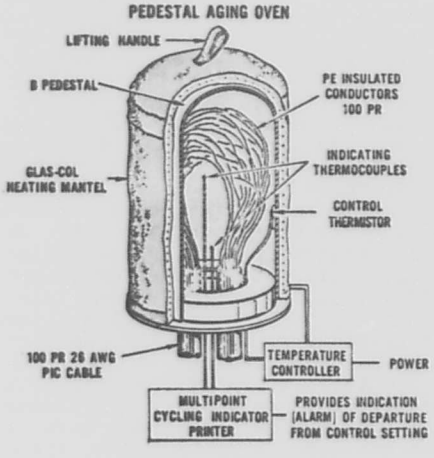

FIGURE 1

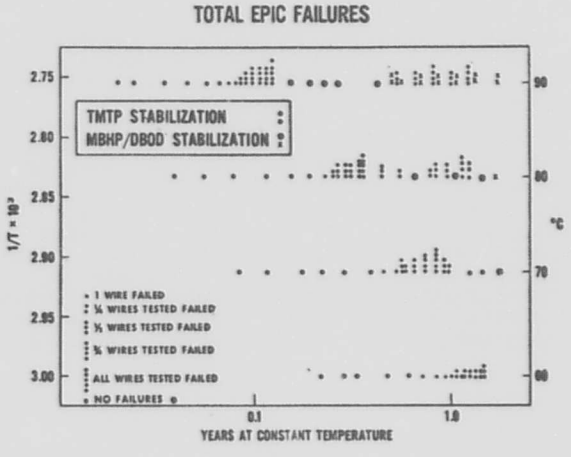

FIGURE 4

RAPID ISOTHERMAL DTA TESTING FOR CONTROL OF STABILITY IN POLYOLEFINS

J. B. Howard, H. M. Gilroy and E. Kokta
Bell Laboratories
Murray Hill, New Jersey 07974

Summary

The performance of a new six-place semi-automatic differential thermal analysis instrument designed primarily for rapid, precise routine quality control testing of stabilized polyolefin plastics is summarized. The apparatus is demonstrated to meet its design intent.

In the course of experiments exploring the versatility of the instrument, an unanticipated catalytic effect was observed by which reactive fragments from an earlier oxidative decomposition appear capable of inducing premature failure in otherwise sound polyolefin specimens. The significance of this observation is discussed.

Introduction

Makers and users of wire and cable have a common interest in the stability of the organic materials incorporated into these structures: the makers because they wish to maintain a reputation for quality and because they must be able to manufacture these products with a minimum of down-time on the extrusion line, the users obviously because they engineer for reasonable service life with a minimum of field problems. Fulfillment of these parallel aims requires that tests be made on both raw material and finished product to ensure that a suitable level of stability is present in each. Inasmuch as the raw materials involved are normally purchased against a control specification, the material supplier also has an interest in testing his wares against the stated requirements. Testing takes time and time equates to money, so the raw material supplier, cable manufacturer and ultimate purchaser all have a common commitment to the establishment of rapid, precise methods for assessing stability.

The materials to be discussed in this presentation are the polyolefins: low- and high-density polyethylene, and polypropylene. The test is an isothermal differential thermal analysis (DTA) procedure designed specifically for rapid quality control testing on a routine basis. It makes use of semi-automatic apparatus capable of measuring the failure times of six individual specimens independently and simultaneously. A prototype of the instrument was briefly previewed in an earlier paper.[1]

Description of the Apparatus

The present model embodies a number of mechanical and electronic refinements, providing improved control and greater sensitivity as a result of superior noise immunity. It consists of two units, a control console and a furnace module (Figure 1). The furnace itself, except for its isolation from the electronic components, is the same as the one designed by R. F. Westover for the prototype apparatus.[2] The core of the furnace is a circular platform about 42 mm in diameter, fitted with seven platinum resistance thermometers, the six serving as specimen sensors arranged in a regular hexagonal pattern around the reference sensor at the center (Figure 2). This platform rides in a chrome-plated brass cylinder equipped with a band heater and a control sensor. A solid-state proportioning controller maintains the pre-selected temperature to ±0.12°C or better.

A stream of pure oxygen, regulated by a pressure-reducing valve and a flowmeter on the front of the module to a rate of 200 ml/minute, is preheated by passage through a length of copper tubing wrapped around the outside of the heater band, and then passes up a helical groove cut into the shaft carrying the platform with its sensors. This flow of gas serves two purposes: the preheated stream provides the oxidizing atmosphere of the test chamber, and, under control of a small lever-valve on the front of the module, an unheated portion is diverted to lift the platform the 25 mm to the top of the heated cylinder for specimen loading. This loading is accomplished with the aid of a small hand-held device which positions all six specimen dishes on their respective sensors simultaneously, after which the same valve lever returns the platform to operating position and automatically starts a set of timers in the control console, an individual timer for each specimen. The removal of the dishes from the previous run and their replacement by a fresh set requires only a few seconds, so that the temperature of the furnace chamber normally drops only about 1°C during the operation and regains its preset level in under two minutes. A small Teflon cover put into place manually after the furnace has

been closed helps to minimize heat loss from the top of the specimen chamber.

The control console houses the electronics, including the temperature controller for the furnace and a digital potentiometer control for setting said temperature at the desired level. On the lower front panel are the aforementioned timers (digital units reading to 0.1 minute) and six warning lights which indicate when a given timer has been stopped by termination of the induction period for the associated specimen. There are also individual controls for setting the base line and trigger voltages for each of the six channels, and provision for plugging in a sensitive millivoltmeter or recorder to monitor these. The upper panel carries a digital thermometer reading to 0.02°C, which continuously displays the temperature of the furnace as indicated by the output of the reference sensor circuit.

Modes of Operation

This apparatus was designed specifically for rapid quality control testing on a go-no-go basis against a stated minimum failure time at a specified temperature. When the induction period of a given specimen terminates and the exotherm accompanying the oxidation reaction produces a voltage differential between the sensors for that specimen and the reference larger than a preset minimum, a relay is triggered and the timer for that particular specimen is stopped. If this event occurs before the specified minimum time has elapsed, the specimen constitutes a failure. If, on the other hand, none of the six specimens has failed when the specified time is reached, the group is recorded as passing, the instrument reset and the specimens replaced with a fresh set of six. Closing the oven automatically restarts the timers. There is thus almost no lost time between runs, and the number of determinations per shift depends primarily on the duration of the minimum failure time specified. If, as an example, this is 25 minutes, over 100 specimens can be tested in an 8-hour shift by a single operator using only one instrument. By suitably staggering the starting times, an operator can handle two, or even three instruments, so that the potential economies in testing time are substantial compared with conventional DTA procedures.

Obviously, the apparatus can also be used to determine the actual failure times of large numbers of specimens in a relatively short time simply by allowing each set to run until all six have failed. This approach can provide insight into the extent of variability within a given sample, since a statistically satisfactory number of determinations can be completed with relative ease.

It should be noted that the failure time established by the automated procedure will not normally be identical with the induction time for the same sample determined from a recorder chart in the usual manner by extrapolation of the rising exotherm back to the base line. This is a consequence of the type of automation employed, which depends for its end point on the development of a small but finite preselected level of exotherm by the specimen. It is exactly analogous to the "t_x" of oxygen absorption, the time required for the specimen to consume "x" milliliters of oxygen per gram, which also differs from the induction time (t_i) determined by corresponding backward extrapolation of the rising curve of oxygen consumption as the oxidation reaction proceeds. In each case, the two types of end point are more nearly equal for samples whose oxidation curves ascend steeply from the base line (curves "A" of Figures 3 and 4), and most different when the rise is very gradual (curves "B" of the same figures). Thus "induction time" is not strictly an accurate designation for the readout provided by the automatic timers, whence our choice of "failure time" (t_f).

The automated apparatus can also be used to determine the more familiar extrapolated induction time when this is desirable, as for calibration, because it is equipped with output jacks through which the amplified voltage differential between the specimen and reference sensors can be switched to a suitable recorder and a conventional DTA plot obtained for the necessary extrapolation. The new instrument thus has the potential for two additional modes of operation over and above the routine control function for which it is primarily intended. In each of the three, its isothermal operation and multiple specimen capacity offer attractive potential savings of testing time, plus greater freedom from certain cross-contamination hazards than is possible when a multiplicity of specimens are tested in a single dish, a practice which has been suggested as a time-saving device.[3]

Repeatability of Results

The first criterion of acceptability for a proposed control test is good precision, or repeatability of results. When the material being tested is a polyolefin, sample inhomogeneities can present a major problem in proving in the new test. The scatter of results for which compositional variations are responsible is, unfortunately, only too often attributed to the test procedure instead of being recognized as a characteristic of the sample. Troublesome inconsistencies have been shown to arise, particularly in low-density polyethylene, from a number of sources, among them poor

solubility and migration of the stabilizers.[4] Most antioxidants and metal deactivators, while soluble in or at least miscible with the polyethylene melt during mixing, tend to separate out in the solid state where they are virtually insoluble and exist as discreet and often surprisingly mobile phases.[5,6] In order to minimize obfuscation from this source, the specimens employed in establishing the precision of the new six-place apparatus were punched from freshly prepared films of low-density polyethylene 0.25 mm thick, stabilized with 0.05% by weight each of tetrakis [methylene 3-(3',5'-ditert.butyl-4'-hydroxyphenyl) propionate] methane and N,N'-dibenzal-(oxalyl dihydrazide). This composition is designated "Sample A". The specimens, which weighed approximately 4 mg, were tested in oxygen at 200°C on preoxidized copper inserts in aluminum dishes, with the criterion of failure the development of 0.05°C differential between the specimen and reference sensors.

For a universe of 132 determinations, the variation between successive specimens in any one of the six positions was found to be essentially the same as that between positions in any one run (cf. Table I). The overall average failure time was 25.29 ± 1.29 minutes. Being based on the largest number of determinations among all the data available, this level of reproducibility is taken as most truly representative of the inherent capability of the instrument. It compares uncannily closely with the standard deviation of ± 1.30 minutes found earlier for similar specimens in a commercial single-specimen apparatus.[7]

Having established the basic precision of the instrument with an ultra-uniform sample of one of the three materials with which it is most likely to be used, the next task was to determine its performance with the others. For a typical high-density polyethylene (Sample B), stabilized with 0.10% each of the same ingredients and tested under the same conditions, an average failure time of 52.14 ± 1.69 minutes was found (Table IIA). Similarly, for a polypropylene (Sample C) stabilized with 0.50% of bis-[ethylene 3-(3',5'-ditert.butyl-4'-hydroxyphenyl)propionate]sulfide and 0.10% N,N'-dibenzal-(oxalyl dihydrazide), the mean failure time was 50.22 ± 2.25 minutes, again under the same test conditions. In each of the latter series of tests, only 42 determinations were involved. This may be a factor in the larger standard deviations found but there are doubtless others as well. One possibility is discussed below.

Absence of Stabilizer Transfer

The second criterion to be met by candidate apparatus for control testing of several specimens at one time is the ability to identify the occasional nonconforming specimen in a group, the others of which meet the stated requirement. The need for caution in this regard in DTA testing was demonstrated by Marshall et al,[3] who reported that when an inadequately stabilized specimen was included in the same dish with several satisfactory ones, stabilizer from the latter migrated into and measurably improved the performance of the former. Roe and his associates have confirmed that this migration can be extremely rapid at even moderately elevated temperatures.[6]

In the six-place apparatus, reliance is placed on a stream of oxygen moving rapidly from the periphery of the chamber, across the specimens and out the top center to minimize cross-contamination. To determine whether transfer of stabilizer is in fact circumvented by this gas flow under normal operating conditions, combinations were tested of poorly stabilized specimens of each of the three polyolefins intermixed with others of the corresponding well-stabilized sample for which results have been given above and in Table IIA.

For the low failure-time materials, Sample D consisted of the same low-density polyethylene as Sample A, but stabilized only with 0.10% of 4,4'-thiobis(3-methyl-6-tert.butyl phenol) but no metal deactivator; Sample E was the same as sample B but with one-third of the total stabilizer package; while sample F was a commercial polypropylene containing a proprietary stabilizer system. The results of the tests involving appropriate combinations of these specimens are given in Table IIB.

In brief, no evidence whatsoever was seen of stabilizer migration from better- to less well-protected specimens. In no case did any of the poorer materials show an increase in failure time when tested in the presence of well-stabilized specimens. In this sense, the kinetic atmosphere of the test chamber proves to be effective and the automated apparatus performs its intended functions in a highly satisfactory manner.

Catalytically Induced Premature Decomposition

To carry our examination of the new instrument well beyond the limits of what might normally be anticipated in routine control testing, extreme combinations of specimens were assembled to study the effects of poorly stabilized or totally unstabilized material on normal or "good" specimens of the same, or even of different polymers, since mixtures of one polymer type with another might sometimes be tested in actual practice. The results of these experiments are shown in Table IIC. Here a totally unanticipated phenomenon is evident in the

data. In each case where specimens with substantially different failure times were tested together, the better-stabilized material failed more quickly than when tested alone. It thus appears that gas-borne fragments from an earlier oxidative decomposition are capable of catalyzing premature failure in otherwise sound specimens.

In tests where only a single polymer type was involved, the magnitude of this catalytic acceleration was found to be moderate (about 5-7 minutes) for the polyethylenes, but in polypropylene it was observed to be as large as nearly 20 minutes, or about 40% of the original oxidative time. The relative effects are totally consistent with the native susceptibilities of these polymers to oxidation. It was also noted that unstabilized material produces an apparently larger, but perhaps merely a more rapid effect on well-stabilized specimens than does corresponding semi-stabilized material. This was found to be true for all three polymers. Oddly, the "incubation time" for the induced catalytic degeneration appears, on the basis of limited experimentation, to be shortest for low-density polyethylene where the net effect is least. This may be only a reflection of the relative concentration of stabilizer in the disordered phase of the low-density polymer, which is the more susceptible portion of the material, compared with that in the corresponding areas of the more crystalline high-density polyethylene where the same weight percent of additive results in a proportionately higher actual concentration in the residual noncrystalline regions. In the case of polypropylene, an extended "incubation time" can be rationalized in light of the much higher overall level of stabilization present.

Limited testing in which polymer types as well as stabilization levels were deliberatedly intermixed indicates that even more serious catalytic effects can result than for homogeneous groups of specimens. The most pronounced degenerative activity was observed when specimens of unstabilized polypropylene were alternated, three and three, with those of HDPE Sample B. In this combination, the failure time for the latter showed a decrease of 57% from its value when tested alone. In general, the same overall relative activities appear to obtain as found previously, with polypropylene producing by far the largest and high-density polyethylene the smallest catalytic action, while that of low-density polyethylene is slightly, but significantly, greater than for its high-density homolog. Again, the relative activities are consistent with the known oxidative susceptibilities of the three polymers.

Significance of the Findings

Insofar as the original objective of this study is concerned, the newly recognized phenomenon has only minor impact. It suggests that redesign of the top of the furnace chamber to preclude intermingling of the atmospheres flowing over the several specimens would undoubtedly be worthwhile, and indeed a simple modification intended to achieve this is being undertaken. This redesign may serendipitously result also in a simplified, one-handed specimen loading device. The new information in no way vitiates the usefulness of the six-place instrument for routine testing purposes. In its present form, this apparatus remains fully capable of meeting the original design intent of rapid, precise quality control testing on a routine basis against a predetermined minimum failure time requirement. It is necessary only that a simple set of operating rules be observed. Obviously, there is no problem when all six specimens in any group exceed the required minimum time. Nor is there if only one of the six fails to pass. If, however, two or more specimens fail to meet the required minimum, all except the first failure must be regarded as potentially questionable and the samples they represent must be retested. With this simple procedure, the advantages of rapid, automated routine testing are available for all three polymers discussed.

In using the six-place apparatus on a nonroutine basis to determine the actual failure times of the individual specimens, some additional restrictions should be observed since it appears unwise to test together specimens of widely differing failure times. This imposes no particular hardship since testing of this type normally involves several replicates for reasons of statistical assurance, and with the new apparatus, six can be tested in less than the time normally required to test one.

The real significance of the phenomenon revealed in these experiments extends well beyond the original limited objective of the study. The data reported suggest that when active oxidation begins in a polyolefin, the ensuing decomposition literally floods the adjacent atmosphere with reactive fragments capable of "seeding" premature oxidation in any other polyolefin in the vicinity, whether in the close confines of thermoanalytical apparatus, in the perhaps less congested interior of an air oven, or under other circumstances. A rapidly moving stream of gas is quite evidently inadequate for preventing the innoculation of other polyolefins nearby. On the basis of present knowledge, it appears that oxidative decomposition of intensity

sufficient to induce premature failure of the kind found in these experiments occurs only under extremely vigorous conditions, as at quite elevated temperatures, and the phenomenon is probably inoperative under normal use conditions for these materials. Possible bearing on the behavior of polyolefins in processing equipment, particularly in the presence of catalyst residues or copper, may be worth considering, however.

Since the design of the new instrument is well-adapted to the insertion of a mass spectrographic probe, study of the decomposition fragments might contribute usefully to the analysis of oxidation mechanics.

Summary

A six-specimen isothermal DTA apparatus designed specifically for rapid quality control testing of polyolefins is described and typical failure times reported for low- and high-density polyethylenes as well as for polypropylene. The new instrument is demonstrated to be equal in precision to good commercial DTA apparatus designed for single-specimen use.

It is pointed out that the type of automation employed for determining the end of the induction period on a routine basis with the new apparatus is exactly analogous to one of the common ways of reporting oxygen uptake data, the time (t_x) required for the specimen to consume "x" milliliters of oxygen per gram. Just as this differs slightly in numerical value from the induction time (t_i) determined by the oxygen uptake apparatus, so does the failure time (t_f) established by the new instrument in its semi-automatic operating mode differ slightly from the induction time as normally determined by either the new instrument or by conventional DTA or DSC apparatus through back-extrapolation of the exotherm on graph paper.

No evidence is found of stabilizer migration between specimens in the new instrument as has been reported for other multi-specimen DTA techniques.

The test data reveal instead a startling new phenomenon operating in the reverse direction: the catalysis of premature oxidative failure by reactive fragments charged into the atmosphere during early decomposition of one of the specimens. This catalysis seems to require a moderate "incubation time", so that it does not interfere excessively with the use of the new six-place instrument for its intended purpose of routine control testing. It does, however, warn of a possible new kind of interaction between specimens in any grossly accelerated oxidative testing of the polyolefins, including oven tests. Perhaps more importantly, it may have bearing on the behavior of these materials in processing equipment under certain conditions of operation, particularly in the presence of potential activators such as copper, certain pigments, or adventitious catalyst residues.

Acknowledgments

The authors wish to thank D. R. Falcone, W. I. Vroom and R. F. Westover for assistance in the design and assembly of the apparatus, Prof. D. J. Shombert for improvement of the noise immunity of some of the circuitry, and Dr. W. L. Hawkins for helpful comments and suggestions.

References

1. J. B. Howard, Polymer Eng. Sci. 13, 429 (1973).
2. Technical details of the construction and circuitry will be given in a forthcoming paper by R. F. Westover and his associates.
3. D. I. Marshall, E. J. George, and J. M. Turnipseed, Polymer Eng. Sci. 13, 415 (1973).
4. J. B. Howard, Proc. 21st Int. Wire and Cable Symp., pp. 329 ff. (December 1972).
5. H. E. Bair, Polymer Eng. and Sci. 13, 435 (1973).
6. R. J. Roe, H. E. Bair and C. Gieniewski, J. Appl. Polymer Sci. 18, 843 (1974).
7. H. L. Gaupp, unpublished information (BTL).

John B. Howard received a B.S. from the Sheffield Scientific School of Yale University in 1963 and immediately joined the Technical Staff of Bell Laboratories. He was involved in many phases of research and development on thermoplastics for wire and cable applications. Mr. Howard was active in standards work for the plastics industry for many years. At the time of his death in September 1974 he was Supervisor of the Plastics Wire and Cable Coating Group of Bell Laboratories at Murray Hill, New Jersey.

Harold M. Gilroy received a B.S. in Chemical Engineering from Newark College of Engineering in 1975. He is a Member of the Technical Staff of Bell Laboratories, having joined Bell in 1960. Prior to that time he was employed by Atomics International, responsible for coolant support systems for organic reactors. At present he is engaged in the development and application of polyolefins for wire and cable.

TABLE I

REPRODUCIBILITY OF FAILURE TIMES FOR SAMPLE A*

Failure Time (t_f) - Minutes at 200°C on Copper

Position 1	Position 2	Position 3	Position 4	Position 5	Position 6
29.2	23.6	29.3	25.5	27.7	27.5
26.0	25.6	29.1	25.7	26.1	26.1
26.6	25.7	26.3	25.4	27.1	26.5
27.8	27.3	26.6	25.4	26.7	26.7
27.5	26.7	26.8	26.2	25.0	25.8
25.6	24.8	26.4	26.2	27.5	26.0
25.7	27.3	23.1	25.8	26.6	25.7
27.8	24.7	26.0	24.6	26.4	28.7
24.8	24.8	23.3	25.2	26.6	24.2
23.1	25.7	24.4	23.8	24.2	24.2
22.8	23.4	24.1	23.6	25.7	26.0
23.3	25.1	25.5	23.0	25.4	25.1
23.5	25.3	25.4	23.4	24.8	27.6
23.7	25.9	23.5	24.4	25.9	23.3
23.1	26.0	23.6	22.9	24.8	24.8
24.0	24.1	23.7	23.2	24.7	25.4
23.6	24.1	25.0	24.4	24.7	24.5
22.6	24.3	27.5	26.8	24.6	25.2
24.3	25.4	26.4	24.9	25.4	25.2
25.5	24.7	26.0	24.0	24.7	24.7
24.9	25.4	24.7	25.7	25.9	24.8
22.9	25.8	25.1	25.0	25.7	25.8
Average 24.73	25.30	25.54	24.81	25.74	25.60
Stand.Dev. 1.82	0.98	1.73	1.09	1.01	1.10

Grand Average: 25.29

Standard Deviation: 1.29

*For composition, cf. text

Elena Kokta is a member of the Plastics Chemistry, Research and Development Department, Bell Laboratories, Murray Hill, New Jersey. She received a B.A. degree in chemistry from Fairleigh Dickinson University in 1973 and joined Bell Laboratories immediately thereafter. At the present time, she is engaged in studies of polyolefins for wire and cable.

TABLE II

FAILURE TIMES OF SPECIMENS TESTED IN VARIOUS COMBINATIONS AT 200°C IN OXYGEN

SAMPLES*	No. of Replicates	Failure Time (t_f) Min.	Δt_f (Min.)
(A) SIX SPECIMENS OF SAME SAMPLE			
A (LDPE)	120	25.29 ± 1.29	
B (HDPE)	60	52.14 ± 1.69	
C (PP)	42	50.22 ± 2.25	
D (LDPE)	60	2.45 ± 0.30	
E (HDPE)	30	23.40 ± 1.08	
F (PP)	42	12.11 ± 1.27	
(B) STABILIZER MIGRATION CHECKS**			
D (Tested with A)	21	2.25 ± 0.16	0
E (Tested with B)	21	22.86 ± 2.03	0
F (Tested with C)	24	11.72 ± .10	0
(C) EVIDENCE FOR PREMATURE CATALYTIC DECOMPOSITION**			
A (Tested with D)	21	23.28 ± 0.85	-2
A (Tested with unstab. LDPE)	21	17.79 ± 1.03	-7 1/2
B (Tested with E)	21	47.03 ± 1.13	-5
B (Tested with unstab. HDPE)	24	45.27 ± 2.16	-7
C (Tested with F)	24	36.58 ± 3.01	-13 1/2
C (Tested with unstab. PP)	21	30.93 ± 3.18	-19
B (Tested with unstab. LDPE)	24	41.16 ± 3.26	-9
B (Tested with unstab. PP)	18	29.20 ± 3.76	-30
C (Tested with unstab. HDPE)	18	43.35 ± 7.50	-7

*For composition, cf. text

**Three specimens of each sample per test group.

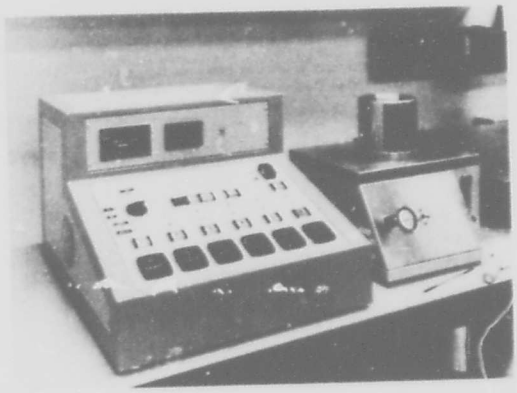

FIGURE 1

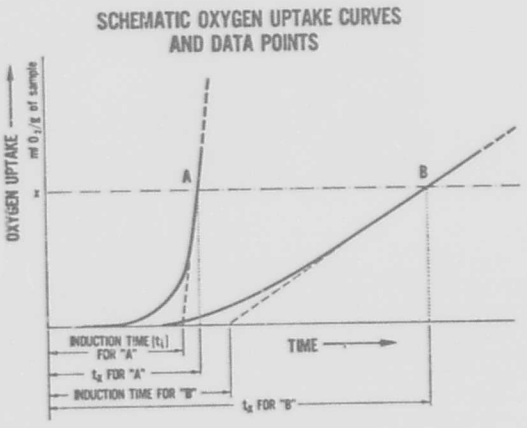

FIGURE 3

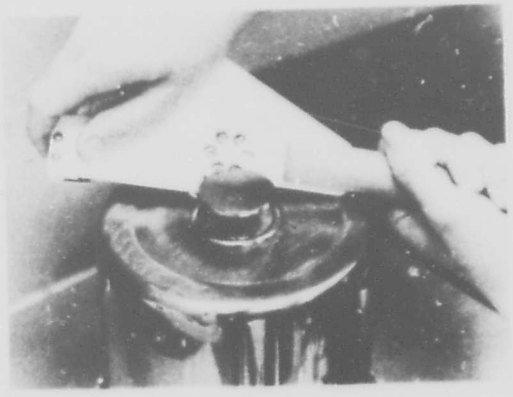

FIGURE 2

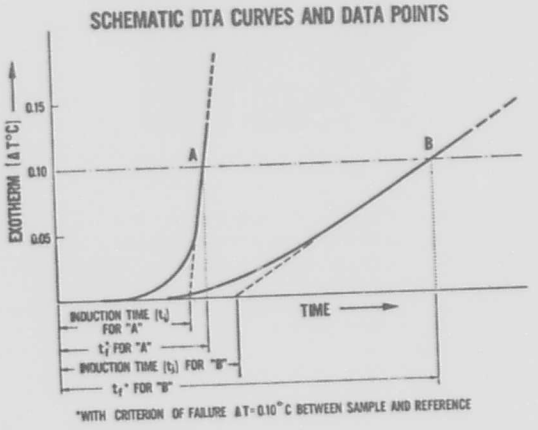

FIGURE 4

CELLULAR INSULATION AS AN ANSWER TO MATERIAL CONSERVATION

E.D. Metcalf
Telecommunications Division
Anaconda Wire and Cable Company
Sycamore, Illinois

Abstract

The polyolefin shortage in the United States has prompted serious consideration of all possible ways to save materials in cable manufacture. One approach offering considerable potential is the substitution of cellular insulation for solid insulation in filled telephone cables. While there has been some reluctance to make this change in the past, a study of the problem areas indicates that most of the concerns can be resolved and only a minimal sacrifice in overall performance would be anticipated. On this basis, the long term availability and cost of polyolefin materials will probably be the deciding factor.

Introduction

With the shortage of petroleum-base polymers in this country, both cable manufacturers and users have been faced with the problem of extending materials. In reviewing possible conservation measures, one significant material reduction becomes immediately obvious. This is the use of cellular insulation as a substitute for solid in Filled Telephone Cables.

When filled type cables were introduced in this country 5 or 6 years ago, the same electrical characteristics were required that had been provided for non-filled cables. Since the filling compound had a dielectric constant of 2.1 and was used to replace air with a dielectric constant of 1.0, it was necessary to increase the interconductor spacing to produce the same mutual capacitance. This was accomplished by going to heavier conductor insulation which increased both the size and the weight of the cable.

With this construction, however, the dimensions could be reduced by lowering the dielectric constant of either the filling compound or the insulating material. The British, who first introduced filled telephone cable, were concerned with the size problem from the start and chose to immediately adopt cellular insulation. Several other countries have also followed their lead but in the United States there has been a reluctance to make this change. This hesitancy appeared to stem from concern over both the processing and performance characteristics of cellular insulation and there was no strong impetus to push the needed engineering and development investigations.

About 12 or 15 months ago, however, the picture was changed - a new impetus was added. This impetus was the polyolefin shortage which has clouded the supply picture for the next several years. There was now a strong justification for the engineering work required and several manufacturers picked up the challenge. The use of cellular insulation for filled telephone cable in the United States now began to receive some serious attention.

Reduction in Material Usage

What are the savings in critical materials that now make cellular insulation more attractive? They not only include insulation but also filling compound and jacketing materials. And this fast growing filled construction already represents far more than half of the exchange area cable market requirements.

In looking at a typical conductor size used in this cable, the solid insulation for 22 AWG wire would be 0.053 inches overall diameter using polypropylene copolymer. Since telephone cable design is based on mutual capacitance, the dielectric constant which is 2.25, controls this diameter. The weight of insulation for one thousand feet of this conductor would be 0.67 pounds. This is based on an insulation thickness of .014 inches.

Now, looking at this same 22 AWG conductor with cellular polypropylene insulation, the mutual capacitance again is the controlling design factor which determines the insulation thickness. With cellular material, based on a typical 30% gas content, the effective dielectric constant now changes from the previous 2.25 to 1.82. This means that the insulation overall diameter can be reduced from 0.053 to 0.047 inches. Likewise, the weight of insulation is reduced from 0.670 to 0.335 pounds per thousand feet.

What the change to cellular insulation accomplishes is shown graphically in Figure 1. The insulation thickness with cellular compound has been reduced 0.003 inches or 21% on the basis of the lower dielectric constant. The volume of insulation, based on cross-sectional area, is reduced 28%. The weight of insulation in turn is affected by both the 28% reduction in volume and the 30% reduction in density. This means the weight of insulation per thousand feet of conductor can be reduced by 50% with the change to cellular material.

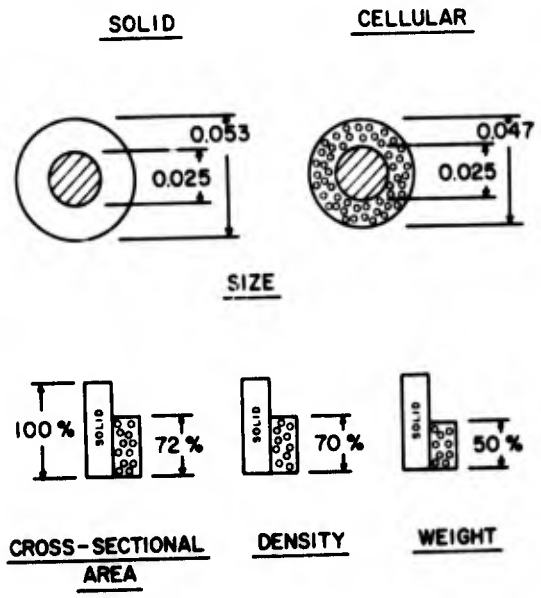

FIGURE 1. Comparison of solid versus cellular polypropylene insulation.

As stated previously, the reduction of critical materials does not stop at this point - other cable components are also involved. If the diameter of the insulated conductors are decreased, the overall diameter of the stranded pairs is likewise reduced. This means that less compound is required to fill the void areas around the conductors and over the core. Also, both the inner and outer diameters of the jacket can be reduced. Taking a representative range of cable sizes using 22 AWG conductors, Figure 2 shows the reduction of materials by percent that would be realized with the change to cellular insulated filled cables. As can be seen, the overall reduction is of a magnitude that is difficult to ignore.

COMPONENT MATERIALS	-22 AWG FILLED CABLES-			
	25 PAIR	100 PAIR	400 PAIR	900 PAIR
INSULATION	50 %	50 %	50 %	50 %
FILLING COMP.	7 %	18 %	20 %	21 %
JACKET	5 %	10 %	20 %	25 %

FIGURE 2. Reduction of petroleum-base materials used with change from solid to cellular insulation.

Carrying this further, percent reductions in petroleum-base materials have been estimated for the typical average cable size and projected to 1975 anticipated cable requirements. Figure 3 shows a rough estimate of materials savings for the entire telephone industry on this basis. As can be seen, a reduction of 50 million pounds could be made in insulating materials, alone. Besides this another 37 million pounds could be saved in filling compound and jacketing materials. This means that a total of 87 million pounds of petroleum-base materials could be conserved in 1975 if cellular insulation was adopted for filled telephone cable by all manufacturers in the United States.

COMPONENT MATERIALS	PERCENT REDUCTION	POUNDS REDUCTION
INSULATION	50 %	50,000,000
FILLING COMP.	15 %	25,000,000
JACKET	10 %	12,000,000
TOTAL	22 %	87,000,000

FIGURE 3. Estimated reduction in material usage for entire telephone cable industry with change from solid to cellular insulation for filled cable.

Product and Process Considerations

Now what are the areas of concern that caused the reluctance to change to cellular insulation. Basically, they involve manufacturing problems, electrical capabilities, long term stability and material compatibility. While cellular insulation has been used in other countries, the base materials, cable design and customer requirements in this country are all sufficiently different to warrant thorough evaluation.

In looking at the manufacturing problems, one of the areas of greatest concern has been whether a completely consistent product can be produced using cellular insulation, without excessive scrap. This question can probably best be discussed by first reviewing the process for making solid insulation.

With a typical extrusion insulating line, the bare conductor is pulled from a supply reel and through the extruder head and sizing die by a variable speed capstan. Insulating compound is fed into the extruder hopper, heated, and forced around the moving conductor at a preset rate. By varying the speed of the capstan, the overall diameter of the insulation can be controlled. The bare conductor is preheated before entering the extrusion head to provide the optimum physical properties of the insulating compound.

In telephone cable, the most important electrical characteristic is mutual capacitance which is primarily controlled by the capacitance of the insulated conductor. With solid insulation, which has a fixed dielectric constant, the capacitance is controlled by varying overall insulation diameter. This can be accomplished by measuring the diameter by hand micrometer or continual gauging head and the capstan speed regulated either by hand or servo-system to hold the required diameter.

Now with cellular insulation, the process becomes somewhat more complicated because both the diameter and the percent gas or density must be controlled to provide the required capacitance. The gas is generated by a blowing agent added to the insulating compound prior to extrusion. Whether this is done by the compound supplier or the cable manufacturer, a very precise control of quantity and dispersion of blowing agent is especially critical for consistent density.

As with solid insulation, the overall diameter can be measured by hand or gauging head and controlled by speed regulation. However, the percent gas or

density will vary with any change in process temperature or pressure as well as with line speed and insulation cooling quench point. For this reason, capacitance control with cellular insulation is not the simple operation it is with solid material. Because stable heat conditions are reached slowly in an extruder, because compounds vary from batch to batch, because different colors influence density and for many other reasons, it is impossible to simply set conditions and expect the line to produce a consistent product. In reality, a continuous check of both density and diameter must be made to provide the close control of mutual capacitance and capacitance unbalances required by the telephone industry.

This is one area that has greatly concerned cable manufacturers since the electrical requirements in this country are generally more severe, and present insulating facilities in most cases are not equipped to provide the control needed. The answer to the problem, obviously, is to install completely automatic control systems for the insulating lines and this means a very extensive investment on the part of the manufacturer. This consideration, of course, would be weighed heavily by the manufacturer in making the decision to change to cellular insulation.

The automatic facilities required must first include an in-line diameter gauge with a feed-back circuit which will control the line speed and thus hold the diameter to a close tolerance. Second, the conductor pre-heater must automatically vary the amount of heat to match any line speed change. Third, all extruder heater controllers must be of the proportioning type to eliminate any abrupt temperature changes.

Along with this equipment, an in-line capacitance monitor must be added which is the only way the density or percent gas can be continually checked. With this monitor, automatic controls must be provided for compound melt temperature regulation and/or quench water entrance position to make corrections in density as required. Finally, some form of interlink between the automatic diameter control and capacitance control must be provided so that neither will overreact relative to the other.

The equipment described above is all currently available and it will provide completely automatic control. Using this equipment, it has been proven that the electrical consistency required for cellular insulated telephone cables in this country can be provided. Along with this conclusion, however, the substantial cost of control equipment and added scrap must be factored into the picture.

On the basis that product uniformity is feasible, the next consideration is physical characteristics of cellular insulation. The basic questions are how its performance compares with current requirements and whether it can withstand the rigors of high speed processing techniques. Since polypropylene has been our standard material for solid insulation, the investigation was based on this material.

The first step taken was to check the physical characteristics of cellular insulation to current industry standards. Figure 4 shows a comparison of 22 AWG cellular insulation with 0.011 inch wall thickness and 30% gas to REA requirements for solid polypropylene insulation. As can be seen from the table, the cellular insulation meets all the requirements currently specified for solid polypropylene.

TEST	REA REQUIREMENT	CELLULAR INSULATION
TENSILE	3000 PSI – MIN	3300-PSI
ELONGATION	300 %-MIN	570 %
COLD BEND	0 FAILURES AT -40° C	0 FAILURES
SHRINKBACK	1/8" MAX	< 1/8"

FIGURE 4. Comparison of cellular insulation physical characteristics to current REA requirements.

A further comparison of the general physical characteristics of cellular polypropylene was made with solid low density polyethylene, solid high density polyethylene and solid polypropylene. Again, 22 AWG insulation was used for this study. Test results for the comparison are shown in Figure 5. From the table, it can be seen that cellular polypropylene insulation, in almost every test, is physically superior to solid low density polyethylene insulation which was the industry standard for many years. It also exceeds solid high density polyethylene in tensile, abrasion and some types of compression resistance. Solid polypropylene as would be expected, is superior to cellular in all these areas.

TEST	CELLULAR	LDPE	HDPE	PPE
TENSILE – PSI	3300	2400	3200	3800
ELONGATION – %	570	650	590	600
COMPRESSION RESIST. – LBS 2" MANDREL	165	155	145	185
COMPRESSION RESIST. – LBS 1/8" DIA MANDREL	35	40	55	55
ABRASION RESISTANCE CYL REV X 1000	200	150	60	410

FIGURE 5. Comparison of physical characteristics of cellular polypropylene with solid low density polyethylene, high density polyethylene and polypropylene.

The abrasion and compression resistance tests were added in this series as a key to the ability of cellular insulation to stand up under the abuse of high speed processing techniques. The areas of concern are passage through guide eyelets and around sheaves or any points of compression or impact. From the test results, it is obvious that cellular insulation must be treated more carefully than solid polypropylene in processing. Because of this, it may be prudent to exclude 26 AWG from the cellular construction for at least the initial start.

Besides these manufacturing considerations, there is also the question as to whether overall plant output will be reduced with cellular insulation. Here, the area of basic concern is the insulation processing rate with the major problem centering around the adequate cooling of the insulation. Because cellular material is more fragile than solid material at elevated temperatures, heat removal must be more

complete to prevent deformation in handling. It has been found that with either a more efficient cooling system or longer cooling trough, high speed extrusion of cellular insulation is possible. The investigation has generally shown that with automatic control equipment and an efficient cooling system the through-put speeds of cellular insulation can be equal to those of the equivalent solid insulation.

After having explored the manufacturing problems, the next area of concern is cable design. Primarily, the consideration is whether a cellular insulated product would be capable of meeting the electrical characteristics required for filled telephone cables. In designing and testing the product, it was found that in most cases the construction could be tailored to meet present industry standards as they exist. The characteristics that would be the same as for solid insulation filled cable are listed below:

1.) Average Mutual Capacitance

2.) RMS Deviation of Mutual Capacitance

3.) Pair-to-Pair Capacitance Unbalance

4.) Pair-to-Shield Capacitance Unbalance

5.) Crosstalk Loss

6.) Mutual Conductance

7.) Copper Resistance

8.) Resistance Unbalance

9.) Insulation Resistance

The principal area of deviation would be in the dielectric strength of the insulation. When 0.014 inches of solid insulation is replaced with 0.011 inches of cellular insulation incorporating 30% gas, it cannot be expected that the same dielectric strength will be provided. Testing of finished cables would indicate that the following dc voltages would be reasonable for conductor to conductor requirements:

19 AWG - 4,500 volts
22 AWG - 3,600 volts
24 AWG - 3,000 volts
26 AWG - 2,400 volts

Likewise, it would also be in order to reduce the conductor to shield test from 15,000 to 10,000 volts dc. This would make all voltage requirements the same as for non-filled, single jacket cables. In discussions with telephone operating personnel, it has been expressed that these requirements would be considered generally acceptable for filled type cables.

One other effect of the change to cellular insulation for filled cable would be found in attenuation at PCM carrier frequencies. As discussed earlier in this paper, when filled cable was introduced it was necessary to increase the spacing between conductors to provide the same mutual capacitance. Because of this increased spacing, the attenuation for 22 AWG filled cable was reduced approximately 17% over air core (non-filled) type at T-1 carrier frequencies of 772 kHz. Now, however, with the change to cellular insulation for filled cable, the distance between conductors can be reduced so that the reduction in attenuation over air core cables would be approximately 8% instead of 17%. Figure 6 shows the relationship of attenuation to frequency for solid and cellular insulated filled and solid air-core cables. As can be seen from the graph, the change in attenuation for either type filled insulation would be insignificant at voice frequencies.

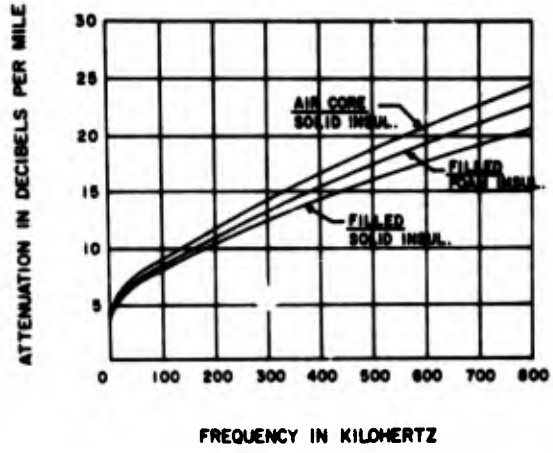

FIGURE 6. Comparison of attenuation versus frequency for 22 AWG air core and filled type cables.

Having established the electrical characteristics of the cellular insulated filled cable, the next major concern was the long term electrical stability. At higher frequency operation, the deterioration of the primary electrical parameters becomes much more critical than at voice frequency. Electrical stability must be an important consideration with more and more circuits being used for high frequency carrier equipment.

The first step in this area of investigation was to check the experience of those who have been using cellular insulation for several years. Discussions with the British Post Office indicated that they had not experienced any appreciable deterioration of the electrical characteristics since they adopted cellular insulation. Several papers have been presented on this subject at previous Wire and Cable Symposiums. Also, while Canadian experience has been limited to a shorter period, they likewise report no problems with electrical deterioration.

To further prove-out the stability of the combination of cellular insulation and filling compound used in this country, an accelerated aging test was run for one year. A 4,082 foot length of 50 pair, 22 AWG Alpeth type filled cable with cellular insulation was used for the test. This cable was held at a temperature of 168 F for five days and then returned to room temperature for two days. At the end of the two day cooling period, the electrical parameters were measured and the cable again brought to 168 F for five days. This cycle was continued for 52 weeks and the percent change in average mutual capacitance is shown in Figure 7.

As can be seen from the graph, the entire change over the year of accelerated aging was only about 3.5%. It should also be noted that the curve is leveling off at that point. Since under normal conditions a buried cable would not see service at 168 F, the logical question is how this relates to normal use. By extrapolation, based on the Arrhenius

equation, the 52 week cycle shown would be roughly equivalent to 45 years at a ground temperature of 50 F. The results of this test certainly help dispel much of the concern over long term capacitance change due to filling compound migration into the gas cells.

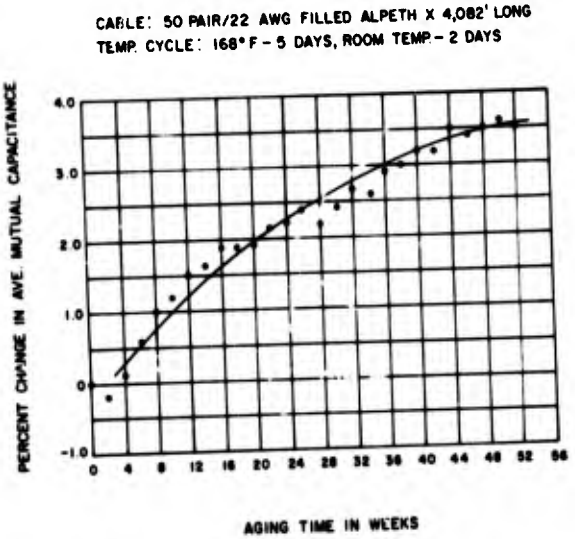

FIGURE 7. Effects of accelerated aging on mutual capacitance of cellular insulated, filled cable.

In the way of further investigation into stability, approximately 1000 feet of 25 pair, 22 AWG Alpeth type filled cable with cellular insulation was buried in the test plot at our Communication Products Engineering Center. Several other cables were also buried in the same trench and all were terminated on a distribution frame in our Pilot Plant for ease of testing. The cables were placed at a depth of 30 inches with 10 inches of soil immediately over the cables. Above the soil, 10 inches of pea gravel was provided and a one inch plastic pipe with holes spaced at one foot intervals was placed in the center of the gravel area. The remainder of the trench was filled with soil.

The plastic pipe was provided to insure that the cables were subjected to wet conditions. A predetermined amount of water was metered through the pipe on a bi-weekly basis. For the first 64 weeks, the electrical characteristics were checked every four weeks. Because characteristics remained stable, the test schedule was changed to a quarterly basis at that time.

Figure 8 shows both average mutual capacitance and average mutual conductance for the cable over the past 2 year period. As can be seen, these characteristics have remained remarkably stable with only small cyclic changes in mutual capacitance which were due to winter and summer ground temperature variations. For all practical purposes, the cable has remained completely stable and this performance again helps to dispel concern over electrical stability of cellular insulation in filled cable constructions.

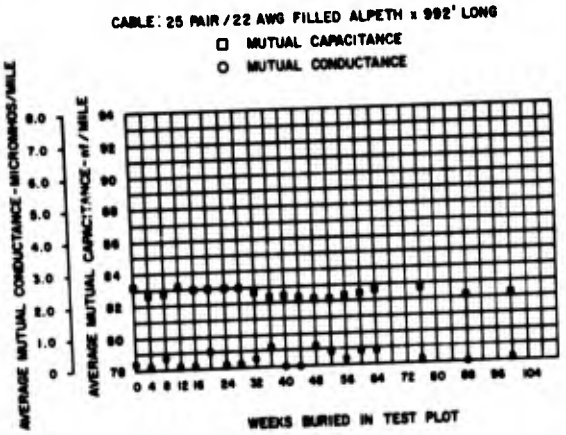

FIGURE 8. Electrical characteristics of cellular insulated, filled cable buried in test plot.

In this investigation, the same polypropylene and filling compounds have been used for the cellular construction that are currently used with solid insulation. Checks for compatibility with the cellular material have been made using oxygen uptake, DTA and oven aging procedures. Because these accelerated tests are run at high temperatures, filling compound present will migrate into the gas cells. Since the same migration would not be the case at normal installed temperatures, the validity of such testing for predicting the life of the insulation has to be questioned. Based on oven testing at reduced accelerated temperatures, there would appear to be about a 3 to 5 degree C reduction in aged performance rating for cellular versus solid insulation. This would tend to corroborate data reported in previous papers and will be confirmed as long term testing progresses.

To augment this overall investigation, several field installations have been made with cellular insulated filled cables. These cables will be monitored on a programmed basis to substantiate laboratory test results reported in this paper.

Conclusion

In summary of this investigation, the telephone cable industry could save approximately 1 billion pounds of petroleum-base materials in the next ten years if they were to change to cellular insulation for filled cable. With regard to concerns over manufacturing, the study would indicate that these problems could be resolved but special handling and control equipment amounting to more than 5 million dollars for the industry would be essential and scrap rate would probably increase 2 or 3 percent. Most standard requirements of the product could be met except for some sacrifice in voltage breakdown strength and possibly a slight reduction of safety factor in long term stability. In general, the change would provide a reduction in material costs but much of these savings would have to go into increased production costs.

On the basis of this analysis, it would appear that the concerns over the use of cellular insulation for filled telephone cable in this country can be resolved and the change will be dictated largely by availability and cost of petroleum-base materials. At the time of publication, the critical polyolefin shortage has been eased somewhat but the need for long term conservation will continue to grow. This temporary relief is a welcome windfall to the industry since it allows time for the further testing needed to more completely establish the overall performance characteristics of the product.

References

1. J.P. McCann, R. Sabia and B. Wargotz
   Characterization of Filler and Insulation in Waterproof Cable.
   18th IWCS, December 1969

2. G.A. Schmidt
   Methods for Life Prediction of Air Core Cables and Filled Cables.
   22nd IWCS, December 1973

3. C.J. Aloisio and E.D. Nelson
   Effect of Water and Petroleum Jelly Migration on Capacitance of Plastic Insulated Cables.
   22nd IWCS, December 1973

4. S. Verne, A.A. Pinching and J.M.R. Hagger
   Long-term Stability of Fully Filled Cables.
   22nd IWCS, December 1973

Emerson D. Metcalf is Manager of Product Development for the Telecommunications Cable Division of Anaconda Wire and Cable Company and is located at their Engineering Center in Sycamore, Illinois. He has been associated with Anaconda for the past 15 years in various engineering positions.

Mr. Metcalf holds a B.S. degree in Mechanical Engineering from Georgia Tech. His background includes 8 years with Western Electric Company, Inc., in communication cable engineering and 4 years with Borden Chemical Company Subsidiaries in plastic processing. He has also served two years with the U.S. Navy as an Engineering Officer.

PROPERTIES OF A CELLULAR COMMUNICATIONS CABLE JACKET*

by
Lester Bragg and Irving Galperin
Continental Copper and Steel Industries, Inc.
Hatfield Communications Products Division

SUMMARY

A foamed ethylene copolymer jacket has been developed at a range of densities from 0.63 to 0.87 gm/cm^3. These foamed jackets have been found to be functional and pass industry standards.

Use of the foamed jacket is projected to provide a materials savings of 10 to 30%.

INTRODUCTION

The use of foamed dielectrics has been accomplished by several investigators. [1-3] Reasons for using these dielectrics range from reduction of overall cable size to consumption of less compound. However, the use of foamed cable jackets has not been discussed.

The major reason for the development of a foamed jacket is the savings effected through the reduction in compound consumption i.e. greater yield from every pound of compound. In an era of short polyolefin supply this consideration can be a critical factor in maintaining continuous production. In spite of this advantage a foamed jacket must, nevertheless, provide adequate protection for the cable plus, exhibit all the functional properties of a conventional jacket.

Experimental

Communication cables with foamed jackets have been made in pair count sizes from 6 pair through 25 pair for direct burial, at densities ranging from 0.63 gm/cm^3 to 0.87 gm/cm^3. The base resin used was a standard communications jacket compound, of density 0.93 gm/cm^3 containing a low density polyethylene copolymer with 2.6% weatherable carbon black.

Foamed Cable Jacket Properties

Typical jacket properties are shown in Table 1. The foamed jacket has passed REA PE-39 test requirements.

Tensile properties as well as failure mode behavior was found to be satisfactory and comparable to conventional jacket.

Impact resistance at room temperature and low temperature were comparable to standard jacketing.

Oven heat aging and oxidative stability as measured by Differential Thermal Analysis were found to be equal to standard jackets.

Mechanical Property Assessment

The main concern with regard to the acceptability of a new jacket for burial applications is that the jacket must survive the ground installation procedures without damage to the jacket. In order to do this, the new jacket must be at least as tough as a conventional jacket and have sufficient flexibility so that underground installation can be accomplished without undue tension. To better understand the foamed jacket performance in comparison to the standard jacket and to enable us to predict its performance in the field, a detailed mechanical property evaluation was undertaken.

Tensile strength, elongation, initial modulus, yield strength, stress-strain curve area and stress-relaxation values were determined, analyzed, compared with the standard jacket and related to projected field performance.

Tensile strength and elongation remained high at densities from 0.75 to 0.87. The 0.63 density foam was lower in these properties. (Fig 1&2). Initial modulus (Fig. 3) was lower as the density was reduced. The air resulted in a less stiff structure. A less stiff structure would result in greater ease of handling and could be a real advantage since installation into a ground trench is much easier when a cable coming off a reel unreels without any undue resistance as a result of excessive stiffness.

Yield strength is a parameter which is very important in any deformation behavior because a material will behave elastically up to its yield value and then start to deform. The jackets at densities of 0.75, 0.83 and 0.87 had higher yield strength values than those of the standard jackets (Fig. 4).

Stress-strain curve area is a measure of jacket toughness. Again compounds at densities of 0.75, 0.83, and 0.87 were good; demonstrating values which were either equal to or higher than those obtained for the standard jacket. A material with a greater stress-strain curve area can withstand impact and deformation more readily, without jacket rupture. (Fig. 5)

Stress-Relaxation rate is a measure of creep and relief of strain under stress. As the density decreased, the stress-relaxation rate increased. (Fig. 6). This is the result of the presence of air. The air in

*Patent Pending

effect acts as a plasticizing agent. The foamed jacket when compared to the standard jacket manifests more rubberlike characteristics.

Field Trials

Extended field trials are underway with direct burial cable. So far, these tests show an advantage for foam jacket in greater flexibility. Toughness compared to standard jacket, appears to be satisfactory. The abrasion resistance has been found to be adequate in direct plowing. The crush resistance indicates an improvement over the standard jacket in that the foamed jacket provides a cushioning effect to the cable core absorbing some of the impact. Tests are being made, both in the laboratory and in the field, to determine the moisture penetration characteristics.

Material Savings

The real plus for use of cellular jacket is the savings in jacket compound. The savings in compound amounts to a minimum of 10% at higher densities and a saving of up to 30% at lower densities.

CONCLUSION

1. Communications cable of pair count sizes 6 through 25 have been made with jacket densities from 0.63 to 0.87.

2. Jacket densities of 0.75, 0.83 and 0.87 had adequate mechanical properties and were superior to the standard jacket in toughness, flexibility, and manifested a more rubberlike character.

3. The foam jacket has passed REA PE-39 tests.

4. Field trials are currently in progress that show promise of a new jacket with improved toughness and greater flexibility.

5. The use of cellular jacket is projected to result in a compound savings of 10 to 30%.

Future of Foamed Communications Jacket

The future of cellular jacket for communications usage is dependent on customer acceptance. At this writing, the field testing is being done in burial applications.

We intend to broaden our investigation by field testing larger cables. So far, our considerations have been towards REA applications with buried cable usage. However, other possibilities include aerial and CATV cables and these areas should be examined as well. The attractive savings in compound usage should be a significant incentive for increasing interest in cellular jackets for communications applications.

ACKNOWLEDGEMENTS

The authors wish to express their thanks to Continental Copper and Steel Industries, Inc., Hatfield Communications Products Division for permission to publish this paper and to our associates who helped in the development of this product.

Appreciation is given to REA for encouragement in finding ways of conserving compound.

REFERENCES

1. "Foam-Skin, a Composite Expanded Insulation for Use in Telephone Cables." E. J. Gouldson, Mrs. M. Farago and G. D. Baxten. Proceedings of 21'st International Wire and Cable Symposium, December, 1972.

2. "Extrusion of Telephone Cable Insulation Using Expandable Medium Density Polyethylene Compounds." J. K. Normanton, Proceedings of 21'st Wire and Cable Symposium, December, 1972.

3. "Cellular Polyethylene Insulated Fully Filled Cable with High Dielectric Strength." S. M. Beach, D. F. Cretney and J. Rushin, Proceedings of 22'nd Wire and Cable Symposium, December, 1973.

Lester Bragg is Chief Process Engineer for Continental Copper and Steel Industries, Inc., Hatfield Communications Products Division, Hillside, New Jersey. Joining CCS in 1960 he has been involved in Building and Communications Products. Mr. Bragg attended Howard University and is a member and past officer of the Society of Plastics Engineers.

Dr. Irving Galperin is Materials Specialist for Continental Copper and Steel Industries, Inc., Hatfield Communications Products Division, Hillside, New Jersey, and is involved in the development of new products. He received his doctorate in Physical Chemistry in 1957 from Case-Western Reserve University. Dr. Galperin is a member of the Society of Plastics Engineers.

Table I

TYPICAL CABLE JACKET PROPERTIES

PROPERTY	A.S.T.M. METHOD	REA-PE-39 SPECIFICATION REQUIREMENTS	LOW DENSITY POLYETHYLENE COPOLYMER JACKET	CELLULAR POLYETHYLENE COPOLYMER JACKET
Melt Flow Rate (% increase from new material)	D-1238-65-T	Less than 50	14	7
Tensile Strength (P.S.I)	D-470-67T	1700 Minimum	2200	2300
% Ult. Elongation	D-470-67T	400 Minimum	550	600
Environmental Stress Cracking	D-1693-66	0/10 Failures Maximum 96 hours	0/10 Failures 100 hours	0/10 Failures 100 hours
Shrinkback (%) 100°C		5% Maximum	2.3	1.8%
Impact -30°C		2/10 Failures Maximum	No Failures	No Failures
Differential (1) Thermal Analysis Induction Time (Min.)			>30	>30
Oven Heat Aging (100°C) for 168 hours				
% Retention of Tensile Strength			90%	95%
% Retention of Elongation			100%	100%

(1) = 200°C, Oxygen

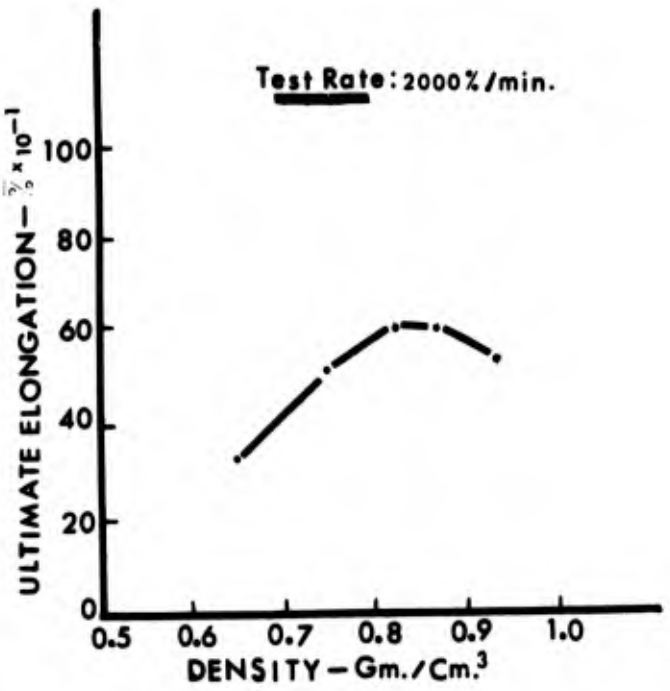

Fig. 2 Change in ELongation with Density

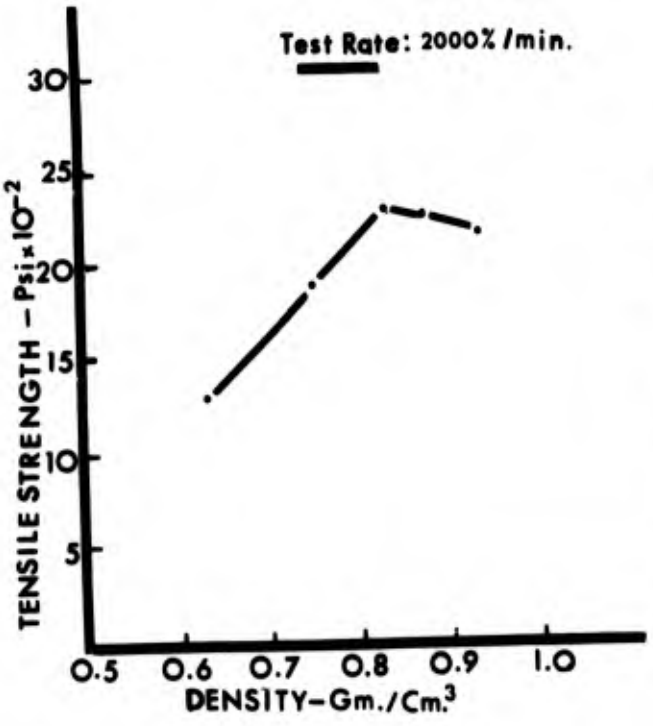

Fig. 1 Tensile Strength vs. Density

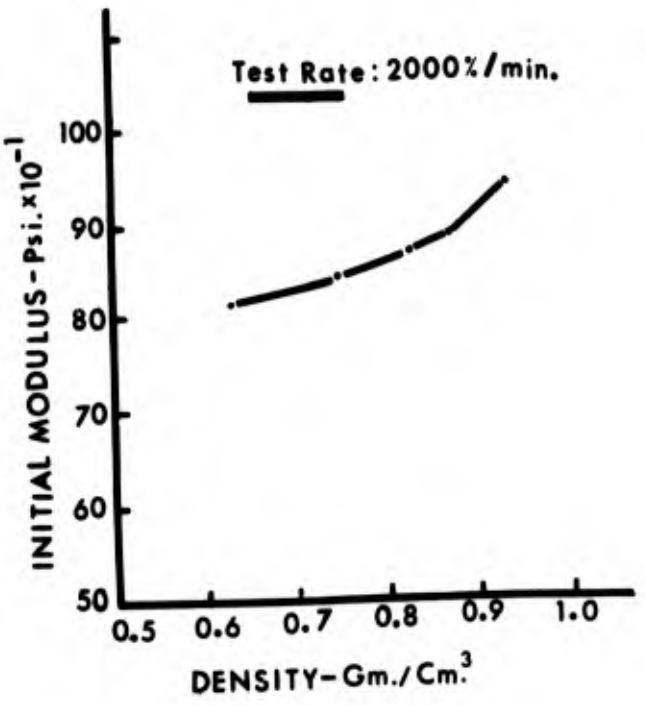

Fig. 3 Stiffness Levels

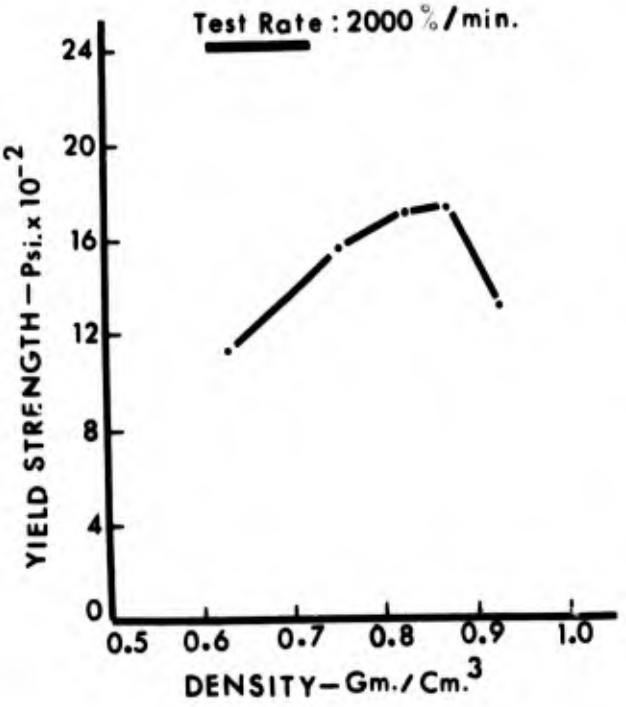

Fig.4 Yield Strength vs. Density

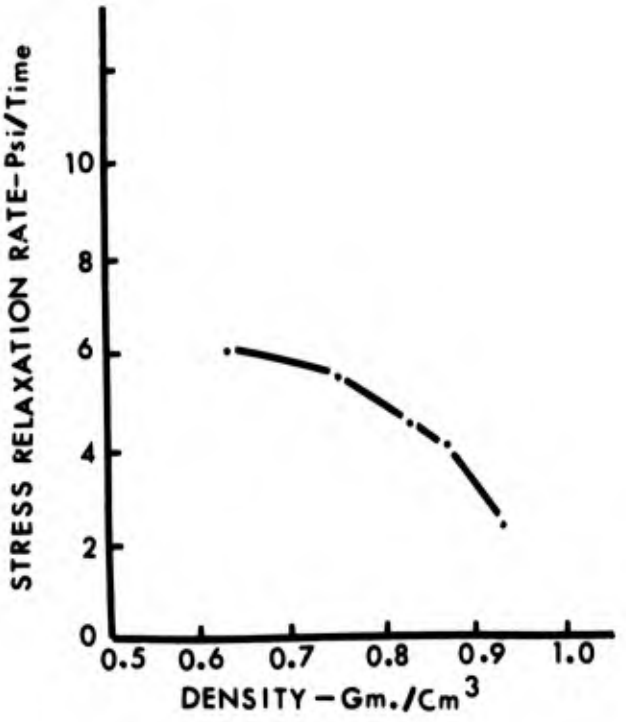

Fig.6 STRESS RELAXATION RATES

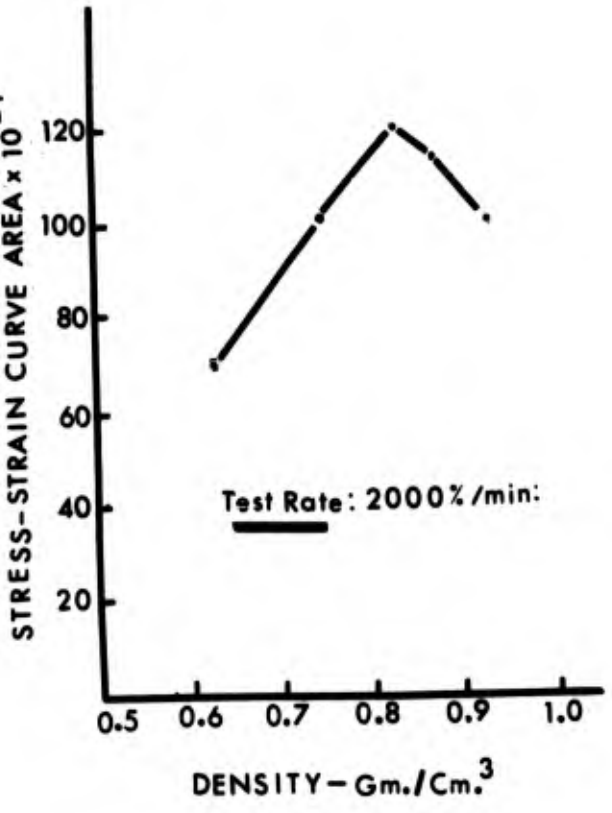

Fig.5 Jacket Toughness

RAW MATERIAL INSPECTION FOR EXPANDABLE POLYOLEFIN INSULATIONS

by
D. I. Marshall and J. M. Turnipseed, Western Electric Company
and
F. K. Wight, Bell Telephone Laboratories
Norcross, Georgia

Abstract

Gas-expanded insulations for communication cable wires made by extrusion of polyolefins containing blowing agents such as azobisformamide, are now coming into widespread use. The combination of resin and blowing agent seriously complicates the problem of characterizing either component by typical inspection methods. Procedures have been developed for separating blowing agent from polyethylene pellets, for optical determination of azobisformamide, and for measurement of pertinent physical and electrical properties of the resin in the presence of unreacted blowing agent. Melt flow and oxidation induction time can be effectively measured in the presence of reacting blowing agent. Some alternative approaches are described.

Similar methods can be used also for dry blends of resin with blowing agent.

Background

The concept of expanded communication wire insulation is not a new one. The Bell System and the television antenna lead industry have made foamed wire insulations for about 20 years. They use low density polyethylene expanded up to about 50% gas by volume. Numerous innovations in designs, materials and processes have appeared in the intervening years. The first large volume telephone cable application appeared in Japan in 1958[1]. This also, was insulated with low density polyethylene. A significant step was taken about that time with the introduction of the azobisformamide (ABFA - azodicarbonamide) blowing agents. These opened the way to the manufacture of extruded expanded insulations with higher melting polyolefins such as polypropylene and high density polyethylene.

Today the growth of expanded insulations is very rapid. This is partly attributable to shortages of materials, bringing on urgent need for material savings, but growth would have occured even with more plentiful supplies because its time had arrived in a technical sense. Mass production of high quality extruded expanded insulations such as those described in a companion paper[2] is now possible using various methods and materials typified by those discussed here. Material shortages and rising prices have only given us larger returns for our development efforts.

Western Electric now manufactures three main types of expanded insulations. One is made from high density polyethylene, another from polypropylene, and the third, mentioned above, from low density polyethylene. Among these, there is rapid growth in the use of the high density polyethylene materials. This growth is the result of the availability of readily processable compounds of expandable high density polyethylene containing the new non-plating versions of azobisformamide.

Along with the large scale use of expandable insulation materials there arises the need for material inspection systems. These are needed to help qualify new sources of material, to assess the quality of successive shipments, and to help in diagnosing causes of any problems that may arise in processability or product performance. This report describes some inspection methods that have been used for both polyethylene compound and polypropylene preblend. The methods in use at this writing are regarded as preliminary answers to the present need. Improved methods are expected later.

Expandable High Density Polyethylene

A compound of high density polyethylene with ABFA first appeared about 1960[3]. This material did not catch on because the industry was not yet ready for it. Polypropylene was also available in combination with blowing agent, and the volume of expanded product was not sufficient at that time to support the two competing systems. Later the intermediate density compounds were introduced and adopted in Europe[4]. The appearance of non-plating modifications of ABFA helped to accelerate progress in use of these systems. Recently the high density expandable compounds were reintroduced at a time when their applications were ready to grow.

Polypropylene Dry Blend

The expandable polypropylenes on the market include both powder blend and coated pellet types of combinations of resin with blowing agent. The latter first became available about fifteen years ago. We have worked mostly with the powder blend type in recent years. But either of these confronts the user with different kinds of inspection problems compared to the polyethylene compounds, and the application of conventional methods is sometimes not practical. We have developed a few special methods for the powder blend material.

Blowing Agent Analysis

The ABFA in the polyolefin is a key ingredient for successful processing. It is important, therefore, to be able to measure the amount and type of blowing agent present. Important characteristics of blowing agent are blowing temperature, gas yield, bubble size, and the effectiveness of plate-out preventing additives. The ultimate answer to all of these is obtained only in extrusion trials, but methods of measuring them without insulating wire are available. Extrusion trial without wire is one example of a cost-saving evaluation method. Also, blowing temperature, gas yield, and relative processing fluidity of a compound can be measured in principle using a special modified version of a Brabender Torque Rheometer[5]. Thus far, we have relied on the use of methods for analyzing the compound for its ABFA and ash content. The ABFA content shows potential gas yield and ash content confirms the amount of silica type plate-out preventing additive.

The chemists might think of a number of possible approaches to the analysis for blowing agent content. We have developed methods based on a spectrophotometric procedure for the determination of the concentra-

tion of ABFA, which in the presence of an appropriate solvent shows a strong absorption band in the visible wavelength region. For this reason, quantitative determination of its concentration will not be affected by typical colorless additives found in polyolefins.

The procedure requires first the use of a solvent which will remove the blowing agent from the resin. A solvent system of 70% xylene and 30% dimethyl sulfoxide (DMSO) was found to extract the ABFA from hot swollen polyolefin. Alternatively a mixture of 92% xylene and 8% DMSO will dissolve both the polyolefin and the ABFA. The resin can be precipitated from this solution by cooling.

Extraction of ABFA from polyethylene therefore can be accomplished in either of two ways. One is to heat the 70-30 solvent system and polyethylene together and extract the ABFA from swollen resin melt. The system is then cooled to solidify the resin, and the liquid poured through a filter. Three stepwise extractions by this method can yield a quantitative result.

In the alternative procedure the resin is first dissolved in pure hot xylene, sufficient DMSO is added to dissolve the ABFA but not enough to precipitate the polyethylene. Polyethylene is then precipitated by cooling the solution. DMSO is added to bring the fluid to a 70-30 ratio. The mixture is then filtered to remove the polymer, and the filtrate is examined with the spectrophotometer.

In the case of a powder blend, the separation of ABFA from polymer is a much simpler problem. The powder is merely treated with 70-30 solvent mixture and filtered to produce a solution similar to those obtained from the polyethylene solutions.

The absorption of the ABFA solution is measured at 419 nm and the concentration of ABFA is calculated using a Beers law plot of absorbance vs. known concentration.

The molar extinction coefficient of ABFA in this system (absorbance-liters per mole-cm) was found to be 54.155. Figure 1 shows the calibration plot and the good linearity between absorbance at 419 nanometers and concentration of ABFA. With the extraction procedure or the powder blend system we generally work with solutions containing 15 to 18 milligrams/100ml. Under these conditions the amount of ABFA content in the resin can be readily measured to an accuracy of about 3%. With the precipitation method more dilute solutions are used and somewhat more refined analytical skill is required for this level of accuracy.

Some typical results of analyses are given in Table 1.

A simple method of testing material for gas yield was developed based on the use of a piston type rheometer as a volume measuring apparatus. The cylinder was packed with a carefully weighed charge at a temperature below the blowing agent decomposition temperature. The piston was applied with a relatively low pressure level. The temperature of the cylinder was then programmed upward at a rate of about 5°F per minute and the displacement of the piston was measured as a function of time. Figure 2 shows the plot of volume versus time when this method was applied to polypropylene powder blend containing pure ABFA blowing agent. The volume first shrinks as melting proceeds. It then increases because of the combination of thermal expansion and gas formation. Ultimately the volume levels out and decreases as gas begins to escape. By making a correction for thermal expansion one obtains a measure of the amounts of foaming under a known pressure and temperature.

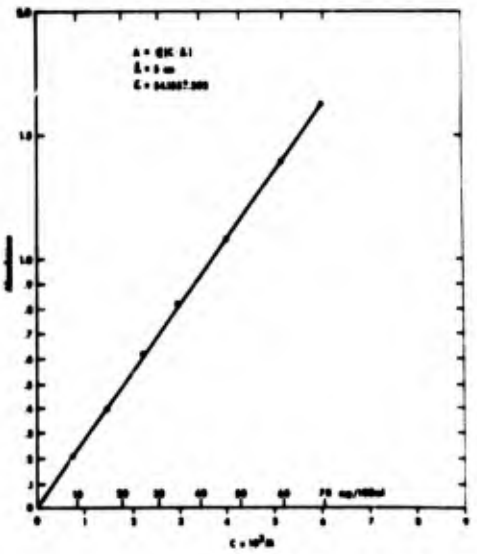

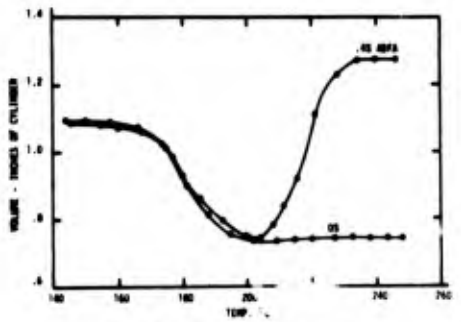

Figure 3 shows a plot of % expansion versus blowing agent content for a number of samples prepared for calibration purposes. The plots were measured at more than one pressure in the search for an optimum for correlation with extrusion performance. The plots show not only gas yield as a function of blowing agent content, but also the solubility of the gas mixture as a function of pressure. Careful work yielded blowing agent content less precise than that obtained with the chemical analysis method, therefore the volume expansion method is not preferred for blowing agent measurements.

Physical Property Measurements

Our expanded high density polyethylene insulation was based on the same type of polyethylene as that used for solid high density insulation, namely ASTM D-1248, Type III-5. Having established that the expected blowing agent is present, it remains to examine the resin and other additives. If one is interested in measuring

the same properties that he would expect to measure on solid high density polyethylene, then the problem is to adapt the desired procedures to the reactive blowing agent compound. This requires either removing the blowing agent or learning how to test the combination.

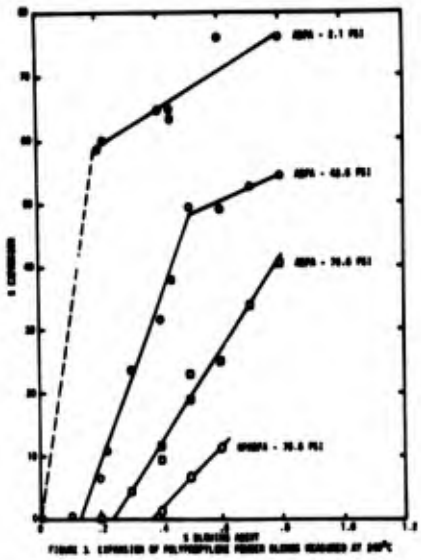

A method that has been used with low density polyethylene containing p,p'oxybis (benzene sulfanyl hyrazid), which decomposes at temperatures in the range of 150-160°C, was to decompose blowing agent on a hot roll mill. After the gas was formed and expelled the resin could then be inspected by the same methods that would be used for solid insulation compounds. When this method was tried with the high density polyethylene, too much heat was required to decompose the ABFA. The severe heat exposure destroyed some of the properties that were to be measured. An alternative method was to examine material containing unreacted blowing agent. This was found to be effective for most properties.

Mechanical and electrical properties require the use of molded sheets. Sheets were compression molded under conditions which would not decompose blowing agent. This requires careful control of the temperature and time cycle. The sheet can be cooled in the press or removed and quenched in water. We have preferred the quenched sheet because of the faster press cycle and because the quenched material has closer similarity to material quenched on wire. Quenching causes lower density and yield strength, but the requirements can be adjusted to compensate for this change.

Polypropylene is commonly tested for physical properties using injection molded specimens. Because polypropylene has a higher melting temperature and thus requires a higher molding temperature, molding without decomposition of blowing agent was not attempted. At this point we are depending on specification of the resin type, which is ASTM D2146 Type II-3, and testing of the extruded foamed insulation.

Examples of mechanical and electrical properties of polyethylene are shown in Table 1. Mechanical properties were measured according to ASTM D638 using Die C of ASTM D412. Electrical properties were measured according to ASTM D257. Density of moldings was measured by ASTM D1505, and density of pellets was measured by an air displacement picnometer.

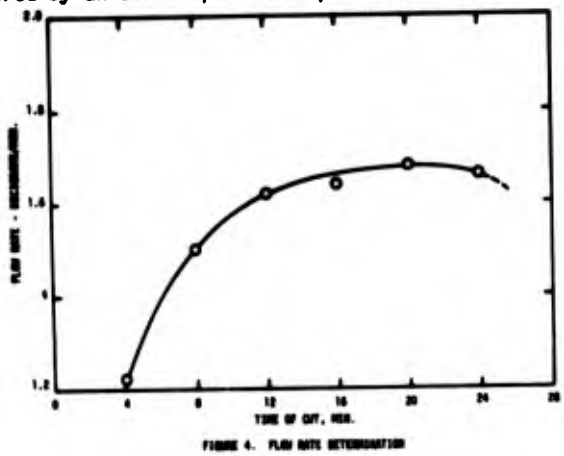

Thermal Properties

A valuable index of molecular size in polyolefins is melt index. ASTM D1238 as commonly used is not applicable to expandable compositions without serious error, because it assumes a material to be relatively stable. A modified technique based on Condition E was used for both polyethylene and polypropylene compositions. Blowing agent reaction occurs at the 190°C test temperature but the effects of the reaction have been minimized by changes in the procedure.

The cylinder is charged with a 2 gram sample in the case of readings higher than 1.0 decigram per minute, or with a 1.5 gram sample in the case of readings lower than 1.0. The material is tamped for only one minute before the weight is applied and readings are started. The cuts are made at 2 to 5 minute intervals until flow slows, choosing the interval to yield a specimen more than two inches long. Flow rate passes through a maximum as illustrated by Figure 4. It first increases as the material is heating, but ultimately decreases because the sample is expended or because foaming has occurred. The two largest cuts are weighed to obtain a result.

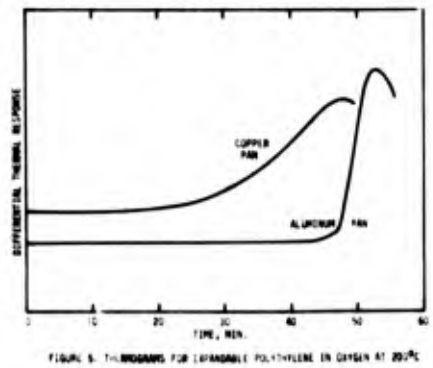

Another thermal property of value for indicating the amount of antioxidant present is the oxidation induction time at elevated temperatures. This is performed as described in two recent papers.[6] The test is commonly performed in a copper pan of a differential thermal analyzer. It was found, however, that the presence of copper in combination with blowing agent reaction products interferes with the induction time test. By using an aluminum pan the interference was avoided. Figure 5 illustrates typical tests on polyethylene in copper and aluminum pans. The thermogram for heating of the material in nitrogen is first recorded to show the approximate melting temperature of the polymer. This helps to identify the polymer, indicating whether it has only one transition or more. Two or more transitions confirm examples of block copolymers or blends. When the sample has reached the desired temperature the atmosphere is changed to oxygen and the isothermal oxidative induction action is recorded.

TABLE I

TYPICAL INSPECTION DATA ON POLYOLEFINS

		Polyethylenes			Polypropylene
Property	Units	Source A	Source B	Source C	Powder Blend
ASTM Content	%	0.57	.56	--	.59
Pellet Density	Gms/ml	.94	.94	.91	--
Molded Density, Quenched	Gms/ml	.945	.942	.942	--
Press Cooled	Gms/ml	.954	.946	.946	--
Melt Index	Gms/10 Min	.60	.70	.90	1.2
Tensile Yield, Quenched	PSI	3050	2830	2750	--
Press Cooled	PSI	3490	3040	3140	--
Elongation, Quenched	%	900	900	1000	--
Press Cooled	%	610	>350	640	--
Dielectric Constant	-	2.33	2.32	2.32	--
Dissipation Factor	-	.0005	.0005	.0005	--
Oxidative Induction Time at 200°C	Minutes	50	50	50	[illegible]
Insulation Resistance	Ohms	10^{15}	10^{15}	10^{15}	--

Raw material pellets tend to vary in oxidative induction time. More uniform results are obtained by taking specimens from molded sheets or melt index extrudate. In the case of polypropylene it was found that the material from the melt index extrudate yielded much more uniform induction times than the original powder blends. The difference is evidently attributed to mixing in the melt index tests. Typical flow and induction time data for both polymers are listed in Table I.

Miscellaneous Quality Tests

Having examined resin and additive mixtures for composition and properties, there may be questions about homogeniety of a material. Some tests were carried out, therefore, to reveal nonuniform mixing of additives. Such tests are valuable tools in cases where a correlation with performance can be shown.

One example of a test that is sensitive to compound uniformity is oxidative induction time, as mentioned above. Another example was seen in some of our work on compounding of low density expandable material. Several small lots of material were prepared. It was found that the material could be foamed in a picture frame type compression mold to reveal some features of its foaming behavior. Figure 6 illustrates the results of the moldings. The nonuniformity was found to arise from poorly mixed compounds in the case of some of the laboratory lots. Separation of chips into size ranges was carried out to confirm that the cause was nonuniformity of the material before it was chopped.

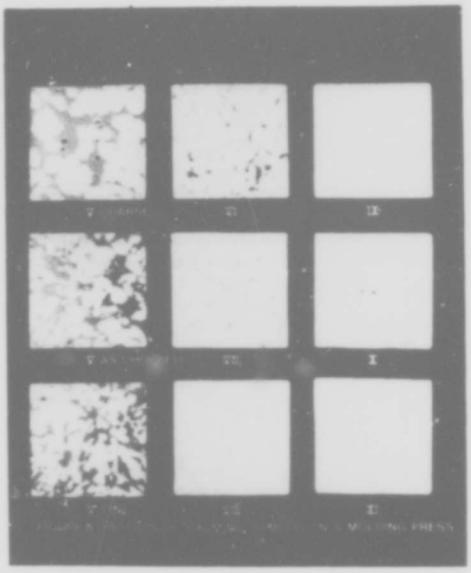

Similar experiments were tried for the high density polyethylenes, but with little success. The .050 inch (1.25 mm) solid sheets molded directly from pellets, however, were found to show differences in composition in cases of opacity differentials or particle agglomerates. These can be useful observations in cases where processing problems are encountered and heterogeneous material is suspected as a cause.

Conclusion

By assembling test methods such as those described here, a set of material requirements can be devised and made the basis for a material specification. We have not attempted to include all known methods for examining expandable compositions nor have we attempted to predict any methods for the future, but have attempted to outline what we consider interesting recent development work on the subject.

Acknowledgement

The authors are grateful for important contributions from Mrs. V. Boehm in the development of some of the blowing agent analysis details, from Mrs. B. Merriday in the developments of some of the physical methods, from Mr. C. Rey for work on chemical and electrical measurements and from Mr. S. L. Craton for much of the physical and electrical test work.

References

1. Rokunohe, M., Yoshida, Z., Miyamoto, H., Mizuno,S. and Okutani, T., U.S. Patent No. 3,068,126, December 11, 1962.

2. Mitchell, D. M. and Webster, G. H., Proceedings of the 23rd International Wire and Cable Symposium, Atlantic City, N.J., December 3-5, 1974.

3. Pusey, B. B., "Cellular Insulation for Communication Cable", 10th Annual Wire and Cable Symposium, Asbury Park, N.J., November 29 - December 1, 1961.

4. Normanton, J. K. "Extrusion of Telephone Cable Insulation Using Expandable Medium Density Polyethylene Compounds." 21st International Wire and Cable Symposium, Atlantic City, N.J., December, 1972.

5. Hogson, T. C., Carefoot, D. B. and Sampat, P., Journal of Cellular Plastics 9, No. 6, pp 3-7, December, 1973.

6. Howard, J. B., DTA for Control of Stability of Polyolefin Wire and Cable Compounds. Polymer Engineering and Science 13, 429-34 (1973). Marshall, D. I., George, E. J., Turnipseed, J. M. and Glen, J. L. ibid, pp 415-21

Donald I. Marshall is a Senior Staff Development Engineer with Western Electric Company's Cable & Wire Product Engineering Control Center, Norcross, Georgia. He holds a Ph.D. in Physical Chemistry from the University of Texas. He joined Union Carbide Corporation, Bound Brook, N. J. in 1948 and Western Electric at Princeton, N. J. in 1958, moving to the Georgia location in 1971. His work has included polymer characterization, melt rheology, and process research in extrusion, molding, and calendering. He is presently engaged in development of plastic material application in communication wires and cables. He is a member of ACS, SPE, and the Society of Rheology.

John M. Turnipseed is a Development Engineer engaged in materials research and development programs in Western Electric's Wire and Cable Product Engineering Control Center, Atlanta Works. He received his M.S. degree in Analytical Chemistry from the University of Virginia in March, 1972. His specialty involves the application of modern analytical instrumentation for investigating the properties of materials. He is a member of ACS and AAAS.

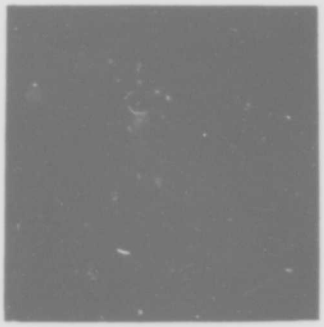

F. R. Wight is a member of the Technical Staff of Bell Laboratories, Norcross, Georgia in the Materials Engineering and Chemistry Group. Mr. Wight received a B.S. degree from the University of Florida, M.S. from the University of Rochester, and Ph.D. from the University of Georgia in Organic Chemistry. He joined Bell Laboratories in 1972.

EFFECT OF PETROLEUM JELLY FILLER ON LOW DENSITY POLYETHYLENE TELEPHONE CABLE JACKETING

R. BOSTWICK

Union Carbide Corporation
Bound Brook, New Jersey

SUMMARY

Accelerated aging studies were made at 60 and 70 C to measure the effect of petroleum jelly filler compound on low density polyethylene telephone cable jacketing, using actual cables and also extruded pipe. No serious effects were measured on properties important for such jacketing. Time-temperature relationships were also studied on pressed plaques.

INTRODUCTION

There have been a number of papers published in the past several years on the effect of petroleum jelly filler on low density polyethylene insulation. However, a literature survey turned up only one reference to low density polyethylene jacketing and this was not very detailed.[1] Accordingly, a study was begun to measure the long-term stability of such jacketing in contact with filler.

ACCELERATED AGING OF CABLES

A two pair Witco 5B-filled cable core for a buried wire construction, with a 30 mil jacket of Union Carbide DFDA-0588 Black 9865 extruded directly over filler, was obtained and stored at 60°C and 70°C as 4" cut lengths. Samples were removed at intervals and tested for tensile strength and ultimate elongation by ASTM D412-68, using the "D" die and a testing rate of 20 inches/minute. Results (average of three specimens) are shown in Tables I and II for an aging period of one year. The data show some scatter, but there is clearly some increased in tensile strength and decrease in ultimate elongation at both temperatures. However, no clear trend with time of storage is apparent. Assuming that a steady state with regard to absorption of the jelly by the polyethylene was reached in four weeks, averaging the data points from four weeks to one year shows a decrease in ultimate elongation to 87% of original in the 70°C aging and to 92% of original in the 60C aging. This would not seem to be a cause for concern.

A multi-pair, Witco 5B-filled cable, 65 mil jacket of DFDA-0588 Black 9865, extruded over a corrugated copper shield coated with filler was likewise stored at 60°C and tested as above.

The cable was used up at four months and the results are shown in Table III. In this case, there was practically no change in tensile strength and ultimate elongation, presumably because of the lesser availability of filler to the polyethylene jacket. Similar averaging of the data as above shows a 98% retention of tensile strength and a 96% retention of ultimate elongation.

The Witco 5B filler is reported to be a low oil petroleum jelly modified with 8% of a low molecular weight polyethylene and stabilized with 0.5% antioxidant, supplied by Sonneborn Division, Witco Chemical Co.

ACCELERATED AGING OF FILLED PIPES

A more extensive study was made by using one inch pipe of nominal 90 mil wall thickness extruded from two Union Carbide jacketing compounds - DFDA-0588 Black 9865 and DFDA-6055 Black 9865. The pipe was prepared in the laboratory, cut into short lengths, corked at one end, hot-filled with Witco 5B filler and stored in an upright position at 60°C and 70°C as shown in Figure 1. Pipe was used as being more like extruded cable jacketing than the pressings used so often in studies of this kind. Pipes were withdrawn at intervals, cleaned, weighed and tested for the properties below.

Melt Index - ASTM D1238-70
Environmental stress crack resistance, 10% Igepal, 21 days, % failure - ASTM D1693-70
Tensile Strength and ultimate elongation - ASTM D412-68 (D-die), testing rate of 20 inches/minute
Low temperature brittleness, F_{50} - ASTM D746-73

The ESCR test specimens were cut transversely to obtain the severest test condition; the other test specimens were cut longitudinally. Unfilled pipes were included in the program as controls.

Data from these studies are shown in Tables IV through VI. Table IV shows a six months' study of filled pipe and unfilled controls of DFDA-0588 Black 9865 aged at 70°C.

Absorption from the filler by the polyethylene at this temperature was essentially complete in a month and leveled off at ∿8.5 percent. Increase in melt index followed the same pattern, leveling off at ∿0.80 from an original value of 0.37 on the extruded pipe. The ESCR testing showed no failures at all in any of the filled pipes. In tensile properties, a slight decrease in ultimate elongation was shown for the filled pipes, with the average of the five weeks to six months data giving a decrease to 91% of the original value. A similar averaging of the control data gives 98% of the original value. Tensile strength showed an immediate decrease of 20% from the hot-filling operation itself, which is probably due to strain-release in the pipe from the 110-120°C temperature of the hot filler. Further loss in tensile strength beyond that, again averaging the five weeks to six months data, was 7%. Low temperature brittleness showed some loss with the LTB, F_{50} value rising from -87°C to -72°C for the filled pipes and to -82°C for the controls, using an average of the seven weeks to six months values in each case.

Table V contains similar data for aging at 60C. The effects are similar but at reduced levels. Weight increase leveled off at ∿5% and melt index rose to ∿0.6. The ESCR testing again showed no failures. Tensile strength showed no loss from the "after-fill" value; averaging of the five weeks to six months data shows a loss in ultimate elongation of only four percent. Low temperature brittleness again showed some loss, with the LTB, F_{50} value rising from -87C to -81C for the filled pipes, using an average of the five weeks to six months values.

A similar study on pipe prepared from DFDA-6055 Black 9865 is shown in Table VI. The pipe stored at 60C is from a different lot of compound than the pipe stored at 70C and the control pipe, so that the original values are slightly different. A different lot of Witco 5B filler from that of the -0588 study was used, which may account for the higher absorption values at 60C shown in Table VI. In other respects, the results are similar except that the -6055 compound was less affected in low temperature brittleness and actually showed an improvement in this property in the 70C aging. During the hot-filling, care was taken to keep the temperature below 110C and the loss in tensile strength on filling was minimal.

ANALYSIS OF AGING RESULTS

The aging temperatures of 60 and 70 C were chosen because these are the highest temperatures the jacketing could reasonably be exposed to. Once the cable has been installed, and in the case of filled cable this means usually burial and pedestal connections, the most significant properties to be maintained are elongation and environmental stress crack resistance. These properties are shown above to be maintained essentially unchanged. Equilibrium absorption from the filler into the polyethylene jacketing is reached in one to two months and no unusual effects developed during continued storage after this point. In one of the two jacketing compounds studied, there was some increase in low temperature brittleness, but this is not considered to be serious.

TIME/TEMPERATURE DEPENDENCE OF FILLER ABSORPTION

Several studies were undertaken on the time/temperature dependence of filler absorption and the effect of jacket thickness. The results are shown in Figures 2-5. This work was done with DFDA-0588 Black 9865 and the second lot of Witco 5B filler.

Figure 2 shows weight increase vs. time for 75 mil plaques totally immersed in filler at room temperature, 40C, 60C, and 70 C. The 70 C samples leveled off at 8.7% absorption within two months, and the 60C sample leveled off at 7.9% absorption within four months. At room temperature, and 40 C, absorption is still continuing after 14 months, with the 40 C sample at 7.3% and the room temperature sample at 5.0%. It is obvious that significant absorption takes place at room temperature.

The effect of thickness is shown in Figure 3. Specimens ranging in thickness from 50 to 90 mils were totally immersed in filler and are being stored at room temperature. It is obvious that the percentage increase in weight with time is inversely proportional to the thickness.

A cable jacket is exposed to filler only from the inside. Figure 4 shows the difference between one-side, and two-side exposure. This was done with one inch pipe of 90 mil wall, stored at 60C. There is an obvious difference in speed of filler absorption and a small difference in the final level reached (8.5% vs. 8.0%).

Summarizing, speed of absorption as well as the final level reached is influenced in the expected direction by temperature, time, thickness and one-side vs. two-side exposure.

POLYETHYLENE IN THE MELT

In the jacketing crosshead extrusion process, polyethylene compound is extruded at melt temperature of up to 225 C, or perhaps even higher. If the filled core is unshielded or if the shielding is itself covered with filler, then the jacketing is in contact with filler at those high temperatures for some finite period of time and at decreasing temperatures as the construction cools. It is legitimate to ask what the interaction might be between the polyethylene and the filler at these conditions.

The results of an experiment to shed some light on this is shown in Table VII. The procedure was to prepare an 8" x 8" x 50 mil plaque, weigh it and place it into a 75 mil cavity mold. This was then heated in a press at the temperature indicated. The pressing was removed, quickly smeared with filler as indicated, cooled as shown and then reweighed after cleaning off excess filler. The data show that under extreme conditions, as much as 17% of filler can be absorbed. Of course, the polyethylene cannot really hold this much and sweat-out quickly occurs at normal temperatures. The data also show that smearing both sides is more severe than smearing only one side, and as might be expected, absorption rises with increasing temperature of contact and time of contact at the high temperatures.

The condition in the last column of one-side smearing and cooling immediately after contact at 190 C is not so far removed from what can actually occur in a cable jacketing operation. Even with efficent cooling, a jacketing operation where the jacket is extruded directly over an uncovered filled core can be expected to lead to a 3% or higher absorption of filler.

CONCLUSIONS

Low density polyethylene jacketing will absorb significant amounts from petroleum jelly filler depending upon time, temperature, jacketing thickness and other conditions of exposure. With Witco 5B filler and two Union Carbide jacketing compounds, an ultimate level of 8-9% absorption is possible. No physical properties are degarded sufficiently to impair functionality of the jacket.

REFERENCES

1. McCann, J.P., Sabia, R. and Wargotz, B. "Characterization of Filler and Insulation in Waterproof Cable", Eighteenth International Wire and Cable Symposium, 1969.

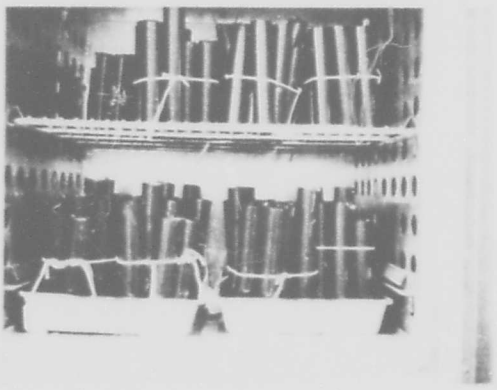

FIGURE 1

AGING OF PIPES

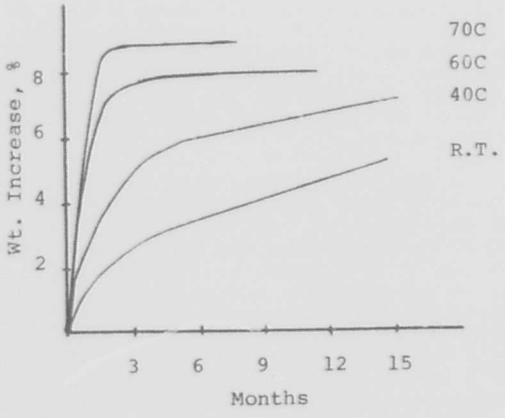

FIGURE 2

FILLER ABSORPTION OF 75 MIL PLAQUES

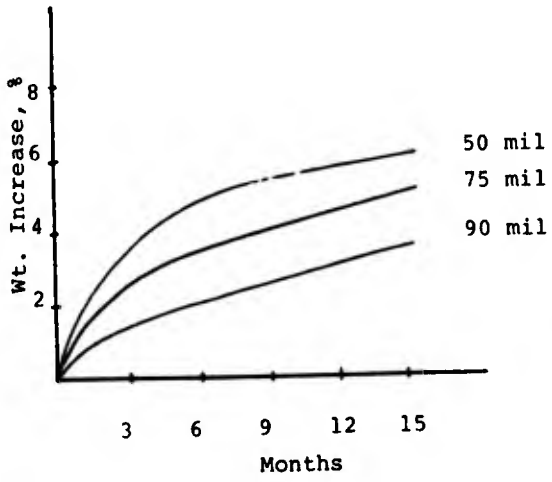

FIGURE 3

FILLER ABSORPTION AT ROOM TEMPERATURE

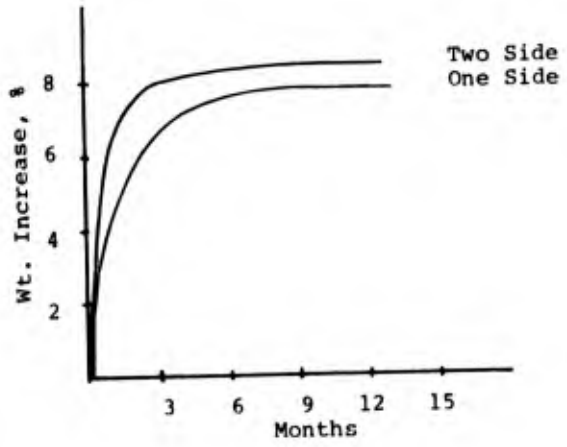

FIGURE 4

FILLER ASBSORPTION OF PIPE AT 60 C

TABLE I

AGING OF FILLED CABLE AT 70°C

Time	Tensile Strength		Ult. Elongation	
	PSI	% of Original	%	% of Original
Original	1640	100	473	100
One Week	1990	121	426	90
Two Weeks	1370	84	436	92
Three Weeks	2270	138	386	82
Four Weeks	1750	107	413	87
Six Weeks	2050	125	416	88
Eight Weeks	2010	123	370	77
Three Months	1920	117	466	99
Four Months	1930	118	363	77
Six Months	1730	106	363	77
Nine Months	1920	117	413	87
One Year	2380	145	466	99

TABLE II

AGING OF FILLED CABLE AT 60°C

Time	Tensile Strength		Ult. Elongation	
	PSI	% of Original	%	% of Original
Original	1640	100	473	100
One Week	1870	114	430	91
Two Weeks	1500	92	440	93
Three Weeks	2150	131	460	97
Four Weeks	1780	109	396	84
Six Weeks	2120	129	433	92
Eight Weeks	2190	133	440	93
Three Months	2080	127	440	93
Four Months	2080	127	446	94
Six Months	1925	117	406	86
Nine Months	2150	131	453	96
One Year	2340	143	470	99

TABLE III

AGING OF FILLED CABLE AT 60°C

Original	2010	100	613	100
Two Weeks	1820	91	586	96
Four Weeks	1820	91	593	97
Six Weeks	2020	101	583	95
Eight Weeks	2100	105	603	99
Ten Weeks	1940	97	583	95
Three Months	1970	98	596	97
Four Months	1890	94	580	95

TABLE IV

STORAGE OF DFDA-0588 PIPE AT 70°C

FILLED WITH WITCO 5B

	Wt. Increase %	ESCR M.I.	ESCR % Failures	T.S., PSI	U.E. %	LTB F50,°C
Original	-	0.37	0	2365	695	-87
Filled	0.3	0.42	0	1900	685	-87
2 Weeks	5.9	----	0	1940	665	---
3 Weeks	7.3	----	-	----	---	-78
25 Days	8.0	0.78	-	----	---	---
5 Weeks	8.0	0.78	0	1770	625	-83
7 Weeks	9.1	0.85	0	1820	640	-68
10 Weeks	8.2	0.77	0	1650	615	-74
4 Months	8.0	0.75	0	1920	615	-75
6 Months	8.7	0.90	0	1710	655	-69
		UNFILLED (CONTROL)				
Original	-	0.37	0	2365	695	-87
2 Weeks	-	0.36	20	2070	715	---
3 Weeks	-	----	-	----	---	-83
5 Weeks	-	0.35	0	2100	695	-87
7 Weeks	-	0.41	0	2160	705	-81
10 Weeks	-	0.37	0	2330	655	-78
4 Months	-	0.35	0	2180	705	-87
6 Months	-	0.36	0	1920	640	-82

TABLE V

STORAGE OF DFDA-0588 PIPE AT 60°C

FILLED WITH WITCO 5B

Original	-	0.37	0	2365	695	-87
Filled	0.3	0.42	0	1900	685	-87
2 Weeks	2.6	0.48	0	2000	675	---
25 Days	3.5	0.48	0	1970	660	-76
5 Weeks	5.2	0.55	0	1910	675	-82
7 Weeks	4.6	0.56	0	1950	645	-81
10 Weeks	3.6	0.56	0	1930	745	-80
4 Months	4.5	0.58	0	2080	635	-86
6 Months	5.2	0.65	0	1950	635	-78
		UNFILLED (CONTROL)				
Original	-	0.37	0	2365	695	-87
2 Weeks	-	----	0	2090	705	---
25 Days	-	0.36	0	2320	745	-83
5 Weeks	-	0.37	0	2160	715	-82
7 Weeks	-	0.35	0	2220	665	-86
10 Weeks	-	0.38	0	2070	695	-79
4 Months	-	0.37	0	2280	720	-90
6 Months	-	0.37	0	2010	675	-88

TABLE VI

STORAGE OF DFDA-6055 PIPE

FILLED - STORED AT 60°C

Original	-	0.33	0	2070	655	-100
Filled	0.3	0.38	0	1900	635	-100
2 Weeks	4.4	0.56	0	1800	635	-88
1 Month	6.2	0.62	0	1900	665	-96
2 Months	6.8	0.68	0	1840	605	-86
3 Months	7.1	0.74	0	1840	625	-91
4 Months	7.1	0.78	0	1880	620	-93
5 Months	6.8	0.72	0	1870	605	-95

TABLE VI CONTINUED

FILLED-STORED AT 70°C

	Wt. Increase %	M.I.	ESCR % Failures	T.S., PSI	U.E. %	LTB F50, °C
Original	---	0.29	0	2030	670	-88
Filled	0.4	0.31	0	1930	700	-87
2 Weeks	6.1	0.56	0	1770	620	-84
1 Month	8.4	0.67	0	1700	600	-85
2 Months	7.4	0.69	0	1770	635	-88
3 Months	9.4	0.75	0	1730	595	-93
4 Months	7.9	0.75	0	1910	580	-91
5 Months	9.3	0.70	0	1920	625	-94
6 Months	8.2	0.55	0	1930	665	-92

UNFILLED - STORED AT 70°C

Original	---	0.29	0	2030	670	-88
2 Weeks	---	0.30	0	2080	680	-92
1 Month	---	0.31	0	2070	685	-89
2 Months	---	0.30	0	2110	685	-95
3 Months	---	0.30	0	2020	675	-93
4 Months	---	0.31	0	2040	635	-93
5 Months	---	0.30	0	2120	655	-100
6 Months	---	0.30	0	2200	670	-100

TABLE VII

MOLTEN -0588 AND FILLER

	Weight Increase, %			
	Both Sides Smeared[1]			One Side Smeared[2]
Temperature, °C	Press[3]	Water[4]	Bench[5]	Bench[5]
190	16.9	8.0	10.7	3.8
150	13.1	6.7	6.9	3.1
120	7.7	4.0	4.3	2.1

1. Smeared with a total of 10 grams Witco 5B filler.
2. Smeared with 8 grams Witco 5B filler.
3. Held in press for 2 minutes after smearing, then cooled in press.
4. Thrown into cold water after smearing.
5. Let cool on lab bench after smearing.

Robert Bostwick
Union Carbide Corp.
P. O. Box 670
Bound Brook, N. J. 08805

Robert Bostwick has been with Union Carbide Corporation in the R&D Laboratories at Bound Brook, N. J. since 1947 except for 1953-56 when he was with Minnesota Mining and Manufacturing Company. He has a B.A. and M.A. in Chemistry from Columbia University. He is presently in the Wire and Cable Product Group, with responsibility for telephone cable jacketing materials. He is a past President of the Newark Section of the Society of Plastics Engineers.

SHEAR & FLOW CHARACTERISTICS OF WATERPROOF PETROLATUM - BASED CABLE FILLER COMPOUNDS

J. J. Kaufman, T. E. Luisi

Witco Chemical Corporation

New York, New York

Abstract

During the past several years, filled cable has become a large portion of the total production of polymer insulated telephone cable (PIC). A review of the filler material used in the United States indicating characteristics at its inception and changes that are occuring is given. Emphasis is placed on the chemical, physical and functional properties of the filler material required by the cable manufacturer; trends in these data are presented with an extrapolation to possible future requirements. New laboratory test procedures for evaluating flow characteristics in relation to shear stability of these cable filler materials are discussed.

Introduction

Shortly after the practice of burying PIC cable was adopted, it became apparent that such cable was susceptible to subsurface moisture. This moisture caused the degradation of electrical properties and, at times, complete electrical failure. Approximately ten years ago, the British attacked this problem directly by replacing the air in the cable with a hydrophobic material thereby precluding the entry of water into the cable. The material used was, what the petroleum industry calls, a petroleum grease. The choice was a good one since this material was inexpensive, hydrophobic, electrically acceptable and compatible with the other components of the cable. In 1969, at the 18th International Wire & Cable Symposium, Bell Laboratories introduced their approach to waterproofing telephone cable, i.e. the now well-known polyethylene/petroleum jelly or "PE/PJ" compounds.(1) These compounds were designed to meet the more severe temperature extremes to be found in the United States as well as the more stringent electrical performance requirements necessitated by the desire to transmit over longer distances, and at higher frequencies.

In 1973, steps were taken in the United States to introduce a polyethylene-free petroleum hydrocarbon system sometimes referred to as "single component system" (SCS). This product fulfilled the physical, as well as the electrical performance required of the PE/PJ type product. Due to the narrower molecular weight distribution, the single component cable fillers have lower melting points and viscosities and are softer at low temperatures (36°F) than the PE/PJ compounds.

Petrolatum Composition and Structure

To better understand the problems associated with the development of filling compounds we will briefly review the composition and structure of petrolatum which is the principal constituent of the various compositions.

Petrolatum is a complex mixture of petroleum hydrocarbons consisting of straight chain paraffins, branched isoparaffins and naphthenic and aromatic structures. The graphical form of typical structures are depicted in Figure #1.

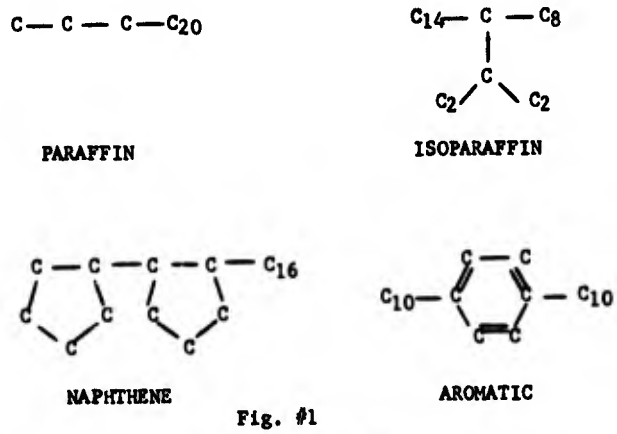

Fig. #1

The composition of petrolatums used in the manufacture of cable filling compounds can be typically characterized as straight chain molecules: 2-5%; branch chain molecules: 10-25%; molecules containing aromatic and/or naphthenic rings: 80-90%.(2)

The petrolatum in the PE/PJ compounds contain structures which have approximately 20 to 50 carbon atoms per molecule. In addition, there are an almost "infinite" number of configurations for molecules of the same carbon atom number. The physical and functional character of the petrolatum is determined by the ratio of the different molecular structures present in it's composition. This ratio is dependent upon the source of the crude oil from which the petrolatum is derived. Higher levels of paraffins give a harder, brittle product. Conversely, higher concentrations of isoparaffins, naphthenics and aromatics lead to a softer product. Petrolatums having melting points from 100°F to 140°F cannot be used by themselves as filling compounds and require modification by incorporating compatible higher melting point additives.

Current Systems Prevalent in the United States

PE/PJ - These systems consist of low molecular weight polyethylene added at various levels to petrolatum plus a stabilizer.

"Single Component" - Earlier in the paper, reference was made to a petroleum grease. This is

a fraction extracted from the heavy distillate of crude oil. It contains molecules with carbon atoms in the range of C_{20}-C_{80}. As previously mentioned, it consists of a mixture of many structures which influence it's performance as a cable filler material. It is possible to fractionate this petroleum grease deriving from it a number of fractions of different melting points and molecular weights. By fractionating and selectively combining some of these fractions, a product can be obtained which is not too hard at low temperature and yet gives the desired high temperature performance for a cable filling compound. This SCS has an advantage over the PE/PJ type in that it does not have the skewed molecular weight distribution and the inherent non-uniformity problems that may arise due to the wide molecular weight distribution found in the PE/PJ systems.

Relationship of Crystallization to Shear and Flow

The use of polyethylene with it's much higher melting point and molecular weight when added to petrolatum significantly affects the rheology of the system. This effect on the liquid-solid transition of PE/PJ is a function of the cocrystallization of the polyethylene and the petrolatum. In the PE/PJ compounds crystal size is dependent upon the molecular weight, molecular weight distribution and the concentration of the polyethylene, together with the cooling rate and the degree of shear imposed during crystallization. The smaller the individual crystal, the larger the total crystal surface area provided by a given concentration of polyethylene. The resultant increased density gives a harder material with an increased resistance to flow. For a given polyethylene in a static PE/PJ System (i.e. zero shear) whose cooling rate is moderate to slow, relatively large, macrocrystals are formed.(3) The resultant compound will have a higher flow temperature and be harder than the same compound which is subjected to shear in the solid state. This is shown graphically in Figure #2 where the macrocrystals have a block-like, laminar structure which after shearing becomes a random dispersion of crystal fragments, Figure #3.

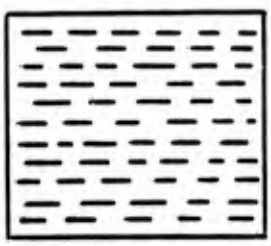

LAMINAR ORIENTATION

Fig. #2

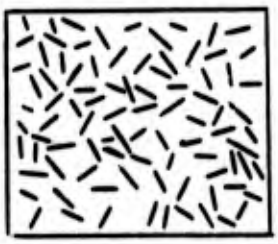

RANDOM ORIENTATION

Fig. #3

This change in structure resulting in a softening of the product, is termed "hardness loss" in petrolatum technology. It should be noted, that if the amount of surface presented by the polyethylene crystals in the sample is sufficiently large, the disorientation produced by shear becomes much less significant in terms of effect on flow. However, such a product does tend to be undesireably hard. In Table #1, the effect of shear on flow using the Western Electric Flow Test (App. 1-e) is demonstrated. Controlled shear was obtained using a standard grease worker (App. 1-b - ASTM D-217). It should be noted that with the sheared samples the conditioning prescribed in the W.E. Test must of necessity be eliminated, since melting the sample would negate the effect of shearing. A review of the data confirms that the currently used systems (PE/PJ and "Single Component System") are sensitive to shear in the solid state and care must be exercised in the manufacture of the cable.

The Ideal Filling Compound

An ideal filling compound should have the following properties:

Hydrophobic - It must not be soluble in nor absorb water.

Compatible - It must not have any significant effect on other components of the cable.

Stable - Under field conditions, it should be oxidatively and thermally stable.

Non-melting - It should not melt nor flow at temperatures below 70°C.

Soft - It should not become excessively hard nor brittle at low temperatures.

Adhesive - It should adhere well to the cable components, but be readily removable for splicing.

Cohesive - It should not embrittle or crack over the temperature range of field exposure.

Electrical - It must meet established electrical criteria.

Non-toxic - It must be dermatologically safe and non-volatile under normal handling.

Uniform - There should be no phase separation when cycled through the temperature range of field exposure or if subjected to shear.

Inexpensive - It should be relatively inexpensive and not add more than a nominal cost to the cable.

The PE/PJ and SCS satisfy, to an acceptable degree, most of the above requirements. However, they do have several limitations. As reported, these solid state products are shear sensitive and are, therefore, normally introduced into the cable as liquids. This may, in some cases, lead to voids occurring in the cable due to shrinkage of the filler material during cooling. Since cable filler materials are a mixture of many isomers of different molecular weights rather than a single chemical species, there is a possibility that classification or phase separation may occur under a given set of circumstances. However, we are not aware of any reports citing phase separation as a failure mode in the field.

Table #1

EFFECT OF SHEAR ON FLOW*

Loss, Weight %

Sample	A European Type	B PE/PJ	C PE/PJ	D SCS	E GEL
Zero Shear					
149°F	0	0	0	0	0
160°F	0	0	0	0	0
176°F	1.5	0	0	0	0
190°F	-	0.5	0.1	67.0	0.1
Moderate Shear (60 Cycles)					
149°F	62.5	70.5	56.8	96.0	0
160°F	-	-	-	-	0
176°F	-	-	-	-	2.0
Severe Shear (10,000 Cycles)					
149°F	70.0	47.8	52.0	98.0	0
160°F	-	-	-	-	-
176°F	-	-	-	-	1.2

*W.E. Flow Test - 2 hours

Table #2

PHASE SEPARATION TEST

Loss, Weight %

Sample	A	B	C	D	E
Zero Shear					
149°F/2 Hrs.	0.1	8.4	0.5	8.7	0
Severe Shear (10,000 Cycles)					
149°F/30 Min.	94.3	22.8	5.2	92.7	0

Gel Cable Filler

A new generation material which has all the advantages of the PE/PJ and single component materials as well as good shear stability has been developed. The physical and functional properties of such a material would allow it to be filled "cold" into the cable as a soft solid. In addition, it is highly resistant to phase separation and would, therefore, constitute an excellent cable filler material. The data for the gel system in Table #1 in contrast with the current systems indicate a product that is stable under shear.

Laboratory Test Procedure Critique

One of the many problems associated with the evaluation of filling compounds has been trying to determine by laboratory techniques how a compound will perform physically in the cable. The "flow test", (App. 1-c) was developed by Bell Laboratories to predict temperature at which a filler would flow from a cable. While the test proved successful, in establishing a minimum criteria, a direct correlation between what would happen in a cable and the test itself has not been established.

Our Laboratory is examining this problem and is developing procedures which it is believed would more accurately predict the drip or flow temperature of the compound in the cable. A procedure developed in our laboratory to determine the effects of temperature, temperature cycling, and shear on the flow characteristics of filling compounds is the Phase Separation Test (App. 2). It is a severe test of the phase stability of filling compounds under stress. Data appear in Table #2. Comparing the data of Tables #1 & #2, the Phase Separation Test appears more severe than the Western Electric Flow Test, but sufficient data has not been collected to allow a definitive statement to be made. This test may also be used to evaluate the effects of temperature cycling on filling compounds.

An established procedure under evaluation is the Ubbelohde, drop point of grease method (App. 1-e). In Table #3 flow temperatures of the samples are recorded using this method.

Table #3
DROP POINT OF GREASE (IP 31/66)

Sample	A	B	C	D	E
Zero Shear/°F	203	206	200	184	>250
Severe Shear/°F	155	183	161	126	>250

Examining the data from Tables #1, #2 and #3 we observe consistent differences in samples A and D vs. B and C. Whereas each sample is adversely affected by shear, the effect of the polyethylene in samples B and C can be observed. From the earlier discussion on crystallography, we might conclude that severe shear would contribute to an increase in surface area of polyethylene compared with a moderately sheared sample resulting in an improvement in flow characteristics of the severely sheared sample. This is confirmed in Table #1 where the weight % loss is less for severely sheared samples of B and C vs. the moderately sheared samples. The effect of the polyethylene on rheology after severe shear is also noticeable in Table #2 where the weight % loss is less for B and C than A and D. Similarly in Table #3 B and C have higher flow temperatures. By each method of evaluation sample E is essentially unaffected.

PHYSICAL PROPERTIES OF FILLER COMPOUNDS

	A	B	C	D	E
Melting Point					
Drop, ASTM D-127, °F.	206.4	207.5	207.5	202.7	N.A. *
Congealing, ASTM D-938, °F.	179.0	185.0	181.0	177.5	-
Drop Point, IP 31/66, °F	203	206	200	184	>250
W.E. Flow Test**°F	175	206	199	190	-
Cone Penetration					
1) Petrolatum, ASTM D-937, 77°F., 0.1 mm	44	105	60	69	88
Lubricating Grease, ASTM D-217, 77°F., 0.1 mm					
2) After 60 double strokes	206	275	230	204	210
" 10,000 double strokes	321	315	313	315	314
Hardness Loss (2-1 = HL)	162	170	170	135	122
Viscosity					
Kinematic, ASTM D-445, SUS @ 210°F.	-	-	-	81	N.A. *
SUS @ 266°F.	62	565	74	-	-
Needle Penetration					
Petroleum Waxes, ASTM D-1321, 36°F., 0.1 mm	55	53	52	65	49
Electrical Properties					
Dielectric Constant, ASTM D-150, K @ 10^5Hz	-	2.18	2.13	2.10	2.11
K @ 10^6Hz	2.22	2.15	2.15	2.14	2.14
Dissipation Factor, ASTM D-150 D = tan delta, 10^5Hz	.0017	0.0001	0.0002	0.0001	0.0004
10^6Hz	.0023	0.0004	0.0007	0.0006	0.0007
DC Volume Resistivity, ASTM D-257 OHM-CM	1.5×10^{16}	1.1×10^{15}	2.7×10^{16}	2.4×10^{15}	2.2×10^{15}

* NA = Test not applicable to gels.

**Western Electric "Flow At Elevated Temperature" - Temperature of Flow

Table #4

In Table #4 data are presented on the various types of petrolatum based filling compounds that have been used to date as well as a new "gel" or "cold fill" type. Under Melting Point, data are given using the D-127, D-938, (App. 1-a) and the Western Electric Flow Test which is run to failure. These tests have been used extensively. Also included is the Drop Point Of Grease method which is simpler and quicker than the Western Electric Flow Test and offers a close comparison to it in the case of non-sheared samples. The comparison does not hold up as well when comparing samples subjected to shear (Table #1 vs. Table #3). Samples B and C perform better in Table #3 than might be expected from the data in Table #1. These differences may be explained by both the composition of the compounds and the conditions of testing.

The cone and needle penetration (App. 1-b) data in Table #4 are indicative of hardness at a specified temperature. The hardness loss represents the difference in hardness between sheared and non-sheared samples. This may be interpreted to represent changes in the crystal structure and orientation induced by shear.

Compatibility With Cable Sheathing

To evaluate the compatibility of filling compound with low density PE sheathing compound, samples of extruded tubing were made from jacket grade PE (Union Carbide DFDA-0588). The tubing was cut into 6" lengths, weighed, calipered, and plugged at one end. The tubes were then filled with the cable compounds under test and placed in a 160°F air circulating oven for 840

hours. Between 350 and 500 hours a light oily film was noticeable on the exterior of the tubing. At the end of 840 hours the tubes were cleaned, weighed and calipered. Weight change and wall thickness data appear in Table #5.

PERMEABILITY COMPARISON
(160°F./840 Hours)

	B	C	D	E
Zero Shear				
Change in Wt., Wt. %	10.7	7.5	9.8	6.9
Change in Caliper, %	7.9	4.6	4.6	2.1
Severe Shear				
Change in Wt., Wt. %	9.2	7.8	10.3	7.5
Change in Caliper, %	3.8	2.4	3.8	1.6

Table #5

Differences are noticeable between compounds. While some plasticization of the jacketing material occured, as measured by weight gain and wall thickness it was concluded that there was no significant effect on the sheath by any of the compounds. It is our understanding that Union Carbide confirms our observation.(4)

Summary

The data presented in this paper indicate that while progress is being made, additional work is required to predict from laboratory procedures the behavior characteristics of filling compound in the finished cable. Our Laboratory is continuing work in this area and is interested in joining with others concerned with this problem in test procedure evaluation programs.

Cable filling compounds have been on the scene for only a few years and while admittedly not perfect, have on the whole done a creditable job. We believe the new generation of gelled filling compounds now on the horizon represent a significant advance.

References

1. "Characterization of Filler and Insulation in Waterproof Cable", J. P. McCann, R. Sabia, B. Worgotz; 18th International Wire and Cable Symposium.

2. "Aspects of the Constitution of Mineral Oils", K. Van Nes and H. A. Van Westen; Elsevier Publishing Co., N.Y., 1951.

3. "Manufacturing Waterproof Telephone Cable", R. A. Conser, T. A. Heim, and L. D. Moody; 19th International Wire and Cable Symposium.

4. "Effect of Petroleum Jelly Filler on Low Density Polyethylene Cable Jacketing", R. Bostwick; 23rd International Wire and Cable Symposium.

Appendix I

Testing Methods and Procedures

Physical Methods

a. Melting Point
"Drop Melting Point of Petroleum Wax Including Petrolatum" ASTM: D 127-63; IP: 133/64

"Congealing Point of Petroleum Waxes, Including Petrolatum" ASTM: D 938-71; IP: 76/64

b. Penetration
"Cone Penetration of Petrolatum", ASTM: D 937-67; IP: 179/68
"Cone Penetration of Lubricating Grease", ASTM: D 217-68; IP 50/69
"Needle Penetration of Petroleum Waxes", ASTM: D 1321-70

c. Viscosity
"Kinematic Viscosity of Transparent and Opaque Liquids", ASTM: D 445-72; IP: 71/66

Electrical Methods

d. Dielectric Constant, Dissipation Factor
"A-C Loss Characteristics and Dielectric Constant (Permittivity) of Solid Electrical Insulating Materials", ASTM: D 150-70
DC Volume Resistivity
"D-C Resistance or Conductance of Insulating Materials", ASTM: D 257-66

Functional Properties

e. Flow Resistance
"Flow at Elevated Temperatures", Western Electric MF-17000, Section 1061 modified as per W.E. MS 62072, Issue 2, October 5, 1972.
Flow Temperature
"Drop Point of Grease", IP: 31/66
Phase Separation
"Phase Separation Test", Witco: AM No. 240.

Appendix II

Phase Separation Test

Apparatus:
1. Funnels - Analytical, 58°, Kimax, 55 mm diameter (i.e., Sargent Welch S-35309-C)
2. Beakers - Griffin, low form, with pourout (i.e., S-W No. S-4675-J) 150 ml
3. Glass Cutter - Tubing, Griffin (i.e., S-W No. S-39955)
4. Glass Rod - KG-33 Glass, Kimax, 4 mm diameter (i.e., S-W No. S-40087-D)

Preparation of Apparatus:
1. Funnels - Remove part of the stem using the Griffin tubing glass cutter. Leave approximately a 10 mm stem. Fire polish in a bunsen burner flame.
2. Tapered Glass Rod - Draw the 4 mm diameter glass rod in a bunsen burner flame to give an approximate 20 mm taper (i.e., 4 mm to 1 mm). Total length of rod 100 mm.

Procedure:
1. Obtain tare weights on a funnel and beaker for each specimen. Prepare duplicate specimens.
2. Place assembled funnel, beaker and tapered glass rod in an oven at 100°F. to pre-condition for 0.5 hour minimum.

3. Heat test sample to 260°F. minimum, (or 25°F. above the cloud point, whichever is greater). Stirring frequently, allow the sample to cool to 240°F. (or 10°F. above the cloud point, whichever is greater). At 240°F., remove the funnel assembly from the oven and immediately pour the sample into the funnel. Fill the funnel to the rim (~30 grams). Be sure not to overfill the funnel. Allow the filled assembly to cool to ambient (approximately 0.5 to

1.0 hours).
4. When the sample has reached ambient, carefully and gently twist and pull the glass rod out of the funnel and sample. Care should be observed to avoid disturbing the sample-rod interface anymore than necessary.
5. Weigh the filled funnel (without rod). Record this value.
6. Replace the funnel in the beaker. Place this assembly in a forced-draft oven at the desired test temperature.
7. At the end of the oven testing time, remove the assembly, being careful not to jar or shake the assembly so as to cause any drops to fall from the funnel stem into the beaker. Allow the assembly and sample to cool.
8. Reweigh the beaker, if anything has flowed into it. Record this value.
9. Determine weight % flow at T°F. and time t.

(Speaker)
Thomas E. Luisi
Witco Chemical Corporation
277 Park Avenue
New York, New York 10017

Tom Luisi is Manager of Market Development for the Sonneborn Division of Witco Chemical and currently acting as Product Manager for Telephone Cable Products. He has been with Witco for 18 years in various technical marketing functions. Tom is a graduate of the City College of New York. He has a B.S. Degree with majors in chemistry and meteorology.

(Co-author)
J. J. Kaufman
Witco Chemical Corporation
Petrolia, PA 16050

John Kaufman is Director of R&D for Wax and Related Products for the Sonneborn Division of Witco Chemical. He graduated from the University of Pittsburgh with a B.S. in chemistry. John is a member of the Joint Committee on Wax Testing sponsored by ASTM and TAPPI.

SYSTEM EVALUATION AND PROTECTION OF CONDUCTOR INSULATION IN OUTSIDE PLANT

Louis Ance and Joseph P. McCann
Rural Electrification Administration
Washington, D. C.

Abstract

Samples of high density polyethylene conductor insulation are randomly cracking after relatively short exposure in field installations. Analysis of the cracked samples and the environmental exposure conditions indicate a combination of sunlight, heat, and antioxidant evaporation are primarily responsible for the rapid deterioration of the system. Methods for protecting the conductor insulation in field installations are discussed. A redesign of the housings and the use of a bag type enclosure are recommended.

Introduction

The basic premise of designing a working telephone system is to insure that all of the parts intermesh and function as intended. The system design should be based on a thorough understanding of the performance requirements of the system as well as of the individual component parts which comprise the system. This study would involve specialists and laboratory personnel who have some part to play in the design and fabrication of the component parts. It requires technical coordination between personnel in overlapping fields in achieving the best in the system design. Using this systems approach, this paper has proceeded to analyze the present field failures of conductor insulation, and has attempted to correlate the random cracking of conductor insulation with a breakdown of the system design. In this analysis, we have pinpointed several areas in the system design where additional safeguards should be applied, either prior to cable installation or in the field, to provide a long-term reliable telephone system.

Background to System

A. Cable Development

The REA telephone program can be considered to have gone through three periods of plastic-insulated cable development. The first period, from 1954 - 1965, utilized low density polyethylene insulation in aerial and buried plant. A great deal of this cable plant is still in use in our borrowers' systems without any problems from the standpoint of conductor insulation cracking. The requirement for low density polyethylene conductor insulation was discontinued in REA specifications in approximately 1965. Santonox was the primary antioxidant used in the insulation without any copper inhibitor.

The second period of development begun in 1963 extended until approximately 1972 requiring the use of high density polyethylene as conductor insulation for both aerial and buried aire core cables. Santonox was the principle antioxidant used in these cables. To the best of our knowledge no copper inhibitors were used in the insulation.

From 1967 until the present time ethylene/propylene copolymers constituted a portion of the conductor insulation. These ethylene propylene copolymers used proprietary antioxidant systems, and were tested according to ASTM D2342 for stability to oxidation. Ethylene propylene copolymers for insulation were used in aerial and air core type buried cables.

The third period of cable development has been in the area of filled telephone cables. The requirements for basic cable conductor insulation continues to also be high density polyethylene or ethylene propylene copolymer. Because of the possible extraction of antioxidants and stabilizers by the filler material, the industry has become cognizant of potential conductor insulation failure due to loss of stabilization. This awareness has created a need for new stabilizer systems and also the methods and kinds of tests performed.

Splicing, Design and Application of Housings

One of the original considerations in the development of buried plant was the elimination of exposure of the plant to storms and other damage from the elements at a cost low enough for application in rural areas. Another major consideration in the design of buried wire and cable was the provision for a corrosion-resistant shield adequate for electrical protection and mechanically strong enough to prevent damage from ground rodents, such as gophers.

During this development almost no thought was given to the housing other than serving as a mechanical protection for the above-ground appearances of wire and cable. In the initial field trial of buried plant, a section of transite pipe was modified to serve as a housing for the protection of above-ground appearances of buried cable.

Two types of housings were adopted as standard units in the REA program. The channel type housings are made up of three parts; a back plate, an upper cover plate and a ground line cover plate formed into a "U" shape and secured to the back plate to form a rectangular column. See Figure 1. The dome type housings are made up of three parts; a top cover shaped like a dome and fastened to a cylindrical shaped base which is mounted on a closed "U" stake. See Figure 2.

It was during the testing of the completed plant that the amount of condensation found in the housing was affecting the electrical performance of the system. Due to the condensation problem in the housing, it became a requirement in the proposed specification at that time that all units must be free breathing.

Holes were drilled in the experimental housings in order to reduce the condensation within these units. The earlier designed system required the use of terminal blocks and load coils equipped with buss bars attached across binding posts. Leakage occurred between buss bars and ground. The terminal blocks and coils equipped with buss bars were later eliminated as standard items.

In 1960 a revision of REA Standard PC-2 was made to include the use of split cable guards to be

placed over the splice bundles to protect them from mechanical and electrical damage. In examining systems which were built in 1960 through 1965 with splice bundles protected by split cable guards, no cracking of insulation has been found to date. The only cracking found to date during this period is where split cable guards had been removed for maintenance purposes. In 1966 a revision of PC-2 was made to delete the requirement for the use of split cable guards over exposed conductors due to the fact that the installers almost never would replace these guards when removed for maintenance purposes. Most of the reports received to date regarding cracking of conductor insulation cover systems which were built in 1966 and later.

In February 1972 with the advent of filled cables in the REA program, interim splicing procedures were issued requiring that all exposed conductors in terminal housings be repacked with filling material and wrapped with muslin tape. Due to the difficulty of reentering housings containing filled splice bundles, it was decided that another method was needed to protect the exposed conductors.

The protection needed has to be some sort of covering which would provide protection for conductors from sunlight, condensation, dust and snow. Several materials were tested to determine which product would be best suited for this application. A polyfoam type material was selected at this time since it showed the best all-around physical and mechanical properties. The polyfoam material is formed into a bag which is positioned over the splice bundles and secured into position at the lower end of the bag using sealing blocks.

Systems Analysis

A. Field Results:

The industry is aware of the deterioration of the low density polyethylene conductor insulation in air core telephone cables in housings under normal operating conditions.[1, 2] The deterioration of low density polyethylene insulation first became evident in the housings in the Southwestern area of the United States. Further instances of insulation deterioration have been reported in the more northern areas of the country. The Bell Telephone operating companies commenced treating the cracked insulation by spraying all of the conductors.[3] The prediction of longer life for the high density polyethylene insulation in cables, using the same antioxidant system in air core cable, has not materialized. (Table 1) Complaints from REA field engineers concerning the deterioration of high density polyethylene insulation are being received.[4] Several reports of ethylene propylene copolymer insulated cables in REA Telephone Companies show the same pattern of deterioration of these polymers. The map (Figure 3) shows the largest majority of complaints in the South. However, we have also received complaints from as far north as Minnesota and Michigan.

The time for these failures to occur varies from 1963 to 1971 (construction date) with the majority of complaints being for those systems built in 1966. To date we have received many field complaints on conductor insulation failures of which at least twenty have been confirmed by our staff.

The type of failures we have noticed are shown in Figures 4, 5 and 6. These failures show both fading of the conductors due to exposure to sunlight as well as circumferential cracking in unstressed areas indicative of oxidative instability. We have had one report of cracking which was analyzed due to heat aging. We have been able to obtain samples of cracked insulation from the field which shows fading is random in effect and the same conductor will be faded and cracked in one area and not in another area.

During a recent inspection trip on one REA borrower's project, conditions were found in several housings as follows:

1. Housing: Channel type, installed 1965 - 1966.
   Condition: Good.
   Insulation: No cracking or color fading.
   Location: Cable Rt. 1-24, Well shaded.

2. Housing: Channel type, installed 1965 - 1966.
   Condition: Very poor mating surfaces; can see some conductors.
   Insulation: Color fading and cracking.
   Location: Cable Route 1-26, no tree coverage; gets sunshine most of day.

3. Housing: Channel type, installed 1965 - 1966.
   Condition: Very good; all hardware in place.
   Insulation: Slight color fading and cracking.
   Location: Cable Route 1-28. Well shaded all day.

4. Housing: Channel type, installed 1960.
   Condition: Fair; all hardware in place.
   Insulation: No fading or cracking; conductors protected by split cable guards and vinyl tape.
   Location: Cable Route 2-1; located in sun most of the day.

5. Housing: Channel type, installed 1960.
   Condition: Very good; all hardware in place.
   Insulation: No fading or cracking; conductor protected by split cable guards and vinyl tape.
   Location: Cable Route 2-2; located in sun most of the day.

6. Housing: Channel type, installed 1960.
   Condition: Very good; all hardware in place.
   Insulation: No fading or cracking. Conductors protected by split cable guards.
   Location: No coverate, open area, cable route 2-3.

7. Housing: Channel type (BD 2) installed 1960.
   Condition: Fair
   Insulation: No fading or cracking, conductor protected by split cable guards.
   Location: Open area; cable route 2-4; load point.

8. Housing: Dome type BD3; installed 1961.
   Condition: Good
   Insulation: No fading or cracking - conductor protected by split cable guards.
   Location: Cable route 5-8, No tree coverage.

9. Housing: Dome type BD3; installed 1961.
   Condition: Excellent
   Insulation: No fading or cracking conductors; protected by split cable guards.
   Location: Cable route 5-12A; open area.

10. Housing: Dome type BD3; installed 1961
    Condition: Fair

Insulation: No cracking but slight fading of colors across the top of cable loop not protected by split cable guards.

Location: Cable route 5-14; open area; load point.

11. Housing: Dome type BD3; installed 1961.
Condition: Very good.
Insulation: No fading or cracking conductors protected by split cable guards.
Location: Cable route 5-17; Open area; no shade trees.

Discussion

We have had several reports of cracked ethylene propylene copolymer insulation in housings. These reports indicated that the cables in question had been installed in the last five years.

We have not received any reports of cracked insulation occurring in aerial cable plant even though such insulation is the same as in buried type cables. The antioxidant systems in both types of cables are the same and one should expect similar results in both types of plants.

(4,5,6) At least three individual field reports have verified that insulations made up of either low density polyethylene or high density polyethylene, if properly protected from sunlight or volitization and evaporation of antioxidant will last for a longer time period. The most unique example of this oxidative stability is reported from Death Valley, California. The Bell System type "B" housings used were similar to the REA BD-2 housings. These cables were installed in 1962 with the housings completely sealed. No degradation of the conductor insulation was found on a recent inspection. The average temperature was 100°F with recorded temperatures over 130°F. In addition, another older telephone system in Iowa was visited by REA personnel to determine reasons why the original cable plant did not show evidence of cracked insulation. From inspection it was noted that all of the cable splice loops were protected by polyethylene split cable guards and in some portions of the loop by two half lapped layers of 7-mil vinyl tape. The housings, both channel and dome types, in these instances were not sealed to provide sunproofness or restrict air flow. The original cable plant was installed in 1960 and subsequently a number of replacement cables were installed in a portion of the route in 1966 using the same older housings. No protection was provided for the newer cables in the housings. Only the replacement cables showed evidence of cracked insulation.

An analysis of the cable system in the housings showed the following patterns of failure as observed in previous studies:

1. Degradation occurred only in the housings.

2. No degradation occurred under the jacket.

3. No degradation occurred under taped areas with the jacket restored.

4. The colors, white and red, with the highest percentage of Ti O_2, deteriorated first.

5. Levels of antioxidant concentration in the insulation were higher under the areas not exposed versus the areas exposed.

6. Deterioration occurred generally in both the stressed and unstressed areas.

7. No reported deterioration of black colored insulation.

In addition to these observations, the following have been noted:

1. Color fading of the high density polyethylene insulation.

2. Little or no deterioration of insulation completely sealed to light and restricted air circulation.

3. Reenterable housings are more susceptible to cracked insulation.

4. Housing designs allow light to enter.

5. Improper maintenance procedures.

6. Improper construction procedures.

7. No ultraviolet stabilizer or copper deactivation to provide sunlight and thermal protection.

These findings are based on observations and examinations of field samples from operating telephone systems. The opinion of field personnel in the Southwest is that the insulation installed over eight years ago in all probability will require replacement if maintenance protection is not immediately provided.

To date the samples of cracked conductor insulation in the REA borrowers' systems is primarily low density and high density polyethylene in air core cables. We have had reports of polypropylene cracking of which only one case has been substantiated. The report indicated that the cable in question had been installed in 1969. With filled cable conductor insulation we have had no reports of trouble in the systems. This lack of trouble could be the result of our system protection concept instituted in 1971.

Examination of Field Samples

The samples returned from the field have been examined for oxidative stability by Differential Scanning Calorimetry (DSC) in oxygen at 200°C. In most cases the area of exposed cracked insulation in the cable showed an oxidative induction time of zero to two minutes. (7,8,9,10,11) The insulation area under the tape, cover guards, and sheath showed a time greater than two minutes. The effect of color was also apparent. (Table 2) The black insulation exhibited no cracking in the exposed area in the area under the cable cover guard and sheath. The white and red insulation showed the greatest incidences of cracking than any of the other colors. (See Figure 7) In the lower pair size cables, the red and white colors of insulation appear more often than the other colors. Therefore, the basic colors code should reflect these colors which will provide the greatest protection from ultraviolet light. In instances where direct sunlight entered the housings one-half of the longitudinal surface of the red insulated conductor had turned (faded) white while the other half was still red. Several of the samples obtained from the field have demonstrated this type of failure. The melting point range (DSC) gave temperatures of 125 - 130°C for low density polyethylene and 135 - 140°C for high density polyethylene. (12) The density and intrinsic viscosity of the black insulation did not change significantly in

the exposed and unexposed areas. The white insulation had a change in density from 0.955 under jacket to 0.988 for the exposed, and an intrinsic viscosity of 1.98 under jacket to 0.54 for the exposed. Molecular weight (Mw) decreased from 15 x 10^4 to 2.5 x 10^4.

Laboratory Studies:

Weatherometer Testing

Samples of conductor insulation were tested in a weatherometer for fading and cracking.[13] The samples were checked after each fifty hours of testing. The insulation was selected from five cable samples returned from the field and included the following types:

1. Filled ethylene propylene copolymer conductor insulation - 1971.

2. Unfilled ethylene propylene copolymer conductor insulation - 1969.

3. Unfilled high density polyethylene - 1971.

4. Unfilled high density polyethylene - 1967.

5. Unfilled high density polyethylene - 1967.

These samples represented a good cross section of cable from different manufacturers, as well as various type antioxidant systems.

The data shows that the black and white insulation did not change to any considerable degree after 194 hours of testing. The other colors showed considerable fading using either the ethylene propylene copolymer or high density polyethylene insulation. The following colors showed deterioration for both types of conductor insulation:

(1) Orange	(6) Brown
(2) Red	(7) Blue
(3) Yellow	(8) Gray
(4) Violet	(9) White
(5) Green	(10) Black

The cable samples listed in descending order of deterioration are as follows: 2, 1, 3, 4, and 5.

This test data correlates with our field samples which show fading and cracking except for the white. Other tests with the same weatherometer showed after 250 hours (equivalent to 1 year exposure in Florida) the ethylene propylene copolymer insulation cracked badly including the white insulation.

Samples of the conductor insulation from these cables were twisted into pigtails and tested in a rooftop environment for two months in Washington, D. C. Most of the various cable samples faded in color. The red conductor in all of the cables exhibited the same red/white striped appearance as the sample recovered from the field. The yellow conductor of sample two cracked upon bending. These tests are continuing.

In addition to the weatherometer test, white high density polyethylene on #22 AWG copper conductors was aged in an air circulating oven at both 70° and 90°C (See Figures 8 and 9). One set of samples was open and a second set was sealed. After oven aging, the samples were tested for residual oxidative stability in DSC. Air tight samples at 70°C and 90°C oven temperatures gave 82 min. and 59 min., respectively after 107 days in the oven. Under these same conditions the open air samples gave 54 min. and 40 min., respectively. A second set of samples immersed in petrolatum for 1 week at 70°C showed the following induction time at the 70° and 90°C levels for air versus sealed samples. Air tight samples after immersion in petrolatum at 70°C and 90°C oven temperatures gave 90 min. and 46 min. DSC oxidative stability respectively after 107 days in the oven. Under these same conditions, the open air samples gave 50 min. and 34 min., DCS respectively. In both cases the closed samples showed considerably longer induction times than the open air samples.

Conclusions and Recommendations

The system design concept of defining the cracking of conductor insulation, emphasizes the responsibility of the manufacturer and the accessories suppliers to be aware of the ultimate requirements their products must meet. The data shows that sunlight can enter the housings and that free breathing type pedestals are presently being used or have been used by the Independent Telephone companies. These conditions are not being reflected in the laboratory tests which are used to evaluate stabilization systems. In cases where no volatilization of the anti-oxidant occurs or sunlight is allowed to enter the system, low density polyethylene and high density polyethylene have performed satisfactorily.

The use of a bag or enclosure to guard against these additional hazards, plus the addition of stabilizers including ultraviolet light types in the bag itself, are recommended. The newer housings have been designed with mating surfaces such that they give protection to the cable from sunlight and free air flow.

As a result of these series of tests we find that the present color code of our telephone cables merits changing. In low pair size cables, the white insulation comprises the first five pairs, while the red insulation comprises the next five pairs. Field samples show that of all the colors these two colors are the most affected by oxidation and heat. We, therefore, recommend changing the color code of cables to the use of black for the first five pairs and another distinguishing color which is highly resistant to ultraviolet light for the next pairs.

We also recommend that research personnel become better acquainted with the end product in order that their testing procedures may reflect the conditions under which the end product is used.

Acknowledgments:

This paper represents the combined efforts of many people in the telephone industry. We especially wish to thank the REA field engineers and area personnel for obtaining field samples and data from their operating telephone companies. In addition, we appreciate the fine cooperation of the many companies and laboratories who have provided laboratory testing and technical data for this paper.

References

1. Evaluation of Thermal Degradation in Polyethylene Telephone Cable Insulation, B. B. Pusey, et al, 20th International Wire and Cable Symposium, 1971, p. p. 209 - 216.

2. Stabilization Problems with Low Density Polyethylene Insulations, John B. Howard, 21st International Wire and Cable Symposium, 1972, p.p. 329 - 341.

3. Treatment of Degraded PIC Insulation in Pedestal Closures associated with Buried Plant, J. W. Shea, 21st International Wire and Cable Symposium, 1972, p. p. 70 - 74.

4. Field Reports - REA Field Engineers (21 Reports)

5. FAR - Louis Ance, Insulation Cracking - Iowa 520, April 23-24, 1974.

6. Telephone Terminal Housings Temperature and Degradation, Topo-Bag Field Condition Tests, Death Valley, California - Robert A. Knoss, Roart Plastics, Inc., August 1973.

7. Letter from E. I. DuPont de NeMours & Company to J. P. McCann - from W. F. Jensen dated 7/12/74.

8. Letter from Hatfield Wire & Cable to J. P. McCann from Dr. I. Galperin dated 3/25/74.

9. Letter from Bell Telephone Laboratories, to J. P. McCann from Glena Kokta dated 4/2/74.

10. Letter from Superior Continental Corporation, to Lou Ance from B. Pusey dated 7/19/74.

11. Letter from Union Carbide Corporation, to Lou Ance from R. J. Turbett dated 6/25/74.

12. Letters from Roart Plastics, Inc., to Lou Ance from Bob Knoss dated 4/30/74, 6/17/74, 7/23/74 and 9/4/74.

13. Letters from Atlantic Richfield Co., to J. P. McCann from Kent Fudge dated 7/7/74 and 8/4/74.

BIOGRAPHY

Joseph P. McCann graduated from University of Maryland with a B.S. in Chemistry in 1956 and Newark College of Engineering with a M.S. in Engineering in 1968. He is presently an Outside Plant Engineer with the Rural Electrification Administration. Previously, he was associated with Bell Telephone Laboratories and is co-inventor of their design for filled cable.

Louis Ance is on the staff of the Outside Plant Branch of REA's Telephone Operations and Standards Division. Previously he was a manager of Product Engineering, System Equipment Plant, Superior Cable and Equipment Division, Hickory, North Carolina. Most of his work has been in the field of outside plant application and designing and is the holder of 6 patents in Telephony.

TABLE I

REPORTS OF CRACKED INSULATION

SAMPLE	LOCATION	INSTALLATION DATE	DATE CRACK REPORTED	MATERIAL
1	Texas	-----	5/9/74	
2	Kansas	-----	5/14/74	
3	Texas		2/1974	L.D.P.E.
4	Missouri	-----	----	H.D.P.E.
5	Iowa	1961	4/1974	L.D.P.E.
6	Iowa	1966	1/1974	H.D.P.E.
7	Missouri	1966	1/1974	H.D.P.E.
8	Tennessee	-----	4/1974	
9	Oklahoma	-----	11/1973	L.D.P.E.
10	Oklahoma	-----	2/1974	
11	Arizona	1966	12/1973	H.D.P.E.
12	Arizona	1966	8/1973	H.D.P.E.
13	Texas	-----	12/1972	
14	Tennessee	-----	10/1973	
15	Texas	1963	10/1973	L.D.P.E.
16	Texas	-----	8/1973	
17	Nebraska	1970	----	H.D.P.E.
18	Florida	1969	6/1974	H.D.P.E.
19	Minnesota	1968	8/1974	H.D.P.E.
20	North Carolina	1969	9/1974	Ethylene, Propylene Copolymer

TABLE 2

CRACKED INSULATIONS FROM FIELD SERVICE, CATEGORIZED IN GAUGE AND COLOR . . . NUMBERS REPRESENT CRACKED INSULATIONS FROM POPULATION STUDIED

19 GAUGE	22 GAUGE	24 GAUGE	26 GAUGE
White --- 21	White --- 3	White --- 7	White --- 6
Slate --- 5	Slate --- 1	Red --- 3	Orange --- 2
Blue --- 4	Blue --- 1	Brown --- 1	Red --- 2
Orange --- 3		Green --- 3	
Green --- 2		Violet --- 2	
		Yellow --- 2	
		Blue --- 1	
		Slate --- 1	

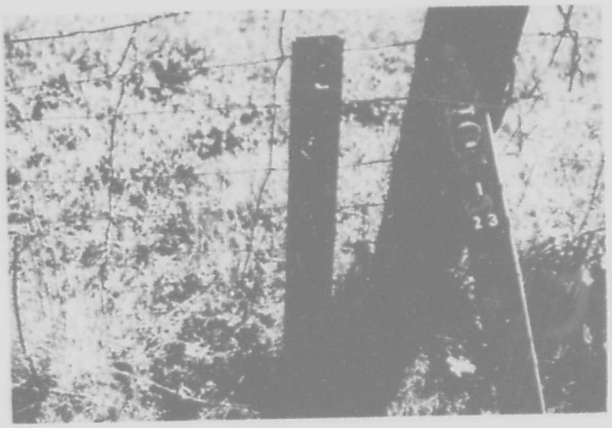

FIGURE 1

CHANNEL HOUSING

FIGURE 2

DOME PEDESTAL

MAP of CONDUCTOR INSULATION CRACKING

FIGURE 3

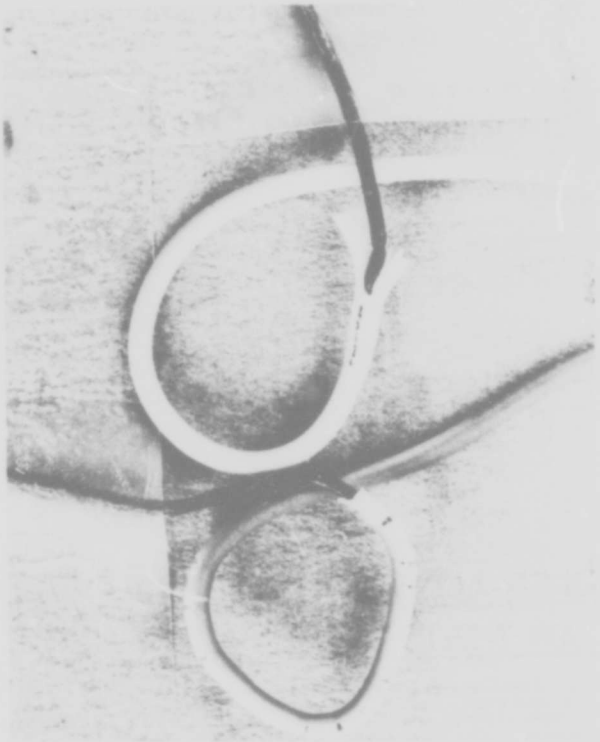

FIGURE 4
RED/WHITE CONDUCTOR

FIGURE 5
CRACKED HIGH
DENSITY POLYETHYLENE

FIGURE 6

CRACKED POLYPROPYLENE

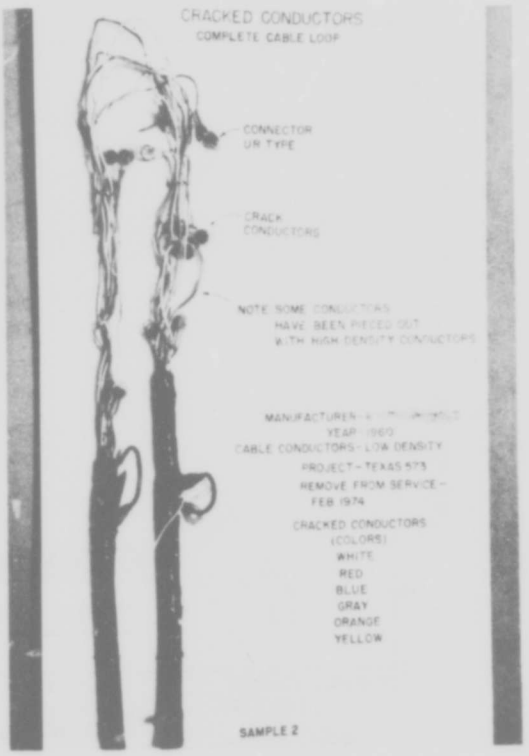

FIGURE 7

CRACKED INSULATIONS FROM FIELD SERVICE

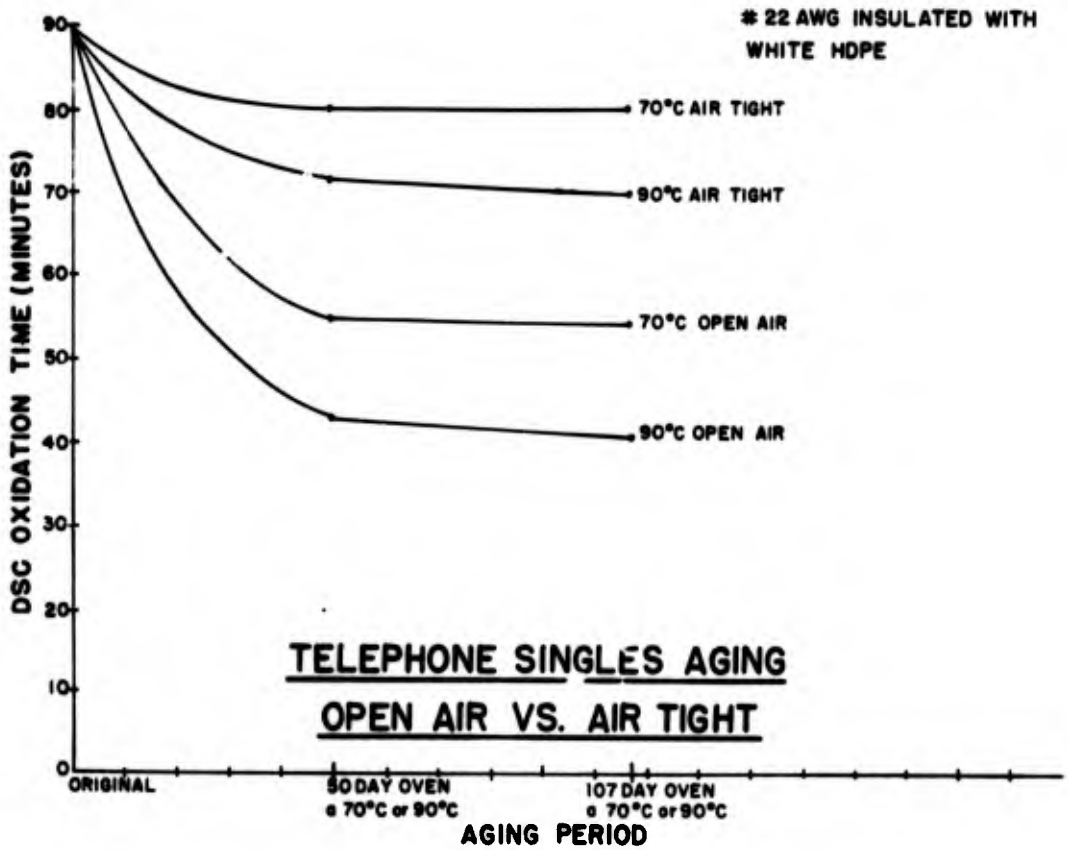

FIGURE 8
TELEPHONE SINGLES AGING

OPEN AIR VS. AIR TIGHT

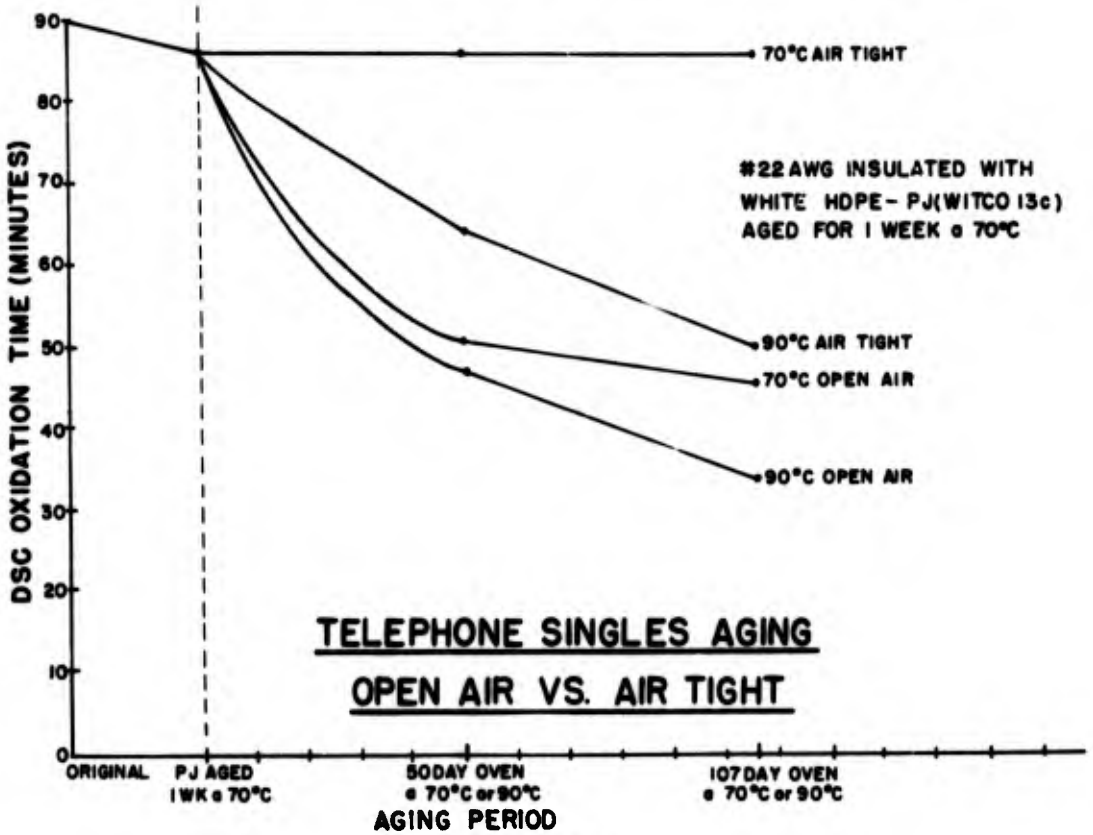

FIGURE 9
TELEPHONE SINGLES AGING

OPEN AIR VS. AIR TIGHT

NEW MULTI-PAIR SUBMARINE CABLE

K. Suzuki
Nippon Telegraph and Telephone Public Corp.
Tokyo, Japan

R. Sawada
Ocean Cable Co., Ltd.
Yokohama, Japan

Introduction

Japan consists of four main islands and many other small ones. Polyethylene-insulated polyethylene-sheathed multi-pair submarine cables (hereinafter referred to as PE-P submarine cable) have been used as short-distance communication cables to connect these islands. Failures of such cables have occured at a rate of fifty times a year. Forty percent of them was caused by fishing and trawling equipment or ship anchors while thirty percent was caused by natural mechanical abrasion or corrosion.

Sea water penetrates into the cable core over a wide range of cable length, once its sheath is subject to damage for any reason. Then a fairly long cable length must be replaced to repair the failure. It was also found that corrosive gas such as hydrogen sulfide (H_2S), which is generated in the sea bottom environments, permeates into the cable through its sheath and causes insulation failure. Reduction of such failures is very important in order to improve performance reliability and reduce maintenance cost of the system.

This report describes new multi-pair submarine cables for shallow water use, specially designed to meet the above requirements.

Cable Design

Cable Structure

As shown in Table 1 and Figure 1, the new cables consist of cable core, sheath and armoring. Features of the new cable are as follows.

1) A compound is forced into the air space of the core to prevent water penetration into a cable core.
2) The sheath consists of an inner sheath and an outer sheath, with a polyethylene laminated aluminum layer, which is longitudinally wrapped over the inner sheath, to prevent the corrosive gas from permeating into the core.
3) The armoring consists of an anti-corrosive layer covered steel wires and serving layers of synthetic high molecular weight materials to improve durability.

The differences between new cable and conventional PE-P submarine cable are shown in Table 2. A layer type assembly construction is used for a cable core of not more than 100 pairs. For a cable core of not less than 200 pairs, however, a unit type assembly is used to improve splicing and terminating work efficiency.

Electrical Characteristics

Typical frequency characteristics of

Table 1. CABLE STRUCTURE OF JELLY-FILLED LAMINATED SHEATHED SUBMARINE CABLE (EXAMPLE)

Cable	Cable Core Diameter (mm)	Sheath (1)		Sheath (2)		Armor Wires		Serving	Overall
		Thickness (mm)	Outside Diameter (mm)	Thickness (mm)	Outside Diameter (mm)	Diameter (mm)	Number	Thickness (mm)	Diameter (mm)
0.5 mm 20 Pairs	8	1.7	11.5	2.5	16.5	6.6	12	1.5	37
0.65 mm 30 Pairs	12	1.7	15.5	2.5	20.5	8.6	11	1.5	45
0.65 mm 200 Pairs	31	2.0	35	2.5	40	6.6 8.6	23 24	1.5	81
0.9 mm 100 Pairs	29	2.0	33	2.5	38	8.6	17	1.5	63

* Sheath (2) contains a polyethylene laminated aluminum layer.

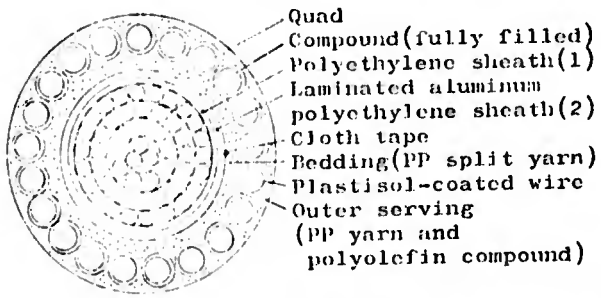

Figure 1. Jelly-filled Laminated Aluminum Polyethylene Sheathed Submarine Cable (Layer Type)

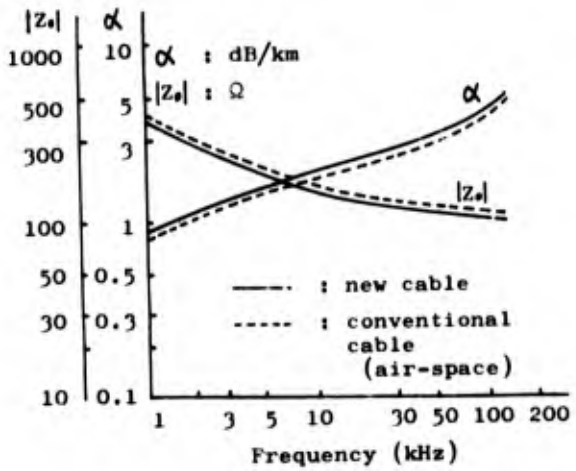

Figure 2. Frequency Characteristics of Secondary Constant (Core Diameter 0.9 mm)

secondary constants are shown in Figure 2. As the cable core is filled with compound, the cable attenuation indicates an increase of about 15% over that of an air-space core. Since this cable is used for short-distance communication, an increase of cable attenuation matters little, while other electrical properties are reasonable.

Basic Approach for New Design

Waterproofing

A filled cable core construction has already been adopted for some land buried cables, so that the core is protected from water penetration when the sheath is damaged. Submarine cables are naturally required to have more superior waterproof chracteristics than land cables, because of higher water pressure in location where undersea cable is generally installed and greater difficulties of repair operations.

Filling Compound

The filling compound must meet requirements of innoxiousness to insulating and sheathing materials, excellent electrical and waterproof characteristics, good processability and moderate cost.

Some compounds, based on petrolatum or

Table 2. DIFFERENCE BETWEEN NEW CABLE AND CONVENTIONAL CABLE

Structure		Conventional Cable	New Cable
Cable Core	Core Space	Air Spaced	Fully Filled
	Insulation Thickness	conductor 0.5 mm : 0.25 mm 0.65 mm : 0.25 mm 0.9 mm : 0.30 mm	conductor 0.5 mm : 0.15 mm 0.65 mm : 0.20 mm 0.9 mm : 0.27 mm
	Stranding Type	layer type	20,30 50,100 pairs : layer type 200 400 pairs : unit type
Sheath		PE one layer	PE double layer with aluminum layer
Armor Wire	Anti-corrosive Layer	tarred or PVC covering(not adhesive)	plastisol coated
	Wire Diameter (mm)	4.5 or 6:one layer 4.5 and 8:double layer	6.6 or 8.6: one layer 6.6 and 8.6: double layer
Outer Covering	Serving	jute yarn	PP split yarn
	Compound	tar-pitch type	polyolefin type

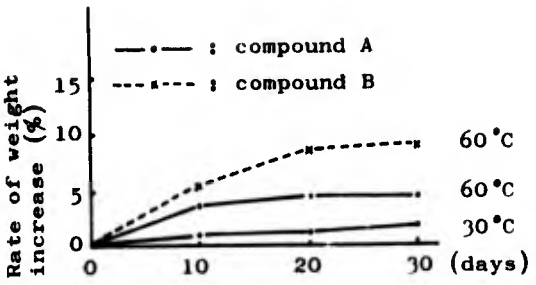

Figure 3. Weight Change of PE in Filling Compound

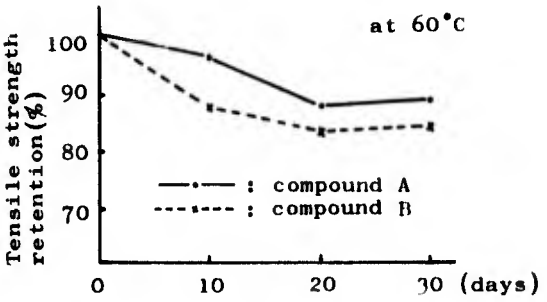

Figure 4. Tensile Strength Change of PE in Filling Compound

polybutene and low molecular weight olefinic polymer were considered satisfactory in meeting these requirements.

Test results showing the effects of compound A and compound B on polyethylene sheets are shown in Figures 3 and 4. The tests were made on molded low density polyethylene sheets immersed in the compound at temperatures of 30°C and 60°C. Changes in weight with time are shown in Figure 3 and changes in tensile strength in Figure 4. Figures show that compound A, consisting of polybutene and low molecular weight olefinic polymer, is less noxious to polyethylene compound than polybutene compound B blended with other materials. The filling compound is applied to the core in the core assembly process and is additionally coated over the core in the sheath extruding process.

Waterproof Characteristics

The following laboratory test was made on the watertight characteristics. One end of a five-meter length of cable was set in a hydraulic test vessel with open ends. A pressure of five kg/cm^2 was maintained for six days. However, no water-leakage at the outer end of the cable was found. A 1.5-km-long field trial cable was laid and left for a week with one open end on the sea bottom at a 90-meter depth and the other end on land for continuous observation of cable characteristics. It was found that sea water penetrated into the core as far as 11.5 meters from the undersea cable end. No change was seen, however, in insulation resistance, cable attenuation or other electrical characteristics.

Another field trial cable, 100 meters in length, was laid at a five-meter depth on the sea bottom with one open end and the other end sealed. Two four-mm-diameter holes had been made previously in the sheath. The sea water penetrated one meter from the open end, but no substantial penetration was seen at the holes in the sheath. These experiments show that the new cable has sufficient waterproof characteristics.

Prevention of H_2S Gas Permeation

As described previously, H_2S gas reacts with a copper conductor and produces copper sulfide. The product, copper sulfide, then grows, with time, in the polyethylene insulation to tree-like states to cause insulation failure. Such failures sometimes occured within two to six years after the cables were laid.

Polyethylene laminated aluminum sheath, where aluminum tape is wrapped longitudinally around the cable with overlap, was considered a most effective countermeasure to the gas corrosion. It was further observed that adhesion between the overlapped aluminum tapes has a considerable effect on prevention of gas permeation. Some experiments proved that H_2S gas permeation, when an adhered overlap sheath is used, is reduced to a sixteenth of that with non-adhered overlap sheath, while non-adhered overlap sheath's permeation is about a thousandth of a conventional polyethylene Sheath's permeation. Based on these results, a double polyethylene sheath with adhered-overlap aluminum layer was finally developed for the new cable.

Test cables were laid where sulfide -treeing trouble has actually occured to determine the degree of conductor discoloration (turns black) as an index of gas corrosion. Discoloration occured in several months with conventional polyethylene sheath. With polyethylene laminated aluminum sheath with adhered overlap, however, no discoloration was seen after more than three years. The results proved the effectiveness of polyethylene laminated aluminum sheath.

Many surveys were made of sea bottom environments on possible cable routes. Conductor discoloration was also checked for many existing conventional PE-P submarine cables in operation. From such studies of sea bottom pollution, it is reasonable to apply the double polyethylene sheath with adhered -overlap aluminum for all undersea cables.

Armoring for Cable Protection

Armor Wire

Two types of wires were formerly in use for armoring in Japan. One was a traditional tarred steel wire and another was an anti -corrosive steel wire with an extruded polyvinylchloride (PVC) compound layer over an individual steel wire. The layer was normally 0.5 mm thick. The thickness is desired, however, to be as thin as possible, to cut down on the gap between armor wire windings from a standpoint of mechanical characteristics of the cable, such as elongation, twist and breaking strength. A thinner layer is also helpful to prevent a cable failure caused by some fishing and trawling equipment penetrat-

ing into the cable core through gaps between wires. The thinner the layer is, however, the more susceptible it is to be crushed by compression when the cable is being handled. Adhesion between PVC layer and steel wire proved to be a convenient solution to the defect. An anti-corrosive steel wire with 0.3mm thick PVC layer adhered to steel wire has been developed from these consideration. Two types of manufacturing processes have been developed; one produces a plastisol coated wire and another produces an adhesive PVC covered wire.

A plastisol compound consists of polyvinylchloride paste resin, plasticizer, stabilizer and other additives. The compound is coated on the steel wire covered with a bonding agent and then is baked at a high temperature, resulting in the plastisol coated wire. An extrusion process is used to get the adhesive PVC covered wire. Bonding agent application and heating operated in tandem with extrusion make the PVC layer adhesive to steel wire. Products by the two processes are rather similar in characteristics, but plastisol coated wire was chosen for the cable in subject due to superior performance of adhesion.

Table 3 shows one example of mechanical characteristics of anti-corrosive armor wires. Table 4 shows mechanical characteristics of armor wire after it was laid in the sea bottom for ten months. The Table shows that anti-corrosive layer of wires without an outer serving shows some degradation in its abrasion resistance. Further detailed study proved, however, that its material itself does not show any degradation and apparent degradation comes from fine surface scratches made during cable laying . This was proved by an experiment where samples buried in a beach for six months, but with no scratches at all, did not show any degradation.

It is well known that armor wire is consumed by electrical corrosion where electrical current flows out from wire to sea water. The electrical current is sometimes caused by tidal current action and terrestrial magnetism as well as by induction from outside power sources. A new steel armor wire splicing procedure is being studied to improve its anti-corrosion characteristics. The new procedure aims at electrical insulation between lengths of spliced wires, and it is expected that such armor wires will be less susceptible to electrical corrosion.

Outer Covering

1) Servings

Cutched or tarred jute yarn has been used for bedding or outer serving. These treated yarns do not have enough anti-rotting characteristics. Additionally, particular attention must be given to coal tar noxiousness during cable manufacture.

Polypropylene-jute yarn (hereinafter PP-jute), a mixed spinning with polypropylene

Table 3. ANTI-CORROSIVE WIRES MECHANICAL PROPERTIES

Property	PVC Covered WIRE (not adhesive)	Adhesive PVC Covered Wire	Plastisol Coated Wire	Test Method
Wire Diameter (mm)	5	8	8	Micrometer
Anti-corrosive Layer Thickness (mm)	0.5	0.3	0.3	
Bonding Strength (kg)	0	110	140	Tensile load necessary to strip a 9.5-mm-long coating layer from wire.
Abrasion Resistance (number of times)	8	14	10	Number of grinder revolutions until wire surface is exposed. (load : 1 kg)
Scratch Resistance (number Of times)	145	500	480	Number of scratching times until wire is exposed. (load : 1 kg)
Compression Crush Strength (ton/3.5 mm width)	0.9	2.6	2.8	Compression load when anti-corrosive layer breaks.

Table 4. COMPARISON BETWEEN ANTI-CORROSIVE WIRES BEFORE AND AFTER UNDERSEAS IMMERSION

Test Item	10 Months After Immersion	
	A	B
Bonding Strength (kg)	150	133
Abrasion Resistance (number of times)	9	6
Scratch Resistance (number of time)	479	372
Compression Crush Strength (ton)	2.8	2.8

Notes : A : with outer serving
B : without outer serving

fibre and jute fibre, was considered one solution of the problem. It has high tensile strength and excellent anti-rotting characteristics, but it is rather costly. As an improved solution, polypropylene split yarn has been brought into consideration. It is made of an abrasion resistant polypropylene compound. A stretched PP film is split mechanically to form meshes, like a net, then it is twisted into yarn. Figure 5 indicates relation between yarn weight (denier) and breaking strength. Also, abrasion resistances of different yarns are shown in Figure 6. It was estimated that a yarn weight of over 10,000 deniers is necessary to meet mechanical strength requirements. Use of two- or three -ply yarn was studied for its increased abrasion resistance. From an economical consideration, however, single ply yarn of 12,000 or 15,000 deniers was finally used for outer serving and that of 10,000 deniers for bedding.

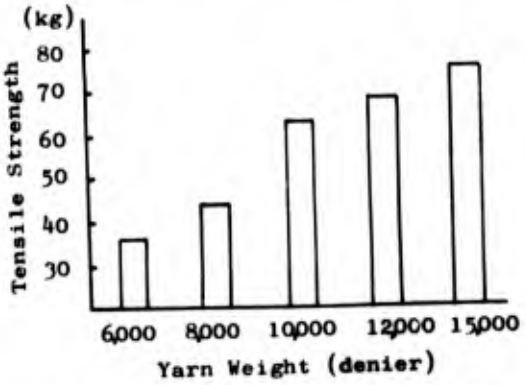

Figure 5. Tensile Strength vs. Yarn Weight

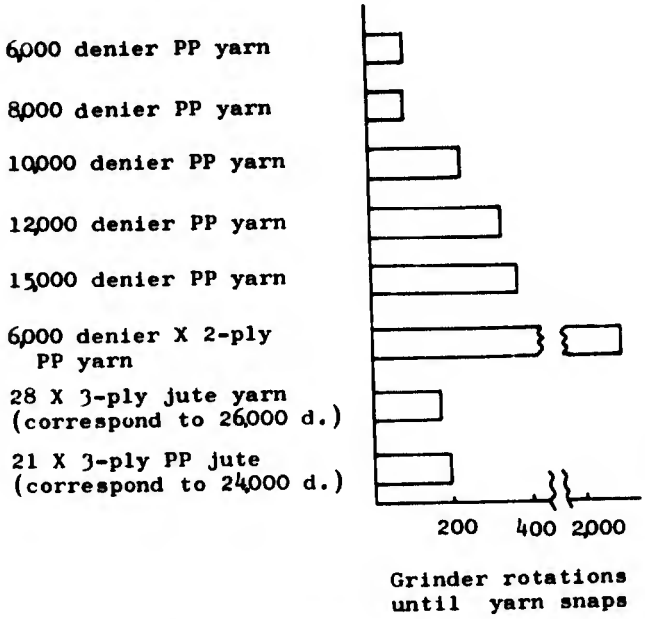

Figure 6. Abrasion Resistance of Yarns

2) Flooding Compound

Flooding compound used for PP yarn outer serving is required to only act as a bonding agent between PP yarn and armor wires, but not as a rot resistant. Conventional tar -pitch type compound proved not to bond firmly enough with PP yarn. It is also attended with environmental pollution difficulties. A new flooding compound consisting of olefinic polymer, was developed to meet the requirements.

Properties of new compound are contrasted with conventional ones in Table 5. Its softening point was determined to be so high that it does not become sticky at higher temperature environments. The new compound, light brown in color, dirties laying operators and laying gears very little.

Table 5. FLOODING COMPOUND PROPERTIES

Compound	Softening Point (°C)	Penetration (25°C,100g) (0.1 mm)
New Compound	155	25
Tar-pitch Type Compound	43	160
Asphalt Type Compound	53	30

3) Mechanical Characteristics of Armor

Two mechanical tests, Squeeze crush test and Drag abrasion test, were made on the armored cable to check protection effect of the armoring.

a) Squeeze crush test

As shown in Figure 7, the test cable is wound around a fixed iron cylindrical pole 240 mm in diameter at an angle of 45 degree. The cable is given a reciprocating sliding motion under a specified tension of three tons. Appearance of cable surface is checked to determine how it is subject to damage due to crushing on the iron pole surface. The actual number of repeated motions causing breaking of outer serving and exposure of armor wires was checked. Table 6 shows test results on three kinds of cables differing in outer serving layer.

b) Drag abrasion test

Test cables are dragged on a concrete road to test abration characteristics of the cable. The same three kinds of cables as those used for Squeeze crush test were tested.

These tests proved that the new design of outer serving is much superior in protection effect to the conventional type outer serving consisting of jute yarn and tar-pitch type flooding compound. It was also proved that the combination of PP yarn and asphalt

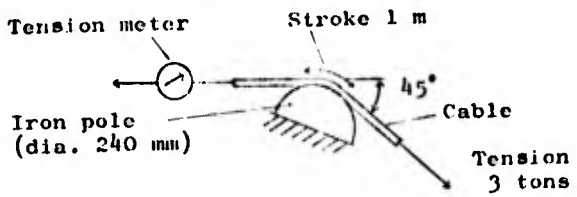

Figure 7. Squeeze Crush Test

type compound is a little inferior in effect to the newly designed serving. Tnis comes from the weaker adhesion characteristics between yarn and compound.

Table 6. SQUEEZE CRUSH RESISTANCE OF OUTER COVERING

Outer Covering	Drawing Times Till Coverings Break
PP Yarn/New Compound	9
PP Yarn/Asphalt Type Compound	6
Tarred Jute / Tar-pitch Type Compound	2

Actual New Cable Use

The first trial cable was laid in October, 1972. Since then, about 24 km of new cable (nine sections) were laid by July, 1974. All the cables have been kept in good operation, except that one length of cable was damaged by a ship anchor. Besides, the new type of cable armoring has been used for a trunk submarine coaxial cable 108 km in length (two sections).

Conclusion

Improvements and backgrounds have been described for new multi-pair submarine cable consisting of jelly filled core, anti-sulfurizing barrier and anti-corrosive armoring. New cable has been widely applied in Japanese waters. It is expected that the new cable will reduce the failure rate and also the length of replacement cable needed for failure repair.

Kinya Suzuki
Nippon Telegraph and Telephone Public Corp.
1-1-6 Uchisaiwai-Cho,
Chiyoda-ku, Tokyo,
Japan

Dr. Kinya Suzuki, Staff Engineer of the Engineering Bureau, NTT, is responsible for the research and development of submarine coaxial cable systems and submarine cable burying system. He received his D.E. degree from Kyoto University in 1960. Dr. Suzuki is a member of the Institute of Electronics and Communication Engineers of Japan, of the Institute of Electrical Engineers of Japan, and of the Institute of Engineering on Ocean Environment, International Electronics and Electrical Engineering.

Ryozo Sawada
Ocean Cable Co., Ltd.
1 Deta-Machi,
Kanagawa-ku, Yokohama,
Japan

Ryozo Sawada is Section Chief of Research and Development Laboratory, Ocean Cable Co., Ltd., and is mainly engaged in the research and application of materials for telecommunication cable. He received his B.E. degree in industrial chemistry from Shizuoka University in 1955, and is a member of the Society of Polymer Science of Japan, and the Institute of Electronics and Communication Engineers of Japan.

NEW COPPER DEACTIVATOR FOR POLYOLEFINS

by

K. YAMAGUCHI, T. YOSHIKAWA, H. KISHI
M. MASAKI and N. SAKAMOTO
Ube Industries, Ltd.
Tokyo, Japan

SUMMARY

As a consequence of screening tests of many chemical substances, two new chemical compounds designated as 3J-15 and 3J-26 have been found to be efficient copper deactivators for polyolefins. They do not impair the physical and electrical properties and appearance of polyolefin insulations.

Various tests on them proved that they prolong the lives of polyolefin insulations more markedly than a typical one of conventional copper deactivators. The results of DSC and other tests indicate that both of the new copper deactivators are particularly effective for polyolefins which contain cupric ion in high concentrations.

It is noteworthy that both deactivators exhibit a remarkable synergism when they co-operate with antioxidant. They can significantly lengthen the weathering lives of polyolefin insulations as measured by weather-o-meter.

INTRODUCTION

It has been shown recently that premature failure of polyolefin insulations of telephone cables is largely due to the copper-catalyzed oxidative degradation of polymeric substances. To minimize this effect, therefore, it is proposed to apply copper deactivators to polyolefin insulations. In the United States it is considered that incorporations of selected copper deactivator into polyethylene or polypropylene is essentially necessary to adopt the optimum design of persistent cable insulations.

From practical point of view, however, the copper deactivator has to satisfy following essential requirement; it is highly copper-deactivating but does not impair the insulating properties of polymers; it is not lost by migration even when the polymer insulation is exposed to a warm ambient temperature for a long period of time; and it is resistant to extraction by water or petroleum-jelly to which the polymer insulation might be exposed in the jelly-filled cable.

Pusey, Chen and Roberts[1] presented a paper before the 20th International Wire and Cable Symposium to discuss the field failure of low density polyethylene telephone cables within the splicing enclosure and referred to the degradative effect of copper conductor. This study was followed by a very detailed report of Howard[2] at the 21st Symposium. He analytically studied the premature brittle failure of low density polyethylene telephone cable insulations in terms of interaction of a number of variables of which involvement of copper in oxidative degradation was emphasized.

At the 22nd Symposium the authors[3] made a brief mention of the compounds which showed a considerably excellent copper-deactivating effect of polyethylene insulations. The present paper describes the copper-deactivating properties of two new compounds which evolved from the former reagents by further modification. The compounds we deal with in this article are effective for low density polyethylene, high density polyethylene and polypropylene in the presence of metallic copper or cupric ion.

EXPERIMENTALS

Base Polymer

The polyolefins used for the preparation of the samples are given in Table 1.

Table 1 The polyolefins* used for the evaluation of copper deactivators.

	Low Density Polyethylene	High Density Polyethylene	Polypropylene**
Melt Index	0.25	0.30	3.0
Density	0.926	0.947	0.90

* Stabilized by a maximum irreducible amount of antioxidant.
** Ethylene-propylene block co-polymer.

Sample Preparation

Blending of additives into the polyolefins was carried out in a Brabender Plastograph.

The film (0.25 mm) and copper screen laminate (1.0 mm) of polyolefin were formed by compression at 190°C under a pressure of 300 Kg/cm^2. The polyolefin insulated conductors (26 AWG) were also prepared. The pig tail specimens were made conventionally from the insulated conductors and were subjected to thermal stress cracking test.

DSC Measurement

The DSC apparatus of Rigaku Denki Ltd. equipped with an oxygen supply line was used. The induction period of the onset of exothermic peak due to oxidation was measured for the film of polyolefin at 200°C in oxygen.

Aging and Weathering Tests

Aging tests were performed for film, laminate or insulated wire in an oven heated at a constant temperature by hot air circulation.

Weatherability was measured by a weather-o-meter furnished with xenon lamp at a black panel temperature of about 60°C with intermittent spray of water.

The aging or weathering performance is expressed by the time of resistance to the onset of brittleness on the film or insulation.

Oxygen Uptake Test

The oxygen uptake of insulated conductor was measured by the volumetric method.

RESULT AND DISCUSSION

Effect of copper deactivator on the properties of polyolefins

In Table 2 are given the properties of our copper deactivators, i.e., 3J-15 and 3J-26. Their effect on the properties of polyolefins are also given.

Both of them are innoxious, white powder with a sharp melting point and hardly soluble in water or organic solvents. They give no adverse effect to processability of polyolefins and cause no discoloration. The electrical properties of polyolefins containing them are satisfactory for cable insulation and comparable with the values in the parentheses for a commercial copper deactivator known as highly effective and designated as MDA-1 throughout in the present paper.

Table 2 Properties of the new copper deactivators and the polyolefins containing them.

Property of copper deactivator		3J-15	3J-26	
Melting point (°C)		253	193	
Color		white	white	
LD_{50} (g/Kg)		> 24.13	> 7.03	
Properties of polyolefins containing the copper deactivator		**3J-15**	**3J-26**	**MDA-1**
LDPE*	$\tan\delta \times 10^6$	66	63	(65)
	ε	2.28	2.28	(2.28)
HDPE**	$\tan\delta \times 10^6$	62	69	(56)
	ε	2.32	2.32	(2.32)
PP***	$\tan\delta \times 10^6$	158	170	(153)
	ε	2.24	2.24	(2.24)
Surface of insulation		excellent		
Color and odor		no	no	no
Processability		excellent		

* Low density polyethylene with 1000 ppm of Irganox 1010 and 1000 ppm of copper deactivator.
** High density polyethylene with 1000 ppm of Irganox 1010 and 1000 ppm of copper deactivator.
*** Ethylene-propylene co-polymer with 4500 ppm of Irganox 1010 and 3500 ppm of copper deactivator.

Loss tangent and dielectric constant were measured at 1 MHz.

Low density polyethylene

The induction periods of the low density polyethylene films measured by DSC at the temperature of 200°C in a stream of oxygen are shown in Figs. 1 and 2.

Fig. 1 shows the relation between the induction period and the amount of cupric stearate added to the polyethylene which contains 1000 ppm of the antioxidant Irganox 1010. As shown in the figure, the addition of 500 to 1000 ppm of cupric stearate to the polyethylene sharply reduced the induction period. Zero induction period was obtained when 1000 ppm of cupric stearate was added.

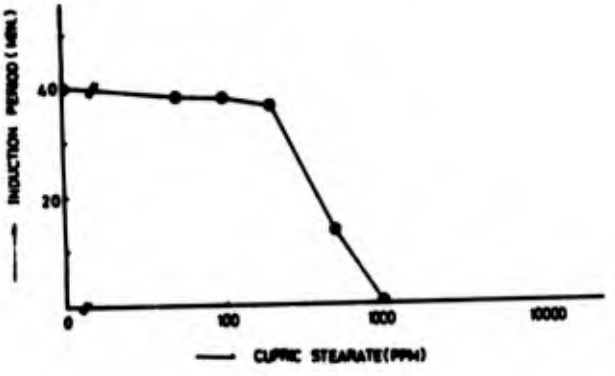

Fig. 1 Effect of cupric stearate on DSC induction period of low density polyethylene with 1000 ppm of Irganox 1010.

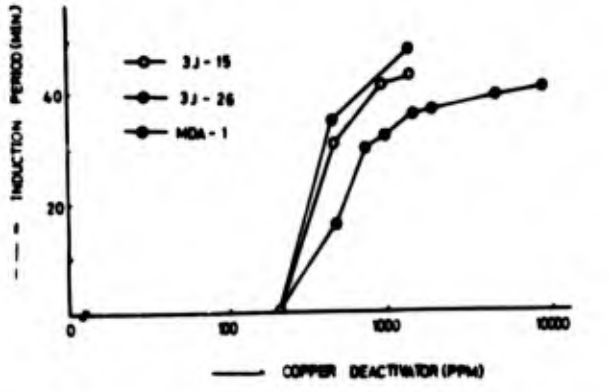

Fig. 2 Effect of copper deactivator on DSC induction of low density polyethylene with 1000 ppm of Irganox 1010 and 1000 ppm of cupric stearate.

Fig. 2 shows the revival of the induction period of the polyethylene whose induction period was once reduced to zero by addition of 1000 ppm of cupric stearate. It is seen that the copper deactivators revive the lost initial induction period and raise it up to about 40 minutes. About 1000 ppm of either 3J-15 or 3J-26 is sufficient to regain the initial induction period, whereas more than 5000 ppm of MDA-1 is necessary to revive the stability of copper-free polyethylene.

Fig. 3 shows the induction periods for low density polyethylene samples free from copper, which contain Irganox 1010 (1000 ppm) and various amounts of the copper deactivators. The figure shows that no perceptible change in induction period is observed when copper substrate is absent. This means that the copper deactivators are not harmful to copper-free polyethylene.

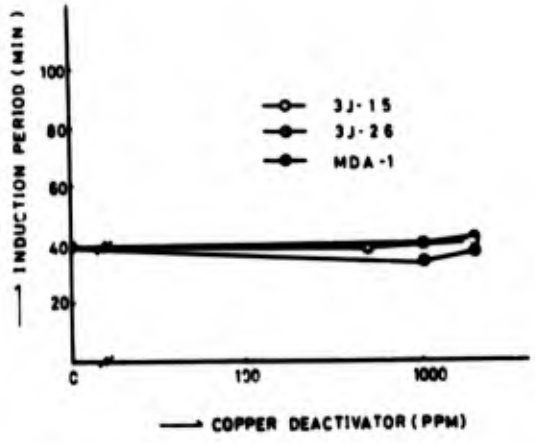

Fig. 3 Effect of copper deactivator on DSC induction period of low density polyethylene free from copper, containing 1000 ppm of Irganox1010.

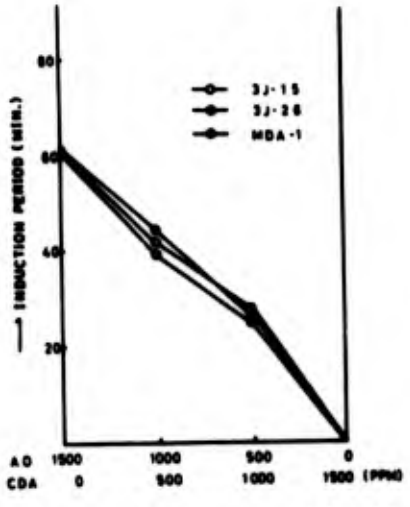

Fig. 4 Irganox 1010 (A.O.): Copper deactivator (C.D.A.) ratio versus DSC induction period of low density polyethylene free from copper

Of interest is the interaction between antioxidant and copper deactivators. In the absence of cupric ion, copper deactivators little improve the aging performance of polyethylene. This is true even when the antioxidant is present. The induction period changes nearly linearly with the quantity of antioxidant as shown in Fig. 4. The effects of antioxidant and copper deactivators are, therefore, assumed to be simply additive, indicating that there is no interaction between two stabilizers.

Strikingly different are the results when the polymer contains 1000 ppm of cupric stearate, as given in Fig. 5 in which the content of Irganox 1010 plus that of copper deactivator is kept constant at 2500 ppm, but the ratio between both additives is varied.

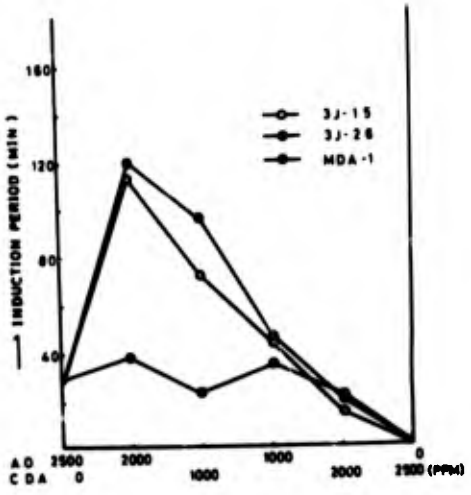

Fig. 5 Irganox 1010: copper deactivator ratio versus induction period of low density polyethylene containing 1000 ppm of copper stearate.

The plot of induction period versus stabilizer ratio is no more linear. Remarkable sensitizing (or synergistic) effect is observed between 3J-15 and Irganox 1010, as well as between 3J-26 and Irganox 1010. A sharp peak of induction period appears at A.O. : C.D.A. ratio of 200 : 500. This means that the optimum ratio of Irganox 1010 to 3J-15 or 3J-26 would lie near 4 : 1.

On the other hand, the synergistic effect is scarcely recognizable in the combination of Irganox 1010 and MDA-1.

Fig. 6 gives the induction periods of oxygen uptake of the low density polyethylene insulated conductors measured at 180°C in oxygen atmosphere. It is seen that the copper deactivators considerably prolong the induction period, as deduced from the comparison with the control sample which contain no copper deactivator; the induction periods of the samples stabilized by 3J-15 and 3J-26 are as long as 3 and 4 hours, respectively, while that of control sample is only 12 minutes.

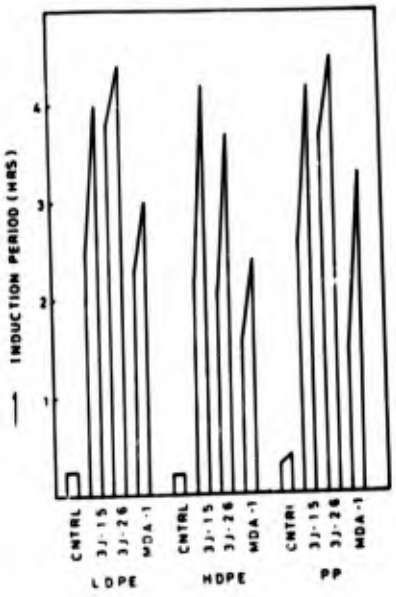

Fig. 6 Effect of copper deactivator on induction period of oxygen uptake at 180°C on polyolefin insulated conductors.

Polyethylene :	Irganox 1010	1000 ppm
	Copper deactivator	1000 ppm
Polypropylene:	Irganox 1010	4500 ppm
	Copper deactivator	3500 ppm
Control :	Irganox 1010	
	1000 ppm (polyethylene)	
	4500 ppm (polypropylene)	
	Copper deactivator	none

The aging test of pig tail specimens of the insulated conductors mentioned above in a circulating air oven at 100°C is now being carried out. Thus far, no thermal stress cracking has been observed after 2000 hours of aging.

High Density Polyethylene

The possible interaction between antioxidant and copper deactivator was studied with high density polyethylene containing various quantities of cupric stearate, in a similar manner to the case of low density polyethylene.

Fig. 7A to 7C show the induction periods of high density polyethylene containing 500 to 4000 ppm of cupric stearate. They are stabilized by the combination of Irganox 1010 with copper deactivator whose total content is constant (4000 ppm) but their ratio is changed.

The figures show that the combination of Irganox 1010 with either 3J-15 or MDA-1 exhibits a remarkable synergistic effect for high density polyethylene, but the effect of 3J-15 is always superior to that of MDA-1. Except for the case where the concentration of cupric stearate is extremely high (4000 ppm), the optimum composition (A.O. : C.D.A. ratio) is seen in the range from 3 : 1 to 7 : 1.

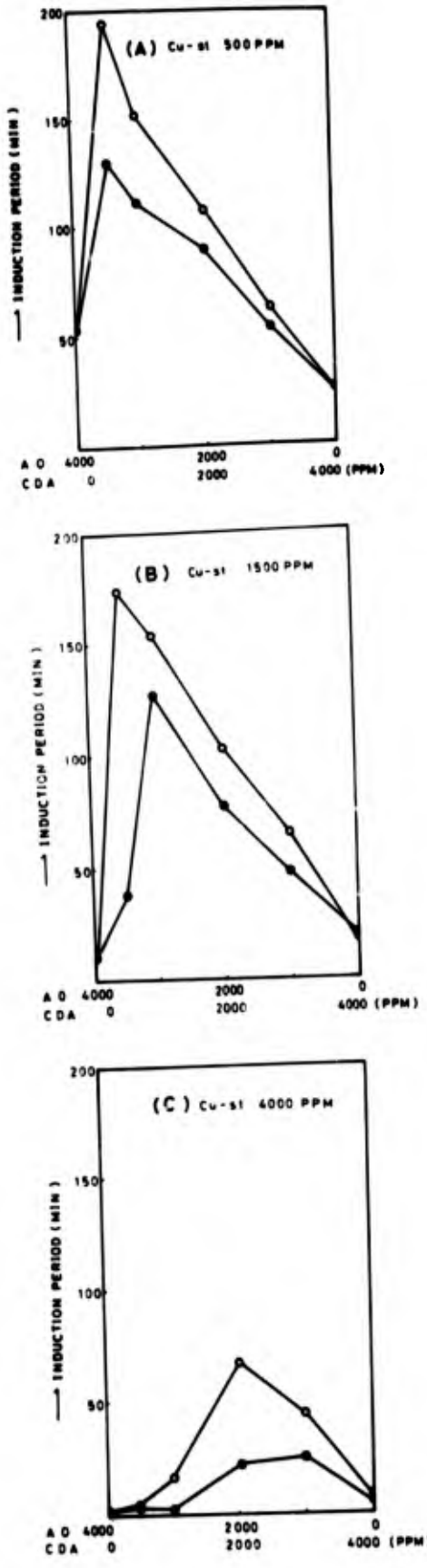

Fig. 7 Irganox 1010 (A.O.) : Copper deactivator (C.D.A.) ratio versus DSC induction period of high density polyethylene containing various amount of cupric stearate.

The stability in oxygen atmosphere of high density polyethylene insulated conductor was already referred to in Fig.6. The induction period of samples stabilized with 3J-15 or 3J-26 is about 3 to 4 hours in contrast to the control sample whose induction period is as small as 12 minutes.

The aging test of pig tail specimens of insulated conductor is being carried out in a similar way to that of low density polyethylene. No thermal stress cracking has been observed at 2000 hours of aging.

With a view to estimating the stability of jelly-filled polyolefin insulated conductors, the samples were dipped in hot (85°C) petrolatum for 18 hours, wiped and then placed in an air oven kept at 100°C. As given in Table 3, in contrast to the life of 6 days for the control (no copper deactivator), the sample stabilized with 3J-15 or 3J-16 give the longer aging life, i.e., 16 and 18 days, respectively.

Table 3 The aging life (100°C) of high density polyethylene insulation after contact for 18 hours with petrolatum heated at 85°C.

Copper deactivator	control	3J-15	3J-26	MDA-1
Aging life (days)	6	16	18	14

Polypropylene

The synergistic effect of the Irganox 1010 copper deactivator combination for polypropylene was measured by the aging test performed at 150°C with the films of polypropylene containing either cupric stearate or copper dust. The amount of the additives in total was kept at a constant value.

Fig. 8 shows the results of experiments with the system in which cupric stearate (1000 ppm) is the copper source. It is seen that both 3J-15 and MDA-1 exhibit the synergistic effect when combined with Irganox 1010, the optimum ratio of A.O. to C.D.A. spreading in a wide range between 3 : 1 to 1 : 3.

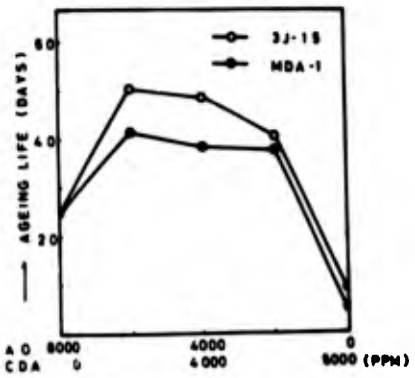

Fig. 8 Irganox 1010 : Copper deactivator ratio versus aging life (150°C) of polypropylene containing 1000 ppm of cupric stearate.

The results of experiments made with samples containing copper dust (1.5 phr) are shown in Fig. 9. Both 3J-15 and 3J-26 combined with the antioxidant display a synergistic effect, the optimum ratio of A.O. to C.D.A. being around 3 : 1 in each case.

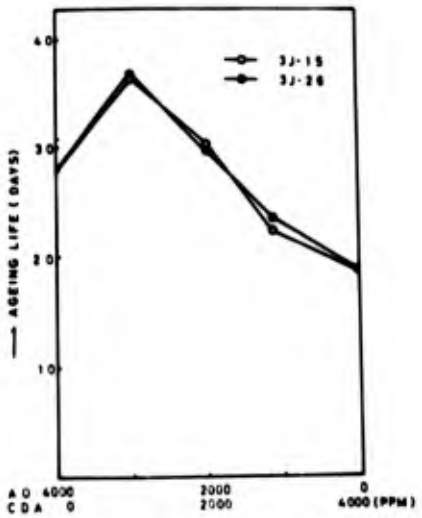

Fig. 9 Irganox 1010 : Copper deactivator ratio versus aging life (150°C) of polypropylene containing 1.5 phr of copper dust.

The samples of polypropylene containing Irganox 1010 and copper deactivators in four different ratios were prepared and subjected to aging and weathering tests ; the compositions of stabilizer pairs are given at the bottom of Fig. 10.

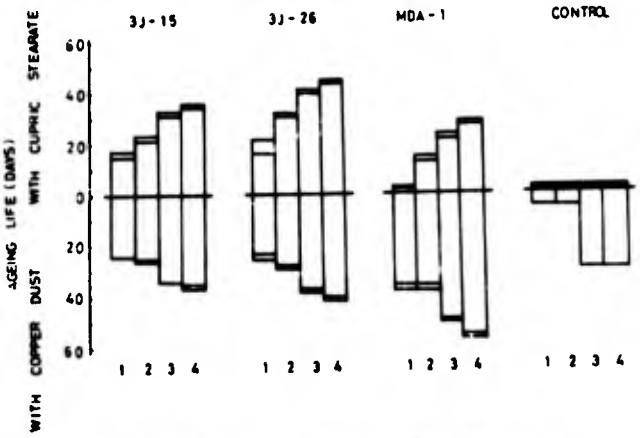

Fig. 10 Aging life of polypropylene samples containing cupric stearate (3000 ppm) or copper dust (1.5 phr) stabilized by the combination of Irganox 1010 (A.O.) and copper deactivator (C.D.A.) in the ratios of ;

1.	A.O.	1000 ppm	C.D.A.	3000 ppm
2.	A.O.	1000 ppm	C.D.A.	5000 ppm
3.	A.O.	4000 ppm	C.D.A.	3000 ppm
4.	A.O.	4000 ppm	C.D.A.	5000 ppm

Fig.10 shows the result of the aging tests. It is seen that all of the copper deactivators are effective in lengthening the aging life of the polypropylene samples containing copper. In the presence of cupric stearate, 3J-15 and 3J-26 display markedly superior effect to that of MDA-1. Since the aging life for the control (containing only cupric stearate) was found to be always nearly zero, it may be assumed that both 3J-15 and 3J-26 possess the ability to stabilize the polypropylene insulation which is highly contaminated with cupric ion.

Fig.11 gives the result of the weathering test for the polypropylene samples which contain the antioxidant, copper deactivator and the copper source. Their amounts are the same as are given in Fig. 10. It is shown that both 3J-15 and 3J-26 exhibit a high ability to give a long weathering life to polypropylene which contains either copper dust or cupric stearate. As shown in Fig. 11, the polypropylene samples which contain cupric stearate are stabilized by 3J-26 to such an extent that failure has not been observed even after 60 days of weathering.

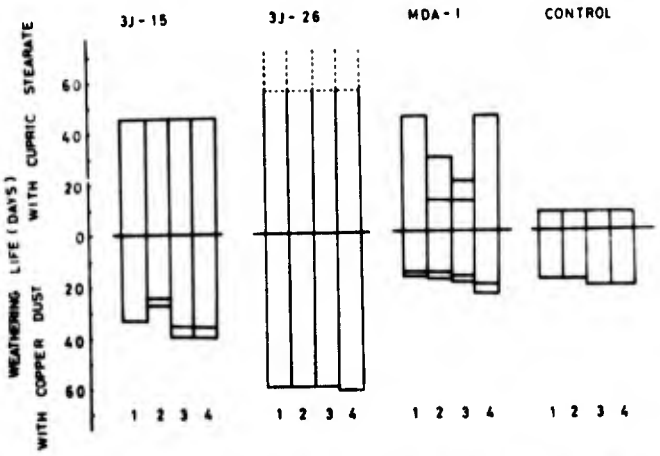

Fig. 11 Weathering life of polypropylene samples containing Irganox 1010 and the copper deactivator. Their amounts are the same as given in Fig. 10.

The oxygen uptake experiment of insulated conductor as already referred to in Fig.6, shows that the polypropylene insulation containing 3J-15 or 3J-26 affords the induction period of about 3 and 4 hours, respectively in contrast to 12 minutes for the control.

The aging test of pig tail specimens of polypropylene insulated conductor is being carried out in a similar way to that of polyethylene insulations. At 2000 hours of aging, no indication of thermal stress cracking on the insulations has been observed.

The resistance of the copper deactivators against extraction from polypropylene insulation by hot petrolatum is demonstrated by the results given in Table 4. A series of experiments was run to confirm the effect of antioxidant added to petrolatum. It was proved that the polypropylene insulation containing 3J-15 keeps the longest aging life in both series.

Table 4 Aging life (100°C) of polypropylene insulation after contact for 18 hours with petrolatum heated at 85°C.

Copper deactivator	control	3J-15	3J-26	MDA-1
Aging life (days)				
Series A*	4	10	6	7
Series B**	6	17	7	15

* Reagent grade petrolatum was used.
** Petrolatum containing 0.5% of Irganox 1010 was used.

Table 5 shows the result of the aging test of the copper screen-polypropylene laminate in the oven heated at 200°C. The laminates stabilized by Irganox 1010 - 3J-15 or Irganox 1010 - MDA-1 are not degraded by this procedure.

Table 5 Aging test of copper screen - polypropylene laminate at 200°C for one hour

Additives (ppm)			Result of test
Irganox 1010	3J-15	MDA-1	
-	4000	-	failed
1000	3000	-	not failed
2000	2000	-	not failed
3000	1000	-	not failed
-	-	4000	failed
1000	-	3000	not failed
2000	-	2000	not failed
3000	-	1000	not failed

CONCLUSION

The newly developed copper deactivators 3J-15 and 3J-26 exceedingly stabilize the polyolefin insulations against the copper induced oxidative degradation as demonstrated by various laboratory tests. Very small amount of 3J-15 or 3J-26 is sufficient to check the effect of copper when an antioxidant such as Irganox 1010 is present since both copper deactivator and antioxidant form a synergistic system. One of the striking characteristics of 3J-15 and 3J-26 is ability to improve the weatherability of copper-containing polyolefins.

The long-term aging test at lower temperatures and the natural weathering test are being undertaken.

REFERENCES

1) B.B. Pusey, M.T. Chen and W.L. Roberts, Proc. 20th Int. Wire and Cable Symp., 209-217 (1971)
2) J.B. Howard, Proc. 21st Int. Wire and Cable Symp., 329-341 (1972)
3) K.Yamaguchi, S. Hoshino, H.Kishi, T. Nagasawa and H. Harakawa, Proc. 22nd Int. Wire and Cable Symp., 30-37 (1973)

Koji Yamaguchi
Ube Industries, Ltd.
7-2, Kasumigaseki 3-chome,
Chiyoda-ku, Tokyo, Japan

Koji Yamaguchi was born in 1925. He received his B.S. degree in fuel engineering from Kyoto University in 1949. He joined Ube Industries, Ltd. in the same year and worked for 10 years at the Central Research Laboratory in Ube, then for three years at the Department for Planning in Tokyo. In 1963, he joined the construction of Ube's first high pressure polyethylene plant in Chiba as the assistant manager in techincal division. Since then he has been the chief of the research and development activities of UBE polyethylene and polypropylene. He is presently the manager of technical division of polyethylene and polypropylene.

Hidehiro Kishi
Ube Industries, Ltd.
7-2, Kasumigaseki 3-chome
Chiyoda-ku, Tokyo, Japan

Hidehiro Kishi was born in 1935. He received a B.S. degree in applied chemistry from Kyushu University in 1959 and joined Ube Industries, Ltd. in the same year. Initially he worked at Ube Fertilizer plant. He has been engaged in the research and development of high pressure polyethylene since 1963. He is presently an assistant manager of polyethylene and polypropylene technical department.

Toshio Yoshikawa
Polymer Research Laboratory
Ube Industries, Ltd.
Ichihara City, Chiba, Japan

Toshio Yoshikawa was born in 1933. He received a B.S. degree in applied chemistry from Nagoya University in 1956 and joined Ube Industries, Ltd. at the same year. Initially he worked at the Central Research Laboratory and he is now a chief researcher of Polymer Research Laboratory. Since joining Ube Industries, Ltd., he has been working mainly in the field of organic synthesis. He published several papers in this field and holds many patents on stabilization of polymers.

Mitsuo Masaki
Polymer Research Laboratory
Ube Industries, Ltd.
Ichihara City, Chiba, Japan

Mitsuo Masaki was born in 1937. He received his B.S. in 1959 from Yokohama National University, and M.S. in 1961 and Ph.D. in 1964 from Tokyo Institute of Technology, respectively. He had done researches in the field of organic chemistry until 1968, when he joined Ube Industries as a chief researcher of Polymer Research Laboratory wherein he has been working in the same field. He is a member of Japanese, German and American chemical societies. He has published many papers on the journals of these societies, and holds several patents.

Nagayoshi Sakamoto
Polymer Research Laboratory
Ube Industries, Ltd.
Ichihara City, Chiba, Japan

Nagayoshi Sakamoto was born in 1941. He received a M.S. degree in applied chemistry from Hiroshima University in 1967 and joined Ube Industries, Ltd. at the same year. Initially he worked at the Central Research Laboratory. He is now a research staff of the Polymer Research Laboratory. Since joining Ube Industries, He has been working in the field of stabilization of polyamide and polyolefins and holds several patents on polymer stabilization.

CIRCULAR/PLASTIC--A NEW GENERATION OF CONNECTORS

Patrick Lannan
AMP Incorporated
Harrisburg, Penna.

Abstract

In describing a new family of all-plastic circular connectors, this paper demonstrates how a combination of materials and geometry can lead to better overall connectors with increased reliability for a wide variety of applications. Although this is the only family of all-plastic circular connectors on the market today, it is the forerunner of a new concept in commercial connectors that combine the desirable advantages of cylindricals with the cost and weight advantages of plastic-bodied connectors.

The connectors described are molded from heat-stabilized, flame retardant, Se-1 thermoplastic, and have built-in contact protection, positive keying, etc. Both sealed or unsealed versions for panel mounting or free hanging applications are covered, as are standard and reverse sex versions as well as pressurized bulkhead feed throughs. The stamped-and-formed crimp-type contacts accept wires from AWG #8 to #28 and either pins or sockets snap readily into either plug or receptacle housings. Screw machine and solder contacts are also discussed.

A technical paper about an all-plastic circular connector family brings up an interesting pair of questions--why circular and why plastic?

Why Circular?

An easy way out of this question is to state that these connectors are circular because circular connectors are the single most widely used multi-pin connectors in the electrical and electronic industry.

Naturally, there are some very sound reasons for this popularity. One of these reasons is the very favorable weight-to-strength ratio that the circular shape has over other geometric forms.

Another benefit is that the standard rotating coupling mechanism of circular connectors eliminates the need for separate jackscrew hardware. Also, the inherent mechanical advantage found in rotating couplings eliminates the need for additional mechanical devices as the contact densities increase and the mating and unmating forces become greater.

Perhaps one of the most attractive advantages of circular connectors is their versatility. They can be modified and changed to a considerable extent without destroying their basic "standard" characteristics.

Why Plastic?

Naturally, circular plastic connectors cannot be judged "better" when used in applications or environments where metal is essential. But plastic does have considerable advantage over metal in connectors where weight-savings is a prime or even secondary design consideration. Molded plastic connector housings are less expensive to fabricate than their metal counterparts, and modern plastics have the strength and durability of metal in many cases and can stand some fairly hostile environments as well.

The light weight of the plastic, which is less than 50% of the weight of an equivalent metal shell connector, is also of benefit in many applications.

The Need

A great many industrial and commercial applications require a connector that is better than the inexpensive soft shelled connectors used in the appliance industry, yet these applications do not require connectors built for use in a military environment. In the past, it has been necessary to use these metal shell connectors designed primarily for military and aerospace applications, as these were the only choice for a connector to meet the reliability requirements. The plastic connector described in this paper is designed specifically for these high reliability commercial and industrial applications. The first requirement was to design a low-cost light-weight connector that would satisfy these commercial and industrial requirements without sacrificing performance and reliability. An additional constraint was that the connectors should have the same ease of use by customers as the standard metal cylindrical connectors, including the features of minimum number of parts, cable clamps, etc. The result was a product line known as the CPC connectors or the Circular Plastic Connector family illustrated in Figure 1. The fact that these connectors are currently used in aircraft, trucks, tractors, farm machinery, computers, computer peripherals, business machines, television sets, test equipment, etc. is an indication that needs for this type of connector exist in the commercial and industrial marketplace.

Figure 1. The Circular Plastic Connector Family.

Connector Body

The most obvious difference between these connectors and the military versions is that the construction is completely of plastic. The bodies are made of glass-filled nylon which is rugged and resistant to many types of chemicals. The coupling ring is also made of a resilient thermal plastic and the back shell strain relief is made from the glass-filled nylon. These materials are not only resistant to corrosion, but are very rugged. When one of our Field Engineers ran over a mated pair of connectors with a truck having dual wheels, the connectors remained operable. This is a severe test for any connector either metal or plastic.

In order to furnish effective keying five individual keys are provided to prevent mismating. Clocking is not provided, but inter-contact keying is provided in all the connector series. This provides a great deal of flexibility when many connectors are used in the same area.

A square buttrus type thread was chosen for the coupling ring rather than fine threads or a bayonet coupling. Bayonet couplings are notorious for their failures under vibration and fine threads take too many turns to provide full connector engagement. This coupling ring has two thread segments 180^{0} opposed to provide the mechanical advantage to engage and disengage the connector. With a double lead thread design, it requires that the coupling ring be rotated not more than 1/2 turn to begin thread take-up. This ring is also positioned on the plug such that the plug body must enter into the receptacle and have the proper alignment prior to thread engagement. This prevents the possibility of cross plugging the connector and thereby protects the pins in the receptacle from possible damage. This has proven to be an excellent compromise between bayonet and threaded type couplings. A readily felt detent is incorporated to provide a locking action and ensure full connector engagement.

One of the design goals was to minimize the role of the end user. In the Series I and III connectors the body and the mounting flange and housing is all one piece instead of the separate insert and shell arrangement of standard circular connectors. In the Series II connectors, two moldings are required to provide the inner geometry required for the rear release feature. However, these are bonded together at the factory and so as far as the user is concerned, it is still one piece.

The pin contacts, which are generally agreed to be the most vulnerable component in an electrical connector system, are protected in the receptacle housing by a skirt which extends from the mating face of the connector and completely encircles the pin contacts. This skirt extends about 1/8" beyond the pin tips so that a foreign object must penetrate into the receptacle area to damage the contacts. We believe this feature is essential even in commercial environments.

The skirt's five keys ways for polarization, further ensures contact protection. These key ways, in conjunction with the corresponding keys in the plug, ensure that the two connector halves are in perfect alignment before the possibility of a pin and socket engaging or even touching each other.

Circuit identification is provided by raised molded-in numerals on the rear face of the connectors and on the mating faces.

These connectors are recognized under Underwriters Laboratories Incorporated, component recognition program and are CSA approved. The product line has been submitted for VDE and other foreign approvals.

The field versions of this connector use the same components as the unsealed version. An "O" ring is used for a circumferential seal to protect the contact interface when the connector is mated. A neoprene boot is used to protect the rear of the male or female plug when a jacketed cable is used. This has been tested for operation under 30" of water for one hour. Rear individual wire seals and cable seals with strain relief will be available in the future.

Configurations

Four shell sizes currently form the basis of this connector family. These are shell size 11, size 13, size 17 and size 23. The shell sizes as in metal circulars are based on the diameter of the body in 1/16ths of an inch as indicated in Figure 2.

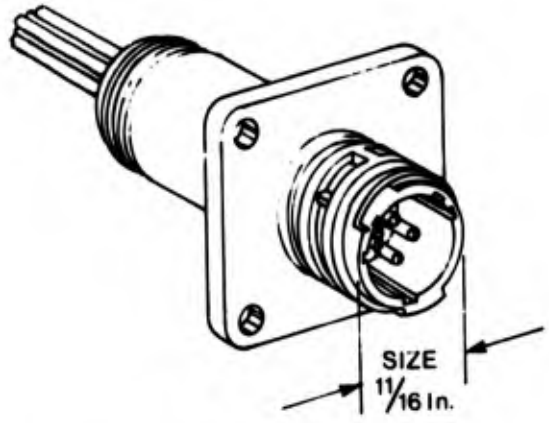

Figure 2. Shell sizes are based on body diameter.

This range of sizes allows for connectors with from 3 to 63 contacts. The best method of presenting sizes is to define one series of connectors at a time. The Series I standard density connector or 13 ampere contact types have the following sizes available:

Size 11	-	4 contact
Size 13	-	9 contacts
Size 17	-	16 contacts
Size 23	-	37 contacts

The reverse sex versions of this connector series are:

Size 11	-	4 contacts
Size 17	-	14 contacts
Size 23	-	37 contacts

The Series II or 7 1/2 ampere contacts are high density rear release versions. These of course have a greater number of positions. The sizes currently tooled are:

Size 11	-	8 contacts
Size 11	-	9 contacts
Size 17	-	28 contacts
Size 23	-	63 contacts

The reverse sex versions of this series are the:

Size 11	-	8 contacts
Size 17	-	28 contacts
Size 23	-	57 contacts

Size 17-16 in the Series I has a reverse sex version that is a size 17-14 and the 23-73 in Series II has a reverse sex version of 23-57. This is necessary due to the area occupied when the sex of the contacts is reversed.

The Series III, or 35 ampere contact, versions have a more limited selection due to the space required. There are no connectors available in size 11 or 13 versions. The standard sex versions are:

Size 17	-	3 contacts
Size 23	-	7 contacts

The reverse sex versions of these connectors are the same as the standard sex or:

Size 17	-	3 contacts
Size 23	-	7 contacts

Of course, as with any product line, there are specials. Some of these are the 23-22. That is a shell size 23 with two power or 35 ampere contacts and 20, 13 ampere contacts. As this connector is used in the trucking and machine industry, the 13 ampere contacts accept #14 AWG wire with an insulation diameter of .150". Standard 13 ampere connector versions accept a wire insulation diameter of .125" in order to obtain higher density.

The 17-3C is a size 17 shell with one twinax contact for shielded unbalanced lines and two 13 ampere signal contacts.

Contacts

The performance of any connector is first dependent upon the contacts being reliable. This entails such elements as contact resistance, contact retention, contact life, conductor termination and insulation support. When designing the Circular Plastic Connectors it was decided to build a connector line based on proven contacts used in other large volume product lines rather than design new contacts. This not only takes advantage of the long history of proven contacts, but allows the user to introduce the product into his equipment using the same contacts he has been applying in his rectangular connectors. This obviates adding more engineering time, drawing numbers, testing and approvals. This standardization of contacts affects inventory, volume purchases, application tooling and field repair tooling.

For a complete connector family it is necessary to have contacts with a broad range of current carrying capabilities and different densities. As a result, three contact sizes were selected--a 7 1/2 ampere size, a 12 ampere size and a 35 ampere size. Each contact size was used to designate a series.

The first series uses the 13 ampere size 16 contact, which many of you know as MIL-C-28748 type. This is referred to as the III+ contact when it is stamped and formed and as the Type II contact when it is the screw machine equivalent. Both are front release crimp-snap-in contacts. The three retention tines ensure excellent contact retention. They are available with many plating options and cover a large range of wire sizes from #14 AWG through #30 AWG with insulation diameters up to .150 outside diameter. The platings available are tin-plated contacts, gold flash over all the contacts, selectively plated gold over nickel plate, and heavy gold over nickel plate. A new low cost one-piece stamped and formed contact is also available for this connector series. The series using this contact is designated as Series I or Standard Density.

The high density version was designed using contacts that are also available as screw machine contacts

Figure 3. Contacts for Series I Connectors.

(MIL-C-24308), stamped and formed versions, and stamped and formed versions with insulation support. All these contacts are interchangeably used with commercial and military versions of other connector families. These are 7 1/2 ampere contacts and are on approximately .109 centers and are known as the Series II connectors in the Circular Plastic Connector family.

Figure 4. Contacts for Series II Connectors.

The power connectors use a stamped and formed blade type contact rated at 35 amperes. Heat rise testing has indicated this contact can actually carry 48 amperes with a 30°C temperature rise. These are called Series III. Automatic application tooling has been well proven for all these contact types. This tooling includes bench type crimping machines, stripper crimpers and high speed AMPOMATOR machines for volume applications.

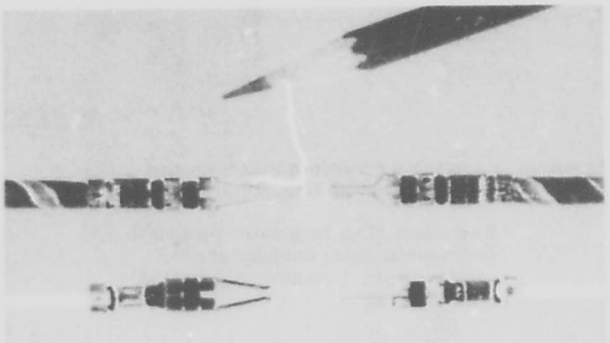

Figure 5. Contacts for Series III Connectors.

Metal vs. Plastic

This connector series was not designed to a military specification, but to an internal specification requirement. One of the connectors most commonly used in commercial applications are connectors built to MIL-C-005015E (Navy). The following chart shows a comparison of performance requirements of connectors to this specification when using crimped removable contacts and the circular plastic connectors specification.

MIL-C-005015E (NAVY)	Circular Plastic Connector 108-10024 (AMP)
Magnetic Permeability	
Test wired or unwired connectors with an instrument conforming to MIL-I-17214. Permeability shall be less than 2.0.	Not required.
Maintenance Aging	
Insert, remove and resinsert all contacts one time. Forces are measured. Mate and unmate connectors 10 times. Nine additional cycles of extraction/insertion on 20% of contacts. Insertion/removal force measured on half the contacts during the ninth cycle. Contact insertion and remc forces shall not exceed the value shown:	Insert, remove and reinsert all contacts one time. Mate and unmate the connectors 10 times. Nine additional cycles of extraction and insertion of 20% of contacts. Connectors must meet all subsequent test requirements. Purpose of procedure is to provide accelerated aging of the contacts, locking mechanism, coupling ring, etc., prior to environmental exposure.
Contact Retention	
Axial loads are applied to the mating end of individual contacts. Contact displacement is measured under load. Test is performed with cable clamps tightened and removed. The individual contacts shall withstand the specified loads without dislodging or having a displacement exceeding 0.025 inch.	All contacts that were subjected to 10 cycles of maintenance aging have an axial load applied to the mating end. Contact displacement is measured under load. Cable clamps are removed during test. The individual contacts shall withstand the specified loads without dislodging or having a displacement exceeding 0.012 inch.
Insulation Resistance	
Reistance is measured between adjacent contacts, unmated connectors, at room temperature. Resistance shall be greater than 5000 megohms at room temperature and greater than 1.0 megohm at elevated temperature.	Resistance is measured between adjacent contacts, connectors mated at room temperature. Resistance shall be greater than 5000 megohms.

Contact Size	Insertion/Extraction Force (Pounds, Maximum)
16	20
12	25
8	30
4	40
0	40

Contact Size	Axial Load (Pounds, Minimum)
16	25
12	25
8	40
4	50
0	50

Contact Size	Axial Load (Pounds, Minimum)
20	10
16	10
8	25

Dielectric Withstanding Voltage

The specified test potential is applied between adjacent contacts and the contacts and shell, connectors mated and unmated, at sea level and altitude.

Service Rating	Test Voltage (Volts-RMS) Sea Level	70,000 Feet
Inst.	1000	260
A	2000	360
D	2800	400
E	3500	440
B	4500	480
C	7000	560

No evidence of breakdown or flashover.

A test potential of 1200 volts RMS is applied between all adjacent contacts and the contacts and mounting hardware at sea level.

No evidence of breakdown or flashover. Leakage current shall not exceed 2 ma.

Thermal Shock

a. Connectors . . unmated.
b. Numbers of cycles . . 5.
c. Temperature extremes . . - 55°/+125°C.

No evidence of damage detrimental to connector operation.

a. Connectors . . mated.
b. Number of cycles . . 5.
c. Temperature extremes . . -55°/105°C.

No evidence of damage detrimental to connector operation.

Water Pressure

Mated connectors are immersed in tap water to a depth of 6 feet for a period of 48 hours. Insulation resistance is measured at the end of the 48 hours while immersed.

No evidence of leakage. Insulation resistance shall be 100 megohms or greater.

Mated connectors are immersed in tap water to a depth of 30 inches for a period of 1 hour. Insulation resistance is measured and a potential of 400 volts RMS applied for 5 minutes while immersed.

No evidence of leakage. No voltage breakdown or flashover. Insulation resistance shall be 1000 megohms or greater.

Durability

Connectors are mated and unmated 500 times with the coupling rings removed.

No evidence of damage detrimental to connector operation.

Connectors are mated and unmated 200 times as in service.

No evidence of damage detrimental to connector operation.

Vibration

a. Connectors . . mated.
b. Amplitude . . 15G's peak.
c. Frequency . . 10 to 2000 Hz.
d. Duration . . 12 hours.
e. All contacts wired in series with a current of 100 milliamperes flowing. Monitor for discontinuity of 10 micro-seconds or greater.

No physical damage nor loss of continuity of 10 micro-seconds or greater.

a. Connectors . . mated.
b. Amplitude . . 15G's peak.
c. Frequency . . 10 to 2000 Hz.
d. Duration . . 12 hours.
e. All contacts wired in series with a current of 100 milliamperes flowing. Monitor for discontinuity of 10 micro-seconds or greater.

No physical damage nor loss of continuity of 10 micro-seconds or greater.

Moisture Resistance

Mated connectors are tested in accordance with method 106 of MIL-STD-202 (10 days exposure). Insulation resistance measured at end of test period while at the high humidity.

Insulation resistance shall be 100 megohms or greater.

Mated connectors are tested in accordance with method 103 of MIL-STD-202 (96 hour exposure). Insulation resistance measured after 4 hour conditioning period at room ambient conditions.

Insulation resistance shall be 100 megohms or greater.

Shock

a. Connectors . . mated.
b. Wave form . . half-sine.
c. Gravity units . . 50.
d. Duration . . 11 milliseconds.
e. All contacts wire in series with a current of 100 milliamperes flowing. Monitor for discontinuity of 10 micro-seconds or greater.

No physical damage nor loss of continuity of 10 micro-seconds or greater.

a. Connectors . . mated.
b. Wave form . . half-sine.
c. Gravity units . . 50.
d. Duration . . 11 milliseconds.
e. All contacts wired in series with a current of 100 milliamperes flowing. Monitor for discontinuity of 10 micro-seconds or greater.

No physical damage nor loss of continuity of 100 micro-seconds or greater.

Corrosion

Mated connectors are exposed to a 20% salt spray test for a period of 48 hours. Connectors shall be unmated and mated one cycle before any subsequent tests.

Connectors must meet all subsequent test requirements.

Mated connectors are exposed to a 20% salt spray test for a period of 48 hours.

Connectors must meet all subsequent test requirements.

Contact Resistance

Voltage drop measured in accordance with MIL-C-23216. Probe points 6 inches apart.

The voltage drop shall not exceed the specified values.

Contact Size	Wire Size	Test Current	Max. Drop (Millivolts)
8	8	46.0A	30.0
8	10	33.0	37.0
12	12	23.0	60.0
12	14	17.0	55.0
16	16	13.0	60.0
16	20	7.5	55.0

Probe points on the current-carrying conductors 13mm back from each end of the mated connector.

The voltage drop shall not exceed the specifield values.

Contact Size	Wire Size	Test Current	Max. Drop (Millivolts)
8	8	46.0A	55.0
8	10	33.0	37.0
12	12	23.0	46.0
12	14	17.0	31.0
16	16	13.0	56.0
16	18	10.0	50.0

Fluid Immersion

Unmated connectors are fully immersed in the following fluids:

a. Hydraulic fluid (MIL-H-5606) - 20 hours.
b. Lubricating oil (MIL-L-7808) - 20 hours.

Connectors shall mate properly after immersion.

Not required.

Insert Retention

Inserts, less accessories, are subjected to the specified axial loads, load varies with shell size.

Inserts shall not be dislocated from original positions or damaged.

Not required.

External Bending Moment

Mated connectors are subjected to the load specified for the particular shell size.

No evidence of damage at 3X magnification.

Not required.

Air Leakage

Not required.

Receptacle connectors are subjected to a pressure differential of 30 pounds per square inch at a temperature of -55°C. Leakage rate shall be measured.

Leakage rate shall not be greater than one atmospheric cubic inch per hour (4.55×10^{-3} cubic centimeters per second).

Temperature Life

Not required.

Mated connectors are subjected to an ambient temperature of 105°C for a period of 200 hours.

Connectors must meet all subsequent test requirements.

Torque to Couple/Uncouple

Not required.

Force required to mate and unmate the plugs from its counterpart receptacle is measured.

Force must not exceed the value specified for each shell size.

Impact

Not required.

Plug connectors, wired as for service, are dropped from a height of 32 inches, by a pendulum action, to strike a steel plate. The number of drops is 8 and the plug is oriented for each drop to expose a different surface for test.

Plug and accessories must not break and plug must mate with receptacle.

Summary

This paper has described a line of connectors that is complete including standard sex connectors, reversed sex connectors, flange, flange mounted plug and receptacles, cable mounted plug and receptacles, free hanging plugs and receptacles, bulk-head feed throughs.

These reliable economical connectors should find many additional applications in the industrial and commercial market place as well as in "design to cost" military applications.

Patrick E. Lannan graduated as an EE from Rochester Institute of Technology in 1939. He has held positions as Senior Research Engineer, Stromberg Carlson Co.; Vice President and Director, Designers of Industry Inc.; Vice President Frontier Electronics; Vice President Drexel Dynamics and Division Chief Engineer, International Resistance Co. In his present position of Product Manager at AMP Incorporated, he is responsible for coordinating all marketing efforts relating to multi-position pin and socket connectors produced by the Connector Products Division of the Connector and Component Products Group.

FLAT CONDUCTOR CABLES FOR EXTREMELY HIGH TEMPERATURE APPLICATIONS

Walter S. Rigling
Martin Marietta Aerospace
Orlando, Florida 32805

SUMMARY

Flat conductor cables have been developed which are capable of operating at temperatures ranging from -65°C to 350°C. The cables, a 25-conductor signal cable and a 3-conductor power cable, were continuously roll laminated as prototypes and then fully characterized at temperatures from -65°C to 350°C. Electrical, mechanical and physical characteristics were evaluated in these tests.

As a result of the successful completion of the prototype development, production lengths of 3000 feet were fabricated. These cables were also subjected to rigorous testing, including flexing endurance at 350°C. The results of the tests and a discussion of the cable performance are presented.

As in the development of any article which challenges the state-of-the-art many problems and frustrations were encountered. Their nature and their solutions are discussed along with guidelines for avoiding them in the future.

As a result of this development an extremely heat resistant family of flat conductor cables are now available. These cables can be fabricated using standard roll laminating equipment. While their primary application is for elevated temperature environments they also provide a large current overload factor when used in more moderate temperature applications.

INTRODUCTION

Flat conductor cables employ conductors made from copper strips slit from copper foil or round strands rolled into a rectangular cross section. These conductors are typically insulated with two layers of film, collated and bonded under heat and pressure using roll laminating techniques.

The insulating films are either all-thermoplastic or are thermosetting films bonded with thermosetting or thermoplastic adhesive. The highest temperature rating in MIL-S-55543, 200°C, is applied to polyimide film bonded with flourinated ethylene propylene (FEP). The program discussed had as its goal the production of two 2-inch wide flat conductor cable designs, one with 3 (0.010 X 0.500 inch) conductors and the other with 25 (0.004 X 0.040 inch) conductors capable of meeting electrical and mechanical test requirements at 350°C. Because of this extremely high temperature requirement, it was recognized that conventional constructors or material combinations would not be adequate.

PREINSULATED - WOVEN CONSTRUCTION

While a polyimide film insulation was available, there was no known adhesive that could survive this temperature under flexing conditions. Therefore, roll laminated constructions were initially ruled out. This left, as an alternate construction, preinsulated flat conductors woven together with high temperature resistant glass yarns.

Because the overall thickness of the insulation, including woven yarns, could not exceed 0.012 inch (adder) it was essential that the materials selected could be applied as films or as multiple pass varnishes. This approach would make it possible to maintain the required wall thickness and concentricity. With this as a goal, eight material systems were selected for initial screening. The materials listed in Table I were first subjected to thermogravimetric analysis (TGA) by monitoring weight loss as the temperature was increased at a rate of 3°C per minute (Figure 1). The most heat resistant insulation material was number 4, polyimide film (Kapton supplied by DuPont), which resisted degradation beyond 500°C under the short term conditions. The most heat resistant composite construction was number 5.

TABLE I

CANDIDATE INSULATION MATERIALS

Figure Number	Resin System	Condition
1	Rhodia Kerimid 501 Polyamide-imide film	Cured 24 hours @ 480°F
2	Rhodia Kerimid 500 Polyamide-imide varnish	Cured 24 hours @ 480°F
3	DuPont "Liquid H" Polyimide	Cured 24 hours @ 480°F
4	DuPont KAPTON Polyimide Film	As received
5	*Wire Insulation Composite	As received
6	Fluorinated Ethylene Propylene Film	As received
7	Ciba Geigy P105A Polyimide	Cured 1 hour @ 550°F
8	Hexcel HX-575 Polyimide (prepreg)	Cured 24 hours @ 480°F
9	Hexcel HX-675 Polyimide (prepreg)	Cured 24 hours @ 480°F
10	Rhodia Kerimid 601 Polyimide "B" Stage Resin	Cured 24 hours @ 480°F

* 0.1-mil FEP adhesive bonded single layer 1.0-mil polyimide film, 2/1 lap with polyimid overcoat.

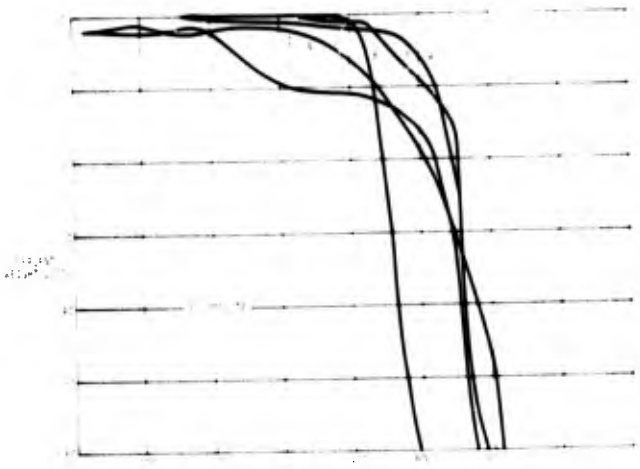

Figure 1. Thermogravimetric Analysis of Candidate Materials

While the FEP bonding layer in the composite insulation melted at the 350°C test temperature, the mechanical integrity of the composite was maintained by the overcoat and the wrapped construction. It was concluded that this construction would be satisfactory for the test cable; however, there was some concern over embrittlement of the polyimide overcoat as a result of aging at 350°C. During the search for a more flexible overcoat material, a polyamide-imide varnish (Kerimid 500), supplied by Rhodia Corporation, was evaluated. When applied as a varnish over the composite insulation it exhibited greater flexibility after 24 hours at 350°C than did the "liquid H" varnish. Beyond 24 hours, it exhibited approximately the same degree of embrittlement.

ROLL LAMINATED CABLE DEVELOPMENT

Although there was a great deal of confidence that the preinsulated woven construction would meet program requirements, the possibility of applying the polyamideimide to the polyimide film as an adhesive caused the program to be redirected toward the development of a roll laminated flat conductor cable. This action was based on the fact that roll lamination is a faster more economical method of construction and that the finished product could be used with existing flat conductor cable hardware and termination equipment.

Experimental samples of 2-mil polyimide film coated with 2-mil polyamideimide dried adhesive were obtained from Circuit Materials Company. A 25-conductor test cable was press laminated in the laboratory and after aging at 350°C for 288 hours the specimen remain flexible. The success of this initial specimen provided the necessary encouragement to implement an investigation into the feasibility of fabricating longer lengths of cable using roll laminating equipment.

The experimental roll lamination was performed at Parlex Corporation with 2-mil Kerimid coated, 2-mil Kapton film. A wide range of variables were investigated and included preheat of the adhesive coating on the film as controlled by the time against the rollers, the speed of tape traveling between the rollers, the pressure of the rollers on the tape, and the surface of the film that is laid against the rollers.

While greater than 10 combinations of parameters were tried, the basic results were always the same. At temperatures below 288°C the appearance of the laminated films was good with very few voids discernable. As the temperature of the rollers was increased, the voids became more numerous until at over 340°C the bonding layer was totally blistered. Attempts were made to drive off solvent in the adhesive prior to reaching the rollers; however, little success was achieved. In addition, while the bond after laminating was somewhat greater than the initial prelamination bond, the final result was not considered acceptable.

Various attempts were made to improve the product, including hard silicone rubber rolls, lower temperatures with steel rollers and high pressures, and longer term - lower temperature (175°C) post cures. As a result of the data and experience gained, it was agreed that preproduction lengths should be attempted. Consistant with this discussion, both 3-conductor and 25-conductor prototype cables were laminated. Both cables, while passing water immersion dielectric strength testing, exhibited marginal bonding of the adhesive layer to the insulating film and did not show a complete encapsulation of the conductors by the adhesive. Nonetheless, the cable was a distinct improvement over the original prototype attempt.

The results of these experiments clearly demonstrated the feasibility of roll laminating a flat conductor cable capable of meeting program technical requirements by using the polyamide-imide adhesive on the polyimide insulation film. There remained, however, two major problems. The first concerned the elimination of bubbles during lamination and after post cure and the second concerned the improvement of the Kerimid to Kapton bond.

Based on limited runs performed at MSFC, which utilized adhesive coated film that had been dried for 15 minutes at 121°C, there was an indication that bubble free lamination may be achieved by using a film containing something less than the 23% solvent supplied in the film used for the initial runs.

In an effort to verify this theory three lots of Kapton film coated with Kerimid containing 28%, 20.4% and 9.9% solvent were shipped to Parlex. Unfortunately, attempts to produce a suitable cable with the low solvent material was unsuccessful since the flow of the Kerimid was drastically reduced. It was apparent that, in order to obtain adequate tack and flow of the Kerimid at reasonable pressures and temperatures (177°C), greater than 20% solvent was required.

At the same time a parallel investigation was being conducted into means for improving the Kerimid to Kapton bond. While it was significant that the material to date had been processed with the adhesive on the glossy side of the Kapton film, the most important factor in developing an improved bond was the discovery that 3-mil film exhibited substantially better and more consistant bondability than the 2-mil film. Examination of the surfaces of 2 and 3-mil Kapton film using the scanning electron microscope (SEM) exposed no significant difference in surface roughness between the films. When questioned as to the reason for the difference in bondability between the films DuPont specialists were unable to explain it; however, they were aware of this fact. In addition, their experience shows that 5-mil Kapton has the greatest bondability and the 1-mil has the least. From this point, it was agreed that 3-mil Kapton would be used for all future cable and that a 2 to 3-mil thick layer of Kerimid adhesive would be used for the next prototype cables.

In the fabrication of the first prototype cables, several approaches using combinations of rubber rollers were tried. The most successful cable fabricated was a 25-conductor version using two steel rollers at 177°C at a speed of 2 feet per minute. This cable had good adhesion to all interfacing materials and the fill between conductors was excellent.

Although the fill and adhesion of the second three conductor cable prototype was considerably better than that previously supplied, the rubber roller did not sufficiently deform the Kapton film to ensure fill of the Kerimid adhesive against the edge of the thick (0.01 inch) conductor. A grooved steel roller was considered a necessity for future 3-conductor cables.

The validity of this decision was verified by the fabrication of a third 3-conductor prototype. The effect of the grooved rollers was apparent with fill along the edges of the conductors complete and the interlaminar bond excellent.

With both prototype cable types successfully laminated, it remained for a post cure cycle to be developed that would drive out the solvent without adversely affecting the interlaminar bond of the cable and without introducing bubbles in the adhesive layer.

The solvent content in the adhesive layer after the cable has been laminated was still approximately 15%. This solvent, which is N-Methyl Pyrolidone, if allowed to remain will cause severe blistering when the cable is subjected to the 350°C test temperature. A great deal of effort was expended in the process of optimizing a practical post cure cycle. It was found that a long term-low temperature cure was necessary prior to implementing shorter term-higher temperature steps. It was further determined that any attempt to accelerate release of the solvent by shortening the time at elevated temperature would cause blistering. The time-temperature relationship for the 25-conductor cable post cure cycle was finalized as follows:

121°C-16 hours, 177°C-4hours, 200°C-4 hours

232°C-4 hours, and 260°C-24 hours.

The final consideration in the optimization of the cure cycle was the elimination of the severe darkening of the Kapton film as the result of the post cure. This problem was overcome by continuously purging the curing oven atmosphere with nitrogen. While there remained a certain degree of darkening, the cured cable was completely translucent and not opaque as was the cable that was cured in air. The use of nitrogen also eliminated slight embrittlement of the film that was noted after the post cure in air.

It was expected that the post cure cycle developed for the 25-conductor cable would also be applicable to the 3-conductor cable. Unfortunately, the additional thickness of adhesive that results along the edge of the 0.010-inch thick conductor contains a proportionately greater amount of solvent which must be released slowly if bubbles are to be prevented. The 121°C starting temperature was too high for this cable and after much testing the following cycle was selected:

24 hours at 68°C, 8 hours each at 94, 108, 121, 135, 149, 178, 204, and 232°C, and 24 hours at 260°C.

Even after this extended cure, small bubbles were observed in the adhesive layer adjacent to the conductor. Exhaustive testing was undertaken in an attempt to eliminate these bubbles; however, no way was found to completely avoid the evolution of randomly dispersed 1-mm and smaller diameter bubbles.

With the successful fabrication and test of the prototype cables, it remained for the 3000-foot production lots to be fabricated. Based on the thorough background and experience gained in the development of the previous cables no major problems arose in the fabrication of these production cables. Due to this being the first attempt at long lengths, moderate difficulties were encountered while attempting lengths over 100 feet; however, the following percentages of various lengths were produced:

3 conductor-over 100 feet-72%, over 50 feet-14% over 25 feet-14%, 25 conductor-over 100 feet-50%, over 50 feet-12%, over 25 feet-38%

Testing of the production cables was successfully completed after post curing using the cycles previously developed.

TEST SUMMARY

The laminated and post cured cables successfully met the comprehensive test requirements described below. In addition to meeting the electrical requirements, there was no visual indication of mechanical or physical degradation.

1. Insulation Resistance - wet - 500 megohms per 1000 feet between each conductor and water and adjacent conductors.

2. Dielectric Withstanding Voltage - wet - 1500 volts (DC) between adjacent conductors, all conductors and water.

3. Moisture Resistance - Insulation resistance of 50 megohms per 1000 feet minimum when tested as described above after six days humidity cycle (MIL-STD 202/106).

4. Insulation Flaws - 1500 volts (DC) between all conductors and wet sponges on the surface with a minimum 0.2 second contact time.

5. Thermal Shock - After 5 cycles from -55° ± 5°C to 350°C ± 15°C the shrinkage was not greater than 1/8 inch, either end of cable. The cable passed dielectric withstanding after this conditioning.

6. Flammability - All cables extinguished immediately after removal of the flame.

7. Flexure Endurance - Withstood 800 bending cycles around a 1-inch diameter mandrel at both -55 ± 5°C and 350 ± 15°C, see Figure 2. All conductors were connected in series with maximum fault duration of one microsecond.

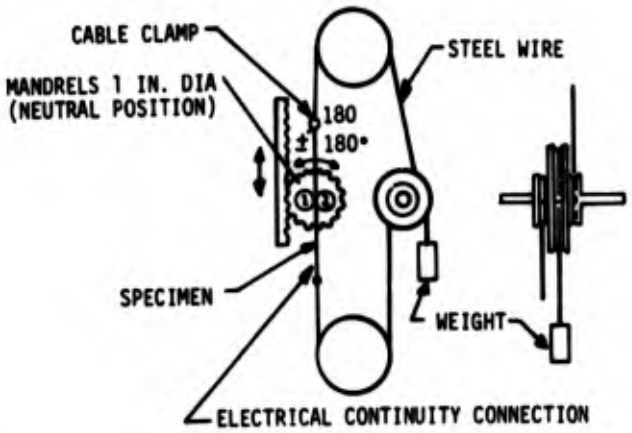

Figure 2. Flex Test Fixture

CONCLUSIONS

The many material, design, fabrication, and analysis factors involved in the successful development of flat conductor cables capable of operation at temperatures of 350°C have been assessed in this program. While it was the original goal of the program to produce the cables using preinsulated flat conductors woven together using high temperature yarns, it is of major significance that, through the innovative application of new adhesive materials and processing techniques, it was ultimately possible to provide roll laminated cables similar to those presently used for lower temperature applications.

The success of the program is attributed to the cooperative efforts of the industrial team that supported Martin Marietta Corporation's Orlando Division in the development of these cables which essentially double the operating temperatures of previous cables. This team, consisted of the Parlex Corporation, Circuit Materials Company, Rhodia Inc. Polymide Division, and the DuPont Film Department.

This program was sponsored by the Research and Process Technology Division of NASA Marshall Space Flight Center under Contract No. NAS8-29076.

WALTER S. RIGLING

Mr. Rigling is supervisor of the Electrical Materials Laboratory of Materials Engineering Laboratories. He is responsible for the research and development of electrical and electronic materials and processes designed to cope with extraordinary requirements of missile and electronic systems. Some of Mr. Rigling's responsibilities are printed wiring, thin films, dielectric materials, molding and insulating compounds, wire and cable, and micro-module packaging and special installation techniques.

Mr. Rigling is known in the industry as an advocate of new techniques and test procedures. He has presented several papers on the subject of electrical insulation materials and processes.

Mr. Rigling is a member of the IEEE, and SAMPE technical societies and a member of several IPC committees. He received a degree in electronics from Temple University in 1951 and a BS degree in Business Management from Florida Southern College in 1971.

CONNECTOR - FLAT CABLE COMPATIBILITY

Gerald C. Smith and David A. Luzadis

The Bendix Corporation
Electrical Components Division
Sidney, New York 13838

INTRODUCTION

Mass termination can be one of the advantages of using flat cable, whether it contains round or rectangular conductors, and is an important factor to consider in obtaining compatibility between flat cable and electrical connectors. A great variety of flat cables and connectors have been developed to meet the multitude of user applications and along with this, various termination techniques have also been developed. These termination processes vary from stripping and soldering to crimping and/or piercing systems with each method requiring certain contact design configuration which accommodates the termination process and the conductor geometry.

More recently a joining method called Energy Pulse Bonding (EPB) has been developed which offers some unique advantages in providing a reliable, cost effective production oriented system and improved compatibility between the various flat cables and a relatively simple contact geometry.

EPB PROCESS THEORY

Energy Pulse Bonding (EPB) is not exactly new but an application of the old science of thermo-compression bonding. Through the use of thermal energy and mechanical force a two stage condition between joining metals is obtained. First, plastic flow of the asperity points disrupts surface contaminates and oxides producing intimate contact between large areas of the two metals. Secondly, accelerated molecular diffusion across the interface serves to establish a metallurgical bond.

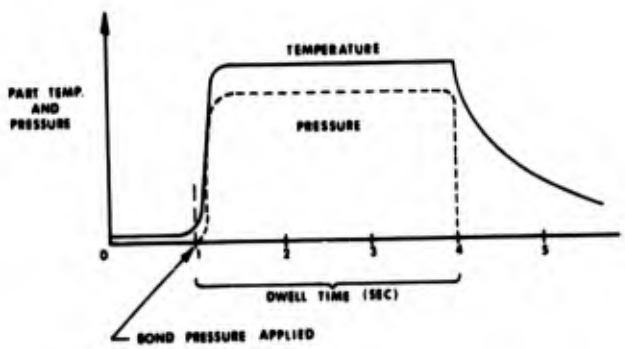

Figure 1

Thermal energy and mechanical force are simultaneously applied to the joining metals in the form of a unified bond pulse of controlled amplitude and duration (Figure 1).

Since metals are not free of contaminants and/or oxides and contain many asperity protrusions the mechanical force disrupts the insulating mechanisms and flattens various asperities obtaining a very necessary condition of intimate contact between greater surface areas. Without intimate contact molecular diffusion will not take place and without asperity deformation large voids will exist which may detract from a good metallurgical bond. Theoretically molecular diffusion does occur at all temperatures above absolute zero, but, to obtain reasonably short bond times, higher temperatures are utilized to accelerate the diffusion rate, which varies with different metals. The bond temperatures used are normally in the realm of 50% to 75% of the melting point for the conductor material.

Since bonding temperatures are significantly below the conductors melting point the formation of brittle intermetallics or cast microstructures, which occur in fusion types of welding are eliminated. The pulse duration or bond time is dependent on bond temperature and type of metal being joined, and has been limited to six seconds or less in most cases.

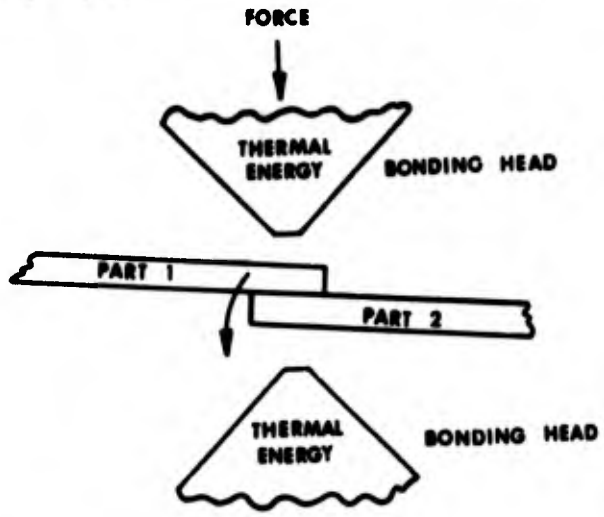

Figure 2

The energy pulse is applied by a pair of specially designed continuously heated bonding heads mounted and aligned in a vertical plane (Figure 2). One is stationary and the other is mounted in the moving arm of a pneumatic press which supplies the required mechanical force. The temperature of each bonding head is independently controlled to provide various combinations of thermal profiles, as desired. The application time for

the bond pulse is electronically controlled from the time of contact between the bonding heads and parts to be joined.

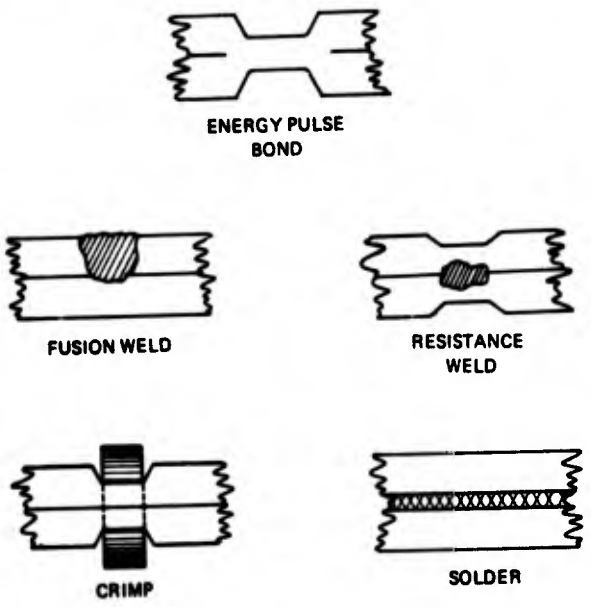

Figure 3

The EPB process differs from other terminating techniques (Figure 3) offering unique advantages over the others. Since joining does occur by diffusion no detectable nugget containing brittle intermetallics exist such as in resistance and TIG welding. EPB does not require additional low melting filter materials such as in soldering nor external mechanical fasteners or special contact designs as used in crimping techniques.

EPB FEASIBILITY

With a theoretical understanding of the process and general equipment requirements, an evaluation of application feasibility was made. Test vehicules of bare and insulated metals consisting of the more common materials found in flat cables and connector contacts were joined and evaluated for joint resistance and mechanical strength. Mechanical strengths were determined by both tensile and peel tests. Effects of process parameter variation on resulting bonds for various materials were determined by process plots (Figure 4). This was accomplished by evaluating peel strength data of joints made from varying bond pressures (deformation) and bond temperatures. If failure occured at the joint interface it was noted by an (O) and if the parent metal failed it was noted by an (X) and an area of bond deformation versus bond temperature can be described in which good or acceptable joints are obtained. These plots can be cataloged for various materials and combinations of materials and recorded in a cookbook for reference to obtain proper bond parameters and allowable variations of each parameter. This does provide a method of assuring quality joints.

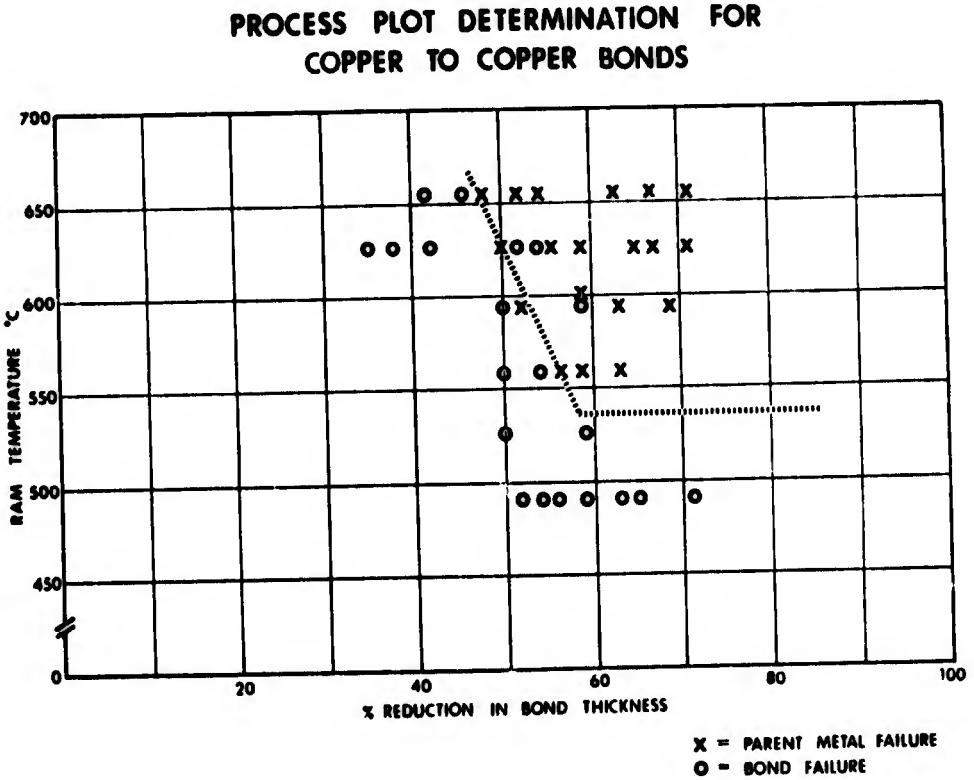

Figure 4

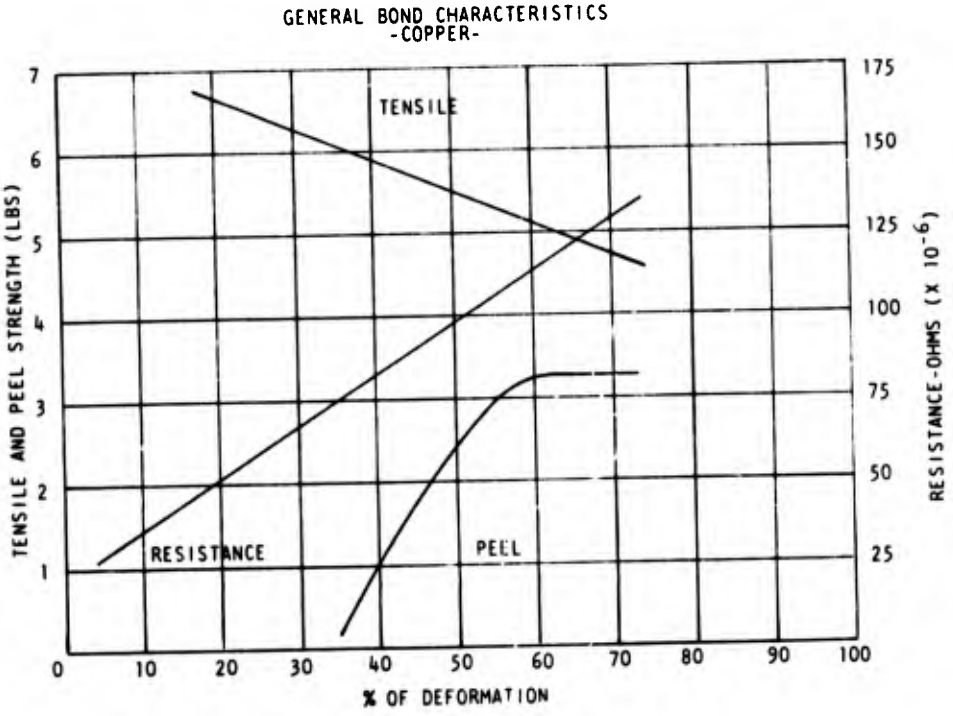

Figure 5

Curves shown in Figure 5 indicate the general mechanical and electrical characteristics of an EPB termination. Tensile strengths decrease with joint deformation due to deceased cross sectional joint area, however, the peel strength increases to a maximum at which point the parent metal fails instead of the joint interface. Normal joint tensile strengths were between 80% and 90% of the original conductor strength where peel strengths averaged between 35% and 50% of the original conductor tensile strength.

The joint resistance, including both material bulk and contact resistance increased with deformation, again due to reduced cross sectional area.

BOND STRENGTHS & RESISTANCES OF JOINTS MADE BY VARIOUS PROCESSES

BOND TYPE	TEST MODE	$\bar{X}$ LBS.	σ	NO. OF SAMPLES	$\bar{X} \sim, S$ X 10^{-6}	σ	NO. OF SAMPLES
Solder	Peel	1.12	0.72	17	93	23.44	12
Fusion Weld	Tensile (1)	6.98	1.72	18	264	102.09	14
Resistance Weld	Peel	0.53	0.39	18	155	26.61	12
Crimp	Peel (2)	6.10	0.27	12	590	196.55	18
EPB	Peel	4.12	0.41	29	98	8.97	12

(1) Fusion weld geometry made peel tests impossible.

(2) Peel tests on crimped conductors are not completely valid but are included for comparison.

Figure 6

In comparing the resulting data with that of other processes for the same materials, the EPB joints were superior in most cases or at less equivalent to those formed by other techniques (Figure 6). For peel tests, where direct comparisons could be made, solder and resistance welding, EPB was superior in both average strength and joint strength variations. Other fusion welded samples were joined so that the test was actually of tensile strength and not peel strength. For crimped samples the crimping device was included in the joint area and definitely should provide a higher peel strength characteristic. However, in comparing these same crimp joints for contact resistance, they were found to be inferior to those of the other processes, with EPB again providing lower resistance on a more consistent basis.

The bonds formed by EPB were also evaluated for mechanical and environmental characteristics such as thermal shock, vibration, salt spray, industrial gas and flexing strength with satisfactory results.

EPB ADVANTAGES

With an understanding of how EPB works and its joining capability demonstrated, what does it offer in terminating flat cable and electrical connectors?

Energy Pulse Bonding offers several distinct and unique advantages over other available termination methods. These include (1. solid state bonding, (2. direct termination of insulated conductors, (3. simultaneous joining of multiple joints, (4. termination of various conductor geometries, (5. good parametric control and (6. good contact termination density.

As was stated earlier, the bonds result from molecular diffusion between joining surfaces at less than material melting temperatures. This eliminates the chances of brittle joint interfaces, consequently weakening bonds around the nugget normally formed by material melting.

A big advantage is the capability of terminating insulated conductors, eliminating an extra stripping operation and reducing costs. This is accomplished by utilizing the thermal energy from the continuously heated bonding heads to either vaporize and/or sublimate or sufficiently soften the insulation to a point where it can be displaced by the mechanical force of the ram and its bond surface geometry (Figure 7). Removal of different insulations requires a variety of bond profiles which must be compatible with the metal joining requirements. A good method for determining this compatibility is through the use of Thermo-Gravimetric Analysis (TGA). TGA plots weight loss versus temperature for a particular material (Figures 8, 9 and 10). From the plots it is noted that some insulations have complete weight loss at compatible bond temperatures, while others may leave a small percentage of residue. Another condition is that some insulations (polyimide) require significantly higher temperatures and do stress the process capability. With the discovery of new insulation materials, each

BONDING TOGETHER OF TWO PIECES OF INSULATED FLAT CABLE

a. Start of bonding process

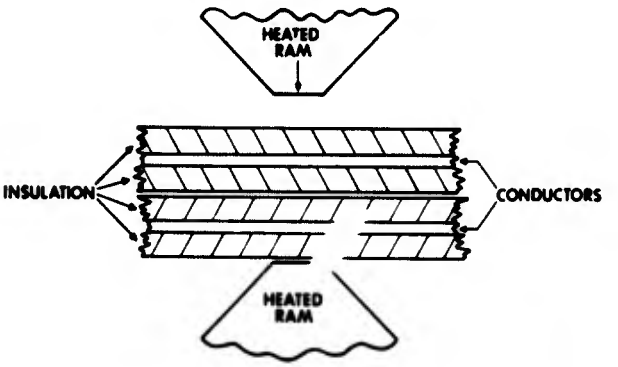

b. Bonding process completed

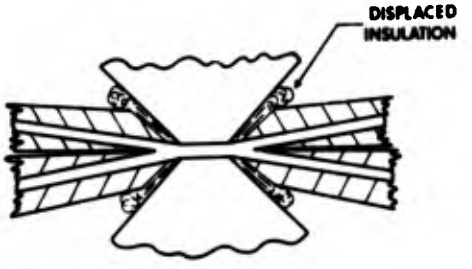

Figure 7

must be evaluated to determine the effects of the use of EPB and this can be accomplished by either TGA or actual bond samples. In studying micro-photographs (Figure 11) no significant quantity of entrapped insulations have been detected.

A big plus for EPB is in its capability of simultaneously bonding multiple numbers of conductors. Since the bonding heads consist of a simple geometrical surface of desired length, multiple contacts, in a single plane, may be joined simultaneously, making the system a natural for flat cables. This multiple joining along with a reasonably fast bond cycle (1.5 to 6.0 seconds) provides for mass termination.

Another inherent advantage is that the terminating surfaces are not a sophisticated geometry. This simplifies the connector contact design and allows the termination of either round or rectangular types of conductors. Again this is a cost reduction in savings on contact design and one termination system for both types of conductor geometries. One requirement is the need to provide a surface area width sufficient to accommodate conductor deformation, especially for round conductors.

The EPB process is accomplished by three basic bond parameters, (1. temperature, (2. pressure and (3. time and all three are readily controllable. Controllers for all three parameters are highly perfected to provide reliable parametric control of the

THERMO - GRAVIMETRIC ANALYSIS

INSULATION TYPE: POLYESTER 1

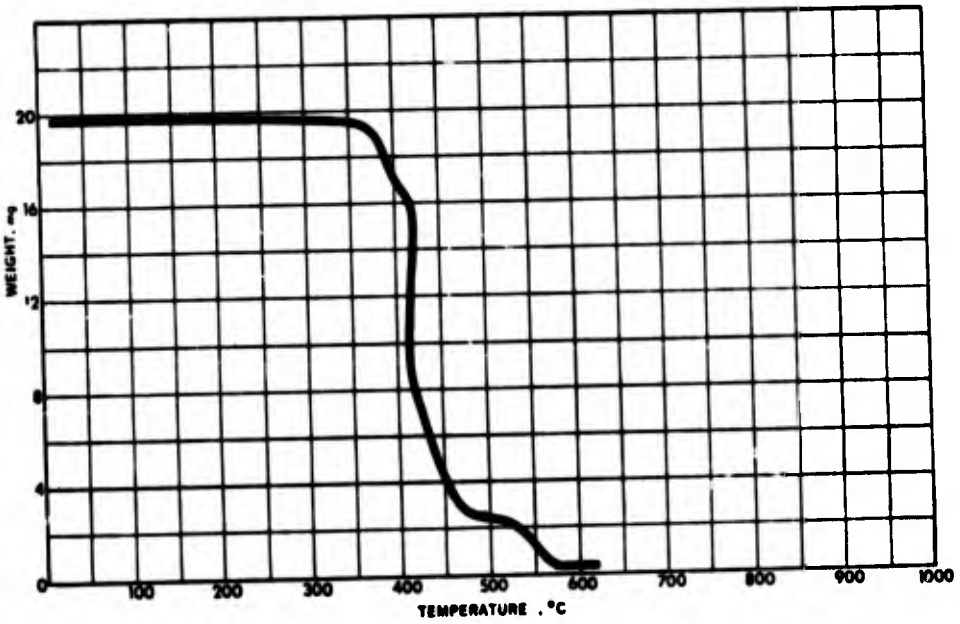

Figure 8

THERMO - GRAVIMETRIC ANALYSIS

INSULATION TYPE: POLYESTER 2

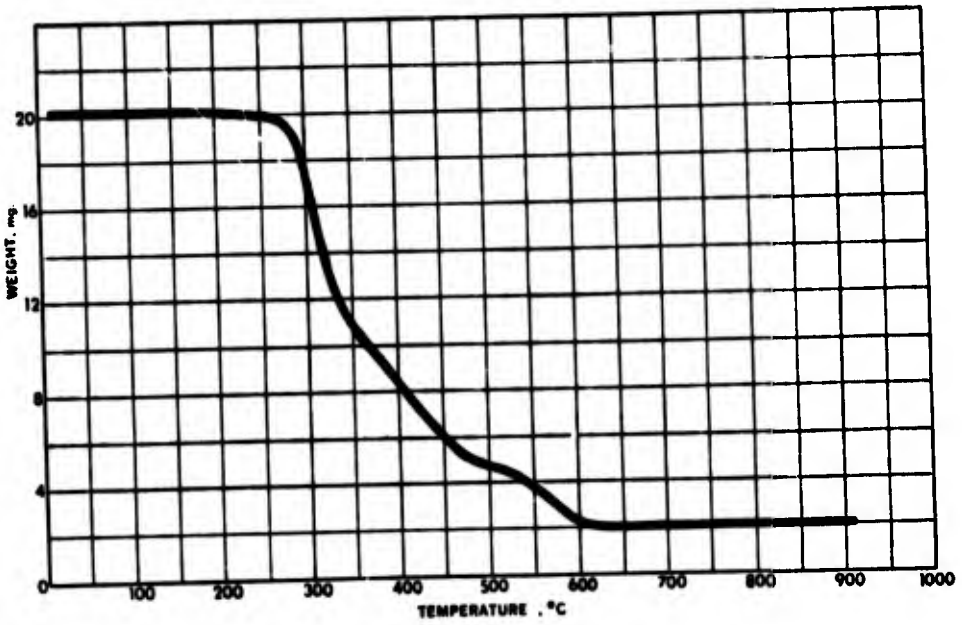

Figure 9

THERMO - GRAVIMETRIC ANALYSIS

INSULATION TYPE: POLYMIDE

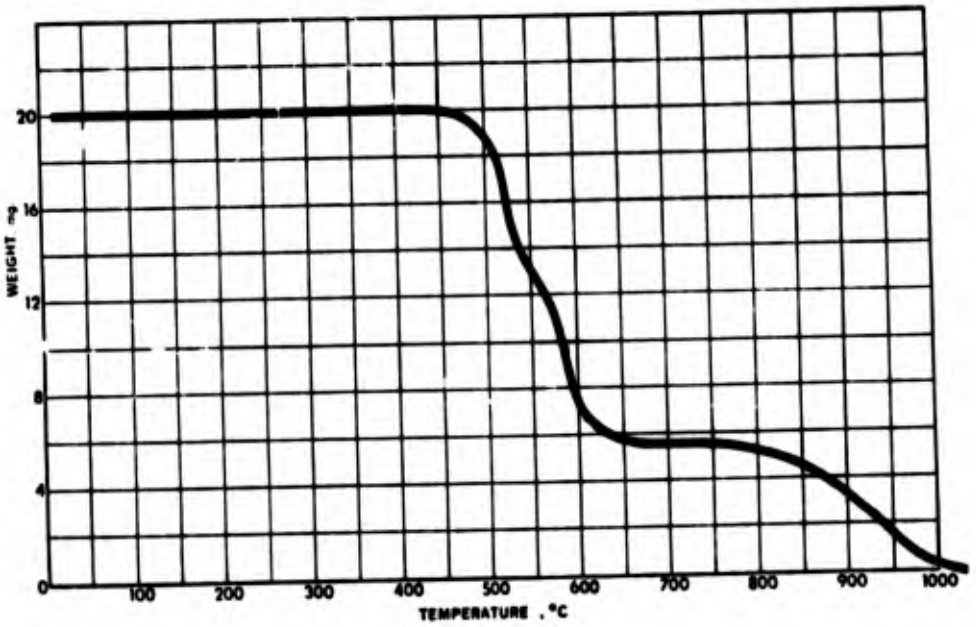

Figure 10

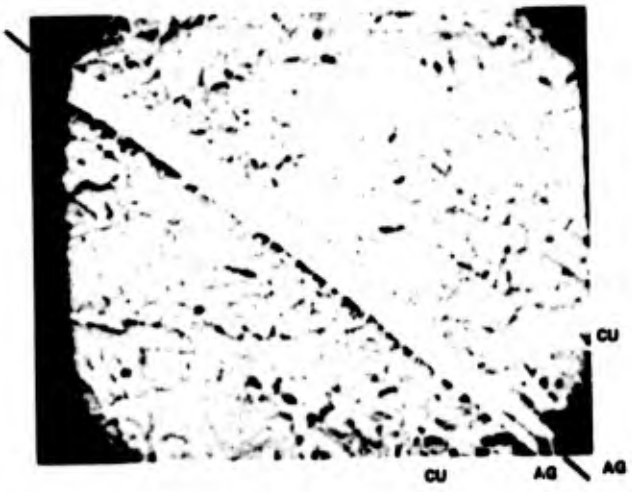

AG PLATED CU
EPB
AG PLATED CU
(FEP INSULATION)
X 1500

Figure 11

EPB process and each parametric value is within a realistic magnitude. Both terminating surfaces, contact and bonding head, are simple geometry, allowing for high termination densities within line contact spacings in the order of 0.050 inches. More complex tails of termination techniques require greater spacings.

CONNECTOR

To utilize advantages offered by the EPB termination process a flat cable-connector has been developed by Bendix and connector cable assemblies evaluated for pertinent functional characteristics. The test results indicate more than satisfactory characteristics for a non-environmental connector-cable assembly.

The connector design offers a simple configuration providing low profile and minimized weight through the use of a single piece molded body. Since the molding is a thermoplastic material, a technique known as Reflow Dielectric Retention (RDR) is used to reform the body geometry to provide contact retention and cable strain relief. This process has been the subject of other papers. Reflow Dielectric Retention utilizes thermally heated rams to heat and reform the material through mechanical force to obtain desired features in the molding once contacts and cable are properly installed. This eliminates the need for a second part to perform these functions.

Contact design is a tapered cantilever beam tuning fork, which minimizes engaging forces and contact resistance and allows placement on 0.050 inch center spacings for greater densities. The termination area is a simple flat surface 0.025 inch wide by approximately 0.075 inch in length.

The connector-cable termination is then obtained via EPB by locating the flat cable conductors overlapped with the termination

NEW FLAT FLEXIBLE COAXIAL CABLE AND MASS TERMINATION TECHNIQUE FOR HIGH-SPEED DIGITAL APPLICATIONS

William L. Schumacher
AMP Incorporated
Harrisburg, Penna.

Keeping pace with tomorrow's need for signal efficiency and shielding is the purpose of a new novel multiconductor flat flexible ribbon coaxial cable for the digital processing industry. Disclosed are physical and electrical attributes with capabilities for mass stripping and termination, placing this cable into today's need for economic reality.

Electronic equipment circuit advancements have already reached the stage where the transmission line is of prime importance. Cross talk, transmission speed, and efficiency needs of the equipment are forcing a change to coaxial cable. In order to achieve this transition to coax in the most economical fashion, a newly designed ribbon coax cable has been produced. Its unique construction permits mass termination of a true coaxial cable.

Coax cable in single and flat multiple conductor form has been available for many years. All previous multiple ribbon forms have been basically ribbonized constructions of various individual cables.

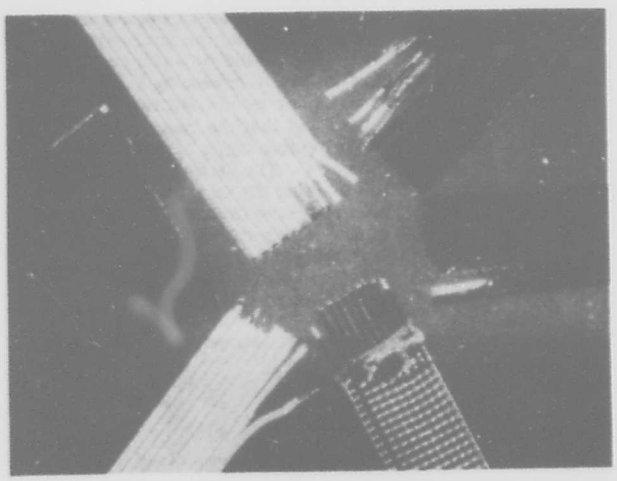

Figure 1. Typical versions of individual coax cables in ribbon form.

Whether woven, laminated, chemically bonded, or heat bonded together in order to make a neat, flat package, the termination of the cables is still an individual, tedious operation. This high handling cost was a contributing reason for the development and use of open air flat cable having a defined impedance. These use round and/or flat conductors, and can be mass terminated. Digital electronic equipment speeds are now near or past the capability of these open constructions. The new coax cable, described in this paper, has the mass termination capability of the open air construction, along with the inherent coax characteristics and capabilities.

Mechanically, the new ribbon coax uses individual multiconductor lines. Each individual cable in the ribbon has its own center conductor, dielectric and shield. The center conductor size, dielectric material, and variations of the dielectric outside diameter are

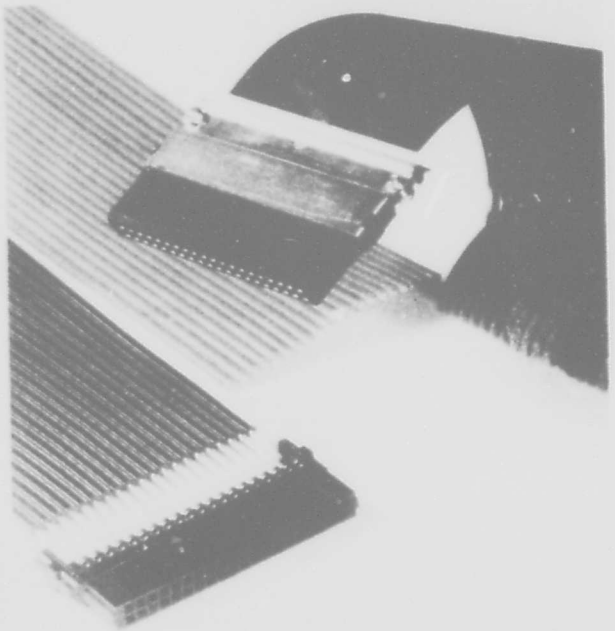

Figure 2. Coax cable constructed to AMP Incorporated design.

varied, to provide different cable characteristic impedances. Solid wire center conductors are used for ease of wire stripping and termination. Each center conductor is located on predictable centerline to centerline spacing. The shield is of a foil and drain wire construction. The aluminized Mylar TM shield totally covers the coax core while the solid drain wire acts as a low resistance path and the shield terminating means. The drain wire locations are also of prime importance. They are located on predictable spacings the same as the center conductors. With both center conductors and drain wires in known locations, mass stripping and terminating is now possible.

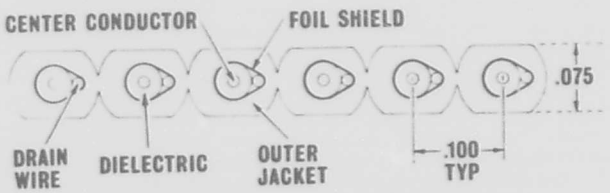

Figure 3. Cross section of AMP coax ribbon cable.

The stripping action removes the foil shield with the cable jacket, exposing the drain wire and center conductor. Depending on the application, the dielectric on the center conductor may be stripped off or left in place. Where the dielectric is left on the center conductor, the slotted-beam wire termination technique is used with its dielectric displacing capability. The same slotted beam technique can be used on bare center conductors and the

bare drain wires. The dielectric may be left in place, as an insulator to positively prevent shorting at a connection.

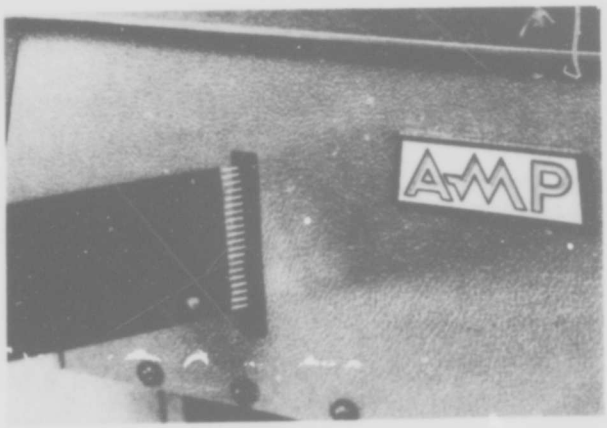

Figure 4. Ribbon coax cable stripping machine.

At the time of writing this paper, 50 ohm cable on .100 center-to-center spacing and 95-ohm cable on .150 spacing have been produced. Seventy-five ohm and 93 ohm on .100 centers, and 95 ohm on .125 centers are being tooled. Test results on the 50 ohm cable will be used for discussion in this paper.

Cable construction is a blend of decisions based upon size considerations for mass termination, cable electrical efficiency, and economics. Considering that conduction loss in the dielectric and resistive loss in the center conductor are the two major sources of loss in a coaxial cable ([1, 2, 3]) these were chosen carefully. A balance between the low characteristic impedance cable and high impedance construction cable on a given center-to-center space of the cable indicated that a #28 (.0126 Dia.) center conductor could be used for 50 ohm cables, and a smaller size #30 (.010 Dia.) would best function in the 75 and 93 ohm cables. The larger the center conductor, the lower the resistive and skin effect losses. Below 1 GHz, attenuation is mainly resistive loss while skin effect has increasing effect at higher frequencies. The conductor material being used is solid copper, tin plated. The dielectric for the higher impedance cables is a foamed polypropylene or polyethylene in order to keep the physical size within the .100 center-to-center spaces. The 50-ohm cable uses solid polypropylene. The balance of low dielectric constant for high impedance designs with the high dielectric constant of the low impedance cable makes the dielectric outside diameter more of a common size. This common size spaces the drain wire to one side in a smaller tolerance zone area. The foamed material gives a propagation delay time about 13% better than teflon, and the solid polypropylene is about 5% slower. Nominal time delay for the solid material is 1.54 nano seconds/ft., and 1.29 for the foamed. Generally, rise time degradation is effected by the cable lenghts[4]. Dielectric loss is dominant in lengths of approximately 3 ft. or less. In long lengths of over 30 ft., the dielectric loss has already taken its toll, and now resistive loss is primary. Between 3 and 30 feet length, the cable loss is a combination of both. The dielectric power factor is very close to that of teflon, thus providing similar transmission capability.

Shield construction resulted from the desire to have some means of easy mass termination. Braid is not easily gang stripped nor terminated. A single solid wire at a known location can be controlled. The foil completes the shielding of the coax core. The foil can be easily removed with the jacket during the gang strip sequence.

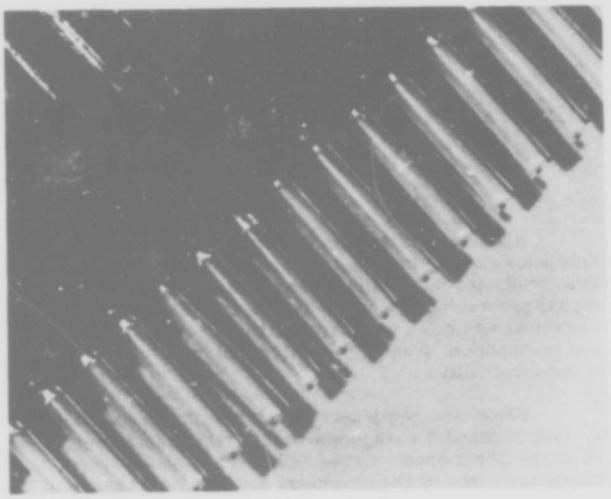

Figure 5. Gang stripped ribbon coax cable.

This stripping action exposes the drain wire where it can be easily controlled for termination. Braid uses not only expensive copper, but also adds bulk. The technique of aluminum foil shielding has had about fifteen years of practical use in service. Because of the many plus features, the foil drain wire shield is used.

It has been stated that the spacing of the center conductors with respect to each other, and the drain wires with respect to each other, is of prime importance. This oriented spacing provides the key to producing various type terminations onto boards, or into connectors. It would be appropriate to point out that the spacing tolerance is not very critical, providing there is no great accumulative overall tolerance. The stripping action removes the jacket and foil, leaving the exposed drain and center conductors. These now have the capability to be moved slightly left or right. The termination techniques have the capability for adjusting the conductors to match the contact location. The close space tolerance required in an enclosed fixed construction is minimized.

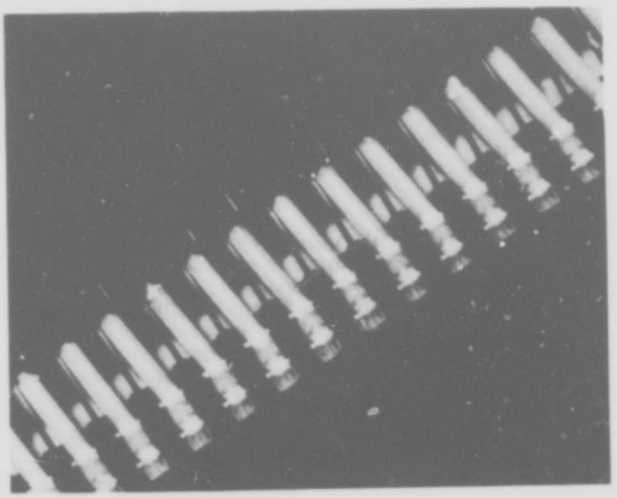

Figure 6. Mass terminated ribbon coax cable showing signal side of connector.

Cable of this new construction has been produced with the foil and drain wire to the inside against the dielectric, as well as foil on the outside with the drain

wire pressed against it. Both methods show the characteristic impedance values, as indicated by TDR, to be quite stable. Minimal variation was observed along the length of the cable using either method.

To check the bend or crush resistance of the cable, the 50 ohm cable was checked for insulation resistant, dielectric withstanding voltage, and impedance on a TDR. A 30 inch length of cable was checked as produced, after being clamped in a 90° bend, and after a 3 hour hold while still being clamped in an 80°C ambient.

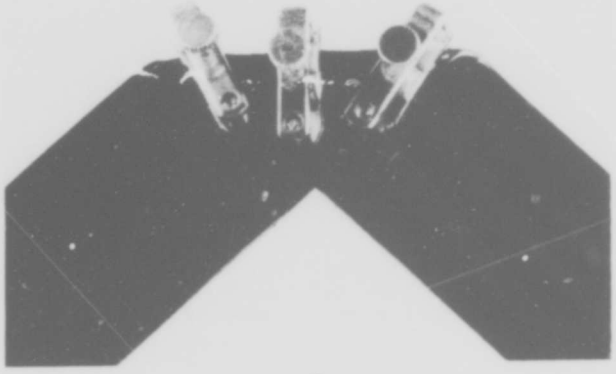

Figure 7. Cable clamped in 90° bend position.

All lines passed all 60 second dielectric withstanding voltage tests held at 1.5 Kv dc. The insulation resistance was 3.4×10^8 megohms average initially, 3.7×10^8 megohms average bent 90°, and 8.8×10^7 megohms average after the 80°C heat age. The bend caused approximately a 0.3 ohm rise in characteristic impedance (Zo) at the bend, a 0.75 ohm increase at the bend while at elevated temperature, and a permanent change of 0.3 ohms Zo over its full length after returning to room ambient. All readings were within 50 ± 1.75 of the 50 ± 3 ohm tolerance of the cable.

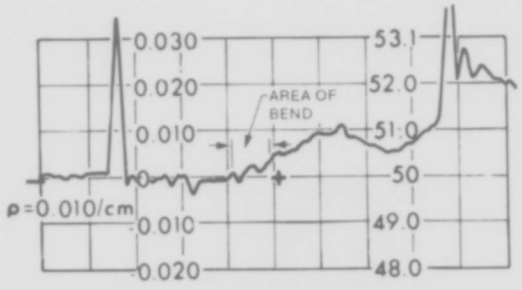

Figure 8a. Unbent "as produced" cable.

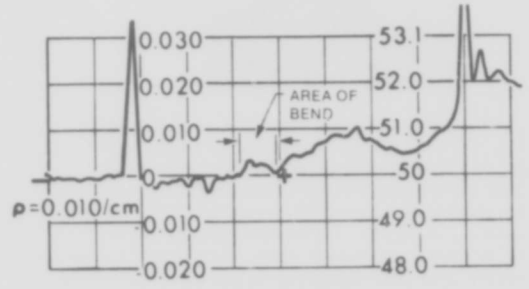

Figures 8b. Cable bent 90 degrees.

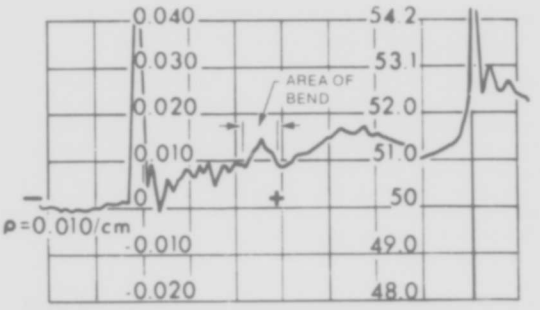

Figure 8c. Cable bent, at 80°C ambient after three hours soak.

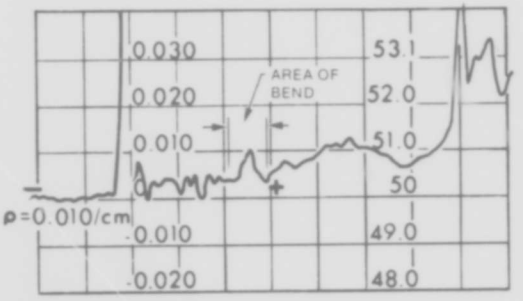

Figure 8d. Cable at room ambient after three hour 80°C soak.

The shielding efficiency between adjacent lines of the cable was checked by Sweep RF and Digital methods. Using a Wavetek 2001 and an HP8551, a 11 ft. 10 inch piece of 50 ohm ribbon coax cable was swept from 0 to 1400 MHz. The spectrum analysis between adjacent pairs indicated the minimum isolation was approximately 36 db at the 730 MHz level. In the 125 MHz frequency range of ECL - 10,000, the isolation was greater than 60 db.

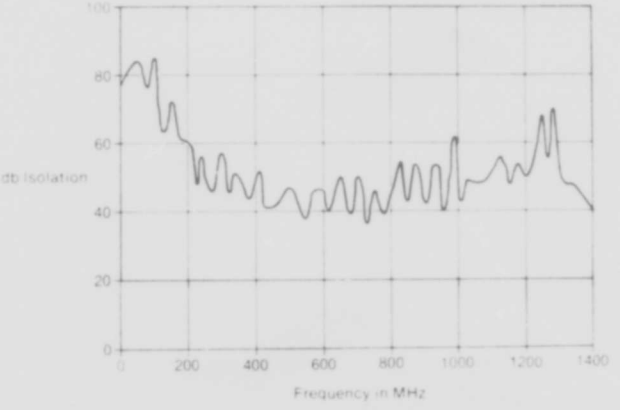

Figure 9. 50 ohm ribbon coax spectrum analysis of cross talk isolation.

The digital cross talk was checked by using an HP 1415. Braid coax (RG-174) and twisted pair were also checked at the same time, to give a comparison to the new foil ribbon coax construction. Using a 1 nano second rise time, the backward cross talk coefficient K_B could not be detected on the braided and ribbon coax, and was considered as being less than 0.04%. The twisted pair K_B was 9%. The forward cross talk coefficient K_F was .00044 nano second/ft. for the ribbon coax. Braided coax K_F was .00024 and twisted pair K_F was .030. Where K_F (ns/ft) x

rate of rise (volts/ns) x cable length (ft) = volts of cross talk and K_B (%) x signal (volts) = volts of cross talk.

In logic families that use high speed, such as the ECL - 10,000, there are four prime contributing factors in the line interconnections. These are propagation delay, attenuation, cross talk, and mismatch reflections.[5] Wm. R. Blood, Jr. states[6] that in MECL circuits the parts specified to drive transmission lines will drive coaxial cables over distances limited only by the bandwidth of the cable. In addition, he indicates the shielding in coaxial cable gives good isolation from external noise.

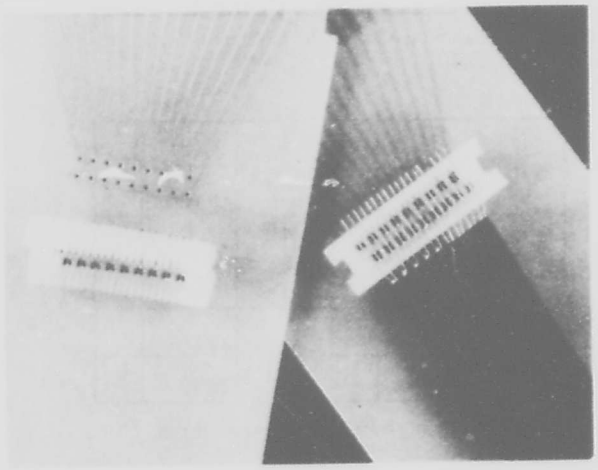

Figure 10. Ribbon coax application to a fixed printed circuit board.

The objective in developing and producing this flat flexible ribbon coaxial cable has been to meet today's and tomorrow's requirements for high speed applications. The cable saves valuable material and assembly time, while providing the excellent transmission capability required.

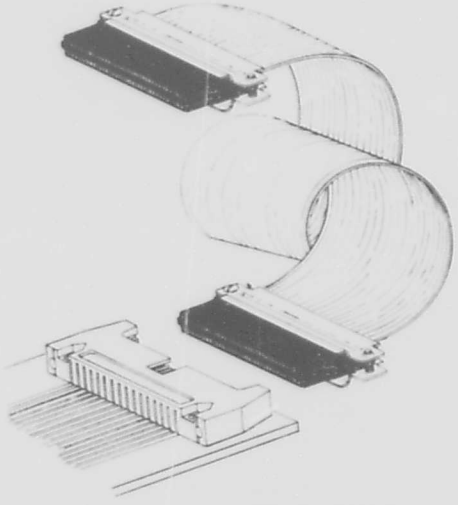

Figure 11. Ribbon coax connector application.

The author wishes to acknowledge the excellent backing of the program by management, Mr. J. L. Boscov and his staff for providing early productive product, Mr. J. H. Huber and his ardent development effort, and Mr. J. C. Latimer and his test laboratory personnel.

References

1. R. Wigington, Transient Analysis of Coaxial Cables Considering Skin Effect, PROCEEDINGS OF THE IRE, Feb., 1957.

2. O. Kerns and F. Kirsten, "Pulse Response of Coaxial Cables", File No. CC2-1B(1) Rev. July 29, 1966, Lawrence Radiation Laboratory, University of California, Berkeley.

3. F. Kirsten and L. Proehl, "Physical Characteristics of Coaxial Cables", File No. CC2-2C(1), Rev. May 31, 1966, Lawrence Radiation Laboratory, University of California, Berkeley.

4. Norris S. Nahman, "A Note on the Transition (Rise) Time Versus Line Length in Coaxial Cables". IEEE Transaction on Circuit Theory, March 1973.

5. Tom Balph, "Avoid ECL - 10,000 wiring problems". ELECTRONIC DESIGN 18, September 2, 1972 and "Interconnection Techniques for Motorola's MECL 10,000 Series Emitter-Coupled Logic", Application note 556, Motorola, Inc., 1972.

6. William R. Blood, Jr. "MECL System Design Handbook", 2nd Edition, Motorola Semiconductor Products, Inc.
MECL - Trademark of Motorola Inc.

William L. Schumacher is Manager of Development Engineering, COAXICON-RF Division, AMP Incorporated. He has been working in the electrical/electronic field with RCA and AMP Incorporated since obtaining his BSEE degree from the University of Missouri in 1949. He is a senior member of IEEE. He has had patents issued and pending in connector construction, crimp techniques, high application rate terminations, coaxial contacts, and RF transmission techniques and products.

MASS WIRE INSULATION DISPLACING TERMINATION OF FLAT CABLE

Donald J. Doty and George A. Patton

AMP Incorporated

Abstract

It has been often said that, widespread usage and application of flat cable has been restrained because of the lack of a suitable and reliable termination technique. A highly innovative new development has made possible the first insulation-displacing, mass terminating connector that can terminate both round and flat conductor cable.

The same connector can be used to terminate twisted pair flat cable providing the unique capability of a single connector that is suitable for every variety of flat flexible cable used in low and medium frequency signal termination.

This paper covers the technical aspects of "Displation", the insulation-displacing termination phenomena and describes the associated tooling that permits mass wire termination.

Several examples of mass-terminated 50-position telecommunications connectors are illustrated using laminated, bonded, woven, extruded, etched, and ribbon cable.

Design Objectives

The general requirements for a permanent wire connection suitable for use in telephone central office equipment were listed by VanHorn[1] in the pioneering work of BTL on the wrapped-wire termination. These requirements, with the very slight modifications to make them applicable to the termination to be discussed, are:

1. Intimate contact must be achieved between wire and terminal.
2. The points of contact should be gas-tight to withstand corrosion.
3. The minimum dimension of the gas-tight area should be great enough so that it does not decrease appreciably during the expected life (40 years) because of corrosion or relaxation of stresses wire and/or terminal.
4. The sum of the areas of intimate contact should be equal to or greater than the cross section of the wire, to prevent local heating.
5. The connection should be mechanically stable so that forces applied during shipping, handling, installation and subsequent maintenance activities will not dislodge the wire and break the points of intimate contact.
6. The wire should not be excessively deformed or embrittled so that it may break due to normal handling and service stresses.

These requirements are equally valid today as they were 20 years ago, and they form the design objectives established for the CHAMP wire termination. The following paragraphs describe this new termination method and how it meets these objectives.

Basic Termination Concept

Stamped and formed from high conductivity beryllium copper, the wire terminating area resembles an inverted "U" as shown in Figure 1. Each leg of the "U" contains a wire slot with precisely controlled dimensions.

An insulated wire fits loosely into the uppermost portion of the slot. As the tool pushes the wire deeper into position, the "funnel shaped" area of the slot displaces the insulation and restricts the conductor. Additional downward

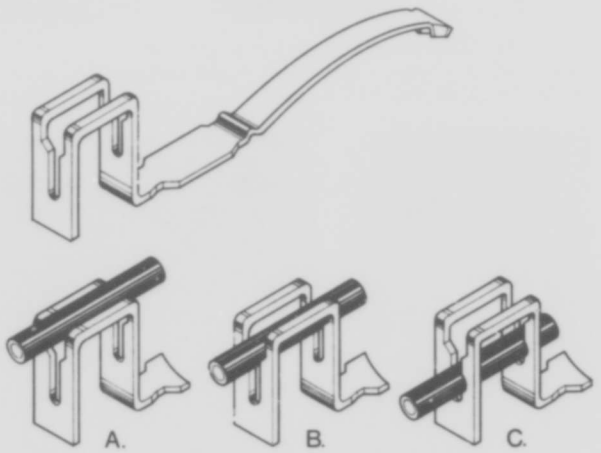

Figure 1. In use wire fits loosely into upper portion of slot (a), "funnel shaped" area displaces insulation (b) and, conductor is forced into narrow bottom portion of slot (c).

movement of the tool forces the conductor to fit into the confines of the narrow parallel portion of the slot where electrical contact is made. During this process, the conductor deformation displaces oxides or other contaminants that may exist on the conductor surface producing a clean metal surface to aid in effecting a stable electrical resistance. The wiping action that takes place as the conductor is forced deeper into the slot produces a similar cleaning of the terminal slot walls.

Residual spring energy in the terminal causes the two side walls of the slot to function like opposing cantilever beams maintaining the constant pressure necessary to ensure intimate metal-to-metal contact.

The two slots (front and rear) are of different widths. The front slot functions in the manner just described. The rear slot is wider and deforms the conductor to a lesser degree serving as insulation support and strain relief. The cross sectional photomicrographs shown (Figure 2) illustrate the type and amount of deformation that typically takes place on round conductor solid wire.

---

[1] R.H. VanHorn, "Solderless Wrapped Connections--Part III, BSTJ 32, No. 3, May, 1953, P.591-592.

CHAMP is a Trademark of AMP Incorporated

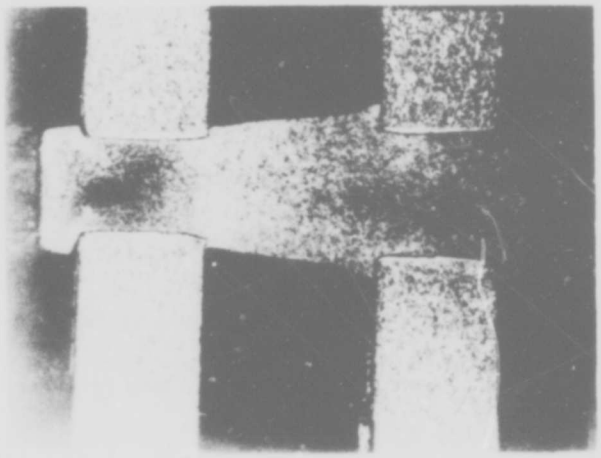

Figure 2a. Relationship of conductor and slot dimensions is shown in this view. Front slot is on the left, rear slot on the right.

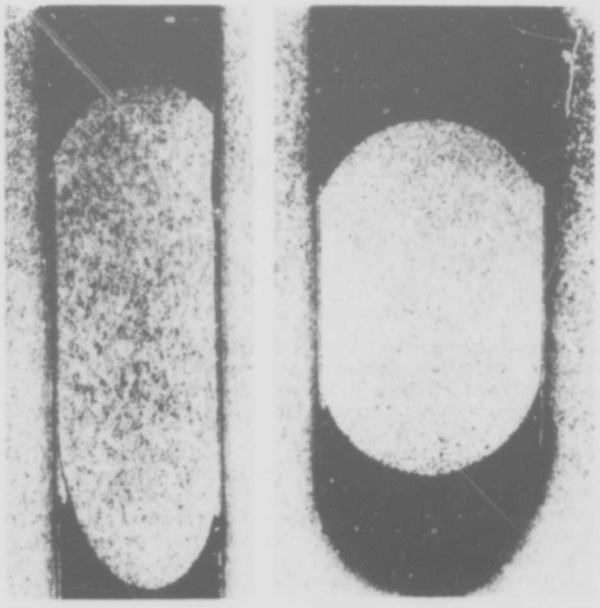

Figure 2b. Figure 2c.
Amount of conductor deformation is readily seen in this view of front slot (2b), while deformation is somewhat less in rear slot (2c).

Wire Deformation and Contact Area

When the wire is inserted into the slot of a CHAMP terminal, plastic deformation of the wire takes place. The original circular cross section of the wire is changed to shapes corresponding to the sketches in Figure 3. It is conceivable that the wire deformation may occur with or without longitudinal extrusion of the wire. Therefore, to calculate the contact area formed by deformation of the wire two cases are considered. In Case I, the original circular wire cross section is simply truncated in producing the final shape obtained in the slot region, which may also implicitly assume that longitudinal extrusion occurs. In Case II, no longitudinal extrusion occurs, and the total cross section of the wire remains constant during deformation

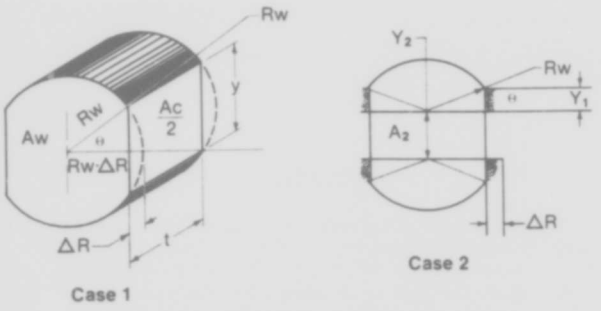

$$\frac{\Delta D}{Dw} = \frac{\Delta R}{R} = K$$

Figure 3. Minimum and Maximum Wire Deformation.

in the slot region. The real case lies somewhere between these extremes.

For either case, we get the expression for the ratio of contact area to wire cross section are:

$$\frac{A_c}{A_w} = \frac{4t}{\pi D_w}\,[f(k)]$$

Where, For Case I,

$$f_{(1)}(k) = 2\sqrt{2k - k^2}$$

Case II,

$$f_{(2)}(k) = \sqrt{2k - k^2} + \frac{\pi\theta}{180(1 - k)}$$

The functions f(k) are plotted in Figure 4. It is apparent that with a terminal stock thickness approximately equal to the wire diameter, a 10% reduction of

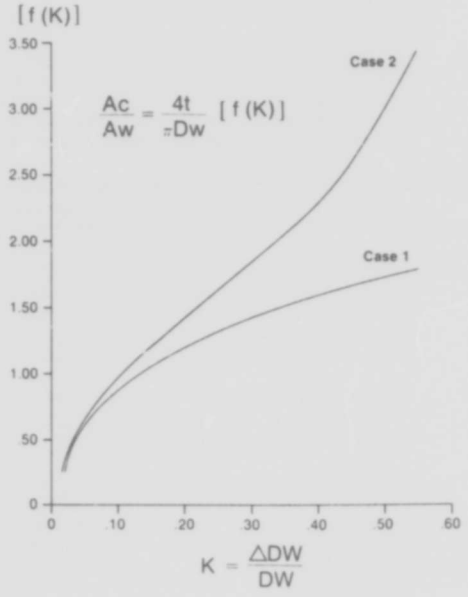

Figure 4. Deformation and Contact Area Relationship.

area of all connector contacts and simultaneously terminating all joints.

To make this operation cost effective and usable for high volume connector quantities, a production oriented line of machines and tooling has been designed allowing for expansion into various contact numbers. The system is designed to provide completed EPB operation of 20 seconds per connector independent of contact numbers, but dependent on bond head length. As an example, with a 50 contact connector, over 8000 terminations per hour can be made. It is possible to perform both the terminating and reflow operations on the same press. Installed costs for both terminating and reflowing using an unburdened labor figure could be less than $0.0025 per line. When adding this to connector costs and then comparing this total to other methods of terminating and associated hardware, only then can a true installed cost evaluation be made.

BIOGRAPHY

Gerald C. Smith
Senior Engineer
Microelectronics Products

Mr. Smith received an Associate Degree in Applied Sciences for Electrical Technology in 1959 from Broome County Community College. Working on a continuing educational program, he received a Bachelor of Arts degree from Utica College of Syracuse University in May 1972 with a major in Physics.

Joining Bendix-ECD immediately following graduation in 1959, Mr. Smith started as a Junior Laboratory Technician performing calibration and repair work on various test equipment. In 1960 he transferred into a new group, the Electrical Standards Laboratory. Here he was concerned with maintaining electrical and environmental standards and advancing calibration techniques for the division, and was advanced to the position of Senior Laboratory Technician. In 1969 he was promoted to Test Engineer assisting in operating the Standards Laboratory and was assigned to work on special projects of high voltage pulse measurements, electrical energy measurements and as a consultant in various measurement problems.

In 1971 he was assigned to the position of Senior Engineer in the division's Microelectronics Group with responsibilities in special connector programs and technical investigations into a new joint bonding program.

Mr. Smith has authored technical papers entitled "Constructing Fixtures for Using MSLD", and "Energy Pulse Bonding".

wire diameter by the slot will produce a total contact area greater than the wire area. For the specific case of a #24 wire in the 50 position connector:

$$D_w = 0.020 \text{ inch}$$

$$t = 0.010 \text{ inch}$$

and

$$\frac{A_c}{A_w} = 0.636 f(k)$$

In the contact slot, $K \sim 20\%$, and

$$\frac{A_c}{A_w} \sim .636(1.3) = .827$$

In the "strain relief" slot, $K \sim 5\%$, and

$$\frac{A_c}{A_w} \sim .636(.6) = 0.3816$$

So the total contact area in the two slots is:

$$A_c = 1.2 A_w$$

Contact Resistance

In all CHAMP terminals, the cross section of the terminal is greater than that of the wire being terminated. However, even when the true area of intimate contact between wire and terminal is equal to or greater than the wire area, there arises a "constriction" resistance at the interface because of the abrupt change in cross section area. Defined as the "Minimum Constriction Resistance of Full-Area Contact,"[2] it is a resistance which must be added to the calculated (or measured) bulk resistance of the contacting members--wire and terminal--to obtain the overall resistance of the connection as normally measured. In a sense, this "minimum constriction resistance" reflects the inability to utilize the entire terminal cross section for conduction at regions close to the interface.

It is possible to calculate the minimum constriction resistance by application of Possion's equation. For practical purposes a sufficiently accurate approximate can be obtained from the simple Holm formula for constriction resistance:

$$R_c = \frac{\rho}{2d}$$

where ρ = resistivity of the large contact member, d = diameter of small wire. For #24 AWG Copper wire and beryllium copper terminal, this gives:

$$R_c = \frac{3.93 \times 10^{-6} \text{ micro-ohm-inch}}{2(20) \times 10^{-3} \text{ inches}} = 98 \text{ microhms}$$

This is the value of constriction resistance expected in the CHAMP termination when full-area contact has been achieved, and when the cleaning action during wire insertion has been effective in removing all films from the contact interface. It should be noted that this minimum value applied even when the total contact area is greater than the cross section of the wire. When the true contact area is less than the wire area, the constriction resistance will be larger than the above value.

Terminal Force/Deflection and Residual Energy

A complete "strength of materials" analysis of force deflection characteristics[3] performed on CHAMP terminals indicates that the resilience of the terminal structure is

$$\delta = 0.426 \frac{\text{mils}}{\text{pound}}$$

where δ is total deflection inches and F is contact force in pounds between wire and each slot side. The differential spring rate than is

$$\frac{dF}{ds} \sim \frac{2.35 \text{ pounds}}{\text{mil}}$$

Empirical curves have been established to give the contact force as a function of wire deformation. Figure 5 indicates that with #24 wire, the contact force ranges from 6.7 pounds at a minimum 20% deformation to 8.0 pounds for a maximum 34% deformation.

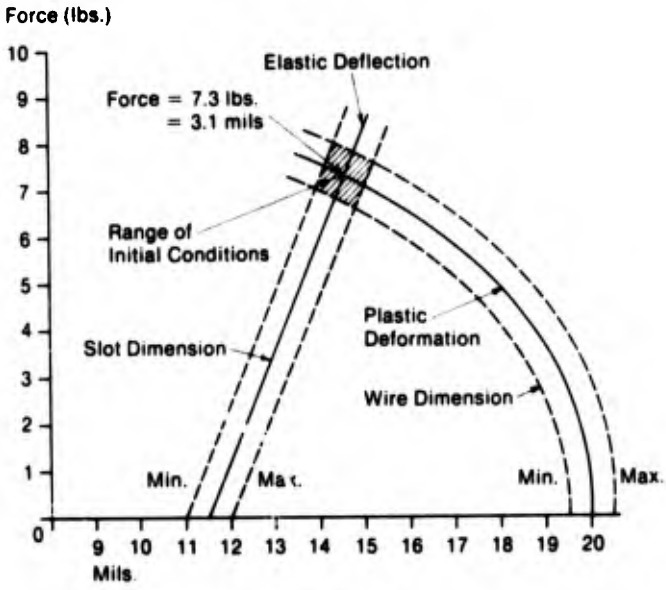

Figure 5. Relationship of Contact Force to Terminal Deflection and Wire Deformation

To confirm the force deflection characteristic obtained from the strength of materials analysis, and to identify regions of maximum stress, the terminal was treated by finite element analysis.[4] The results of this analysis indicate that the average terminal stresses are relatively low and well below the 110 KSI yield stress for beryllium copper. Since the wire is plastically deformed during insertion in the slot, it is apparent that the average unit stress in the wire is high. In fact, it is at the yield point for the wire. In evaluating the stored elastic energy in the two members, it has been found that for (AWG #24), 98% of the stored energy resides in the terminal, a highly desirable situation with respect to the ability to maintain contact forces over a long period of time.

Creep

The wire can be expected to contribute most to creep and stress relaxation in the termination because it is under higher unit stress than the terminal and be-

[2] J.H. Whitley, "Minimum Constriction Resistance of Full-Area Contacts", AMP Research Note #21, January 7, 1966.

[3] G. A. Patton & J. H. Whitley "Appendix I, The Force Deflection Characteristic for the Slot Terminal, Termination Analysis of AMP 50 position (25 pair) Cable Connector" Report #110-6009, February 1973.

[4] M.A. Oliver "Appendix II, Finite Element Analysis of 50 Position CHAMP Connector, Termination Analysis of AMP 50 Position (25 pair) Cable Connector," Report #110-6009, February 1973.

cause the terminal alloy is more resistant to creep. Data on compressive creep of copper wire is scarce, especially at low temperature. It is believed that an estimate based on tensile creep data will represent a worst-case situation. Under compression, creep is inhibited by the "friction hill" effect at the contact faces. The wire is also strain-hardened in the region under compression, which improves creep characteristics.

Tensile data indicates that 1% creep in copper is a large amount to be obtained at room temperature even with high stress. At normal room temperature, the total creep is more usually given as fractions of a percent. The wire dimension in the slot (for AWG #24) is about 14.6×10^{-3} inches. If this dimension decreases by 1%, it represents a "deflection" of 146 microinches which must be accommodated by the elastic deflection of the terminal. The terminal deflection is normally $\delta = 3100$ microinches. The indicated terminal deflection after creep is then $\delta = 2953$ microinches, which implies that the contact force will be reduced to $F' = 6.96$ lbs.

The 5% reduction in contact force is considered reasonable and safe, and is greater than that which would actually occur, since as the force diminishes the stress decreases and the creep rate decreases.

To reduce the contact force to one-half its initial value, the total creep of the wire must be greater than 10%. This is 10 to 100 times the creep actually expected in service.

Mechanical Stability

Potentially the most serious weakness of single wire-in-slot connections is mechanical disturbance of the contact interface due to externally-imposed forces and torques on the wire. The double slot of the CHAMP terminal is effective in eliminating this weakness. The separated slots reduce the effect of bending moments. The strain relief slot, being wider, does not appreciably deform (and hence weaken) the wire as much as the contact slot.

So the CHAMP termination is purposely designed to withstand the forces of handling shipping, and maintenance activities. Actual field experience with the "standard" CHAMP termination has proven the efficacy of the approach.

Performance With Different Conductor Types

Solid Wire--Original design centered around solid wire and extensive testing has been performed with solid conductors. These tests included; heat aging (244°F for 33 days), temperature cycling (MIL-STD-202D, Method 102A, ConditionD), moisture resistance (MIL-STD-202D, Method 106C), as well as shock, vibration, industrial gas, and salt spray. The heat age test results shown in Figure 6 are typical of the data obtained.

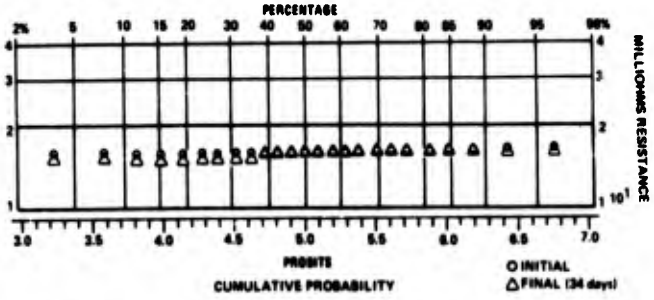

Figure 6. Solid Conductor Millivolt Drop

Stranded Wire--Investigations indicated that satisfactory performance will also be obtained with stranded wire in a terminal designed for solid wire. The feasibility of this approach has been confirmed by preliminary testing. Testing covering electrical characteristics and the effects of stress relaxation, temperature cycling, thermal shock, moisture, shock and vibration, etc. has been in process since early 1972.

Figure 7 is typical of the preliminary test results obtained with stranded wire. To obtain the data presented in Figure 7, initial millivolt drop readings were taken, and the samples were subjected to 99°C for 16 hours, then exposed to -15°C for 30 minutes. The samples were then subjected to vibration cycling. The first segment of vibration was 5 to 31 cycles/sec. for 12 sweeps with sweeps of 6 minutes. The second segment of vibration used 31 to 100 cycles/sec. for 12 sweeps; with 12 minute sweeps. After vibration testing, the samples were placed in a humidity chamber for 4 cycles of 24 hours each. No termination tested exceeded 2 milliohms change in resistance. Heatage exposure of 244°F for 33 days produced similar results.

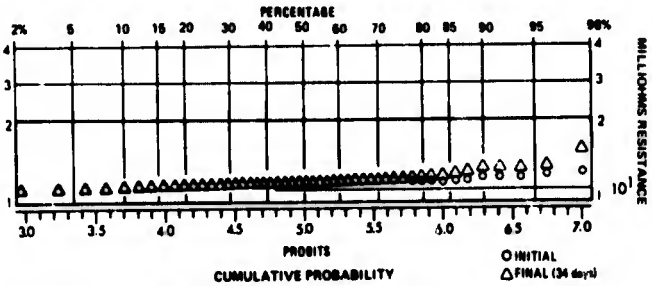

Figure 7. Stranded Wire Millivolt Drop

Flat Conductors--The flat conductors found in flat conductor flexible cable required special consideration. To prevent the insulated flat conductors from folding away from the slot walls during insertion, a forming support device was designed. This supporting member is basically a square wire that serves as a mandrel over which the insulated flat conductor is formed as it is pressed down into the terminal slot as shown in Figure 8.

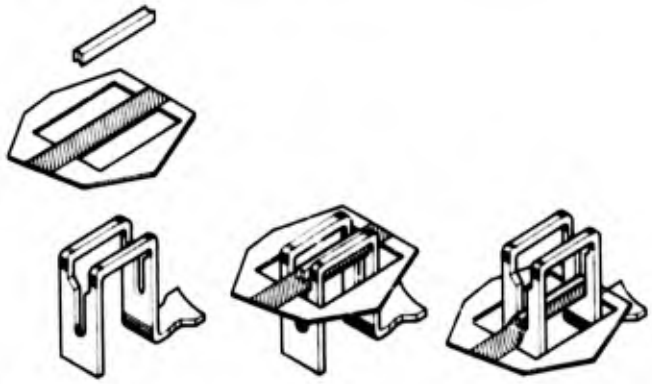

Figure 8. Terminating Flat Conductors.

Besides serving as a forming device, the square wire remains in the terminal slot providing the mass and rigidity required to adequately deflect the terminal beam members. Thus, with the addition of the square wire support device, the basic terminal accepts the flat conductors used in flat conductor flexible cable.

The only cable preparation required is a simple die cutting operation to provide clearance windows between conductors. There is no requirement to remove the insulation as it is displaced during termination. Figure 9 illustrates this and also the "stuffer" wire assembly.

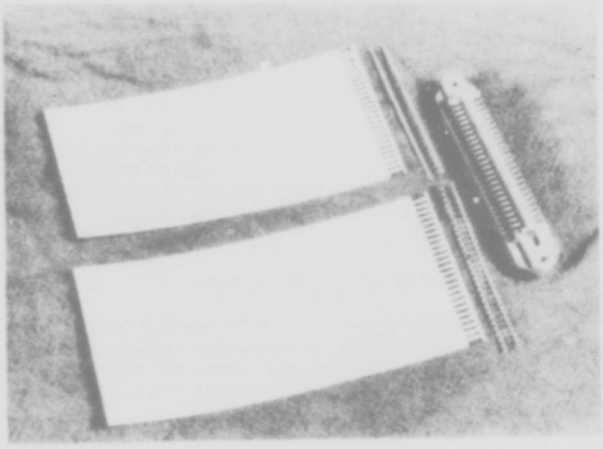

Figure 9. "Stuffer" wires are pre-positioned on .085" centers by insulating carriers.

The same testing performed for stranded wire terminating was performed on flat conductor terminations. The data presented in Figure 10 is typical of the results obtained.

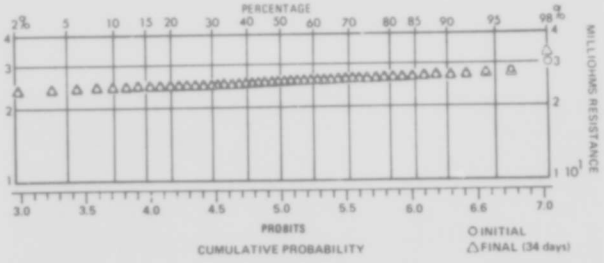

Figure 10. Flat Conductor Millivolt Drop.

Although the test program is still underway and formal results are not yet available, early data indicates that the same terminal that provides suitable performance with solid and stranded wire can also be used with flat-conductor flexible cable.

The photomicrograph shown (Figure 11) is typical of the results obtained by terminating flat conductor cable with the "stuffer" wire.

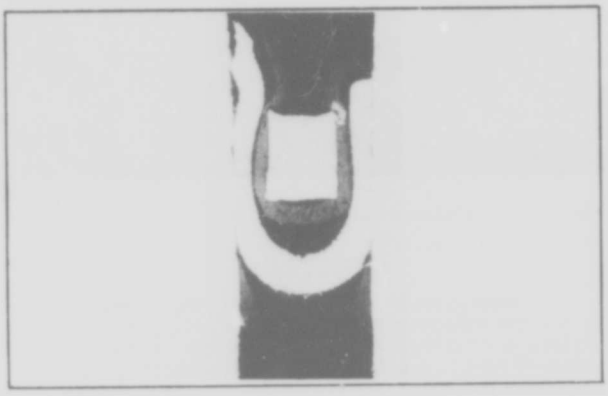

Figure 11. The square "stuffer" wire provides the backup support necessary to bring the thin flat conductor into intimate contact with the terminal slot.

Pair-At-A-Time Machine

Designed specifically to terminate multiple pair round conductor communication cables to CHAMP connectors, the machine shown in Figure 12 simultaneously cuts to length and terminates two wires. With the connector loaded in the machine and the cable clamped in position, the operator locates the appropriate pair of wires as indicated by a revolving color-code wheel and pulls the wires down over a guide bar. Completion of this action trips the two microswitches that actuate the machine. After the machine terminates each pair of wires it automatically indexes the connector and color-code wheel to the next position.

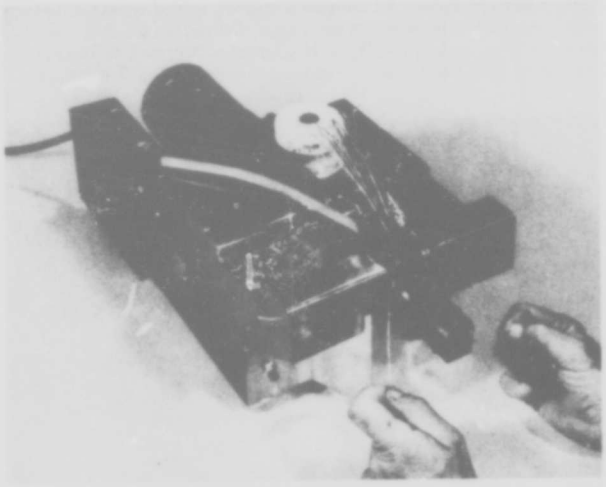

Figure 12. Pair-At-A-Time Machine for 25-pair Communication Cables.

Including the time required to load the machine and identify and position the wires, the total time required to terminate a 25-pair cable is approximately two minutes. The machine operates from 110 vac and requires less than two amperes.

Mass Termination In The Field

The manual tool concept used with these connectors lends itself readily to mass termination. The manually operated tool illustrated in Figure 13 simultaneously cuts to length and terminates all conductors for a given connector.

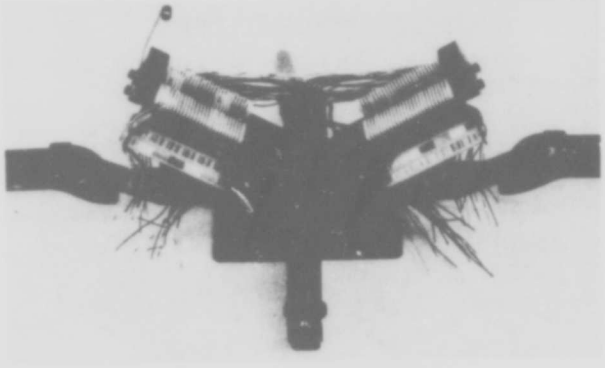

Figure 13. Hand Tool for mass termination of 25-pair communications cable.

In use, a connector is loaded into the tool, all wires dressed into position in a comb-like holder, the wire holding fixture swung into place, and a single closing stroke of the handles terminates all conductors. For 25-pair communication-cable or other cables requiring wire positioning, this entire sequence requires less than six minutes.

For flat cables with round conductors which are not located on the same centerline spacing as the terminals, a simple slit and form operation is required in order to fan the individual wires into the combs for mass termination.

The straight action manual tool shown in Figure 14 is specifically designed to mass terminate flexible flat cable, flat conductor or round conductor (solid or stranded) with conductors located on the same centerline as the connector. The tool is totally self contained and can fully terminate up to a 64-position connector in less than 2 minutes.

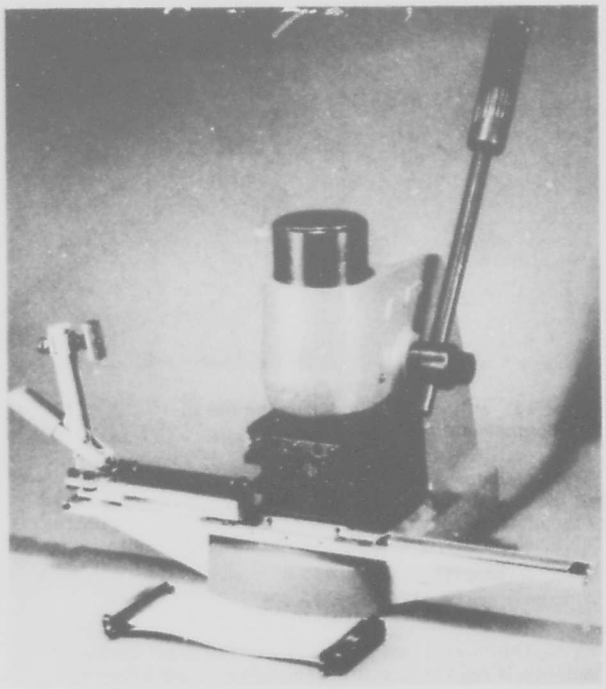

Figure 14. Straight Action Hand Tool for Flat Cables.

Mass Termination in The Factory

For higher production rates a fully automatic mass-terminating machine is shown in the artist's conception

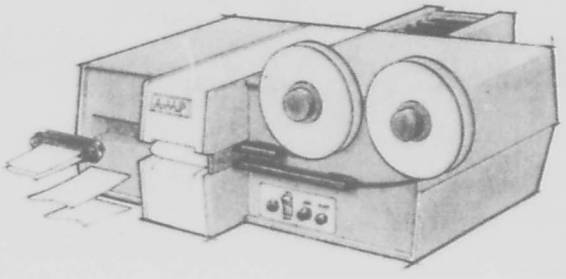

Figure 15. Fully Automatic Mass Terminating Machine.

of Figure 15. Feasibility of terminating up to a 64 position connector with flat cable having either round (solid or stranded) wire or flat conductors in less than 10 seconds has been established. For flat conductors, the square "stuffer" wire assemblies are fed to both sides of the connector. For round conductors, the stuffer feed mechanism is uncoupled or the reels removed completely from the machine. Connectors are magazine loaded. This machine is intended specifically for cables with conductors on the same centerline spacing as the terminals.

Flat Cable Applications

Although the various types of flat cable (bonded, woven, extruded, laminated, and etched) pose different terminating problems, each of these commonly available types can be successfully mass terminated in the same CHAMP connector.

Laminated Cable

Since laminated cable is available with conductors located on the same centerline spacing as the terminals in standard CHAMP connectors, the termination process is simple and straightforward. After the insulating web has been window punched to provide clearance between the individual conductors, the entire cable is positioned on the connector and all the conductors terminated simultaneously in the manual tool shown in Figure 14. The cable illustrated in Figure 16 was terminated in this manner in less than one minute.

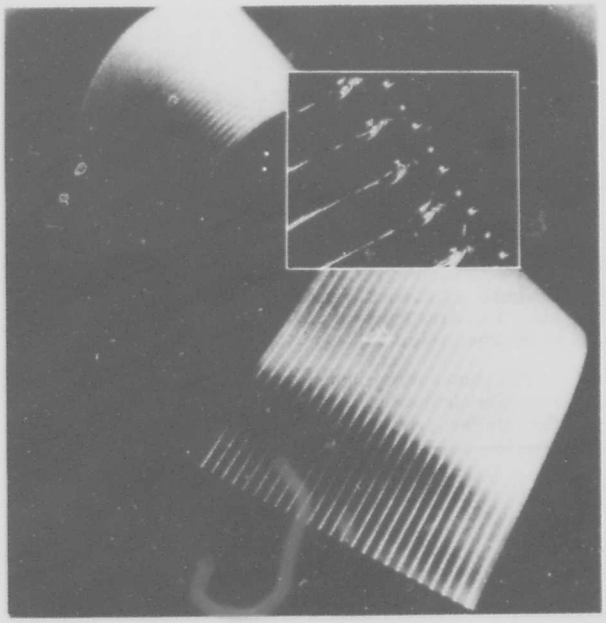

Figure 16. Laminated Cable.

Bonded Cable

To terminate parallel-conductor bonded cables, such as the one shown in Figure 17 it is necessary to separate and fan the conductors into position with a simple fixture. Once the conductors are located in their respective positions, they can all be terminated simultaneously.

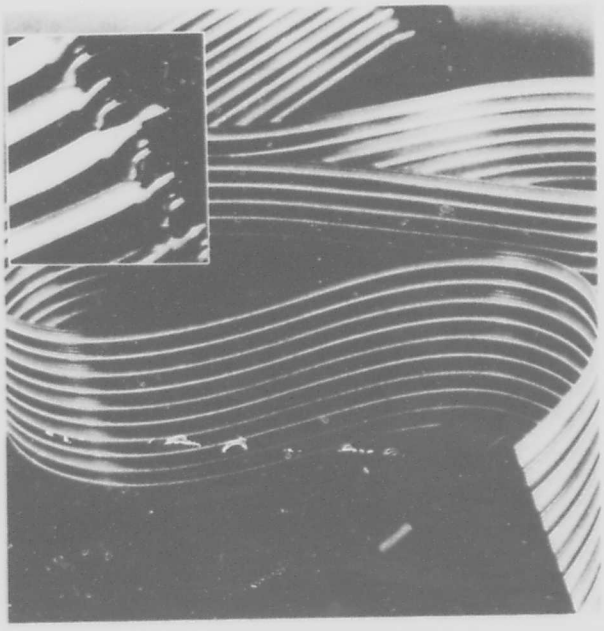

Figure 17. Parallel-Conductor Bonded Flat Cable.

Twisted pair bonded cables like the one in Figure 18, are slightly more complex to terminate since each wire of each pair must be visually identified, separated, and positioned. However, once the individual wires are properly positioned the entire cable can be mass terminated like parallel-conductor cable.

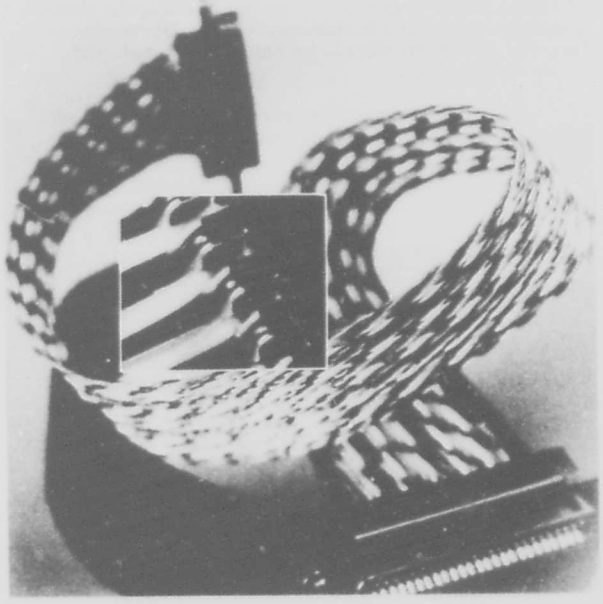

Figure 18. Twisted-Pair Bonded Flat Cable.

Woven Cable

Woven Cable, such as that shown in Figure 19 is also available in both parallel-conductor and twisted-pair versions and is terminated in a manner basically similar to that used for bonded cable.

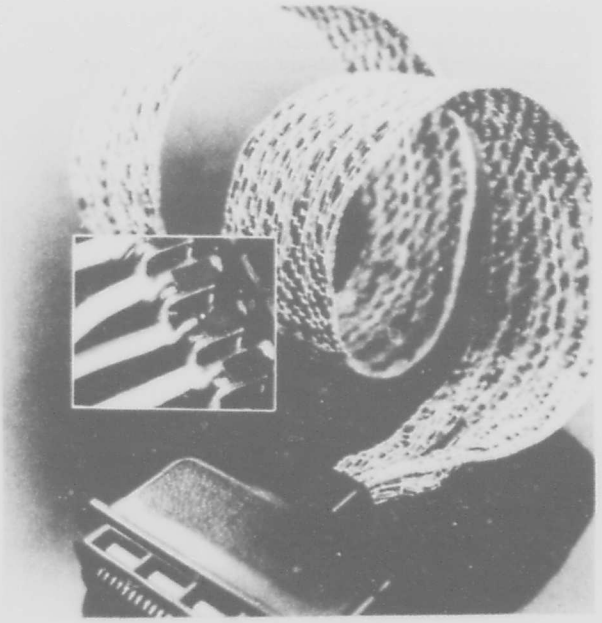

Figure 19. Woven Cable.

Jacketed Cable

The term "jacketed cable" is meant to include any flat cable protected with a relatively thick extruded or laminated plastic jacket such as that illustrated in Figure 20. The cable itself can be either extruded, bonded, or laminated. Several types are available and some include a copper or aluminum shield on one or both sides of the

Figure 20. Jacketed Cable.

cable beneath the outer jacket. Once the outer jacket has been stripped to the proper length, the cable is terminated like any other flat cable. Shield continuity is carried through with a simple grounding clip.

Flat Conductor Cable

The preferred flat-conductor cables which should be considered for mass-termination are those with conductors located on the same centerline spacing as the terminal with which they are to be used. It is also recommended that the conductors be over .025" wide to produce adequate contact area. Fortunately these two requirements pose no great problem since such cable is readily available from a variety of sources. Before terminating the cable shown in Figure 21 a simple punch die cuts "window" openings between adjacent conductors. These openings are sized to fit over the insulating barriers between each terminal, and are located away from the leading edge of the cable leaving a continuous "tie bar" of insulation on the leading edge of the cable. All openings were cut simultaneously.

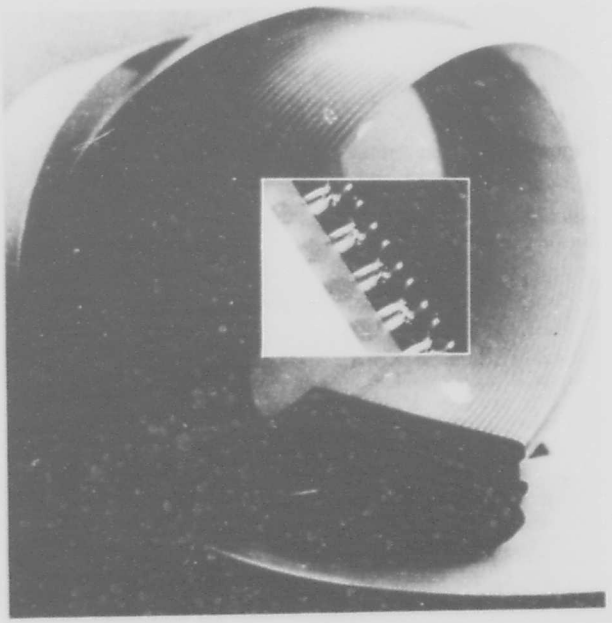

Figure 21. Flat Conductor Cable.

An integral strip of square "stuffer wires" (insulated from each other) is then positioned over the cable and all conductors terminated simultaneously.

The uninterrupted insulation "tie bar" provides the terminated cable with enhanced tensile strain relief. Additional flexure strain relief is provided by a close-fitting rib inside the rear cover of the connectors.

Etched Cable

Etched cable, flat flexible circuitry, with conductors on the same centerlines as the connector can be terminated in the same manner as just described for flat conductor cable (Figure 21).

Ribbon Cable

Ribbon cable which is essentially individual round conductor (solid or stranded) wires laminated between two plastic carrier strips and located on the same centerlines as the connector is terminated in the same fashion as laminated cable. (Figure 16).

It is possible to terminate this type of cable (Figure 22) without die cutting windows if the dielectric carrier strip is of the proper thickness and durometer.

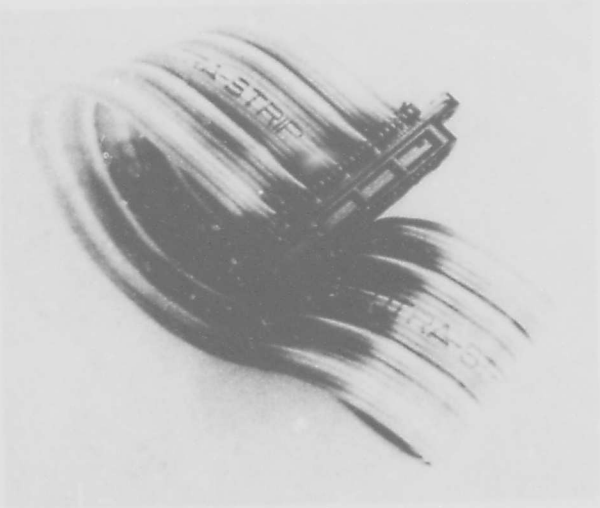

Figure 22. Spaced Paralled Conductor "Ribbon" Cable.

CONCLUSION

The design objectives established at the onset of the CHAMP connector development program have been met, and the resultant terminating technique has been proven suitable for mass termination. Solid wire, stranded wire, and flat conductor cable have demonstrated satisfactory levels of performance when terminated in standard CHAMP connectors. Tooling has been developed to terminate 25-pair communication cable and flexible flat cable of bonded, woven, extruded, laminated, and etched construction.

The CHAMP connector concept has brought mass termination of flat cable, and effective wire management one step closer to reality.

Donald J. Doty is Manager of Development Engineering, Communications Products Division, AMP Incorporated. A graduate of Rutgers University with a Bachelor of Science Degree in Engineering, he has more than 20 years experience in the design and manufacture of electronic components and equipment, including microwave and UHF components, and printed circuits.

WIDE BAND LEAKY COAXIAL CABLE

FOR A 800 MHz BAND

by

T. Kishimoto
Japanese National Railways
Tokyo, Japan

H. Kitani, Y. Nagai, Y. Miyamoto
Sumitomo Electric Industries, Ltd.
Yokohama, Japan

ABSTRACT

This paper concerns a newly developed wide band leaky coaxial cable (LCX) for a mobile communication system on 800 MHz band, and describes the basic designs of the large diameter (72D) cable structure and the advanced slot array cut on the outer conductor for a wide band use.

Two different typical size cables, the 72D (new size) and the 50D (former size) LCX, are discussed for the 800 MHz band use. Through the experimental evaluations, the wide band coupling characteristics have been examined over 300 MHz to 1,000 MHz.

In addition to these basic properties of the new LCX, the system construction method and some future applications are discussed in the paper. The field test in the practical system construction has been applied now by using about and 800 meter length new 72D LCX line installed along the railway track in the Railway Technical Research Institute of the Japanese National Railways. It is expected that the coupling level change along the LCX line will decrease within ±5 dB in total. A unit repeater length at 860 MHz can be enlarged to about 1.3 kilometers by arranging several types of the new 72D LCX with different leakages in cascade.

1. INTRODUCTION

In general, in the carrying forward a scheme of a mobile radio communication system, one of the last technical problems is the countermeasure to insure excellent communication quality covering over the desired service region in whole. Especially in the case of a train radio communication, any interruptions of communication channels cannot be permissible even though inside tunnels or in poor electromagnetic field regions.

Up to this time, various kinds of open type wired-wireless transmission lines were proposed. A leaky transmission line of coaxial structure with slot array cut on the outer conductor, which was developed for train radio communication in tunnels about 7 years ago [1], is recognized as one of the most desirable transmission lines to fulfil the above mentioned problems.

Figure 1 shows the cable structure and the shape of the particular slot array whose properly spaced slots convey a leaky wave and form a uniform radiation field along the cable for good coupling with mobiles. As a result of the good performances of the many field tests and practical feasibility studies, the Japanese National Railways (JNR) has decided to adopt the LCX as shown in the figure, and has proceeded to install the LCX train communication system to the JNR lines, as well as the Sanyo New Trunk Line.

For the present, the 150 MHz and 400 MHz bands allocated for the ordinary mobile radio communication channels are the main aiming frequency ranges for the LCX manufactured in Japan. However, considering the present situation of confused radio channels and the insatiable need for communication, it is anticipated that the utilization of the 800 MHz band will be done for mobile radio communication.

Heretofore, there is no example of an LCX for 800 MHz band use, nor is there a report of it. In the paper, the design of a new LCX for 800 MHz band, the basic properties of the developed cables and the system construction method, etc. are discussed.

2. CONSIDERATIONS OF THE LCX FOR 800 MHz BAND

There are two approaches to the realization of the LCX for 800 MHz band. One is only to reform a slot array for 800 MHz band using the former size cable structure, and the other both the slot array and the cable size.

Owing to the former method, it is natural that the transmission loss will increase considerably on 800 MHz band. Figure 1 indicates the former type cable structure (50D) for 400 MHz band use. The basic heat loss of the cable approaches 36 dB/km at 860 MHz, and the less the coupling loss, the more the transmission loss increases by the amount of the increased radiation. Those increased transmission losses on 800 MHz band inherently invite the contraction of the repeater spacing.

The other method acompanied by the moderate increase of cable size will be expected to compensate the increased loss. On the occasion of decision on the cable size, the following three technical problems were investigated.

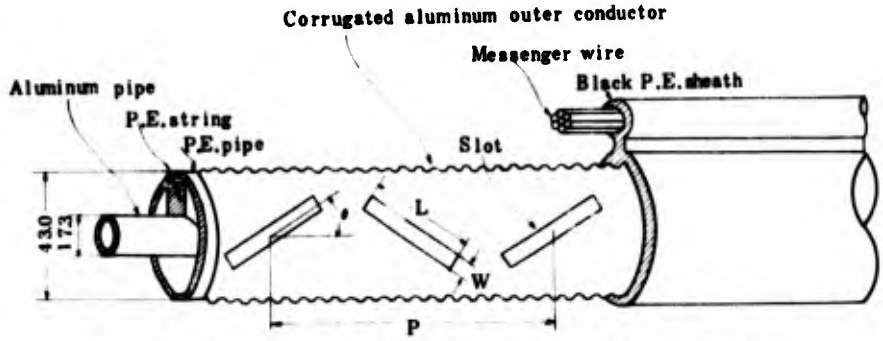

Fig. 1 Cable Structure of a LCX (50D) with a zig-zag slot array

(1) To compensate the increased loss on 800 MHz band

(2) Not to enlarge cable size to excess, so that the coaxial transmission mode may be a TEM-mode and each slot may operate under the nonresonant condition.

(3) Not to impair the flexibility of a cable.

3. CABLE STRUCTURE OF THE NEW LCX

Figure 2 shows the cross-sectional view of the newly developed LCX (72D) for 800 MHz band, as the result of the investigation described the above. The inner conductor is a corrugated copper pipe (av. diameter; 27.5mm), and the outer conductor is a corrugated aluminum tape with the advanced slot array which is longitudinally applied to the coaxial structure (av. diameter; 65mm). In order to protect the slot parts from deformation and cracks through the manufacturing process and the cable installation, the outer conductor is backed by a lamination of plastic films. As the insulation structure of the coaxial, the natural polyethylene string of a square cross-section spirally wound on the inner conductor and the plastic tapes wound around the spiral string structure are applied. The spiral polyethylene string has comb-like cuts periodically, which assist the winding operation and give flexibility to the cable. The cable jacket is sheathed by the black polyethylene, and the overall diameter of the cable is 72mm.

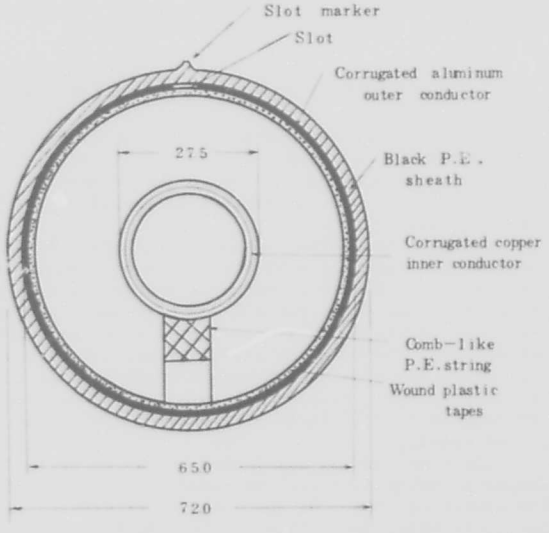

Fig. 2 Cross-sectional view of the new LCX (72D)

Figure 3 shows the manufactured cable samples of the 72D and 50D LCX.

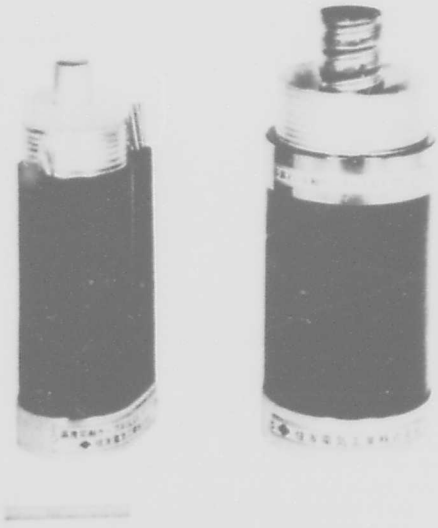

Fig. 3 Manufactured cable samples of 72D and 50D LCX

4. SLOT ARRAY DESIGN

4-1 Basic Theory of Radiation Condition

As a typical example of the former slot arrays, the zig-zag slot array [1] is shown in Fig. 1. It is well known that a coaxial structure with closely spaced slots on its outer conductor conveys surface wave modes, while that with properly spaced slots conveys leaky wave modes. On this, the subject of great interest to us is a leaky wave transmission.

In general, these periodical slot structures on the outer conductor induces many kinds of space harmonic modes of different phase constants in the outer space around the cable. For the conventional zig-zag slot array, the radial phase constant γ_n of the n-th order space harmonic mode is given by;

$$(\gamma_n)^2 = \left(\frac{2\pi}{\lambda}\right)^2 - \left(\frac{2\pi}{\lambda_g} + \frac{2\pi n}{p}\right)^2 \qquad (1)$$

where λ, λ_g, ν, p and n represent a wavelength in free space, a waveguide wavelength, a contraction ratio of λ_g to λ ($\nu = \lambda_g/\lambda$), a repetition interval of slots and an arbitrary integer, respectively.

The n-th order space harmonic mode begins to radiate outwards in the radial direction when γ_n is a real number, so that the radiation regions (or the leaky wave regions) of space harmonics are illustrated in Fig. 4.

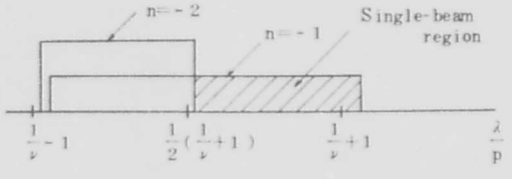

Fig. 4 Radiation regions of space harmonic modes in case of a zig-zag slot array

In the figure, the single-beam radiation pattern can only be attained where n=-1, and the ratio of upper and lower frequency limits is two times. On the other hand, the region of $\lambda / p > (1/\nu + 1)$ in the figure means that of surface wave modes, and the region of $\lambda /p < (1/\nu + 1)/2$ means that of multibeam radiation patterns which spoil the coupling characteristics owing to the interferences among plural space harmonic waves of different phase constants with one another.

The advanced slot array which is adopted to the new LCX discussed in the paper is characterized by its sinusoidally varing source-intensity distribution that makes it possible to greatly extend the single-beam radiation region. Figure 5 shows the practical implementations of the slot array based on the above thinking.

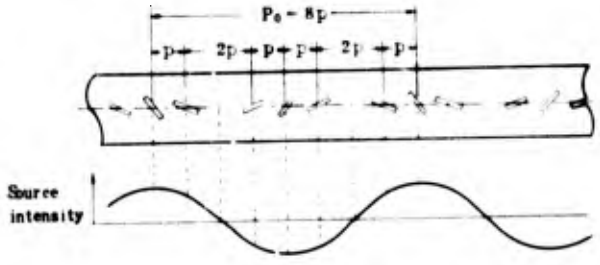

Fig. 5 Advanced slot array for wide band use

In the advanced slot array shown in Fig. 5, the phase constant in the radial direction γ_n of n-th order [2] the space harmonic mode can be expressed as follows;

$$(\gamma_-^n)^2 = \left(\frac{2\pi}{\lambda}\right)^2 - \left(\frac{2\pi}{\lambda}\right)^2 \left[\frac{1}{\lambda} - \frac{\lambda}{P_0} - \frac{n\lambda}{p}\right]^2$$

$$(\gamma_+^n)^2 = \left(\frac{2\pi}{\lambda}\right)^2 - \left(\frac{2\pi}{\lambda}\right)^2 \left[\frac{1}{\lambda} - \frac{\lambda}{P_0} + \frac{n\lambda}{p}\right]^2 \qquad (2)$$

where p and P_0 are the minimum slot intervals and the repetition period of the sinusoidal change in the slot array, respectively.

The radiation regions in the case of the above mentioned slot array can be got under the condition $(\gamma_{\pm}^n)^2 > 0$ in Eq. 2, and graphically drawn as shown in Fig. 6.

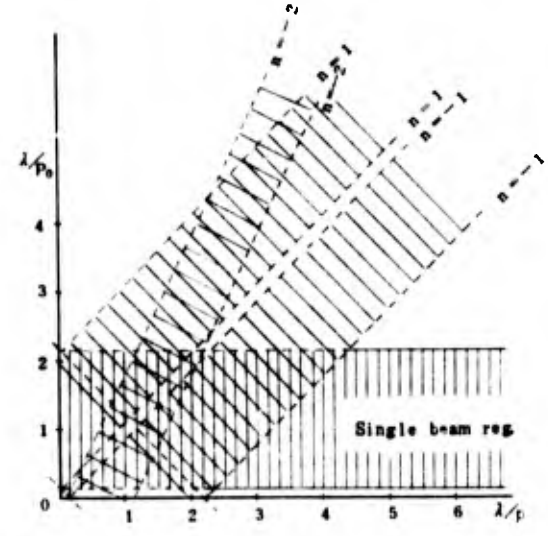

Fig. 6 Radiation regions of space harmonic modes in case of the advanced slot array

In the figure, the region which is bounded with lines n=0 and does not overlap with other radiation regions represents a stable single-beam radiation. Since such a radiation pattern is most desirable for mobile communication applications, the design of the slot pitches P_0 and p should be determined in relation to the wavelength to be used, so that the parameters λ/P_0 and λ/p may fall in the single-beam region all over the frequency band necessary to the desired mobile communication system.

When the slot pitches P_0 and p are chosen properly according to the above procedure, the ratio of upper and lower frequency limits for the single-beam leaky wave can be seven times, in case of the selection P_0=8p as shown in Fig. 5. When the degree of approximation of the sinusoidal source-intensity distribution is improved, the ratio will come up to 19 times in case of $\nu = 0.9$.

4-2 Radiation Property of Leaky Wave

The radiation beam angle of leaky wave is naturally frequency responsive. When the angle θ is defined as Fig. 7, the relation between θ and λ/P_0 can be calculated from Eq. (2) as follows;

$$\theta = \arcsin\left(\frac{\lambda}{P_0} - \frac{1}{\nu}\right) \qquad (3)$$

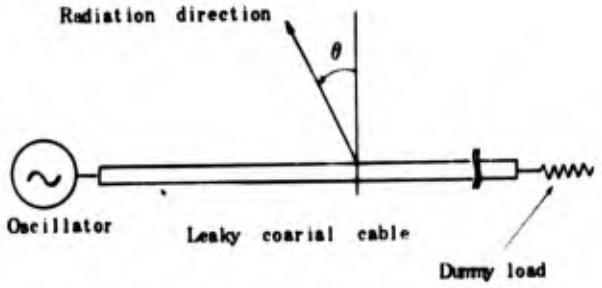

Fig. 7 Definition of radiation beam angle

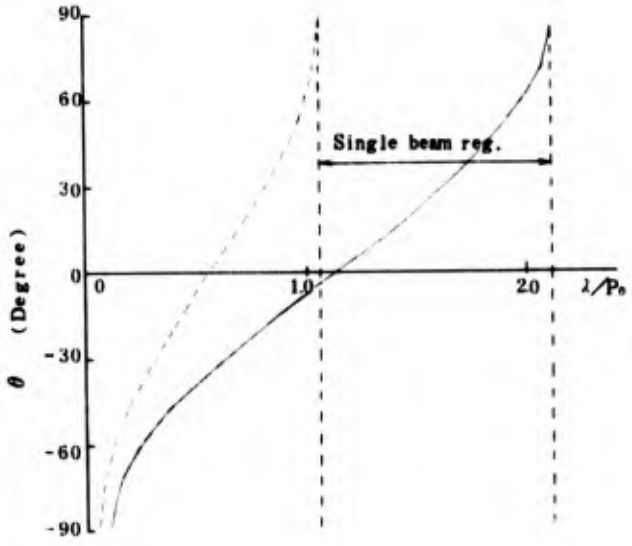

Fig. 8 Property of radiation beam angle vs. λ/P_0

Figure 8 shows the property of radiation beam angle θ vs. λ/P_0 owing to Eq.(3). In the figure, the dotted line indicates the angle of the next higher order mode of space harmonic wave in the case of the zigzag slot array of uniperiodicity P_0, which means the limitation of the single beam radiation region. In the case of the advanced slot array of dual periodicity P_0, p, the undesired radiation of the above mentioned higher mode is inherently suppressed, and the superior wide band radiation characteristics can be realized. Figure 9 shows the example of the radiation pattern in the horizontal plane including the cable axis measured by using the new 72D LCX of 2 meter length at 860 MHz. The measured radiation beam angle is good consistent with the caculated value.

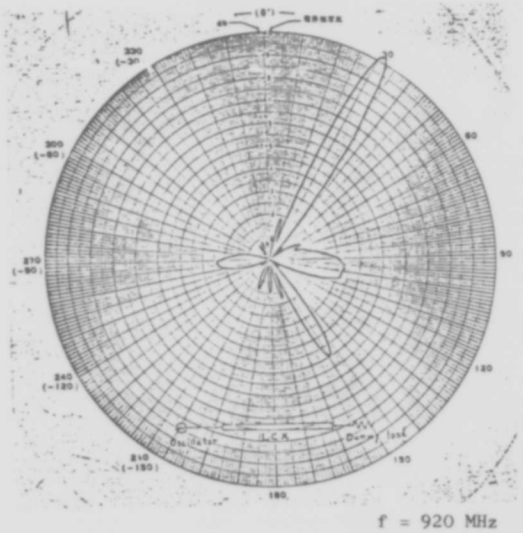

f = 920 MHz

Fig. 9 Example of measured radiation pattern of the new 72D LCX

The frequency accorded with the condition of the radiation angle $\theta = 0$, the broadside radiation, means the resonance in the array of slots, and is represented as the following relation.

$$f_r = \frac{\nu \bar{C}}{P_0} \qquad (\bar{C} : \text{light velocity}) \qquad (4)$$

When such a resonance occurs, the value of the input reflection coefficient of the cable exceeds the allowable limit, and the transmission and radiation characteristics may be unstable close to the resonance frequency. These resonances will occur at all integral times of the basic resonance frequency indicated in Eq.(4). In designing the advanced slot array, care must be taken such that these resonance frequencies are not included in its operating frequency band.

5. EXPERIMENTAL EVALUATION OF THE NEW LCX

Four types of the 72D LCX with different leakages have been manufactured on the basis of the cable and slot designs described above. In this chapter, the basic characteristics of their test cables are mainly discussed.

5-1 Coupling Loss Characteristics

Figure 10 shows the frequency characteristics of the coupling loss concerning four types of the LCX. The amount of coupling losses are usually defined as the ratio of the transmitted power inside the cable to the coupled power by a mobile antenna in a decibell unit. The coupling loss measurements were done by the standard construction method as shown in Fig. 11.

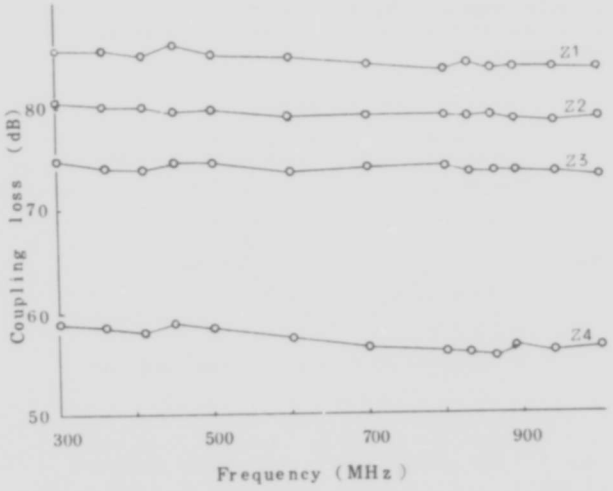

Fig. 10 Coupling loss characteristics of the 72D LCX

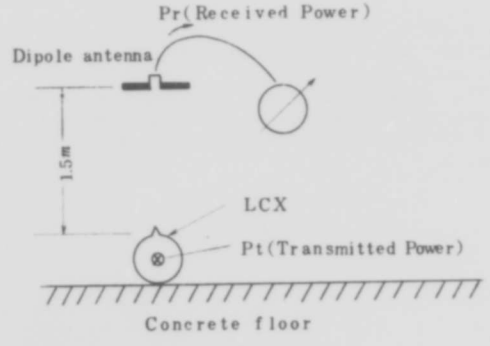

Fig. 11 Standard construction method of coupling loss measurement

It can be seen from the experimental result in the figure, that the new 72D LCX has a coupling loss of about 85, 80, 75 or 55 dB just as expected, and that the wide band and the flat coupling characteristics is realized from 300 MHz to 1,000 MHz.

Figure 12 for example shows the recorded charts of coupling loss measurement, whose coupling level changes can be seen as very small and stable, as for both 400 MHz and 800 MHz bands.

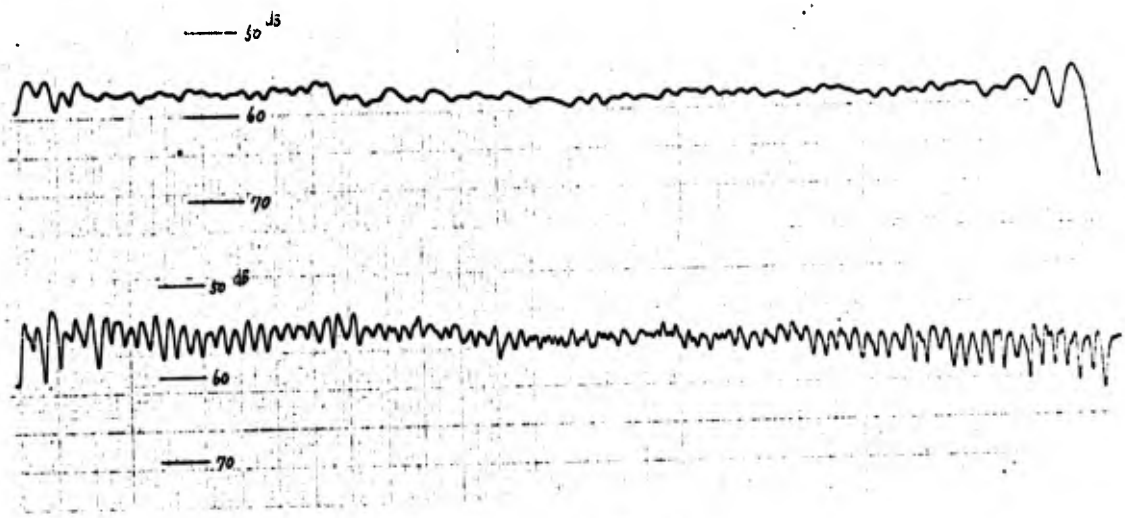

Length of Test LCX	:	50 meters
Installation Method	:	LCX extended onto the concrete floor
Receiving Antenna	:	Half wave length Standard Dipole antenna
Antenna Separation	:	1.5 meter upper the LCX

Fig. 12 Measured data of coupling characteristics of the test cable

5-2 Transmission Loss Characteristics

Figure 13 shows the measured results of transmission loss characteristics as to the four type cables. The measurements were carried out on the same concrete floor as in the previous experiment.

It can be observed that the basic heat loss at 860 MHz reduced to about 23 dB/km, and that the increasing tendency of the loss values according to the decrease of coupling loss on 800 MHz band is more noticeable than that on 400 MHz band.

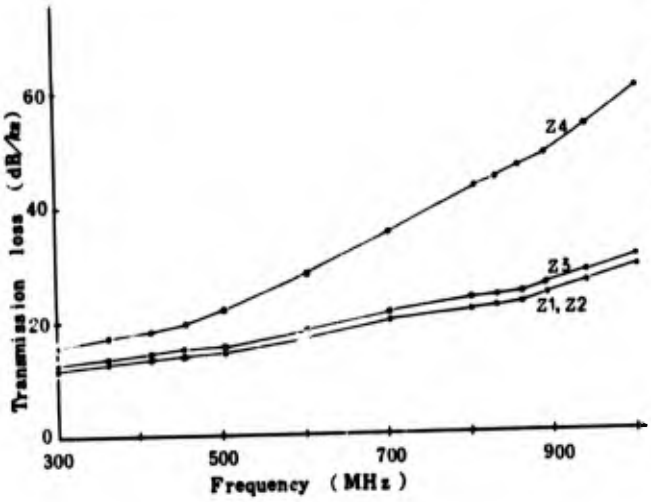

Fig. 13 Transmission loss characteristics of the 72D LCX

5-3 VSWR Characteristics

Frequency characteristics of the VSWR measured by the test cables are shown in Fig. 14. Two large peaks of the VSWR are observed in the figure, which agree with the resonant frequencies of the slot array. The VSWR characteristics other than the above mentioned resonance points are below 1.2 in whole, which is agreeable for good connection to radio equipment.

According to these measurements, the new type wide band LCX was found to be well suited to the use in not only 400 MHz band, but also 800 MHz band.

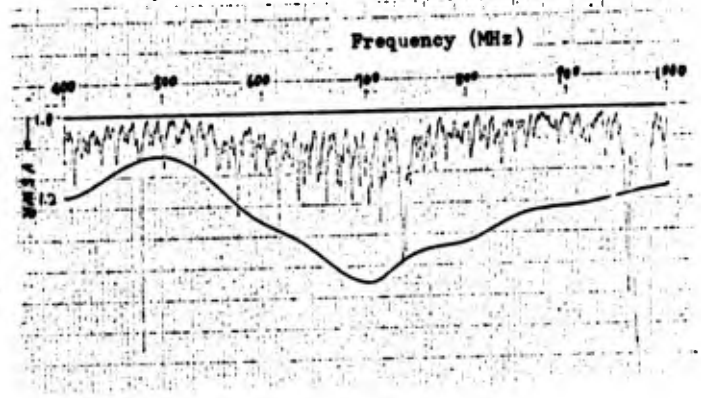

Fig. 14 VSWR characteristics of the 72D LCX

6. FIELD EVALUATION OF THE NEW LCX

Four types of the aforementioned 72D LCX have been installed on the wayside of the railway track in the RTRI of JNR in order to evaluate these new cables through a field test. Figure 15 illustrates the system construction and the coupling level diagram of the field test, where the graded design method by arranging four types of the cables with different

leakages in cascade is introduced to decrease a coupling level change as small as possible.

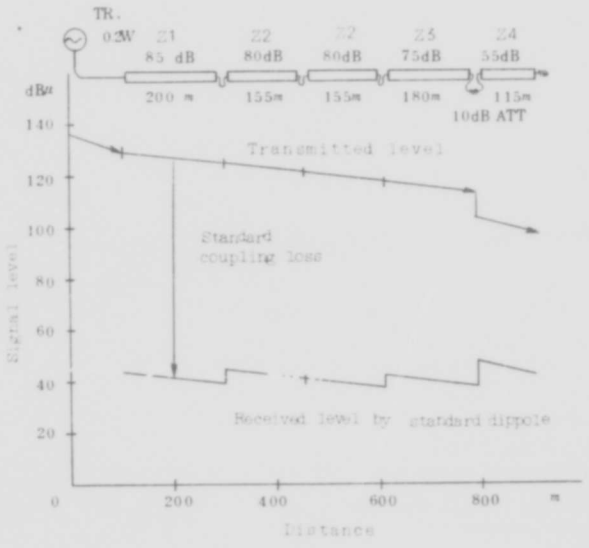

Fig. 15 System construction of the field test and its standard level diagram (at 830 MHz)

Figure 16 and 17 show the appearance of the field test system, and a part of the cable joint, respectively. The new train antenna for 800 MHz band as shown on the left hand side in Fig. 16 is equipped for good coupling with the new LCX line. The antenna consists of 8 elements of radiation slots in a plane which are cooperated-fed so as to get a good beam-matching with the LCX in whole 800 MHz band. Its isotropic gain comes up to 12 dB.

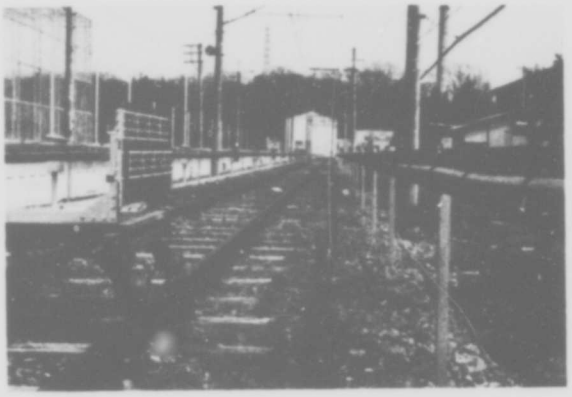

Fig. 16 Appearance of the field test system

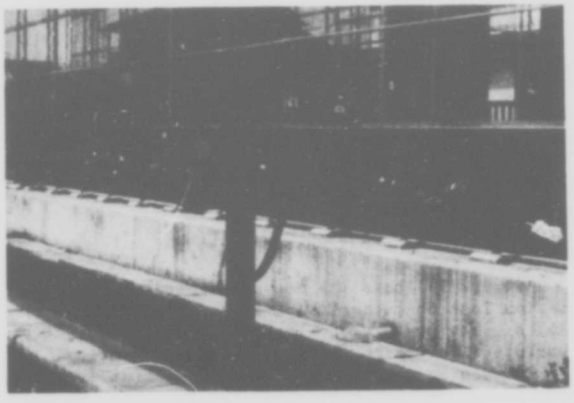

Fig. 17 Part of the 72D LCX joint

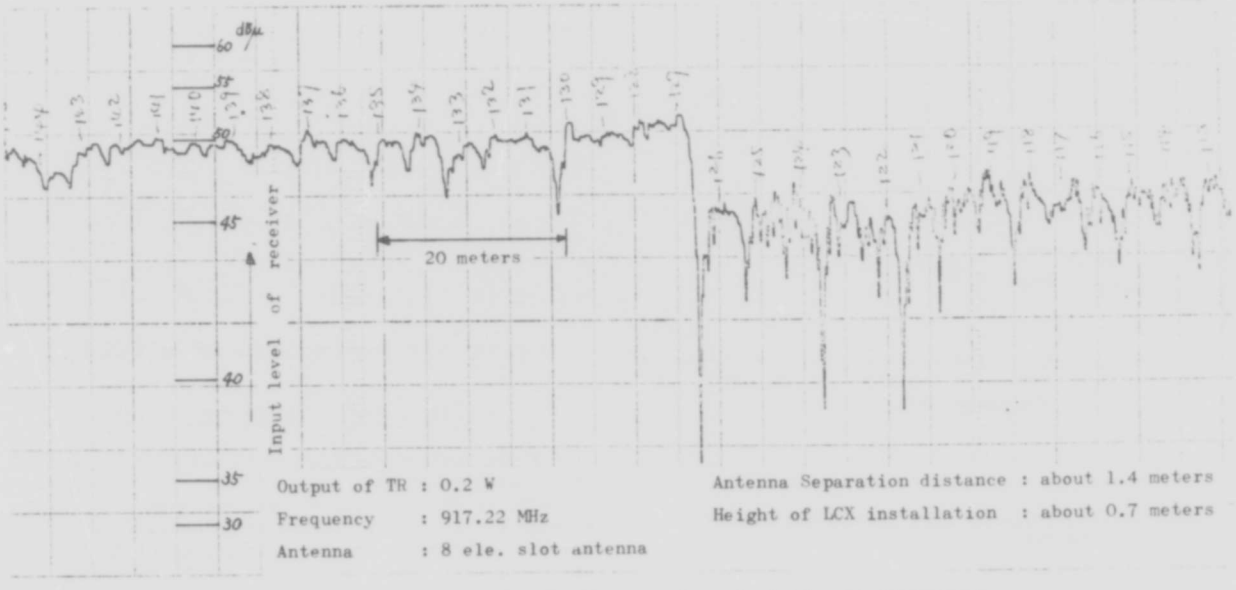

Fig. 18 Measured data of coupling characteristics in field test

Examples of the measured data of the coupling characteristics between the 72D LCX and the train antenna are shown in Fig. 18. The coupling level fluctuations are considerably suppressed by using the antenna. At the parts of the graded steps, the adjustment of the electrical length of the joint-cable was done so as to satisfy the co-phase condition of the radiation fields between the adjacent LCX.

As the first step of the field test, it has been confirmed that the basic characteristics of the new LCX are displayed as expected. Hereafter, the problems of the stability of the LCX line, the improvement of the coupled level fluctuation and some applications of transmissions will have been investigated.

7. SYSTEM CONSTRUCTION AND FUTURE APPLICATIONS

Figure 19 shows the relations of the standard coupling loss vs. transmission loss at 860 MHz, as the result of the experimental reduction. From the relation in the figure, the LCX system construction for 800 MHz band mobile radio communication is simply designed as shown in Fig. 20. Practically, proper margins of coupled level should be included in correspondence with the cable installation condition and the system requirements, in addition to the basic system level diagram.

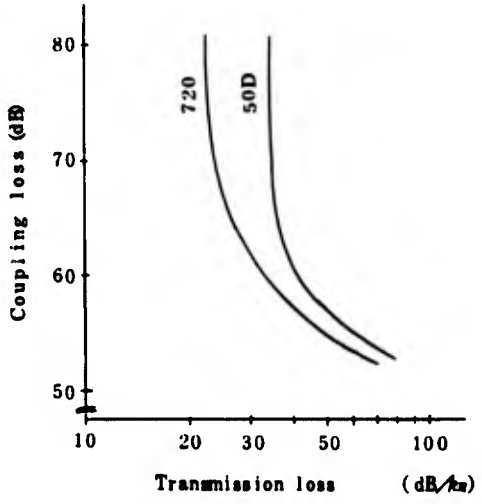

Fig. 19 Relation between coupling loss vs. transmission loss (at 860 MHz)

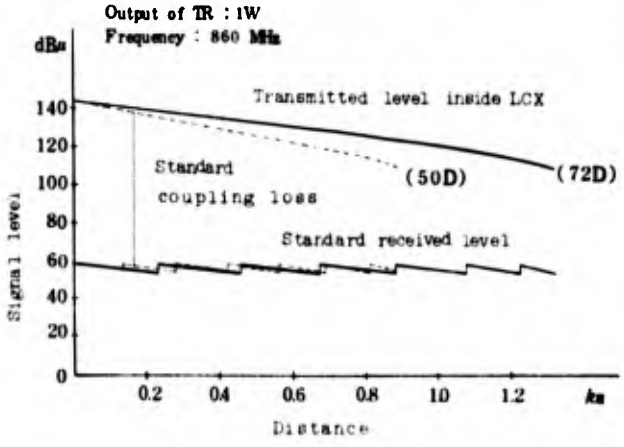

Fig. 20 LCX system construction for 800 MHz band

As seen in Fig. 20, the graded design method in 5 dB step is adopted, and the standard repeater spacing will be enlarged to about 1.3 kilometers. On the other hand, the repeater spacing will reduce to about 0.9 kilometers, in the case of the 50D system.

The features of the LCX can be summarized as the wide frequency band radiation characteristics for a good coupling with mobiles, and the low loss transmission characteristics with no leakages. In other words, the transmitted signal in the cable below a certain frequency cannot leak out as described in chapter 4. These two features enable the integration of both mobile communication and ground-to-ground communication systems by one line of cables. Figure 21 shows an example of frequency allocations. The lower part of the frequency bands is used for ground-to-ground communications, and the higher part for mobile communications, as in the figure.

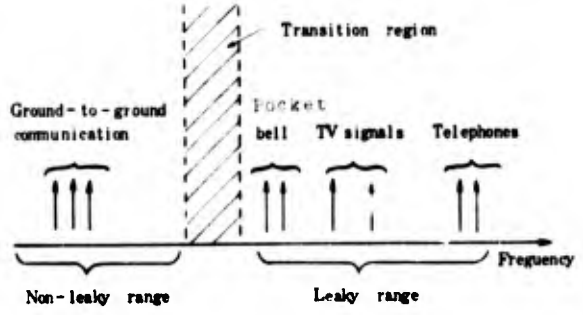

Fig. 21 Frequency allocation of LCX system

8. CONCLUSION

The newly developed wide band LCX for 800 MHz band has been examined through theoretical and experimental investigations, for the two different cable sizes, the 72D (New size) and the 50D (Former size). The wide band radiation characteristics of the advanced slot array of dual-periodicity has been confirmed over 300 MHz to 1,000 MHz. The basic system construction method and the possibility of future applications of LCX have been mentioned, too.

Nowadays, the JNR proposes the introduction of leaky coaxial cables endowed with wide band characteristics of 400 MHz to 800 MHz band, in consideration of the need for the large capacity mobile communication in high speed railways in the near future.

The good results presented in the paper will be expected to provide a reliable basis for the earnest investigation of their introduction.

REFERENCES

(1) T. Baba et al.; "Leaky Coaxial Cable with Slot Array" Paper of IEFE Symposium on A.P., Sept., 1968

(2) N. Kurauchi et al.; "Wideband Leaky Coaxial Cables" Paper of IECE of Japan, Vol. 54-B No. 11, 1971

Toshihiko Kishimoto

Railway Technical Research Institute of JNR
2-38, Hikarimachi
Kokubunji-shi, Tokyo
Japan

Toshihiko Kishimoto received a B.S. degree in Electrical Communication Engineering from Osaka University in 1954.
He then joined the Japanese National Railways, and engaged in electric design and investigation of microwave network, research of train communication, etc.
Mr. Kishimoto is now Senior Engineer of the Communication Laboratory of the R.T.R.I. of JNR.

Hiroshi Kitani
(Speaker)

Sumitomo Electric Industries, Ltd.
1 Taya-cho, Totsuka-ku
Yokohama, Japan

Hiroshi Kitani received a B.S. degree in Electronic Engineering from Osaka University in 1962 and joined Sumitomo Electric Industries, Ltd. in the same time.
He has been engaged in the development of TV broadcast antennas, microwave and millimeter waveguides, leaky waveguide and leaky coaxial cable.
Mr. Kitani is now Senior Engineer of Communication Systems Dept., and a member of the Institute of Electronics & Communications Engineers of Japan.

Yasunobu Nagai

Sumitomo Electric Industries, Ltd.
1 Taya-cho, Totsuka-ku
Yokohama, Japan

Yasunobu Nagai received a B.S. degree in Electrical Communication Engineering from Waseda University in 1959.
He then joined Sumitomo Electric Industries, Ltd., and engaged in development of communication cables and CATV coaxial cables.
Mr. Nagai is now Senior Engineer of Communication Systems Dept.

Yoshio Miyamoto

Sumitomo Electric Industries, Ltd.
1 Taya-cho, Totsuka-ku
Yokohama, Japan

Yoshio Miyamoto received a B.S. degree in Electrical Communication Engineering from Osaka University in 1968.
He then joined Sumitomo Electric Industries, Ltd., and engaged in research and development of leaky wave transmission lines.
Mr. Miyamoto is now a member of Communication Systems Dept., and a member of the Institute of Electronics & Communications Engineers of Japan.

LARGE SIZE LEAKY COAXIAL CABLE FOR 400 AND 800 MHz FREQUENCY BAND

T. SAKO, T. NARUSE, H. YASUHARA, T. KATO

The Fujikura Cable Works, Ltd., Tokyo, Japan

ABSTRACT

A leaky coaxial cable (LCX) is an extremely good medium as a wave guide for wireless communication system. We have been studying the basic transmission characteristics of leaky coaxial cables and have continued development of practical applications.

A large leaky coaxial cable for 350-900 MHz in addision to conventional LCX was developed by the improvement of a radiating slot arrangement. To reduce transmission loss at high frequency, the cable O.D. was enlarged about 77mm and the insulation was composed of double layers in order to reduce equivalent permittivity. In this paper, transmission characteristics and performance of this cable are described and experimental results are given.

1. INTRODUCTION

With the recent progress in communication systems, studies have been made to use leaky coaxial cables to develop previously-unknown vehicular communications in weak electric field regions and for inter-communications in tunnels and buildings.

Although a wireless system is usually used for vehicular communication, a wired system also offers advantages. With a wired system, electromagnetic waves can be transmitted while enclosed within certain space (space division). When this space is extended to surrounding space along wires, it covers the disadvantage of a wireless system and serves as an effective medium of vehicular communication. Recently, it has been possible to use as extremely limited frequency band for vehicular communication. For this reason, the need for using a frequency band efficiently occasionally surpasses economic factors. Space division by a wired system is extremely advantageous in such cases.

Leaky coaxial cables have been developed against such a background. They were first applied to railway communication when free space propagation of 150 MHz and 400 MHz bands were used.

Vehicular communication in tunnels is extremely important in Japan because transport routes pass through many mountains. A radio induction system (50-250 KHz) using a parallel wire line is also frequently used. But it has some serious disadvantages, including difficult installation and maintenance, (secure connection of cables and antennas), and large connection level fluctuations. Leaky coaxial cables can solve these difficulties. A non-radiation inductive wave from open coaxial cables was used in the first stage of application. Subsequent development brought about radiating leaky coaxial cables with zigzag slots on the outer conductor.

LCX has already been put into practical use in Japan. Up to now it has been utilized in the 150-400 MHz frequency band, but this range will be extended to the 800 MHz band in the future as vehicular communication matures. But, if conventional cables are adapted for the 800 MHz band, the cable will cause more attenuation than occurs in the 400 MHz band, thus the repeating section should be shortened. Therefore we have studied a large size LCX in order to reduce the attenuation factor.

Since leaky coaxial cables have some remarkable properties, serving both as transmission lines and antennas, their application has been extended to several fields, such as highway communication, remote vehicle control, telemetering and wireless telephone systems.

The remainder of this paper discusses the basic properties, design and experimental results of leaky coaxial cables with major emphasis on railway communication.

2. THEORETICAL BACKGROUND

2-1. Leaky waves

Assume a completely conductive wide surface with a slit of infinite length, as shown in Fig.1. The slit is excited from one region (1). The electric field on the slit goes through with a phase change in the direction of the slit (direction z).

$$E_0 = A\exp(-j\beta_g z) \quad \cdots\cdots\cdots\cdots\cdots\cdots (1)$$

in which A: constant

β_g: propagation constant

When the region (I) is a hollow wave guide or a coaxial cable, β_g may be considered as phase constant. The electromagnetic field that is produced in the space of the region (II) by this electric field consists of the following three components in a cylindrical co-ordinates (r, θ, z), shown in Fig.1.

$$H_z = -\frac{Akr^2}{2\omega\mu_0} H_0^2(krr)e^{-j\beta_g z}$$

$$H_r = \frac{\partial^2 Hz}{kr^2 \partial z \partial r}$$

$$E_\theta = -\frac{\omega u_0}{\beta_g} H_r \quad \Big\} \cdots\cdots\cdots\cdots (2)$$

in which

$$k_r^2 = k_0^2 - \beta_g^2 \quad \cdots\cdots\cdots\cdots (3)$$

$k_0 = \omega\sqrt{\varepsilon_0 \mu_0} = \frac{2\pi}{\lambda}$: propagation constant in the region (II)

H_0^2 : 0 order, Hankel Function of the second kind

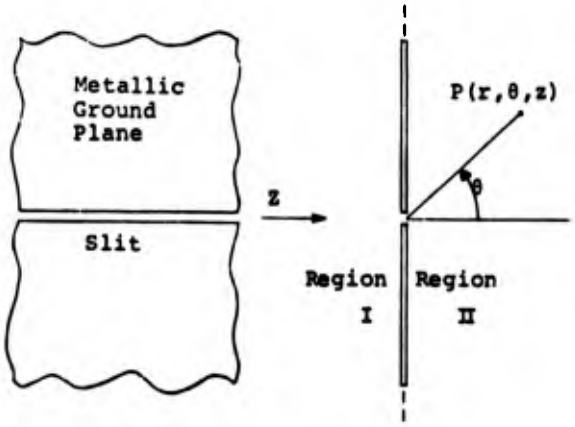

Fig.1 Infinite slit on conductor plane

The electromagnetic field of the region (II) is calculated bolow by using the equation (2).

$$E_\theta = j \frac{Akr}{2} \cdot H_1^2 (k_r r)^{-j\beta_g z} \quad \cdots\cdots (4)$$

The electro magnetic field in an adequate far region ($k_r r >> 1$) is calculated below.

$$E_\theta = -\frac{Akre^{j\frac{\pi}{4}}}{\sqrt{2\pi k r r}} e^{-j(k_r r + \beta_g z)} \quad \cdots (5)$$

The energy flow in r direction per unit area in a sufficiently far region is given below.

$$S_r = \frac{1}{2} R_e(E_\theta H_z) \doteq \frac{Re(kr)}{2\omega\mu_0} |E_\theta|^2 \quad \cdots\cdots (6)$$

Note that $R_e(k_r)$ means the real part of k_r in the above equation. So, if k_0 is larger than β_g in the equation (3), energy flow of r direction exists in the region (II). The equation (7) shows propagation constant β_g and k_0 with phase speed.

$$\beta_g = \frac{\omega}{v_g}$$

$$k_0 = \frac{\omega}{v} \quad \Big\} \cdots\cdots\cdots\cdots (7)$$

In other words, v_g (the phase speed of exciting electric field) must be larger than v (phase speed in the region II) to produce radiation wave in the region II .

In this case, radiation wave is plane wave whose equiphase surface is propagating from direction at the angle of ξ shown in Fig. 2.

$$\xi = \tan^{-1}\left(\frac{\beta_g}{k_r}\right) = \sin^{-1}\left(\frac{\beta_g}{k_0}\right) = \sin^{-1}\left(\frac{v}{v_g}\right) \cdots (8)$$

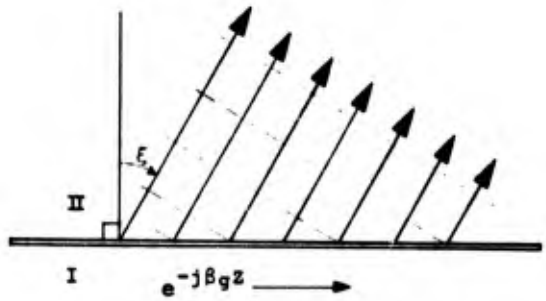

Fig.2 Leaky wave from the slit

When energy leakage from a transmission line over a semi-infinite length forms plane wave, this transmitting wave with radiation is called leaky wave.

However, TEM waves in coaxial cables are slow waves and v_g is smaller than v. Therefore kr is pure imaginary figure and the equation (6) can be written as $S_r = 0$.

But, it is possible to replace an infinite length slit with periodic slots to increase apparent phase velocity for obtaining effective radiation from TEM waves in coaxial cables. When a conductor's flat surface has exciting slots repeated at the cycle of P in a line, the excited electric field becomes a periodic function of the period P. The excited electric field (Equation 1) can be shown by Fourier series development with En as amplitude modulus, as shown below.

$$E_\theta = \sum_{n=-\infty}^{\infty} En \cdot \exp\{-j(\beta_g + \frac{2\pi n}{p})z\} \quad \cdots\cdots (9)$$

In other words, propagation constant is expressed as $\beta_g + 2\pi n/p$. For this reason, radiation waves also consist of numerous spacial harmonic waves based on the period P. The radiation direction of each harmonic waves are as shown below.

$$\xi n = \tan^{-1}\left(\frac{\beta_g + \frac{2\pi n}{p}}{krn}\right) = \sin^{-1}\left(\frac{\beta_g + \frac{2\pi n}{p}}{k_0}\right) \cdots (10)$$

in which $krn^2 = k_0^2 - (\beta_g + \frac{2\pi n}{p})^2 \quad \cdots\cdots (11)$

It gives a radiation field only when krn is a real number as mentioned previously.

2-2. Radiation from coaxial cables

To obtain radiation from a TEM wave transmitting in a coaxial cable, it must have slot for cutting the wall current flowing on the external conductor, like a waveguide, or slots that leave wall current uncut must be excited by a post or other methods. Slanted zigzag slots on the external conductor, as shown in Fig. 3, are ordinarily convenient for practical use and manufacturing. Since one set of zigzag slots is in about one wave length of the transitted electric field, the direction of axial fields components (Ez) generated by these slots are reversed to be cancelled and circumferential field component (Eθ) are directed to the same direction.

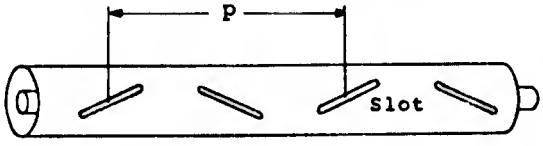

Fig.3 Slanted zigzag slots

Therefore, the longitudinal electric field components (Ez) are suppressed, while perpendicular (circumferential) electric field components (Eθ) alone remain to allow the radiation of circumferential leaky waves.

To quantatively determine leakage from cable, the coupling loss (Lc) between a standard half wave dipole antenna and a cable is defined as the equation (12).

$$Lc = -10 \log \frac{pr}{pt} \quad \text{.....(12)}$$

pr: power received by antenna

pt: power to be transmitted in cable

For measurement, a cable is laid on the ground and a half wave dipole antenna is moved longitudinally abobe the cable. Although electric field strength changes a little longitudinally, the average read out is used as coupling loss.

The phase constants (direction Z) of electromagnetic field components (E_θ, Ez field components) radiated from the slot layout shown in Fig. 3 are as given below.

$$\beta_{\theta n} = \beta_g + \frac{2\pi n}{p} \quad (n = \pm 1, \pm 3 \ldots) \quad \text{.....(13)}$$

$$\beta_{zn} = \beta_g + \frac{2\pi n}{p} \quad (n = 0, \pm 2, \pm 4 \ldots) \quad \text{....(14)}$$

The radiation direction is as follows from the equation (10).

$$\sin\xi_n = \frac{\lambda}{\lambda_g} + \frac{n\lambda}{p} = \sqrt{\varepsilon_s} + \frac{n\lambda}{p} \quad \text{.....(15)}$$

ε_s : Equivalent dielectric constant in coaxial cable

λ_g : Wave length in coaxial cable

Fig. 4 shows the radiation direction at $\lambda/\lambda_g = 89\%$. It is known that krn is a real number in the case of n<0. The basic mode is in the case of n = -1 and it radiates backwards. Backward waves are peculiar to a periodic structure. The range for basic mode ($E_{\theta-1}$) radiation alone is given below.

$$\frac{1 + \sqrt{\varepsilon_s}}{2} < \frac{\lambda}{p} < 1 + \sqrt{\varepsilon_s} \quad \text{.....(16)}$$

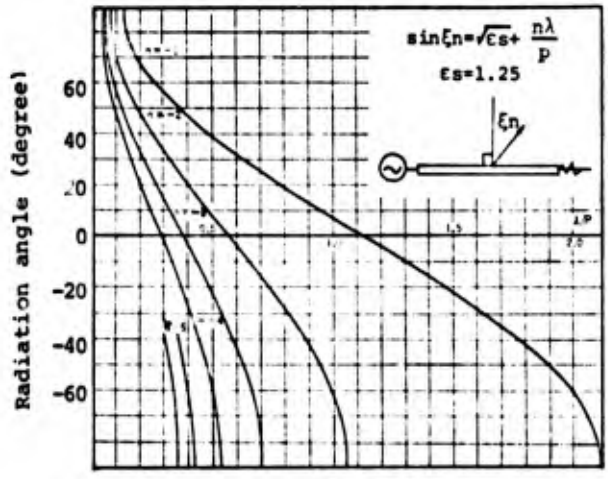

Fig.4 Radiation angle

Since other spacial harmonic waves of n = -2 or less exist simultaneously at $\lambda/p \leq (1 + \sqrt{\varepsilon_s})/2$, a longitudinally uniform field cannot be obtained. One of the features of a leaky coaxial cable with slanted slots is that the amount of coupling can be changed considerably by changing slot length-angle combination. Fig. 5 shows an example in case of large size leaky coaxial cable. It is important data for actual cable designing.

2-3. Extention of usable frequency band

In the case of a leaky coaxial cable with a single zigzag slots, the usable frequency band is limited to the range of equation (16). Currently, 150 MHz and 400 MHz bands are widely used for wireless communication systems. Recently, and 800 MHz band has also been developed.

The frequency band can be extended to a certain extent by changing the dimensions and layout of zigzag slots. As equation (13) shows, n = -1, -3 ..... is finite and n = -2, -4 ... is zero for the component E_θ. Therefore, a five times wider band becomes available by cancelling n = -3($E_{\theta-3}$). Various methods are available for this purpose. In view of easy fabrication, the method of cutting many slots at equal intervals, (as Fig. 6 shows) was used for this study.

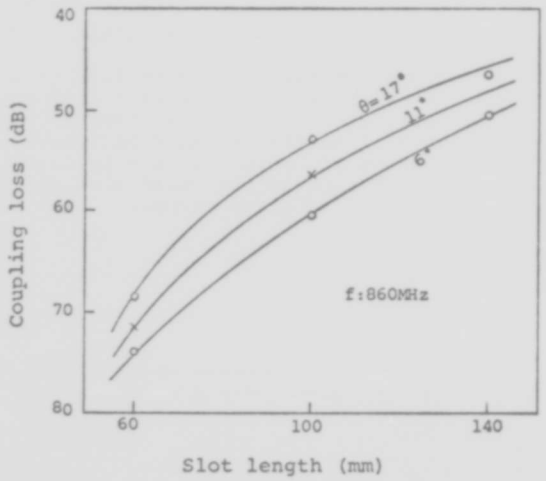

Fig.5 Coupling loss of various slot dimentions

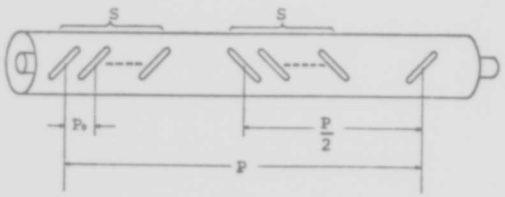

Fig.6 Wide band slots arrangement

When the excited field is expressed with equation (9), its higher harmonic components are expressed by the following equation

$$En = A(n,\theta,l,p)\sum_{k\neq 0} \exp\left(j\frac{2\pi n}{p}kp_0\right)(1-e^{-jn\pi})$$

$$= A(n,\theta,l,p)\cdot(1-e^{jn})\frac{1-\exp\left(j\frac{2\pi n}{p}sp_0\right)}{1-\exp\left(j\frac{2\pi n}{p}p_0\right)} \quad \cdots(17)$$

in which $sp_0 < \frac{p}{2}$

A (n,θ,l,p): Constant determined by slot inclination and dimensions

The second modulus of equation (17) shows that En is equal to zero for an even number n because of the symmetry of the slots. The third modulus shows the effect of multi-slots. The following condition must be satisfied to obtain En = 0 at n = -3.

$$\frac{2\pi n}{p}sp_0 = 2r\pi \quad (r = 0, \pm 1, \pm 2 \cdots)$$

$$sp_0 = \frac{p}{3} \quad \cdots\cdots\cdots\cdots\cdots\cdots(18)$$

Therefore, a wide band region can be used by selecting such numbers of slots (s) and slot intervals (p_0) that satisfy equation (18).

3. Description of the cable

Various sizes of leaky coaxial cable are tabulated in table 1. The series is similar to 50Ω type Antenna Feeder cable, but a little different in means of permittivity.

Table 1

	Inside dia. of outer conductor	Frequency band
20D type LCX	ab.21mm	150MHz
32D "	ab.32mm	"
43D "	ab.43mm	150, 400MHz
77D "	ab.69mm	400, 800MHz

Smaller cable has already been used in practical application, but it causes more attenuation in 800MHz band than occurs in 400MHz band. Therefore cable like the 77D type is required. This paper reports a new 77D type leaky coaxial cable. The details of its physical structure are shown in Fig. 7,8, 9.

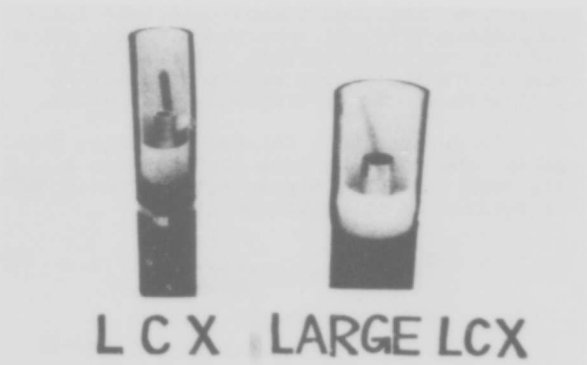

Fig. 7 Photograph of the LCX

Fig. 8 Photograph of PE-disks

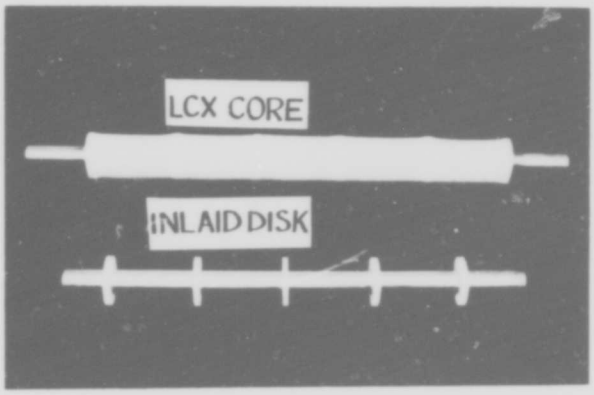

Fig.9 Photograph of the LCX core

It has Aℓ-pipe made by the tape forming method as the inner conductor which may be corrugated if easy bending is required. Insulation formation is a combination of PE-disk inlaid at suitable interval and extruded onto PE-pipe. PE-disks are made by injection molding method. The outer conductor is wrapped longitudinally with laminated 0.2mm thick Aℓ-tape and is covered with a PE-sheath.

The zigzag arrangement of two parallel slanted slots(s=2, p =p/6) made in the outer conductor, is able to suppress spacial harmonic waves, so that the available frequency is from 350MHz to 900MHz, while the radiation angle is kept within ±30 degrees. The calculated radiation angle is shown in Fig.10. The specially designed machine for punching slots in Aℓ-tape is capable of making slots for the 150-800MHz band and others.

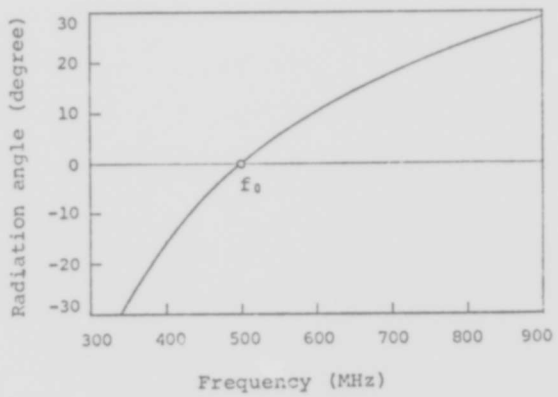

Fig.10 Radiation angle from the large LCX

A comparison of the cable design between the new 77D type leaky coaxial cable and the popular 43D type leaky coaxial cable is shown in Table 2. The equivalent relative permittivity of new LCX is lower than conventional 43D LCX because of disk insulation.

Table 2 Cable Design

	43D LCX	77D LCX
Dia. of I.C.	17.2mm	27.8mm
Dia. of Insulation	PE-string 39mm	PE-disk 63mm
	PE-pipe 43mm	PE-pipe 69mm
Cable O.D	ab 50mm	ab 76.5mm
Permittivity	1.27	1.17
Characteristic Impedance	50Ω	50Ω

4. Electrical performance

Fig. 11 shows one example of measured coupling level. It is clearly seen that the field fluctuation is very small.

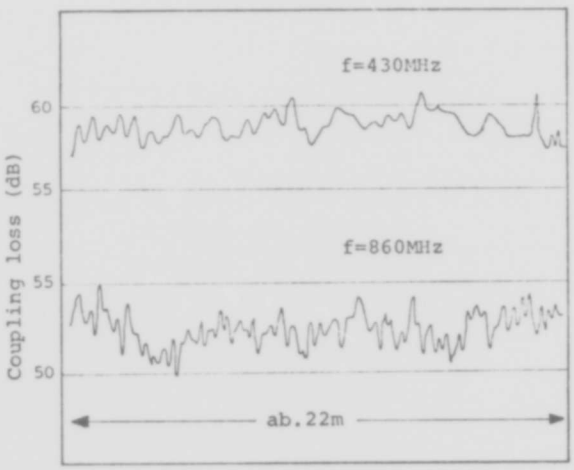

Fig.11 Radiation uniformity along the cable

Coupling loss defined by the equation (12) is measured to be graphed in Fig. 12 for the cables with four different values of coupling loss. The real line shows a cable on the ground and the dotted line shows one on a concrete surface. It is evident from Fig. 12 that a difference depending upon frequency is observed at about a 6dB decrease in the 800MHz band compared to the 400MHz band for cables which radiate great amounts of energy. But, this phenomenon does not occur strongly in less radiating cables which have short radiating slots. So, this frequency characteristics of coupling loss seems to depend on the radiating slot length. Some difference of coupling loss due to the places where the cable is laid is considered that the effect of reflected waves appeared.

Fig. 13 shows the measured gain and phase directivity pattern. An antenna installed 0.5m from a slot front is used as the reference in the figure.

The external radiation field from a cable of constant coupling loss decreases linearly due to basic transmission loss because of radiation. The total measured transmission loss is shown in Fig. 14. Transmission loss increases sharply when coupling loss falls to 50dB especially in the 800MHz band. This is probably due to loss of surface wave component.

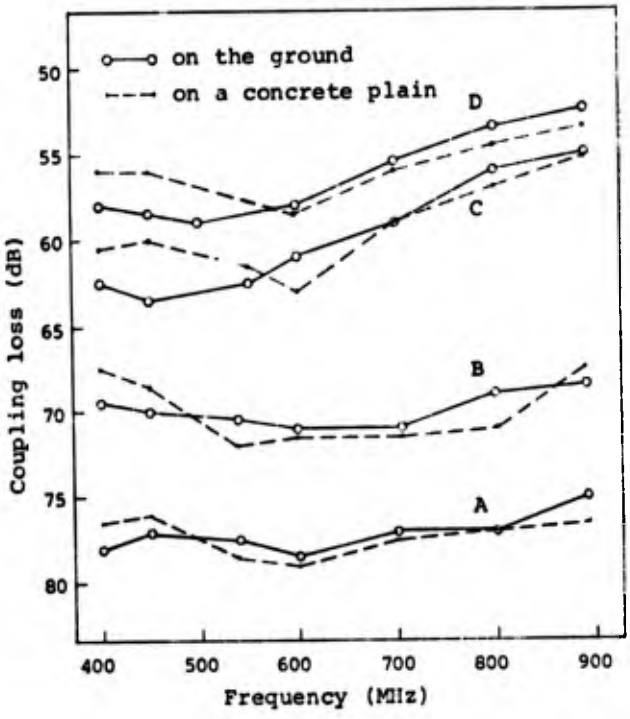

Fig.12 Coupling loss VS. frequency

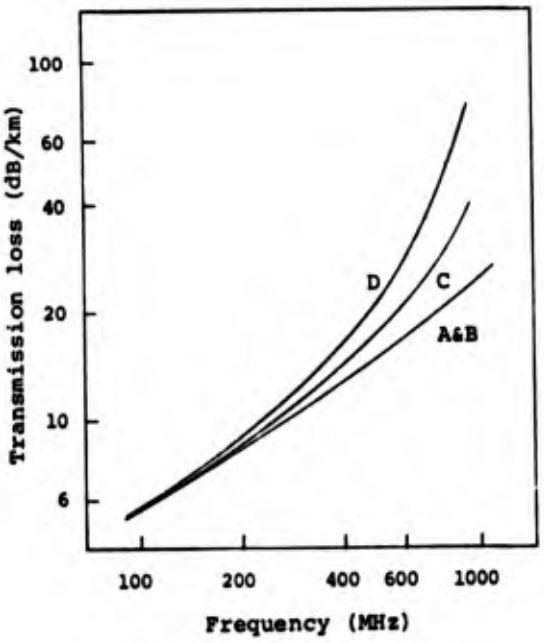

Fig.14 Transmission loss

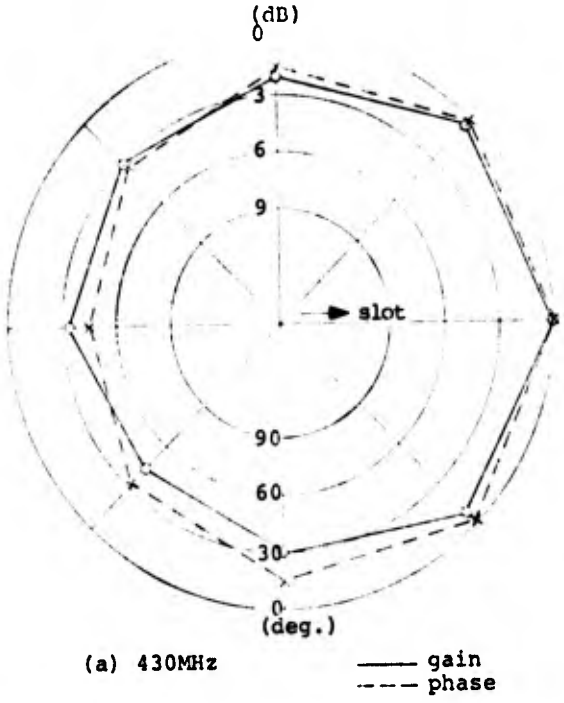

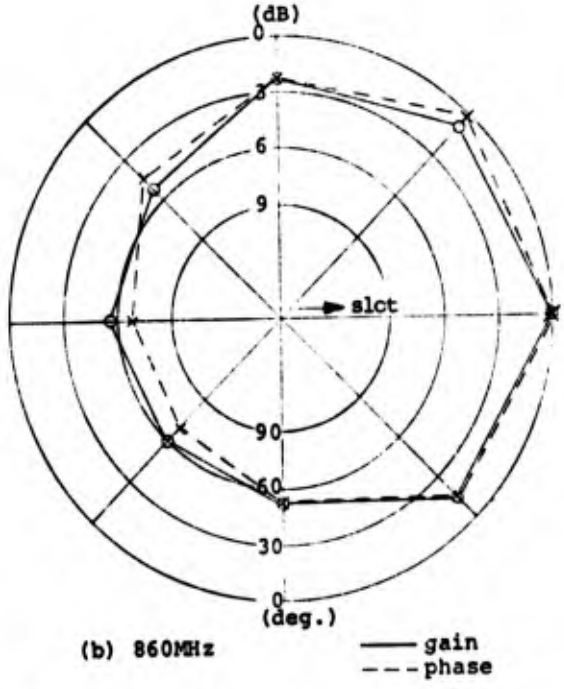

Fig.13 Radiation pattern of the LCX

The relation between coupling loss and transmission loss is extremely important for designing as actual system. Fig. 15 shows the experimental results.

Structual return loss (equivalent to V. S.W.R.) of the cable is shown in Fig.16. The measurement was achived by the frequency sweep method. The resonance frequency is clearly evident from the figure and, except for near that frequency, V.S.W.R. is fairly good.

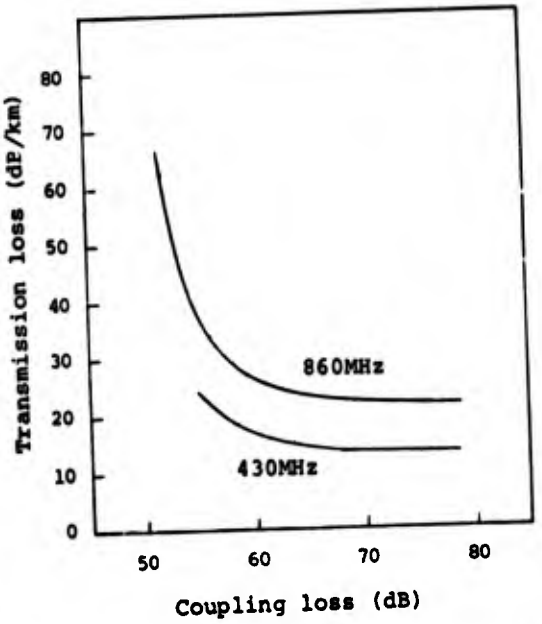

Fig.15 Coupling loss VS. transmission loss

5. Effects of environmental conditions on radiated electric field

Since leaky coaxial cables are often installed along railways and in tunnels, their radiation characteristics, including environmental conditions, must be studied. When a cable is installed on a tunnel wall or on the ground between two rails, the interference between radiation waves and wall reflected waves sharply changes the electric field intensity and increases fluctuation. The cable-wall plane distance and the reflection coefficient of the wall may be considered as parameters.

Measurements with a dipole antenna show that the level of radiating field is high and fluctuation is extremely small when a cable is installed on the ground. However, the properties sharply deteriorate when a cable is off the ground by as much as about a 1/4 wave length. This is evident from experimental measurement, the results of which are shown in Fig. 17.

Fig. 18 shows a measurement taken in a tunnel. A cable was installed on the wall, but it had a flat concrete surface as well as an uneven surface due to tunnel construction.

Field drop-out of radiation field occurs due to obstacles such as electrified poles. Although a drop-out of 15dB was found with dipole antenna measurements, an extremely good result was obtained with a travelling wave antenna. And it has been confirmed that neither a thick PE-pipe nor an inorganic cover have great effects on radiation.

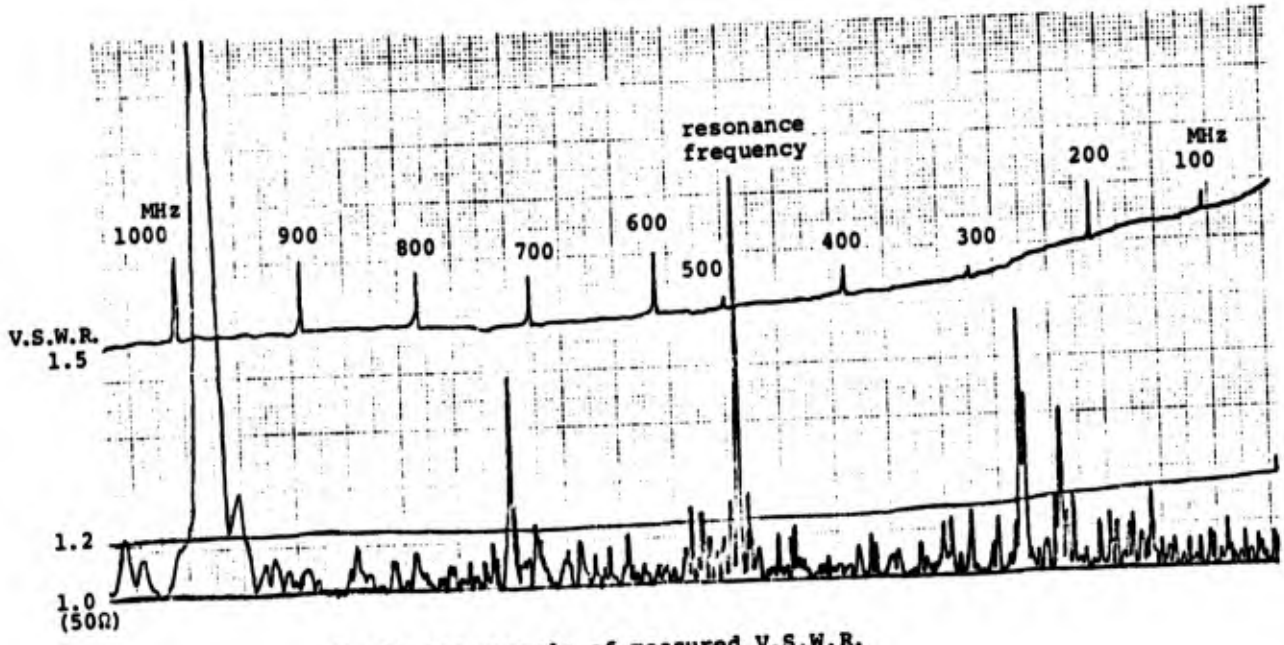

Fig.16 One example of measured V.S.W.R.

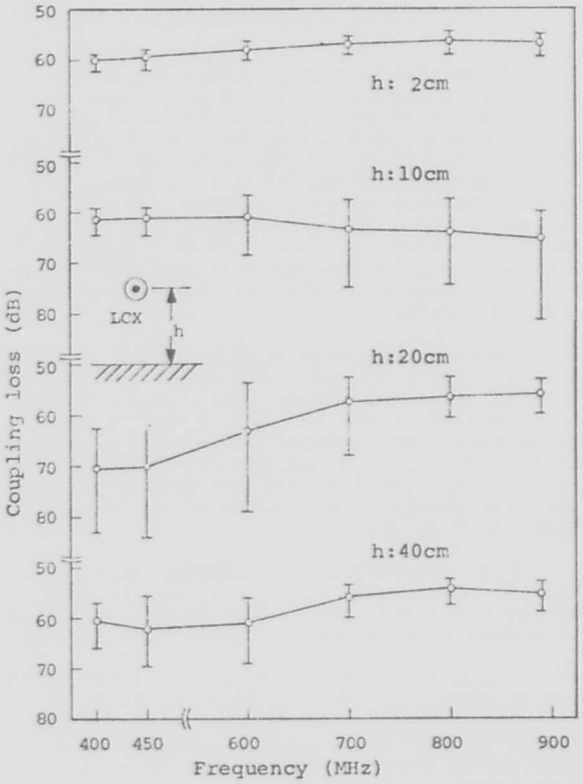

Fig.17 Coupling loss changes by the distance (43D LCX)

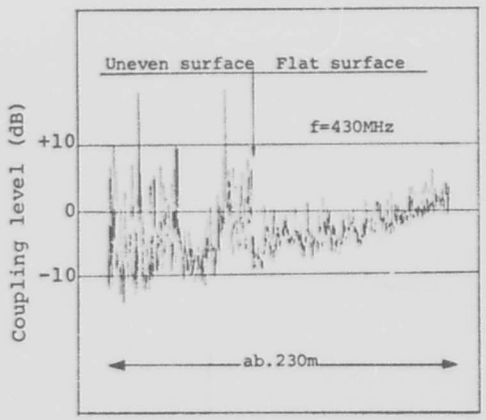

Fig.18 Measured radiation field in a tunnel

When a cable is suspended beside a metallic fence, fluctuation increases sharply probably due to complicated radiation mode generated between the metallic surface and the cable. Radiation field fluctuation also increases when a cable without a messenger wire is supported by metal or lashing wire.

Another effect of a wall is some increase of cable attenuation. When the leaky coaxial cable approaches a wall, cable attenuation increases mainly due the loss of surface wave component, and a cable of larger leakage is more influenced by earth or wall.

6. Conclusion

This paper outlined the basic properties of the leaky coaxial cable especially for 400 and 800MHz bands. In some measurements, adequate results were obtained for extending the frequency range up to 900MHz by using a new large size leaky coaxial cable. These cables have been developed for use in various fields and are ready for practical application. Further development and application are expected in the future.

7. Acknowledgements

The authors express their deep appreciation for the cooperation of the Japanese National Railway and our company staff.

TETSUZO SAKO,
Manager
Telecommunication systems Dept.,
Telecommunication Cable Division, The Fujikura Cable Works, Ltd.,
5-1, Kiba, 1-chome,
Koto-ku, Tokyo, Japan.

Mr. Sako received his B.E. degree in electrical engineering from Kyushu University in 1953. He then joined the Fujikura Cable Works, Ltd. and was engaged in design, research and development of telecommunication cable, cabtire cable and control cable. Since 1970, he has been supervisor of the telecommunication system engineering group.
He is a member of the Institute of Electronics and Communication Engineers of Japan.

TOSHIHIDE NARUSE,

Assistant Chief,
Telecommunication Cable Engineering & Development Dept., The Fujikura Cable Works, Ltd., 1440 Mutsusaki, Sakura-shi, Chiba-ken, Japan.

Mr. Naruse received his B.E. degree in electrical engineering and M.E. degree in engineering from Waseda University in 1963 and 1965 respectively.
He then joined the Fujikura Cable Works, Ltd. and has been engaged in research and development of telecommunication cable.
He is a member of the Institute of Electronics and Communication Engineers of Japan.

HIKARU YASUHARA,
(Speaker)

Senior Engineer,
Telecomminication Cable Engineering & Development Dept., The Fujikura Cable Works, Ltd., 1440 Mutsusaki, Sakura-shi, Chiba-ken, Japan.

Mr. Yasuhara received his B.E. degree in electronics engineering from Tokyo University in 1966. He then joined the Fujikura Cable Works, Ltd. and has been engaged in research and development of telecommunication cable.
He is a member of the Institute of Electronics and Communication Engineers of Japan.

TAKAMASA KATO,

Engineer,
Telecommunication Cable Engineering & Development Dept., The Fujikura Cable Works, Ltd., 1440 Mutsusaki, Sakura-shi, Chiba-ken, Japan.

Mr. Kato received his B.E. degree in electrical engineering from Tohoku University in 1970. He then joined the Fujikura Cable Works, Ltd. and has been engaged in research and development of telecommunication cable. He is a member of the Institute of Electronics and Communication Engineers of Japan.

RELATING TRANSFER IMPEDANCE TO COAXIAL CABLE RADIATION

by Keneth A. Simons
Simons and Wydro Associates
Hilltown, Pa. 18927

Summary

The effectiveness of the shield surrounding a coaxial cable is characterized in terms of two basic parameters: the transfer impedance, and the capacitive coupling impedance. These can be computed in some cases, but in general some kind of test fixture is required. Once these quantities are established a difficult question arises: Given the shielding parameters, how does one arrive at the degree of radiation to be expected in a given situation or, conversely, the energy to be expected within the cable when immersed in a known field? This paper describes some experiments conducted using cables with known parameters in an attempt to find a suitable technique for answering the question. Tests were made using calibrated antennas both with fixed position and variable frequency, and with fixed frequency and variable position.

The Transfer Parameters

In relation to a shielded coaxial cable the transfer impedance is defined by:

$$Z_T = \frac{\Delta V_2}{I_1 \Delta X} \qquad (1)$$

where Z_T is the transfer impedance, in ohms per meter.

ΔX is an incremental length of cable (very short compared to a wavelength) in meters.

I_1 is the current flowing on the inner surface of the shield at this point, in amperes.

V_2 is the resulting voltage drop along the outer surface for this length.

In practice this impedance may be resistive (for DC and very low frequencies), inductive (at high frequencies, with braided shields), or have any phase angle at all depending on the skin effect, and the way the above factors combine at any given frequency.

There is another mechanism which allows transfer of energy from a shielded cable, which involves capacitive coupling. In the past this effect has been called the "Transfer Admittance" with the symbol "Y_T", measured in micro-siemens per meter.

However, at a recent meeting of Working Group 1 (Screening Efficiency) of IEC Subcommittee 46A it was agreed that this terminology was confusing and cumbersome, and the capacitive effect is now to be described in terms of the "Capacitive Coupling Impedance" with the symbol "Z_F", to be expressed in the same units as the Transfer Impedance, i.e. milli-ohms per meter. The relationship between this new unit and the mutual capacitance per unit length between the inside of the cable and the surrounding environment is given by:

(Note: The development of this and the other relationships in this section are detailed in Appendix I.)

$$Z_F = Z_{01}\, Z_{02}\, 2\pi f\, C_{12} \qquad (2)$$

where Z_F is the Capacitive Coupling Impedance, in ohms per meter

Z_{01} is the characteristic impedance of the cable, in ohms

Z_{02} is the characteristic impedance of the outer surface of the shield in relation to the surrounding electrical environment, in ohms

f is the frequency, in Herz

C_{12} is the mutual capacitance between the inner conductor and the environment, in farads per meter

Measurement of the Transfer Parameters

The IEC has standard methods, in use for many years, for the measurement of the Transfer Impedance and the Capacitive Coupling. The Transfer Impedance fixture, the "Triaxial" arrangement, is diagrammed in Figure 1.

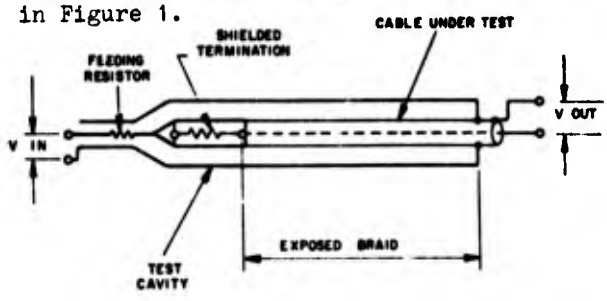

FIGURE 1
THE IEC TRANSFER IMPEDANCE TEST FIXTURE

A known current is caused to flow along the outside surface of the shield of the sample under test by applying a known voltage to it through a "feeding resistor". The inner system is terminated at the feeding end by a carefully shielded resistor equal to its characteristic impedance; and at the other end by a voltmeter having the same impedance which measures the output voltage due to the known current. At frequencies where the system is shorter than 0.3 wavelength the transfer impedance is given by:

$$Z_T = \frac{V_2}{V_1} \cdot \frac{2R}{\ell} \qquad (3)$$

where V_1 and V_2 are the input and output voltages respectively

R is the feeding resistor, in ohms

ℓ is the length of exposed shield, in meters

The IEC method for measuring mutual capacitance uses the "quadraxial" fixture diagrammed in Figure 2.

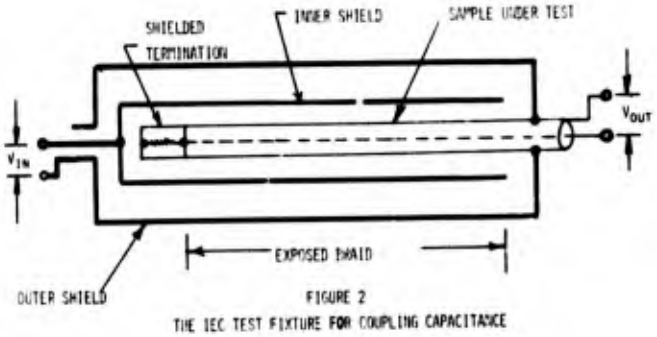

FIGURE 2

THE IEC TEST FIXTURE FOR COUPLING CAPACITANCE

The coaxial system, involving the outer surface of the cable shield and the inner surface of the tube surrounding it, is dimensioned to give a characteristic impedance approximating that of the cable under test. At frequencies where the system is electrically short the mutual capacitance is given by:

$$C_{12} = \frac{V_2}{V_1} \cdot \frac{1}{\pi f Z_{02} \ell} \qquad (4)$$

where C_{12} is the mutual capacitance in farads

V_1 and V_2 are the input and output voltages respectively. in volts

f is the measuring frequency, in Herz

Z_{02} is the characteristic impedance of the sample in ohms

ℓ is the length of the exposed shield, in meters.

Although both of these methods suffer from the restriction that the sample must be electrically short (e.g. 1 meter at 30 MHz), in many cases they are adequate. The IEC standard maximum transfer impedance for single-shielded cables larger than 5mm, for example, is 100 milli-ohms per meter at 30 MHz. The performance for higher frequencies is controlled by the result of much experience which shows that, above 30 MHz, the transfer impedance for this construction is no worse than directly proportional to frequency. However, there is need for a reliable method for measuring the shielding parameters directly at higher frequencies.

To meet this need, allowing measurements on longer (2 or 3 meter) samples and at higher frequencies (up to 1 GHz) the author has proposed to the IEC the "Terminated Triaxial" fixture diagrammed in Figure 3.

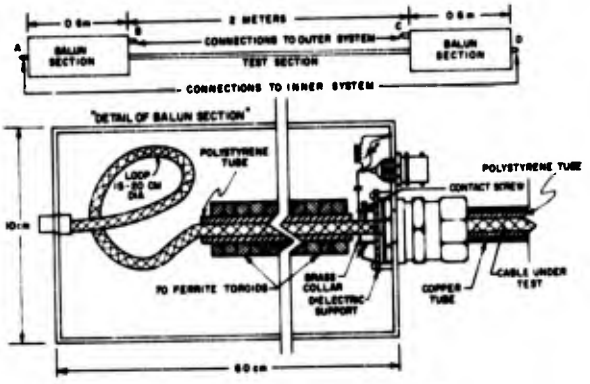

THE TERMINATED TRIAXIAL FIXTURE

FIGURE 3

In this method both the inner and the outer coaxial systems are terminated at both ends in their characteristic impedances. When this is done and when, in addition, the wave velocity in the outer system is matched to that in the inner (by choice of dielectric material) the "forward" response, i.e. the ratio of the input voltage at port "B" to the output voltage at port "D", is proportional to the Transfer Impedance at any frequency. (This assumes that there are no capacitive effects.) Under these conditions:

$$Z_T = \frac{V_2}{V_1} \cdot \frac{2Z_{01}}{\ell} \qquad (5)$$

where Z_{01} is the characteristic impedance of the outer system

The "reverse" response, under these same conditions, varies rapidly with frequency, following the law:

$$V_2 = \frac{V_1 Z_T \ell}{2Z_{01}} \cdot \frac{\sin x}{x} \qquad (6)$$

where x is the sum of the electrical lengths of the two systems, in radians

This function reaches maxima when x is an even multiple of $\frac{\pi}{2}$, and minima when x is an odd multiple.

Since, in the absence of coupling capacitance, the relationship between forward and reverse response is known, its presence is indicated when this relationship does not exist and its magnitude can be calculated from the forward-reverse ratio. The computed response for this fixture for certain assumed conditions, including a constant transfer impedance of 10 milli-ohms per meter, is shown in Figure 4 plotted between 0 and 500 MHz.

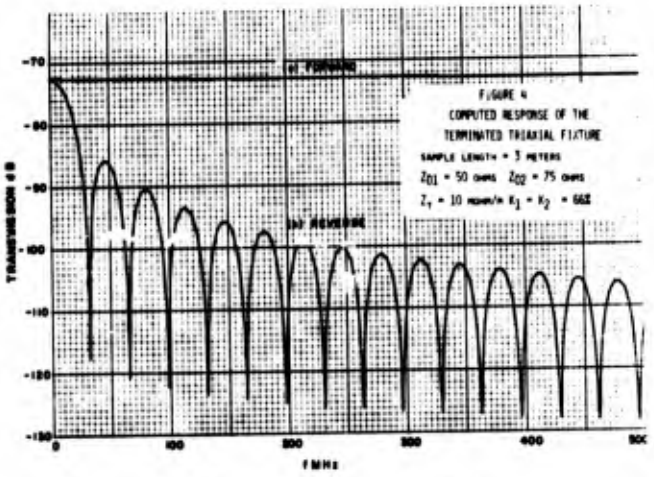

This shows the constancy of the forward response, and the $\frac{\sin x}{x}$ variation of the reverse response. In this case the minima fall at odd multiples of 33 MHz, the frequency at which the sum of the two electrical lengths is one-half wavelength.

To establish that the computed response has validity, tests were made with simple homogeneous shields for which the transfer impedance could be computed. Figure 5, for example, shows the computed transfer impedance (solid line) for a particular thin copper shield in the frequency range 0 to 10 MHz.

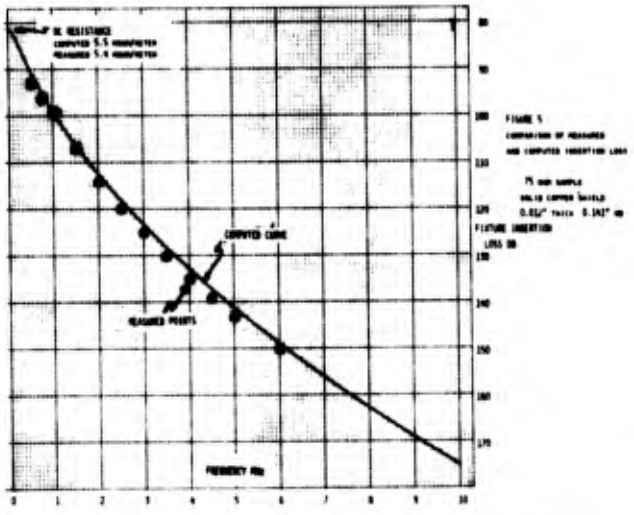

The values measured on the terminated triaxial fixture between 0.5 MHz (the lower frequency limit of the particular fixture used) and 6 MHz (at which frequency the sensitivity limit of the test was reached) are shown as plotted points. One other point on the curve, the DC resistance, is also shown.

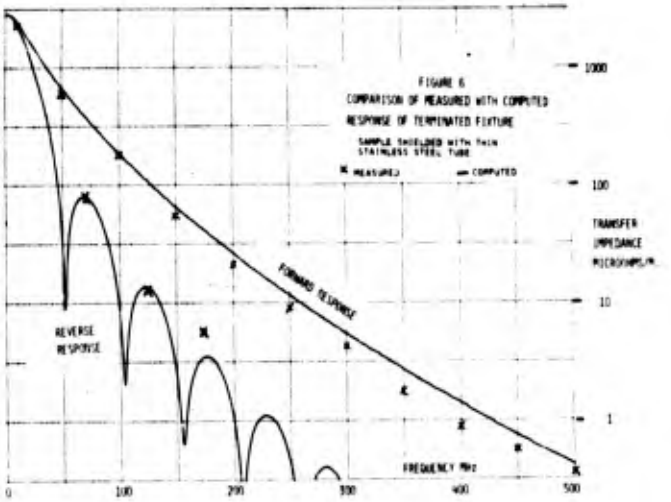

Figure 6 shows a comparison of the computed (solid) response (both forward and backward) and measured points for a thin-wall stainless steel tube, chosen because its resistivity was high enough to provide a measurable transfer impedance over the full frequency range to 500 MHz. These results indicate that the performance of this fixture is predictable, with reasonable accuracy, in the frequency range for which it is intended. When this fixture is used for testing a sample the response can be tested with four possible connections: two "forward" responses (B to D and C to A) (referring to Figure 3), and two reverse responses (B to A and C to D). For a uniform sample, the two responses in the same direction should agree, and lack of agreement indicates lack of uniformity. For a sample with no capacitive effects the relationship between the forward and the reverse responses is that described above; any other relationship indicates the presence of capacitive effects. Figures 7a and 7b show, for example, the response of a sample of the RG59 A/U cable used in the tests described at the end of this paper.

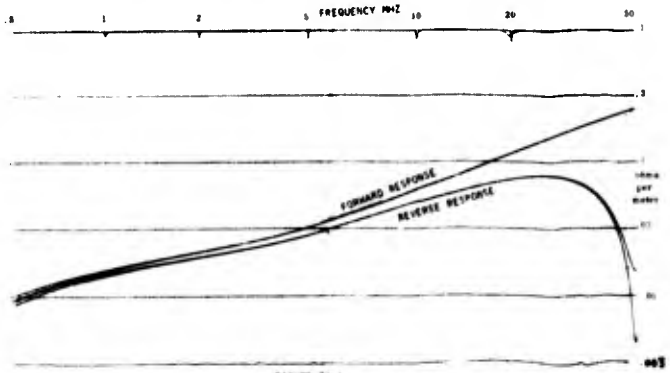

FIGURE 7(a)
THE MEASURED TRANSFER IMPEDANCE OF THE RG59/U CABLE USED IN THE TESTS 0.5 to 50 MHz

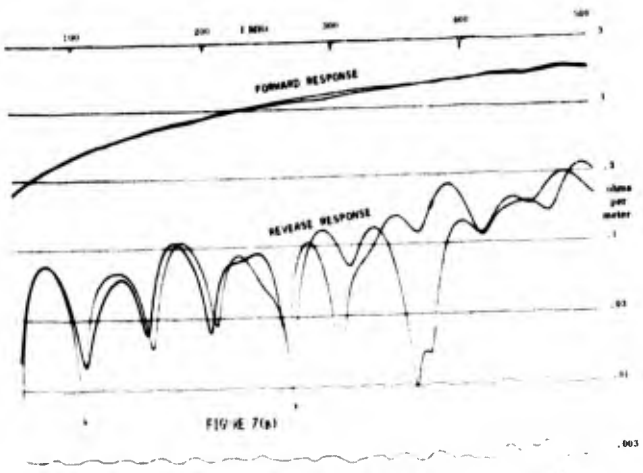

THE MEASURED TRANSFER IMPEDANCE OF THE RG59/U CABLE USED IN THE TESTS 50 to 500 MHz

By applying the criteria described above it is evident that this was a uniform sample with relatively little capacitive coupling.

Antenna Tests - Half-Wavelength Dipoles

In order to measure the radiation from cables under semi-realistic conditions, i.e. with several hundred feet of cable strung on poles, it was necessary to use test antennas. Before proceeding with those measurements, tests were made on the antennas in the attempt to answer, experimentally, these very basic questions:

1. The usual formulas for antennas apply rigorously when their spacing is very large compared: (a) to one-half wavelength (so that one is in the far-field of the other) and (b) to the physical dimensions of each so that they are, in effect, point sources. How closely can they approach each other without major deviations from the predicted response?

2. Tests must be carried out with the antennas located a short distance above the ground. What is the effect of the ground on the response?

3. In the real-life situation there are, within the general area in which the tests are carried out, many metallic conductors, telephone and power lines, automobiles and, inescapably, the cables feeding the test antennas. Do reflections from these conductors produce major deviations from the computed response?

The antennas used in these tests were constructed by mounting two collapsible whips on a section of PVC pipe, and connecting their inner ends through a ferrite-cored "balun" to a coaxial cable (to minimize the currents on the braid of the connecting cable. Each whip consisted of 11 sections and tests were carried out at frequencies corresponding to the measured resonance (as determined by the frequency of best impedance match) of various integral numbers of sections. In the initial test two such antennas were mounted ten feet apart and ten feet above the ground in a relatively clear area beside the laboratory building of the Jerrold Electronics Company. The antennas were about 75 feet from the building and from nearby power lines. The test was carried out by setting each of the two antennas successively to each of seven lengths, and measuring the power loss between their terminals. For each setting the frequency of the test signal was swept over a relatively narrow band centered on the corresponding resonant frequency. A General Radio Model 1710 Network Analyzer was used for the tests. In this instrument a narrow-band (10 kHz) receiver is continuously tracked with the transmitter so that loss measurements can be carried out without major interference from air signals. Loss calibration was accomplished by substituting a precise calibrated attentuator for the two antennas. The resulting loss-frequency plots are shown in Figures 8 (for horizontally polarized antennas) and 9 (for vertical polarization). To avoid confusing the plots of Figures 8 and 9, the loss calibration is shown separately, to the same scale, as Figure 10.

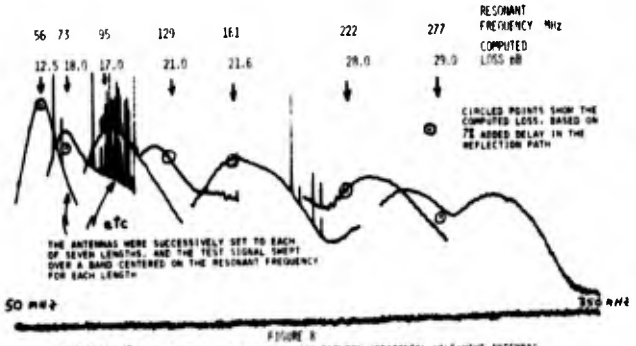

FIGURE 8
COMPARISON OF THE MEASURED AND COMPUTED LOSS BETWEEN HORIZONTAL HALF-WAVE ANTENNAS
ANTENNAS WERE TEN FEET APART AND TEN FEET ABOVE THE EARTH

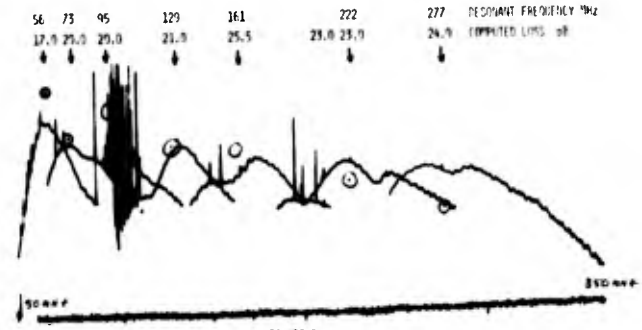

FIGURE 9
COMPARISON OF THE MEASURED AND COMPUTED LOSS BETWEEN VERTICAL HALF-WAVE ANTENNAS
CONDITIONS THE SAME AS FOR FIGURE 8

In making these plots it was necessary, to avoid creating interference, to use the lowest levels allowed by the sensitivity of the test set. As a result each local air signal created a "spike" where the receiver swept past its frequency. The occurence of these spikes can be seen more clearly on

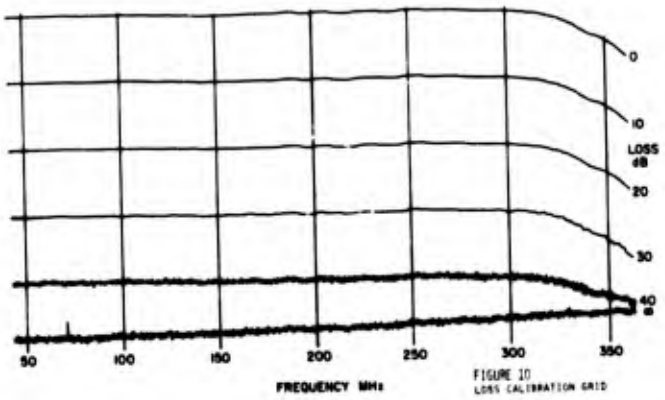

FIGURE 10
LOSS CALIBRATION GRID

Figure 11, which shows the receiver response with the transmitter disconnected. In effect, this plot must be mentally subtracted from Figures 8 and 9 to obtain the antenna losses.

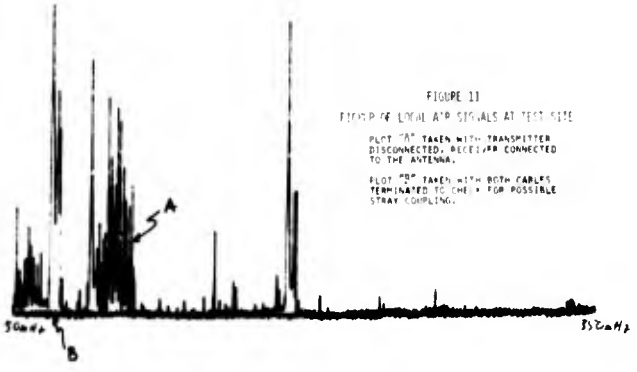

FIGURE 11

PLOT "A" TAKEN WITH TRANSMITTER DISCONNECTED, RECEIVER CONNECTED TO THE ANTENNA.

PLOT "B" TAKEN WITH BOTH CABLES TERMINATED TO CHECK FOR POSSIBLE STRAY COUPLING.

Comparison of Measured With Computed Antenna Response

As a check on these measurements, the loss between two antennas was computed by the method described in Appendix II. The loss-frequency characteristic was computed for three cases: for two half-wavelength antennas in free space; for the two antennas over a perfect reflector; and for the two antennas over a reflector providing 100% reflection but with an added delay in the reflected wave of 7%. The 7% figure was used because it provided an excellent agreement with the measured response for the horizontal case. The computed responses for the three cases are illustrated in Figure 12. The computed losses at each of the resonant frequencies are shown superimposed on each of the measured plots (Figures 8 and 9) and they are also listed in Table I.

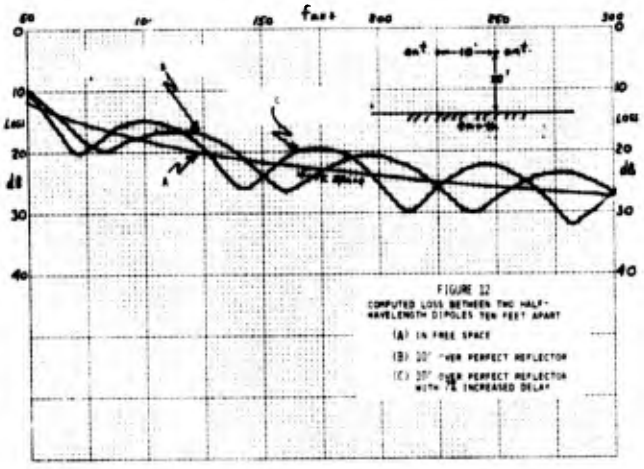
FIGURE 12

COMPUTED LOSS BETWEEN TWO HALF-WAVELENGTH DIPOLES TEN FEET APART

(A) IN FREE SPACE

(B) 20' OVER PERFECT REFLECTOR

(C) 20' OVER PERFECT REFLECTOR WITH 7% INCREASED DELAY

Table I

No.of Sects.	Resonant Freq.	Meas. Loss H.Pol.	Meas. Loss V.Pol.	Comp. Loss 100% Ref. 7% Delay Increase	Comp. Loss Free Space
11	56mHz	12.5dB	17	12.69	11.98
8	73	18	20	19.97	15.09
6	95	17	20	15.07	17.38
4	129	21	21	21.09	20.04
3	161	21.6	25.5	20.62	21.96
2	222	28.0	23	26.67	24.75
1.5	277	29.0	24	30.54	26.67

Several conclusions can be drawn from these comparisons. Agreement between the modified theory and the measured response for horizontal polarization is quite satisfactory(±2 dB). It is much less so for vertical polarization (± 5 dB). The former agreement tends to indicate that the errors due to the proximity of the two antennas and to other conductors in the area are relatively unimportant. There are two reasons why the results were not as good in the vertical case. In the first place, it is fundamental in regard to the reflecting properties of the earth that it closely approximates a perfect reflector for horizontally polarized waves, while the phase and amplitude of the reflected wave are very much affected by the nature of the soil, the angle of incidence and the frequency for vertically polarized waves. In the second place, the construction of the whip antennas was such that, in the horizontal case, they were at right angles to the feed cables, so that relatively little interaction might be expected. When the antennas were rotated to the vertical plane the lower half of the dipole was about a foot from the feed cable and parallel to it. In this case there is no question that there was considerable interaction between the cable and the antenna, which undoubtedly contributed to the deviation of the measured response from that computed.

There is no doubt that a vertically polarized antenna can be constructed for which this effect is important.

Loss vs. Frequency Measurements With Long Cable Samples

To provide a simple way of describing the efficiency of the shielding of any system, I have chosen to define a "System Shielding Factor". This factor is simply the increase in the loss (measured in decibels) that occurs when one of the two antennas, in the situation described above, is replaced by a "system", the nearest approach of the system being held at the same distance as the spacing of the two antennas, and the height of the system above ground being the same as the height of the two antennas. Having established these spacings, loss-frequency measurements were carried out by setting the lengths of the receiving antenna successively to each of the seven positions and sweeping the frequency as before. By comparing the loss measured in this case with that measured with the two antennas, the "System Shielding Factor" could be established for any given system at any one of the resonant frequencies.

As an initial test, a 200 foot piece of the RG59/U cable whose transfer impedance had been determined (see Figures 7 (a) and (b)) was strung on wooden poles at an average height of 10 feet above the earth. One of the test antennas previously described was mounted 10 feet away from the cable and 50 feet from the end at which the test signal was introduced. Its length was set to each of the seven positions used before, and the frequency swept as before. The result is illustrated in Figure 13.

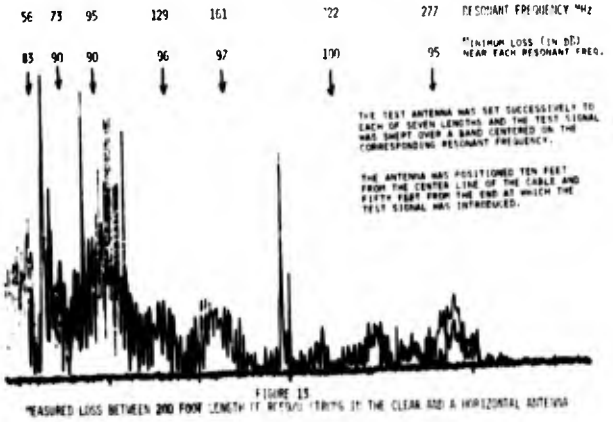

FIGURE 13
MEASURED LOSS BETWEEN 200 FOOT LENGTH OF RG59/U STRUNG IN THE CLEAR AND A HORIZONTAL ANTENNA

The response varies very rapidly with frequency, undoubtedly due to the fact that the outer surface of the shield constitutes, in effect, a long-wire antenna with many resonances and a complex directional pattern. The plot is also confused by the local signal "spikes" referred to above. It is, however, possible to estimate, at each resonant frequency of the test antenna, the peak response, and these figures are noted on the plot. The test antenna was then rotated to the vertical position and another series of plots was made, with the result shown in Figure 14. Again the maximum responses are noted.

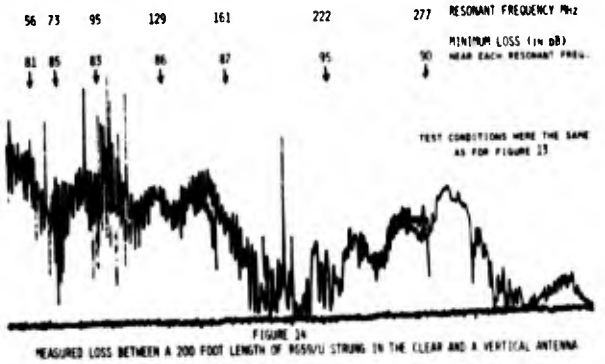

FIGURE 14
MEASURED LOSS BETWEEN A 200 FOOT LENGTH OF RG59/U STRUNG IN THE CLEAR AND A VERTICAL ANTENNA

These tests made on an isolated piece of cable might be useful in evaluating the shielding performance to be expected when a cable is used in a similar situation, e.g. as a CATV drop cable. In many cases, for example in the case of a CATV feeder or trunk cable, the cable is surrounded by lashing wire, and runs parallel to and closely associated with many other wires and cables. To get some idea of the effect that might be expected from such a situation, tests were made in which a 100 foot piece of the same RG59/U cable was strung along a complex array of cables that is used as a test facility at the laboratory. The plots obtained in this situation are shown in Figures 15 and 16.

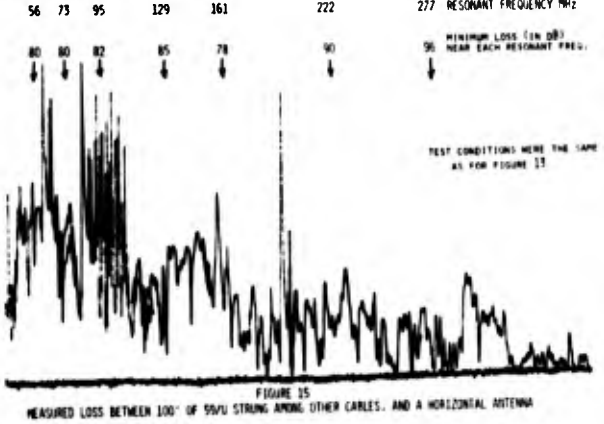

FIGURE 15
MEASURED LOSS BETWEEN 100' OF 59/U STRUNG AMONG OTHER CABLES, AND A HORIZONTAL ANTENNA

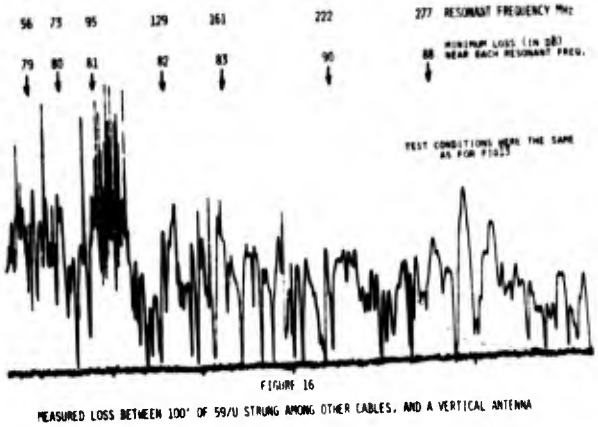

FIGURE 16
MEASURED LOSS BETWEEN 100' OF 59/U STRUNG AMONG OTHER CABLES, AND A VERTICAL ANTENNA

In an attempt to reduce these data to more manageable form the System Shielding Factor was computed corresponding to the major response in the vicinity of each resonant frequency. These data were further corrected for the measured transfer impedance of the cable used.

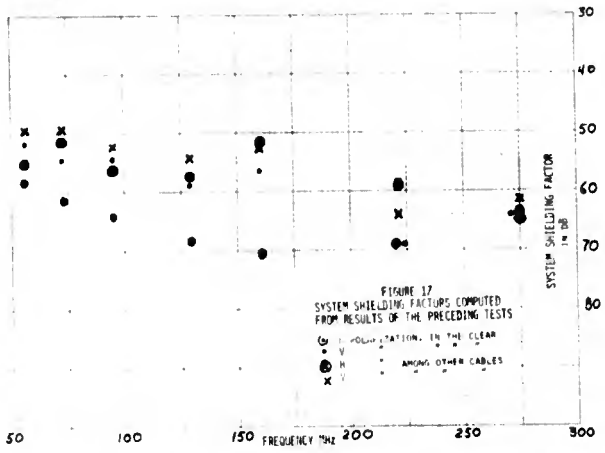

The result, shown in Figure 17, summarizes the results of the shielding vs. frequency tests in terms of the System Shielding Factor corresponding to a constant transfer impedance of one ohm per meter. This plot shows some interesting trends. The complex system, with many cables surrounding the test cable, showed generally poorer shielding than the simple system with the isolated cable, as evidenced by the fact that most of the crosses are above the dots on the plot. The shielding appeared to be poorer for vertical polarization than for horizontal, as evidenced by the fact that most of the points with circles around them are below the others on the plot. Finally, there seems to be a general, but slight, tendency for the shielding to improve at higher frequencies. With the limited amount of data available, it is obviously not possible to generalize, but these results pose some interesting questions for the future.

Loss vs Antenna Position Measurements With Long Cable Samples

Since the energy intercepted by the test antenna is a rapidly varying function of both the frequency and the antenna position, it seemed likely that useful results could be obtained by holding the frequency constant and varying the antenna position. Tests were made at spot frequencies corresponding to the resonant frequencies of the test antenna. At each frequency the antenna was moved parallel to the cable under test in such a way that its spacing from the cable and its height above ground were approximately constant at 10 feet. The antenna was physically connected to a cord which was wound on drums geared to a DC potentiometer; this, in turn, provided an X axis drive for the X-Y Plotter, so that the plots are linear with distance horizontally, and linear with decibel loss vertically. Some samples of the resulting plots, where the antenna was moved for a distance of 100 feet along a piece of the same RG59/U, are shown in Figures 18 to 21 inclusive.

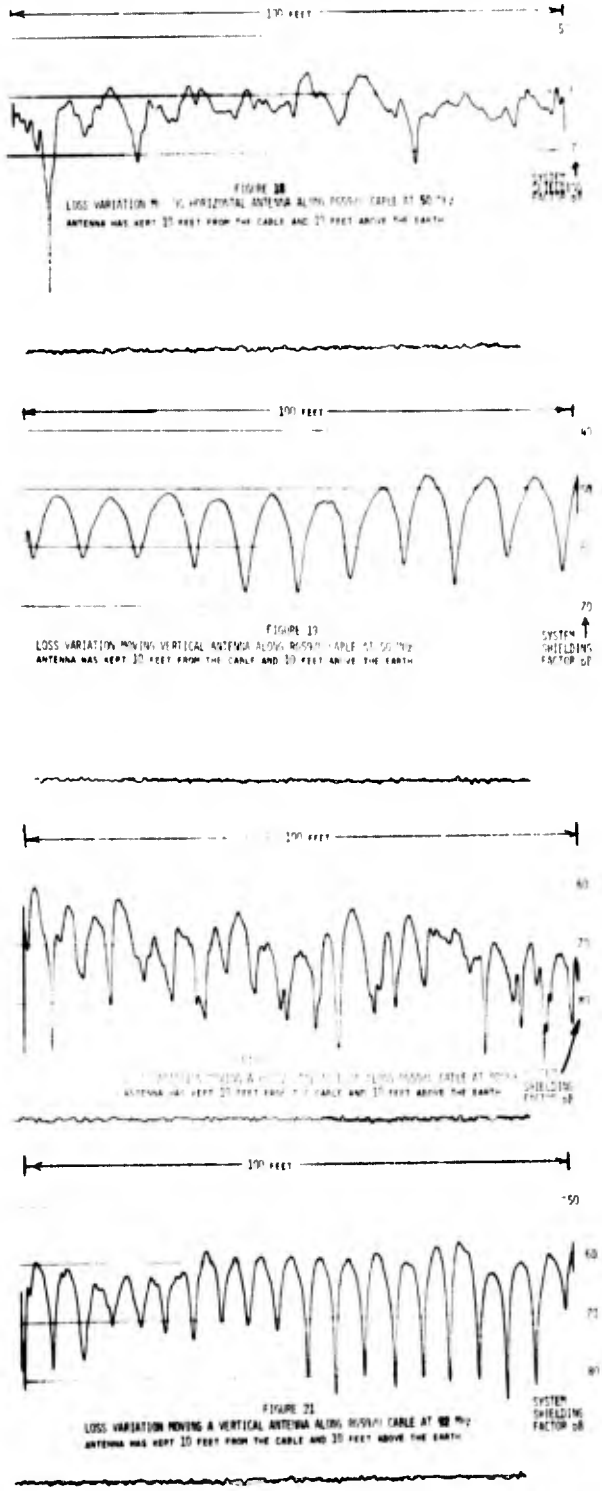

On each plot the calibration lines represent the System Shielding Factor corrected to a Transfer Impedance of one ohm per meter. Inspection of these plots shows several interesting facts. The peak Shielding Factors near the center of the cable agree quite well with those found by the other method and plotted on Figure 17. This would indicate that essentially the same information can be found by either method. Again the shielding for vertical polarization

appears to be poorer. For some reason the energy picked up by the antenna appears to vary in a more regular manner for vertical polarization than for horizontal.

Conclusion

This paper has presented some of the fundamentals in regard to cable shielding and shielding test fixtures, and described some of the tests made in an attempt to correlate Transfer Impedance with signal leakage under somewhat realistic conditions. There is not sufficient data to provide any conclusive results. Based on experience with these tests, it is the author's opinion that the better of the two methods is the second, employing fixed frequencies and variable position. A great deal remains to be done to refine this technique. To have a technician walk along the sample, dragging a feed cable behind him and trying to estimate the height and spacing of the antenna represents a very crude approach. Much greater accuracy and repeatability could be achieved by arranging some kind of track for the antenna, and a form of telemetry so no connecting cable would be required. Another major improvement would be achieved by providing the test area with a highly reflective metallic ground plane so that, particularly for vertical polarization, the environment would be more closely calculable. With these improvements it would seem that this approach could provide a powerful technique, not only for relating the Transfer Constants to real life, but for making meaningful measurements of the radiation characteristics of cables as well as a variety of devices used with cable.

APPENDIX I

The Developement of Equations 2 Through 5

Equation 2: The Relationshipe Between Z_F and C_{12}

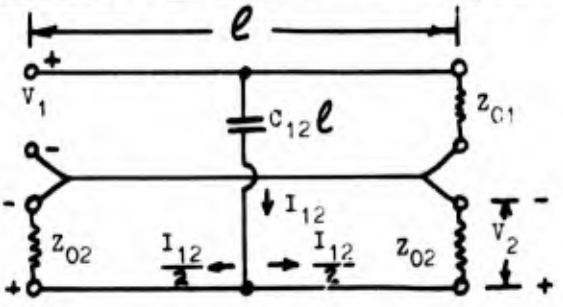

Figure 22

Referring to Figure 22, consider a section of shielded cable which is very short compared to a wavelength, and which is terminated at both ends by its characteristic impedance (System 2). Assume that it is surrounded by a second shield, so that the outer surface of the cable and the inner surface of the shield form another system which is terminated at the right-hand end by its characteristic impedance (System 1). Further assume that the two systems are coupled by a mutual capacitance $C_{12}\ell$, where C_{12} is the mutual capacitance per unit length, and ℓ is the length. Also assume that the coupling reactance is very large compared to the characteristic impedances, then:

$$I_{12} = \frac{V_1}{X_{12}} \text{ and } V_2 = \frac{I_{12}Z_{02}}{2} = \frac{V_1 Z_{02}}{2 \cdot X_{12}}$$

$$\text{since } X_{12} = \frac{1}{2\pi f \cdot C_{12}\ell}, \quad V_2 = \frac{V_1 \cdot Z_{02} \cdot 2\pi f C_{12}\ell}{2} \quad (7)$$

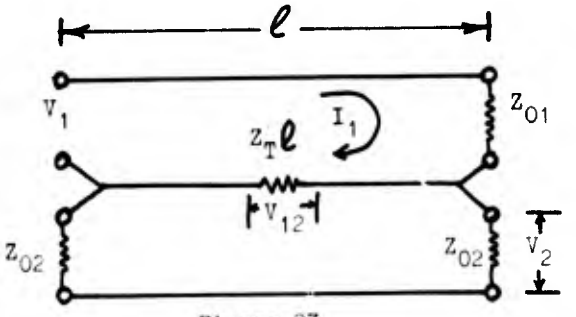

Figure 23

Now, referring to Figure 23, consider two similar systems coupled by a mutual impedance $Z_T\ell$ which is very small compared to the characteristic impedances. Z_T is the transfer impedance per unit length. In this case:

$$I_1 = \frac{V_1}{Z_{01}} \text{ and } V_{12} = I_1 Z_T \ell = \frac{V_1 Z_T \ell}{Z_{01}}$$

$$\text{and thus } V_2 = \frac{V_{12}}{2} = \frac{V_1 Z_T \ell}{2Z_{01}} \quad (8)$$

To find the value of the IEC "Capacitive Coupling Impedance" (Z_F), which is a fictitious transfer impedance giving the same output voltage as that due to C_{12}, it is only necessary to equate the output voltages in equations 7 and 8, replacing Z_T in 8 by Z_F:

$$\frac{V_1 Z_{02}^2 \, fC_{12}\ell}{2} = \frac{V_1 Z_F \ell}{Z_{01}^2}, \text{ so:}$$

$$Z_F = Z_{01} Z_{02}^2 \pi f C_{12}, \text{ which is equation (2).}$$

Equation (3), the Response of the IEC Transfer Impedance Fixture

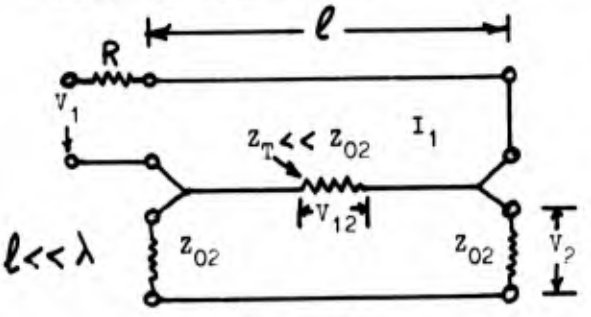

Figure 24

$$I_1 = \frac{V_1}{R} \text{ and } V_{12} = I_1 Z_T \ell = \frac{V_1 Z_T \ell}{R}$$

$$V_2 = \frac{V_{12}}{2} = \frac{V_1 Z_T \ell}{2R} \text{ so } Z_T = \frac{V_2}{V_1} \cdot \frac{2R}{\ell}$$

which is Equation (3).

Equation (4): The Response of the IEC Quadraxial Capacitance Test Fixture

Refer to Figure 22. This circuit diagram applies to the fixture in question, except that there is no terminating resistor in the outer system of the IEC fixture, i.e. Z_{01} is omitted. Since its absence has no effect on V_1, equation (7) applies equally in this case:

$$V_2 = \frac{V_1 Z_{02} 2\pi f C_{12} \ell}{2} \quad \text{so} \quad C_{12} = \frac{V_2}{V_1} \frac{1}{\pi f Z_{02} \ell}$$

which is Equation (4).

Equation (5): The Response of the Terminated Triaxial Test Fixture (Forward Direction)

Refer to Figure 23. This circuit diagram applies to the forward response of the fixture in question except that, when the velocities in the two systems are matched, there is no restriction on the length. Thus:

$$V_2 = \frac{V_1 Z_T \ell}{2 Z_{01}} \quad \text{(Eq. 8), so } Z_T = \frac{V_2}{V_1} \frac{2 Z_{01}}{\ell}$$

which is Equation (5).

APPENDIX II

THE INSERTION LOSS BETWEEN THE TERMINALS OF TWO HALF-WAVELENGTH DIPOLES

In Free Space:

The power density at a distance due to any transmitting antenna is given by:

$$P_D = \frac{G P_T}{4\pi D_m^2} \qquad (9)$$

Where: P_D is the power density in watts per square meter
G is the power gain of the antenna relative to an isotropic radiator.
P_T is the radiated power
D_m is the distance in meters

The effective "capture area" of any receiving antenna is given by:

$$A = \frac{G\lambda^2}{4\pi} = \frac{G}{4\pi}\left(\frac{300}{F_{MHz}}\right)^2$$

Where: A is the capture area in square meters.
λ is the wavelength in meters
F_{MHz} is the corresponding frequency in megaherz

The output power from the receiving antenna is found by multiplying the power density by the capture area:

$$P_R = P_D A = \frac{G P_T}{4\pi D_m^2} \frac{G}{4\pi}\left(\frac{300}{F_{MHz}}\right)^2$$

and the power ratio is $\frac{P_R}{P_T} = \left(\frac{300G}{4\pi D_m F_{MHz}}\right)^2$ (10)

For half-wavelength dipoles G = 1.64 so this reduces to:

$$\frac{P_R}{P_T} = \left(\frac{39.15}{D_m F_{MHz}}\right)^2 = \left(\frac{128.4}{D_{ft} F_{MHz}}\right)^2$$

and the insertion loss = $20\log_{10}\left(\frac{128.4}{D_{ft} F_{MHz}}\right)$ dB

Over a Perfect Reflector:

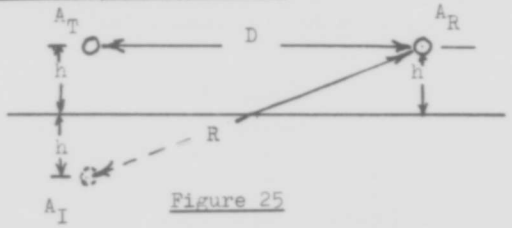

Figure 25

A_T represents the transmitting antenna
A_R the receiving antenna, and
A_I an "image" antenna hypothesized to allow convenient treatment of the reflected wave.
H is the perpendicular distance from each antenna to the reflector
D is the spacing between the transmitting and receiving antenna
R is the spacing between the image antenna and the receiving antenna

$$R = \sqrt{D^2 + (2h)^2}$$

The output of the receiving antenna was computed by assuming that A_T and A_I radiated equally, the resulting output power from A_R being determined by summing the two components at A_R. The magnitude of each component was found by using Equation (10) for each frequency and for the two paths. The phase of each component was found by assuming a delay equal to the electrical distance in each path, with an assumed 180° phase reversal at the point of reflection.

Keneth A. Simons
Simons and Wydro Associates
Hilltown, Pa.

Keneth A. Simons has a B.S. in Electrical Engineering from the University of Penna. He has worked in electronics since 1930, in television since 1939. During over 20 years spent with Jerrold Electronics Corp., the pioneer CATV company, he held, among other positions that of Vice-President of R. and D.

He has recently left Jerrold to join Walter Wydro in a firm acting as consultants to the cable manufacturing and CATV industries.

He has published numerous technical articles and a "Technical Handbook for CATV Systems." He is a member of Working Group 1 (Screening Efficiency) and Secretary of Working Group 2 (CATV Cables) both of Subcommittee 46A (RF Cables) of the I.E.C.

STRUCTURAL RETURN LOSS ASSOCIATED WITH 2.6/9.5 COAXIAL CABLE FOR 60 MHz ANALOGUE SYSTEMS AND HIGHER CAPACITY FUTURE DIGITAL SYSTEMS

J.R. Osterfield
Pirelli General
United Kingdom

S. Longoni & A Manilii
Industrie Pirelli S.p.A.
Italy

SUMMARY

The structural return loss (SRL) must be considered when using coaxial cables at high frequency. The causes of SRL peaks occurring during the manufacture of coaxial cable are discussed and the measurement of SRL by the c.w. burst method is described.

A simplified method is suggested for measuring the returned power in discrete bands, a parameter of interest to system designers considering coaxial cables for digital operation. The paper compares the results achieved with those of a conventional method.

The effect of SRL on the design of two layer 2.6/9.5 disc insulated coaxial pair cable is considered. A prototype design of 18 tube cable is shown to exhibit SRL peaks resulting from tube distortion caused by interaction between layers. New designs of cables are discussed involving the extensive use of fillers and the variation of stranding lay within a cable length to minimize the effect of the SRL peaks.

INTRODUCTION

The 2.6/9.5 disc insulated coaxial pairs have been operated at 12 MHz in Europe and Japan giving capacities of 2700 two way voice channels per pair of coaxial tubes. Even in the United States the common L4 system with a capacity of 3600 channels operates below 18 MHz. Hence an adequate control of quality for system performance has been possible by checking the uniformity of impedance and the tube end impedance of coaxial cable by short pulse echoes [1] to ensure discrete impedance irregularities are not built into the transmission system. The sine squared 50 nsec wide pulse used with its spectrum of 20 MHz amply covered the bandwidth for system performance.

Now, however, 10800 channel systems are being commissioned for FDM systems operating to 60MHz with talk of higher capacity systems in a digital mode. The use of 10 nsec and 2 nsec wide test pulses could provide bandwidths of 100 MHz and 500 MHz respectively but owing to the cable attenuation present at these high frequencies pulses particularly of the latter width are unlikely to penetrate far into the cable. Also the transmission performance of cables at high frequencies is influenced by small periodic irregularities which are sufficiently small, if considered individually, not to be discernible by the 50 nsec and 10nsec wide pulse test. Because the small reflections from the irregularities are equidistant they sum in phase at particular frequencies giving rise to peaks of reflected energy commonly known as SRL peaks.

CAUSES OF SRL PEAKS IN CABLE MANUFACTURE

The outer conductor of our 2.6/9.5 coaxial tube is made from a copper tape which is formed longitudinally with its edges butting and is held together by tension in the steel screening tapes which are applied overall. Should pressure be applied to one point on the surface of a tube and this point of application rotated helically along the tube, non uniform distortion will occur each time the pressure is applied to the tape seam. This may be represented schematically in Figure 1a as a series of equally spaced irregularities. The energy reflected from each irregularity will be in phase for a fundamental frequency having a wavelength twice the distance between irregularities and for all harmonics of it.

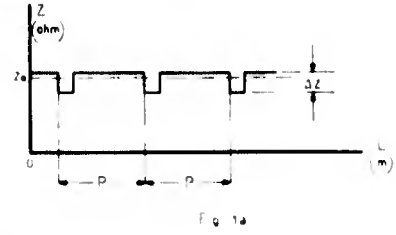

Fig. 1a

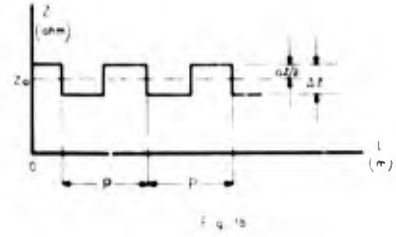

Fig. 1b

Fig. 1 Schematics of impedance irregularities.

A special case is given by symmetrical irregularities, shown schematically in Figure 1b, which could occur with cyclic variations in the copper tape thickness. In this case all even harmonics will cancel.

An example of the effect on SRL peaks of unsatisfactory tape is shown in Figure 2a. As predicted the second harmonic is shown not to be present. A plot of the sinusoidal variation in mass is shown in Figure 2b. The frequency of the fundamental has been superimposed on weight measurements and gives good agreement.

The tolerances of thickness of the order of a few micrometres currently asked for the 12 MHz cables, are already near the practical limit of control by normal measurement techniques. It should be possible, however, to alter the manufacturing processes of the tape perhaps with a change of roller diameters to ensure the period of irregularities is reduced to push the fundamental frequency above 60 MHz to a region where so far the requirements on SRL peaks are less severe.

The deformations produced from the periodic thickness and width of copper tape are also influenced by the mechanical stability of the tube. Non uniformity in the degree of anneal along the tape and in the working

of it during the tube forming process could lead to fluctuations in the amount of tape edge reopening before the steep taping heads. This would add importance to any variability in steel tape tension.

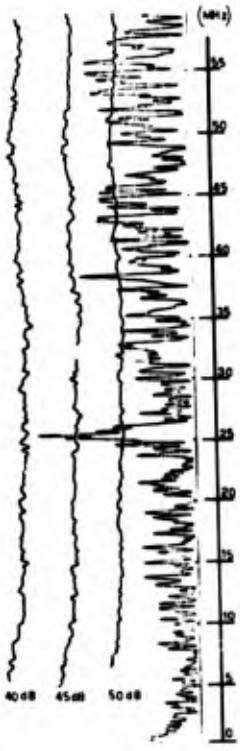

Fig. 2a

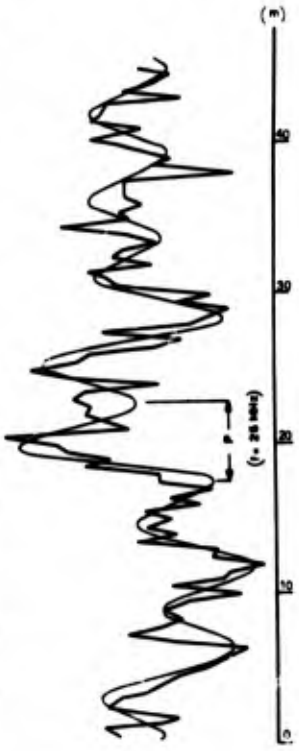

Fig. 2b

Fig. 2 SRL peaks arising from symmetrical variations in the dimensions of copper tape.

Although copper tape is probably the major cause of SRL peaks resulting in the manufacture of tube, other possible causes are given in Table I.

Table I Causes of Periodic Irregularities in Tube Manufacture

Causes of Irregularities	Period (mm)	Fundamental frequency (MHz)
Capstan	3770	38
Steel tape supply bobbin		
- outer turns	4230	34
- inner turns	2470	59
Take-up bobbin	3160	46
Centre conductor supply bobbin		
- outer turns	1760	82
- inner turns	1476	98
Copper tape pad		
- outer turns	1480	98
- inner turns	346	420
Disc applicator	999	145

As the tubes are laid up with almost complete detortion the cable strand closing die will exert a pressure against the tape seam of each tube once for each revolution of the carriage, Figure 3a.

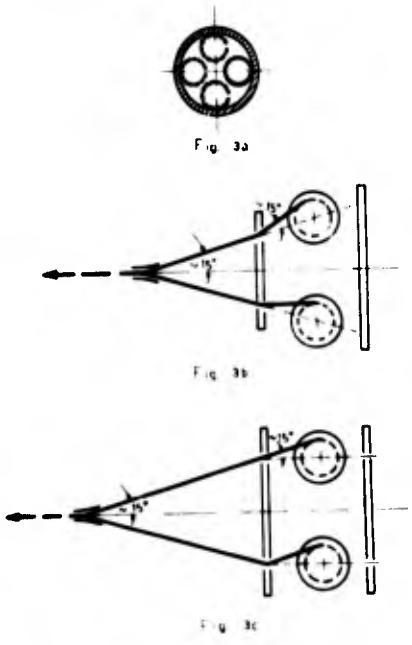

Fig. 3 Tube configurations on stranding machines.

At the caterpillar or capstan of the strander sufficient pressure must be applied to the tubes to pull the cable core through the machine and it will be applied to each tape seam at intervals of the stranding lay. On the take up drum the tape seam will again be subjected to a periodic pressure from the weight of the layers of laid up cable.

Perhaps the most interesting area is that of periodic irregularities arising from inclined or parallel cradle pay off bobbins, Figures 3b and 3c. In the former case Coriolis acceleration accounts for a pulsating pay off tension related to the speed of rotation of the carriage and the angle of inclination. In the latter case each tube is subjected to additional bending in a plane rotated around its circumference for each turn of the carriage. It has been found in practice that for our machine with an angle of inclination of about 15° the effect of Coriolis acceleration is not significant for a carriage speed of 12 rpm.

Although our stranding machines are designed to be torsion free observations, by marking the tubes with a longitudinal line corresponding to the seam of the copper tape at the pay off bobbin, show a random variability of torsion at the stranding die. The variation which is not the same of all tubes is probably influenced by the distance between payoff and stranding die, by intermediate supports which limit the free catenary of the tubes and from the type and stability of the pay off bobbin braking system. While the irregular torsions of the tubes favourably assist with a reduction in the size of the SRL peaks with diffusion of the periodic irregularities, any resulting irregular movement of the tubes away from their desired geometrical position can be serious if the non-uniformity of distance between adjacent tubes

causes a tube to stand proud of the layer. It will then be exposed to greater pressures, than the other tubes, from the capstan and the weight of the layers of other turns.

During the rewinding processes associated with other manufacturing stages some movement of the tubes occurs which distributes them more equally in the space available. Those deformations within the elastic limit are therefore given a chance to relax with a resulting improvement in quality. Eventually a point is reached where the tubes start to deteriorate with continued reworking of the cable core. Of course, those irregularities which are permanently deformed may become worse. Generally the worst peak may deteriorate by 1 to 2 dB with an average improvement for the rest of the tubes in the cable being much more marked when the quality is poor.

It has been shown [2] that the magnitude of the SRL peaks is a function of the magnitude of the irregularities, the cable attenuation and the length of cable involved. Also the magnitude of harmonics is effected by the proportion of distorted tube relative to the period of the irregularities. Depending on the asymmetry of the irregularity period the SRL peak at the fundamental may be of smaller amplitude than the harmonics.

CW BURST TEST METHOD

The conventional method of assessing SRL relies on measuring the ratio of the reflected to the incident wave at the cable end using an r.f. bridge and a c.w. signal. By sweeping the frequency an assessment of the bandwidth can be made. However, above 50 MHz difficulties arise from residual vswr in the connectors and in the matching of the cable to the bridge. The problems may be overcome [3] by pulsing the c.w. at any particular frequency through suitable gating, and sampling the reflected signal when it is free from the incident c.w. burst. The signal at the end of the cable can be displayed against time graphically, Figure 4.

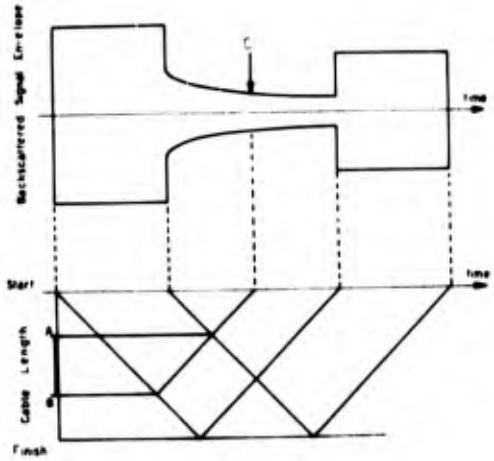

Fig. 4 Reflection of c.w. burst signal

As the speed of propagation is the same for the incident and reflected waves the position of the waves with respect to length along the cable and time may also be displayed. The back scatter received at the end of the cable is from the reflections as a result of interaction of the incident burst with a particular segment of cable. Thus the segment AB is the result of sampling at C a finite time after the burst. By increasing the length of burst the segment of cable will be increased.

In practice the point C must be sufficiently behind the burst to allow its tail to decay. Hence the burst time should be twice the propagation time down the cable less twice the time to sample after the burst. In this manner the reflections from most of the cable will be obtained. Normally the sampling point C is 50 nsec after the burst thereby gating out the first 7m of cable. A schematic of the test equipment is given in Figure 5.

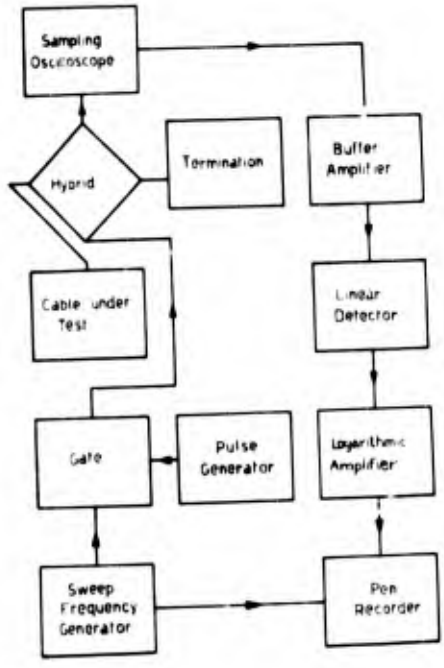

Fig. 5 Block diagram of c.w. burst

The length of the lead to and from the bridge is important since multiple reflections occur between the ends of each lead following the end of the c.w. burst. As the majority of the energy in the leads is dissipated in the terminations and not from cable attenuation short leads are chosen to decay the signal more quickly. In order to sample 50 nsec after the burst the leads are restricted to about 2m. The gate is also critical because it is used to mask out the incident signal during the sampling of the reflected signal. The HP modulator Type 10514A works well in this function.

Although the c.w. burst measurement was developed for the measurement of SRL peaks it is sensitive to the presence of significant discrete irregularities particularly when these are near the end of the cable. The trace given in Figure 6a shows the effect of a 64 dB irregularity (measured with a 50 nsec pulse) 15m from the end of the cable. The result of gating out this irregularity is shown in Figure 6b.

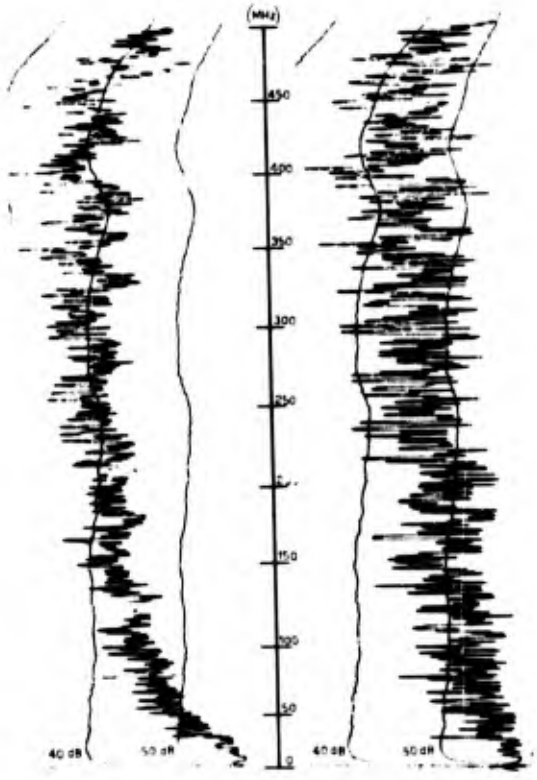

Fig. 6a Fig. 6b

Fig. 6 The effect on a SRL trace of a 64 dB discrete irregularity 15m from the end of the cable and the result of gating it out.

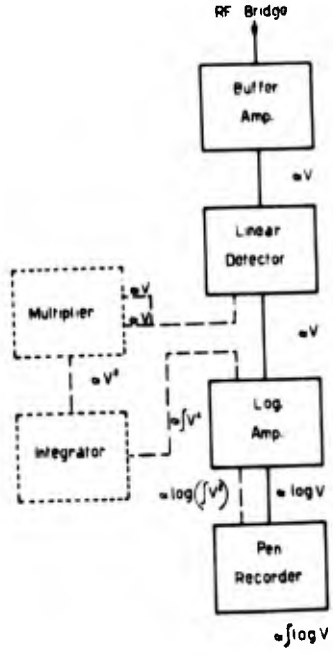

Fig. 7 Block diagram of the measurement equipment for the mean power returned.

MEASUREMENT OF MEAN POWER RETURNED

There is a growing opinion that the average power returned should be specified especially for high frequency digital performance. Already the British Post Office is requesting that the mean power returned in any 10 MHz band should meet certain limits for coaxial cable systems which will eventually be worked in a digital manner [4].

A novel method of monitoring this parameter is a 10MHz moving band across the required bandwidth. The technique involves modulating the sweeping frequency with a 10 MHz signal by applying a sawtooth waveform to the sweep generator and averaging the output obtained. The voltage existing at the linear detector output of the c.w. burst equipment should be squared and integrated, Figure 7, before being presented to the logarithmic amplifier. However, since the voltage at the output of the logarithmic amplifier ($20 \log_{10} V$) can be recorded equally as power ($10 \log_{10} V^2$) the slow response time of the pen recorder will provide an integrated output. Good agreement between the two methods, Figure 8, is achieved so long as the SRL peaks do not exceed 30 dB.

By modifying the c.w. burst equipment to modulate the sweeping frequency with a 10 MHz signal, at the flick of a switch the measurement of power in band can be easily plotted on the SRL trace of each tube, for instance during the flyback of the sweep generator.

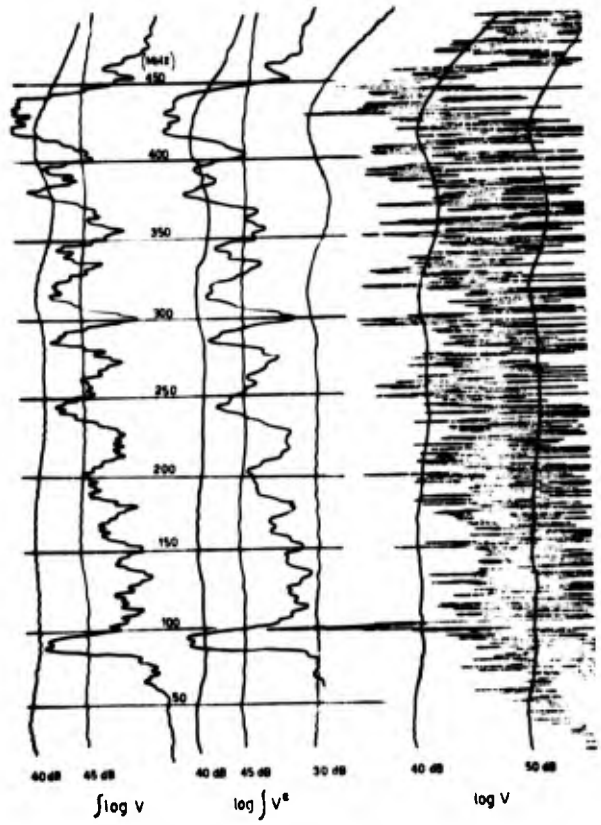

Fig. 8 Traces of the mean power returned compared with the original SRL signals.

MODIFICATIONS TO CABLE DESIGN TO MODERATE SRL PEAKS

In the design of cables to reduce SRL peaks precautions are taken to reduce to a minimum the pressures between tubes in the same layer and between each tube and all others in adjacent layers. In an early design an inadequate belt between the two layers of an 18 tube cable caused SRL peaks at the frequency relating to a combination of the lays of the two layers, Figure 9a. The SRL trace figure 9b, for a tube from the centre of the cable, shows no signs of the interaction as the frequency involved is above 600 MHz.

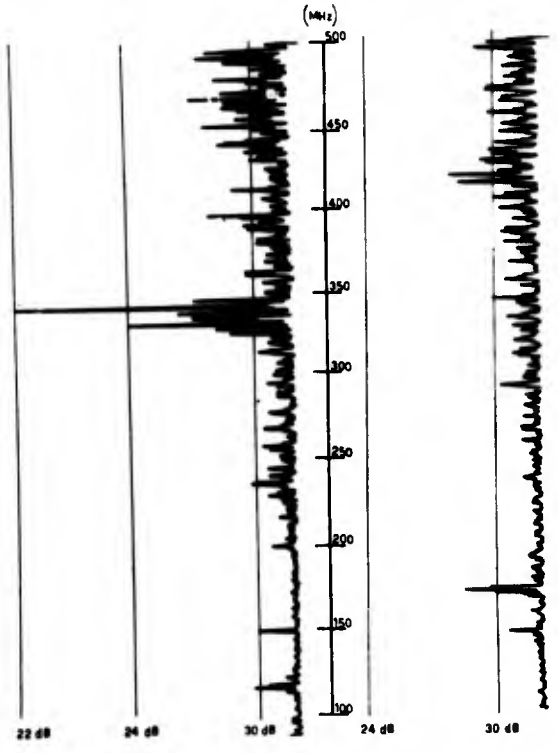

Fig. 9a

Fig. 9b

Fig. 9 SRL traces of any early design of 18 tube cable.

Design criteria can be condensed into four rules:-

(1) The bedding under each layer should be of excess diameter to that required for a perfect geometrical lay up of tubes to allow some room for re-adjustment subsequent to the stranding operation.

(2) The surface of the bedding should be as regular as possible using suitably deformed interstitial fillers in the layer below.

(3) The softest belt possible should be adopted making extensive use of crepe paper alternated with smooth paper tapes all applied with a low tension.

(4) Maximum protection of the external layer of tubes should be obtained by the use of a soft belt or by the adoption of deformable interstitial elements of sufficient size that they protrude with respect to the layer of tubes.

In the application of these rules it was noted that in the 18 tube cable sufficient room was created in the outer layer to allow space for 13 tubes. The 13th element is used to contain a group of control quads. The construction, Figure 10a, is being used by the BPO for its first 100 mile 60 MHz installation. Two experimental Italian constructions adopting the same principles are given in Figure 10b and 10c. Results for these two cables are given in Table 2 below.

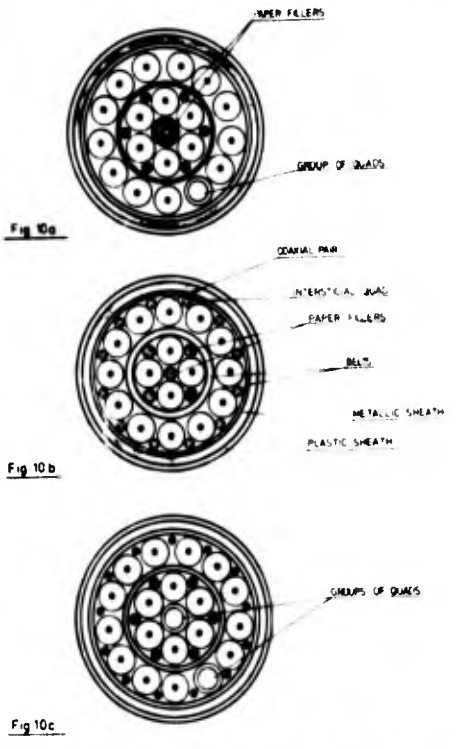

Fig. 10 Lay ups of multilayer coaxial tube cables.

Table 2 Results from Experimental Lengths of 16 Tube and 18 Tube Cables

	16 tube (4 + 12)			18 tube (6 + 12)		
	1st layer (dB)	2nd layer (dB)	Total (dB)	1st layer (dB)	2nd layer (dB)	Total (dB)
Fundamental SRL peak - mean - worst	28.5 27	31.6 27	30.8 27	26.9 24	31.0 26	29.[illegible] 24
2nd harmonic - mean - worst	34.0 32	29.3 26	30.5 26	34.2 30	34.9 34	34.7 30
3rd harmonic - mean - worst	35 35	33.1 29	33 29	34.9 34	34.9 34	34.9 34
Power in 100MHz band - mean - worst	39.2 38	36.7 34	37.3 34	35.9 34	39.7 38	38.4 34
Power in band after the worst 3 - mean - worst	40 40	39.7 38	39.7 38	39.8 39	40 40	39.8 39

Generally the SRL peaks of the centre tubes are worse than those in the outer layer. This is not because the tubes make two passes through the stranding machine but because of the shorter stranding lay used.

The recommendations suggested to minimise SRL peaks do lead to some increased costs resulting from increases in cable diameter, and from a slow down in the

stranding operation. The use of thick crepe paper incurs frequent machine stops for pad changes. Also the use of fillers increases the machine loading time and necessitates greater care on the part of the operator to prevent crossover of the elements during stranding.

It has been argued that with the use of long lay lengths the advantage from the greater spacing between irregularities is off set by the lower cable attenuation from a corresponding lower fundamental frequency. With the c.w. burst technique it is a simple matter to record the magnitude of the SRL peaks for increasing lengths of cable by adjusting the width of the c.w. burst. The value of the fundamental SRL peak has been plotted against cable length for two different stranding lays, Figure 11. The solid curves shown have been derived theoretically from an assumption of the reflection coefficient. It can be seen that for equal lengths of cable the longer the stranding lay, the lower the SRL peak.

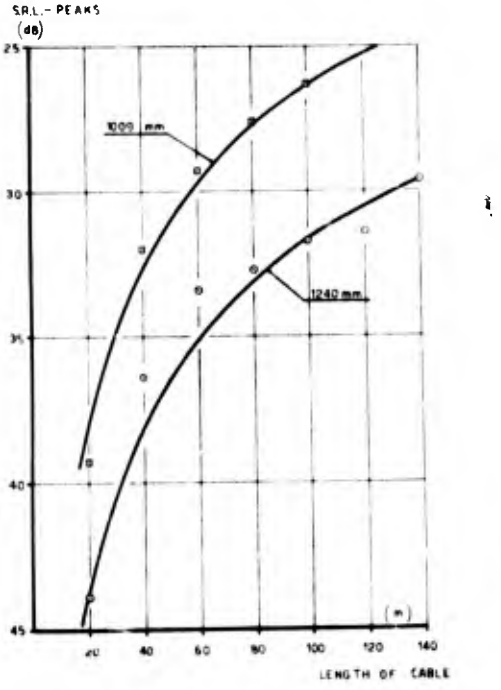

Fig. 11 Variation of the magnitude of the fundamental SRL peak with cable length.

Measurements of the SRL on 8 tube cables manufactured with and without fillers lead to results (average SRL peaks) which confirm the improvement possible with long lays, Figure 12. The improvement in the fundamental is less marked when fillers are used, which is possibly because of the improved quality achieved. Since the SRL peaks generated at the harmonic frequencies will depend only on the percentage of deformed tube in each period between irregularities and the magnitude of these irregularities, they will not alter with a change of stranding lay. The results confirm the theory that the lengthening lay effects the distance between deformations but does not reduce their magnitudes.

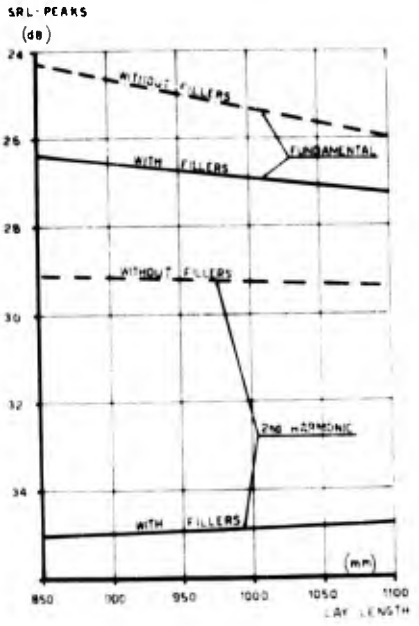

Fig. 12 Schematic of the effect of fillers on the SRL peaks of 8 tube cable for different stranding lays.

Trials with the use of a continuously variable stranding lay have shown the possibility of reducing large SRL peaks associated with the stranding lay. The cable was laid up with a range of lay determined by a choice of gears. The variations were obtained by means of a PIV box driven from a reduction motor. In one experiment a triangular variation to alter the lay between 880mm and 1100mm in a period of 50m was adopted. The results are given in Figure 13.

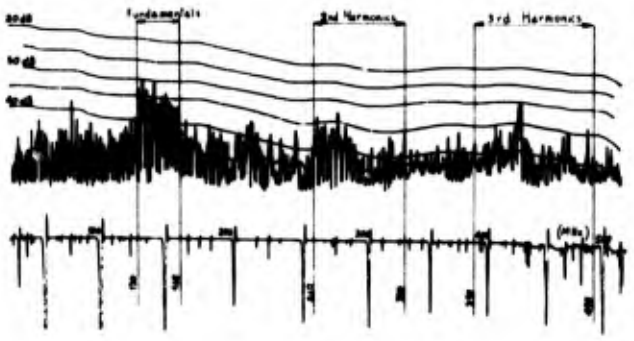

Fig. 13 SRL trace of a continuously variable lay.

The trial was carried out with 8 tube cable. The results obtained although numerically limited are sufficient to indicate the fundamental characteristic of the variable stranding lay. The SRL peaks are distributed in a relatively uniform manner in the intervals determined by the fundamental frequencies corresponding to the extreme values of lay. Although the continuously variable stranding lay reduces the magnitude of the SRL peaks it does not reduce the amount of energy being reflected. Hence with such a technique the power in band requirements of the BPO

are unlikely to be achieved. To overcome the difficulty a change of lay by discrete steps has been tried.

Stranding commences with the longest lay possible until the fundamental SRL peak reaches an arbitrary value for the length of cable involved. The lay is then reduced by an amount that will ensure that the new fundamental peak does not overlap the tail of the first. The process is repeated once or twice more until half the desired length of cable is stranded. Then the second half of the cable is stranded as a mirror image of the first.

The SRL traces of three and four lay designs for 750m lengths of 4 tube cable are shown in Figure 14a and 14b. In the latter case the mean power in band is displayed which is shown to fall well within the requirements of the British Post Office.

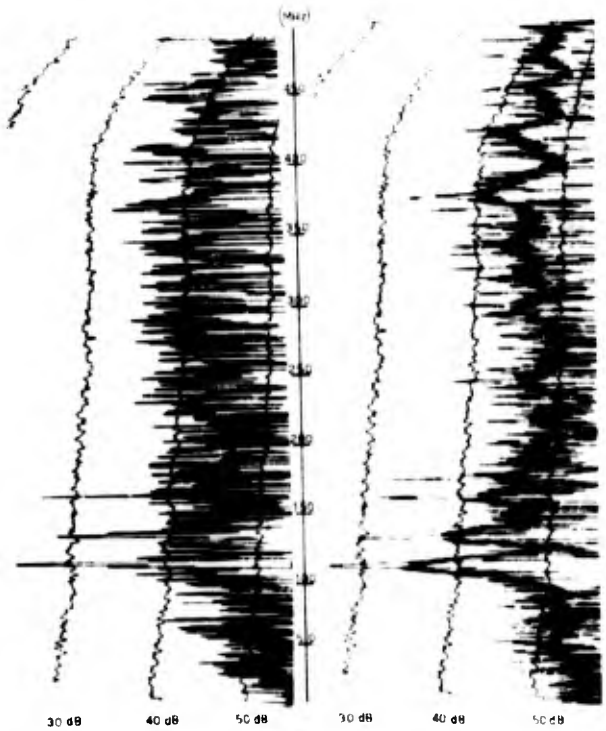

Fig. 14a

Fig. 14b

Fig. 14 SRL traces of a change of lay be discrete steps.

CONCLUSIONS

The paper has shown the important causes of SRL peaks in the manufacture of disc insulated coaxial pairs particularly in two layer constructions. The problem should be tackled in three phases, cable design, tube manufacture and stranding of the cable.

The cables should be designed to have minimum pressure between the tubes by building up the belt between layers and by the use of interstitial fillers. In addition the softest possible belts should be used over the laid up tubes by making extensive use of crepe paper applied with a low tension.

In tube manufacture, the quality of the copper tape plays the major role in the generation of SRL peaks.

Peaks through other causes can be controlled by good maintenance of the machinery. The principle causes of SRL peaks at the stranding stage arise by the deformation of the tubes in the strander closing die, from the pressure exerted by the caterpillar or capstan and from the size of the barrel of the take up drum.

Trials with the use of a continuously variable lay have shown the possibility of reducing large SRL peaks associated with the stranding lay. In order to also improve the returned power characteristic a change of lay by discrete steps has been tried.

The analytical work described above has only been possible by the quick and accurate assessment of SRL peaks uncluttered by mismatches from cable terminations or test leads. This has been possible by the use of the c.w. burst and power in band techniques evolved.

REFERENCES

1. E. Baguley and F. B. Cope: "A Pulse Echo Test Set for the Quality Control and Maintenance of Impedance Uniformity of Coaxial Cables". British Post Office Electrical Engineers Journal, Vol. 44, Part 4, January 1952.

2. J.A. Olszewski and H. Lubars: "Structural Return Loss Phenomenon in Coaxial Cables". Proceedings of the IEEE, Vol. 58, No. 7, July 1970.

3. G. Rosman: "Assessment of Coaxial Cable for Frequency-Division-Multiplex Transmission by Means of a C.W. Burst Test Signal". Proceedings of the IEE, Vol. 117, No. 1, January 1970.

4. British Post Office Specification CW 217A for Cable Coaxial 2.6/9.5F (4, 6, 8 and 18 pairs).

J. R. Osterfield
Pirelli General
Southampton, England.

J. Richard Osterfield born in 1931 has a general science degree and a master's degree in mathematics achieved at the University of London. He is a member of the IEE. He joined the GEC Research Laboratories in 1955 to work on telephone cable problems and transferred to Pirelli General in 1960. He is manager of the Telephone Cables Research and Development Department.

S. Longoni
Industrie Pirelli S. p. A.
Milan, Italy.

Sergio Longoni born in 1927 has a master's degree in electrical engineering achieved at the University of Milan, Italy. He has been with Pirelli since 1951 and presently is the manager of the Telephone Cables Research and Development Department.

A. Manilii
Industrie Pirelli S. p. A.
Milan, Italy.

Aldo Manilii born in 1931 has a master's degree in electrical engineering achieved at the University of Rome, Italy. He has been with Pirelli since 1959 and presently is the manager of the Telephone Coaxial Cable Research and Development Laboratory.

MICROCOAXIAL CABLES IN THE PCM MEDIUM BIT RATE ITALIAN TELECOMMUNICATION NETWORK AND THEIR DEVELOPMENT

P. Calzolari
A. Manilii
Industrie Pirelli S.p.A., Milan, Italy

G. Paladin
F. Scrofani
S.I.P. - Società Italiana Per l'Esercizio Telefonico p.A., Rome, Italy

Summary

After a brief historical introduction on the development of the microcoaxial cable, the present situation of the Italian digital network, in which this type of cable is widely used, is described.
A cost comparison between PCM systems at 120 and 480 channels (8 and 34 Mbit/s) on microcoaxial cable and FDM systems at 960 and 2700 channels on 1.2/4.4 mm coaxial cable (4 and 12 MHz) is given.
Future developments in the use of the microcoaxial cable both in the analogue and digital transmission are examined, making reference in particular to television and video-telephone signals.
The paper describes the constructional and electrical characteristics of the present microcoaxial cables, their manufacturing lines and the cable links reliability.

1. History

A cable particularly suitable for digital medium bit rate transmission in the trunk network was studied in 1967.
The problem was approached at first by considering two possible alternative:

a) a cable made up of two or more quad units for each transmission direction, each properly screened to obtain the same transmission characteristics given by independent quad local cables;

b) a cable with microcoaxial pairs that from a manufacturing point of view would be less expensive than the conventional coaxial pairs currently used in FDM transmission over long distances.

Solution a) was discarded after preliminary tests showed that it would not be possible to manufacture such cables with the same type of quads and units used in the manufacture of standardised local cables.

A small diameter coaxial pair (0.65/2.6 mm) insulated with cellular polyethylene was then designed, initially without outer steel screen. The outer steel screen would not be necessary if the digital transmission has a bit rate higher than the value at which the near-end cross-talk noise is of the same level as the thermal noise ('critical' frequency of about 6 to 7 Mbit/s).

In the same year the fundamental parameters of an integrated digital transmission system using microcoaxial cables were defined with a bit rate of about 8 Mbit/s and a repeater spacing of 4 km.[1] Afterwards the feasibility of digital transmission at 34 Mbit/s, with a repeater spacing of 2 km, was examined.
However, at a later date, it was decided to adopt a conventional construction with outer steel screen in order to obtain a cable which is not only better for medium bit rate digital transmission, but also suitable for analogue transmissions of different kinds.[2]
The present dimensions of the microcoaxial pair are 0.7/2.9 mm.

2. Microcoaxial Cable Network Development

As already stated, the microcoaxial cable was designed as a carrier for digital systems at 8 Mbit/s (120 channels) and at 34 Mbit/s (480 channels). It was also planned for use in FDM transmission at 900 channels to meet some specific requirements of the Italian telephone network, e.g. supergroup transmission, connections between exchanges and radio-relay links located some miles away, etc.
The results of a cost comparison between PCM systems on microcoaxial cable (120 and 480 channels) and conventional FDM systems on 1.2/4.4 mm coaxial cable (960 and 2700 channels), as a function of the link length and the number of circuits forecast for the next twenty years, are shown in Fig. 1.

The costs included the installed cable, its accessories and the line and terminal equipment. Some degree of approximation had of course to be accepted when evaluating the 480 channel systems, which are just now in a trial phase (a 480 channel connection approximately 20 km long was installed in the Milan area in early 1974), but the actual costs of the above systems will not affect, in our opinion, the results of the comparison.

The area under curve A represents the range of optimum use for PCM 120 channel systems.
Conventional low frequency or high frequency systems, mainly with 12 channels, on symmetric pair cables (e.g. 0.9 mm DM cables) were used for such links in the past. The area bordered by curve B represents the range of optimum use for PCM 480 channel systems, while the area bordered by curve C represents the optimum range for FDM systems with 960 channels on 1.2/4.4 mm coaxial cables. The upper side of the diagram refers to 2700 channel systems on 1.2/4.4 mm coaxial cables. It has been forecast that the medium distance link of the Italian trunk network (with a length of approx. 15 to 100 km) should not exceed in 20 years a maximum number of approx. 10 000 circuits.
The links therefore fall within the optimum areas of PCM systems bordered by curves A and B.
The above conclusions could be subject to some slight modifications when the PCM systems with 1920 channels (140 Mbit/s), on 1.2/4.4 mm coaxial cable, now still in a trial phase, are operating.
Up to 1974, S.I.P. (the Italian Telephone Operating Company) installed a total amount of approx. 70 000 km of coaxial pairs.

3. Characteristics of the Link

The problem of the link reliability received a great deal of attention, due to the high number of circuits that can be carried on microcoaxial cable systems (a 48 microcoaxial pair cable equipped with 480 channel systems carries 11 520 circuits).
In order to improve reliability many protective measures were studied and implemented, the most important being:

a) cable laying at a 70 cm depth in a cement trough;

b) almost in all links, an aluminium sheath was adopted. This, besides improving the cable mechanical strength, provides an effective protection against damages caused by induced overvoltages;

c) a 4 mm thick polyethylene overall jacket which greatly improves the cable dielectric strength;

d) a galvanized steel shielding wire laid approx. 25 cm over the cable in order to obtain a remarkable reduction in the voltage break-down stress due to lightnings;[3]

e) pressurisation of all links using continuous flow gas pressure systems with pressure alarm gauges along the cable route; this allows immediate detection of pressure losses which are signalled to the manned terminals.

All links are designed for their maximum capacity, i.e. with repeater spacings of 2 km for 34 Mbit/s systems. Metallic housings were installed where the line equipments will be located. It is worthwhile pointing out that also 900 channel FDM systems have repeater spacings of 2 km.
Splicing methods are, generally speaking, conventional.
Statistical pulse echo measurements, carried out on all links, did not reveal impedance reflections exceeding the values to be expected for random allocation of the cable lengths.
A higher tolerance of the impedance range, in relation to the one required by the 1.2/4.4 mm coaxial cable links, used for analogue system transmission, allows remarkable savings in splicing costs.
An approximate comparison of splicing costs between 1.2/4.4 mm and 0.7/2.9 mm coaxial cables is shown in Fig. 2.
Microcoaxial cables splicing costs are approx. 50% lower than those of 1.2/4.4 mm coaxial cables with the same number of coaxial pairs.
This investigation covered only links with lengths in the range of 40 to 120 km.

4. Considerations on the Electrical Characteristics of Digital Network

The multiplexing hierarchy that was studied for digital transmission was not only suitable for the characteristics of the microcoaxial cables, but also for those of digital radio links at 13 GHz.[4]
This hierarchy (see Fig. 3) was standardised in Europe by CEPT (Conférence Européenne Des Administrations Des Postes Et Télécommunications).
The transmission at 8,448 Mbit/s takes place with a ternary code type 1B/1T (each binary pulse is converted into a ternary pulse).
The transmission at 34,469 Mbit/s is carried out using a ternary line code type 4B/3T (4 binary pulses are converted into 3 ternary pulses). The line bit rate is then $3/4(34{,}368) = 25{,}776$ Mpulses/s.

As far as the regenerators are concerned, an automatic gain control is provided in order to obtain regenerative sections having attenuation values which fall within a fixed interval, with adequate margins of safety.
The values of the line attenuation limit at the Nyquist frequency f_o (half the frequency of the pulses) are found with the following equations:

$$(\alpha + \Delta\alpha)\sqrt{f_o}\,(h + \Delta_1 h) = A_{max}\ \text{dB}$$

$$(\alpha - \Delta\alpha)\sqrt{f_o}\,(h - \Delta_2 h) = A_{min}\ \text{dB}$$

where:

α = 8.9 dB is the cable attenuation at the frequency of 1 MHz, for 1 km length and at the temperature of 10°C;

$\Delta\alpha$ = 0.7 dB is the variation range of α, i.e.: 0.4 dB for the cable differences and 0.3 dB for thermal variations within 10 ± 15°C;

f_o = 4,224 MHz for 8,448 Mbit/s;

f_o = 12,888 MHz for 34,368 Mbit/s;

h = 4 km for intermediate sections at 8,448 Mbit/s;

h = 2 km for terminal sections at 8,448 Mbit/s and all regenerative sections at 34,368 Mbit/s;

$\Delta_1 h$ = + 0.1 km
$\Delta_2 h$ = - 1.0 km
} are the tolerances for the actual length of the regenerative sections compared with the nominal one

On the basis of the above data, the regenerators must operate within the following attenuation ranges:

- intermediate regenerators for 8,448 Mbit/s: 50.6 to 80.9 dB at 4,224 MHz
- terminating regenerators for 8,448 Mbit/s: 16.8 to 41.4 dB at 4,224 MHz
- regenerators for 34,368 Mbit/s: 29.4 to 72.4 dB at 12,888 MHz

5. Improvements in the Cable Characteristics

The characteristics of today's microcoaxial pairs are the result of a thorough investigation carried out on the first cables manufactured.
In fact the coaxial pairs are subjected to torsional stresses both during manufacture and subsequent stranding. Such strains could cause a rapid decay in their cross-talk performance, mainly at high frequency.
An experimental and theoretical study on this phenomenon was carried out and several measures to improve the pair were suggested, among which the most significant were the lapping of two paper tapes in opposite directions on the coaxial pair and the reversal of the edges of the iron and copper tape overlappings.

6. Description of the Standardised Cables

a) 0.7/2.9 mm Microcoaxial Pair

The microcoaxial pair manufactured at present consists of a central copper conductor 0.7 mm in diameter, insulated with cellular polyethylene. The diameter over the insulation is approx. 2.9 mm. Besides the circular one, other forms of insulation could be used, for instance a shaped cross section.
The outer conductor is a copper tape 0.1 mm thick, applied longitudinally with an overlapping covered by a longitudinal screen (a steel tape 0.1 mm thick). The pairs are manufactured in such a way that the edges of the copper and steel tapes are always far from each other and their overlappings are in opposite directions. Two paper tapes with opposite lay are applied overall, thus increasing the mechanical strength and, at the same time, providing insulation between the coaxial pairs.
The finished pair, very strong and compact, has an outer diameter of approx. 4 mm. This diameter is respectively 2/3 and 1/3 of outer dimensions of the pairs standardised by C.C.I.T.T. (1.2/4.4 mm and 2.6/9.5 mm). The reduced dimensions and the much simpler manufacturing process described later, lower the cable costs and, as a consequence, the cost of the system.

b) Cable Constructions

Coaxial cables covered by the Italian Standards may have 12, 24, 36 or 48 pair configuration, the pairs being stranded in concentric layers together with a number of 0.6 mm polyethylene insulated quads for control and supervisory services.
A 0.6 mm pair with perforated insulation is always provided (the holes are suitably spaced along the insulation) in order to make the fault localization easier in case of water penetration, even in absence of pressurisation and to achieve a greater reliability in promptness of the warning.
The standardised constructions are given in Table 1.
Standard lengths are 500 m long, a sub-multiple of the regeneration section of 4 km (8 Mbit system) or 2 km (34 Mbit system).

Table 1

Standardised constructions and approx. diameters over the concentric laying-up, before lapping, of coaxial pair cables

Number of coaxial pairs	Constructions				ø
	Centre	1st Layer	2nd Layer	3rd Layer	approx. mm
12	4Q+1QA	12T			21
24	4Q+1QA	10T	14T		26.5
36	3Q	1Q+1QA+6T	14T	16T	32
48	6Q+1QA	10T	16T	22T	34.5

where: T = 0.7/2.9 mm coaxial pair
Q = 0.6 mm service PE insulated quad
QA = 0.6 mm alarm PE insulated quad, one pair having perforated insulation

As can be seen from the table, standardised cables, consisting of up to 48 pairs with concentric configuration, have been manufactured up to now. This type of construction easily covers the present traffic demand as well as future forecasts for the medium distance Italian network in which the microcoaxial cable is used; however, the concentric cables with more coaxial pairs (e.g. 60 coaxial pairs) could be manufactured when stranding machines with this capacity are available (the stranding operation can be carried out also in more than one single pass).
For the types of cables now used, the concentric construction is economically more advantageous than assembling a number of microcoaxial units (e.g. 6 or 12 for each unit).
If larger distribution cables are required, i.e. above 100 pairs, for ease of handling and flexibility as well as the reliability of the cable in operation the unit type construction could be more advisable.

No remarkable differences in the electrical characteristics have been noted between the unit or the concentric cables (i.e. a cable with 48 coaxial pairs made of 8 groups each consistuted by 6 coaxial pairs or several concentric layers).

Since the dimensions of the coaxial pair are very similar to those of a 0.9 mm quad or multiple twin both having, for instance, a mutual capacitance of 38.5 nF/km, it is possible to substitute some of these elements with microcoaxial pairs without changing the basic construction of the original symmetric circuit cable.
For manufacturing reasons, if cables of this type are to be designed, it is advisable to position the coaxial pairs around the centre.

c) Core belt, sheath and outer coverings of the cable

The stranded pairs are lapped with paper tapes in order to achieve a dielectric strength of the cable higher than 3000 V D.C. (or 2000 V A.C.) and a reliable protection against damages that might occurr during manufacture (i.e. extrusion of the aluminium sheath) or during splicing operations.

The belt usually consists of flat and creped paper. Metallized and semiconductive paper tapes are added for aluminium sheathed cables.

Coaxial cables are aluminium or lead alloy sheathed since, due to the importance of the links, direct burial or duct laying is preferred. The metallic sheath is applied tightly on the core belt in order to prevent movements between core and sheath during the cable life.

The choice between aluminium or lead depends on the characteristics of the two metals; the aluminium sheath is preferred where severe vibration damage is feared (laying along highways where bridges and walls are frequent), and where there is the need for a reliable protection against lightnings or damage due to induced voltages caused by power lines.
The lead alloy (Pb-Sb or Pb-Sn-Cd) is used mainly under standard laying conditions, for example along streets with normal traffic or in ducts in town areas. In this case the lead sheath is also preferred for easy handling.

The metallic sheath is covered with a polyethylene jacket having a high resistance to stress cracking, thus ensuring protection against corrosion. The jacket is suitably thick in order to provide a high dielectric strength, since in Italy there is widespread danger of lightning damage.
Aluminium sheathed cables may be steel armoured for additional mechanical protection, but this is done mainly to improve the screening factor. This armour, made of bituminized steel tapes, is covered by a suitably treated jute serving (e.g. treated with pentachlorofenillaurate) or by an overall polyethylene jacket.

Table 2 gives the standardised coverings, together with the approximate diameters for each type of construction. It should be noted that four types of outer coverings are provided for each construction and that for aluminium sheathed cables the manufacturing characteristics and the dimensions up to the first polyethylene jacket are the same.

Table 2

Standard coverings

Protection Composition	Approximate outer diameters mm			
Designation	12 coaxial pairs	24 coaxial pairs	36 coaxial pairs	48 coaxial pairs
AE	36	42	48	50.5*
AENJ	45.5	51	58.5	61
AENE	47	52.5	60	63
L_2E	36	42	48	50.5*

* see Fig. 5

where:

A = aluminium sheath

E = polyethylene jacket

N = steel tape armour

J = treated jute serving

L_2 = lead alloy sheath

d) Electrical Characteristics

During the entire manufacturing process electrical and physical controls are carried out on the coaxial pairs using statistical sampling methods.
Thanks to the intrinsically good characteristics of the coaxial pair, a manufacturing process under normal control ensures finished cables of good quality; specifically uniformity of the impedance and low levels of cross-talk between pairs are achieved without difficulty.

The electrical characteristics specified for the coaxial cable are given in Table 4; the typical values measured on finished cables are given later as follows:

- Distribution of pulse-echo impedance (see Fig. 5)
- Distribution of 'corrected values' of pulse-echo attenuation (see Fig. 6)
- Cross-talk (see Figures 7, 8 and 9)
- Attenuation at 1 MHz (see Table 3)
- Capacitance at 800 Hz (see Table 3)
- Characteristic impedance versus frequency (see Fig. 10).

Table 3

Attenuation at 1 MHz and 10°C dB/km		Capacitance at 800 Hz nF/km
8.97	minimum	55.2
9.02	average	55.5
9.06	maximum	55.8

Table 4

Coaxial Cable Electrical Characteristics

- Ohmic resistance at 20°C			maximum value
inner conductor		ohm/km	49
outer conductor		ohm/km	17
- D.C. insulation resistance			minimum value
		MΩ·km	10 000
- D.C. dielectric strength			minimum value
between conductors		V	1 500
between conductors and earthed metallic sheath		V	3 000
- Corrected attenuation of sine-squared pulse echos having half amplitude duration of 50 ns			minimum value
- 100% measurements		dB	38
- 50% measurements		dB	46
- Pulse-echo impedance measured with sine-squared pulses having half amplitude duration of 50 ns			
- 100% measurements		ohm	75 ± 2.5
- 90% measurements		ohm	75 ± 2
- Attenuation at 1 MHz at 10°C (measured on a 2 km length)		dB	8.9 ± 0.4
- Cross-talk (measured on a 2 km length)	at 60 kHz		0.5 to 20 MHz
minimum N.E.X.T. attenuation	dB	80	135
minimum equal level F.E.X.T. attenuation	dB	70	95

In order to obtain approval for use in many situations and operating conditions, other important electrical characteristics were considered and measurements were extended beyond the frequency range now used for the cable, for example :

- Attenuation up to 200 MHz (see Fig. 11);
- Phase velocity and delay up to 200 MHz (see Fig. 12);
- Structure return loss up to 60 MHz (see Fig. 13);
- Corona discharge level at 50 Hz: higher than 1000 V;
- Impulse strength with 10/800 amplitude waveform: higher than 5 kV.

A correlation was found between impulse tests and D.C. breakdown tests carried out with a rapid increase in voltage. The breakdown voltage is affected by the degree of expansion of the insulation and by the regularity of the insulation process.

- Screening factor at 50 Hz for aluminium sheathed cables: see Table 5.

Table 5

Intrinsic Screening Factor (K)

(reference to the cables of Table 2)

Longitudinally induced voltage (50 Hz) V/km	Type of cable								
	Number of coax. pairs	12		24		36		48	
	covering type	AE	AENJ AENE	AE	AENJ AENE	AE	AENJ AENE	AE	AENJ AENE
50	K (screening factor : calculated values)	0.4	0.12	0.35	0.10	0.3	0.07	0.25	0.06
100		0.4	0.09	0.35	0.08	0.3	0.06	0.25	0.05
250		0.4	0.08	0.35	0.07	0.3	0.05	0.25	0.04
500		0.4	0.21	0.35	0.19	0.3	0.08	0.25	0.06
1000		0.4	0.25	0.35	0.22	0.3	0.15	0.25	0.13

e) Manufacturing process

The cable is manufactured on a cellular polyethylene insulating line, a coaxial pair forming line, a stranding machine and conventional machinery for the application of the outer protective coverings.
The extruding line, see Fig. 15, does not differ substantially from the ones used for cellular polyethylene insulation of other high quality telephone cables. It should be noted that considerable improvements were and are still being made in the extrusion technique of expanded materials both for small cores (e.g. microcoaxial pairs) and for large cores (e.g. for CATV cables). As far as the insulation is concerned, besides cellular polyethylene, polypropylene copolymers and other expandable polymers could be used.

The modern extrusion lines now available can manufacture cores with remarkable dimensional and structural uniformity at high speed, with higher output and lower scrap rates.
The microcoaxial pair is currently manufactured at speeds between 200 and 250 m/min on an extruder with a 60 mm screw (2½ inches).
The extrusion line is equipped with a series of automatic controls to ensure good quality of the extrusion and uniformity of the insulation capacitance.
Uniform pay-off and heating of the central conductor and coiling of the insulated conductor on to the take-up reel must be provided.
Automatic setting and monitoring devices checking the main characteristics of the line allow the process to function reliably for an extended period of time.

Once the insulated central conductor is made, the manufacturing process consists of lines equipped with forming tools for the copper outer conductor and the steel shield tape and with heads for the application of the binding paper tapes.

Other materials could also be employed for the outer coverings, substituting paper, with the purpose of improving the bonding capacity and the pair strength.

Fig. 14 shows a vertical forming machine oper-

ating at a speed of 15 m/min.
The mechanical characteristics of these machines influence the electrical performance of the cable, during the pair formation, and for that the forming process must be properly controlled.

The stranding machine used has 60 floating cradles.
These machines are conventional in construction but need some arrangements so as to match the mechanical characteristics of the coaxial pair, which are different from those of other telephone elements such as pairs, quads or unit quads (see Fig. 16).

The machinery for the application of the metallic sheaths and the outer covering is conventional.

7. Future Developments

New developments in microcoaxial cable system technology are mainly directed towards its use for television and video-telephone transmission. For this application the transmission could be in analogue form in local networks and in digital form in trunk links.
A research study is now in progress on analogue -digital converters with redundancy reduction for video-signals.
The purpose of this study is the possibility of converting: 1) a video-telephone signal (with 313 lines and at approx. 1 MHz band) into a digital signal at approx. 2 Mbit/s; 2) a television signal (with 625 lines and at approx. 5 MHz band) into a digital signal at approx. 34 Mbit/s.
It would then be possible to transmit 16 video -telephone signals or 1 television signal over a microcoaxial pair.
The problems to be solved in the transmission of digital video signals are mainly related to the development of a satisfactory coding system.
As far as the analogue transmission of a number of video-telephone signals on microcoaxial pairs is concerned, it will be necessary to develop wide band amplifiers and FDM multiplex equipment (see Table 6).

Table 6

signals	transmitted band (approx. values) MHz	repeater spacing km	repeater maximum gain dB
1 TV (FDM)	3 to 10	2	60
1 VT (FDM)	0.6 to 2	4	53
4 VT (FDM)	2 to 10	2	60

The simplicity of video signal transmission in analogue rather than digital form is counterbalanced by the signal to noise ratio which decreases with the increase of the connection length. The length of analogue transmission links is therefore limited.
For television signals this length is approx. 24 km with a signal to noise ratio of 55 dB.

8. Conclusions

The microcoaxial cable, at first designed specifically to match the requirements of medium bit rate digital transmission, was later modified to make it suitable for a wider range of applications.
This cable is now under consideration by C.C.I.T.T., together with other standard 1.2/ /4.4 mm and 2.6/9.5 mm coaxial pairs.[5]

Microcoaxial cables are extensively used in Italy for the transmission of digital signals at 8 and 34 Mbit/s in medium distance trunk links. These signals are currently generated by telephone PCM multiplex equipments. The conversion of television and video-telephone signals into digital signals is under study. The microcoaxial cable is going to be also used in digital systems for the interconnection of digital switching exchanges and in analogue systems for video-telephone and television signal transmission.

Acknowledgments

The authors wish to thank the managements of Industrie Pirelli and S.I.P. for the opportunity to perform this work and permission to publish the present paper.

References

1. G. Paladin: "Nuovi portanti fisici per la trasmissione di segnali PCM a media velocità". XV Convegno Internazionale delle Comunicazioni, Genoa , October 12-15, 1967.

2. S. Longoni, P. Calzolari, A. Portinari : "New Italian Types of Cables for PCM and FDM transmission". 19th International Wire and Cable Symposium, Atlantic City, December 3, 1970.

3. G. Luoni, A. Morello, P. Ronzani: "Lightning Protection of Buried Coaxial Cables". 21st International Wire and Cable Symposium, Atlantic City, December 5, 1972.

4. M. Decina: "Planning of a Digital Hierarchy". I.E.E.E. Trans. on Comm., Vol. COM 20, February 1972.

5. C.C.I.T.T. Comm. Sp. D, TD N. 28-4, Geneva, 1-11 April, 1974.

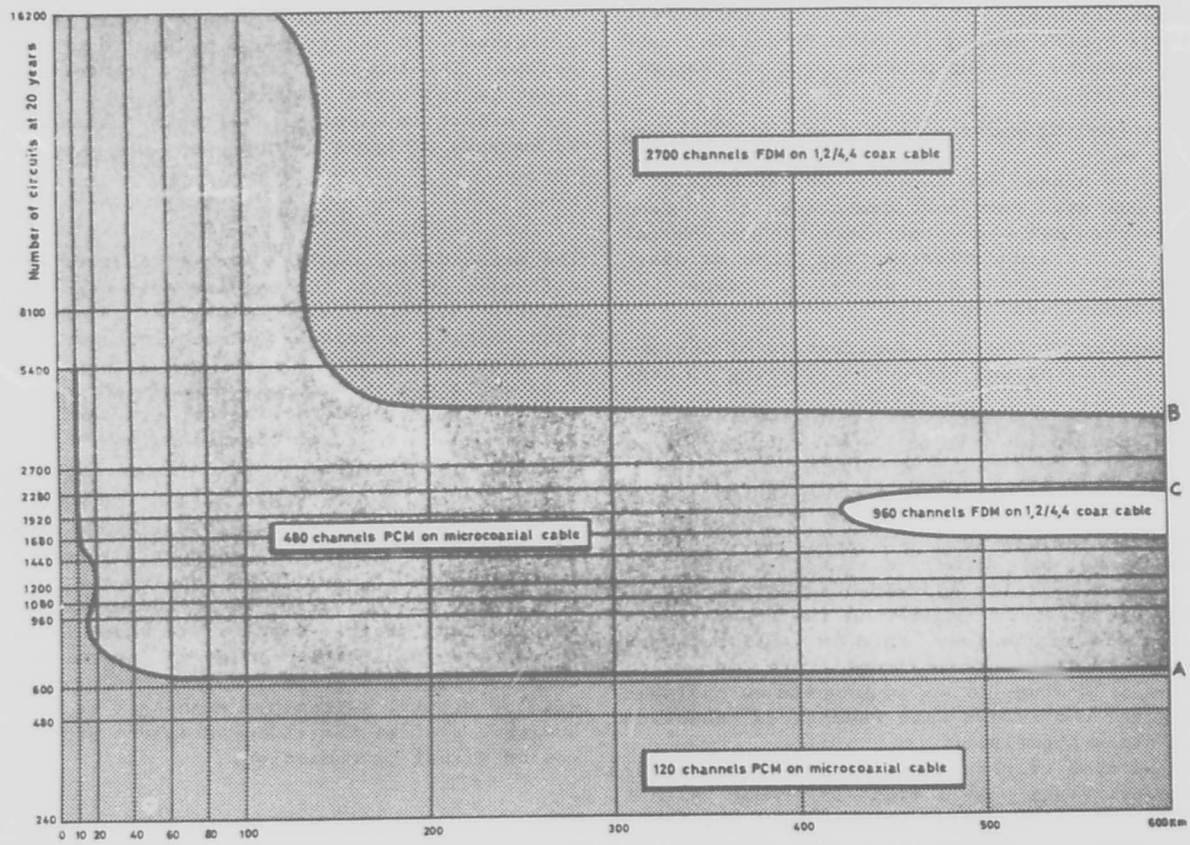

FIG. 1 - Cost comparison between PCM systems on microcoax. cable and conventional FDM systems on 1.2/4.4 mm coax. cable.

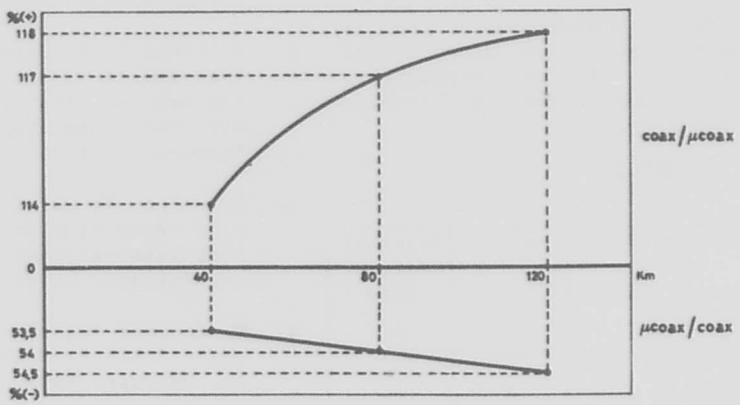

Fig.2 - Reciprocal jointing cost between microcoax and 1,2/4,4 coax

C_1 = SYMMETRIC PAIR CABLES

C_2 = MICROCOAXIAL CABLE WITH REPEATER SPACING OF 4 KM

C_3 = MICROCOAXIAL CABLE WITH REPEATER SPACING OF 2 KM

C_4 = 1.2/4.4 MM COAXIAL CABLE WITH REPEATER SPACING OF 2 KM

R_1 = ON-OFF RADIO LINK AT 13 GHZ

R_2 = RADIO LINK WITH 4-PHASE SHIFT KEYING (4-PSK) AT 13 GHZ

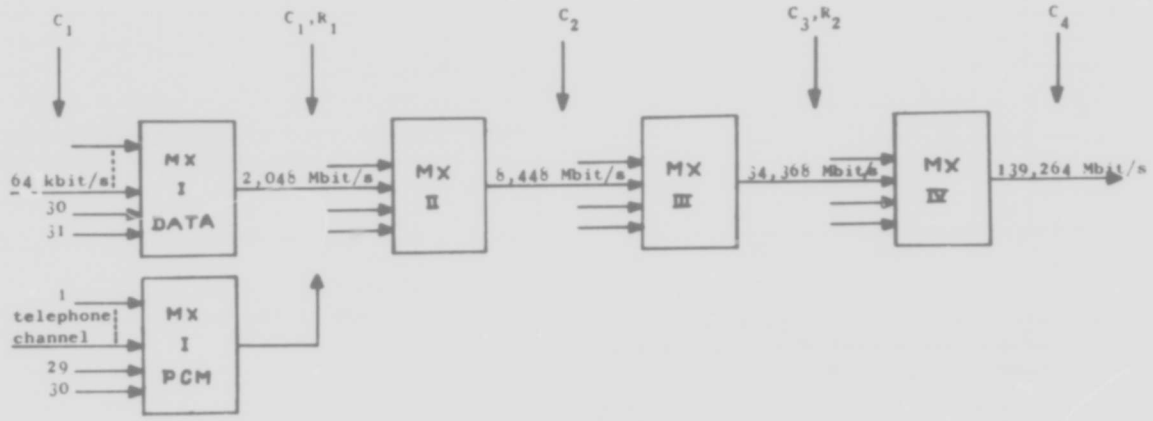

FIG. 3 - Digital multiplexing plane and relevant carrier systems.

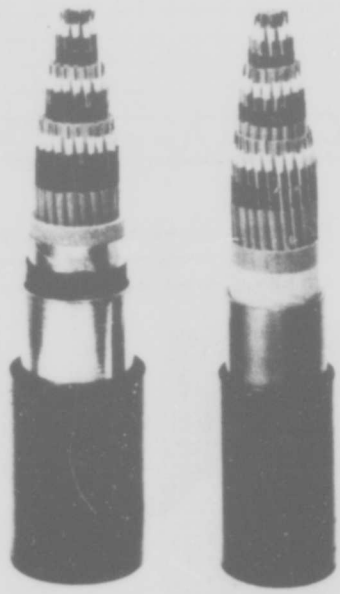

FIG. 4 - Microcoaxial cables, aluminium or lead alloy sheathed (48 coax. pairs).

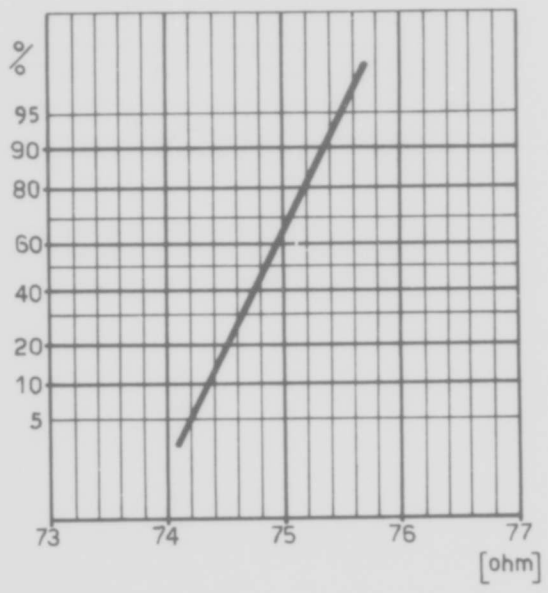

FIG. 5 - Pulse echo impedance distribution (50 ns pulse).

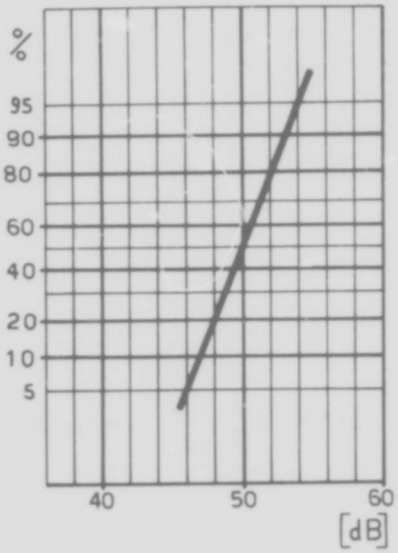

FIG. 6 - Distribution of the pulse echo worst values with distance correction (50 ns pulse).

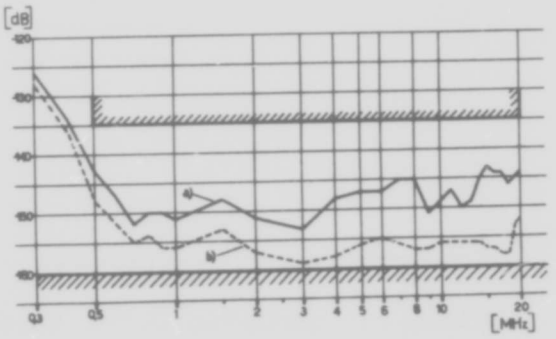

FIG. 7 - Near end cross-talk diagram 0.3 to 20 MHz:
a) 100% of the measurements
b) 90% of the measurements

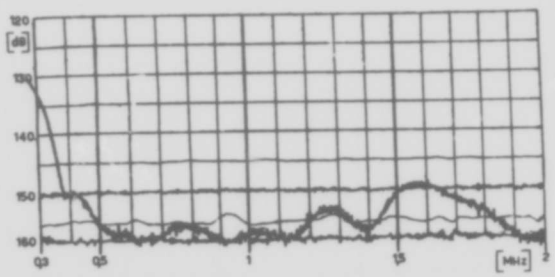

FIG. 8 - Near end cross-talk diagram plotted by swept-frequency equipment up to 2 MHz, between adjacent pairs.

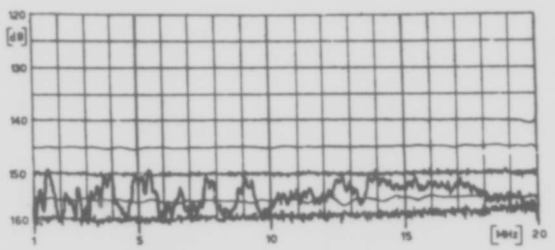

FIG. 9 - Near end cross-talk diagram plotted by swept-frequency equipment up to 20 MHz, between adjacent pairs.

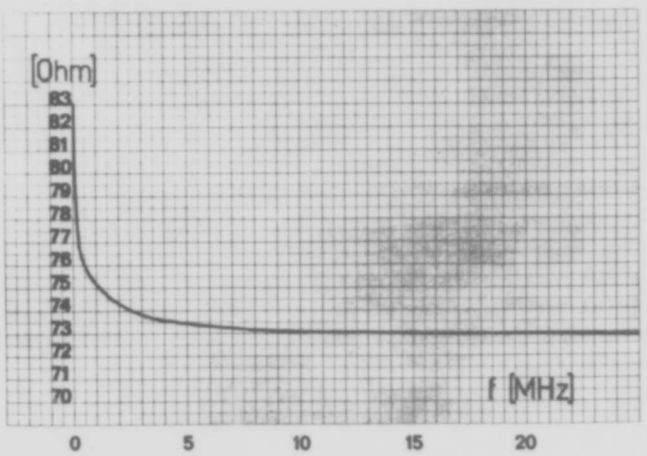

FIG. 10 - Characteristic impedance of 0.7/2.9 mm coax. pair vs. frequency

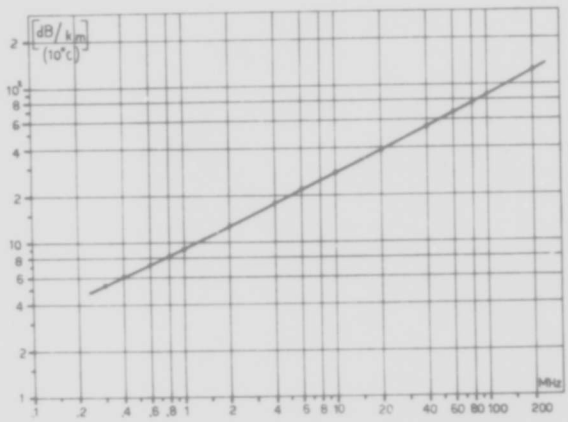

FIG. 11 - Attenuation versus frequency up to 200 MHz (at 10°C).

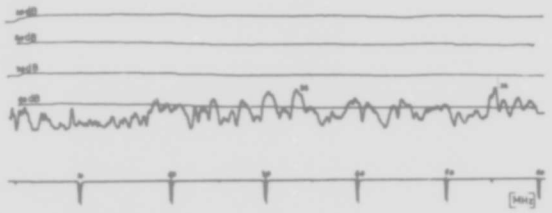

FIG. 13 - Typical structure return loss spikes diagram up to 60 MHz.

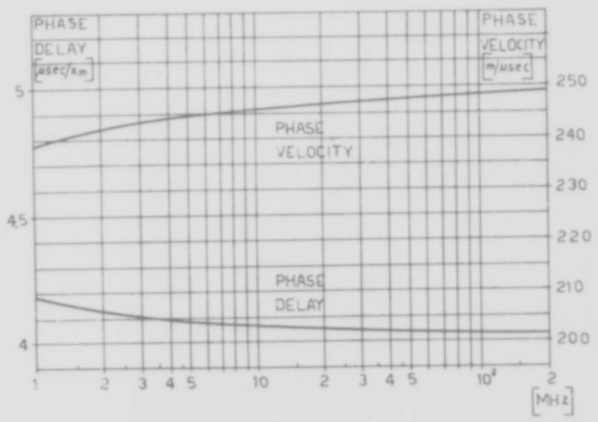

FIG. 12 - Phase velocity and delay versus frequency up to 200 MHz.

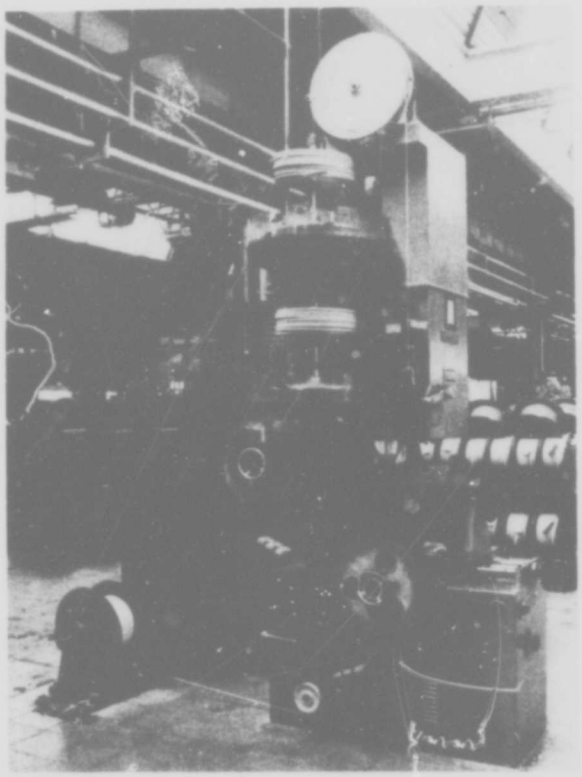

FIG. 14 - Forming vertical machine

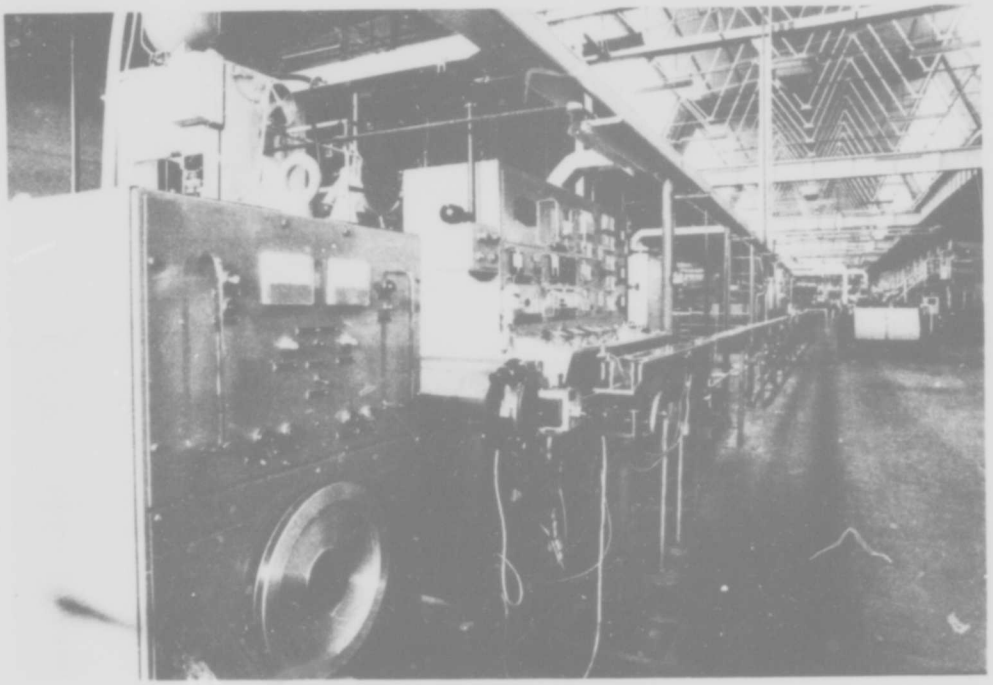

FIG. 15 - Extruding line.

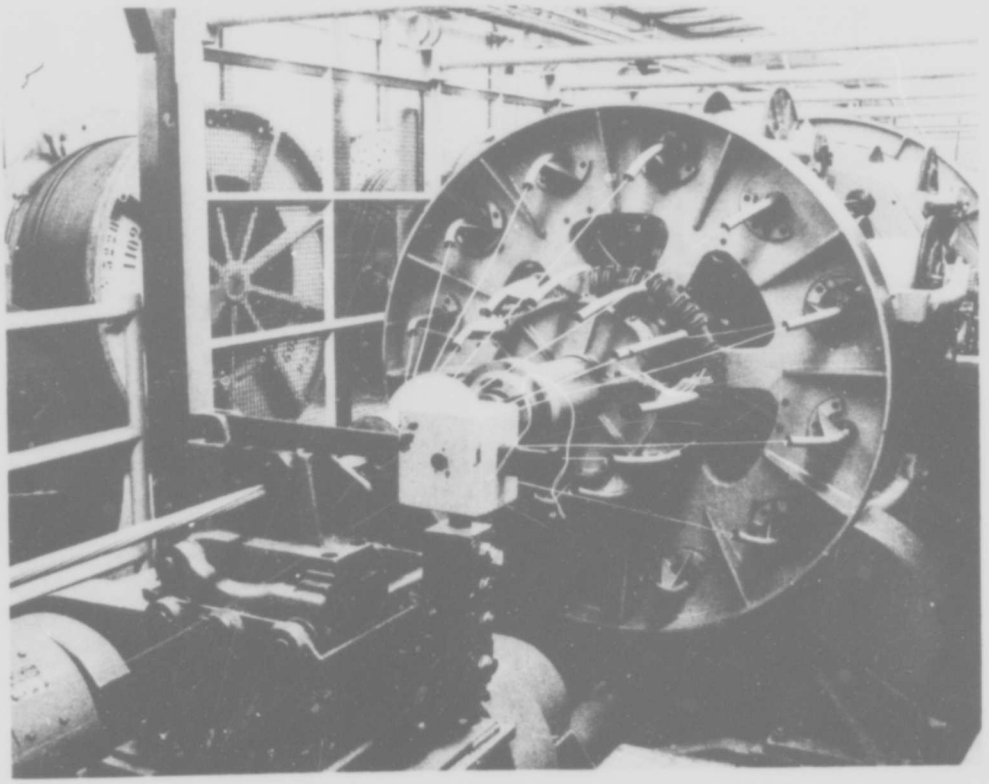

FIG. 16 - Front view of a cage of the stranding machine.

P. Calzolari
Industrie Pirelli S.p.A.
Milan, Italy.

Born in Bologna in 1931, he graduated from the University of Bologna with a B.S. degree in Electrical Engineering in 1955.
He joined Industrie Pirelli in 1956 and has been associated with the manufacture and then the design of telephone cables since that time.
He is now Manager of the Telecommunications Cable Design Department.

G. Paladin
S.I.P. - Società Italiana Per l'Esercizio Telefonico p.A., Rome, Italy.

Doctor's degree in Electrical Engineering and "libera docenza" in electrical communications. In 1949 he joined SIP, the Italian Telephone Operating Company, where is at present engaged in the research and development field.
Since 1970 he is associate professor of digital communications at the University of Naples.

A. Manilii
Industrie Pirelli S.p.A.
Milan, Italy.

Born in Rome in 1931, he has a master's degree in Electrical Engineering achieved at the University of Rome. He has been with Pirelli since 1959 and presently is the Manager of the Coaxial Telephone Cable Research and Development Laboratory.

F. Scrofani
S.I.P. - Società Italiana per L'Esercizio Telefonico p.A., Rome, Italy.

Born in Rome in 1930. Electrical Engineering degree from Rome University.
In S.I.P., the Italian Telephone Operating Company, he is at present engaged in planning development and installation of trunk cable plants and associated equipment.

AN APPROACH TO CROSSTALK COUPLING REDUCTION OF PAIR TYPE CABLE

Masami Yotsuya, Seiki Minematsu, Akira Itoh

Dainichi-Nippon Cables, Ltd. Osaka, Japan

Summary

Design philosophy for twist length selection and pair arrangement within a cable was established, considering the effect of fluctuation in twist length on crosstalk coupling. High frequency signal transmission cables under this new design philosophy are satisfactory insofar as crosstalk coupling is concerned.

1. Introduction

With the recent growing demands for video and data transmission, urgent needs arose for new multipair cables suitable for broad-band signal transmission. To send higher frequency signals over a pair type cable, the reduction of crosstalk between pairs would be a key problem.

The study of crosstalk in communication cables is quite old. Up to now, much has been revealed by much valuable work. Nevertheless, no decisive theory has been reported as yet, which is capable of directly connecting actual crosstalk phenomena in a cable with relevant cable structure. One of the reasons why the phenomena are difficult to interpret lies in the fact that crosstalk is affected by many intricate factors, including cable structural irregularities. Crosstalk is more or less based on statistical quantities, which are distributed along the line length as well as in cross-section of a cable. Therefore, it is especially important to determine actual patterns of these distributions to establish a reasonable connection between crosstalk and cable structure.

Pulse crosstalk measurement is a well known method to visualize crosstalk coupling distribution along the cable length. In developing video transmission twisted pair cables, a new sophisticated system of pulse near-end crosstalk measurements has been built up at Dainichi-Nippon Cables Telecommunication Laboratory. With their aid, crosstalk coupling between pairs has been investigated to establish a new design philosophy and new processing conditions for the cables.

2. Experimental Cables

The experimental cables are composed of twisted pairs of 0.9mm copper conductors insulated with foamed polyethylene. In assembling pairs, units are formed with 7 or 19 pairs, which are cabled together into a cylindrical core. Over each unit, an aluminum shield is provided to prevent interference from circuits in other units. Finally, a laminated aluminum-polyethylene jacket or a corrugated steel sheath with a protective jacket, depending on its application, is covered over the cable core.

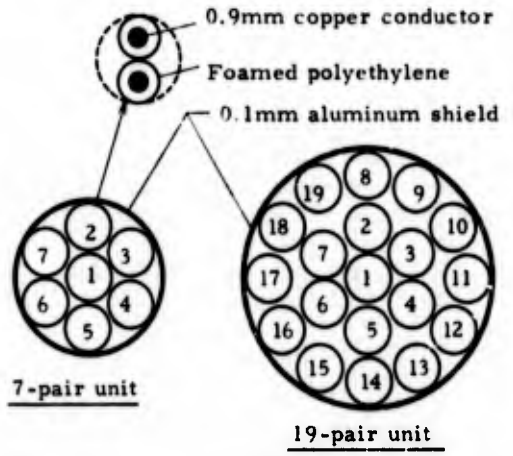

Note : Numerical figures denote pair-numbers

Fig. 1 Unit Construction

Figure 1 illustrates the pair arrangement within the units. These one-pair-center arrangements are expected to relieve somewhat the problem of structural irregularities, thus resulting in better crosstalk characteristics, because they are the most resistive to possible dislocation during cabling process.

Table 1 shows the representative electric characteristics of the cables. The transmission properties versus frequency are also given in Fig. 2. These cables were designed for applications in base-band video communication system of short or medium distances, such as on-premises connection of video equipment or private interoffice trunks over

Table 1 Electrical Properties

Characteristic Impedance	(at 5 MHz)	140 Ω
Mutual Capacity	(at 1 KHz)	33 nF/km
Attenuation	(at 5 MHz)	15dB/km

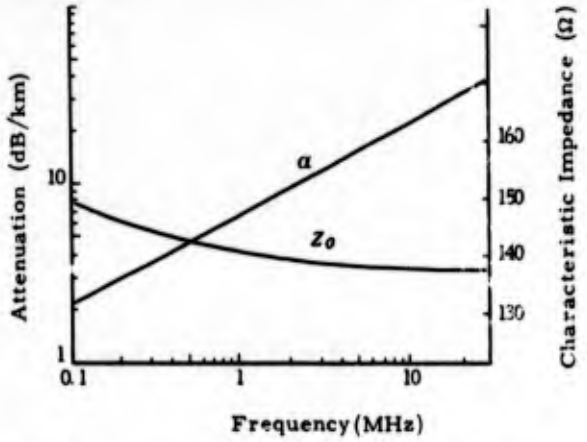

Fig. 2 Transmission properties of test cable

distances of a few kilometers. In practice, no preference is given to use of expensive line repeaters, consequently low attenuation in cable is especially required.

3. Pulse Near-End Crosstalk Measurement

3.1 Principle of the Measurement

As is shown in Fig. 3, when both disturbing and disturbed circuits have the same transmission properties of γ and Z_0, far-end crosstalk X_f and near-end crosstalk X_n are defined by

$$X_f = \frac{V_2(l)}{V_1(l)} = \int_0^l Z_f(x)\,dx \tag{1}$$

$$X_n = \frac{V_2(0)}{V_1(0)} = \int_0^l Z_n(x) e^{-2\gamma x}\,dx \tag{2}$$

where $Z_f(x)$ and $Z_n(x)$ are the quantities called far-end and near-end crosstalk coupling coefficient, respectively. They are given by

$$Z_f(x) = \omega \left| \frac{Z_0}{4} K(x) - \frac{1}{Z_0} M(x) \right| = k(x) - m(x) \tag{3}$$

$$Z_n(x) = \omega \left| \frac{Z_0}{4} K(x) + \frac{1}{Z_0} M(x) \right| = k(x) + m(x) \tag{4}$$

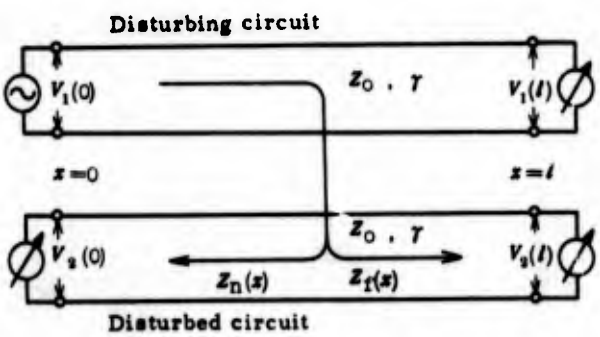

Fig. 3 Near-end and far-end crosstalk coupling

In the above formulas, $K(x)$ is capacitance unbalance, $M(x)$ mutual inductance, $k(x)$ capacitive coupling and $m(x)$ inductive coupling. Each of them shall have a value per unit length at x; and ω is the angular frequency of the applied signal.

When making an analysis on statistical properties of $Z_f(x)$ and $Z_n(x)$, the expected values of $|X_f|^2$ and $|X_n|^2$ can be written in the form [1]

$$\langle |X_f|^2 \rangle = 2\overline{Z_f^2} \int_0^l (l-x)\varphi_f(x)\,dx \tag{5}$$

$$\langle |X_n|^2 \rangle = \overline{Z_n^2}\, \frac{1-e^{-4\alpha l}}{2\alpha} \int_0^\infty \varphi_{n(x)} \cos 2\beta x\,dx \tag{6}$$

where α is attenuation constant, β phase constant, $\varphi_f(x)$ and $\varphi_n(x)$ normalized autocorrelation functions of $Z_f(x)$ and of $Z_n(x)$, respectively. It is shown by Eqs. (5) and (6) that both effective far-end and near-end crosstalk attenuations, which are defined by $(-10 \log \overline{X_f^2})$ for far-end and by $(-10 \log \overline{X_n^2})$ for near-end, can be determined by r.m.s. value of coupling distribution along the length and their normalized autocorrelation functions.

In general, the pulse near-end crosstalk measurement is useful to obtain actual distribution of crosstalk coupling. First, let us assume a lossless cable. When a step pulse with risetime t_r is applied to a disturbing circuit, the wave-form of crosstalk voltage, observed at the near-end terminal of the disturbed circuit, represents crosstalk coupling averaged per resolution length of the applied pulse. Then its normalized autocorrelation function $\Phi(t)$ can be expressed in the approximate form [2]

$$\Phi(t) \fallingdotseq 1 - \frac{t}{l_r} \quad (0 < t < t_r) \tag{7}$$

where t is the time scale for observed wave-form on an oscilloscope.

In the case of actual cables, however, a transmission circuit has an attenuation loss. Thus, an observed wave-form would be somewhat deformed due to the attenuation. The farther a crosstalk point from the near-end, the larger the difference in amplitude between original and observed waves. Therefore, amplitude correction of the observed wave-form must be made, to determine the real crosstalk coupling distribution. This can be accomplished by taking into account risetime of applied pulse and attenuation constant of cable circuits. [2]

3.2 Measurement Method and Results

Figure 4 shows a pulse near-end crosstalk measuring method diagram. During measurement, a step pulse with 15 ns risetime is applied to the disturbing circuit. A crosstalk voltage appears in the disturbed circuit and returns as a wave to the near-end. The wave is received through the sampling convertor into the digital memory, in which the wave form is digitally memorized. The wave can also be monitored by an oscilloscope or

X-Y recorder connected to the output terminals of the digital memory. The digital memory is equipped with a calculating function which can compute, without delay, the r.m.s. value of the coupling distribution as well as its autocorrelation function, using the memorized data.

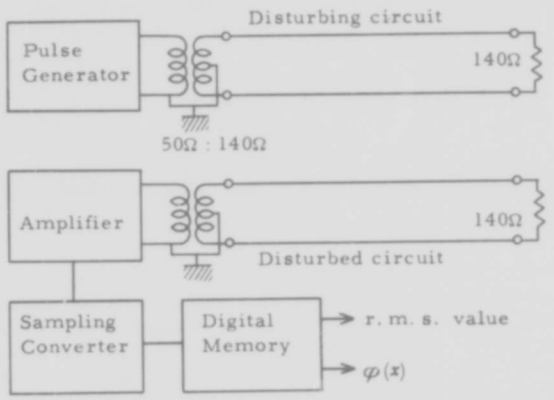

Fig. 4 Circuit for measuring pulse near-end crosstalk

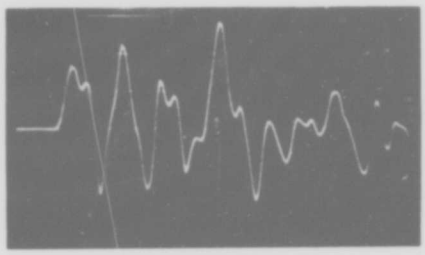

Fig. 5 Typical pulse near-end crosstalk wave-form

Figure 5 shows a typical wave-form example of pulse near-end crosstalk between pairs of properly selected twist lengths. Its normalized autocorrelation function is given in Fig. 6, from which it is seen that approximation of the function can be made by Eq. (7).

The longitudinal variation of r.m.s. values of measured crosstalk couplings along a 500 meter length are plotted in Fig. 7. Each dot represents the r.m.s. value per every 50 meters, being converted in the form

$$Si = 20 \log \frac{ri}{\bar{r}} \qquad (8)$$

where r_i is r.m.s. value at the ith section and $\bar{r}$ average value of all r_i values.

As compared with wide variations, such as 6 to 10 dB, seen in crosstalk attenuations themselves, the longitudinal variations of measured r.m.s. values are very small. In addition to the sampling length of 50 meters, examinations of the effect of sampling section length on variations of

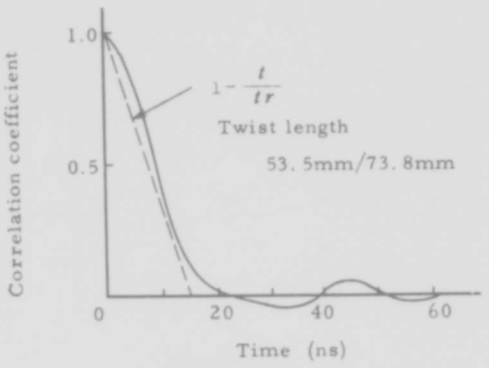

Fig. 6 Typical normalized autocorrelation function for proper twist length

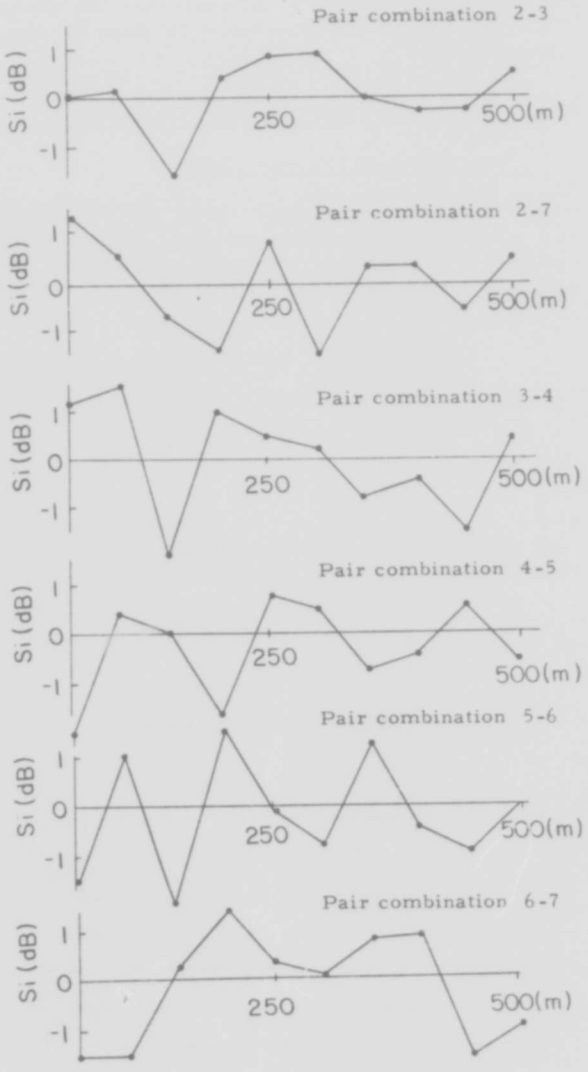

Fig. 7 Longitudinal variation of measured r.m.s. value

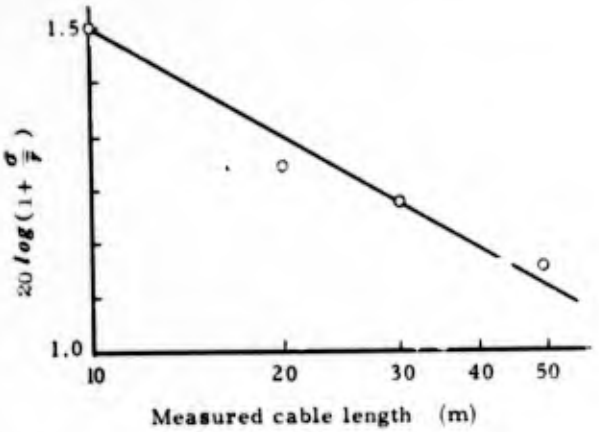

Fig. 8 The effect of measured cable length on the deviation of r. m. s. value

measured r. m. s. values were made. It was found that, when the sampling section length is more than 30 meters, the standard deviation of measured r. m. s. values will be less than 1.3 dB as is shown in Fig. 8. This fact means not only that the pulse near-end crosstalk measurement is useful for accurate evaluation of crosstalk coupling, but also that even a short cable piece of around 30~50 meters is sufficient for evaluation of crosstalk level inherent in the cable.

3.3 Relation between r. m. s. Value and Crosstalk Attenuation

Root mean square value of a pulse near-end crosstalk is directly related with near-end crosstalk coupling coefficient, that is, the sum of capacitive coupling $k(x)$ and inductive coupling $m(x)$, so that it can be related with the crosstalk attenuation. Figure 9 shows the empirical relation between r. m. s. value and effective near-end crosstalk attenuation at 5 MHz for cables 250 meters in length.

On the other hand, far-end coupling, namely

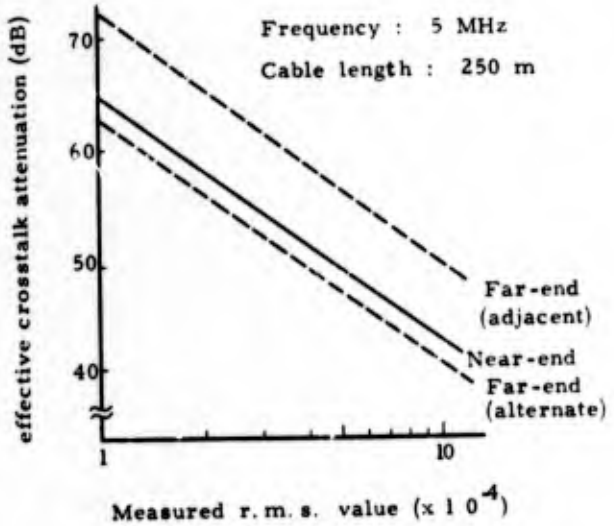

Fig. 9 Experimental relation between r.m.s value and effective crosstalk attenuation at 5 MHz

the difference between $k(x)$ and $m(x)$ has no direct connection with r. m. s. value of a pulse near-end crosstalk. However, some connection can be built up between them by utilizing a quantity, i. e., correlation coefficient, relating $k(x)$ with $m(x)$.

Assume that $\varphi_n(x)$ and $\varphi_f(x)$ in Eqs. (3) and (4) can be expressed as

$$\varphi_n(x) = \varphi_f(x) = e^{-\frac{\pi}{4}\left(\frac{x}{\tau_0}\right)^2} \quad or \quad e^{-\frac{x}{\tau_0}} \tag{9}$$

where τ_0 is autocorrelation length of these functions. When designating, by EFXT, the effective far-end crosstalk attenuation, by ENXT the effective near-end crosstalk attenuation, and by ρ the correlation coefficient between $k(x)$ and $m(x)$, the following relation can be led from Eqs. (3), (4), (5) and (6).

$$EFXT - ENXT = 10 \log \frac{X_n^2}{X_f^2} = 10 \log \left(\frac{1 - e^{-4\alpha l}}{4\alpha l} \cdot \frac{1+\rho}{1-\rho} \right) \tag{10}$$

In general, correlation coefficients between $k(x)$ and $m(x)$ are assumed to have almost the same value, if relative pair combination situations are the same. Therefore, ρ can be empirically back calculated from Eq. (10) for each pair combination situation, using EFXT and ENXT values measured on several test cables. After that, these correlation coefficients can be considered as characteristic constants of any cable of the same design. Correlation coefficients, thus obtained for adjacent and alternate pair combinations of test cables, are given in Table 2, which demonstrates the close relation between capacitive and inductive couplings in adjacent pair combination as well as the absence of such a relation between alternate pairs, suggesting the reduction of capacitive coupling by an intervening pair.

EFXT can now be determined by Eq. (10), on the basis of r. m. s. value of pulse near-end crosstalk, through the known relation between ENXT and the r. m s. value. The curves, thus determined, are also given in Fig. 9. As is seen in Eq. (6), EFXT is independent of line loss, therefore, the following empirical formula is obtained.

$$EFXT = K - 20 \log r - 10 \log \frac{l}{250} - 20 \log f \tag{11}$$

where K = 5. 5, for adjacent pair combination
= -3, for alternate pair combination
r = r. m. s. value of pulse near-end crosstalk, normalized by amplitude of applied pulse
l = cable length (meter)
f = frequency (MHz)

Table 2 Correlation Coefficient between m and k

Combination	ρ
Adjacent pairs	0. 75
Alternate pairs	0. 13

4. Theory Relating Crosstalk with Cable Structure

Although crosstalk is a complicated phenomena, there must be a reasonable interpretation for it. The pulse near-end crosstalk measurement will furnish an effective aid to establishing a theory able to connect actual crosstalk coupling with related cable structure.

4.1 Classical Theory

In developing a mathematical theory pertaining to magnetic coupling between conductor pairs in carrier cables, much important work has been done by N. Kobayashi.[3] To investigate the algorithm of pair twist lengths, he has strictly reduced the Neumann integral to the formula of mutual inductance between two helically twisted pairs of conductors, from which the following facts were induced.

(1) Mutual inductance between pairs can be expressed as an infinite odd term double series of sinusoidal functions.

(2) When a ratio of twist lengths of the pairs is odd to odd, such as 1/1, 3/1 and 5/3, the infinite series has a term directly proportional to length, whereby the magnetic coupling will increase with the cable length.

(3) When the pairs are twisted in the same direction with different twist lengths, and these are sufficiently greater than the interaxial spacing of the conductors of a pair, the mutual inductance can be expressed by superposition of the two periodic functions whose amplitudes and wave lengths are given below;

amplitude	wave length
$0.88\,\frac{a^2}{c}\sqrt{\left(\frac{p_1+p_2}{p_1-p_2}\right)+5.2}$,	$\frac{p_1 p_2}{\lvert p_1-p_2\rvert}$
$\frac{4}{\pi}\,\frac{a^2}{c^2}\,\frac{p_1 p_2}{\lvert p_1-p_2\rvert}$,	$\frac{p_1 p_2}{p_1+p_2}$

where a is the interaxial separation of the conductors of a pair, c the interaxial spacing between the pairs and p_1 and p_2 the twist lengths of the pairs, respectively.
Of particular note here is the fact that the possible value of magnetic coupling between pairs is characterized by a ratio of their twist lengths.

Table 3 shows the r.m.s. values of pulse near-end crosstalk between every adjacent pair, measured on ten 7-pair cables made under the same manufacturing conditions. As compared with the variation of average r.m.s. values in whole pair combinations, the variations of the r.m.s. values for individual combination are markedly small, which demonstrated the dependency of crosstalk coupling on pair combination as well as stabilized manufacturing conditions applied. The large crosstalk values seen in pair combinations 1-7 and 4-5, whose twist length ratio is 3/1, are in accord with results of the theory.

Nevertheless, there remain several questions not explained by the theory. The pair combinations 1-3 and 2-7, for instance, whose twist length ratio is 2/1, one of the most preferable ratios by the theory, brought about crosstalk coupling of the worst level. Quantitative analysis of these measurements by means of twist length ratio is not effective. Magnetic couplings calculated by the above formulas are, in general, less than one tenth

Table 3 Measured r.m.s. Value for Several Pair Combinations

(Sample number = 10, Cable length = 50 m)

Pair Combination *	Twist Length		Twist Length Factor		Measured r.m.s. ** Value ($\bar{r}$)	Standard Deviation	
	p_1 (mm)	p_2 (mm)	$\frac{p_1 p_2}{\lvert p_1-p_2\rvert}$ (mm)	$\frac{p_1 p_2}{p_1+p_2}$ (mm)	($\times 10^{-4}$)	$\frac{\sigma}{\bar{r}}$	$20\log\left(1+\frac{\sigma}{\bar{r}}\right)$ (dB)
1 - 2	120	80	240	48	3.2	0.12	1.0
3	120	60	120	40	8.8	0.17	1.33
4	120	90	360	51.5	3.9	0.09	0.78
5	120	30	40	24	1.9	0.17	1.40
6	120	50	85.7	35.3	1.8	0.06	0.5
7	120	40	60	30	8.8	0.16	1.28
2 - 3	80	60	240	34.3	2.3	0.2	1.57
7	80	40	80	26.7	4.1	0.09	0.76
3 - 4	60	90	180	36	5.5	0.12	0.98
4 - 5	90	30	45	22.5	6.2	0.14	1.10
5 - 6	30	50	75	18.8	0.8	0.12	1.02
6 - 7	50	40	200	22.2	1.9	0.14	1.13

* Refer to Fig. 1

** Normarized by the applied pulse amplitude.

of those obtained by experiments. Above all, there is a knotty problem widely recognized, that is, the accumulation of crosstalk coupling with increasing length of a cable by well known square root law, to which the theory can render no reasonable solution.

Therefore, another approach must be taken to explain actual crosstalk data. When regarding the accumulation of crosstalk, it is probable that random distribution of coupling along length would govern the phenomena. Why does this random distribution take place? The most possible reason must be fluctuation in manufacturing conditions, which may include unbalanced twining and fluctuation in pair twist length, as well as longitudinal variation in wall thickness and dielectric properties of insulation. The incidental fluctuation in interaxial separation between pairs is also a factor.

A series of measurements of pulse near-end crosstalk between pairs, carried out on test cable after the stranding, cabling and jacketing process, proved that the crosstalk was affected very little by the latter two. Twining unbalance and longitudinal variation of coaxial capacitance of wire cause a pair-ground capacitance unbalance, which constitutes a factor to cause indirect crosstalk. However, investigation on many test cables made it clear that this kind of capacitance unbalance, if it is no larger than the order of 30 pF/250m, would not be a determining factor to cause crosstalk at a frequency up to 10 MHz. Consequently, it is estimated that fluctuation in pair twist length, as well as in interaxial separation of pairs, are largely responsible for the crosstalk coupling. Pair-twist length fluctuation is especially likely to play a leading role in the present problem.

4.2 Coupling-Wave Model

The next objective is, therefore, formulation of the effect of twist length fluctuation on crosstalk coupling. Much difficulty is expected in direct incorporation of the fluctuation factor into the classical theory formulas, because they are given in the form of an infinite series of sinusoidal functions whose amplitudes are extremely intricate. Hence, another simplified course shall be taken.

When special regard is paid to the fact that mathematical crosstalk coupling is given by the infinite double series of odd terms, as stated previously, it is expected that the basic pattern of crosstalk coupling longitudinal distribution may be expressed by a product of two independent periodic functions. Since the higher terms of the said series decrease rapidly, these periodic functions can be simulated by periodic triangular waves. Due to fluctuation in pair-twist length, some fluctuation will occur in the waves. As these waves, let us assume the two triangular waves, $f_1(x)$ and $f_2(x)$ shown in Fig. 10, whose half wave-length varies at random, while maintaining each whole wave-length at constant values of p_1 and p_2. The validity of this assumption has been supported by research on actual twist length condition in completed cables, which disclosed a similar pattern of twist length fluctuation, particularly in longer twist lengths.

When designating by q_1 a half of wave-length p_1, by q_2 a half of wave-length p_2, by σ_1 stand-

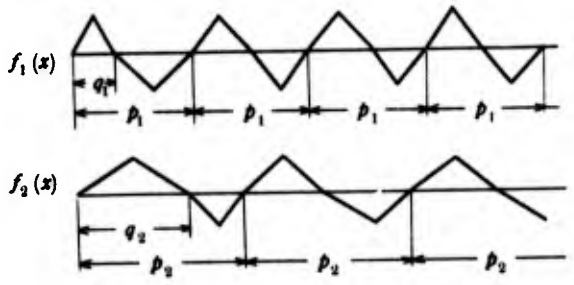

Magnetic coupling $M(x) \propto f_1(x)\, f_2(x)$

p_1 , p_2 Uniform along length

q_1 , q_2 Variation at random along length

Fig. 10 Coupling Model

ard deviation of q_1 and by σ_2 standard deviation of q_2, $f_1(x)$ and $f_2(x)$ can be written in the forms

$$f_1(x)=\frac{2}{\pi}\sum_{n=1}^{\infty}\sqrt{A_n^2}\,\sin\frac{2n\pi}{p_1}x=\frac{2}{\pi}\sum_{n=1}^{\infty}g_n(x)$$

$$f_2(x)=\frac{2}{\pi}\sum_{m=1}^{\infty}\sqrt{B_m^2}\,\sin\frac{2m\pi}{p_2}x=\frac{2}{\pi}\sum_{m=1}^{\infty}g_m(x) \qquad (12)$$

where

$$A_n^2=\frac{1}{2n^4}\left\{1-(-1)^n e^{-\frac{n^2\pi^2}{2}\left(\frac{\sigma_1}{q_1}\right)^2}\right\}$$

$$B_m^2=\frac{1}{2m^4}\left\{1-(-1)^m e^{-\frac{m^2\pi^2}{2}\left(\frac{\sigma_2}{q_2}\right)^2}\right\} \qquad (13)$$

The product of these two periodic waves is given by

$$g(x)=f_1(x)f_2(x)=\left(\frac{2}{\pi}\right)^2\sum_{n=1}^{\infty}\sum_{m=1}^{\infty}\left[A_n^2 B_m^2\right.$$

$$\left.\times\frac{1}{2}\left\{\cos\left(\frac{n}{p_1}-\frac{m}{p_2}\right)2\pi x+\cos\left(\frac{n}{p_1}+\frac{m}{p_2}\right)2\pi x\right\}\right] \qquad (14)$$

If there is no fluctuation in q_1 and q_2, that is, $\sigma_1/q_1=\sigma_2/q_2=0$, it is obvious from Eq. (13) that A_n^2 and B_m^2 vanish when n and m are even. In this case, $g(x)$ is reduced to a double series of only odd terms, which is consistent with classical theory.

Magnetic coupling is presumed to be related with $g(x)$, hence we have

$$M\propto G=\int_0^l g(x)\,dx=\sum_{n=1}^{\infty}\sum_{m=1}^{\infty}\int_0^l g_{nm}(x)\,dx\equiv\sum_{n=1}^{\infty}\sum_{m=1}^{\infty}G_{nm} \qquad (15)$$

where $g_{nm}(x)=g_n(x)\,g_m(x)$, and l is cable length.

4.3 Effect of Twist Length Fluctuation

It is evident from Eq. (15) that the square mean value of magnetic coupling $\overline{M^2}$ can be estimated from square mean value $\overline{g_{nm}^2}$ and normalized

autocorrelation function $\varphi_{nm}(x)$ of $g_{nm}(x)$. Because $g_{nm}(x)$ is a product of two independent functions, $\varphi_{nm}(x)$ is given by $\varphi_n(x)\,\varphi_m(x)$, where $\varphi_n(x)$ and $\varphi_n(x)$ are normalized autocorrelation functions of $g_n(x)$ and $g_m(x)$, respectively.

Although Eq. (14) is led on the assumption that wave-lengths p_1 and p_2 are maintained at constant values, actual wave-lengths fluctuate with the same variance as those of q_1 and q_2 . In this case, square mean values and autocorrelation functions of $g_n(x)$ and $g_m(x)$ are obtained by the following equations, (see Appendix).

$$\overline{g_n^2} = A_n^2 \quad , \quad \overline{g_m^2} = B_m^2$$

$$\varphi_n(x) = e^{-\frac{x}{\tau_n}} \cdot \cos\frac{2n\pi x}{p_1} \tag{15}$$

$$\varphi_m(x) = e^{-\frac{x}{\tau_m}} \cdot \cos\frac{2m\pi x}{p_2}$$

In the above formulas, τ_n and τ_m are autocorrelation lengths of $g_n(x)$ and $g_m(x)$, respectively. Then, designating $\tau_n\tau_m/(\tau_n+\tau_m)$ by τ_{nm} , and $(n/p_1 - m/p_2)$ by $1/P_{nm}$, we have

$$\overline{G_{nm}^2} = 2A_n^2 B_m^2 \int_0^l (l-x)\varphi_{nm}(x)\,dx$$

$$\fallingdotseq 2A_n^2 B_m^2 \int_0^l (l-x)\, e^{-\frac{x}{\tau_{nm}}} \cos\frac{2\pi x}{P_{nm}}\,dx \tag{17}$$

When $l \gg \tau_{nm} \gg P_{nm}$, and if $(n/p_1 - m/p_2)$ is sufficiently large, the following approximation can be made.

$$\overline{G_{nm}^2} \fallingdotseq \frac{A_n^2 B_m^2}{\tau_{nm}} \left(\frac{P_{nm}}{2\pi}\right)^2 l \tag{18}$$

When $(n/p_1 - m/p_2)$ is approximately equal to 0, and again $l \gg \tau_{nm} \gg P_{nm}$, we obtain

$$\overline{G_{nm}^2} \fallingdotseq A_n^2 B_m^2 \tau_{nm}\, l \tag{19}$$

The terms given by Eq. (18) and by Eq. (19) are called here "different wave-length component" and "same wave-length component", respectively. The former represents quantities corresponding with magnetic coupling, produced under different twist length conditions and the latter under t. same twist length conditions. Since both n and m are arbitrary integers, $(n/p_1 - m/p_2)$ has a chance to be approximately equal to zero at any pair combination. Then, the suitability of pair-twist lengths can be estimated by total magnitude of the same wave-length components.

Special regard must be paid to the fact that the two types of components of Eqs. (18) and (19) are inversely affected by $1/\tau_{nm}$, which is a quantity corresponding to fluctuation of twist pair lengths. This fact means, if fluctuation increases, then magnetic coupling due to the same wave-length components will decrease while coupling due to the different wave-length component will increase.

Variation in a pair-twist length is inextricably linked with the pair-twist length itself. Experimental results give the following approximate relation between pair-twist length and its longitudinal variation.

$$\left(\frac{\sigma}{q}\right) \fallingdotseq \alpha q \tag{20}$$

where α is a factor dependent on twist length fluctuation and, in general, is a value between 5×10^{-4} ~ 10^{-3}. Figure 11 shows the effect of twist length ratio on the crosstalk coupling, computed under the conditions of $\alpha = 10^{-3}$ and $p_1 = 30$ mm. Extremely high peaks are seen in the figure when twist length ratios are integers, from which the drastic effect of the same wave-length components is recognized.

When twist length ratio is less than 2.0, crosstalk coupling is mostly determined by the term $\sqrt{\overline{G_{11}^2}}$ in Eq. (15). Therefore, $\sqrt{\overline{G^2}}$ is given by the following approximate formula.

$$\sqrt{\overline{G^2}} \fallingdotseq \frac{1}{2\pi} \frac{A_{11} B_{11}}{\tau_{11}} \frac{p_1 p_2}{|p_1 - p_2|} \sqrt{l} \tag{21}$$

Furthermore, using the relation of Eq. (20), we obtain

$$\sqrt{\overline{M^2}} \propto \alpha \frac{p_1 p_2}{|p_1 - p_2|} \sqrt{p_1 + p_2} = \alpha Q \tag{22}$$

where $Q = (p_1 p_2 \sqrt{p_1 + p_2})/|p_1 - p_2|$, which will be called here twist length factor.

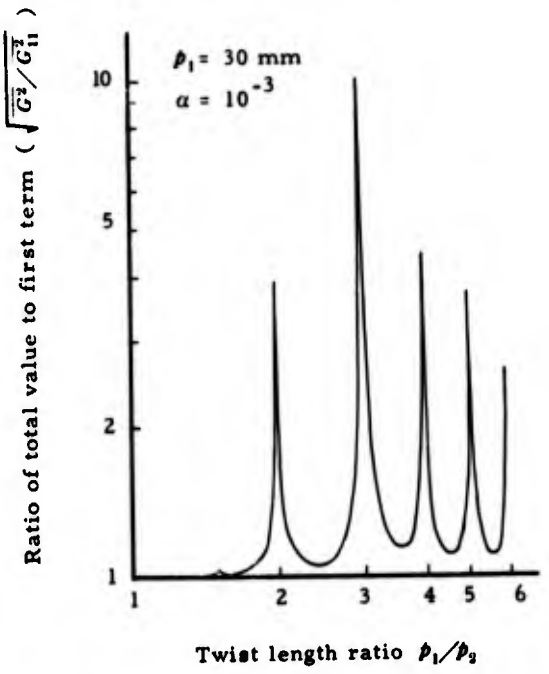

Fig. 11 Effect of twist length ratio on crosstalk coupling

5. Measurement Results

5.1 Effect of Twist Length on Crosstalk Coupling

Relation between Measured r.m.s. Value and Calculated Value Comparisons between measured r.m.s. values of pulse near-end crosstalk and calculated $\sqrt{G^2}$ were made on each adjacent pair combination in test cables. The data are plotted in Fig. 12(a) and (b); (a) for standard test cables and (b) for two reference 7-pair cables whose pair twist lengths range between 30~75.7mm and 51.2~124.3 mm, with each pair being formed with polyethylene twine fillers and a polyester tape overwrap. Calculations of $\sqrt{G^2}$ were carried out according to Eqs. (15) and (17), on the assumption that $\alpha = 1 \times 10^{-3}$. It is evident from these figures that the

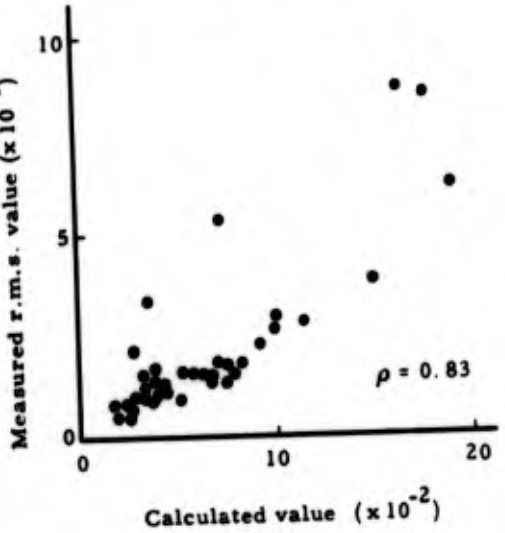

(a) Usual cables

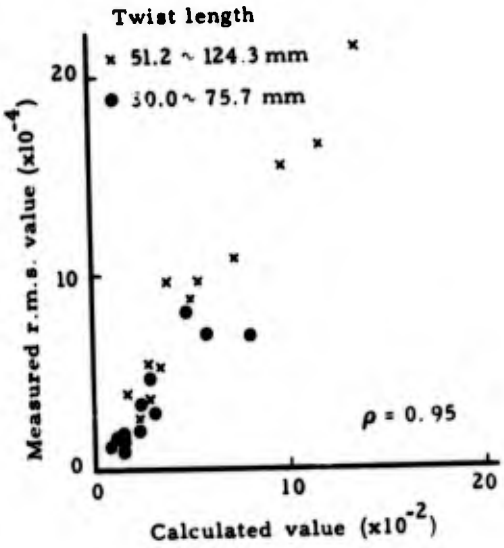

(b) Reference cables

Fig. 12 Relation between calculated value $\sqrt{G^2}$ and measured r.m.s. value for adjacent pairs

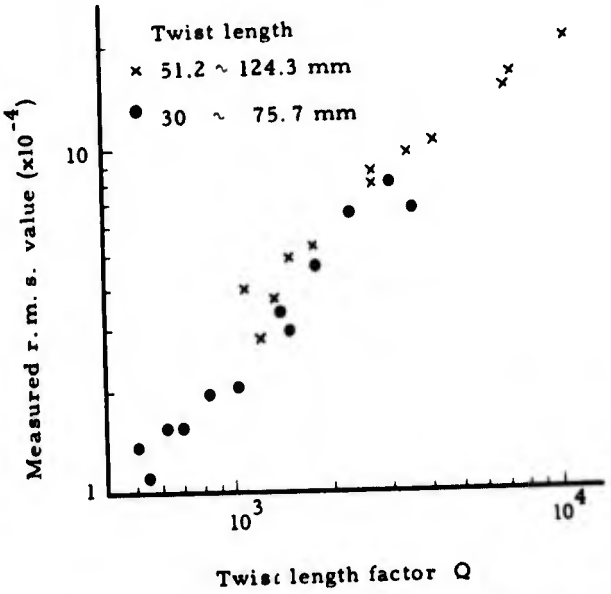

Fig. 13 Relation between twist length factor and measured r.m.s. value

measured r.m.s. values are closely related with the calculated $\sqrt{G^2}$. A rather stronger correlation is seen in the reference cables, which may be attributed to lower fluctuations in interaxial spacing between pairs.

In general, $\sqrt{G^2}$ is mostly determined by $\sqrt{G_{jj}^2}$ or twist length factor Q. This is proved by Fig. 13, which shows the strong correlation between the measured r.m.s. values and Q.

Twist Length Ratio and Autocorrelation Function As explained previously, any interpair crosstalk coupling has many constituents due to both the same and different wave-length components. When a pair-twist length ratio is an integer, the same wave-length components become dominant, therefore, the normalized autocorrelation function of crosstalk coupling will be different from that obtained in case the ratio differs from an integer. Figure 14 shows the measured normalized autocorrelation functions for the twist length ratios of 2/1 and 3/1, which

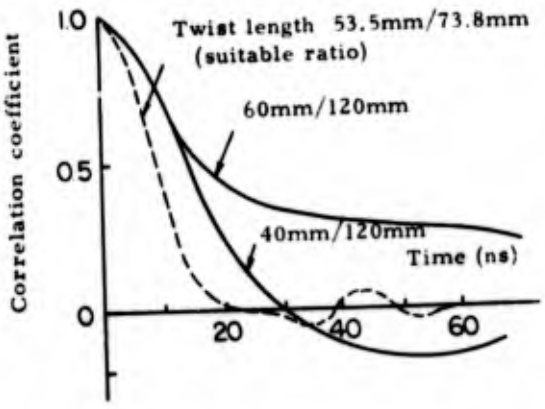

Fig. 14 Effect of twist length ratio on autocorrelation function

are evidently distinguishable by their longer auto-correlation length from the usual one shown in Fig. 6.

5,2 Effect of Manufacturing Conditions and Pair Combination

Effect of Manufacturing Conditions When calculations of $\sqrt{\overline{G^2}}$ are conducted under a fixed value of α, inclination of measured r.m.s. curve, plotted in relation to the $\sqrt{\overline{G^2}}$, is expected to be an index of twist length fluctuation level; the larger the fluctuation, the greater the inclination becomes. Thus, the propriety of cable processing conditions can be discussed by this index. Figure 15 shows the curves for the cables, whose units are formed through two different stranding conditions, A by the usual practice and B by the new conditions modified in the degree of back twist, back-tension in supplying pairs and so on. A remarkable difference is seen between them.

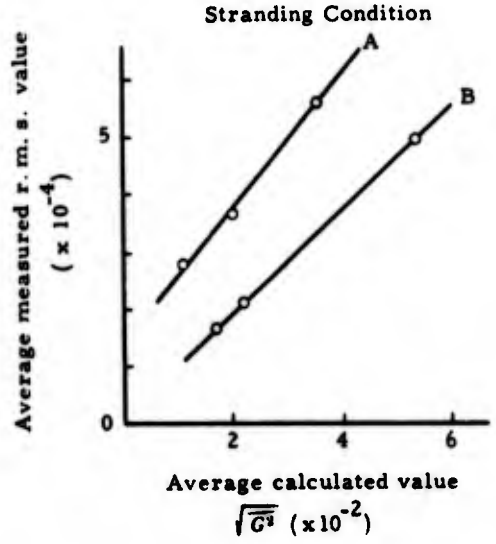

Fig. 15 Variation between different stranding conditions A and B

Table 4 Crosstalk Reduction Effect

Pair Combination		Reduction * Coefficient	Note
Adjacent Pairs		1.0	
Alternate Pairs		1/4 ~ 1/5	
Pairs between Adjacent Layers	I	3/5 ~ 4/5	
	II	1/10 ~ 1/5	

* r.m.s. value divided by that for adjacent pairs

Pair Combination Situations Thus far, discussions have been limited mostly to crosstalk between adjacent pairs. Investigation on pair combinations in other situations is also important. Crosstalk between pairs, separated by an intervening pair or pairs, is affected by their situations as well as by the factor due to the twist length ratio. Separation of the two effects is rather hard. Therefore, an empirical approach was taken to determine a factor representing a crosstalk reduction effect for each pair combination situation.

Figure 16(a) shows the relation between measured r.m.s. values and calculated $\sqrt{\overline{G^2}}$ values for alternate pairs in the same cables as in Fig. 12 (b). Similar curves are plotted in Figs. 16(b) and (c) for two types of pair combinations across adjacent stranding layers; both of situations are illustrated in the figure by denoting as adjacent layer I and II, respectively. These results are summarized in Table 4, in which the ratio of the

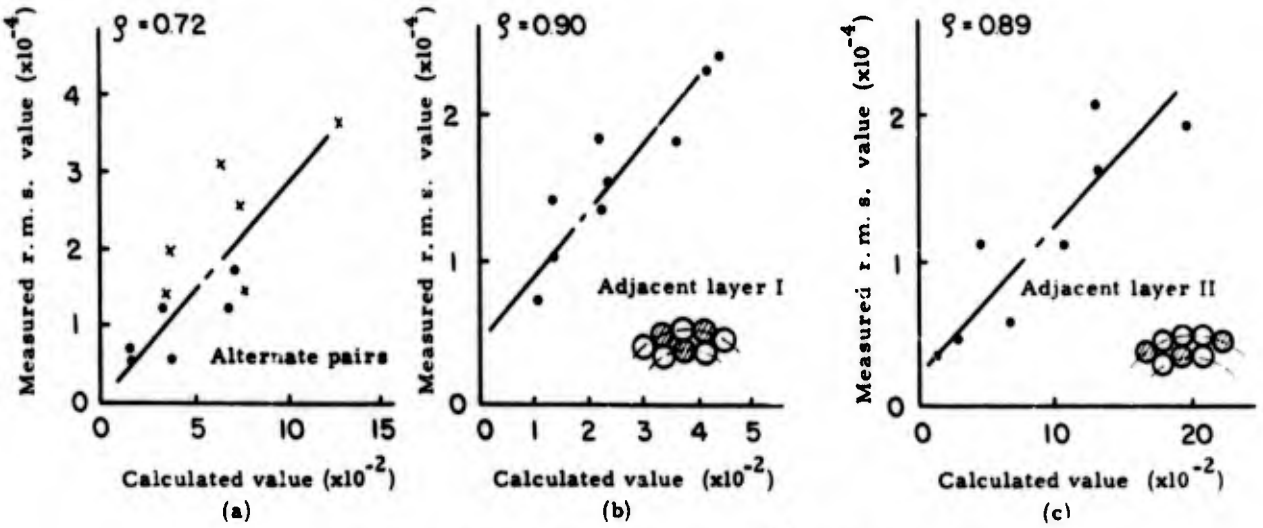

Fig. 16 Relation between calculated value $\sqrt{\overline{G^2}}$ and r.m.s. value for several pair combination

r.m.s. values between given pair situations and adjacent pair combination are given as reduction factors.

6. Crosstalk Attennation of Finally Designed Cables

On the basis of the investigations so far discussed, a series of the most preferable pair twist

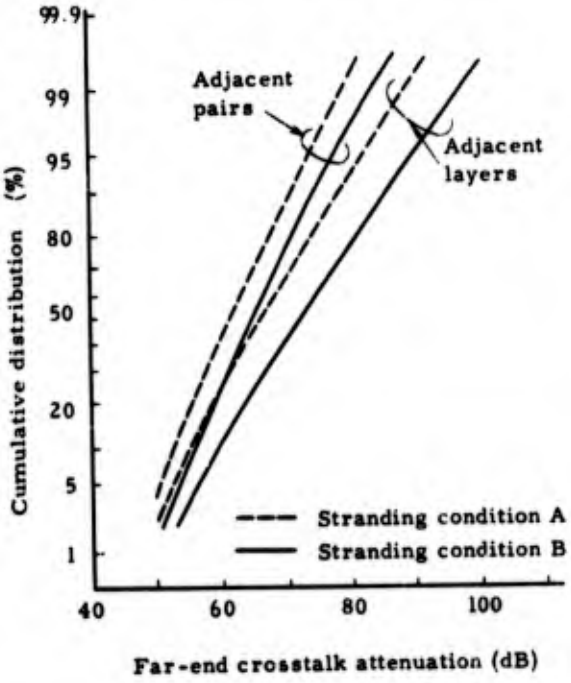

(a) Adjacent pairs and layers

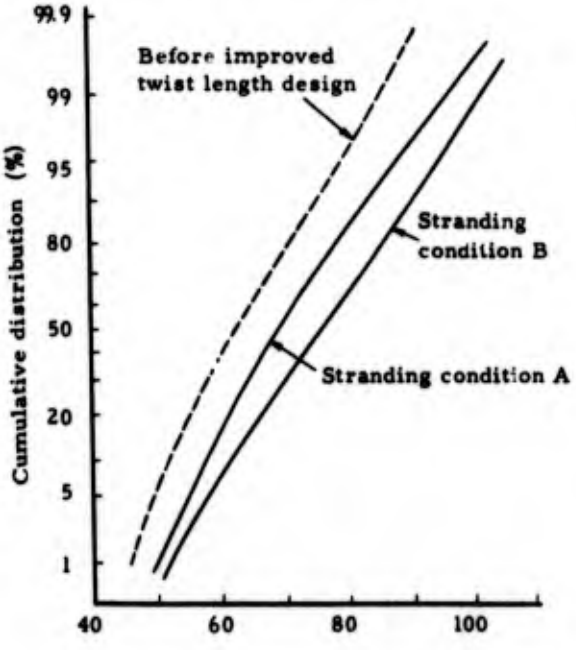

(b) Total

Fig. 17 Cumulative distribution of far-end crosstalk loss at 5 MHz (250 m)

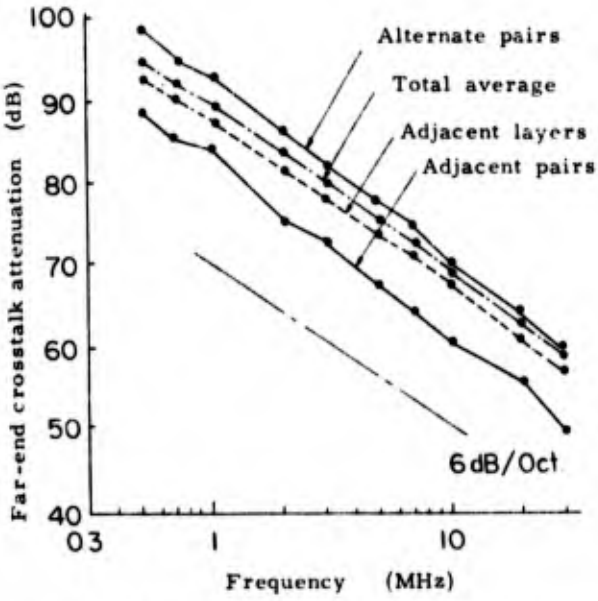

Fig. 18 Change of far-end crosstalk with frequency

lengths and the optimum pair arrangement were determined. These pairs were stranded, under the condition of either A or B, then cabled and jacketed into completed cables.

Figure 17 shows the cummulative curves of far-end crosstalk attenuations per 250 meter length of these cables, measured at a frequency of 5 MHz. For comparison, similar curves for a cable designed under the conventional philosophy are also given in Fig. 17(b). In the figure, (a) is the far-end crosstalk between adjacent pairs as well as between pairs across adjacent layers, and (b) is for the whole pair combinations. Much improvement, attained in crosstalk properties of the cables by the new design, can be seen from this figure Furthermore, it is also ascertained that the newly established stranding condition B improves crosstalk properties by about 5 dB, as compared to the conventional conditions.

Figure 18 shows the variation of far-end crosstalk attenuation with frequencies of finally standardized cables.

7. Conclusion

As the results of the work made on inter-pair crosstalk in video transmission multipair cables, many valuable factors have been disclosed. They are summarized as follows :

(i) Pulse near-end crosstalk measurement is very useful for an exact evaluation of crosstalk coupling inherent in a cable, even if it is of short length.

(ii) The connection between actual crosstalk coupling in a cable and the cable structure can reasonably be made on the basis of quantitative analysis of pair-twist length fluctuation, which would be the "missing-ring" in classical theory.

(iii) Measured crosstalk coupling is proved to be closely related to the calculated value, according to this new theory.

(iv) Optimum selection of pair-twist lengths and pair arrangement can reasonably be conducted by this theory.

(v) Qualification of cable manufacturing conditions can easily be made through use of a correlation diagram between measured crosstalk couplings and calculated values.

(vi) Remarkable improvement has been attained in the newly developed cables under the newly established design philosophy and cable manufacturing conditions.

References

1. H. Kaden, "Impulse und Schaltvorgänge in der Nachrichtentechnik" R. Oldenbourg, München, 1957.

2. S. Minematsu, A. Itoh "Amplitude Correction of Pulse Near-End Crosstalk for Multipair Cables" Dainichi-Nippon Cables, Review, No. 58, Aug. 1974 Osaka, Japan

3. N. Kobayashi, "Electro-Magnetic Coupling Between Quads of Multipair Cable" Research Report No. 1563 Oct. 1961 E.C.L. N.T.T. Japan

APPENDIX

Autocorrelation Function of Sinusoidal Wave Whose Wave-Length Varies Statistically along Its Length.

Because an analytical reduction of autocorrelation function of the sinusoidal function $\cos(\pi x/q)$ is very hard, when length q varies statistically along the length, the periodic rectangular wave, as shown in Fig. A-1, will be considered instead of the sinusoidal wave.

If probability density function $h(q)$ of half wave length is given by

$$h(q) = \frac{1}{\sqrt{2\pi}\,\sigma} e^{-\frac{(q-q_0)^2}{2\sigma^2}}$$

probability $Q_n(\delta, y)$ that a spacing δ, between fixed point x_1 and arbitrary point x_2 in Fig. A-1, involves total n concavities and convexities is expressed by

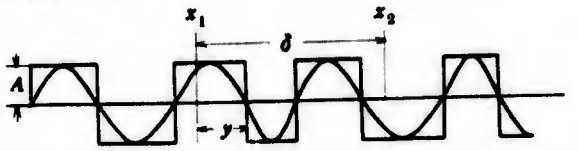

Fig. A-1 Periodical rectangular wave for sinusoidal wave

$$Q_n(\delta, y) = P_r(\delta - y > nq) \cdot P_r(\delta - y < (n+1)q) \qquad (A\text{-}1)$$

where

$$P_r(\delta - y > nq) = \int_{\delta - y}^{\infty} \frac{1}{\sqrt{2n\pi}\,\sigma} e^{-\frac{(x - nq_0)^2}{2n\sigma^2}} dx \qquad (A\text{-}2)$$

$$P_r(\delta - y < (n+1)q) = \int_0^{\delta - y} \frac{1}{\sqrt{2(n+1)\pi}\,\sigma} e^{-\frac{[x-(n+1)q_0]^2}{2(n+1)\sigma^2}} dx$$

Therefore, as the probability $p_n(\delta)$ that a spacing δ between two arbitrary points x_1 and x_2 involves total n concavities and convexities, we obtain

$$p_n(\delta) = \int_0^{\infty} \frac{h(q)}{q} \int_0^{q_0} Q_n(\delta, y)\, dy\, dq \qquad (A\text{-}3)$$

If σ/q_0 is small enough, $p_n(\delta)$ can be approximated to the form

$$p_n(\delta) \fallingdotseq \frac{1}{q_0} \int_0^{q_0} Q_n(\delta, y)\, dy \qquad (A\text{-}4)$$

The average value of products of the wave amplitudes at x_1 and x_2 is given by

$$\overline{f_1(x) f_2(x)} = A^2 \sum_{n=1}^{\infty} (-1)^{n+1} p_n(\delta) \qquad (A\text{-}5)$$

Thus, normalized autocorrelation function $\varphi(\delta)$ of the wave is

$$\varphi(\delta) = \sum_{n=1}^{\infty} (-1)^{n+1} p_n(\delta) \qquad (A\text{-}6)$$

Figure A-2 shows a typical example of computed result of Eq. (A-6). It is reasonable to expect, from Fig. A-2, that the normalized auto-

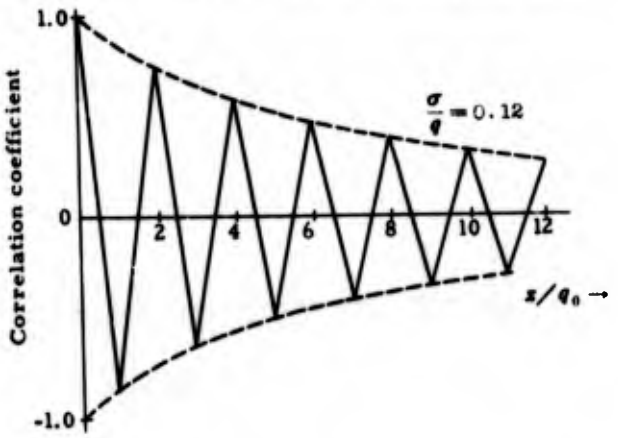

Fig. A-2 Normalized autocorrelation function for periodical rectangular wave whose wave length changes at random

correlation function can be written in the form

$$\varphi(\delta) \fallingdotseq e^{-\frac{x}{\tau}} \cos\frac{\pi x}{q_0} \qquad (A\text{-}7)$$

Autocorrelation length, defined as the change of (τ/q_0) with variation of twist length (σ/q_0) is given in Fig. A-3, from which the following approximate relation is obtained.

$$\left(\frac{\tau}{q_0}\right)\left(\frac{\sigma}{q_0}\right)^2 = 0.14 \qquad (A\text{-}8)$$

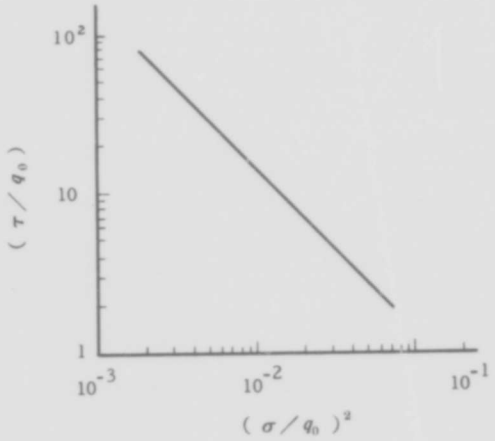

Fig. A-3 Twist length variation effect on the autocorrelation lengths

Masami Yotsuya
Dainichi-Nippon Cables, Ltd.
7-3 Umeda, Kitaku
Osaka, 530 Japan

M. Yotsuya joined Dainichi-Nippon Cables, Ltd. in 1961 after he received his BS degree in Electrical Communication Engineering from Osaka University. He has been engaged in design and development work on communication cables. He is now assistant manager of Design Section, Telecommunication Engineering Department of the present company. Mr. Yotsuya is now a member of the Institute of Electronics and Communication Engineers of Japan.

Seiki Minematsu
Dainichi-Nippon Cables, Ltd.
Kaichiku, Ikejiri, Itami
Hyogo-Ken, 664 Japan

S. Minematsu joined Dainichi-Nippon Cables, Ltd. in 1965 after he received his BS degree in Electrical Engineering from Kobe University. He has been engaged in research and development work on communication cables. He is now a stuff engineer of Telecommunication Research Laboratory. Mr. Minematsu is now a member of the Institute of Electronics and Communication Engineers of Japan.

Akira Itoh
Dainichi-Nippon Cables, Ltd.
Kaichiku, Ikejiri, Itami
Hyogo-Ken, 664 Japan

A. Itoh received his BS and MA degree in Electrical Engineering from Tohoku University in 1969 and 1971 respectively. He then joined Dainichi-Nippon Cables, Ltd., and engaged in research on Communication cables. He is now a stuff engineer of Telecommunication Research Laboratory. Mr. Itoh is now a member of the Institute of Electronics and Communication Engineers of Japan.

INTELLIGIBLE CROSSTALK IN MODERN LOCAL AREA TELEPHONE NETWORKS

H.W. Silcock and D. Sibbald

Standard Telecommunication Laboratories Limited
Harlow, England

Summary

Present trends in the planning of local area networks, together with the advent of quieter exchanges may be expected to reduce the margins available for satisfactory control of intelligible crosstalk between telephone subscribers. Analysis of the incidence of such crosstalk depends on subjective as well as objective considerations.

The factors involved in the control of voice frequency crosstalk are examined, with particular reference to the local area cable, and a basis is given for assessing capacitance unbalance performance directly in terms of the CCITT curves for threshold of intelligibility. The scheme depends on the 'extreme value' method of analysis and the convolution of the various distributions involved - talker level, listener acuity, crosstalk attenuation, etc. The influence of threshold shift due to noise is then considered and, finally, the effects of activity factor are taken into account.

The results of capacitance unbalance measurements on a recent cable design are analysed by this method and used to calculate the risk of intelligible crosstalk for a representative set of conditions.

Introduction

The significance of intelligible crosstalk has long been recognized. When the CCITT recommendations for international circuits were drafted about 40 years ago a great deal of thought was given to this subject and calculations were made to achieve an equitable result.

The control of crosstalk is fundamental to the design of equipment and cables used in telephone circuits and so affects their cost. On the other hand, if crosstalk is present at a sufficiently high level it impairs the privacy of the system.

Little is known about the disturbing effect of intelligible crosstalk except that its syllabic nature must surely distract the affected subscriber from his own call. It is usual therefore to concentrate on the privacy aspect when considering these effects.

Over the past few years renewed attention has been internationally focussed on the subject of intelligible crosstalk, particularly in Study Groups XII and XVI of the CCITT. Administrations and operating companies are naturally sensitive about their networks in this respect and, because various technical changes have been slowly taking place, a need for a review of the subject is now apparent. The technical changes have involved:

- a general improvement in the quality of transducers
- a tendency to increased attenuation in subscribers' lines (requiring higher outputs to line and more sensitive receivers to compensate for the loss in overall level)
- quieter subscribers' lines and less noise introduced by modern exchanges and line transmission systems

finally, the publishing of information and recommendations by the CCITT that have created considerable interest and discussion.

There are many aspects of the subject but this paper will deal only with one important source of intelligible crosstalk - the subscribers' local exchange plant.

Mechanism of Intelligible Crosstalk in the Local Area Network

Considering the subscriber's end of a telephone call, Figure 1 shows the factors which give rise to crosstalk. In this model the sources of crosstalk are the cable and the exchange. Leaving aside human factors, the severity of the crosstalk will depend on:

- power to line of transmitted speech
- sensitivity of the receiving subset
- noise introduced by the exchange and line
- near end crosstalk in cable and exchange.

(Far end crosstalk is not normally a controlling factor). A knowledge of the above parameters and certain others peculiar to the country concerned (such as line lengths, etc) will enable the value of the crosstalk to be calculated, but further information is needed to determine whether the crosstalk is intelligible or merely detectable in the presence of the prevailing noise. Calculations have to take into account variations between the loudness of one speaker and another and also the variation between one listener's hearing and another's. All the factors, including human ones, are statistical in some degree. But as in many other assessments of quality of service, administrations are interested in the general quality of their telephone service and accept the necessity of receiving an answer in a form giving the probability of overhearing in a population of subscribers.

An examination of Figure 1 shows that the mouth-to-ear path of the crosstalk is made up of three parts:

- transmitting part of subset
- cable crosstalk path (for instance)
- receiving part of subset.

Moreover, the assessment is subjective. The normal method of describing mouth-to-ear loss is to make a comparison with a standard speech path (NOSFER): the loss in decibels inserted in the standard to give equal loudness to the model under test is known as its 'overall reference equivalent'. Considerable controversy surrounds this subject in laboratories but for planning purposes the procedure is sufficiently accurate for the moment. The overall reference equivalent may be broken down into the sending reference equivalent of the sending subset (SRE), the receiving reference equivalent of the receiving subset (RRE), and the loss in between (NEXT attenuation). It is very important to note that this approach takes account of the characteristics of the subsets themselves, that

is, how much 'amplification' they introduce. We need to know the reference equivalents of the subsets at the point at which the crosstalk attenuation path is measured and must also remember tnat these equivalents may be dependent on line length due to regulators incorporated in the subsets. The equivalents of subsets are not always quoted alone: for instance in many countries these parameters are often quoted for a typical subscriber's line, and subset equivalents have to be deduced by subtracting twice the line attenuation from the sum of the two equivalents for subset plus line. This operation is obviously dependent on the line lengths prevailing in the country under consideration.

Cable crosstalk is also frequency dependent, but a value measured or calculated at 1 kHz will be sufficiently accurate for our purpose.

Social Crosstalk

As a further indication of complications that can arise, consider Figure 2 which in a simplified way indicates how exchange area cables may be laid out. Main cables from the exchange, often containing very large numbers of pairs, terminate at a suitable cross-connection point. From here much smaller cables (not larger than 100 pairs) proceed to distribution points (DP) serving a number of subscribers (sometimes by a span or two of open wire and sometimes by a small underground cable).

Obviously a customer on DP1 will be more concerned if his conversation is overheard by a neighbour, who will more than likely be also connected to DP1 with both their line circuits in one of the small distribution cables. This we may call 'social crosstalk' and we note that it is potentially more important than crosstalk between a customer on DP1 and one on DP2 or DP3. (Social crosstalk occurs when a subscriber overhearing another telephone conversation not only understands the conversation but also recognizes the voice of the disturbing party).

Crosstalk may also occur in the exchange itself, with no external cables involved, for example, between subscribers on DP1 and DP3, but this is most unlikely to be social crosstalk. Also at this point the difference in levels has been reduced, further improving the position. However, exchange crosstalk cannot be entirely neglected, particularly in view of the very much reduced level of noise in modern exchanges. This is made worse by the general tendency for a reduction in line noise over the last decade. And so a system effectiveness dilemma is approaching - for the economy of the system as a whole, is there a balance required between intelligible crosstalk and noise?

Listener Thresholds for Intelligible Crosstalk

Consideration must now be given to the fundamental curves relating mouth-to-ear loss for detectability or audibility (Figure 3). So that the curves may be generally applicable for all subsets, the ordinate represents the loss which must be inserted between one subset with a zero sending reference equivalent and another with a zero receiving reference equivalent for a constant talking level which gives an output at the subset terminals of -10 VU allowing just detectable or audible speech. Trained listeners are used and the point of detectability or audibility is that at which 50% of listeners think it is higher and 50% think it is lower. The value is termed 'nominal overall reference equivalent' because it has not been obtained directly by comparison with NOSFER.

To make the curves useful a correction has to be made to take account of the average talking level in the country concerned. This is the loudness factor 'c' given in Table 1. This factor not only has a mean value but also a standard deviation. Figure 3 and Table 1 and 2 are taken from CCITT Recommendation G.116 (P.16) - Subjective effects of Direct Crosstalk.

Thus to make use of the curves it is necessary to know for the environment concerned:

- statistics of talker volumes of subscribers
- variation of subscribers' listening acuity. This lies between 4 and 6 dB standard deviation
- receiving reference equivalent of the disturbed subscriber's subset.

The required value of the latter is that of a subscriber's set alone but operating under average line conditions. This is not always available directly and may have to be estimated by subtracting from the receiving reference equivalent of the whole local telephone circuit the attenuation of the line, as previously mentioned. The frequency at which the attenuation is taken varies somewhat according to the gauge of the wires but no great error occurs if 1 kHz is assumed. Attenuation will be of the order of 3 dB.

Figure 3 also gives the curves with and without sidetone, and with room noise and negligible room noise. Note the almost constant difference of about 11 dB between the detectable and audible curves. Equivalent curves may be deduced from basic threshold theory.

Before applying these curves to the present study, it is necessary to consider in some detail the various other factors involved and, in particular, cable crosstalk.

Calculation of Crosstalk from Cable Parameters

Crosstalk Coupling Formulae

If we consider two neighbouring pairs in a short element from a long length of cable (Figure 4), then for practical purposes we may regard the disturbing circuit as a generator whose impedance equals Z_o, the line characteristic impedance, connected by a short length of twin wire to a load also equal to Z_o and the disturbed circuit as a short piece of twin wire terminated at both ends by impedances also equal to Z_o. Ignoring for one moment the problem of inductive coupling and considering only capacitative coupling between the two small sections of circuits, we have between the 4 wires, 6 possible capacitative 'leaks' if we disregard any currents flowing via the earth or cable shield.

In Figure 5, C_{12} and C_{34} are the mutual capacitances of the short lengths of the two pairs and since at voice frequencies their impedance is high compared with Z_o they may be omitted from the calculation. Two crosstalk paths exist; in one the voltage V drives a current through C_{13} then through Z_N and Z_F in parallel and back via C_{24}. The other path is through C_{14} then through Z_N and Z_F in parallel and back via C_{23}. (Other paths through purely capacitative elements may be disregarded owing either to their comparatively high impedance or to the fact that they do not contribute to the current through Z_N or Z_F).

In both cases the currents divide equally between Z_N and Z_F but are in opposite directions. The capacitative current i_c is therefore approximately equal to

$$i_c = \tfrac{1}{4}V \left[\frac{C_{14}\,C_{23}}{C_{14}+C_{23}} - \frac{C_{13}\,C_{24}}{C_{13}+C_{24}} \right] j\omega$$

$$= \tfrac{1}{4}V \left[\frac{(C_{13}+C_{24})\,C_{14}C_{23} - (C_{14}+C_{23})\,C_{13}C_{24}}{(C_{14}+C_{23})(C_{13}+C_{24})} \right] j\omega$$

...(1)

As $C_{13} \doteq C_{14} \doteq C_{23} \doteq C_{24}$,

$$i_c = \tfrac{1}{4}V \left[\frac{C_{13}+C_{24} - C_{14}-C_{23}}{4} \right] j\omega$$

$$= \tfrac{1}{4}V \left[\frac{\Delta C}{4} \right] j\omega$$

$$= \frac{V\,\Delta C}{8}\, j\omega$$

where ΔC in the capacitance unbalance between the two pairs. The wanted signal

$$i = \frac{V}{Z_L}$$

so

$$i_c = i\,\frac{Z_o\, j\omega\, \Delta C}{8}$$

A similar treatment applied to the mutualinductance coupling between the 4 wires gives by the same approach an induced current

$$i_m = i\,\frac{j\omega\,\Delta M}{2Z_o}$$

At the near end of the circuit the two currents i_c and i_m tend to aid one another and at the far end to oppose. (This assumes that the capacitance unbalance is due primarily to variations in the relative geometric positions of the wires, rather than to dielectric irregularities). Therefore we have for the case of near end crosstalk:

$$i_x = i\, j\omega \left[\frac{\Delta C\, Z_o}{8} + \frac{\Delta M}{2Z_o} \right] \qquad ...(2)$$

Since Z_o is relatively high in cables at voice frequencies, the capacitative term of the expression is much larger in magnitude than the inductive term and therefore dominates. Since at the same time the angle associated with Z_o is approaching $/45^o$, the two terms actually combine almost in quadrature for both near end and far end crosstalk.

If the small section of cable under consideration is at a distance ℓ from the end, then if I is the current entering the disturbing circuit

$$i = I\, e^{-\gamma \ell}$$

where γ is the propagation constant; also if I_x is the near end crosstalk current leaving the disturbed circuit due to the coupling within the small section under consideration

$$I_x = i_x\, e^{-\gamma \ell}$$

so

$$I_x = I\, j\omega\, \frac{\Delta C\, Z_o}{8}\, e^{-2\gamma \ell} \qquad ...(3)$$

So far, we have been considering crosstalk coupling due to capacitance unbalance between two neighbouring pairs in a short element of cable, the direction of flow of the crosstalk current clearly depending on the 'sign' of the unbalance (+ or -). In carefully manufactured modern cables, any systematic unbalance effects, for example due to systematic differences in thickness or permittivity of the insulation on the 'a' and 'b' wires of a pair, are (or should be) relatively small and consequently the residual unbalances on different elements of cable tend to be of random magnitude and sign, with a mean value of zero, i.e. they are distributed normally.

In proceeding to longer lengths of cable, it is therefore reasonable to assume that the capacitance unbalance couplings due to the different elements of line combine on a random or power basis, i.e. that the capacitance unbalance squared is proportional to length. At the same time, phase effects are small, since at voice frequencies the wavelength is relatively long (40 km at 1 kHz on 0.5 mm cable). We may therefore calculate the total near end crosstalk coupling between the two pairs by summing the crosstalk power contributions from the various elements of line, only taking account of attenuation effects.

Then from Equation (3), the near end crosstalk contribution (power fraction) from an element of line $d\ell$ at distance ℓ is given by

$$\left| \frac{I_x}{I} \right|^2 = \frac{\omega^2\, \overline{\Delta C^2}\, Z_o^{\,2}}{64}\, e^{-4\alpha \ell}\, d\ell \qquad ...(4)$$

$$= \frac{\alpha^2}{32} \left[\frac{\Delta C_{rms}}{C} \right]^2 e^{-4\alpha \ell}\, d\ell$$

(at voice frequencies) where the line characteristic impedance

$$Z_o = \sqrt{\frac{R}{j\omega C}}$$

α is attenuation per unit length (nepers) $= \sqrt{\frac{\omega CR}{2}}$

R = resistance per unit length

C = mutual capacitance per unit length

$\overline{\Delta C^2}$ = mean square capacitance unbalance per unit length for the particular pair combination (or class of combination) considered

Integrating over a line of length L (assuming no change in the relative position of the two pairs),

$$\text{total NEXT (power fraction)} = \frac{\alpha^2}{32}\left[\frac{\Delta C_{rms}}{C}\right]^2 \int_0^L e^{-4\alpha\ell}\, d\ell$$

$$= \frac{\alpha}{128}\left[\frac{\Delta C_{rms}}{C}\right]^2 \left(1-e^{-4\alpha L}\right)$$

For an electrically short line, this expression reduces to

$$\frac{\alpha^2 L}{32}\left[\frac{\Delta C_{rms}}{C}\right]^2 \qquad \ldots(5)$$

and for an electrically long line, the expression reduces to

$$\frac{\alpha}{128}\left[\frac{\Delta C_{rms}}{C}\right]^2 \qquad \ldots(6)$$

In the general case, the near end crosstalk attenuation is given by

$$\text{NEXT} = -10 \log\left[\frac{\alpha}{128}\left(\frac{\Delta C_{rms}}{C}\right)^2\left(1-e^{-4\alpha L}\right)\right] \text{ dB} \qquad \ldots(7)$$

The effect on crosstalk of varying the parameters R, C or ω may be judged by substituting for α in formulae (5) and (6). For example, whereas quadrupling R (attenuation and impedance doubled) would worsen crosstalk coupling on a short line by about 6 dB, the near end crosstalk on a long line would be worsened by about 3 dB.

Nature of Crosstalk Coupling within a Cable

The make-up of subscriber cables can take a variety of forms. Although cables of conventional layer design are sometimes used, the more usual practice is to employ unit type cables, with units generally of 100, 50 or 25 pairs. Here again, the units themselves may take a variety of forms and may consist of either layers of pairs, bunched pairs, or a number of subunits, typically of the 10-pair size.

Whatever the form of construction, it will be apparent that the distribution of capacitance unbalance couplings throughout the cable is far from homogeneous, the pairs in closest proximity normally having the highest couplings, while well separated pairs, screened from one another by intermediate wires, usually have negligible coupling, except for possible indirect paths via pair-earth unbalance, etc. (It may here be noted that inductive couplings, which become of importance at frequencies above the voice range, are not reduced by screening to the same extent as capacitance couplings).

In units or cables of layer type construction, the largest unbalances usually occur between adjacent pairs in the same layer or between pairs in adjoining layers, although significant couplings can also arise between nominally separated pairs having 'like' twist lengths. However, the remaining pair combinations (which form a large proportion of the total in the unit or cable) tend to have little or no unbalance. Even within small subunits, where all pairs are relatively close to one another (and may all have different twist lengths), there tends to be considerable variation in the size of the pair-pair couplings if the subunit is of conventional make-up, and various mixing schemes have been devised to reduce the distance along the cable over which any two pairs remain in adjacent positions.

Figure 6 illustrates these effects for 10-pair subunits in a recent IKO (Swedish company for ITT) cable design. The curves represent the distribution of capacitance unbalance values for each of the 45 combinations of pairs within the subunit, based on measurements on 80 subunits in a 500 m drum length of 0.4 mm cable.

The tendency for the curves to fall into groups related to the subunit structure can be clearly seen, the 5 classes of combination indicated (nominally adjacent, etc) referring to relative positions in a single layer of 10 pairs.

Extreme Value Analysis

One of the main objects of the present study is to demonstrate a method of assessing the crosstalk performance of subscriber cables regardless of their size or make-up. This is based on 'extreme value' analysis.

It will by now be evident that any one pair in a cable when regarded as the disturbed pair will have significant capacitance unbalance coupling only with certain other pairs when regarded as potential disturbing pairs; the highest of these couplings may be designated EV1 (Extreme Value 1), the second highest EV2, and so on. Similarly, every other pair in the cable when regarded as the disturbed pair will have its own set of extreme values.

In cables employing subunits, the first few extreme values for any one pair will normally arise on pair combinations within that pair's subunit, and a distribution of EV1 values for the pair can be obtained from observations on a large number of subunits. Similarly for EV2 values, and so on.

Corresponding distributions for individual pairs will not usually differ greatly (particularly if some form of mixing has been used within subunits) and it is therefore permissible to combine the separate distributions into a single overall distribution (of EV1 for example) for an average pair. Within 10-pair subunits, each pair will have 9 extreme values (EV1-9) and Figure 7 shows combined distribution curves based on 240 such units contained in two 400 m drum lengths of a recent design of 1200-pair 0.4 mm cable.

Table 3 shows the rms extreme values of capacitance unbalance for each of the 9 curves, together with the first 3 crude power moments (normalized for unit mean power). Also given are the 1 kHz values of near end crosstalk attenuation corresponding to these rms values, calculated for the 400 m length.

It should be borne in mind that significant capacitance unbalance couplings may occasionally occur between pairs in different subunits or units, and these must of course be taken into account in a complete analysis of the cable. Usually, however, the within-subunit couplings tend to control the first few extreme values.

Calculation of the Risk of Intelligible Crosstalk

In order to apply the results of the extreme value of capacitance unbalance analysis to the calculation of the risk of intelligible crosstalk, it is necessary to include or combine all the other variables which enter into the overall speech chain. Some may be regarded as environmental constraints - room noise, line noise, sidetone, etc which act as a mask on the intelligibility threshold whilst others - talker level, listener acuity, subset efficiency, and cable crosstalk attenuation, add directly together to fix the absolute level of speech perceived over the crosstalk path. If the distributions are uncorrelated (and there is no reason to suppose that the vocal level of the disturber is related in other than random manner to the crosstalk attenuation or the disturbed's hearing ability), then if these distributions need to be convolved by adding together their variates expressed in dB type units from the different distributions, the combined distribution of the sum may be obtained by adding together the cumulants of the individual distributions. (If the various distributions to be convolved were all of the normal Gaussian type, then their combined distribution would also be normal and its mean and variance would be equal to the sum of the means and the sum of the variances of its component parts).

It should be noted that capacitance unbalance, taking account of sign, tends to be normally distributed for individual pair-pair combinations, as indicated for example by the general slope of the curves shown in Figure 6. (On the special probability scale used, all folded normal distributions have a standard slope). However, the resultant distribution obtained when these individual folded distributions are combined into a single overall distribution tends to be approximately log normal.

The extreme value distributions of capacitance unbalance with which we are here concerned tend similarly to be approximately log normal (as indicated by the relationship between the moments given in Table 3). Whilst this is in fairly good agreement with the experimental results, a more precise treatment is possible by using the actual extreme value moments in the overall convolution of distributions. This may then be fitted by using a 3-parameter augmented log normal distribution rather than a simple two-parameter log normal.

We now apply the method of calculation just considered to a representative example (0.5 mm cable). The assumptions made are as follows (see Figure 1):

- a median listener with hearing acuity distribution of mean 0 dB and standard deviation 5 dB
- an average speech level 'c' factor of mean +3 dB and standard deviation 4 dB
- an overall reference equivalent (SRE + RRE) of mean -3 dB for a pair of subsets connected together on a zero line (but operating, as far as their line regulators and feeding currents are concerned, as though they were connected to average lines).

  The variation of subset efficiency with line current within the network (taken as having a standard deviation of 2.5 dB) is combined with the variation of near end crosstalk attenuation with which it is correlated (see below)
- a value of 3.5 dB standard deviation has been taken to allow for the combination of performance variations which change with line length: carbon microphone battery supply effect, line regulator effect, and crosstalk attenuation length factor as indicated in Equation (7).

  These 3 effects are added for a particular line length and then weighted in proportion to their occurrence in the network under consideration.
- a typical distribution of local line lengths is as shown in Figure 8. In all cases considered it is assumed that the disturber and the disturbed share the same final distribution point (DP) and are therefore located at approximately the same distance from the exchange.
- the distributions assumed for cable near end crosstalk attenuation are based on the extreme value distributions of capacitance unbalance given in Table 3.

The results obtained by convolving all the distributions are as shown in Figure 9 which gives the probable expectation of a given 'nominal crosstalk reference equivalent' for the first 9 extreme values of capacitance unbalance.

Threshold Shift due to Noise

An important parameter in the estimation of intelligibility is the noise level at the disturbed subset terminals.

If we take 3 levels of exchange noise:

400 pWp (noisy step-by-step exchange)

100 pWp (crossbar exchange specification)

10 pWp (crossbar exchange achieved in practice)

and 3 levels of local area line noise:

100 pWp, 50 pWp and 0 pWp

then for a line of average length having a loss of 3 dB the 9 possible values of noise at the subset terminals in pWp and converted to dBmp are as shown in Table 4.

If the receiving reference equivalent of the subscriber's set on an average line is taken as -4 dB, then the reference equivalent at the subset terminals at the point at which the noise level is evaluated is -7 dB. Either from Figure 3 or from lin ar interpolation in the CCITT table (Table 2) the following values are obtained for the median listener thresholds for intelligible crosstalk (nominal overall reference equivalents):

- Under conditions of negligible room noise:

52.7	55.6	55.0	
53.5	57.2	59.5	T dB
54.5	59.8	67.6	

- Under conditions of +40 dB(A) room noise:

50.1	52.4	53.5	
50.7	53.6	55.4	T dB
51.5	55.6	60.9	

From these 18 values of T dB two have been selected for further study. One, the highest value 67.6 dB, corresponds to a median listener on a quiet modern exchange, with no line noise and a negligible background of room noise. The other value selected, 55.4 dB, corresponds to another median listener on a quiet modern exchange, with 50 pWp line noise on the local circuit and a background of +40 dB(A) room noise. From Figure 9 the probabilities of intelligible crosstalk under these ambient conditions are as shown in Table 5.

Activity Factor

The risk of crosstalk depends not only on the probabilities shown in Table 5 but also on the level of activity on the circuits concerned. Clearly in the middle of the night with no other circuits in use there can be no crosstalk interference regardless of the degree of coupling. If we restrict our consideration to the exchange busy hour, then typical calling rates for residential and business subscribers are as shown in Figures 10 and 11, respectively. The overall rate for any one exchange will depend on the mix of the ratio of business to residential subscribers. But for the sake of example we will consider two rates: 0.025 erlang per exchange connection one way corresponding to a predominately residential case, and 0.2 erlang per exchange connection one way for an exchange with mainly business subscribers.

If the calling rate is denoted by r, then if a subscriber on average receives as many calls as he makes, the bothway overall calling rate is $2r$. If there are n subscribers connected to a particular cable, where n is a reasonably large number, then at any instant in the busy hour there will be on average $2rn$ active subscribers. In the steady state with the births keeping up with the deaths, during the time taken for an average call, all of the subscribers who were connected at the start of the period will have terminated their calls and will have been replaced by others. The probability of a particular subscriber making or receiving a call or being already engaged on a call during the time when you are making a call is therefore 4 times the average busy hour calling rate, namely $4r$.

The probability that your EV1 will be active during a call is $4r$. The probability that your EV1 is not active but your EV2 is active is clearly $(1 - 4r)\ 4r$. The probability that your EV3 is active and your EV1 and EV2 are inactive is $(1 - 4r)\ (1 - 4r)\ 4r$, and so on.

If P_n is the probability of intelligible crosstalk from an active EVn circuit, then the probability that the EVn circuit is active and intelligible during a call is $4rP_n$. The probability that no circuits will give intelligible crosstalk during a call is the product

$$\prod_{1}^{N} (1 - 4rP_n)$$

where N is the total number of pairs from which crosstalk is possible. This product converges rapidly and only the first few terms are required; the risk of intelligible crosstalk is given by the product's complement.

Using the two calling rates and the two threshold conditions as shown in Table 5 the following results are obtained:

- For a residential calling rate the risk of social crosstalk in the exchange busy hour is 0.16% under quiet conditions of no room noise and no line noise, or 0.00074% under conditions of 40 dB(A) room noise and 50 pWp of line noise.
- For a business calling rate the risk of social crosstalk in the exchange busy hour is 1.31% under the unlikely environment of no room noise and no line noise, or 0.0059% under conditions of 40 dB(A) room noise and 50 pWp of line noise.

In all cases a modern exchange has been assumed with a low noise level of -80 dBmp.

Other Factors

Certain factors have been ignored in the calculations, mainly due to lack of information. These include the effects on cable crosstalk of unbalance in the transmission bridges. In defence of this it may be said that such unbalances have much greater effect when cable crosstalk coupling is low, but little at the tail of the distribution, where it is high.

Present Position in the CCITT

The new recommendations (G.116/P.16) that have been introduced in the Green Book, Volumes III (Line Transmission) and V (Telephone Transmission Quality) are confined to publication of the curves shown in Figure 3 together with explanations and examples. However, in the present session the questions are being studied in greater depth. This will certainly mean a review of existing recommendations and this could lead to their modification and possibly the introduction of new recommendations affecting national and international practices.

Conclusions

Margins that in the past ensured good crosstalk performance are in danger of being eroded away. Exchanges are becoming quieter and the use of electronics in supervisory circuits permits a new generation of exchanges with higher possible loop resistances and hence higher overall speech path loss which has to be compensated by additional gain. To this must be added a growing demand by the public for privacy in its telephone conversations.

The local area is particularly susceptible to crosstalk problems as it is the region in which speech level differences are at their highest and where signals are most likely to exist in analogue form. Whilst many of the factors which play an important role in determining whether or not a possible crosstalk path will give intelligibility are not under the control of the network designer, the specifications for capacitance unbalance limits in the local cable are, and will doubtless come under closer scrutiny.

For distributions of the type that arise in cable capacitance unbalance the problem is concentrated in the peak of the distribution rather than in the bulk and a reduction in the spread of readings is just as valuable as an overall improvement in the rms value.

Bearing in mind the likely range of environmental factors that will be encountered in practice, such as room noise, subscriber calling habits, and talking volumes, the cable design on which the measurements were taken would appear to be more than adequate for present day use and to have a fair degree of latitude to meet many of the demands which could be made during its installed life. For, although there must be a future trend towards a reduction in the average overall reference equivalent of connections, this is inevitably accompanied by a partial lowering in the subscribers' vocal level. Furthermore, greater sophistication in subscribers' apparatus circuitry will permit better control of level extremes due to a 'bull' talker or poor line equalization.

In the ultimate future, the problem of intelligible crosstalk will disappear and be replaced by one of impairment due to bit mutilation as digital transmission stretches right to the subscriber's premises. But the vast investment in existing techniques and the inertia to change of the local area network as a whole seem likely to ensure that the task of intelligible crosstalk suppression will remain a challenge to cable and equipment designers for many years to come.

Acknowledgments

The authors wish to acknowledge the assistance and co-operation they have received from their colleagues in ITT Swedish company IKO, at Grimsas who made and measured the cable on which the analysis is based.

The authors also wish to acknowledge the help received from their colleague Harold Williams of STL who was largely responsible for providing material for certain sections of the paper.

The authors especially acknowledge their debt to their friend the late Bent Bulow Jacobsen of STL with whom they had many discussions during the early stages of this study.

Table 1 - Mean values and standard deviations of the loudness factor 'c' for various administrations

Administration	Nominal overall reference equivalent of the disturbing connection	Estimated mean value of factor c $\bar{c}$	Estimated standard deviation of the factor c σ_c
A T & T	dB 10 20 30	dB -2 +2 +5	dB 4
Switzerland	35	+3.5	4
Sweden	10	-6	5
United Kingdom	10 20 30	+3 +4 +5	4.8

Table 2 - Median listener thresholds of intelligible crosstalk as a function of the noise power level at the input to a 0 dB reference equivalent receiving end, for a variety of listening conditions (based on Figure 3)

N dBmp noise power level at input to 0 dB RRE	T dB, nominal overall reference equivalent of the crosstalk path		
	Negligible room noise		+40 dB (A) room noise with sidetone
	Without sidetone	With sidetone	
-100	76.5	75.0	65.1
- 95	75.7	74.5	64.9
- 90	74.0	73.0	64.2
- 85	72.5	72.0	64.0
- 80	70.0		60.5
- 75	67.0		58.0
- 70	63.0		55.0
- 65	59.0		51.5
- 60	54.5		47.5
- 55	49.5		43.0
- 50	44.0		

Table 3 - Extreme value statistics for 1200 pair 0.4 mm cable

Distribution	rms capacitance unbalance (pF on 400 m)	Crude power moments (normalized for UMP) P_1	P_2	P_3	NEXT attenuation at 1 kHz for ΔC_{rms} (dB for 400 m)
EV1	31.814	1	1.642	3.946	93.0
2	21.295	1	1.623	3.826	96.5
3	15.755	1	1.672	4.364	99.1
4	11.825	1	1.681	4.582	101.6
5	9.090	1	1.714	4.424	103.9
6	7.004	1	1.860	5.309	106.1
7	5.276	1	2.187	6.894	108.6
8	3.780	1	3.050	15.965	111.5
9	2.765	1	2.267	14.706	114.2

Table 4 - Possible values of noise at subset terminals

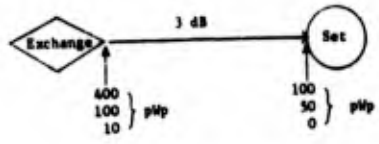

Line noise (pWp)	Exchange noise (pWp)			
	400	100	10	
100	300 (-65.2)	150 (-68.2)	105 (-69.8)	Subset terminal noise (pWp)
50	250 (-66.0)	100 (-70.0)	55 (-72.6)	
0	200 (-67.0)	50 (-73.0)	5 (-83.0)	

Note: Figures in brackets are dBmp

Table 5 - Probabilities of intelligible crosstalk

	T = 67.6 dB (percent)	T = 55.4 dB (percent)
EV 1	1.15	0.0062
2	0.33	0.00090
3	0.11	0.00020
4	0.038	0.000044
5	0.013	0.0000094
6	0.0045	0.0000023
7	0.0015	0.00000051
8	0.00047	0.00000015
9	0.00008	0.00000002

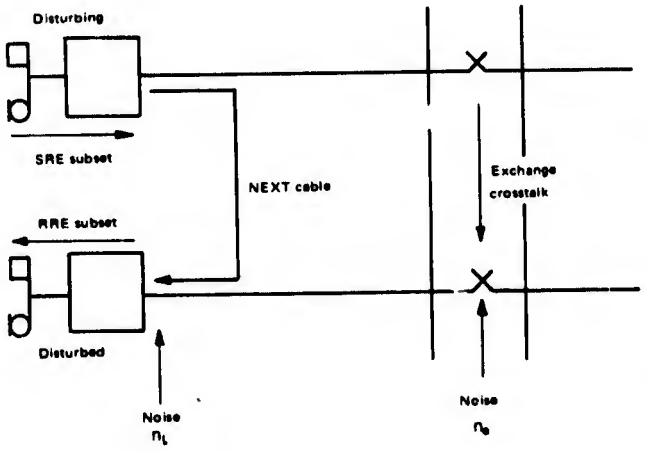

Fig. 1 - Factors giving rise to crosstalk

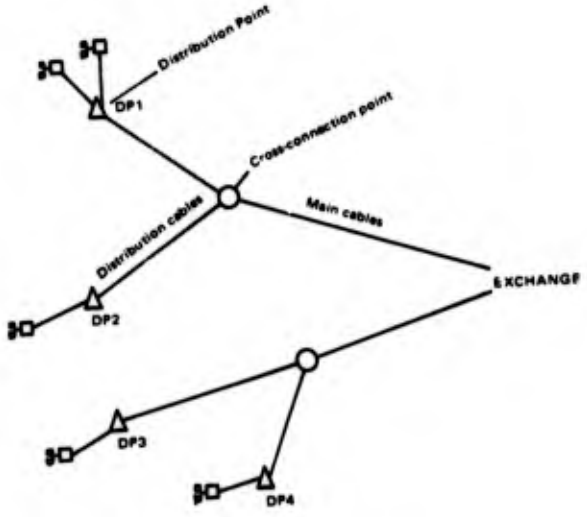

Fig. 2 - Typical exchange area cable layout

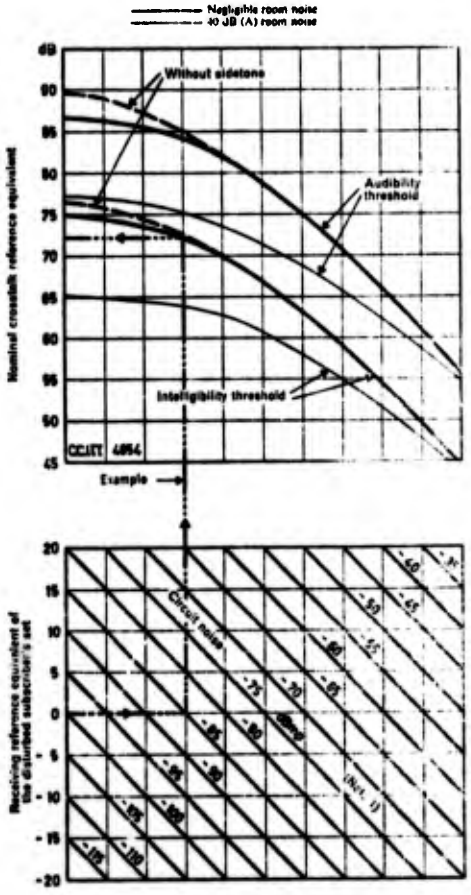

Fig. 3 - Crosstalk reference equivalent as a function of receiving reference equivalent and circuit noise (CCITT Green Book Vol.III, Rec.G.116; Vol.V,Rec.P.16)

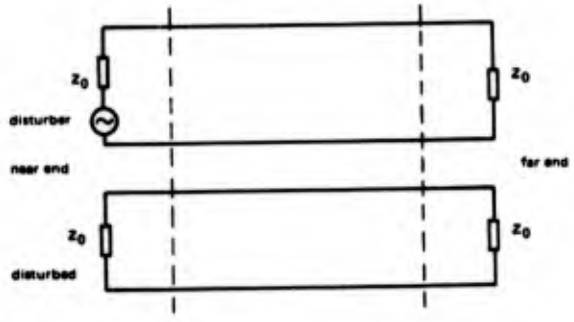

Fig. 4 - Neighbouring pairs in a short element of cable

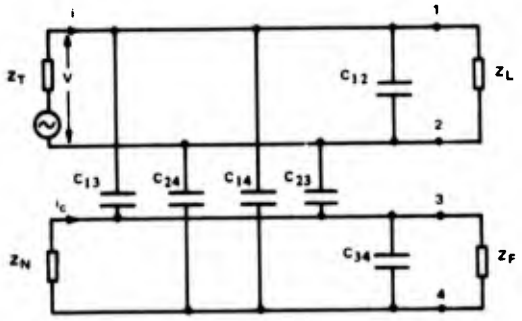

Fig. 5 - Capacitance couplings between short lengths of two pairs

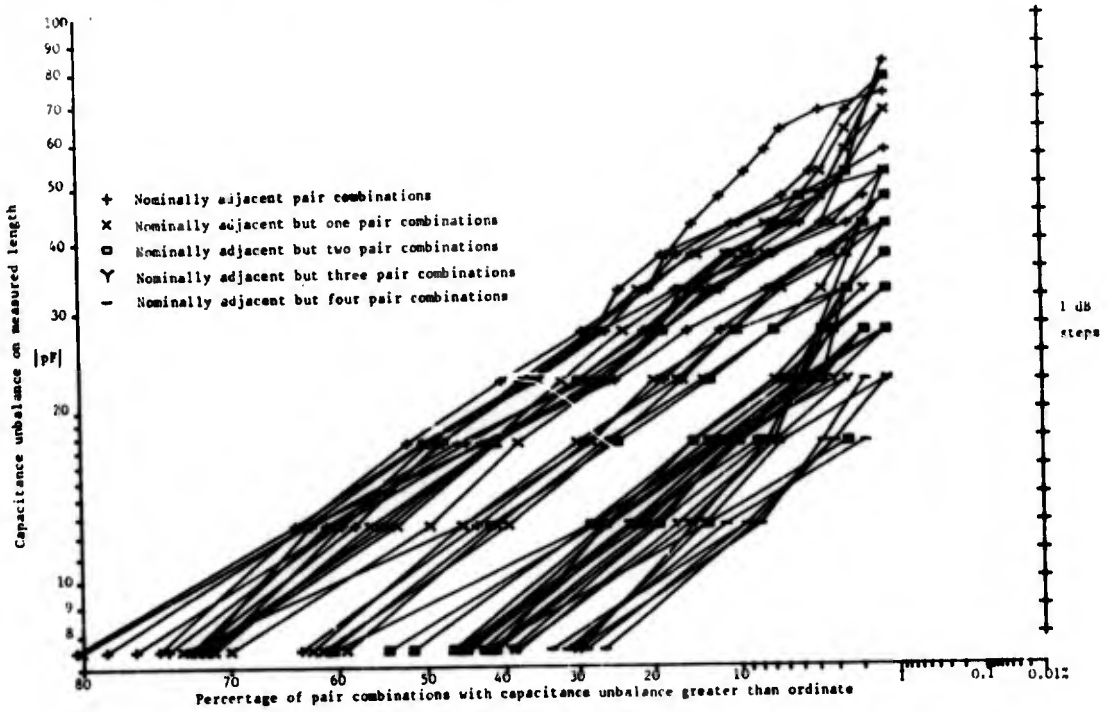

Fig. 6 - Dependence of capacitance unbalance on relative pair positions within 10-pair subunits of 800-pair cable

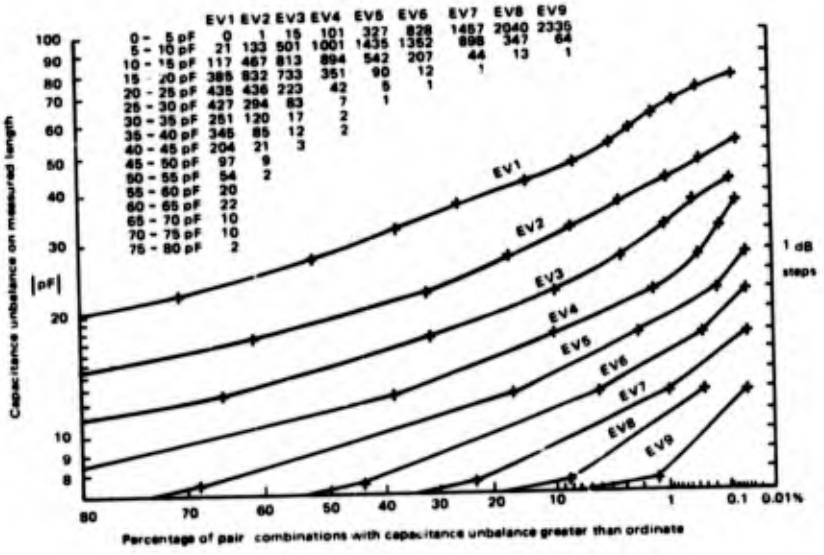

Fig. 7 - Distribution of the first nine largest values of capacitance unbalance in two 1200-pair cables

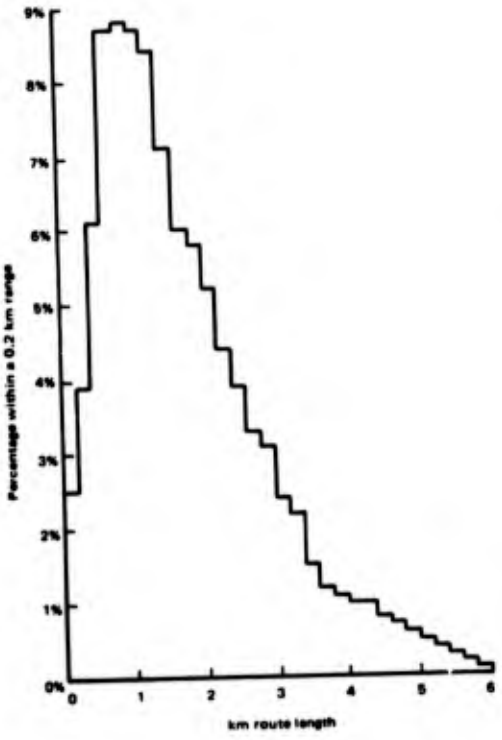

Fig. 8 - Distribution of the length of subscribers' local lines in a typical network

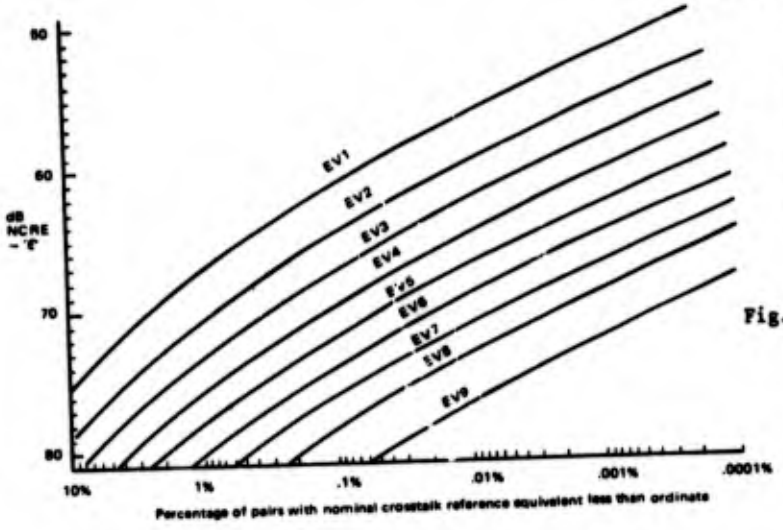

Fig. 9 - Probable expectation of Nominal Crosstalk Reference Equivalent for first nine extreme values of capacitance unbalance

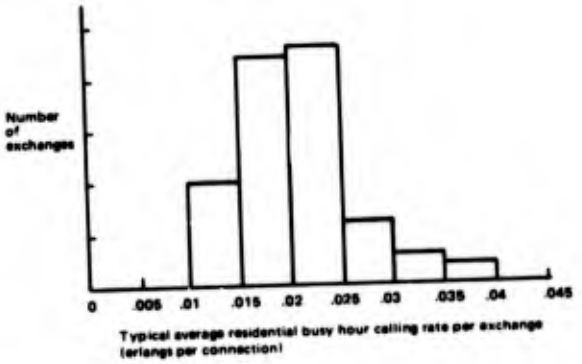

Fig. 10 - Typical calling rates for residential subscribers

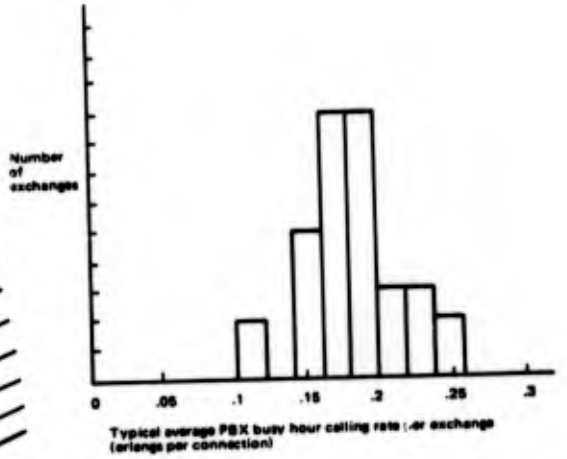

Fig. 11 - Typical calling rates for business subscribers

HOWARD H. SILCOCK* was born in Maidstone in 1916. After studying at University College, Southampton, he received a B.Sc. (London) general degree in 1936, and a B.Sc. (London) special degree in physics in 1937. He then joined the Systems Planning Division of Standard Telephones and Cables and worked on carrier cable and open-wire projects. He later transferred to the newly formed Standard Telecommunication Laboratories, where he has been concerned with crosstalk and other aspects of line transmission, including carrier cable balancing techniques and open-wire transposition schemes.

DAVID SIBBALD* was born in Guildford, England, in 1928. He graduated from London University with a B.Sc.(Hons) degree in Physics and Mathematics in 1951 and joined the Standard Telephones and Cables Transmission Division at North Woolwich the same year. After several years in the STC Apparatus Division he was transferred to Standard Telecommunication Laboratories in 1955, where he has been mainly concerned with various aspects of speech transmission both from the subjective and objective point of view. In recent years he has concentrated on problems arising from the evolution of the subscribers local area network.

* Standard Telecommunication Laboratories Limited, London Road, Harlow, Essex, CM17 9NA, England.

MULTI-PAIR ALUMINUM CONDUCTOR JUNCTION CABLE

H. Fukutomi
Nippon Telegraph and Telephone Public Corp.
Tokyo, Japan

S. Kaibuchi
Nippon Telegraph and Telephone Public Corp.
Tokyo, Japan

A. Toyokawa
The Furukawa Electric Co., Ltd.
Tokyo, Japan

T. Higashimoto
Sumitomo Electric Industries, Ltd.
Yokohama, Japan

H. Chiba
The Fujikura Cable Works, Ltd.
Chiba, Japan

1. ABSTRACT

In 1972, NTT purchased more than 140,000 tons of copper for use as cable conductors, which amounts to 14% of domestic consumption. The average annual demand for this material for the next five years will be about 170,000 tons; approximately 14% of the total.

In recent years, world wide copper supply has been unstable, and lately prices have risen sharply; and exhaustion of copper resources is forecast. Therefore, to ensure a constant and stable supply of cable conductor material, it is important to obtain a substitute material whenever needed. Aluminum as a copper substitute is abundant and has excellent conductivity. NTT has been conducting a development study of aluminum as conductor material for telecommunication cable since 1966.

Since 1971, NTT has twice conducted commercial tests of multi-pair aluminum conductor junction cables, and aluminum conductor cables have become feasible for practical use.

2. INTRODUCTION

In order to cope with the unstable copper supply, NTT has been conducting a development study of aluminum as a cable conductor material for telecommunication cable since 1966, so that we would be able to use it whenever needed. In spite of long experience in the use of aluminum conductor power transmission lines, an aluminum conductor telephone cable was not developed until quite recently, because aluminum conductor cable has inferior physical and chemical properties compared to copper.

However, problems of splicing, corrosion and manufacture of aluminum conductors have been solved by recent technical advances and aluminum conductor cables have become feasible for practical use. In 1971, NTT began commercial tests of 0.8 mm 600-pair EC grade aluminum conductor junction cables, using a total of over 12 km. Since 1973, NTT has been conducting further commercial tests of 0.65 mm 1,000-pair and 0.5 mm 1,800-pair aluminum alloy conductor junction cables using a total of over 12 km in order to develop finer gauge aluminum conductor cables. Good results have been obtained from the commercial tests regarding electrical and mechanical properties and splicing performance.

3. SUPPLY AND DEMAND OF CONDUCTOR MATERIAL

Supply and demand of copper is very sensitive to world political and economic conditions. As shown in Fig. 1, copper price fluctuations are much more violent than aluminum prices, thus the supply situation is very unstable. Copper and aluminum resource demand and supply postures are shown in Table 1 and Table 2.

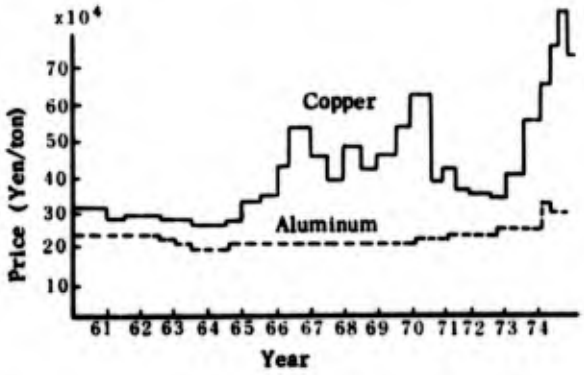

Fig. 1 - Price fluctuations of copper and aluminum

If consumption of copper continues at the current growth rate, presently known deposits of copper resources will last about 20 years, and will be exhausted by 1995-2000. In contrast, aluminum resources may last 53 years even if demand increases and could last 1,000 years if the current annual consumption rate remains the same. Therefore, since aluminum deposits are rich and supply is stable, it is the most suitable material for future conductor use.

On the other hand, the highest percentage of copper used for various cable conductors, (see Table 3), is in multi-pair cables. Therefore, if these conductors are replaced by aluminum, the economic effect will be great. Junction cables are used under stabilized environs, as in ducts or cable tunnels, and seldom need any rejointing once they are installed. Because of these reasons, NTT first began a development study of junction cables.

Table 1 - Resource situations

Resource			Demand for refined copper and aluminum (x 10^3 ton) Present*	2000	Total from present to 2000	Deposits (x 10^8 ton)		
Cu	World		7,067	26,136	468,512	2.9		
	Japan		807	4,022	63,377	0.02		
Al	World	from data of U.S. Bureau of Mines	9,330	min. 45,000 max. 95,000	min. 710,000 max. 1,150,000	35% content	25%** content	Total
		from Rev. del' Aluminum	8,570	99,820	1,250,900	18.6	20.0	38.6

* Cu for 1969, Al for 1968
** Low-quality minerals

Table 2 - Supply life of copper and aluminum resources

Life (years)	Cu	Al
Present demand level	36	1,000
Continuously rising demand	21	53

Table 3 - Percentage of quantity of copper use by kinds of cables

Cable	Percentage (%)
Multipair local cables (including junction cable)	56
Distribution cables	18
Toll cables	9
Switch board cables	5
Coaxial cables	4
SD wires	4
Other cables	4
Total	100

4. ALUMINUM CONDUCTOR MATERIAL AND FOAMED POLYETHYLENE INSULATION

(1) Properties of aluminum conductors:

Aluminum conductor materials are classified as: EC grade aluminum (purity: 99.65% or more) and aluminum alloy (Al and Fe, Mg, Si, Cu, Sb, etc.). EC grade aluminum has high conductivity and is relatively low priced but it is inferior in tensile strength. It is applicable for thick gauge conductors such as 0.8 mm, but, it is unsuitable for conductors as thin as 0.5 mm. Therefore, EC grade aluminum is used for 0.8 mm conductors, while aluminum alloy of higher tensile strength is used for 0.65 mm and 0.5mm conductors in view of manufacturing efficiency.

Table 4 shows the physical and mechanical properties of aluminum conductor material as compared with copper conductors. O grade and H grade indicate degree of "soft" and "hard" work hardening respectively. The relation between tensile strength and conductivity, which is one of the most important relations, is shown in Fig. 2. Generally speaking, the greater the conductivity, the smaller the tensile strength. The conductivity of actually used aluminum conductors is: aluminum alloy -- about 61% IACS (International Annealed Copper Standard). EC grade aluminum conductivity is about 63% IACS. Intermediate degrees of softness or hardness between O grade and H grade are most suitable for aluminum conductors, which are produced so as to correspond to 1/4 H grade. Cable specifications provide standards for tensile strength, elongation, free-bend property, 180° reverse bend property and a wrap test around a wire of its own diameter. The actual measurement values meet the requirements as shown in Table 5.

However, one of the fundamental demerits of aluminum is that it has less tensile strength than copper and, as shown later, this is an impediment to manufacturing efficiency. Other outstanding demerits of aluminum are found in splicing and corrosion.

Aluminum is a chemically active metal and its corrosion mechanism is basically different from that of chemically inactive copper. It is well known that aluminum is severally corroded by improper and wrong use. On the other hand, since aluminum is highly active, it reacts strongly on oxygen in the atmosphere and forms a film of Al_2O_3 on the surface, which works as a protective film, with a resultant increase in anticorrosiveness. The corrosion rate of aluminum is relatively high in the initial stages of exposure to the atmosphere, but in most case it rapidly drops with time and retains an excellent anticorrosive condition.

However, aluminum deteriorates due to contact corrosion with other kinds of metal as copper, brass and iron, when exposed to the air: this is particularly true in seaside areas where salt water spray is carried on the wind.

Table 4 - Physical and mechanical properties of conductors

Item		EC grade Al		Al alloy		Copper	
		O grade	H grade	O grade	H grade	O grade	H grade
Physical Properties	Purity (%)	99.8		99.2		99.9	
	Density (g/cm^3 at 20°C)	2.70		2.70		8.89	
	Conductivity (% IACS)	63.3	61.8	61.3	59.9	101.2	98.8
	Volume resistivity (Ω -cm at 20°C)	2.72	22.80	2.80	2.88	1.70	1.75
	Temperature coefficient of resistance (10^{-3}/°C at 20°C)	4.10		4.05		3.93	
	Coefficient of linear expansion (10^{-6}/°C at 20°C)	23.1		23.1		17.0	
	Thermal conductivity (Cal/°C.cm.sec at 20°C)	0.54		0.53		0.92	
	Specific heat (Cal/g.°C at 20°C)	0.213		0.213		0.092	
	Melting point (°C)	656.8		655.6		108.3	
	Latent heat (Cal/g.atm)	94.6		94.6		48.9	
Mechanical Properties	Tensile strength (kg/mm^2)	9.0	17-25	12.0	23-25	24.5	49.8
	0.2% proof stress (kg/mm^2)	4.0	19.4	5.8	24.7	8.1	46.8
	Elongation (%)	27.3	1.0	21.6	1.0	30.9	1.0
	Modulus (kg/mm^2)	5,400	6,500	5,600	6,900	8,900	10,500
	Hardness (V_H)	26	53	33	62	70	112
	Shearing stress (kg/mm^2)	4.9	–	7.4	–	16	21

Table 5 - Mechanical properties of conductors

Item	Diameter	EC grade Al		Al alloy		Copper
		Measurement value	Requirements	Measurement value	Requirements	Measurement value
Tensile strength (kg/mm^2)	0.8	10.9	9.5	-	-	-
	0.65	-		13.5	12	23.5
	0.5	-	-	13.6		24.0
Elongation (%)	0.8	10	3	-	-	-
	0.65	-		8	3	26
	0.5	-	-	8		25
(Note 1) Free-bend test (times)	0.8	30	15	-	-	-
	0.65	-		30	15	107
	0.5	-	-	39		195
(Note 2) 180°reverse-bend test (times)	0.8	12	6	-	-	-
	0.65	-		16	6	15
	0.5	-	-	17		18
(Note 3) Wrap test around a wire of its own diameter (cycles)	0.8	6	3	-	-	-
	0.65	-		5	3	5
	0.5	-	-	6		6

(Note 1) Free-Bend test

Free-bend tests are performed on the device shown in Figure.

A test piece of bare conductor fixed at the both ends shall be expanded and contracted from 80 mm to zero.

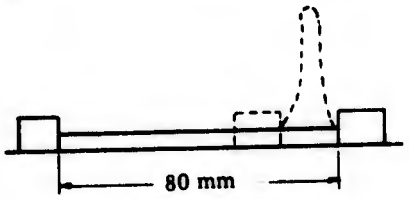

Free-bend test

(Note 2) 180° reverse-bend test

Bend tests are performed on the device shown in Figure.

A test piece of bare conductor shall be bent over a 1 mm radius.

180° reverse-bend test 6"

(Note 3) Wrap test

A piece of bare conductor shall be wrapped round a wire of its own diameter to form a close helix of 10 turns. 5 turns shall be unwrapped and again closely rewrapped in the same direction.

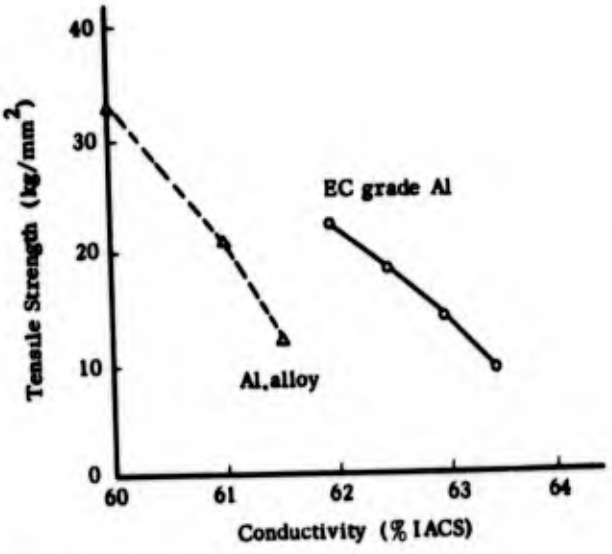

Fig. 2 - Relation between tensile strength and conductivity of Al conductor

Corrosion is roughly divided into the following types:

1) Wet atmospheric corrosion
2) Corrosion in liquid
3) Contact corrosion
4) Crevice corrosion

Wet atmospheric corrosion is a rate decreasing type. The higher the purity, the larger the anticorrosiveness due to Al_2O_3 film. Corrosion in liquid is caused by diluted inorganic acids or alkalis. But aluminum is chemically stable against a solution which is not strong enough to eat into the oxidized film. Electrochemically, aluminum is a base metal. When an electrolyte touches aluminum which is in direct contact with a different kind of metal, a local cell is formed, and in most cases, corrosion of the aluminum is accelerated. This is called a contact corrosion. Metals vary in standard electrode potential according to different electrolytes because they polarize, form a protective film or become passive in accordance with the environment. Generally, aluminum is not contact-corroded by zinc or cadmium, but is heavily contact-corroded by copper, iron or their alloys. Crevice corrosion is especially noted in power cables. When water gathers in a narrow spacing, there concentration cell action arises due to the difference in oxygen content in the water, between the part where the water is in contact with the air and the interior part shut off from the air, and such action causes corrosion. However, as compared with contact corrosion, crevice corrosion is generally so slow to progress that it does not require special attention except in areas near the seashore.

As previously mentioned, aluminum has corrosion problems which are seldom encountered with copper. Therefore these problems become restrictions in manufacture, installation and maintenance of aluminum conductor cables. During manufacture, utmost care should be taken to avoid intermixing of any different type of metal and during installation, a good connector should be used for conductor splicing. Furthermore the spliced parts have to be filled with a suitable compound or the spliced cables have to pressurized.

(2) Mass production and properties of formed polyethylene insulation:

Foamed polyethylene (PEF) is used for conductor insulation of this cable to improve its crosstalk characteristics and space factor. High density polyethylene (HDPE) with good mechanical properties is used for higher manufacturing speed for a thin-walled insulation. For HDPE blowing, a coating method has been applied to the insulation process of subscriber feeder cables with 0.32 mm conductors. This method is suitable for small diameter conductors, but is not an advantage as far as coating speed for larger diameter conductors is concerned. Therefore, an extrusion blowing method is used for aluminum conductor junction cables. This method has been practically used for toll cables with PEF insulation of low-density polyethylene (LDPE), but it has not been applicable to HDPE because the temperature for suitable melt viscosity of HDPE for high extrusion speed was higher than the decomposing temperature (190° - 220°C) of the chemical blowing agent. To solve this problem, it is necessary to reduce the melt viscosity of HDPE to make its extrusion possible at a suitable temperature for the decomposition of the blowing agent, to improve the agent or to develop a method which does not need such an agent. Along

with the recent remarkable advances on blowing techniques, various methods have come into practical use.

For reducing the melt viscosity there are various methods: 1) Swelled polyethylene method wherein a compound of polyethylene and a blowing agent is swelled with an organic solvent prior to extrusion: 2) Method of obtaining low-viscosity HDPE by blending resins having a softening effect, 3) Method of using HDPE having high flow characteristics, and 4) Gas-blow method. Methods 1) 2) 3) are chemical blowing methods using blowing agents, while 4) is a physical blowing method in which gas (chiefly nitrogen) is directly compressed into melted polyethylene without using any blowing agent. Good PEF-insulated conductors can be produced at high speed by all of the methods.

The PEF insulation thus obtained has a thin walled thickness as shown in Table 6 and uniform and closed cells as tiny as 10 μ average, and 30 μ maximum. Its dielectric constant should be around 1.95 from the necessity of making the mutual capacitance 50 nF/km and the insulation thickness equivalent to paper insulation thickness, as a result of which the expansion rate is about 20%. HDPE material has a brittleness temperature of -60°C or under and a melting temperature of 120°C or over. Other properties are shown in Table 7. Tensile strength and elongation fully meet the requirements of the specification and abrasion resistance is also satisfactory.

Table 6 - PEF insulation thickness

Conductor diameter (mm)	0.5	0.65	0.8
Insulation thickness (mm)	0.12	0.15	0.19

Table 7 - Properties of PEF insulation

Cell size	Ave. 10 μ Max. 30 μ
Expansion rate	about 20%
Tensile strength	0.5 mm : 2.2 kg/cm^2 0.65 mm : 2.0 "
Elongation	0.5 mm : 430% 0.65 mm : 450%
Abrasion resistance (NEMA type)	0.5 mm : about 16 times 0.65 mm : about 300 "
Maximum potential gradient	50 kV/mm
Thermal shrinkage (80°C x 24 hr.)	0.75 %
Thermal stress cracking (100°C x 1000 hr.)	No cracks
Environmental stress cracking (50°C x 1000 hr. Aqueous solution of Alkyl-Allyl-Polyoxyethylene)	No cracks

NEMA type abrasion tester
Diameter of abrasion-bar : 4 mm
Stroke : 10 mm
Speed : 60 times/min.
Dead weight :

mm / kg	0.5	0.65
T	0.125	0.21
W	0.5	0.5

(3) Manufacture of PEF insulated aluminum conductors:

In the manufacture of aluminum conductor cables, an exclusive "Wire drawing-annealing-extrusion tandem line" has to be employed to prevent the coexistence of other kinds of metal; especially copper powder. In particular, machines in which aluminum conductors are exposed, such as drawing machines and annealers, must have covers to protect the conductors from factory contamination. Fig. 3 shows an example of an aluminum conductor insulating tandem line. In producing aluminum conductors of a specified size, first aluminum wire is drawn into an intermediate size and fully annealed by a continuous annealer, and then reduced by about 20% by a secondary wire drawing machine. Hardness then is 1/4H - 1/8H. For quadding and subsequent processes, equipment the same as used for copper conductor cable manufacture can be used.

Because of the poor mechanical properties of aluminum, aluminum conductor production efficiency is not so good: insulation extrusion line speed is 60 - 70% that of copper conductor, quadding speed is about 80% and quad stranding and unit stranding speeds are 100%. On the whole, these factors are responsible for high aluminum conductor manufacturing costs.

5. CABLE STRUCTURE

(1) Core structure:

In aluminum conductor junction cable, PEF insulated conductors are twisted into a star quad. The cable core consists of two kinds of units, that is a 25-quad unit and a 50-quad unit, to make the cable core circular. The core structures are shown in Table 8.

The cables used by NTT for commercial tests so far are 0.8mm - 600 pairs, 0.65mm - 1000 pairs and 0.5mm - 1800 pairs. They are only the cables with the max. number of pairs for each conductor size that can be installed in a 75 mm duct. Cables of intermediate numbers of pairs will be produced in the near future.

In PEF insulation, loosening of insulation does not occur, as it does in paper insulation, and the manufacturing defect ratio is so small that spare quads have been entirely done away with.

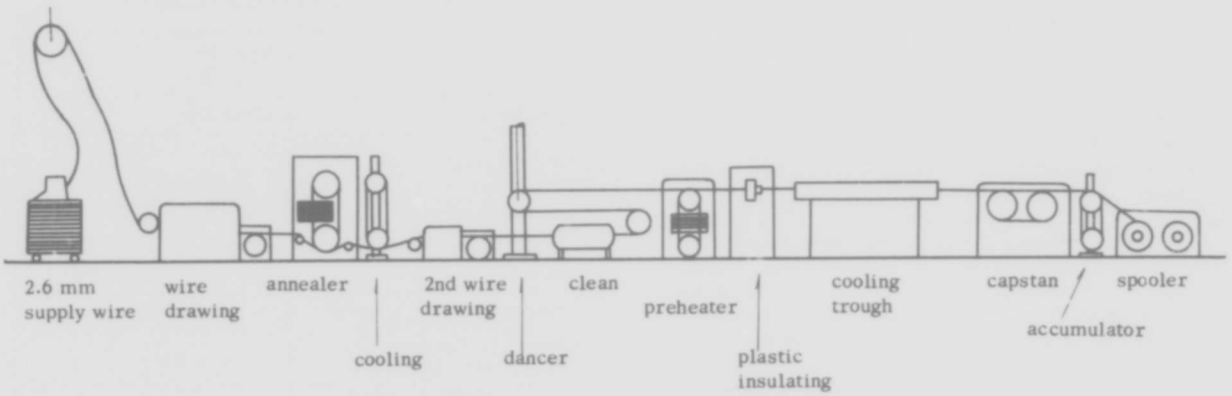

Fig. 3 - An example of manufacturing line of aluminum conductor cable

Table 8 - Core structures

Number of pairs	Number of units in each layer			Total		Remarks
	Center layer	1st layer	2nd layer	25 quad unit	50 quad unit	
600 pairs	*3	*9		12		*: 25-quad unit
1,000 pairs	*4	8		4	8	The rest are
1,800 pairs	1	6	11		18	50-quad unit.

(2) Sheath structure:

The cable core is wrapped with paper and then covered with a laminated aluminum polyethylene (LAP) sheath. In manufacturing LAP sheath, 0.2 mm thick aluminum tape bonded with 1 - 2 layers, 0.05 - 0.06 mm thick, of ethylene-copolymer film (called "laminated tape") on one side, is applied longitudinally with the film side outward over the cable core and a polyethylene jacket is extruded onto it. The heat resulting from the extruded polyethylene firmly fuses the aluminum tape to the inner surface of the polyethylene jacket. The quality of the laminated tape is controlled so that the peel strength of the plastic film of the laminated tape may be 0.3 - 0.5 kg/10 mm in width, and that of the aluminum tape of the laminated sheath may be 3 - 5 km/10 mm in width.

Because the mechanical properties of the cable deteriorate due to springing back of the overlap of the laminated tape, the overlap should be bonded tightly by hot jet, etc. after tape forming. Along with its excellent mechanical properties even higher moisture-proofness can be obtained. Fig. 4 shows the construction of the cable and Table 9 shows the size, weight, etc. of the cable.

Fig. 4 - Cable structure

Table 9 - Cable sizes

Item / Kind of cables	Cable core diameter (mm)	LAP sheath thickness (mm)	Cable diameter (mm)	Cable weight (kg/m)
0.8 mm 600 pairs	58	3.1	64	3.2
0.65mm 1000 pairs	60	3.2	67	3.4
0.5 mm 1800 pairs	62	3.3	69	3.6

6. ELECTRICAL CHARACTERISTICS

One of the greatest differences between aluminum conductor cable and copper conductor cable lies in conductivity. Therefore, resistances of 0.8 mm, 0.65 mm, and 0.5 mm aluminum conductor cables correspond to those of 0.65 mm,

0.5 mm and 0.4 mm copper conductor cables respectively. This is shown in Table 10. Capacitance and inductance of aluminum cable are nearly the same as those of a copper conductor junction cable; about 50 nF/km and about 0.7 mH/km respectively.

Table 10 - Resistance (Ω/km)

Aluminum conductor cable			Copper conductor cable		
Conductor diameter	Ave.	Max.	Conductor diameter	Ave.	Max.
0.8 mm	55.7	60.5	0.65 mm	52.5	56.5
0.65	86.3	94.0	0.5	88.7	93.5
0.5	145.9	155.4	0.4	139.0	147.5

Because of the difference in conductor resistance (R) of the primary constants, there also arises a similar difference in the secondary constants; that is "a one-rank difference". The secondary constants of 0.5 mm aluminum conductor cable as shown in Fig. 5, correspond to those of 0.4 mm copper conductor junction cable.

The static couplings between pairs within a quad used for the commercial tests are small as seen from Table 11, therefore their crosstalk characteristics are good, as shown in Fig. 6. NTT has already discontinued test splicing of copper conductor junction cables, and since the aluminum conductor cable is the same as, or better than, the copper conductor junction cable in crosstalk characteristics, its test splicing could be also abolished. But test splicing has been continued up to now in view of the irregularity of crosstalk characteristics. NTT will hereafter investigate its abolishment.

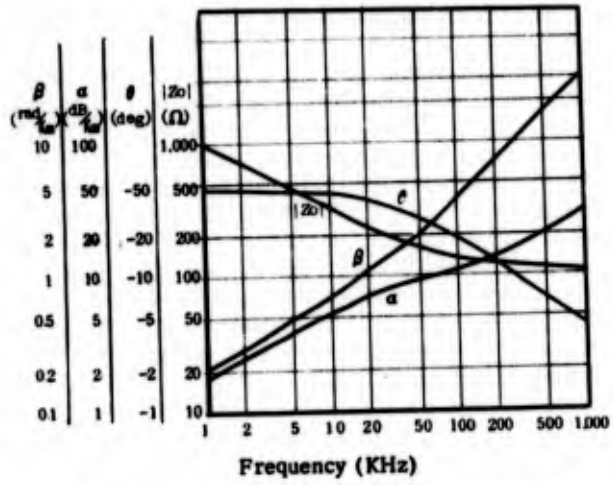

Fig. 5 - Secondary constants of 0.5mm aluminum conductor cable

Table 11 - Static couplings (pF/150 m)

Conductor diameter	Ave.	Max.
0.8 mm	17	195
0.65	16	137
0.5	17	149
Spec. regulation	less than 100	less than 600

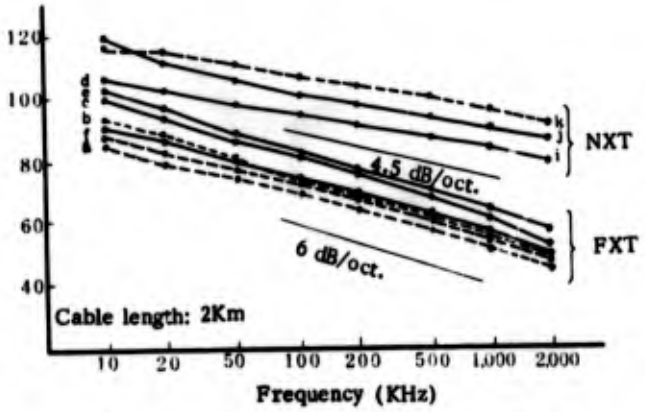

Fig. 6 - Crosstalk on non-loaded circuits of Al conductor Cable

a : Within a quad

b : Between adjacent quads

c : Between every second quads

d : Between every third quads

e : Between every fourth quads

f : Between quads in adjacent layers

i : Between quads in adjacent units (3 rd layer - 3 rd layer)

j : Between quads in adjacent units (2nd layer - 2nd layer)

k : Between quads in adjacent units (1st layer - 1st layer)

7. MECHANICAL AND PHYSICAL PROPERTIES

NTT's conventional underground multi-pair local cables have been paper insulated stalpeth (ST) sheathed. But recently, not only PEF insulation, but also the LAP sheath which is more economical than the stalpeth sheath and equal to or better in various properties have been adopted for junction cables. Aluminum conductor junction cables also use the LAP sheath, which is superior in mechanical and moisture-proof properties.

The LAP sheath is far superior to the stalpeth sheath in bending characteristics: a sharp difference in the number of bendings until aluminum tape or polyethylene sheath develops cracks or bucklings; as shown in Fig. 7. Fig. 8 shows expansion and contraction of the cable sheath when its middle is pulled by a fleeting grip. The expansion and contraction rates of the LAP sheath are about half that of the stalpeth.

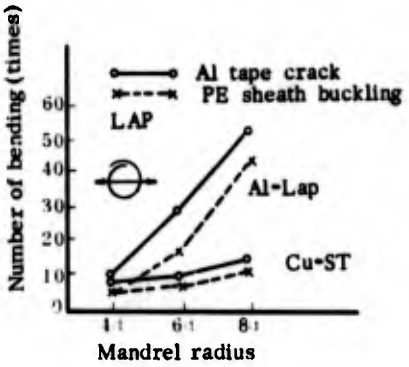

Fig. 7 - Bending characteristics

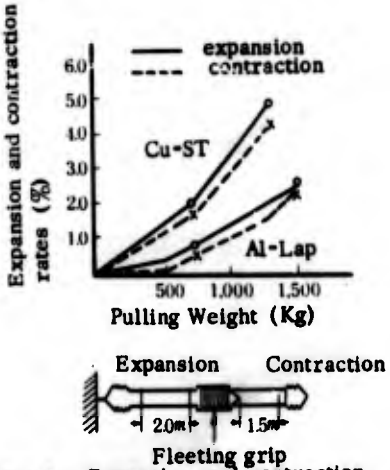

Fig. 8 - Expansion and contraction rates

As compared with PEF insulated copper conductor LAP sheathed cable, aluminum conductor cable has almost the same characteristics, such as torque and compression. However, the aluminum conductor cable shows a little larger deflection in flexibility characteristics, as shown in Fig. 9.

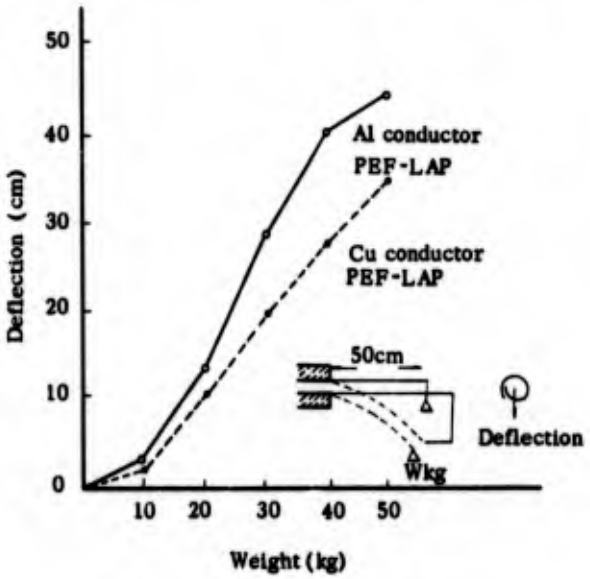

Fig. 9 - Flexibility characteristics

The permeation rate of LAP sheathed cable is calculated as follows:

(1) When the overlap of laminated tape is unbonded

$$G_1 = P. \frac{\pi}{\ell n \frac{8d}{\pi a}}$$

where G_1 = permeation rate (g/hr. cm. mmHg)
d: polyethylene jucket thickness (cm)
2a: overlap gap of laminated tape (cm)
P: permeation rate of polyethylene
$(2.2 \times 10^{-9}$ g/hr. cm. mmHg)

(2) When the overlap of laminated tape is perfectly bonded

$$G_2 = \frac{1}{\frac{1}{G_1} + \frac{1}{G_3}} = P. \frac{1}{\frac{1}{\pi} \ell n \frac{8d}{a} + \frac{}{2a}}$$

where G_2 : permeation rate (g/hr. cm. mmHg)
$G_3 : P \frac{2a}{\ell}$: permeation rate of tape overlap (g/hr. cm. mmHg)
ℓ : overlap width of laminated tape (cm)

For 0.5 mm 1,800-pairs cable, by presuming the imperfection (0.2%) of overlap bonding, the rate is given by the following formula

$$G_{LAP} = G_2 \times \frac{99.8}{100} + G_1 \times \frac{0.2}{100} = 9.7 \times 10^{-12} \text{(g/hr. cm. mmHg)}$$

This value is much smaller than that of alpeth sheath and is near that of stalpeth sheath. LAP sheathed cables may be considered suitable for practical use because it takes 42 years for relative moisture in the cable to reach 20%.

8. ALUMINUM CONDUCTOR SPLICING METHODS

(1) Various splicing methods:

The most difficult problem in using aluminum conductors for a telecommunication cable is splicing. Aluminum conductors are difficult to splice because aluminum is so highly reactionary that it quickly oxidizes and forms an oxide film. The film, though extremely thin, tightly adheres to the aluminum surface and has a high melting point, which makes it difficult to remove the film. Moreover, the film is non-conductive, therefore if aluminum conductors covered with the film are spliced, contact resistance gradually increases until conductibity disappears. Thus it is necessary to remove the oxide film when splicing and to prevent the contact surface from oxidizing again after splicing.

When splicing aluminum conductors and conventional co copper conductors, the problem of contact corrosion also arises. Because of these problems, a simple manual twist, splicing of copper conductors cannot be used for splicing aluminum conductors. Aluminum conductor splicing methods are as follows:

(1) Cold pressure welding
(2) Manual twist and soldering
(3) Arc welding
(4) Ultrasonic brazing
(5) Compression joint
(6) Connector joint

Of these methods, (1) is a method wherein conductors are butted and jointed together under high pressure at normal temperature. This is free from thermal strain and the jointed part is very stable, but it is difficult to join conductors of different diameters and the jointing device has to be large-sized; for this reason, it is used only for factory jointing. Method (2) makes use of aluminum solder, but as it needs a degree of high skill and is inferior in anticorrosiveness, it is not feasible. Method (3) uses arc welding or resistance welding equipment, but the former needs an atmosphere of argon gas, etc., while the latter calls for a large current capacity; so that they are not recommended. Spark welding method was once used, but dropped in consideration of operational efficiency and reliability. Method (4) uses an ultrasonic-wave iron which removes the oxide film with ultrasonic-wave energy. While there is no need to remove the insulation, it leaves something to be desired in mechanical strength, therefore this method is not in use. In method (5) jointing is done by compressing a conductor sleeve, but it has problems of operation and reliability regarding conductors less than 1 mmφ thick. For method (6), various connectors have been developed and reported. They are roughly divided into "clamp types" and "compression types". It is easy to obtain connectors that are high in operational efficiency and reliability, and NTT adopted a clamp type connector that can be used for aluminum conductors with an automatic splicing machine.

(2) Development of connectors:

When aluminum conductors are spliced with connectors the following four technical problems arise:

1) Presence of non-conductive oxide film.
2) Perfect shielding from oxygen required to prevent forming of aluminum oxide at contact surface.
3) Possibility of corrosion from contact with different kinds of metal.
4) Inferior mechanical strength.

A connector which is free from all of these problems has to be developed.

At first, the feasibility of using copper conductor connectors foa aluminum conductors was taken up, but becoause of a problem of reliability, a connector especially for aluminum conductors has been developed. This connector is compsed of a thread outer sleeve and a flat tapered inner pin, while the connector for copper conductor connection consists of a flat outer sleeve and a thread tapered inner pin. In the first commercial test of 0.8 mm - 600 pair aluminum junction cable, a handytool was used for aluminum conductor splicing with this connector, and good results were obtained. However, because this connector had large deviations of contact resistance when used for 0.65 mm and 0.5 mm conductors and since the threading of the inside surface of the sleeve was costly, it was rejected.

On the other hand, since a subsequently improved connector for copper conductors had a high reliability when used for aluminum conductors of various diameters, it was used in the second commercial test with an automatic splicing machine with satisfactory results. However, since the connector tended to somewhat increase contact resistance under accelerated aging tests coupled with moisture, its application is limited to only pressurized junction cable for the time being. There was a need to investigate enlarging the scope of its application to non-pressurized cables and to jelly-filled cables, so an improved connector was developed. Its properties are now being confirmed. Fig. 10 shows the structure of the connector used in the second commercial test.

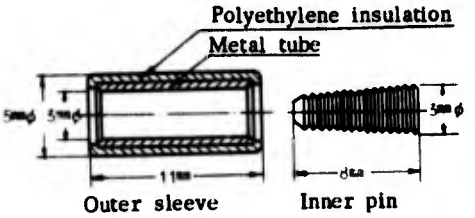

Fig. 10 Connector structure

(3) Connector performance properties:

Combined use of the above connector and the automatic splicing machine facilitates efficient, reliable and stable splicing of aluminum conductors. In other words, when the inner pin is pushed into the outer sleeve, the ridges of the inner pin peel off the oxide film and the insulation from aluminum conductors and the conductors are held rigidly between the inner pin and outer sleeve. As a result the contact surface is gas-tight, a new oxide film does not form, and as shown in Fig. 11 initial contact resistance is small with little deviation. In addition, this value remains virtually unchanged even when subjected to a thermal cycling test, - 20°C~60°C of 200 cycles, or a vibration test, 7 x 10^6 cycles, and it changes only a little even under a thermal shock test, -195°C ~ 70°C of 200 cycles. A sufficient value to hold the conductors is also obtained, and the results of a tensile strength test are shown in Table 12.

Table 12 - Tensile strength distribution of spliced points of conductor

Combinations of conductor diameters (Aℓ - PEF)	Break points		
	Outside of connector	Inside of connector	
	Conductor	100~90%*	90%* under
0.5 - 0.5 mm	91 %	9 %	0 %
0.65-0.65	90	10	0
0.8 - 0.8	100	0	0

* Ratio of tensile strength of break points to that of conductor

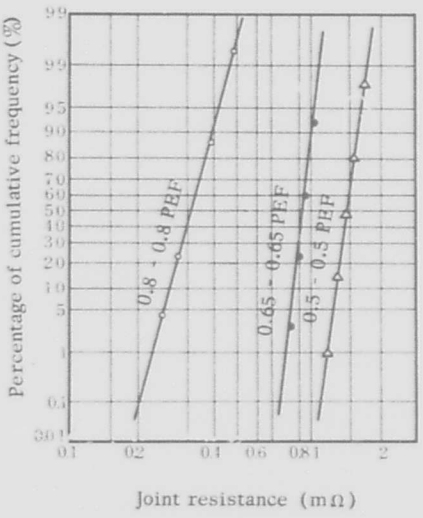

Fig. 11 - Initial joint resistance

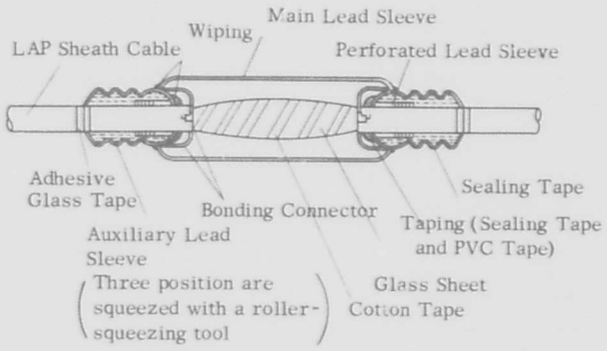

Fig. 12 - The improved auxiliary lead sleeve squeezing method using a roller squeezing tool

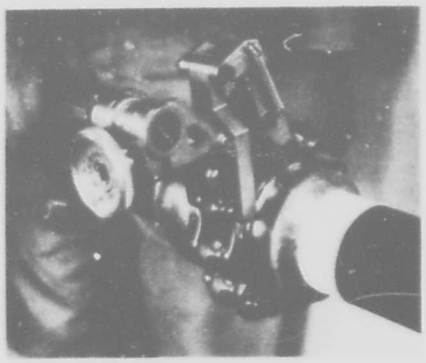

Fig. 13 - Roller - squeezing tool

9. SHEATH JOINTING METHOD

(1) Jointing method:

LAP sheaths are jointed by the conventional auxiliary lead sleeve squeezing method used for paper insulated stalpeth sheathed cables. However, it is different in that instead of using wire squeezing tools for the auxiliary lead sleeve, roller squeezing tools are used to ensure uniform squeeze and to prevent buckling of the sheath, and inner taping is used to obtain more reliable air-tightness. Furthermore, a glass sheet is used to protect the conductor insulation and the connectors at the jointed part from plumbing heat, and a bond for jointing aluminum tape is used for electrical connection of the shield. Fig. 12 shows the construction of the sheath jointing part. The jointing part made by this method is very stable and its air-tightness remains entirely unaffected when subjected to a thermal shock test - $30^{o}C \sim 70^{o}C$ of 100 cycles and a vibration test, 10^{6} cycles.

(2) Jointing tools and materials:

Unlike the wire squeezing method in which the auxiliary lead sleeve is squeezed by a wire squeezing tool, the roller squeezing method squeezes it by coupled rollers. Fig. 13 shows the appearance of the tool. The number of rollers suitable for the size of the auxiliary lead sleeve are selected, and after the rollers are fitted onto the lead sleeve, they are turned around the sleeve. The sleeve is then squeezed gradually, and when a suitable squeeze depth is reached, a warning is sounded, indicating the end of squeezing. The glass sheet is a laminated sheet consisting of glass wool, aluminum foil and a glass cloth. It has a heat shielding effect that does not permit the surface temperature of the conductor splicing part to go beyond $70^{o}C$ at the time of plumbing, and it also has good operational efficiency. The bond for jointing aluminum tape is directly compression-bonded to the LAP sheath, thus ensuring a low-resistance stable electrical connection.

CONCLUSION

As explained previously, various problems of aluminum conductor junction cable have been solved, and the cable has become feasible for practicable application as a substitute for copper conductor cable. However, with the goal of abolishing the necessity for test splicing and establishing aluminum conductor cable manufacturing technology, further commercial tests will be conducted from the autumn of 1974.

It is thought that aluminum conductor cable will prove economical when installed in a cable tunnel, but additional duct construction may often be necessary for installation in a duct. The economical considerations in the latter case are to be further studied, but in view of current soaring copper prices, aluminum conductor cable is economically promising.

NTT began commercial tests on the connector and the automatic conductor splicing machine in 1972, and they are expected to operate commercially in 1974.

HIDEO FUKUTOMI

Nippon Telegraph and
Telephone Public Corp.
1-1-6 Uchisaiwai-Cho,
Chiyoda-Ku, Tokyo,
Japan

Hideo Fukutomi, Staff Engineer, Engineering Bureau, N T T, is now in charge of the comprehensive business regarding the development of outside plant. After jointing N T T in 1956, he was engaged in outside plant construction and maintenance work.

He received his B. E. degree in electrical engineering from Waseda University in 1955, and is a member of the Institute of Electronics and Communication Engineers of Japan.

TAKENOBU HIGASHIMOTO

Sumitomo Electric Industries, Ltd.
1 Taya-Cho, Totsuka-Ku,
Yokohama, Japan

Takenobu Higashimoto is a staff member of communications R & D Department of Sumitomo Electric Industries, Ltd., and is mainly engaged in the development of the aluminum conductor telephone cable.

He received his B. S. degree in Mechanical Engineering from Kyoto University in 1969.

SHUNJI KAIBUCHI

Nippon Telegraph and
Telephone Public Corp.

1-1-6 Uchisaiwai-Cho,
Chiyoda-Ku, Tokyo,
Japan

Shunji Kaibuchi is Staff Engineer, Outside Plant Division, Engineering Bureau, NTT, and is now in charge of the development of outside plant. After jointing NTT in 1959, he was mainly engaged in the design and construction of telecommunication plants.

He received his B. E. degree in electrical engineering from Tokyo University in 1959, and a member of the Institute of Electronics and Communication Engineers of Japan, and that of Electrical Engineers of Japan.

HIDEO CHIBA

The Fujikura Cable Works, Ltd.
1440 Mutsusaki, Sakura-Shi,
Chiba-Ken, Japan

Hideo Chiba is senior engineer, Research & Development Laboratory and Telecommunication Cable Engineering & Development Dept., The Fujikura Cable Works, Ltd. He is engaged in the development of metals for wire and cable, and the production engineering of telecommunication cable.

He received his B. E. degree in metallurgical engineering from Iwate University in 1962, and is a member of the Japan Institute of Metals.

AKIRA TOYOKAWA

The Furukawa Electric Co., Ltd.
2-6-1 Marunouchi, Chiyoda-ku, Tokyo,
Japan

Akira Toyokawa is Assistant Manager, Engineering Section, Telecommunication Division, The Furukawa Electric Co., Ltd., and is mainly engaged in the designing of telecommunication cable.

He received his B. E. degree in telecommunication engineering from Yamagata University in 1961, and is a member of the Institute of Electronics and Communication Engineers of Japan.

MATERIAL SAVINGS BY DESIGN IN EXCHANGE AND TRUNK TELEPHONE CABLE
PART I: WATERPROOF CABLE WITH DUAL INSULATION

By

D. M. Mitchell
Bell Laboratories
Atlanta, Georgia

Abstract

Waterproof cable with dual expanded insulation uses less plastic while retaining service reliability. Aluminum conductor has been incorporated to conserve copper and reduce cost without compromise of design capability. Fine-gauge, low capacitance copper cable using dual expanded insulation can match the performance of 22-gauge pulp cable at carrier frequency, while continuing to provide adequate voice frequency facilities. There are savings both in conductor metal and in more efficient duct use.

INTRODUCTION

As plastic insulation materials become more expensive and their procurement becomes more difficult, design alternatives must be sought to assure the continued availability of telephone cable at reasonable cost. Similar considerations require that an acceptable substitute be found for copper, the traditional choice for general electrical conductor applications.

It is well known that expanded insulation offers two important attributes in meeting the above need:

1. Dielectric constant is lowered, Fig. 1, permitting reduced wall thickness for equivalent capacitance characteristics, Fig. 2.

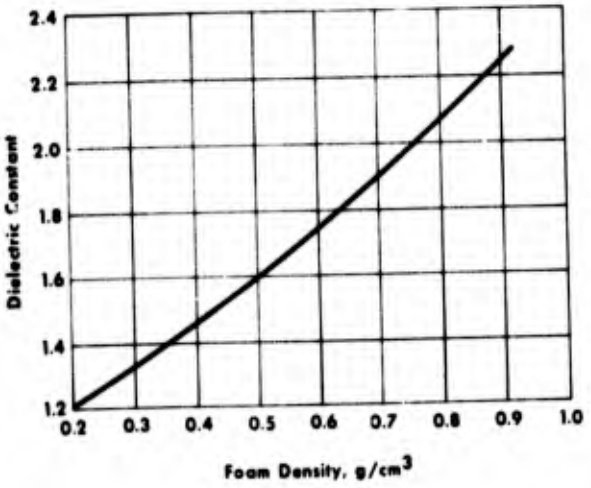

FIGURE 1

DIELECTRIC CONSTANT vs. FOAM DENSITY

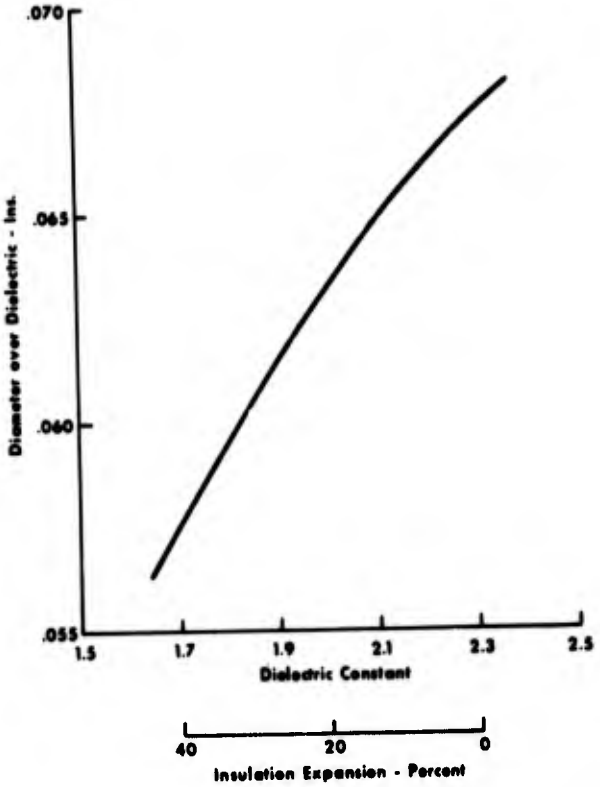

FIGURE 2

20 GAUGE CONDUCTOR HIGH DENSITY POLYETHYLENE

2. A portion of the insulation cross section is occupied by void spaces.

The combined effect is a significant reduction in consumption of insulation material, Fig. 3. Related technology has been the subject of several papers at previous Symposia.[1-10]

Aluminum, by reason of its abundance in the earth's crust and relatively good conductivity, has attracted interest[5] as an economic replacement and critical supplement for copper.

Waterproof cable for buried distribution plant[11,12] has experienced rapid acceptance as a reliable transmission medium with the added advantage that buried installation imposes negligible alteration of the environment. The filling system in waterproof cable is an effective dielectric as well as water-blocking agent. Because it represents a sizeable and growing portion of

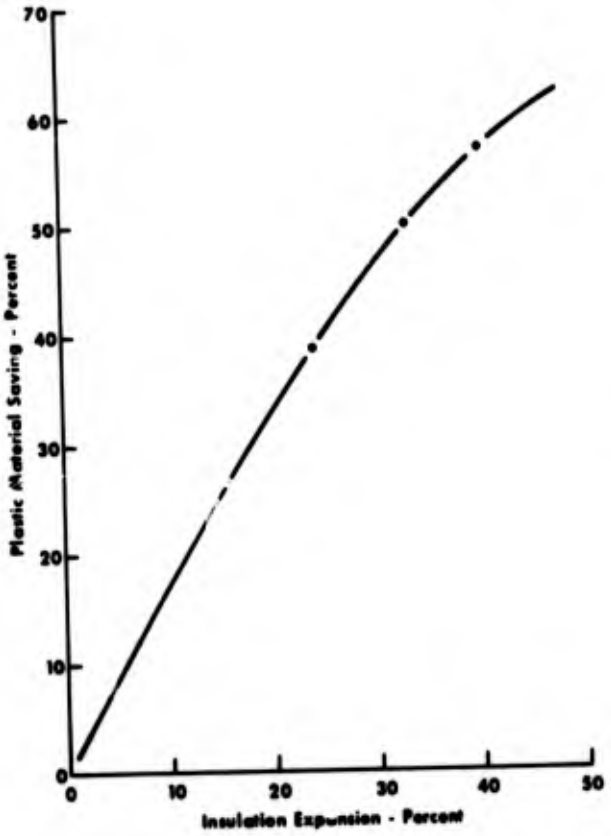

FIGURE 3

20 GAUGE CONDUCTOR HIGH DENSITY POLYETHYLENE

multipair cable production, because maximum benefits can be realized from plastics savings (since heavier equivalent wall thickness is required than for comparable air core PIC), and because it provides a protected environment in which new technology can be safely introduced, waterproof cable has been selected by the Bell system for design modifications in the interest of material conservation and cost savings.

A development program has been undertaken based on the benefits to be derived from expanded insulation in waterproof cable and from the availability of a system utilizing aluminum conductor. The results are reviewed in this paper and represent the joint efforts of Bell Laboratories and Western Electric Procut Engineering Control Center (PECC).

EVALUATION OF EXPANDED INSULATION

The first comparison to be made is that between expanded insulation in general and equivalent solid forms. While expansion provides a means of extending available material supplies and reducing material cost, replacement of solid insulation with an expanded version imposes, in varying degrees, some combination of the following considerations:

a. reduced dielectric strength,

b. less resistance to mechanical damage,

c. greater cable attenuation at carrier frequencies for the same mutual capacitance, due to conductor proximity effects)

d. increased interaction with filling compound in waterproof cable,

e. added complexity in wire insulating and cable manufacturing processes.

A decision to use expanded insulation and the section of a suitable form should be made with these considerations in mind; relative importance can, of course, vary considerably with individual circumstances.

Expanded insulation in its simplest form consists of a cellular structure with more-or-less uniform voids; its use in waterproof cable has been discussed.[9] In the absence of a specific provision to seal the outer surface, or otherwise impede permeation, the possibility exists that surface porosity may permit the entry of filling compound to the cell structure by mass flow, as well as by slower and more limited diffusion mechanisms.[13] The result is a more rapid and possibly more extensive degradation of dielectric properties with time. If, however, the economic benefits of expansion can be achieved while maintaining a continuous outer surface, it is reasonable to expect improvement in dielectric strength and in resistance to mass transfer of filling compound into the cell structure. The latter characteristics, in turn, should contribute to improved resistance to high-voltage breakdown and to reduced change of dielectric properties.

Specialized versions of expanded insulation include controlled structure providing increasingly fine cell size outward from the conductor[10] or the formation of a film seal over a uniformly expanded coating. While both approaches offer improved surface properties, a third possibility, combines control of surface characteristics with other important features.

Dual insulation, Fig. 4, consists of an expanded core of plastic material surrounded by a solid skin having controlled thickness. Foamed core and solid skin are processed in separate extruders and the two melt streams are combined in a one-pass insulation process. The technical features have been discussed at a previous Symposium[6] under the name "Foam-Skin"; the name used here is "dual expanded plastic insulated conductor," or DEPIC.

DEPIC design allows the desirable properties of solid and expanded insulation to be combined in a manner which effectively utilizes the advantages of each. The cellular layer is closest to the conductor where reduced dielectric constant is more effective in lowering capacitance and the solid coating is at the outside for improved surface properties.

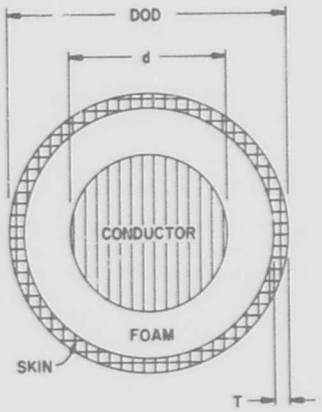

FIGURE 4

DUAL INSULATED CONDUCTOR

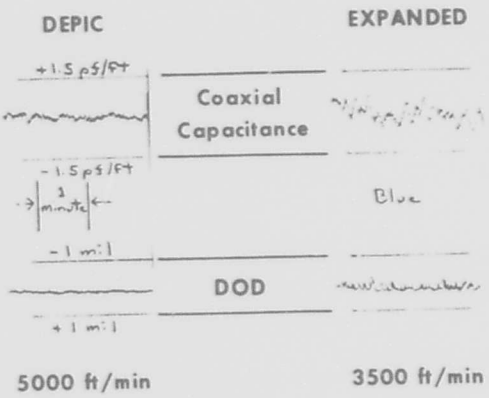

FIGURE 5

Additional features commend the choice of DEPIC for expanded insulation:

a. Pigment can be eliminated from the expanded core of color coded conductors. The dielectric properties of the foam are thus improved since a source of "degradation" is eliminated; furthermore, possible interaction between blowing agent and pigment is avoided, and less pigment is required for given color intensity. Color quality in production wire is comparable to that of solid insulation. Since pigment is confined to the skin where it is relatively ineffective in altering insulation properties, limitation of maximum concentration is less critical.

b. Improved capacitance and diameter control is possible at insulating, Fig. 5, resulting in reduced capacitance unbalance for finished cable.

An offsetting factor of considerable importance in comparing DEPIC to other expanded designs, is the initial investment in additional extruders, specialized die tooling and process control equipment.

Following review of the comparative features mentioned above, DEPIC design was selected for use in waterproof cable within the Bell System. That choice is due in large measure to the process capability which has been developed by the Western Electric PECC organization.

GENERAL DEPIC CABLE DESIGN CONSIDERATIONS

Degree of core expansion and thickness of solid skin are important variables in establishing the physical and electrical characteristics of dual insulation, as well as in determining the economics with respect to solid insulation. Preliminary analysis was made using computer techniques to evaluate a design and cost model for various combinations of conductor diameter, diameter-over-dielectric (DOD), number and spacing of conductors, and the related dielectric constants of the insulation and the surrounding medium.

Based on the analysis and on evaluation of experimental and production wire, nominal expansion levels of 40-to-45% and skin thickness of 2 mils were selected for wire sizes from 17 ga. to 26 ga. From the dielectric properties thus determined and coaxial capacitance values required to meet design mutual capacitance of 0.083 μf/mi, values of DOD were obtained. Typical cross sections of insulated wires are shown in Fig. 6; Western Electric has been able to maintain skin thickness of .002 ± .0002 5-inch on a production basis.

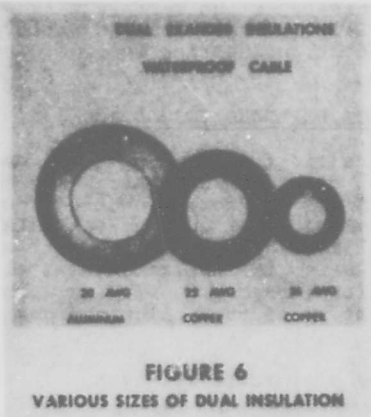

FIGURE 6
VARIOUS SIZES OF DUAL INSULATION

Design conditions have been verified by evaluation of completed cables. Significant size reduction is obtained, Fig. 7, with reduced bending resistance, Fig. 8, for improved handling during unreeling and placement. Transmission test results, Fig. 9, while satisfactory, show an attenuation level higher than that of waterproof cable with solid insulation, although less than that of air core cable.

	DIAMETER (INCHES)	
	Insulation	Core
Solid	.052	1.03
DEPIC	.045	0.88
% Reduction	13.5	14.5

FIGURE 7

DEPIC vs. SOLID INSULATION

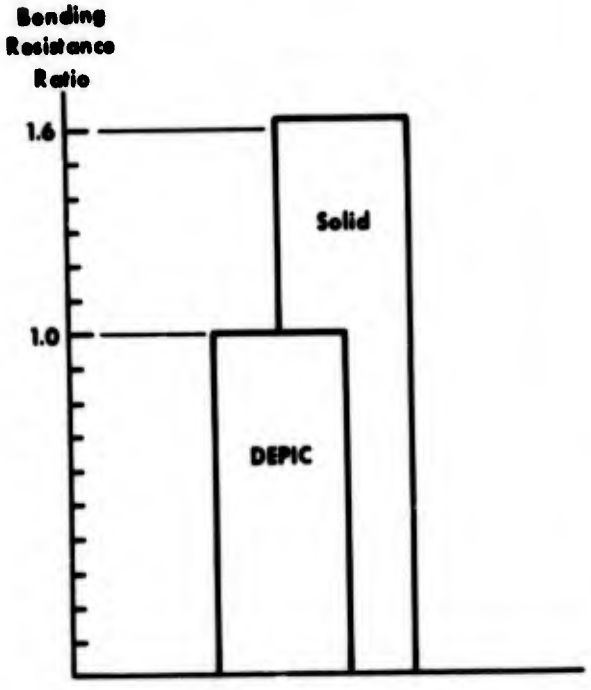

FIGURE 8

WATERPROOF CABLE STIFFNESS @ 0°F

50 PAIR, 22 GAUGE, COMMON SHEATH DESIGN

CABLE	α dB/mi		C μF/mi	
	Before[a] Aging	After[b] Aging	Before[a] Aging	After[b] Aging
Solid Waterproof	20.6	20.3	.083	.082
DEPIC Waterproof	22.3	22.1	.083	.082
Solid Air Core	23.2	—	.083	—

a) Measured @ 75°F

b) Measured @ 72°F after sixty 12-hour cycles, 70°F to 160°F

FIGURE 9

TRANSMISSION CHARACTERISTICS 22 GAUGE CABLE 772 kHz

With the exception of increased attenuation at carrier frequencies, which may require special consideration, DEPIC can be substituted directly for the current solid insulation in waterproof cable system design. Reliable joints can be made with self-encapsulating connectors[14,15] in wires from 17 to 26 gauge. Present filled closures are satisfactory for below-ground splices of current pair-sizes, and standard pedestals and closures (as currently recommended for waterproof plant) are employed for above-ground terminations. Early manufacturing experience has confirmed technical and economic feasibility and a field trial program has verified that normal burial, splicing, and terminating practices are satisfactory.

WATERPROOF DEPIC ALUMINUM CABLE

If copper supplies become critically restricted, the capability to use aluminum conductor may assume an importance overriding technical or economic qualifications. That eventuality, as well as the desire to maintain a flexible economic position and the advent of waterproof cable, has renewed interest within the Bell System in the development of aluminum conductor for exchange cable. The susceptibility of aluminum to corrosion when under electrical potential in the presence of moisture has meant that applications had to be restricted to carefully engineered portions of the plant; however, current waterproof systems technology establishes a level of reliability which renders aluminum conductor technically and economically attractive.

DEPIC design is an effective complement to waterproof aluminum cable. The reduced conductivity of aluminum relative to copper requires an increase of two gauge sizes for comparable transmission properties, but the reduction in DOD which is made possible by dual insulation significantly limits the increase in cable size, e.g. 20

gauge DEPIC aluminum wire is 14% smaller than the solid equivalent, resulting in comparative core diameters as shown in Fig. 10.

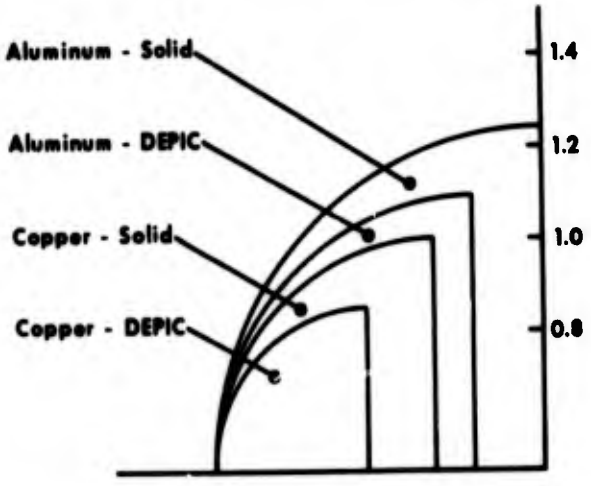

FIGURE 10

RELATIVE CORE DIAMETERS OF COMPARATIVE WATERPROOF CABLES

- INSULATION — 50 %
- FILLING COMPOUND — 22 %
- CORE WRAP — 8.5%
- SHEATH
  - Aluminum — 13 %
  - Steel — 10 %
  - Plastic — 14 %

FIGURE 11

MATERIAL SAVINGS WATERPROOF CABLE DUAL HDPE vs. SOLID PP INSULATION

Waterproof DEPIC aluminum when used in conjunction with encapsulating connectors, filled closures, fixed-count terminals, and filled service wire provides an engineered system for reliable service in buried and underground trunk and feeder applications, as well as certain feeder routes with incidental distribution.

MATERIAL CONSERVATION AND ECONOMICS

The substitution of dual insulation for solid in waterproof cable results in important material savings. An appreciable portion of the insulation volume is occupied by cell structure and reduced dielectric constant permits smaller DOD for the same cable capacitance; thus substantially less compound is required. Resulting smaller core diameters require less filling compound, binders, core wrap, and sheath materials, Fig. 11.

Cost savings, relative to solid insulation, are predicted for waterproof DEPIC cable based on reduced comsumption of insulation and sheath materials as well as increased handling capacities of wire reels, core trucks, and cable reels.

Fig. 12 compares material costs (exclusive of labor and load) for comparable waterproof cables based on August, 1974, prices. Attention is called specifically to the improvement in relative saving, approximately 17 percent vs. 7 percent, which results from the use of dual insulation on aluminum conductor compared to its use on copper. This results from the fact that for aluminum conductor insulation cost is a large portion of material cost.

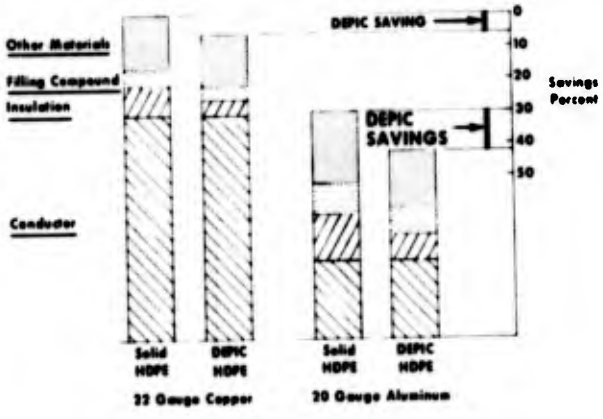

FIGURE 12

RELATIVE MATERIAL COSTS FOR 100-PAIR WATERPROOF ASP CABLE

MANUFACTURING AND SERVICE EXPERIENCE

Western Electric Company, Atlanta, is currently manufacturing 20 gauge, waterproof DEPIC aluminum cable in sizes up to 300 pair. A program for controlled introduction is being administered jointly be AT&T, Bell Laboratories, and Western Electric. 17 gauge, 100-pair aluminum cable has been made and tested. Manufacturing experience has been satisfactory and field reports have indicated no unusual problems in handling, placement, and initial service. Limited commercial quantities of waterproof DEPIC copper cable have been made in 22 and 26 gauge, up to 100 pair and 19 and 24

gauge wire have been insulated. Manufacturing feasibility has been demonstrated and detailed evaluation has shown the design to be practical and reliable. Installation of facilities for DEPIC copper will commence early in 1975.

SUMMARY

The technical feasibility of waterproof DEPIC exchange cable with copper and aluminum conductor has been adequately demonstrated. Important material savings are made possible, reducing demands on available supplies and offering attractive cost savings. Waterproof DEPIC cable offers the user:

1. Reduced cable size with improved handling flexibility,
2. An optional aluminum design which
   a. provides a practical alternate conductor material,
   b. enhances the savings potential of aluminum substitution, and
   C. reduces the increase in cable size for equivalent conductivity.
3. Continued reliability in buried plant.

REFERENCES

1. Dean, N. S., Wardley, B. J., and Walters, J. R., "A Report on the Further Progress made in the Application of Cellular Plastics to Telephone Cable Design and Manufacture," Proc. 18th International Wire and Cable Symposium.
2. Asai, A., Jitsukawa, M., Fujiwara, Y., and Utsumi, A., "A Method for Manufacturing Polyolefin Insulated Communication Cable by Solvent Injection Foaming Process," Proc. 19th International Wire and Cable Symposium.
3. Kato, Y. and Ohshima, H., "A Foaming Process for Wire Insulation," ibid.
4. Tanaka, S., Tsujikawa, A., Ishihara, H., and Ogawa, K., "A New Foamed Polyethylene Insulated Junction Cable for Telecommunication," Proc. 20th International Wire and Cable Symposium.
5. Patout, P., "Pure Aluminum Conductors in Fully Filled Celiular Polyethylene Insulated Telephone Cables," ibid.
6. Gouldson, E. J. Farago, M., and Baxter, G. D., "Foam-Skin, A Composite Expanded Insulation for Use in Telephone Cables," Proc. 21st International Wire and Cable Symposium.
7. Sato, Y., and Yoshida, Z., "A Process of Manufacturing Foamed Polyethylene Insulation by Using Low Hydrocarbon as Blowing Agent," ibid.
8. Normanton, J. K., "Extrusion of Telephone Cable Insulation Using Expandable Medium Density Polyethylene Compounds," ibid.
9. Foord, S. G., "Compatibility Problems in Filled Cellular Polyolefin Insulated Telephone Cables," Proc. 22nd International Wire and Cable Symposium.
10. Beach, S. M., Cretneg, D. F. and Ruskin, J., "Cellular Polyethylene Insulated Fully-Filled Cable with High Dielectric Strength," ibid.
11. Dean, N. S., "The Development of Fully Filled Cables for the Telephone Distribution Network," Proc. 17th International Wire and Cable Symposium.
12. Biskeborn, M. C. and Dobbin, D. P., "Waterproof Plastic Insulated Multipair Telephone Cable," ibid.
13. Aloisio, C. J., and Nelson, E. D., "Effect of Water and Petroleum Jelly Migration on Capacitance of Plastic Insulated Cables," Proc. 22nd International Wire and Cable Symposium.
14. Frey, D. R., Smith D. T., and Pasternak, J. P., "700 Series Connectors for Aluminum and Copper Telephone Cable Conductors," Proc. 21st International Wire and Cable Symposium.
15. Henn. R. W., "Systematic Encapsulated Cable Splicing Connectors for Aluminum and Copper Wires," Proc. 22nd International Wire and Cable Symposium.

D. M. Mitchell
Bell Laboratories
Atlanta, Georgia

D. M. Mitchell is a graduate of Newark College of Engineering, BS-ME. He joined Bell Laboratories in 1954. A major portion of his career has been devoted to ocean cable development. Since 1971 he has been associated with the Transmission Media Laboratory and has been most recently engaged in waterproof cable development.

Acknowledgement: Many colleagues within Bell Laboratories and Western Electric have made important contributions to the Dual Insulation Project; the work of T. S. Dougnerty, Western Electric, Product Engineering Control Center, is particularly noteworthy.

MATERIAL SAVINGS BY DESIGN IN EXCHANGE AND TRUNK TELEPHONE CABLE

Part II: METROPOLITAN AREA TRUNK CABLE

G. H. Webster
Bell Laboratories
Atlanta, Georgia

Introduction

Trunk cables between central offices in cities are characterized by their short runs and high traffic densities. They are placed in ducts which are often limited in number and invariably costly. While many trunks still operate at voice frequencies (VF), the T1 carrier system,[1] which was designed for this market, has gained tremendous acceptance. It provides 24 voice channels on two cable pairs, one for each direction of transmission. The pairs are normally 22-ga. 83 nF/mile pulp pairs so that the T1 repeater spacing is near 6000 ft. and the repeaters can be housed in the oversize manholes provided at this spacing for the loading coils of VF circuits.

Typically when a route needs reinforcement a 900 pair 22-ga. pulp cable will be installed. This is the maximum size of cable for many of the ducts already in place. Initially this cable will provide mostly VF circuits. Growth is accommodated by adding more T1 systems (hence the choice of 22-ga. cable). Regular 900 pair cable accommodates up to 200 two-way systems; transversely screened cable[2] close to 450. Such heavy incursions of T1 raised the question of whether 22-ga. pulp pairs were the optimum for this application even though the T1 system was initially designed around them. It turns out that there are attractive alternatives.

The metropolitan area trunk (MAT) cable which has evolved, is a low capacitance design with 25- or 26-ga. copper conductors and expanded plastic insulation. It has these capabilities compared to 22-ga. pulp cable:

- Matches its T1 frequency loss and at least equals its crosstalk performance.
- Saves 50% or more of the copper and will cost appropriately less.
- Allows 30% to 50% more pairs in a duct.
- At least 35% lighter: easier installation.

Moreover, its VF loss is close to that of 24-ga. cable.

However, the MAT cable is not a straightforward substitute for 22-ga. pulp cable. Not only is its DC resistance unavoidably higher, but both VF and T1 carrier equipments need modification to match its different impedance and loss versus frequency characteristics.

At this writing, experimental MAT cables have confirmed the theoretical designs. Initial studies indicate Bell System savings in cable and duct in the tens of million dollars a year if the MAT cable gains full acceptance. More elaborate studies to determine equipment penalties are proceeding. Whatever the present outcome the cable design principles involved will look increasingly attractive as trends to lower electronics costs relative to cable costs continue.

Attenuation Considerations

Using conventional notation the VF loss of a pair in a multipair cable is well represented by:

$$\alpha_{VF} = \sqrt{\frac{R\omega C}{2}}$$

Here R is the DC resistance of the wire and is inversely proportional to the wire's cross-sectional area. For a wire diameter d and at a given frequency we can write

$$\alpha_{VF} = K_1 \frac{\sqrt{C}}{d}$$

where K_1 is a constant.

If we start with an 83 nF/mile cable pair and hold the diameter of the insulation constant while we shrink the wire

diameter, the reduction in d will cause the attenuation to rise. But about half of this rise will be nullified by the reduction in C, the mutual capacitance of the pair.

At high frequencies, at say 772 kHz, the frequency of maximum power for the T1 carrier system, and in a plastic insulated conductor (PIC) cable where conductance is negligible, an excellent approximation for loss is

$$\alpha_{HF} = \frac{R}{2}\sqrt{\frac{C}{L}}$$

At this frequency the current is carried predominantly by the outer skin of the wire so that the resistance R is proportional to 1/d. Thus:

$$\alpha_{HF} = K_2 \frac{\sqrt{C}}{d} \cdot \sqrt{\frac{1}{L}}$$

where K_2 is a constant.

If we now repeat the wire shrinking experiment, not only does the decrease in C help compensate for the reduced wire diameter, exactly as in the VF case, but there is an increase in the HF inductance L to further mitigate its effect. Overall the HF loss is affected less by the reduction in wire size than is the VF loss.

Percentage changes in the constants of interest for both VF and HF in shrinking wire size from 22-ga. to 26-ga. in PIC pairs can be seen by comparing lines 1 and 2 in Table 1. In the table the metamorphosis is continued in line 3 where 40% expanded plastic is substituted for the solid plastic originally assumed, with the objective of further reducing both losses by reducing C. Finally, in line 4, because the HF loss has now fallen to less than its initial value, some insulation can be removed (the diameter over dielectric (DOD) can be reduced), to restore it to its initial value.

By going through this illustrative sequence we now have a 26-ga. expanded plastic insulated pair design which matches the HF attenuation of a 22-ga. PIC pair, has a 10% smaller diameter and, incidentally, a VF loss some 3% less than that of 24-ga. PIC pair. The material savings in this example are 60% in conductor, 40% in plastic insulation and some 10% in sheathing materials.

Choice of Conductor and Insulation

A primary objective of MAT cable is to match the T1 repeater spacing of 22-ga. pulp cable. That is, the loss is to be 32 dB in the maximum repeater spacing of 6300 ft., equating to 26.8 dB/mile at 772 kHz. The conductor will be of copper (aluminum is too bulky for duct use) and the insulation will be high density polyethylene or polypropylene with an effective expansion near 40%. Effective expansion is named because a dual expanded construction is used consisting of a highly (say 45%) expanded layer of natural material with an outer 2 mil skin of pigmented material. An acronym for this construction is DEPIC: dual expanded plastic insulated conductor. Compared with the non-skinned expanded insulation, DEPIC has advantages in ruggedness and dielectric strength; in manufacture, it avoids interaction of pigments on blowing agents and, also, entrapment of gas by the skin leads to more efficient blowing so there can be less blowing agent and residue. The advantages of this type of construction for waterproof cables have been documented at a previous Symposium,[3] and in PART I of this paper.

TABLE 1: EFFECTS OF STEP-BY-STEP TRANSFORMATION OF CABLE PAIRS

	VF			HF			
	R	C	α	R	L	C	α
1. 22-GA. PIC	100	100	100	100	100	100	100
2. 26-GA. WIRE	253	67	130	151	146	67	102
3. EXPAND	253	55	118	151	146	55	93
4. REDUCE DOD	253	59	122	153	138	59	100

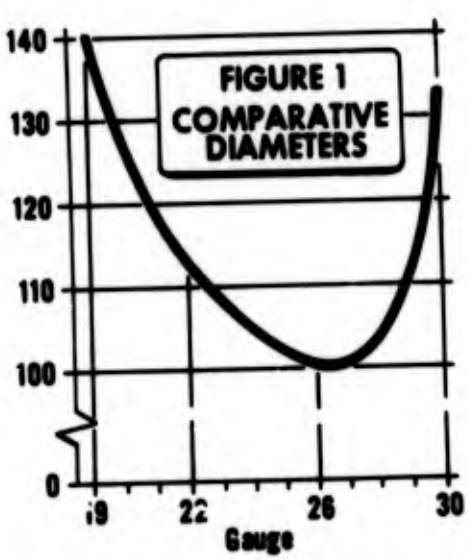

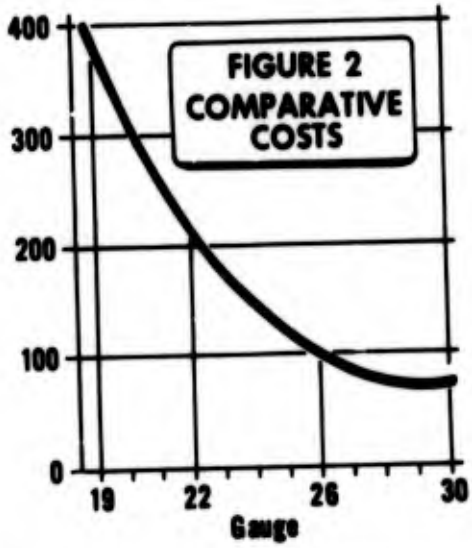

Figs. 1 & 2: EXPANDED PLASTIC INSULATED CABLES GIVING 6300' T1 REPEATER SPACING

Comparative diameters and cable costs for a range of cables having the specified attenuation are shown above. Note first from Fig. 1 that minimum diameters are achieved with 26- to 27- ga. conductors. This is a vital consideration for duct cables. The cable cost curve of Fig. 2 was derived for a particular set of raw material and manufacturing costs and will vary as these change; its general shape will not. It is not surprising that overall cable cost reduces as wire size shrinks because copper is the major cost component. However, the rate at which costs are reducing is quite slow in the range of minimum diameters. It is practical, for manufacture, field handling and splicing, and tolerable DC resistance, to choose conductors not smaller than 26-ga.

Experimental 26-ga. cables, first one of 50 pair and then a 600 pair screened cable, confirmed all theoretical predictions. Results of interest with appropriate pulp cable data for comparison appear in Table 2.

TABLE 2

CABLE CHARACTERISTICS

		26-GA. MAT	PULP 22-GA.	PULP 24-GA.
α dB/kft.	1 kHz	0.46	0.35	0.44
	772 kHz	5.1	5.1	6.2
Z_o	772 kHz	130Ω	95Ω	
$R_{D.C.}$	Ω/kft.	42	16	
C	nF/mi.	58	83	

Prospective MAT Cable Designs

Duct space in cities is so valuable that only large cables are warranted. Also, the cables may include a transverse screen to permit full-fill single cable T1 operation. We calculate that a 1400 pair cable will have an O.D. near 3" and be suitable for pulling into 3¼" square or 3½" round ducts while an 1800 pair cable with an O.D. near 3.3" will be useful for the newer and larger ducts.

As presently proposed both cables will feature:

- 100 pair multiunits (4x25 pair units)
- PIC type color coding within multiunits
- Multiunit identification by position and very elementary binder color code.
- Oscillated layer units and new twist scheme for crosstalk improvement.

There is no strong incentive to improve crosstalk performance over that of 22-ga. pulp cable since that serves the T1 system adequately. However, improvements which add virtually nothing to cable costs cannot be reasonably overlooked in a new cable design.

VF Considerations

The 26-ga. MAT cable design's capabilities for transmitting T1 carrier have been established. However, at least a fair proportion of the pairs, and initially probably the majority, will serve as loaded VF trunks or provide special services. The distribution of lengths of VF trunks in the Bell Network is such that, if the loaded MAT cable cannot match the attenuation of loaded 24-ga. pulp cable, a large number of extra VF repeaters will be needed and their cost will offset an appreciable portion of the projected System savings. VF attenuation figures are given in Table 3. It can be seen that the 26-ga. MAT cable falls short of this objective. However, a MAT cable with a 2 mil larger conductor, increasing it to 25-ga., and still engineered for 6300 ft. T1 repeater spacing, looks satisfactory.

TABLE 3

VF ATTENUATIONS (dB/kft)

	NON LOADED	H-88* LOADED	OTHER LOADING
24-GA. PULP	0.44	0.23	
26-GA. MAT	0.46	0.29	0.26 (H-125)
25-GA. MAT	0.43	0.25	0.23 (H-110)

*88mH at H(=6000') spacing

What are the penalties in this increase in conductor size? While a 26-ga. conductor saves 60% of the copper compared with the 22-ga. conductor it seeks to replace, the 25-ga. conductor saves only 50%. Next, a glance at Figure 1 will show that the 25-ga. cable is, not unexpectedly, larger than that of 26-ga. Fortunately, the increase is less than 2% in diameter. Such a small increase turns out to be insignificant because of the necessary quantization to cable counts in even round hundreds of pairs which will comfortably accommodate a bisecting screen.

Prospects

The T1 carrier system has enjoyed unparalleled success because it could increase twelvefold the traffic carrying capacity of the 22-ga. pulp cables generally available in cities. No less important it is a rugged and reliable system. But 22-ga. 83 nF/mile pulp cables are far from optimized for T1 transmission. The proposed MAT cable is optimized for it in much the same way as LOCAP cable[4,5] is optimized for the T2 system. Moreover, MAT cable can make efficient use of city ducts and, with some compromise (to 25-ga. conductors) can provide acceptable and still needed VF trunks.

Questions to be answered are: At what point in the growth of T1 carrier systems in cities is it worth the time and expense to proliferate repeater designs to match MAT cable? What are the costs of adapting all the VF and signaling equipment which will need to use MAT cable? What is involved in the documentation and training of operating company personnel in the use of the new cable? The monetary rewards of utilizing MAT cable look attractive but the "initiation fees" are high.

Another aspect not previously mentioned is that MAT cable is an air-core plastic insulated cable now being proposed for use in ducts where pulp cables have been supreme for upwards of 40 years. Other papers at this Symposium[6,7] will cover new water detection and removal techniques for PIC cables to ease at least some qualms.

Conclusion

Fine gauge, low capacitance, expanded plastic insulated cables have been designed which can provide both the VF and T1 carrier transmission needs of metropolitan area trunks. Copper savings will be 50 or 60% and duct savings will accrue from a cable having at least 30% more pairs. A major drawback is that virtually all transmission systems using the cables need equipment or instructional modifications. However, if the long term trend of lower electronics costs relative to cable costs continues, and as ducts become more scarce and expensive, the eventual changeover to some type of MAT cable appears inevitable.

References

1. Hoth, D. F., "The T1 Carrier System," Bell Laboratories Record, November, 1962.

2. Roberts, W. L. and Wilkenloh, F. N., "Multipair Cable Shielding for PCM Transmission," Proc. 19th, International Wire and Cable Symposium.

3. Baxter, G. D., Farago, M., and Gouldson, E. J., "FOAM-SKIN, A Composite Expanded Insulation for Use in Telephone Cables," Proc. 21st, International Wire and Cable Symposium.

4. Setzer, D. E. and Windeler, A. S., "A Low Capacitance Cable for the T2 Digital Transmission Line," Proc. 19th, International Wire and Cable Symposium.

5. Durham, R. L., Nutt, W. G., and Refi, J. J., "LOCAP: A Low-Capacitance Cable for a High Capacity System," Bell Laboratories Record, July/August, 1974.

6. DeVeau, G. F. and Dykes, J. D., "Polybutylene-Jacketed Air-Core PIC Cable for Use in Steam Exposed Ducts," Proc. 23rd, International Wire and Cable Symposium.

7. Hardwick, N. E., "Restoration of Wet PIC Cable Using Vaporization Drying," Proc. 23rd, International Wire and Cable Symposium.

G. H. Webster
Bell Laboratories
2000 N.E. Expressway
Norcross, Ga. 30071

Mr. Webster graduated from Manchester University (U.K.) in 1948 with a B.Sc. (Hons. Physics) degree. His professional career has been in the design and development of coaxial and multipair telephone cable, in England with BICC, Canada with Phillips, and since 1957, in the U.S.A. with Bell Laboratories. He is named in eight patents, is a member of I.E.E.E. and, since 1972, has been serving on the committee of this Symposium.

TRANSIENT SHIELDING EFFICIENCIES

of

FERROMAGNETIC CABLE SHIELDS

by

H. D. Campbell
NORTHERN ELECTRIC CO. LTD.
Montreal, Quebec

ABSTRACT

Communication cables are subjected to interference transients having a broad range of magnitudes and frequency components. The shielding efficiencies of ferromagnetic shields, as a function of these variables, are investigated by appropriate test circuit configurations and the use of a high voltage impulse generator as transient current source.

INTRODUCTION

The continuous increase in the use of very high power transmission circuits in conjunction with the rapid growth of communication circuits requires more attention to the problem of electrical co-ordination. Since both information and power are, in effect, being transmitted at higher densities reliability is more critical. Adequate physical separation is often a problem. All these factors increase the need to quantify the shielding efficiencies of communication cable shields.

When ferromagnetic materials such as steel tape armour, or tubular steel sheaths are used in communication cable constructions either for purely mechanical or electrical shielding purposes it is well known that protection from electromagnetic fields tends to be enhanced by the high relative permeability of the ferromagnetic materials provided that the disturbing fields do not cause magnetic saturation of the shielding material. Measurement methods such as recommended by CCITT* are widely used in laboratories to determine the steady state power frequency shielding effectiveness of such constructions as a function of the disturbing magnetic field. Communication circuits are also subjected to high energy transient interference from lightning currents. High frequency transients, generated by high voltage arcs in EHV substations during switching operations, are a source of trouble in associated control circuits.[1]

This paper deals with the shielding response of ferromagnetic shields when subjected to both aperiodic and oscillatory transient currents having peak amplitudes ranging from less than 100 to 15,000 amperes, and a frequency range from less than 400 Hz to 85 kHz.

* International Telegraph and Telephone Consultative Committee.

MEASUREMENT METHOD

The measuring system consisted of a transient current source, a sample test assembly, a current monitor and a voltage response monitor. The schematic of the measuring system is shown in Figure 1.

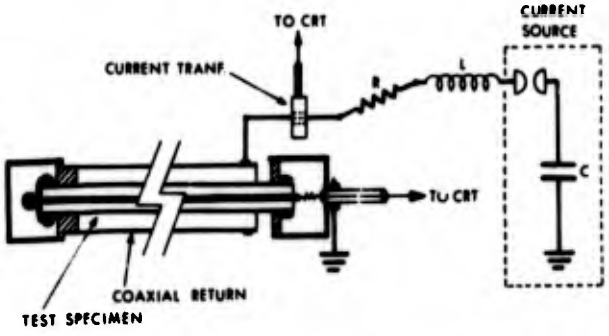

FIG. 1. SCHEMATIC OF TEST CIRCUIT

Transient Current Source

The current source was an 8-stage 1600 kV impulse voltage generator, modified so that any number of the eight 0.5 μF capacitors were connected in parallel as desired. The limitation of this configuration as a high surge current source is the inherent inductance of the current paths associated with the capacitors at the higher positions on the columns. To provide undistorted waveshapes a series inductor must be inserted to increase the rise time; otherwise spurious oscillations occur between the capacitors in the several parallel branches. For this reason the front times of the highest energy aperiodic currents are rather longer than desired (about 15 μs). Furthermore, to prevent underdamped currents the value of the damping resistance must be increased to compensate the increased inductance. In practice, an impulse voltage generator modified in this way does not generate very high peak currents but the time integral of the current, $\int i\,dt$, is in direct proportion to the number of capacitors, thus a wide range of aperiodic waveshapes can be generated with crest values of current sufficient to cause a high level of saturation in the test specimen.

Waveshapes

The transient aperiodic current as a function of time is a fundamental expression for an RLC series circuit. For the over-damped case:

$$i = \frac{E}{L(a_2-a_1)} \left[\exp(-a_1 t) - \exp(-a_2 t)\right] \quad (1)$$

where:

i = current at time, t, in kA
E = source voltage kV
R = resistance in ohms
L = inductance in μH
C = capacitance in μF

$$a_1 = R/2L - [(R/2L)^2 - 1/LC]^{1/2}$$

$$a_2 = R/2L + [(R/2L)^2 - 1/LC]^{1/2}$$

$$R > 2(L/C)^{1/2}$$

t = time in μs

If no series resistance is introduced in the circuit, a wide range of damped sinusoidal frequencies can be generated by choosing appropriate values of inductance and capacitance. For the underdamped case:

$$i = E/\beta L \exp[-\alpha t] \sin \beta t \quad (2)$$

where:

$$\beta = [1/LC - (R/2L)^2]^{1/2}$$

$$\alpha = R/2L$$

and the units are the same as in (1).

If $1/LC >> (R/2L)$

then $\beta = [1/LC]^{1/2} = \omega_o$

where ω_o is the resonant frequency.

Expressions (1) and (2) are introduced here merely to illustrate that the current wave forms can be readily predicted and checked by a programmable calculator.

To generate the desired range of both damped sinusoidal and aperiodic transient currents, two inductors were constructed (Figure 2). The small coil had an overall inductance of 75 μH while the much larger coil had a total inductance of 45 mH. Both coils were suitably tapped to provide a set of intermediate values. The circuit constants of the transient current source had the following range of nominal values:

Capacitance - 0.5 μF to 4.0 μF

Inductance - 8 μH to 45 mH

Resistance - 0 to 45 ohms

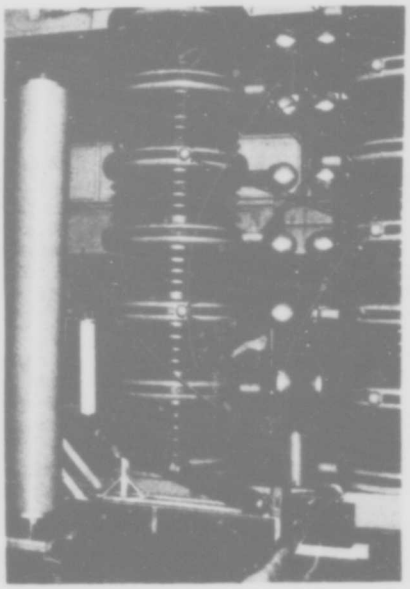

FIG. 2. GENERAL VIEW OF TEST CIRCUIT

Test Assembly

The test assembly was arranged in a coaxial configuration as shown in Figure 1.

Such a coaxial system simulates the sheath earth circuit of buried cable where the cable sheath is one conductor of a sheath earth circuit having some value of surge impedance to a lightning stroke, say about 25 ohms. The coaxial configuration has other advantages; (a) the self-inductance is very low so that the waveshape is independant of the test sample, (b) since the magnetic field is enclosed within the circuit induced ground currents are minimized, (c) current distribution is essentially uniform, and (d) current measurement is simplified because the entire test circuit is maintained at low voltage relative to the generator terminals.

It becomes apparent that the coaxial circuit is similar to a radio frequency surface transfer impedance test configuration where the rf generator is replaced by an impulse current source.

The test specimen was centered inside the 4-inch (10.2 cm) diameter aluminum pipe coaxial return by suitable spacers and short circuited to it at the far end. The length of the coaxial return was made as long as practical (11.0 metres) to minimize end errors. The test specimen consisted of a multi-pair coaxial cable having a corrugated tubular steel sheath (Figure 3) 0.020 inches (0.51 mm) nominal thickness and a mean diameter of 5.97 cm. The entire core assembly, outer coaxial conductors and aluminum longitudinal shield, was short circuited at both ends so that the core assembly was electrically one conductor, short circuited to the

steel sheath at the far end and open circuited at the near end. The terminals of the core assembly were enclosed in heavy aluminum caps (Figure 4). The active length of the test specimen (steel sheath) was 11.1 metres.

The driving current was measured by either of two wide band current transformers as appropriate, i.e. (a) maximum peak current 5000 amperes, sensitivity 0.1 volt per ampere, rise time 20 nanoseconds and (b) maximum peak current 50,000 amperes, sensitivity 0.01 volt per ampere, rise time 20 nanoseconds.

The output of the current transformer, (i), and the voltage response, (e), of the test specimen were fed to a dual channel storage oscilloscope through suitably terminated coaxial leads. The quantity (e/i) is the surface transfer impedance. A camera attachment was used to record both the transient current and the voltage response. The impulse generator and oscilloscope were triggered by a conventional trigatron circuit.

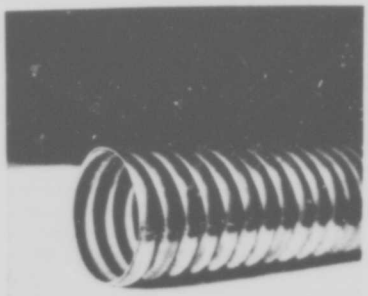

FIG 3 CORRUGATED STEEL SHEATH TEST SPECIMEN

Measurement Errors

As a verification of the accuracy of the test method a coaxial cable test specimen having a seamless tubular aluminum outer conductor was subjected to a series of measurements similar in the range of current amplitudes and frequencies as that of the steel sheath. The transfer impedance of such a nonmagnetic tubular shield may be calculated by the expression due to Schelkunoff[2] where the thickness of the shield is small compared to the radius:

$$Z_T = \frac{Z_o}{2\pi\sqrt{ab}\sinh \gamma t} \qquad (3)$$

where Z_o = intrinsic impedance of the shield.

γ = intrinsic propagation constant of the shield.

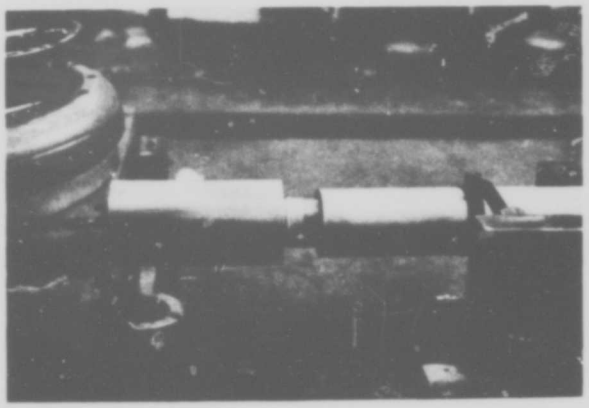

FIG. 4. NEAR END OF TEST CIRCUIT

This expression may be converted to the form:

$$Z_T = \left[\frac{A+B}{2\pi\sigma\sqrt{ab}\delta(A^2+B^2)}\right] + j\left[\frac{A-B}{2\pi\sigma\sqrt{ab}\delta(A^2+B^2)}\right] \qquad (4)$$

where:

Z_T = surface transfer impedance, ohms per metre

a and b = inner and outer radii (metres)

σ = conductivity (mhos per metre)

μ = permeability ($4\pi \times 10^{-7}$ H/m)

t = thickness (metres)

$\delta = (2/\sigma\mu\omega)^{1/2}$ (skin depth, metres)

A = sinh t/δ cos t/δ

B = cosh t/δ sin t/δ

The values calculated by (4) were in good agreement with the measured values. Further checks were performed including comparison of recorded currents to values calculated by (1) and (2) and conventional open circuit and short circuit measurement lead techniques to determine interference and ground loop errors. To eliminate voltage response errors due to ground currents in the voltage measurement lead it was necessary to introduce a high impedance between the CRO and ground. For this purpose an isolating transformer was inserted in the CRO power supply lead. Other methods of introducing the necessary impedance can be used[3]. Suitable modifications were similarily required to the triggering signal circuit. The pulse current transformer, unlike conventional current viewing resistors, is effectively isolated from current carrying parts of the circuit and ground therefore does not introduce group loop problems.

BASIC SHIELDING THEORY REVIEW

A brief review of some basic shielding concepts may prove helpful in the interpretation of the experimental results given later. A current flowing in a tubular shield gives rise to a longitudinal electric field at the inner surface. The ratio of this voltage to the current flowing in the shield is the surface transfer impedance. The voltage response is equal to the product of the current density at the inner surface of the shield and the resistivity of the shield material. It is evident from (4) that the current density at the inner surface is a complex function of the shield conductivity, permeability and thickness; and the driving frequency. It differs both in magnitude and phase to the total current in the shield unless the frequency is zero (i.e. dc) when the transfer impedance Z_T is simply equal to the dc resistance.

Reference to fundamental electromagnetic field theory of plane waves is useful to form a physical interpretation of transfer impedance, as indicated in the following qualitative treatment.

When a travelling plane wave impinges on a conductor, e.g. a tubular shield, it is rapidly attenuated as it passes through the shield. The wave length and velocity of propagation are much different than in free space:

$$\alpha = \beta = [\sigma\mu\omega/2]^{1/2} \quad (5)$$

$$v = [2\omega/\sigma\mu]^{1/2} \quad (6)$$

$$\gamma = 2\pi/\beta \quad (7)$$

where:

v = velocity of propagation (metres/second)
α = attenuation constant (nepers/metre)
β = phase constant (radians/metre)
γ = wave length, (metres)

Expressions (5), (6) and (7) show that the velocity of propagation, attenuation and wavelength of a disturbance at the outside surface of the shield is a function of the permeability, conductivity, and frequency as indicated in (4). If appropriate values for a metallic shield are inserted it becomes apparent that the wave length and velocity of propagation are very much less than in free space, so that both the magnitude and the phase angle change rapidly as the disturbance penetrates the shield. This means that a current flowing on the inside surface of the shield may lag several cycles behind the current on the outside surface, thus there can be several layers of current flowing in opposite axial directions at the same instant. The measured current in a transfer impedance measurement is the vector sum of the currents flowing within the shield while the measured voltage is simply the product of current density at the inside surface and the shield resistivity. The fundamental expression (5) can be utilized to calculate broad approximations of the ratio of the inner surface current to the measured current both in phase and magnitude thus the transfer impedance can be roughly estimated. This concept of current attenuation, although an over simplification, is useful and is utilized later.

In practice the voltage (e) impressed between core and shield may be expressed as a function of the surface transfer impedance (Z_T) when there is a disturbing field:

(a) from lightning currents

$$e = i_s Z_T \quad (8)$$

(b) from a circuit carrying current (i)

$$e = (Z_T/Z_s)\, j\omega M i \quad (9)$$

where:

i_s = current flowing in disturbed cable shield
Z_s = self-impedance of disturbed cable shield circuit
M = mutual inductance
i = current in disturbing circuit
ω = angular frequency

FERROMAGNETIC SHIELDS

Common grades of mild steel are often used as mechanical protection or electrical shielding of communication cables. The power frequency shielding factor (reduction factor) of such constructions is commonly measured and well documented. Although transient[4,5,6] shielding has been given some attention and specially designed cables for lightning protection have been described there appeared to be a need for further investigation. The transfer impedance of ferromagnetic materials subjected to transient electromagnetic phenomena can be characterized by (a) attenuation and phase delay (b) saturation effects, (c) post transient response and (d) residual magnetic effects.

Attenuation and Phase Delay

It is well known that thin nonmagnetic shields, such as the commonly used 8-mil (0.20 mm) longitudinal aluminum tapes, have essentially uniform current distribution at lightning current frequencies so that the transfer impedance is nearly equal to the dc resistance. The high relative permeability of a ferromagnetic material provides a skin effect, or attenuation and phase delay as indicated by (5). Since the value of the permeability (μ) is a function of the current density such that its value is extremely difficult to solve analytically the transfer impedance cannot be solved by (4) and in practice must be measured. An example of the phase delay is shown in Figure 5 where it is seen that the peak voltage response occurs some 30 μs after the current peak. The effect of phase delay is reflected in the ratio of the voltage front time

to the current front time. The front time of both the current and voltage waveshapes were measured in accordance with standard procedure for impulse current waveshapes. The transfer impedance (Z_T) is the ratio of the peak voltage to the peak current.

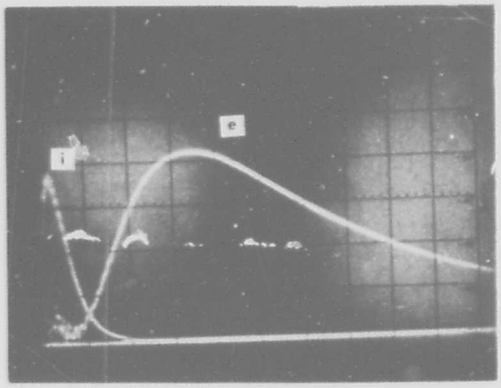

FIG. 5. EXAMPLE OF PRONOUNCED PHASE DELAY

i = 200 amps/cm
e = 0.2 volts/cm
t = 10 μs/cm

Saturation Effects

At 60 Hz, the current density in the test specimen previously described is essentially uniform and the effect of saturation can readily be predicted. A *normal* μ-H curve, (Figure 6) typical of the shield material indicates a maximum value of the permeability μ at a magnetizing field Hϕ of 400 amperes per metre. From Amperes Law:

$$I = H\phi\pi D \qquad (10)$$

where:

Hϕ = magnetic field strength (amperes/metre)
I = sheath current (amperes)
D = mean diameter of sheath (metres)

and $I \simeq 75$ when $\mu_{max} \simeq 2.7 \times 10^{-3}$ H/m

or $\mu_r(max) \simeq 2150$

Furthermore, approximate values hold as given in Table 1.

I(amps RMS)	μ_r
<20	300
20 < I < 500	300< μ_r < 2150
>500	< 300

TABLE 1

These values, in general agreement with known data from 60 Hz shielding factor measurements, illustrate the usual wide excursion of μr as the B-H function is taken over the knee of the curve.

When the frequency is increased slightly beyond 60 Hz to (say) the 3rd, 5th, 7th ... harmonics the current density begins to be non-uniform so that there are, in effect, an infinite number of B-H curves as a function of the thickness of the shield. A mean value of permeability has little meaning, however it is to be expected that saturation effects would be most pronounced in the current range of 20 to 500 amperes. Such saturation effects can be discerned in Figure 7 where the transient current varies from about 170 to less than 20 amperes. The response of the first half cycle, to be discussed later, should be disregarded. The current density and μr can be readily calculated only at the inner surface of the shield, and in this case μr at the inner surface lies on the linear part of the μ-H curve. The distorted response at the higher current values shows that the current density at the outer surface must be over the peak of the curve. At the lower values of current the response becomes linear and the shielding effectiveness less because μr is now on the lower portion of the μ-H curve.

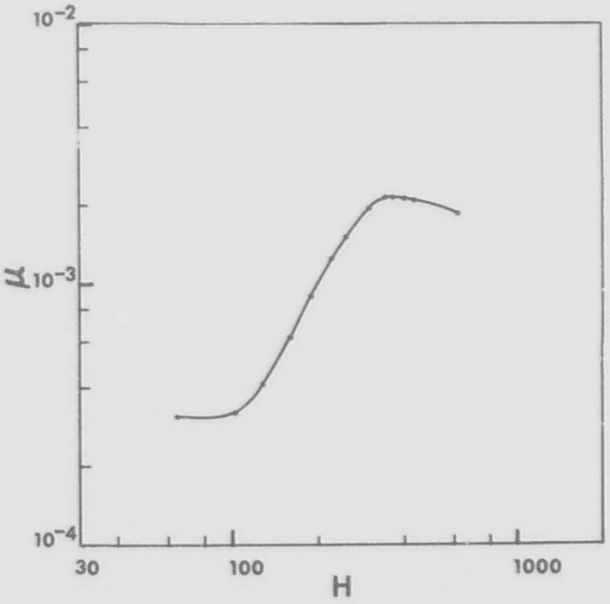

FIG. 6. TYPICAL *NORMAL* μ-H CURVE OF TEST MATERIAL

$\mu = 4\pi \times 10^{-7}$ Henries/metre
H = Amperes/metre

Post Transient Response

From expressions (5) and (6) the phase delay of the pulse response, or the transit time to penetrate the shield, may equal or exceed the duration of the current or driving pulse. Such a pulse is shown in Figure 5 where it can be seen that the current flows on the inside of the sheath for a long time after the driving current has ceased. It should be noted that the driving current does not continuously decay exponentially to zero but has a definite cut off determined by the spark gap spacing. This phenomenon is due to stored magnetic energy.[7] When the driving current ceases the currents within the sheath have an energy content equal to $\frac{1}{2}\mu H^2$ where μ and H are both functions of the current density and sheath thickness, and fall exponentially to zero with a time constant determined by the ratio of the inherent inductivity and resistivity. This post transient delay may be much greater than the phase delay thus the voltage response pulse may have a much lower frequency content than the driving current. The shield can be said to act like a low pass filter.[5]

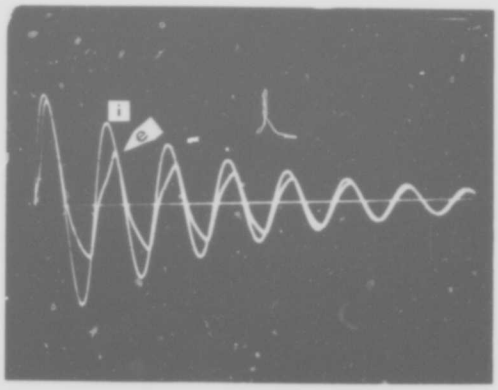

FIG. 7. NONLINEAR RESPONSE AT 362 Hz

i = 100 amps/cm
e = 2 volts/cm
t = 2 ms/cm

Residual Magnetic Effects

Where an aperiodic current pulse is applied to a ferromagnetic shield the magnetizing force (H) rises to some maximum value from zero and finally falls back to zero. The result of the unidirectional field is some residual value of magnetic flux density (B) say 1.8, as indicated on a typical *normal* B-H curve (Figure 8). If the pulse is now repeated the resultant B-H curve excursion will be different and the residual will tend to be increased. If the polarity is reversed the residual will tend to be reduced to zero. The magnitude and direction of the residual magnetism have pronounced effects on the transfer impedance (Figure 9).

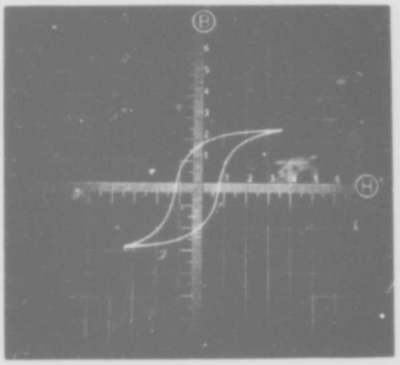

FIG. 8. A TYPICAL *NORMAL* B-H CURVE

When a damped oscillatory transient is applied there is a net current in magnitude and direction such that:

$$\int i\,dt = \pm Q$$

where i is given by (2) and Q is the stored charge of the source. The first half cycle has an effect similar to the aperiodic pulse such that the shield becomes magnetized in one direction while the exponentially decaying transient causes the residual to approach zero. If some residual magnetism remains a repetitive transient will tend to increase the residual, and so on, until an equilibrium is reached, thus the effective value of permeability and the attenuation of current through the shield are not equal for the positive and negative going current. This inequality gives rise to a unidirectional component of current flowing on the inner surface (Figure 10). If the polarity of the transient is reversed (as determined by the initial half cycle) the residual magnetism tends to be reduced to zero. The voltage response of oscillatory transients, repeated such that the direction of the initial current is reversed for each consecutive transient, can be expected to be more symmetrical than if the initial current direction remains constant.

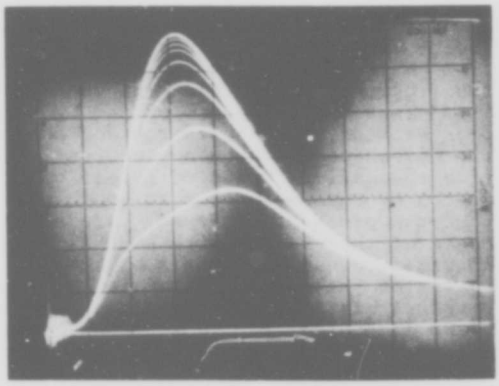

FIG. 9. EFFECTS OF RESIDUAL MAGNETISM (Response to Repeated 7.3/33μs Current +ve pulses of 3300 amperes peak following (-ve) pulses. e = 5 volts/cm
t = 50μs/cm

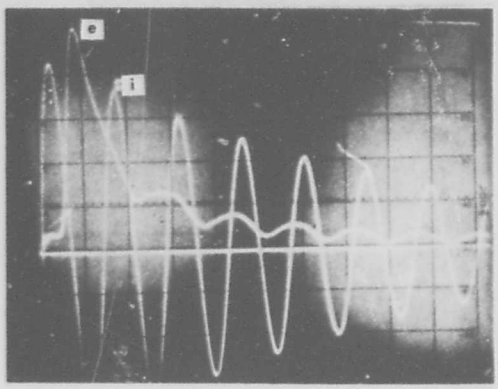

FIG. 10. RESIDUAL MAGNETISM EFFECTS ON THE RESPONSE TO AN OSCILLATORY TRANSIENT

i = 1000 amps/cm
e = 2 volts/cm
t = 20 μs/cm

EXPERIMENTAL RESULTS

The experimental data will now be discussed in some detail.

Aperiodic Transients

The generated aperiodic transients were chosen to simulate lightning currents. Since the available current source has a maximum stored charge of 0.8 coulombs and individual lightning strokes may have a charge magnitude about one order of magnitude greater the experimental aperiodic transients are equivalent to rather modest lightning strokes. Statistical data indicate that about half of the lightning strokes are less than 30 kilo-amperes. If a stroke occurs to a location on a cable remote from its ends the shield current is half the stroke current, or 15 kilo-amperes. A waveshape* of 5/65 micro-seconds is often used to be respresentative of the wide range of lightning current values. In terms of this data the generated transients are roughly equivalent to 50 per cent of the shield transient currents that occur in practice.

The response to the disturbance or current transient may be characterized by (a) the peak voltage, (b) the energy content and (c) the waveshape or frequency content. In practice the maximum value of shield current is limited by the dielectric strength to earth of the protective jacket. The surge impedance of the sheath earth circuit is sufficient to cause dielectric breakdown (pinholes) of the jacket for quite low sheath currents[8]. It is shown in Ref 9 that in such cases the lightning transient diminishes rapidly along the cable because of leakage to the surrounding earth, thus the maximum effect of the sheath current only occurs over a short length of cable. The core to sheath voltage is also attenuated both in respect to magnitude and equivalent frequency as it travels along the cable. Travelling wave effects are not considered; the criteria is simply a comparison to nonmagnetic shields.

The peak core to sheath voltage is, of course, of prime importance because it determines the necessary dielectric strength, core to shield, however the energy and equivalent frequency content may be of interest in the more sophisticated communication circuits. As indicated previously residual magnetic effects must be taken into account in the measurement procedure. Polarity of the charging voltage was reversed several times during the test procedure to demonstrate the pronounced attenuation on the initial reversed polarity transient. In all cases the response was checked for stability by repetition of the pulse so that the recorded results are a worst value. Such procedure was considered to be the better approximation of field conditions. Transfer impedance, (Z_T = E/I where E and I are peak values), is shown in Figure 11 as a function of current density (J) with waveshape* as the parameter. The plot indicates that the transfer impedance rises to the limiting value of the dc resistance from significantly lower values at low current densities. Only the short pulse is highly attenuated.

For purposes of comparison, an 8-mil (0.20 mm) aluminum tape of the same mean diameter has a transfer impedance (dc resistance) of 0.75 ohms per kilometer. The 20 mil (0.50 mm) steel shield, because of its significantly lower conductivity appears to perform less well, in general, than the aluminum tape, although the differences are probably not very significant particularly if current leakage to earth due to sheath pinholes at the higher transient currents is assumed. It should be noted that the steel shield (sheath) is corrugated for adequate mechanical properties, a process that increases the unit length resistance by about 10 per cent. The results confirm that the wave tail primarily determines the value of the transfer impedance.

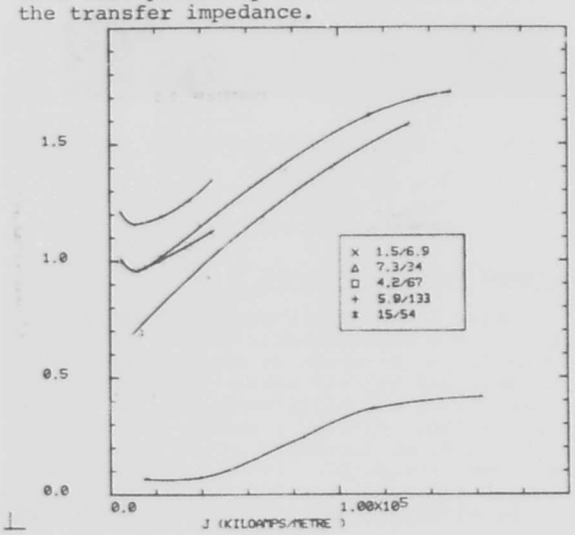

FIG. 11. TRANSFER IMPEDANCE (Z_T) AS A FUNCTION OF CURRENT DENSITY (J); I(Amperes) = 0.0953 J

*Waveshape: $(t_1)/(t_2)$

where: t_1 = front time (μs)
t_2 = time to half value (μs)

If it is of interest to estimate the amount of energy introduced into the cable as a function of the lightning current transient it is only necessary to determine the $\int i^2\,dt$ and $\int e^2\,dt$ for the current wave and the voltage response respectively. The integration can be conveniently executed by use of a computer digitizer interface on the photographed waveshapes. Alternately the integration can be done analytically if it is assumed that the transient rise is linear and the decay is exponential. The assumption is generally valid and it is easily shown that:

$$\int_0^\infty i^2\,dt \simeq I^2\left(\frac{t_1}{3}+\frac{t_d}{1.39}\right) \qquad (11)$$

where:

I = peak current

t_1 = rise time and t_d = decay time

such that $I>0.5I$ when $t_1<t<t_d$

Similarly

$$\int_0^\infty e^2\,dt \simeq E^2\left(\frac{t_1}{3}+\frac{t_d}{1.39}\right) \qquad (12)$$

The energy functions, computed by both methods, yielded results in good agreement.

If the waveshapes are identical then:

$$\int e^2\,dt/\int i^2\,dt = E^2/I^2 = Z_T^2 \qquad (13)$$

From Figures 13 and 14 it is found that the 15/54 current waveshape becomes virtually identical to its voltage response at high current values. The ratio $\int e^2\,dt/\int i^2\,dt$, shown plotted in Figure 12 confirms expression (13) for the 15/54 waveshape. For the current waveshape 1.5/6.9, there is pronounced post transient delay and in this case $\int e^2\,dt/\int i^2\,dt = 12.1\,Z_T^2$ for the lowest current value, thus the transfer impedance does not necessarily indicate even an approximate value of energy transfer.

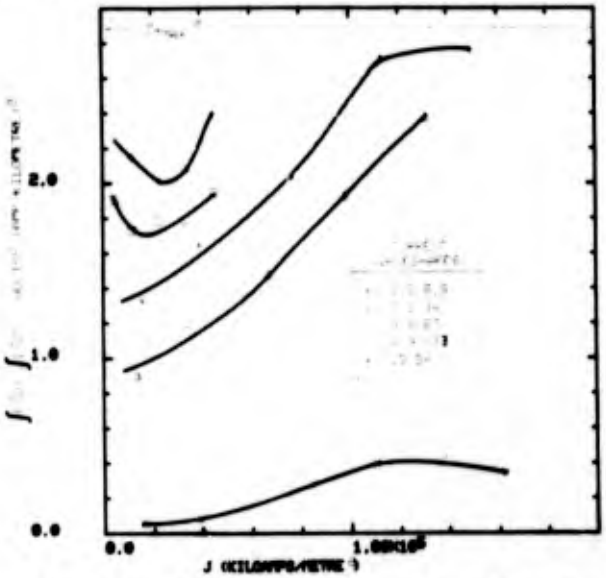

FIG. 12. ENERGY TRANSFER AS A FUNCTION OF THE CURRENT DENSITY (J) I(Amperes) = 0.0953 J

The plots of front time ratios (Figure 13) and time to half value ratios (Figure 14) are of interest in demonstrating the filtering effect on the disturbing current transient. Although no Fourier analysis has been made the effect is seen to be pronounced for the short pulse where the equivalent frequencies in the voltage response appear to be down by as much as one order of magnitude.

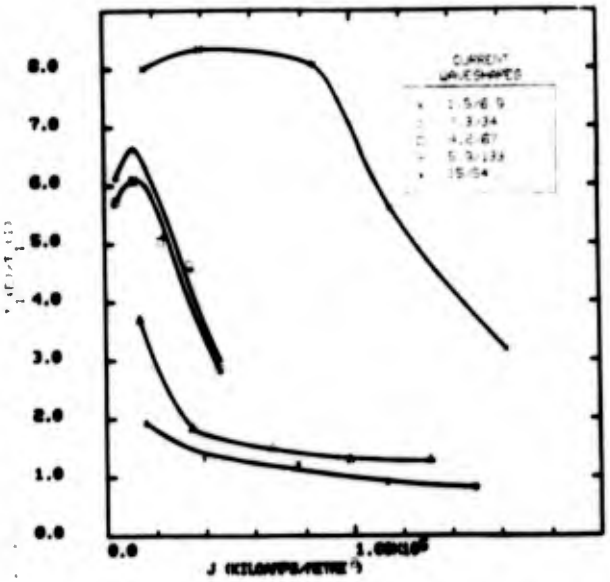

FIG. 13. RATIO OF THE FRONT TIME OF THE RESPONSE (e) TO THE FRONT TIME OF THE CURRENT (i) AS A FUNCTION OF CURRENT DENSITY (J). I(Amperes)=0.0953J

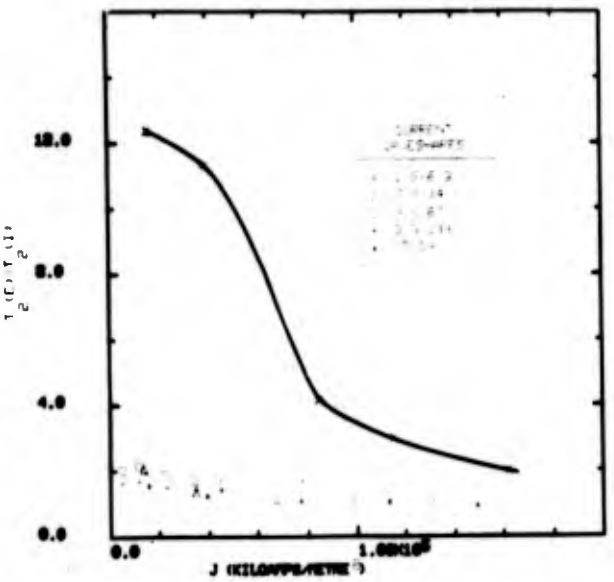

FIG. 14. RATIO OF THE TIME TO HALF VALUE FOR THE RESPONSE (e) TO THAT OF THE CURRENT (i) AS A FUNCTION OF CURRENT DENSITY (J). I(Amperes)=0.0953J

Oscillatory Response

Oscillatory or sinusoidal transients are conveniently generated if the source is underdamped. From (2) the initial peak current, when the damping resistance is very small:

$$I_p \simeq E/(L/C)^{1/2} \qquad (14)$$

The inductance in the circuit used was much greater than the capacitance at low frequencies but began to approach the capacitance value at high frequencies, thus the magnitude of oscillatory currents was constrained by the chosen frequency. It was difficult, in practice, to generate currents less than a few hundred amperes at the high end, or less than a few tens of amperes at the low end of the frequency range. Despite these constraints it was felt that such transients would yield useful shielding data as a function of both frequency and field strength. For example, power frequency harmonics are a source of interference, and their attenuations in a ferromagnetic shield can be expected to be modified by the much higher field of the 60 Hz fundamental, although it is recognized that this mode in a non-linear system cannot be obtained by superposition.

The results of the oscillatory transients are shown in Figures 15a and 15b. The rate of the driving current decay, or decrement, was normally modest and the response considered applicable to a steady state mode. From Figure 15a it is seen that the response of the four current densities converge and approach the dc value at the lowest frequency (362 Hz). Furthermore, improved shielding occurs at the higher current densities when the frequency is increased. These current densities are above the initial saturation level at 60 Hz, indicating the effects of saturation are displaced as a function of frequency. The equivalent inner surface shield current can be readily calculated:

$$I_e = I_{(RMS)} \, Z_T / R_{dc} \qquad (15)$$

where:

I_e = (inner surface current density) X (cross-section area of shield)

R_{dc} = dc resistance of shield (ohms/km)

These values are listed for three different frequencies in Table 2.

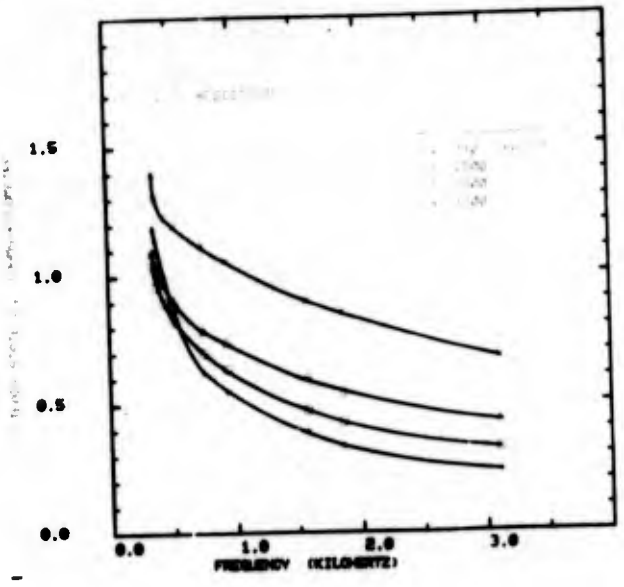

FIG. 15a

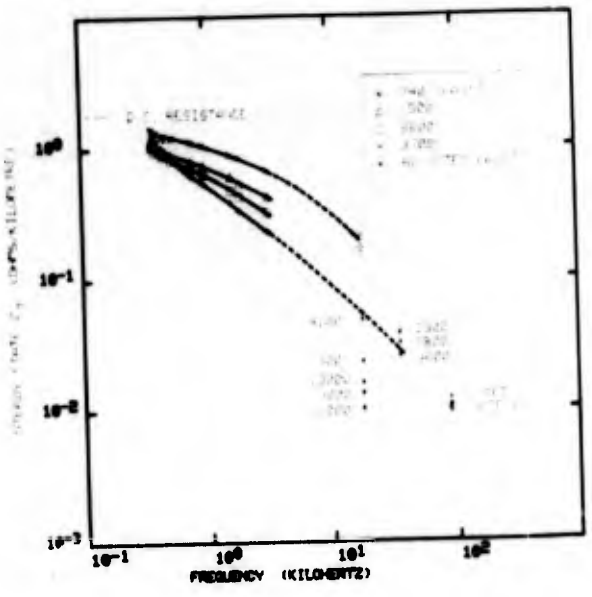

FIG. 15b

TRANSFER IMPEDANCE (Z_T) AS A FUNCTION
OF THE FREQUENCY OF THE DISTURBING CURRENT
I_{RMS}(Amperes) = 0.0953 x (kA/m^2)

NOTE A - Approximate Values

TABLE 2

Shield Current $I_{(RMS)}$	Equivalent Inner Surface Current I_e (RMS) f=1.6kHz	f=3.1kHz	f=17.3kHz
70	37	28	--
140	50	35	--
210	59	40	--
350	81	48	--
390	--	--	11.3
2000	--	--	12.3

When these values (Table 2) are compared to values of permeability versus current (Table 1) it is found that the inner surface of the sheath is operating from about the initial permeability to maximum values of permeability for currents of 70 to 350 amperes respectively. The tabulated values are in no sense an analytical confirmation of the effects of current density (Figures 15a and 15b) but they do have a certain consistent relative order.

The shielding effects at frequencies up to 500 Hz or so are modest and not a strong function of current. In a practical situation harmonics or noise interference is applicable normally to steady state power line currents where the magnetizing force is small therefore the 70 ampere plot is probably resonably representative.

In Figure 15b the frequency range is extended to 85 kHz. For these additional values a procedure of reversing the polarity for consecutive pulses was used. The difference in response (Figures 16a and 16b) is very pronounced, particularily at the higher current values. The driving currents in (a) and (b) are identical but the voltage scale is quite different, 0.5 volts/cm and 10 volts/cm respectively. The phase delay in 16b is evident (~90°) at a peak of about 40 volts. The initial flat response has a value of about one volt at 17μs. This response appears as a peak value of 1.35 volts in Figure 16a. It is clear that there should be no voltage response until the driving current has penetrated the shield so there is an error for at least the initial 17μs. The possibility that the observed response during the whole transient is a resultant of an error signal from test specimen end effects, non-uniform current distribution and the like, cannot be discounted, however, the results do not support this concept, including the initial phase relationships and the fact that the response is fairly constant for quite different levels of current. It is thought that the error is associated with initial high frequency effects when the generator is fired and these effects disappear when the response becomes symmetrical. Appendix 1 includes a series of typical responses.

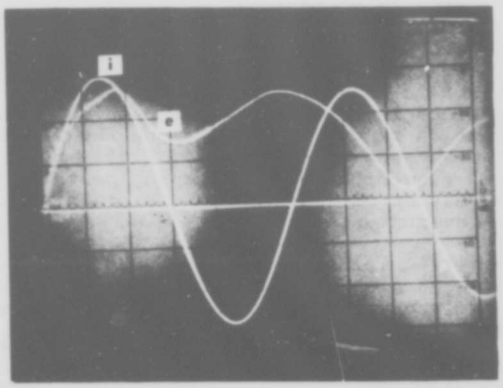

FIG. 16a

RESPONSE WHEN RESIDUAL MAGNETISM IS SMALL

i = 2000 amps/cm
e = 0.5 volts/cm
t = 10 μs/cm

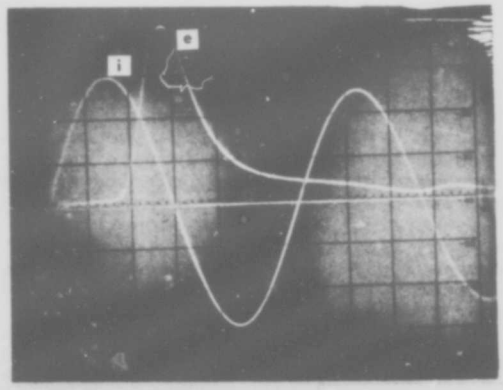

FIG. 16b

RESPONSE WHEN RESIDUAL MAGNETISM IS LARGE

i = 2000 amps/cm
e = 10 volts/cm
t = 10 μs/cm

The high frequency results included in Figure 15b are consistant with the results of Figure 15a indicating that ferromagnetic shields can be subjected to very high steady state magnetic fields at high frequencies without deterioration of shielding effectiveness. This conclusion is supported by Figure 17 where the transfer impedance is plotted as function of current densities. The minimum Z_T values are displaced to the right as the frequency parameter is increased.

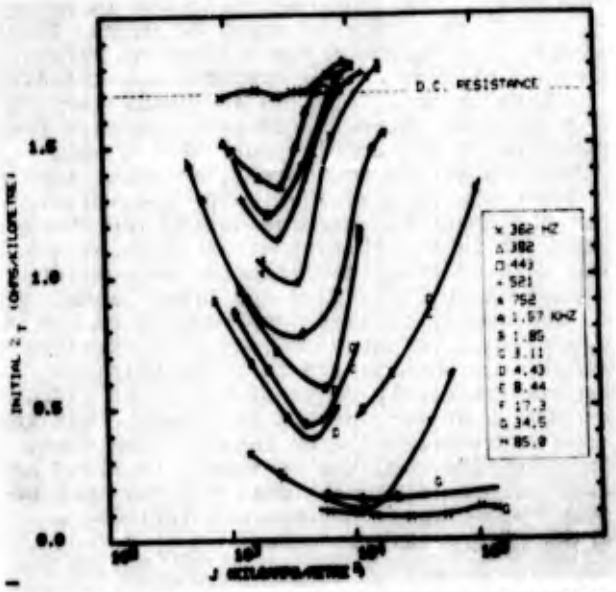

FIG. 17. INITIAL PEAK RESPONSE TO A DAMPED OSCILLATORY TRANSIENT AS A FUNCTION OF CURRENT DENSITY(J). I(Amperes)=0.0953J

The values of Z_T in Figure 17 are computed from the initial peak value of each voltage response (cf Figure 16b).

The data is not sufficiently well documented to draw exact quantitative conclusions. It was obtained while the impulse current source was charged to one polarity only. The first few cycles of each response tended to be asymmetrical even at the lower end of the frequency range. The effect increases with frequency, until finally it becomes totally aperiodic. The transfer impedance at the higher frequencies is about one order of magnitude higher (Figure 17) than values obtained when residual magnetic effects were kept to a low value (Figure 15b). It is evident that the response to a high frequency oscillatory transient is highly dependent on the residual magnitism of the shield. The data in Figure 17 and other observations indicate that if the driving frequency is raised (say to a few MHz) that the response would also be aperiodic at low field strengths. In practice, the shield can be expected to be in a residually magnitized state, the response totally aperiodic and perhaps orders of magnitude greater than expected from steady state measured values. The waveshape of the response resembles a rectified envelope of the driving current.

The data (Figure 17) indicates that at 362 Hz the initial peak of the driving current tends to saturate the shield for all values of current. At higher frequencies the maximum value of effective permeability moves to the right (higher driving current values) until at the higher frequencies measured, saturation effects again occur, the typical U-curve flattens once more and the shield tends to function like a nonmagnetic material.

CONCLUSIONS

Although a corrugated steel sheath of the construction and dimensions described provides reasonably good lightning protection it is, in general, inferior to the common 8-mil (0.20 mm) aluminum tape.

The shielding efficiency is a strong function of the peak current magnitude and its rate of decay. When these quantities are unfavourable, as in the more common lightning transients, the skin effect is small and the shielding effectiveness is primarily dependant on the dc resistance like in nonmagnetic shields. The advantage of the high relative permeability of the steel becomes significantly more effective by modest increases in either the shield thickness or frequency content of the disturbing field.

The voltage response to an aperiodic transient has a greater duration than the disturbing pulse. The shield is, therefore, less effective with respect to energy induced into the cable than the voltage induced.

Because of residual magnetism the electrical history of a ferromagnetic shield can have pronounced effects on its shielding efficiency. With respect to lightning currents this characteristic can result in quite different induced voltages depending on the direction of current flow along the shield. Although such effects are of little practical significance in lightning protection they may be of significance in other shielding environments.

The shielding efficiency with respect to damped high frequency oscillatory transients is greatly reduced by residual magnetism, and in fact, the induced voltage can be completely aperiodic. Under conditions where residual magnetism can be assumed absent the response would be quite different and the shielding efficiency greater by probably more than an order of magnitude.

Steady state field strengths that can be accommodated without saturation effects increase with the applied frequency.

ACKNOWLEDGEMENTS

The author wishes to express appreciation for the contributions of other members of the technical staff of Northern Electric Co. Ltd., in particular to Régis Morin for his continual assistance in making the measurements, compiling the data and preparing the test circuitry.

REFERENCES

(1) H.J.Sutton "Transients Induced in Control Cables Located in EHV Substation", IEEE Trans Power Apparatus and Systems, Volume PAS-89 pp 1069-1081 July/August 1970.

(2) S.A.Schelkunoff "Electromagnetic Waves", D. Van Nostrand, 1943, Chapter 8 p 278.

(3) A.J.Schwab and Josef Herold "Electromagnetic Interference in Impulse Measuring Systems", IEEE Trans Power Apparatus and Systems, Volume PAS-93 pp 333-339. January/February 1974.

(4) F.J.Young "Pulse Shielding by Nonferrous and Ferromagnetic Materials", Proceedings of the IEEE Vol 61 No.4, April 1973.

(5) F.A.Fisher "Voltages Produced by Transient Currents Flowing Upon Shields of Cables", 1970 Lightning and Static Electricity Conference, San Diego.

(6) E.L.Fisher and W.A.Bishop, "Lightning Shielding of Plastic Telephone Cable", presented at the 17th International Wire and Cable Symposium, Atlantic City.

(7) Ryszard Malewski "Measurements of Transient Skin Effect within Nonlinear Conductors", IEEE Trans Power Apparatus and Systems Volume PAS-91, September/October 1972.

(8) D.A.Douglass "Lightning Induced Current on a Buried Multi-Coaxial Cable System", Wire Journal, January & February 1973.

(9) E.D.Sunde "Earth Conduction Effects in Transmission Systems", Dover Publications New York, Chapter 9.

Hugh D. Campbell is a member of R&D staff Northern Electric Co. Ltd., Cable Division and has been engaged in development and electrical measurements of both power and communication cable since joining the company in 1950. He holds a B.S. degree in Electrical Engineering from Nova Scotia Technical College and is a member of the Order of Engineers of Quebec and IEEE.

APPENDIX 1. TYPICAL VOLTAGE RESPONSES

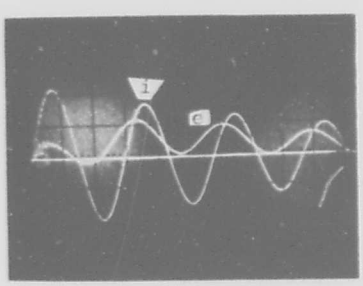

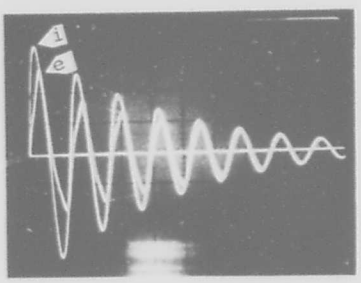

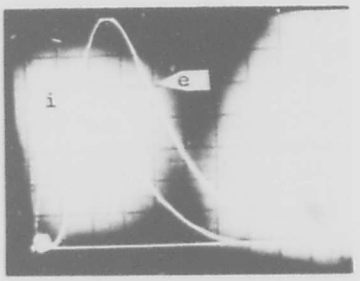

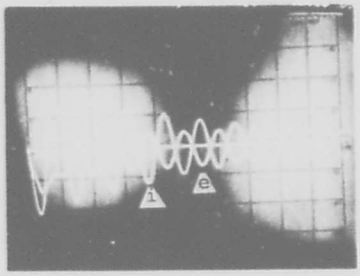

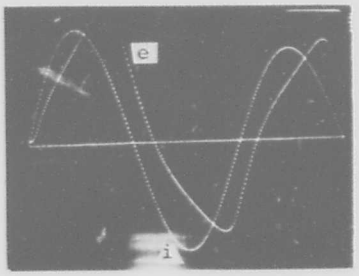

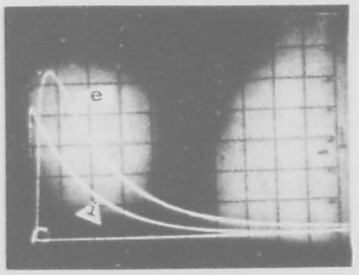

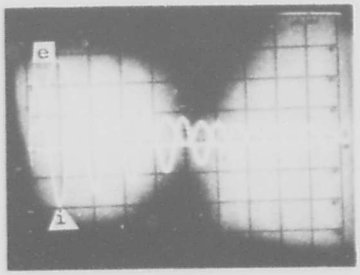

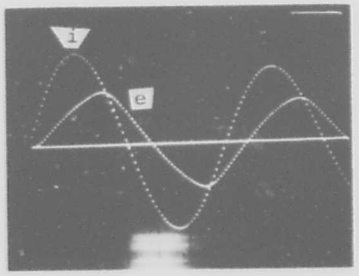

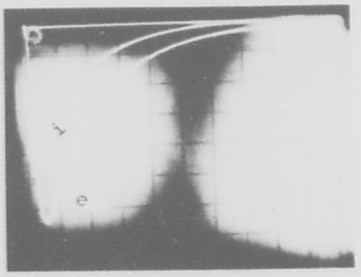

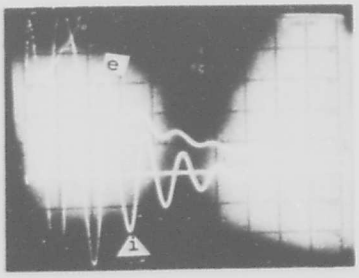

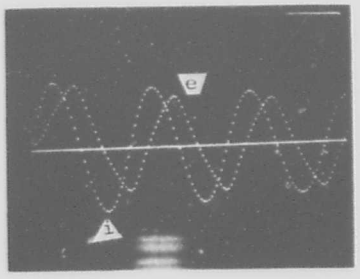

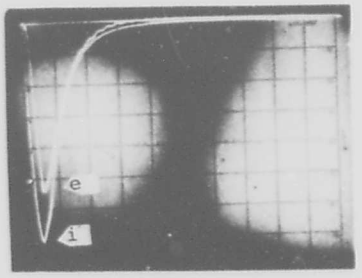

Photo	f(kHz)	Volts per cm	Amps per cm
1 (top)	34.5	0.5	500
2	17.3	0.5	1000
3	17.3	0.5	500
4	85.0	1.0	1000

f(Hz)	Volts per cm	Amps per cm
382	1.0	50
752	0.5	50
1570	0.5	20
3110	0.5	50

Sweep µs/cm	Volts per cm	Amps per cm
10	20	2000
50	10	1000
100	10	1000
50	50	2000

NOTE: Column 1 illustrates typical responses
when (Photo 1 & 2) residual magnetism is weak
(Photo 3 & 4) " " " strong

HIGH STRENGTH, CORROSION RESISTANT CLAD METAL SHIELDING, FOR TELEPHONE WIRE AND CABLE

by

R. Baboian, S. R. Hartley and E. D. Hyman

Texas Instruments Incorporated
Materials and Electrical Products Group
Attleboro, Mass. 02703

Abstract

This paper deals with design parameters for wire and cable shielding materials. The performance of such materials depends on electrical shielding properties, mechanical properties (such as strength) and corrosion resistance properties. Evaluation of currently used shielding materials is based on results of various test programs. The data has been collected and organized such that a direct comparison can be made of the various shielding materials.

Introduction

Design of telephone cables have changed considerably since their inception in the 1880's. Until the early 1950's, the basic design for distribution cable in the communications industry was lead sheathed and paper or pulp insulated aerial and underground duct cable.[1] The use of direct buried cable required variations in the basic design including an asphalt-impregnated jute coating (for corrosion protection of the lead sheath) and a single or double steel tape armor (for additional mechanical protection).

With the introduction of polyethylene as a jacketing material, several combinations of lead and polyethylene were used for direct burial sheath design. However, use of these designs was limited due to cost considerations.[1]

During the 1950's the increasing trend toward the use of direct-buried cable coupled with a short economical supply of lead provided the impetus for development of new cable designs. The aluminum-polyethylene (Alpeth) and steel-aluminum-polyethylene (Stelpeth) sheathed designs were followed by cables incorporating polyethylene insulated conductors (PIC) such as PIC-Alpeth and PIC-Stelpeth.[1]

Installation procedures used during the early period of direct burial of PIC cables frequently caused cable damage leading to sheath faults and conductor grounding due to accumulated moisture. One solution to this problem was the addition of an inner polyethylene jacket and the PIC-PAP (polyethylene-aluminum-polyethylene) design. However, due to severe corrosion of aluminum in the underground environment, the independent cable industry went to a PIC-PCP (polyethylene-copper-polyethylene) design using a copper shield rather than aluminum.[1,2] Mechanical protection requirements for gopher-infested areas was provided by use of a 10 mil copper shield, a more expensive design (PIC-PCPG) compared to others.[1,3]

An extensive R&D effort was conducted in order to develop materials that would reduce shielding costs without serious decrease in corrosion and mechanical properties. As a result of the effort, 8 mil aluminum tape coated on both sides with a 2 mil film of polyethylene was developed as an alternate to 5 mil copper. Substitutes for 10 mil copper include 6 mil copper clad stainless (2 copper/2 SS/ 2 copper) and 6 mil copper alloy 194.[3] In wire sizes, 4 mil copper clad stainless (0.8 copper/2.4 SS/ 0.8 copper) and 5 mil copper clad stainless (0.8 copper/ 3.4 SS/ 0.8 copper) are substitutes for copper and bronze.

The properly grounded sheath performs a number of important functions including:[4] protection from injury and equipment damage if a live power line should contact the cable, protection from electrostatic pickup due to power line voltage, protection from lightning, suppression of induced voltage due to power line currents, suppression of radio frequency pickup, and reduction in cross talk coupling between pairs. In order to function properly, the cable sheath must provide mechanical protection for the cable core during and after installation, keep moisture out of the cable core, and provide electrical conductivity for the life of the cable. Thus, primary properties for the sheath are mechanical strength, electrical conductivity, and corrosion resistance. In addition, the materials should be economic and abundant, easily fabricated and flexible.

Electrical Conductivity

One of the basic requirements for shielding materials is electrical conductivity. The list of metals and alloys along with their resistivities in Table I gives a good indication of their relative potential for use as shielding materials and thickness requirements for equal conductivity. However, in addition to monometals, combinations such as aluminum-steel and copper-stainless steel are used widely to take advantage of the properties of both components. Several examples of cable designs and a description of the shielding materials are listed in Table II.[5] Since

TABLE I

ELECTRICAL RESISTIVITIES
OF METALS AND ALLOYS

Metals and Alloys	Electrical Resistivity Microhm-cm at 20°C
Copper	1.724
Aluminum (1000 series)	2.828
Bronze (CDA 220)	3.92
CDA 194	2.54
CDA 195	3.44
Lead	20.65
Steel (1011)	14
Type 430 SS	60
Type 304 SS	72

a shielding, copper clad stainless, is shown in Figure 1.

Electric and Magnetic Field Shielding

A shield operates in three ways to reduce the field strength within the shield enclosure:[6]

1. A continuous metallic shield will completely screen the electric field from circuits within the shield. (Electric field refers only to the high-impedance field associated with capacitive coupling.)
2. A magnetic material shield will divert the magnetic field away from the conductors inside the shield.
3. Any metallic shield may reduce the magnetic field within it because of eddy currents set up within the material of the shield when exposed to an alternating magnetic field. These eddy currents set up fields which tend to neutralize the disturbing field.

TABLE II

SHIELD RESISTANCE AND COMPOSITION
OF SIX PAIR, 19 GAUGE CABLES

Cable Designation	Metals in Shield	Shield Resistance Ohms per 1000 ft.
P - C - P	5 mil copper	1.13
P - C - P	10 mil copper	0.53
P - A - P	8 mil aluminum	1.20
A - P - A - P	8 mil aluminum + 8 mil aluminum	0.62
A - P - SS - P	8 mil aluminum + 5 mil stainless steel (304)	1.51
P - B - P	5 mil commercial bronze	2.22
P - C SS C - P	6 mil copper clad stainless steel (430) (2 + 2 + 2)	1.35
P - A - SS - P	8 mil aluminum + 3 mil stainless steel (211) adhesively bonded	1.16
P - Cu Alloy - P	5 mil copper alloy 194	1.31
A - P - S - P	8 mil aluminum + 6 mil 1011 steel	1.24
A - P - S - P	8 mil aluminum + 10 mil 1011 steel	0.87

these cables are all six pair 19 gauge, the shielding resistances (ohms/1000 feet) in this table are directly comparable.

The table shows the variation in shield resistance with various metals, the effect of shielding thickness (for example 5 mil and 10 mil copper), the effect of alloying (such as copper, 90/10 bronze and alloy 194), and the effect of combining metals and alloys (for example aluminum with steel and copper clad stainless steel). The advantages of combining metals and alloys to form a shield with composite properties can be obtained while maintaining a shield resistance comparable to other systems (see Table I and II). The configuration of such

The effectiveness of metallic shields in reducing electric and magnetic fields in communication cable is well documented. For example, Gooding and Slade[6] measured the electric field induced voltage in a disturbed circuit (CD) for 1 volt across a disturbing circuit (AB). Metallic shielding applied over CD completely eliminated any coupling between the two circuits with the shield grounded and there was no reading on the voltmeter. However, under the same electric field conditions and frequency range (10-300 kilocycles/sec), over 240

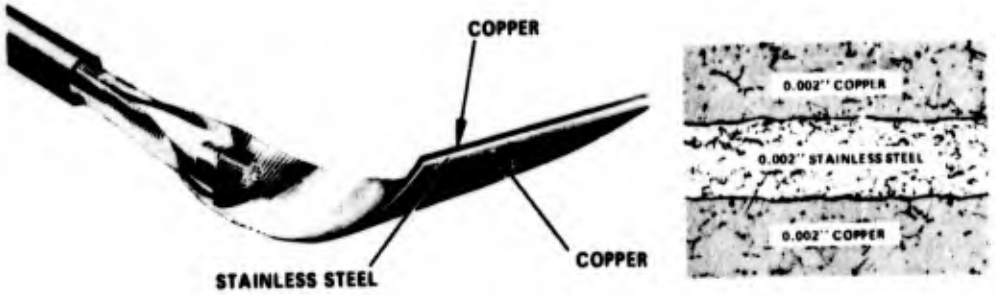

PHOTO OF COPPER CLAD STAINLESS STEEL SHIELDING IN CABLE AND PHOTOMICROGRAPH AT 250X OF Cu/430 SS/Cu CROSS SECTION SHOWING THE INTEGRITY OF THE METALLURGICAL BOND PRODUCED BY A SOLID PHASE ROLL BONDING PROCESS.

FIGURE 1

millivolts induced voltage was measured in circuit CD without metallic shielding.

In order to measure the effectiveness of metallic shielding in screening out electromagnetic fields, Gooding and Slade[6] measured the interference (proportional to the mutual inductance between circuits AB and CD) in volts induced in circuit CD for 1 ampere flowing in AB. Their results are shown in Figure 2 where millivolts in CD are plotted vs frequency for various shielding materials, and the unshielded conditions.

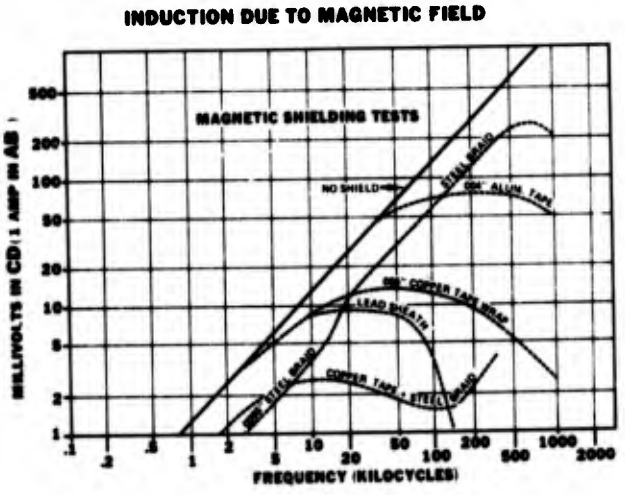

Efficiency of Various Types of Shield in Screening out Magnetic Fields (Ref. 6)

FIGURE 2

Notice that below 10 kilocycles, only steel containing materials are effective including steel braid and a combination of copper tape plus steel braid. Above 10 kilocycles, the steel braid begins to lose effectiveness, whereas the copper (5 mil) tape and lead sheath materials become effective. At 50 kilocycles, no difference is observed in induced voltage between aluminum (4 mils) tape and the unshielded condition, whereas 5 mil copper tape reduces the induced voltage to one-fifth that value. Above 100 kilocycles, aluminum (4 mil) tape becomes effective; however, even at 200 kilocycles, the induced voltage is almost ten times the value observed with copper (5 mil) tape and forty times that for the copper tape plus steel braid combination. Notice that the copper-steel combination is effective at all frequencies including the audio-range.

Additional data on the effectiveness of metal shielding was reported by Fisher et al.[5] Surge currents were applied to the shield of 500 foot lengths of cable and the potentials developed between the shield and conductors were measured in order to determine relative susceptibility to lightning influence.

On the basis of equal shield resistivity, their results show significant reduction in conductor to shield potential with composite shields containing magnetic materials compared to nonmagnetic materials. The results are in agreement with those obtained by Gooding and Slade; i.e., copper-steel and aluminum-steel combinations can be more effective than either component used singularly. Fisher et al also found that copper clad stainless steel was effective in reducing the conductor to shield potential due to the combination of copper with magnetic type 430 stainless steel.[5]

Mechanical Properties

Mechanical strength in cable shielding materials is also required to protect the conductors against rodents and other mechanical abuses such as those encountered using modern installation techniques. The important mechanical properties of materials used in cable shields are listed in Table III. Notice that aluminum has the lowest tensile strength in this group. Copper has a considerably higher value; however, the highest tensile strengths are obtained with alloy 195 and type 430 stainless steel. Copper clad stainless and copper alloy 194 have values intermediate to copper and stainless steels.

In cable size, the effect of thickening the copper tape (5 mil to 10 mil) on the breaking strength can be observed. In order to achieve equivalent breaking strength, aluminum tape must be almost three times as thick as copper. On the other hand, the thickness requirements for equal break strength with copper is reduced significantly by alloying (copper alloy 194) and by combining copper with stainless steel (copper clad stainless).

In addition, the mechanical properties of copper clad stainless vary with cladding ratio. These properties are listed for several cladding ratios in Table V. The tensile strength of copper clad stainless

TABLE III

MECHANICAL PROPERTIES OF SHIELDING MATERIALS

Shielding Material	Temper	Tensile Strength ksi	Yield Strength (0.2% Offset) ksi	Elongation in 2 Inches %	Modulus of Elasticity in Bending kksi
Aluminum	Soft	13	5	40	10
Copper	Soft	34	11	45	17
Bronze (CDA 220)	1/4 Hard	45	35	25	17
Copper Clad Stainless 2 Cu/2 SS/2 Cu	F.A.	47	29	18	17.4
CDA 194	Light Anneal	50	30	29	17.5
CDA 195	Precipitation	80	65	15	17.3
Steel (1011)	Soft	45	30	35	30
Type 430 Stainless	Soft	75	49	25	29

A calculation of breaking strength under load can be made using the tensile strength of the corresponding shielding material. These data are listed in Table IV for several cable size shielding tape materials.

TABLE IV

BREAK STRENGTH OF VARIOUS CABLE SHIELDING TAPES (FOR 2 INCH WIDTHS)

Shielding Material	Thickness (Mils)	Break Strength (Lbs.)
Aluminum	8	208
Copper	5	340
Copper	10	680
CDA 194	6	600
Copper Clad Stainless 2 Cu/2 SS/2 Cu	6	564

increases significantly with decreasing copper/stainless steel ratio. This data has been utilized in the design of new high strength, gopher resistant shielding for communication cable and wire (see Table V for shielding designations).

An important consideration in the use of high strength shielding such as copper clad stainless is thinner tape can be used while maintaining the required mechanical properties.[7] This provides some additional benefits such as easier fabrication[8] and increased flexibility of the cable.[8] For example, the equation for induced stress is[9]

$$S = \frac{3DEt}{2L^2} \qquad (1)$$

under deflection where S is the induced stress (psi), D the deflection (inches), E the modulus of elasticity in bending (psi), t the thickness (inches) and L the

TABLE V

PROPERTIES OF COPPER CLAD STAINLESS SHIELDING MATERIALS

Copper Clad Stainless Shielding Designation	Total Thickness (mils)	Component Thickness (mils) Cu	430 SS	Cu	Cladding Ratio Cu/SS % by Volume	Tensile Strength ksi	Yield Strength (0.2% Offset) ksi	Elongation in 2 Inches %
CCS I	6	2	2	2	33.3	47	29	18
CCS III	4	0.8	2.4	0.8	20	62	41	18
CCS V	4.6	0.8	3	0.8	17.4	63	42	26
CCS IV	5	0.8	3.4	0.8	16	65	43	27

length (inches). For equivalent induced stress in bending, the deflection for 10 mil copper is only one-half that for 6 mil copper clad stainless. The resulting increased flexibility of cable with the thinner clad metal shielding tape provides easier handling and installation, and reduction in cable damage due to buckling.

Gopher Resistance

Resistance to gopher damage in buried wire and cable is an important design consideration. In order to prevent this type of damage, the shielding material must have adequate strength to withstand the forces exerted by this animal. It is recognized that gophers must gnaw on hard objects to wear down their rapidly growing incisor teeth.[3,10,11] In addition, it is believed that they are attracted to disturbed soil such as that found in freshly buried wire and cable trench.[10] These factors, along with the fact that the gopher can be found in over 60 percent of the continental United States, has led to extensive and costly damage to improperly designed wire and cable.

Several studies have been conducted on the effect of shielding material on gopher damage.[3,10-13] Although they have been limited in scope, some important conclusions can be drawn from these investigations. First, variation in thickness and mechanical properties of wire and cable shielding material effects resistance to gopher damage. Second, shielding having steel or stainless steel components are highly gopher resistant. For example, 6 mil copper clad stainless (2 mil stainless steel) was equivalent to 10 mil copper in resistance to gopher attack in cables.[3] Third, in these studies, aluminum and lead shieldings were found to be highly vulnerable to gopher damage.[10,11]

In order to more fully investigate the effects of shielding thickness and mechanical properties on resistance to gopher damage, Texas Instruments Inc. in cooperation with the U.S. Fish and Wildlife Service conducted experiments on wire and cable. Tests were conducted on two pair, industry standard, filled buried distribution wire (REA specification PE-54) and six pair 19 gauge industry standard, filled buried cable (REA specification PE-39). In order to eliminate the effects of other variables, only the shielding differed in each type wire and cable sample.

Ten sections of each wire and cable sample were exposed for 7 consecutive days to each of 10 individually caged gophers (Geomys Bursarius). They were exposed to the gophers through a 2 inch by 2 inch opening in the front of the cage in the horizontal position.

Test specimens were evaluated for damage after exposure using the following rating system:

0 No damage
1 Slight damage, outer jacket scratched but not penetrated
2 Outer jacket penetrated, shield damaged but not penetrated
3 Shield penetrated
4 Shield penetrated and conductors damaged
5 Wire severed

Shieldings were ranked according to score which was obtained by multiplying the number of samples in each damaged category times the category value and dividing the product by the number of gophers in each test.

Test results are listed in Table VI for distribution wire having shieldings of bronze (1/4 hard), alloy 194 (temper 1 and 2), alloy 195 (precipitation temper) and copper clad stainless (fully annealed). Notice the strong dependence of shielding material on resistance to gopher damage. Material temper also affects the performance. For example, heavy annealed alloy 194 (temper 2) did not perform as well as light annealed (temper 1) alloy 194. However, both of these alloy 194 shielding materials are not as resistant to gopher damage as alloy 195, a precipitation hardened material, and copper clad stainless. Results also show that longitudinally corrugated and helically applied shields have similar

TABLE VI

RESISTANCE OF VARIOUS SHIELDING MATERIALS TO GOPHER DAMAGE IN DISTRIBUTION WIRE (REA SPEC PE-54)

Shielding Material (Temper)	Thickness Mils	Score: Longitudinally Applied	Score: Helically Applied
Bronze (CDA 220) (1/4 Hard)	7	3.1	2.7
	6	3.1	2.9
	5	3.5	3.8
	5	3.9	4.1
CDA 194 (Light Anneal)	6	3.3	3.6
	5	3.5	3.7
CDA 194 (Heavy Anneal)	6	3.7	3.7
	5	4.2	4.3
CDA 195 (Precipitation Anneal)	5	3.3	3.1
	4	3.7	4.2
Copper Clad Stainless (Full Anneal) (1.6 mils Copper)	5.6	2.1	-
	5.4	2.1	-
	5.2	2.1	2.3
	5.0	2.1	-
	4.8	2.6	2.7

resistances to gopher damage.

In Figure 3, gopher damage score is plotted vs shielding thickness for bronze, alloy 195, and copper clad stainless (the copper thickness remains constant at 1.6 mils while the stainless steel thickness varies in the composite). Gauge for gauge the order of increasing gopher resistance is bronze, alloy 195, and copper clad stainless. The thicknesses of these shielding materials at equivalent and acceptable levels of gopher damage resistance are: 8 mil bronze, 6.5 mil alloy 195 and 5 mil copper clad stainless (0.8 Cu/3.4 SS/0.8 Cu). Thus, increasing the shielding thicknesses beyond these values would not lead to appreciable increase in resistance, whereas thinner gauges would lower resistance to gopher penetration.

Results with cable are shown in Table VII and Figure 4. For comparative purposes, results with 10 mil copper shieldings are included along with those for alloy 194 (temper 1) and copper clad stainless (the copper thickness remains constant at 4 mils while the stainless steel thickness varies in the composite). Gauge for gauge, the order of increasing gopher resistance is copper, alloy 194 and copper clad stainless. The thicknesses of these shielding materials at equivalent and acceptable levels of gopher damage resistance are: above 10 mils copper, approximately 7.5 mils alloy 194 and approximately 6 mils copper clad stainless (2 Cu/2 SS/2 Cu).

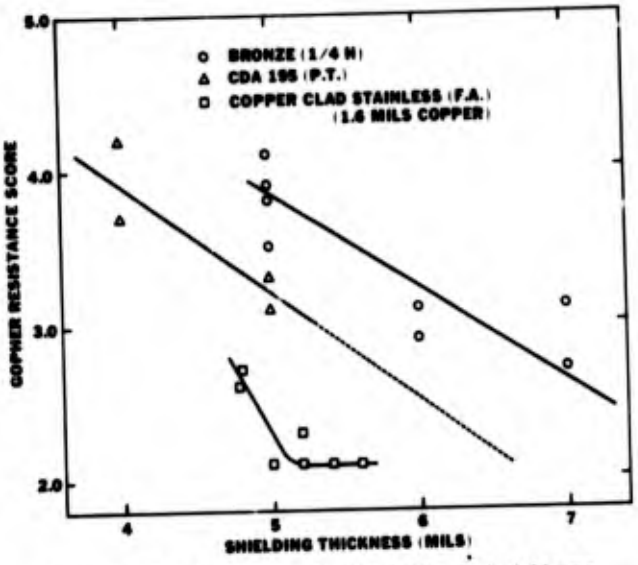

Gopher Resistance of Various Shieldings in Buried Distribution Wire

FIGURE 3

In this study, the correlation of tensile strength with resistance to gopher penetration for monometal shieldings is excellent. However, the higher resistance of copper clad stainless compred to alloy 194 and 195 cannot be explained by the relative overall tensile strengths of the shielding materials

(see Table III). Since the type 430 stainless steel component in the clad material has a higher tensile strength and its abrasion resistance is greater than the alloys, it appears that the clad (laminate) configuration has directional properties such that penetration resistance perpendicular to the clad layers has a more complex relationship with tensile strength. Thus, the stainless steel layer can be regarded as a barrier which is not easily ruptured even at the thinner gauge.

TABLE VII

RESISTANCE OF VARIOUS SHIELDING MATERIALS TO GOPHER DAMAGE IN CABLE (REA SPEC 39)

Longitudinally Applied Shielding Material (Temper)	Thickness Mils	Score
Copper (Soft)	10	2.7
CDA 194 (Light Anneal)	7.5	2.2
	7	2.7
	6	3.6
Copper Clad Stainless (Full Anneal) (4 Mils Copper)	7.5	2.0
	7	2.0
	6.5	2.1
	6	2.3

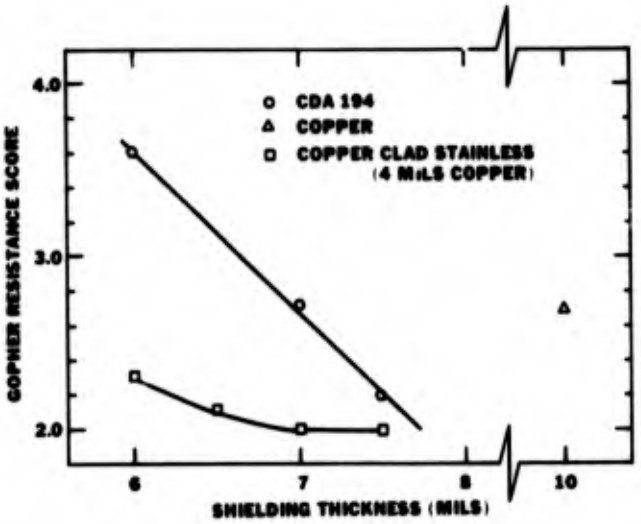

Gopher Resistance of Various Shieldings in Buried Cable

FIGURE 4

Corrosion Resistance

The corrosion behavior of lead sheathed cable has been the subject of investigation for many years.[14-16] However, it has only been recently that newer polyethylene jacketed systems have received attention.[16-24] The polyethylene outer jacket of a telephone cable is the first line of defense against corrosion of the metal shield.[17] However, this jacket is subject to damage due to lightning and rodents and during installation because of equipment, rocks, sand abrasion and handling. In addition, it is now known that moisture passes through polyethylene cable jacket by osmotic permeation when there is a differential vapor pressure.[25]

The problems associated with corrosion of the shield in contact with soil environments became apparent in the early 1960's.[2] Serious deterioration was found in aluminum shields at points where the shield was exposed to moisture. Subsequently, the use of copper shielding in place of aluminum was applied in some cable designs to retard corrosion.[2,26]

The corrosivity of a soil depends on a number of factors including resistivity, pH, aeration, moisture content, and chemical content.[27] These properties vary considerably depending on location. It is, therefore, not surprising that the corrosion resistance of metals and alloys is quite variable from one soil to another. Aluminum, for example, is susceptible to localized corrosion (such as pitting) in the presence of specific ions such as chloride and sulfate and where differential aeration conditions exist.[17] In addition, it is an amphoteric metal and will corrode more rapidly in both highly acidic and highly alkaline solutions than in environments within pH 5.5 to 8.5. Since the pH of soils varies widely from extremely acid (below pH=4.5) to strongly alkaline (above pH=9.1), and the concentration of soluble sulfates and chlorides is high in many areas, it is not surprising to find that rapid corrosion of aluminum has occurred.[27]

On the other hand, copper and many of its alloys are known to have good corrosion resistances in soils. For example, copper on the average is reported to corrode at about 1/6th the rate of steel.[27] The losses in weight and the maximum pit depths of copper and copper alloys in these National Bureau of Standards tests were slight with the following exceptions: in cinders, in soils having high concentrations of sulfides, in acid soils and in soils containing chlorides.

In general, stainless steels have excellent corrosion resistances in soils (including acid soils). Only in high chloride containing soils are types 430 and 304 stainless steels susceptible to localized corrosion such as pitting. The overall high corrosion resistance of stainless steel, however, is in contrast to the poor resistance reported for steel and tin plated steel in various soils.

Several important investigations on the corrosion behavior of various cable shielding materials have been conducted. The most comprehensive study is the cooperative field test program conducted by the U.S. Department of Agriculture Rural Electrification Administration (REA)

and National Bureau of Standards (NBS) in which over 50 cable types having various shielding materials were buried.[20-22] The cable specimens had an annular ring and lateral window exposing the shielding as shown diagramatically in Figure 5. Various underground test sites were chosen according to soil type. Table VIII is a list of these sites along with the soil properties. In this 6-year program, cable specimens are retrieved yearly and rated according to the system in Table IX. Table X is a summary of reported results available through the fourth year retrieval.[22]

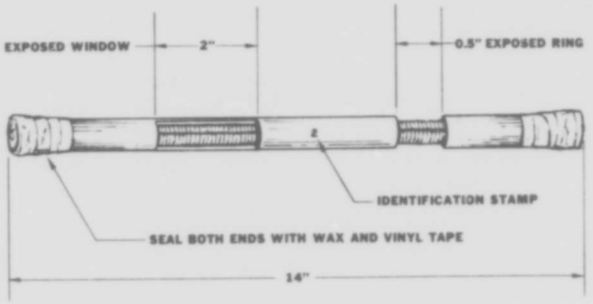

Diagramatic representation of Cable Specimen for Soil Burial Test

FIGURE 5

severe localized corrosion and undercutting of the aluminum occurs. This effect is represented diagramatically in Figure 7.[24]

The most severe corrosion of aluminum occurred in galvanic couples with other metals and alloys such as copper, steel, and stainless steel. In these tests, the aluminum was susceptible to corrosion in

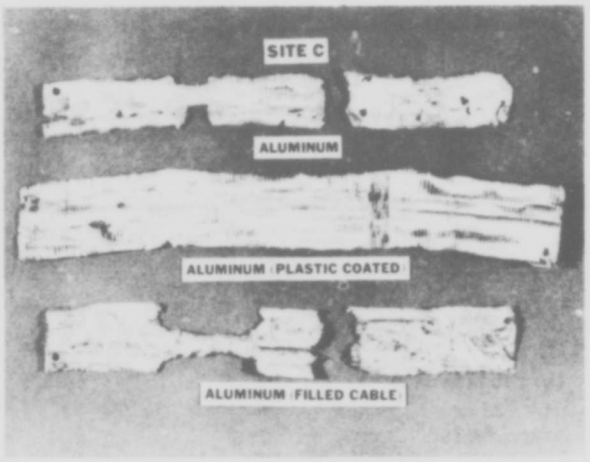

Aluminum Shielding Specimens from REA-NBS Soil Burial Corrosion Test Program

FIGURE 6

TABLE VIII

PROPERTIES OF SOILS AT TEST SITES

Site Ident.	Soil	Location	Internal Drainage of Test Site	Resistivity (Ohm - Cm)	pH
A	Sagemoor sandy loam	Toppenish, Wash.	Good	400	8.8
B	Hagerstown loam	Loch Raven, Md.	Good	5,200	5.8
C	Clay	Cape May, N.J.	Poor	300	4.0
D	Lakewood sand	Wildwood, N.J.	Good	30,000	7.3
E	Coastal sand	Wildwood, N.J.	Poor	55	7.1
G	Tidal marsh	Patuxent, Md.	Poor	300	7.1

The data clearly shows that bare aluminum shielding, even after one year exposure, is susceptible to severe corrosion in certain soils (sites C and G). Attempts to substantially improve the performance of aluminum by coating both sides with plastic or by using filling compound also resulted in severe corrosion of the shielding material (see Figure 6). These results are in complete agreement with those reported elsewhere.[17,18,23,24] For example, Schick found that filling compound (petroleum jelly) prevented the passivation of aluminum, and, therefore, the shielding performed worse than with no coating.[17] Damage sites on coated aluminum provide locations of differential aeration so that even the milder soils and in many cases the aluminum in the shield was almost completely dissipated throughout the full length of the test cable.[20-22]

As expected from previous work, copper and alloy 194 perform well in most soil sites. The ratings in Table X show that the acid soil site (site C) is the most damaging followed by the tidal marsh site (site G). In contrast with aluminum, copper and alloy 194 do not undercut and corrosion is limited to areas exposed at the annular and lateral windows as represented diagramatically in Figure 7.[24]

TABLE IX

RATING CODE FOR THE EVALUATION OF SHIELDS IN CABLE SPECIMENS

Rating	Performance	Degree of Corrosion
10	Excellent	Unaffected - no indication of corrosion.
9	Excellent	Superficial rust or etching on surface.
8	Very good	Uniform metal attack, rust, and/or slight localized pitting.
7	Good	Appreciable pitting over the surface, but no perforations through metal shield. Some minor delamination or dissipation of metallurgically or plastic-bonded metals leaving cathodic metal intact.
6+	Good	Localized pitting: only one perforation in shield by pitting.
6	Good	Localized pitting: 2 to 5 perforations in shield by pitting
5	Fair	Many localized pits causing perforation of shield <5% of shield dissipated by corrosion; extensive delamination of metallurgically bonded metals.
4	Poor	Severe corrosion: pitting to perforation of shield; 5 to 10% of shield dissipated by corrosion; severe corrosion of anodic part of metallurgically bonded metals.
3	Poor	Severe corrosion: pitting to perforation of shield; 10 to 25% of shield dissipated by corrosion.
2	Very poor	Severe corrosion: more than 25% of shield dissipated by corrosion; shield still has electrical continuity along the cable.
1	Very poor	Severe corrosion: shield is close to electrical discontinuity (ELD) due to perforation in shield and dissipation of metal by corrosion.
0	Very poor	Severe corrosion: shield is electrically discontinuous (ELD) due to dissipation of metal by corrosion

One of the most significant contributions of the REA-NBS study is the interesting results with copper clad stainless shielding material. This combination of copper and type 430 stainless steel in the clad configuration provided excellent corrosion resistance. In most soils, the behavior of copper clad stainless shields was identical to that of solid copper shields. However, in the more aggressive soils the corrosion resistant stainless steel provided a barrier which prevented perforation of the shield. Thus, the inner copper layer was unaffected even in the acid soil site so that electrical continuity was maintained. This unique corrosion barrier mechanism is diagramatically represented in Figure 7.[24]

The significance of the behavior of copper clad stainless can be clearly observed by referring to Figures 8, 9, and 10. A site for site comparison of fourth year aluminum, copper, and copper clad stainless cable shielding specimens shows the effectiveness of the stainless steel barrier in preventing perforation of the copper clad stainless shield in all soils.

SUMMARY

Design criteria for cable shielding materials include economics, conductivity, flexibility, fabricability, resistance to mechanical and gopher damage and corrosion resistance. However, the performance of the material depends specifically on the electrical shielding properties, the mechanical properties (such as strength) and the corrosion resistance properties.

In recent years, a clad metal shield composed of type 430 stainless steel metallurgically bonded of copper and stainless steel are combined into a single materials system having unique qualities that cannot be duplicated in a monometal. In the clad metal configuration (Cu/430SS/Cu) the copper component provides conductivity for reducing electric fields while the magnetic stainless steel is effective in reducing magnetic fields.

The stainless steel layer in copper clad 430 stainless steel (Cu/430SS/Cu) provides strength, thus providing resistance to

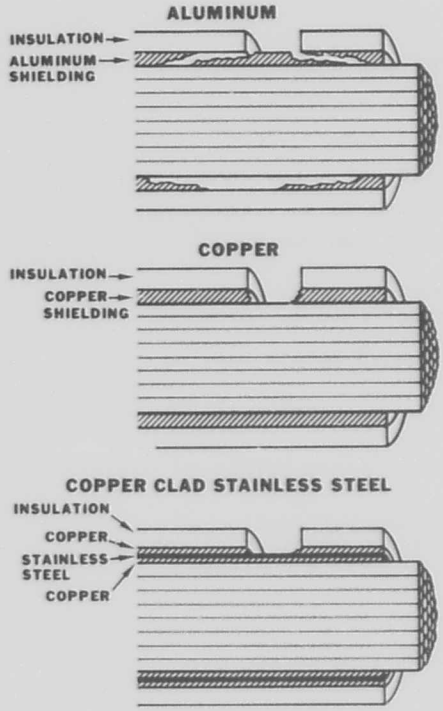

Diagramatic Representations of Corrosion Mechamisms for Shieluings in Buried Wire and Cable

FIGURE 7

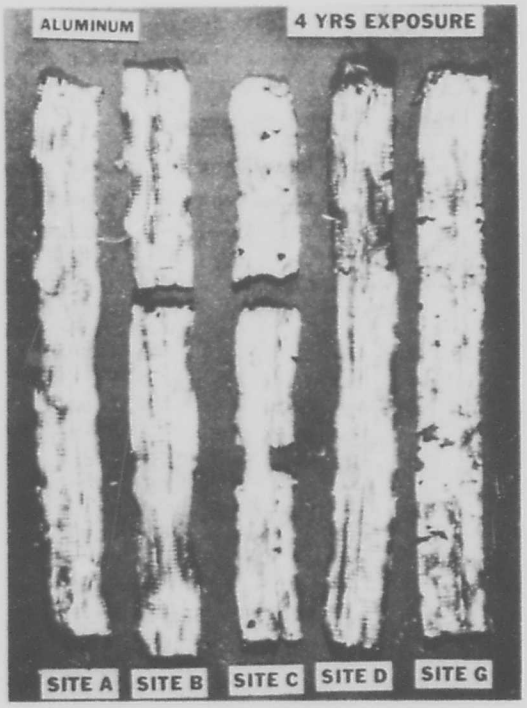

Shieldings from REA-NBS Soil Burial

FIGURE 8

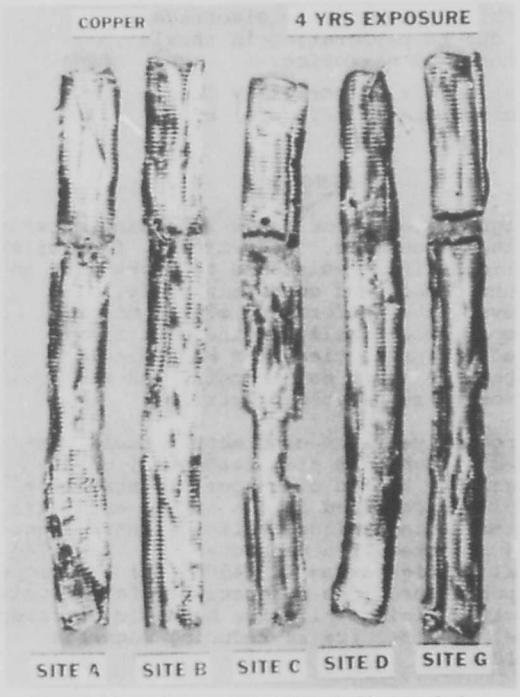

Shielding from REA-NBS Soil Burial

FIGURE 9

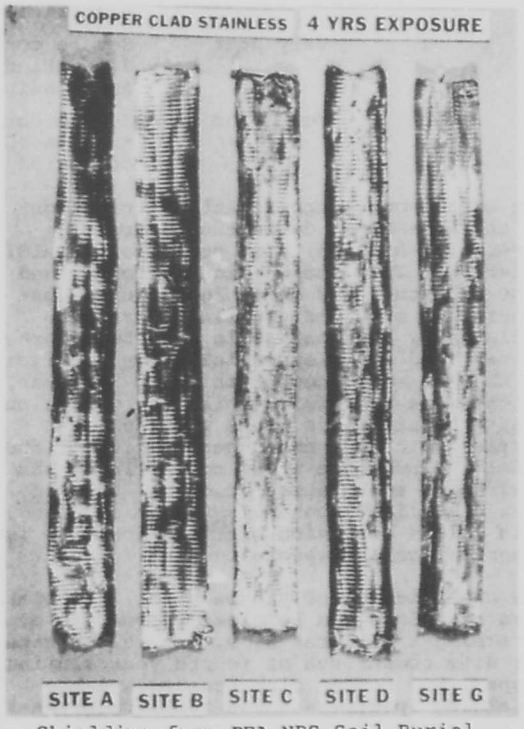

Shielding from REA-NBS Soil Burial

FIGURE 10

TABLE X

PERFORMANCE RATINGS OF SHIELDS IN BURIED CABLE SPECIMENS

System No.	Site	Window Exposure time, years				Ring Exposure time, years				Under Jacket Exposure time, years			
		1	2	3	4	1	2	3	4	1	2	3	4
1	0.008" Corrugated Bare Aluminum												
	A	10	10	9	6+	10	10	9	9	10	10	9	10
	B	9	9	9	9	9	9	9	9	9(8)	9	6	10
	C	5	5	2	1	5	0	2	0	8	5	6	0
	D	10	10	9	10	10	10	9	9	9	10	9	9
	E	10	9	9	-	10	9	9	-	9	9	9	-
	G	0	0	5	6	0	0	5	6	3	5	5	6
2	Same as No. 1 except that system is coupled to copper												
	A	2	0	0	0	1	0	0	0	6	0	0	0
	B	6	0	5	6	6	8	5	2	9	8	5	9
	C	0	0	0	0	0	0	0	0	0	0	0	0
	D	5	5	4	5	5	5	2	5	6+	8	5	5
	E	6	5	5	-	6	5	5	-	8	9	0	-
	G	0	0	0	0	0	0	0	0	0	0	0	0
5	50-Pair, 22 Gauge Cable with 0.008" Corrugated Aluminum with Plastic Film Coating on the Core Side of the Shield. An adhesive outer jacket is then applied. The aluminum edges are also protected at the shield overlap by an experimental process.												
	A	10	10	10	10	10	10	10	10	10	10	10	10
	B	10	10	9	9	10	10	9	9	10	10	10	10
	C	8	9	9	9	5	6	9	5	8	9	10	4
	D	10	10	9	10	10	10	9	10	10	10	10	10
	E	10	10	10	-	9	10	10	-	10	10	10	-
	G	2	0	0	0	0	0	0	0	5	3	6	0
6	Same as No. 5 except that system is coupled to copper												
	A	2	0	0	2	0	0	0	2	1	2	3	3
	B	10	10	9	9	8	5	3	8	8	10	9	9
	C	0	0	0	0	0	0	0	0	0	4	2	0
	D	10	10	5	1	5	0	5	5	5	8	5	5
	E	3	10	10	-	1	6	9	-	10	10	9	-
	G	0	0	0	0	0	0	0	0	4	0	9	0
41	25 Pair, 22 Gauge Western Electric Filled Cable, (15% PE-85% PJ Filling Compound) Uncorrugated 0.008" Aluminum Shield												
	A	10	9	10		10	9	10		10	9	10	
	C	9	10	0		9	5	0		10	10	0	
	G	5	5	10		2	5	10		6	5	6+	
42	Same as No. 41 except that system is coupled to copper												
	A	5	0	0		0	0	0		4	0	0	
	C	0	0	0		0	0	0		0	5	0	
	G	0	0	0		0	0	0		0	0	0	
3	0.005" Corrugated Bare Copper												
	A	10	10	9	9	10	10	9	9	10	10	9	10
	B	10	10	9	9	10	10	9	9	10	10	10	9
	C	10	8	0	0	5	3	0	8	10	9	0	9
	D	10	10	9	9	10	10	9	9	10	10	10	9
	E	10	10	9	-	10	10	9	-	10	10	9	-
	G	10	10	9	9	10	10	9	6+	10	10	9	9

TABLE X (Continued)

PERFORMANCE RATINGS OF SHIELDS IN BURIED CABLE SPECIMENS

System No.	Site	Window Exposure time, years 1	2	3	4	Ring Exposure time, years 1	2	3	4	Under Jacket Exposure time, years 1	2	3	4
4	0.005" Corrugated Bare Copper Alloy (97.5% Copper, 2.5% Iron, 0.02% phosphorus)												
	A	10	10	9	9	10	10	9	9	10	10	10	10
	B	10	6	9	8	10	10	9	8	10	10	10	10
	C	10	10	2	0	10	4	1	1	10	10	9	9
	D	10	10	9	9	10	10	9	9	10	10	9	9
	E	10	10	10	-	10	10	10	-	10	10	10	-
	G	10	10	9	8	10	10	9	8	10	10	9	9
23	0.006" Corrugated Copper-430 Stainless Steel-Copper (2-2-2)												
	A	10	10|10|9	9|10|9	9|10|9	10	10|10|9	9|10|10|9|10|9		10	10	10	10
	B	10	10	9|10|9	9|10|9	10	10	9|10|9	9|10|9	10	10	9|10|9	10
	C	7|10|7	1|10|9	1|10|9	3|6+10	6|10|6	1|10|9	1|10|9	1|5|10	10	10|10|9	9|10|9	9|10|9
	D	10	10	9|10|9	9|10|9	10	10|10|9	9|10|9	9|10|9	10	10|10|9	9|10|9	9|10|9
	E	10	10	9|10|9	-	10	10	9|10|9	-	10	10	9|10|9	-
	G	10	9|10|9	9|10|9	2|10|9	10	9|10|9	9|7|9	2|10|9	10	10	9|10|9	9|10|9

Summary (Contd.)

mechanical and rodent damage. Results of the Denver Wildlife Research Center test program in cooperation with Texas Instruments, Inc. confirm the resistance to gopher damage in cables with the clad metal shielding.

The corrosion behavior of the clad material has been demonstrated by the results of a cooperative program between the Rural Electrification Administration (REA) and the National Bureau of Standards (NBS) and also by Texas Instruments, Inc. Results show that the corrosion behavior of copper clad 430SS (Cu/430SS/Cu) is similar to copper except in highly corrosive soils (such as acid soils) where the stainless steel layer acts as a corrosion barrier preventing electrical discontinuity in the clad metal shielding.

References

1. O. D. McMahon, "How Undergrounding Has Affected Cable Design," p. 53, June, 1973.
2. C. L. Cox, T. E. Tingley, and H. A. Webster, "Problems of Water in PIC Cable,"17th International Wire and Cable Symposium, Atlantic City, New Jersey, December, 1968.
3. J. B. Backlund, "Are Gophers Gaining in Guerrilla War," Telephone Engineer and Management, p. 82, September, 1969.
4. R. L. Harrison, "Telephone Cable Shield Bonding and Grounding," Telephony, p. 37, March, 1974.
5. E. L. Fisher, W. F. Bishop, and E. A. Robinson, Jr., "Lightning Shielding of Plastic Telephone Cable," 17th International Wire and Cable Symposium, Atlantic City, New Jersey, December, 1968.
6. F. H. Gooding, and H. B. Slade, "Shielding of Communication Cable," AIEE Transactions, p. 378, July, 1955.
7. G. H. Parker, "Clad Metals in Cable Construction," 14th International Wire and Cable Symposium, Atlantic City, New Jersey, December, 1965.
8. A. Masciarelli, D. Conroy, and U. U. Savolainen, "Clad Metal Longitudinally Corrugated Shields Applied to Control Cables," Conference on Electric Wire and Cable Technology, New York, June, 1972.
9. "Copper and Copper Alloy Springs," issued by the Copper Development Association, 55 South Audley St., London, W.1.
10. R. A. Connolly and R. E. Landstrom, "Gopher Damage to Buried Cable Materials," Materials Research and Standards, p. 13, December, 1969.
11. R. A. Connolly and N. J. Cogelia, "Can any Cable Armor Stop A Gopher," Telephony, p. 23, June 1970.
12. F. B. Livingston, "Cable Damage by Gophers," Bell Laboratories Record, p. 147, April, 1946.
13. W. E. Howard, "Tests of Pocket Gophers Gnawing Electric Cables," Journal of Wildlife Management, p. 296, July, 1953.
14. G. Schick, "Corrosion of Lead Sheath Cables," private communication, Bell Telephone Laboratories, Whippany, N.J.
15. R. B. Diffenderfer, "Corrosion of Lead Sheathed Cables," Paper 91, National Association of Corrosion Engineers, Chicago, Illinois, March, 1974.
16. P. H. Middleton, "Required Testing and Protection of Buried Polyethylene Jacketed Lead Sheath Coaxial Cables," Paper 80, National Association of Corrosion Engineers, Anaheim, Calif.,

March, 1973.

17. G. Schick, "Effect of Inhibitors on Aluminum Shield in Telephone Cable Sheaths," Paper 107, National Association of Corrosion Engineers, St. Louis, Missouri, March, 1972.

18. G. Schick, "Evaluation of Flooding Compounds for Corrosion Protection of Telephone Cable Shields," Paper 85, National Association of Corrosion Engineers, Anaheim, California, March, 1973.

19. K. E. Bow and T. S. Choo, "Corrosion Resistance of Plastic Clad Aluminum for Cable Shielding, Paper 88, National Association of Corrosion Engineers, Chicago, Illinois, March, 1974.

20. G. A. Lohsl and M. Romanoff, "Corrosion Evaluation of Shielding Materials for Direct Burial Telephone Cables, 17th International Wire and Cable Symposium, Atlantic City, New Jersey, December, 1968.

21. G. A. Lohsl and M. Romanoff, "Progress Report on Corrosion Evaluation of Shielding Materials for Direct Burial Telephone Cables, 18th International Wire and Cable Symposium, Atlantic City, New Jersey, December, 1969.

22. W. F. Gerhold, J. P. McCann, and W. E. Williamson, "Report on Corrosion of Underground Telephone Cable Shielding Materials in Soil Environments after Exposure for Four Years," Paper 87, National Association of Corrosion Engineers, Chicago, Illinois, March, 1974.

23. R. Baboian, "Corrosion Barrier Shielding Materials for Buried Wire and Cable," Paper 81, National Association of Corrosion Engineers, Anaheim, California, March, 1973.

24. R. Baboian and G. S. Haynes, "Corrosion Resistance of Copper Clad Stainless Steel Cable Shielding Materials, Paper 89, National Association of Corrosion Engineers, Chicago, Illinois, March, 1974.

25. E. D. Metcalf, "Smooth New Cable Shield Mops Up Moisture Problems, Telephony, p. 24, April, 1973.

26. Corrosion Considerations in Outside Plant, Rural Electrification Administration Telephone Engineering and Construction Manual, Section 670, December, 1970.

27. M. Romanoff, "Underground Corrosion," National Bureau of Standards Circular 579, U.S. Government Printing Office, Washington, D. C., 1957.

Dr. Robert Baboian is currently manager of the Electrochemical and Corrosion Laboratory in the Product Research Department. He joined Texas Instruments Inc. in September, 1966, as a member of the Scientific Technical Staff of the Research and Development Department.

After completing his Ph.D. work at Rensselaer Polytechnic Institute, he was awarded a Ford Foundation Postdoctoral Fellowship at the University of Toronto and was subsequently appointed Senior Research Associate. Dr. Baboian's work in the field of electrochemistry and corrosion has led to many publications and patents, and he is a member of the Executive Board of several technical societies.

Mr. Steven R. Hartley received a B.S. in Industrial Engineering from the University of Rhode Island in 1968 and has done graduate work in Engineering Management at Northeastern University. He is presently a Product Specialist in the Metallurgical Materials Division of Texas Instruments, Inc. working on the application of metallurgically bonded copper/steel materials systems. Prior to his current position, he was involved with marketing and quality engineering for temperature control and limit switches in the Control Products Division.

Mr. Edward D. Hyman received his Metallurgical Engineering degree from the Colorado School of Mines. His 26 years of industrial experience includes many phases of the metals industry and in capacities as process engineer, superintendent, manager of engineering and plant development. Currently he is the product engineer responsible for cable shielding products as well as other metallurgical materials systems.

A MATRIX INTERCONNECTION SYSTEM FOR AIRCRAFT WIRING

R. A. Bradshaw
Grumman Aerospace Corporation
Bethpage, New York 11714

E. F. Godwin
U.S. Army Electronics Command
Fort Monmouth, New Jersey 07703

Summary

A Matrix Interconnection System for Aircraft Wiring was developed and flight tested by Grumman Aerospace Corporation under U.S. Army Electronics Command contract. The Matrix Interconnection System utilizes flat conductor flat cable (FCFC) and a Matrix Interconnecting Device (MID).

Use of the MID has enabled Grumman to achieve a total systems approach to aircraft wiring which incorporates within its basic design concept provision for growth, circuit change, maintenance, functional test-ability and repair, while providing system performance equal to or better than current wiring concepts.

Introduction

In a conventional aircraft interconnecting system, Fig. 1, subsystem circuits are routed point-to-point with individually insulated round conductor wires. Wires and cables with a common origin and/or destination, or sharing at least some common routing, are assembled into harnesses by lacing, plastic ties or braided covering. To provide electro-magnetic compatibility (EMC) control of the systems during design, installation and test, requirements may be imposed for use of special constructions such as multiconductor twisted shielded, jacketed, or shielded and jacketed cables.

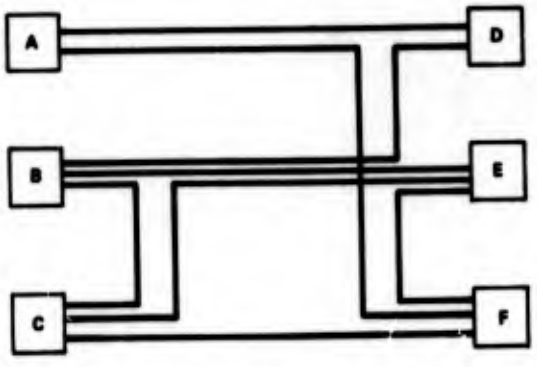

Fig. 1 Conventional Interconnection System.

In the Matrix Interconnection System, Fig. 2, all subsystem interconnecting circuits are routed to a Matrix Interconnecting Device (MID) via shielded and unshielded modular flat conductor flat cable (FCFC) assemblies. Within the MID the circuits are conveyed to removable matrix card assemblies. These assemblies are printed circuit boards with vertical traces on one side and horizontal on the other.

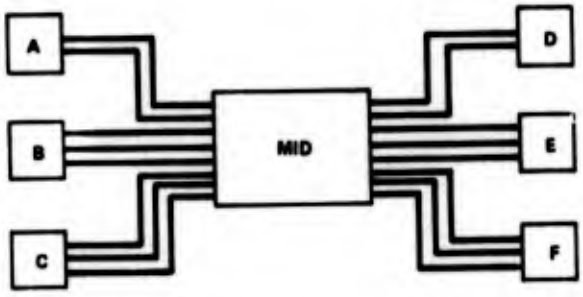

Fig. 2 Matrix Interconnection System

The traces form a matrix pattern with a broad subsystem interconnecting potential. Each matrix card assembly also has a test connector through which all subsystem circuits on the card can be interrogated or monitored without disturbing the subsystem interconnecting wiring.

The Matrix Interconnection System, developed by Grumman Aerospace Corporation, under U.S. Army Electronics Command contract, offers a total systems approach to aircraft wiring design. The basic MID design concept provides for growth, circuit change, maintenance, functional test-ability and repair, and provides EMC systems performance improvement over current round conductor wiring concepts.

To assure the validity of the development program, two Matrix Interconnection Systems were fabricated. One for environmental test and the second to interconnect the navigation and communication subsystems of an Army aircraft. The second Matrix Interconnection System was subjected to extensive systems performance evaluation during ground and flight tests. During these evaluations, performance tests were first conducted with the conventional wiring system to establish a reference from which the performance of the Matrix Interconnection System could be accurately evaluated.

The "base-line" aircraft selected was the OH-6A light observation helicopter equipped with the Standard Lightweight Avionics Equipment (SLAE) package and its associated electronics. On the OH-6A the SLAE and its associated electronics consists of:

- A VHF-FM Radio, for Communication and Homing
- A VHF-AM Radio for Communication
- A UHF-AM Radio for Communication
- A Direction Finder Set
- A Gyromagnetic Compass Set
- Three Communication Control Units, one each for pilot, copilot, and passenger
- A Transponder Set
- A Communication Security Set
- A Transponder Computer
- A Transponder Test Set
- A 28 vdc Power Supply
- A Static Inverter.

The conventional wiring system in the OH-6A utilizes shielded and jacketed single wires, and shielded and jacketed groups of twisted wires to interconnect the ac and dc power, audio, and discrete signals inherent to the SLAE equipments. The OH-6A conventional wiring system was designed and installed to meet the requirements of MIL-W-5088. This specification governs the selection and installation of wiring and wiring devices used for the interconnection of electrical and electronic equipment in aircraft.

System Analysis

To insure that the Matrix Interconnection Systems performance would be equivalent to, or better than the conventional wiring system, an extensive analysis was made of the SLAE equipped OH-6A. This analysis included definition of the electrical components utilized in the conventional interconnection system, SLAE equipment signal levels and characteristics, equipment power requirements and the generation of a wiring diagram for the SLAE equipped OH-6A in matrix interconnection system format. In this format all circuits from each basic electronic equipment, installation item and aircraft interface are defined "point-to-point" from the source to the Matrix Interconnecting Device (MID). In addition all electrical/electronic system interconnections are defined within the MID.

Two exceptions to the Matrix Interconnecting System concept were taken for the program:

- Four coaxial cables, used to transmit classified data between the Transponder Computer and the Transponder receiver/transmitter were not processed through the MID. This deviation was necessary because information on classified signals is difficult to obtain and without it the effects of the MID on the transmission line characteristics could not be predicted nor the completed system accurately evaluated.
- Wiring for the pilot's, copilot's and passengers' headsets was not processed through the MID because it is incorporated into special cable assemblies integral with the headsets or the headset control assemblies.

EMC Analysis

An extensive EMC analysis of the projected OH-6A matrix interconnection system was made early in the program. This analysis was accomplished to insure maximum utilization of flat cable's EMC predictability and repeatability characteristics. The analysis included a theoretical review of magnetic and electrical coupling in FCFC, laboratory tests of FCFC, and resulted in EMC design recommendations for the OH-6A's Matrix Interconnection System. These recommendations consisted of a detailed procedure for assigning circuits to the flat cable conductors, the assignment of areas for the various types of signals within the flat cable layers and a series of design guidelines for the MID and FCFC installation.

In order to assign circuits to the flat cable conductors, each circuit was classified with respect to its type of signal and signal level in accordance with Table I.

Table I

Circuit Classification

Type of Signal	Signal Level
Primary Power (From circuit breaker to the unit)	AC-115V, 400 Hz DC-27.5V
Secondary Power (From Unit to Unit)	AC-26V, 400 Hz DC-less than 27.5 DC-greater than 27.5
Signal Power (REF) (From Unit to Unit)	DC-from OV to ± 10 VDC DC-from ± 10 to ± 28 VDC
Discrete Signals (Step Function)	Bi-Level (OV to ± 5V) Bi-Level (OV to ± 28V)
Digital Signals (DC Pulse Train)	Bi-Level (OV to ± 5V) Bi-Level (O to ± 28V)
Analog Signals (Variable Amplitude and/or Frequency)	AC-(OV to 5 VAC) AC-(OV to 26 VAC)
RF Signals (above 20 KHz)	AC-(OV to 30)

The conversion from the OH-6A conventional round conductor configurations to equivalent FCFC was accomplished in accordance with Table II. The following EMC design parameters were involved during this phase:

- High voltage level discrete and low voltage level analog (or vice versa) signals should not be shielded adjacent to each other in the same layer of flat cable. A minimum of one flat conductor, grounded at both ends, should be used to separate them.
- Two different types of signals with the same signal voltage level may be shielded adjacent to each other in the same layer of the flat cable.
- All leads which are shielded in the conventional system, should be shielded in the Matrix Interconnecting System.
- Spare leads in the flat cable should be grounded at the MID box end only.
- 115 vac and 28 vdc primary power leads should be separated from all other leads with a lead grounded at both ends. Chassis ground or signal ground may be used for this purpose.

Table II Electrical Characteristics Comparison, Round Conductor vs Flat Conductor

ROUND CONDUCTOR-22AWG		FLAT CONDUCTOR	
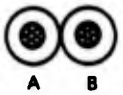 A B TWISTED PAIR	CAPACITANCE 11pf/ft A to B	 A B PARALLEL LEADS	CAPACITANCE 5.68pf/ft A to B
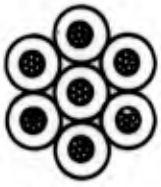 MULTILEADS	Lead-to-Lead 33pf/ft	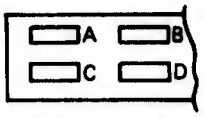 A B C D MULTILAYER	3.07pf/ft A to B 26.59pf/ft A to C
 SINGLE LEAD SHIELDED	Conductor-to-Shield 98pf/ft	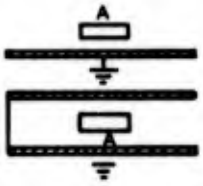 A	63.79pf/ft A to Shield 112.57pf/ft A to Shield
 A B TWISTED PAIR SHIELDED	Conductor-to-Conductor 36.5pf/ft Conductor-to-Shield 62.5pf/ft	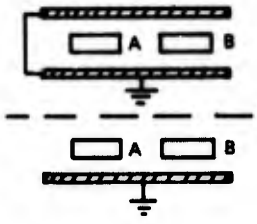 A B A B	0.17pf/ft A to B 112.57pf/ft A to Shield 1.27pf/ft A to B 63.79pf/ft A to Shield
 THREE WIRE-TWISTED SHIELDED	Conductor-to-Conductor 30pf/ft Conductor-to-Shield 52pf/ft	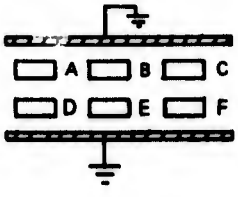 A B C D E F	0.64pf/ft A to B 111.2pf/ft A to Shield 22 pf/ft A to D

REFERENCE – DH 1-4 Series 1-0
AFCS DESIGN HANDBOOK
ELECTROMAGNETIC COMPATIBILITY
SECT-5B2, SUB NOTES 6 (1) & 6 (2)

REFERENCE – ITT Cannon Electric
FLAT CABLE CONNECTOR TERMINATION
SYSTEMS AND DESIGN GUIDES
FIGURES 12 THROUGH 15

- Shielded leads should not be adjacent to the primary power leads. A minimum of one lead grounded at both ends should separate the signal carrying lead from the 115 vac and 28 vdc. A power return may be used for this purpose.

Areas within the FCFC layers were assigned to the different types and levels of signals in accordance with the following EMC design parameters:

- Primary power leads should be allocated to the top or bottom layer. If a second flat cable group is superimposed, the power leads should be on opposite sides of the two groups.
- Primary power leads shall be located away from analog signals.
- Flat cables from one connector interfacing with more than one other connector should have the area assigned per the individuals connectors. In each area, proper shielding and separation procedures shall be followed.

MID Construction

The Matrix Interconnecting Device, Fig. 3, consists of three subassemblies: housing, connector plate and 12 matrix cards. The unit measures 10.0 in. (254 mm) x 10.5 in. (266.7 mm) x 5.5 in. (139.7 mm). Located on two opposite sides of the housing are sixteen input/output connectors accommodating a total of 816 circuits. The OH-6A SLAE package, associated electronics and aircraft interface requires approximately 680 circuits. This leaves 136 spare circuits for future system growth, without change in unit dimension.

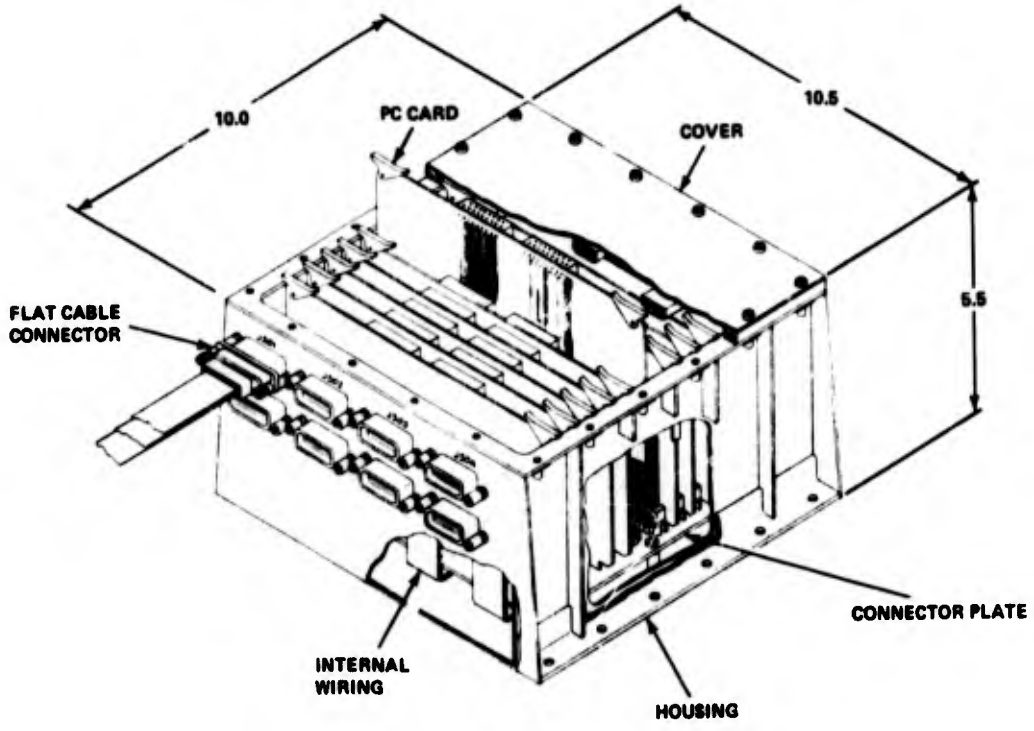

Fig. 3 Matrix Interconnecting Device (MID)

MID Housi g

The housing is constructed of .060-in. thick (1.52 mm) aluminum alloy, 6061 condition "0". This becomes hardened to 6061 T4-T5 during the dip brazing assembly process. Reinforcing ribs are incorporated on the four sides of the housing to prevent diaphragming. Ribs on the connector sides of the housing are located internally. Cut-outs are provided on two opposite sides of the housing for back-panel mounting the sixteen flat cable connector receptacles, eight connectors per side. Each connector receptacle, Cannon part number FCB3C222SIE, accepts 3 one-in. (25.4 mm) cables, each with 17 conductors spaced at .050 in. (1.27 mm) centers. Metal guides are riveted to the inside of the housing to facilitate insertion of the matrix cards.

The cover assembly is of similar dip braze construction. Three stiffener channels are added to the inside of the cover. Hard rubber strips cemented to the inside of these channels act as matrix card retainers. To prevent possible RFI emissions, an RF gasket is used between the cover and the housing.

Connector Plate

The connector plate, which is used to terminate all input/output circuits and for interconnecting between matrix boards, is made from 6061 T-6 aluminum alloy and measures 8.0 in. (203.2 mm) x 8.5 in. (215.9 mm) x .080 in. (2.03 mm) thick. The plate is drilled to a standard hole pattern to accept 1176 contacts of the tuning fork type. The contacts are divided into 12 double rows with each double row having 98 contacts. Four contacts in each group are grounded to the plate to furnish a common ground for shields of the flexible printed circuit cables. Figure 4 shows the termination of the flexible printed circuit cable to the bottom of the connector plate.

Internal wiring between the flat cable connectors and the connector plate is accomplished by use of a flexible printed circuit. This is a 17 conductor flat cable with the conductors spaced at .050 in. (1.27 mm) centers on one end and at .150 in. (3.81 mm) centers at the other. Since all connections in this system are direct point-to-point, all the flexible printed circuits are the same configuration. The cable is shielded on one side with 1 oz. (.031 kg) copper foil. This provides signal separation when the cables are stacked. The narrow end of the flexible printed circuit is terminated to the connector insert wafer by means of a heat shrinkable Multiple Splice Module. The wide end is soldered to the terminal pins on the underside of the connector plate.

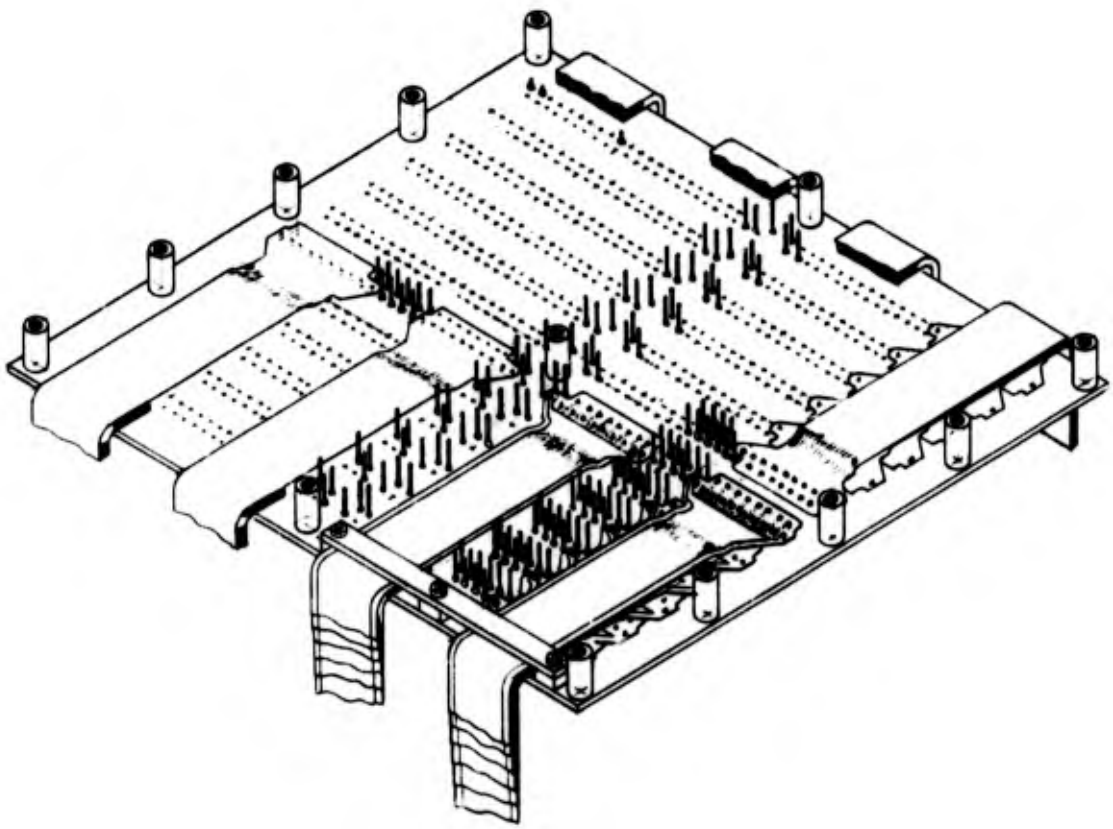

Fig. 4 Connector Plate

Matrix Board Assembly

Each matrix board assembly consists of five parts: the printed circuit board, stiffener, header, test connectors and ejectors. The printed circuit board is .062 in. (1.57 mm) glass epoxy clad on both sides with 2 oz. (.062 kg) copper, and measures 8.600 in. (218.4 mm) x 4.750 in. (120.6 mm). One side of the board has vertical conductors which terminate with a header. The opposite side has horizontal conductors and are used to interconnect two or more vertical conductors by means of soldered wire, eyelets or through plated holes.

The header assembly consists of an aluminum "Z" extrusion with 98 male contact pins which mate with the double rows of female contacts on the connector plate. The header is assembled to the printed circuit board with three rivets and the contacts soldered to the pads provided on the vertical conductors. Provisions are made on the printed circuit board for mounting two test connectors for checking continuity, monitoring system performance and troubleshooting simply by removing the cover from the housing assembly. Two plastic ejectors located on each end of the board are used to facilitate its removal.

Flat Cable Assemblies

While the Matrix Interconnecting concept is compatible with both conventional round conductor wire and flat conductor flat cable, flat cable was utilized for the program because it provided:

- Predictable and repeatable EMC characteristics
- Reduced size and weight through its increased current carrying capacity and physical strength properties
- Modular replaceable assemblies.

Flat Cable Description

The specific cable used was a one-in. (25.4 mm) wide x .012-in. (.305 mm) thick polyimide/flourinated ethylene propylene (Kapton/FEP) insulated cable having seventeen .005 in. (.127 mm) x .025 in. (.635 mm) conductors (approx. AWG 28) on .050 in. (1.27 mm) centers.

Only two variations of the FCFC were required to interconnect the entire OH-6A navigation and communication systems; shielded one side and unshielded. Shielding was accomplished with a .001 in. (.0254 mm) solid copper foil.

A current carrying capacity analysis made on the selected flat cable determined that a single flat conductor, utilizing a 50°C temperature rise, would carry in excess of 3.5 amp. Since the maximum input power requirement of any individual SLAE equipment item could not exceed 3.088 amp, it was evident that the current carrying capacity of the selected FCFC would not be the limiting factor in the Matrix Interconnecting System design. Accordingly, our efforts progressed to a voltage drop analysis.

After calculating the resistance of typical input power circuit configurations used in the existing SLAE equipped OH-6A, calculations were made using one, two, three and four parallel flat conductors. From this effort it became evident that the voltage drop values of the existing conventional OH-6A interconnecting wiring would be difficult to duplicate, even by paralleling conductors and the MID circuits. For this reason an investigation was made to determine if satisfactory equipment performance could be achieved with them. The investigation made clear the fact that the voltage drops occurring in the Matrix Interconnecting System, though larger than those of the conventional OH-6A interconnecting wiring, were reasonable and within the limits set forth in Military Standard 704A, when two, three or four conductors were bussed together.

Flat Cable Connector

The Cannon "FC" series connector, designed and tested to meet the requirements of MIL-C-55544, was selected for use on the program. This connector contains three removable modular wafer inserts which can be used singly or joined with one or two others to terminate individual pieces of flat cable or round wire. They are inserted or removed from the back of the connector; thus, a cable terminated on each end by one of these modular wafers can be installed or removed at any time.

This connector has a cadmium plated cast aluminum shell, gold plated pin and socket contacts, and thermoset plastic modular insert wafers. Coupling is accomplished by jack-screws made of stainless steel.

Flat Cable Termination

Termination of the FCFC to the flat cable connector was accomplished with a Multiple Splice Module (MSM). The MSM consists of individually insulated solder preforms and copper strips with their number and spacing identical to that of the flat connector contacts and flat cable conductors. The solder preforms and copper strips are contained in a heat shrinkable device which is activated by placing the assembly between heated platens for a controlled period of time.

Transition of the Matrix Interconnection Systems FCFC to the existing circular or rectangular connectors of the OH-6A's avionic boxes was accomplished with a variation of the MSM device. This device has size-24 wires on one side which were used to interconnect the contacts of the avionic box connectors.

Design Feasibility Testing

A design feasibility testing program was conducted on the Matrix Interconnection System for Aircraft Wiring. This program demonstrated that the system components were suitable for the intended application and established its performance characteristics with respect to the performance of the OH-6A's conventional round conductor interconnecting wiring.

Environmental Testing

The environmental testing program subjected the Matrix Interconnection System for Aircraft Wiring to the following:

- Thermal Shock- in accordance with MIL-STD-202C, Method 107B, Condition B

- Vibration- in accordance with MIL-STD-810B, Method 514.1, Procedure 1, Time Schedule 1, Curve M

- Physical Shock- in accordance with MIL-STD-810B, Method 516, Procedure 1

- Moisture Resistance- in accordance with MIL-STD-202C, Method 106B with steps 7A and 7B omitted

- Thermal Aging - ten cycles of 125°C for 20 hours followed by 20°C for four hours.

During this testing program 384 flat connector contacts and 384 matrix board contacts were monitored for circuit discontinuities in excess of ten microseconds. In addition 144 circuits were monitored for dielectric strength in accordance with MIL-STD-202C, Method 301, with a test voltage of 1000 vac applied for 60 seconds. Insulation resistance was also measured on these same 144 circuits in accordance with MIL-STD-202C, Method 302, Condition B (500 v ±10%).

The environmental test program disclosed the need for matrix board stiffeners (which were incorporated) and improved environmental resistance in the connector design. During the moisture resistance test sufficient moisture entered the MID through the interstices between the flat connector insert wafers to lower the average insulation resistance values from 10^{10} ohms to 10^{5} ohms.

Ground Testing

An extensive electromagnetic compatibility (EMC) evaluation was accomplished utilizing an OH-6A System Integration Test Stand (SITS). The SITS consisted of an OH-6A mock-up configured with the actual OH-6A SLAE package, associated electronics, antennas, antenna cables, relays and switches.

Two identical tests were performed on the SITS. In the first test the SLAE and associated electronics were interconnected with a duplicate of the OH-6A conventional round conductor interconnecting wiring. In the second test the SLAE and associated electronics were interconnected with the MID and FCFC of the Matrix Interconnecting System.

Test data obtained with the conventional round conductor wiring was used as a baseline from which the Matrix Interconnection System's performance could be evaluated. Testing of both systems was accomplished in a function vs. function matrix format encompassing 29 modes of operation for both interconnecting systems.

The test results obtained reflected an improvement in overall system electromagnetic compatibility when the Matrix Interconnecting System was utilized. In addition, a decrease of 4 dB in measured "noise" level was obtained at the copilot's headset with the Matrix Interconnection System.

Flight Test

Flight testing of the Matrix Interconnection System for Aircraft Wiring was accomplished on an Army model OH-6A helicopter, serial number 17144 during June of 1974. Again two identical tests were accomplished. During the first, the OH-6A was evaluated "as delivered" with the SLAE and associated electronics interconnected with the conventional round conductor wiring. During the second, the aircraft's SLAE and associated electronics were interconnected with the MID and FCFC of the Matrix Interconnection System.

The installation was accomplished by disconnecting, capping, and stowing all connectors and individual circuits that interconnected the SLAE, associated electronics and aircraft interface. The MID was installed in the passenger compartment with an adapter mounting panel and the FCFC system installed alongside the disconnected conventional interconnecting wiring.

Each of the two evaluations consisted of three systems tests: ground, preflight and flight. Data obtained during the evaluation of the OH-6A in the "as-delivered" state was used as a baseline from which the performance of the Matrix Interconnection System was evaluated.

The test results summarized in Fig. 5, showed that the Matrix Interconnection System provided an overall 58% improvement in systems electromagnetic compatibility. Another improvement, also shown in Fig. 5, indicates that with the Matrix Interconnection System installed, the SLAE equipped OH-6A was, for the first time, able to meet the 3 mv requirement of MIL-E-6051.

A major improvement was also made in the Aircraft's Homing. With the conventional interconnecting wiring the Steering Dial was totally unreliable. The aircraft's panel contained a notice: "FM Homing Unreliable". At most frequencies the Steering Dial on the Heading Indicator was 180 degrees out from the direction of the signal source. However, with the MID and FCFC the Homing capability of the aircraft was such that it was either exact, or off by a maximum of five degrees.

It was noted during testing that the aircraft's dials and indicators monitoring engine performance and fuel quantity showed no indication of susceptibility to EMI. Also, turning equipment on or off, landing lights or anti-collision lights, caused no excessive transients to be heard in the earphones.

An unexpected benefit of the Matrix Interconnection System installation in the OH-6A was the significant reduction achieved in the time required to remove and replace avionic boxes despite the fact that it was not an optimum installation.

Conclusions

While providing proven, flight tested performance at least equivalent to current wiring concepts, the basic design concept of the Matrix Interconnection System for Aircraft Wiring has provisions for:

- Growth - through adequate spare MID input/output circuits

- Circuit Change - because all changes are accomplished simply by removing and replacing the applicable matrix card(s)

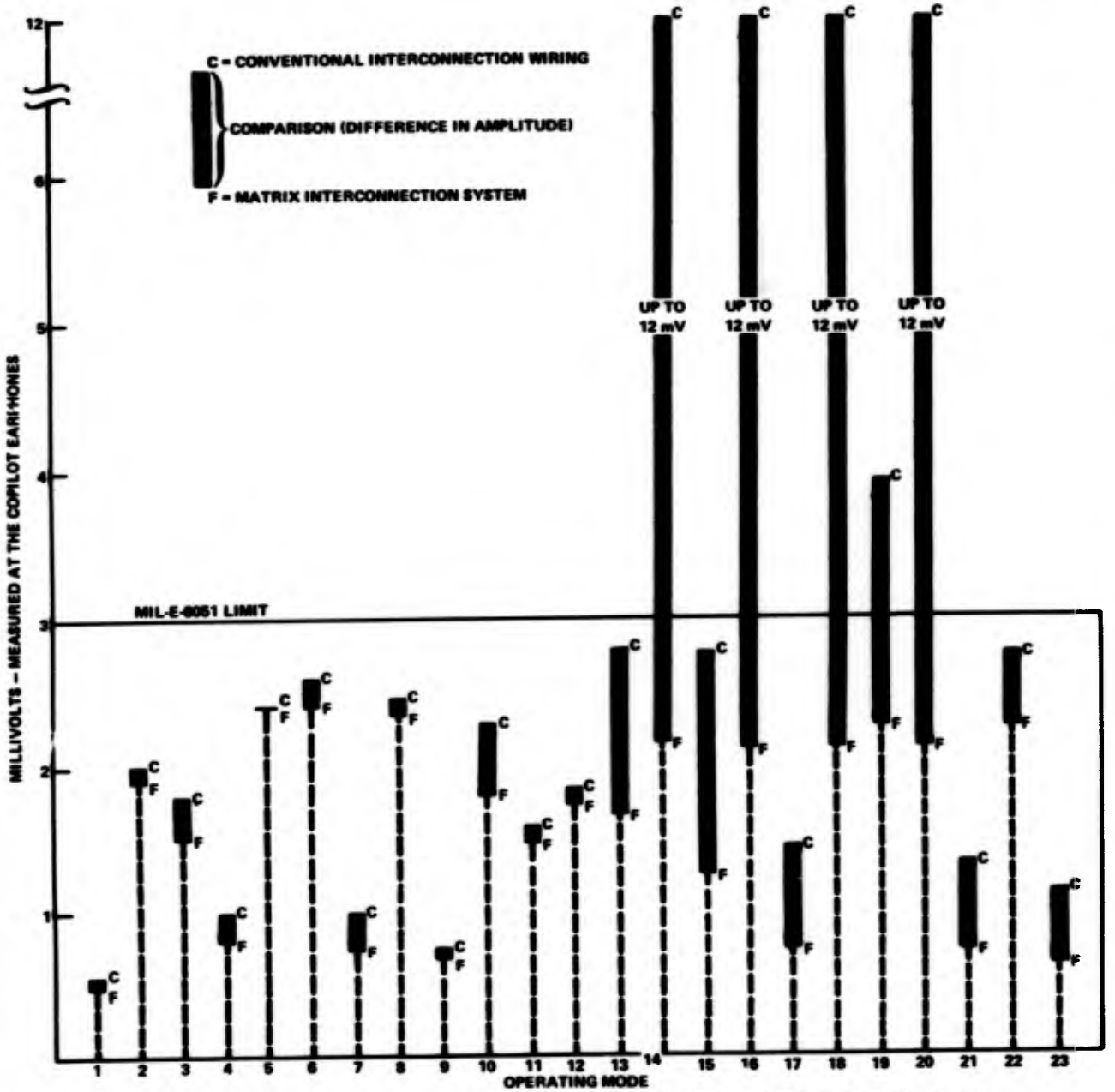

OPERATING MODE	EQUIPMENT TESTED
1	COMMUNICATION CONTROL/COMPASS
2	COMMUNICATION CONTROL/ VHF-FM RADIO
3	COMMUNICATION CONTROL/ VHF-AM RADIO
4	COMMUNICATION CONTROL/ UHF-AM RADIO
5	COMMUNICATION CONTROL/ DIRECTION FINDER (COMPASS POSITION)
6	COMMUNICATION CONTROL/ DIRECTION FINDER (ANTENNA POSITION)
7	COMMUNICATION CONTROL/ TRANSPONDER (IFF, MODE 1)
8	COMMUNICATION CONTROL/ TRANSPONDER (IFF, MODE 2)
9	COMMUNICATION CONTROL/ TRANSPONDER (IFF, MODE 3A)
10	TRANSPONDER (IFF)/ VHF-FM RADIO
11	TRANSPONDER (IFF)/ VHF-AM RADIO (MODE 1)
12	TRANSPONDER (IFF)/ VHF-AM RADIO (MODE 2)
13	COMMUNICATION SECURITY (PLAIN)/ VHF-FM RADIO
14	COMMUNICATION SECURITY (CIPHER)/ VHF-FM RADIO
15	COMMUNICATION SECURITY (PLAIN)/ VHF-AM RADIO
16	COMMUNICATION SECURITY (CIPHER)/ VHF-AM RADIO
17	COMMUNICATION SECURITY (PLAIN)/ UHF-AM RADIO
18	COMMUNICATION SECURITY (CIPHER)/ UHF-AM RADIO
19	COMMUNICATION SECURITY (PLAIN)/ DIRECTION FINDER
20	COMMUNICATION SECURITY (CIPHER)/ DIRECTION FINDER
21	COMMUNICATION SECURITY (PLAIN & CIPHER)/TRANSPONDER (MODE 1)
22	COMMUNICATION SECURITY (PLAIN & CIPHER)/ TRANSPONDER (MODE 2)
23	COMMUNICATION SECURITY (PLAIN & CIPHER)/TRANSPONDER (MODE 3A)

Fig. 5 Flight Test, EMC System Performance Comparison

- Maintenance - through the use of matrix card ejectors, modular input/output FCFC assemblies, utilizing but two types of flat cable and internal flexible printed circuits
- Functional Test Ability - through the use of test connectors on each matrix board, which make it possible to interrogate or monitor circuits without disturbing the subsystem interconnecting wiring
- Repair - through the use of "back-panel" mounted connectors, modular FCFC assemblies, and standard matrix board assemblies.

Acknowledgements

The authors wish to acknowledge the contributions of Messers. B. Lijoi, E. Truslow and J. Brunter of Grumman, and Messers. D. Lichenstein and J. Rubin of the U.S. Army Electronics Command for their significant efforts in development of the Matrix Interconnection System for Aircraft Wiring.

Richard A. Bradshaw (Speaker)
Grumman Aerospace Corporation
Bethpage, New York 11714

Mr. Bradshaw has over seventeen years of engineering experience related to aerospace interconnection technology. For the past seven years he has been employed by Grumman as a Component Application Specialist responsible for wire, cable and aerospace interconnection systems.

Prior to Grumman, he was a Senior Designer of aerospace cable assemblies for a major components supplier. In this capacity he was responsible for the design and supervision of the prototype manufacture of many advanced cabling systems. Mr. Bradshaw attended the State University at Farmingdale, New York and Pratt Institute Evening School, Brooklyn, New York.

E. F. Godwin
U. S. Army Electronics Command
Fort Monmouth, New Jersey 07703

Mr. Godwin attended Rutgers University where he received his B. S. degree. He has been employed by the U. S. Army Electronics Command for over thirty (30) years. During this time he has engaged in research and development activities related to various electronic components. He is presently the leader of the Transmission Electro- Mechanical Devices team of the Electronic Technology and Devices Laboratory, U. S. Army Electronics Command, Fort Monmouth, New Jersey, and is responsible for research and development of wires, cables, connectors and electro-mechanical devices.

He is a member of various industrial/military technical committees and is acknowledged as the Army's spokesman on multi-conductor cables, wires, and cable assemblies.

TRANSMISSION CHARACTERISTICS OF OPTICAL FIBERS

By

A. H. Cherin
Bell Telephone Laboratories, Inc.
Norcross, Georgia

Abstract

Recent developments in optical fiber and source technology have stimulated considerable interest in optical communication systems. Optical fibers with losses of less than 10 dB/km are being fabricated routinely at Bell Laboratories and at Corning Glass Works. In addition, substantial progress has been made in extending the lifetime of GaAs injection lasers. As a result of these developments, optical fibers may soon be used to complement conventional wire pairs and coaxial cables in a wide range of applications.

This paper will review the transmission characteristics of optical fibers. The mechanisms that produce attenuation and time dispersion in the optical fiber medium will be described along with techniques for measuring these quantities. When optical fibers are packaged and placed in cables, small deformations of the fiber axis can occur which alter the transmission characteristics of the fibers. Changes in the loss and time dispersion of the optical fibers due to packaging will also be considered.

Introduction

Since the first low-loss optical fiber was made by Corning Glass Works (CGW) in 1970 (a single-mode silica fiber with a loss of 20 dB/km at 0.6328 um wavelength),[1] a number of laboratories have made multimode optical waveguides with minimum losses of 1.2 to 20 dB/km at various useful wavelengths. Knowledge of the transmission properties of such optical fibers and how they are affected when placed in structures is essential for the proper design of future optical communications systems. To understand these transmission properties, Bell Laboratories has undertaken a program to characterize potentially useful fibers.[2] A number of fibers were measured to determine their transmission loss over a wide spectral range. The dispersion suffered by short optical pulses in traversing a length of fiber was also measured. In this paper, some results from this program will be presented. Transmission loss and pulse dispersion are important parameters that are used in determining the repeater spacing and bandwidth of an optical communications system.

Transmission Characteristics of Optical Fibers

A typical optical fiber, shown in Figure 1, consists of an inner cylinder of glass of refractive index n_1, called the core, surrounded by a cylindrical shell of glass of lower refractive index n_2, called the cladding.[3] As shown in Figure 2, the number of modes that a fiber can support is proportional to the core diameter squared and to the difference between the squares of the core and cladding refractive indexes. For the multimode fibers discussed in this work, a typical core diameter was 75 um with a cladding diameter of 125 um. The refractive index difference between the core and cladding was less than 1% of the core refractive index.

Transmission Loss Mechanisms

Loss occurs in a dielectric waveguide when energy is extracted from the propagating field and reradiated out of the guide or converted to heat. As seen in Figure 3, there are several mechanisms which may cause transmission loss to occur in a fiber waveguide.

1. Material Absorption Loss - Loss due to conversion of energy to heat by impurity atoms in the glass. For example, an important absorbing ion in glass is OH^-. Figure 4 shows the absorption bands due to OH^- in fused silica glass in the .5 to 1.0 um region of the spectrum. Approximately 1.25 parts per million by weight of OH^- will cause a 1 dB/km peak loss in the glass. Approximately 1 part per billion of ion impurities such as Cr^{3+}, Fe^{2+} or Cu^{2+} will cause 1 dB/km peak losses in the glass. High purity glass is required to achieve low loss fibers.

2. Material Scattering - There are different scattering mechanisms in the glass material that can cause loss in the fiber. Rayleigh scattering will always be present in glass materials and determines the minimum possible loss the waveguide can have. Rayleigh scattering is caused by minute dielectric inhomogeneities in the glass. The inhomogeneities may be caused by thermal fluctuations, compositional fluctuations, or phase separations and are on a small scale compared to the wavelength of the propagating energy.[4] A well made high silica glass will cause Rayleigh scattering loss of about 0.9 dB/km at 1.0 um; this loss varies inversely as the fourth power of the wavelength.[5]

3. Waveguide Scattering - Geometric variations in the size of the fiber core and/or index of refraction variations along the length of the fiber will cause transfer of power between guided modes and/or from a guided mode to the radiation field. Fortunately, the scattering losses due to a "rough" interface between the core and the cladding in a well made low loss fiber are small.

4. Other Loss Mechanisms - Radiation loss due to curvature of the guide, loss due to opaque coatings on the surface of the cladding and crosstalk loss between fibers must be considered in designing an optical fiber cable. Proper cable design and choice of

fiber parameters such as cladding thickness and numerical aperture can minimize these loss mechanisms.

Transmission Loss Spectra

Figure 5 is a block diagram of a measuring set used to determine the transmission loss spectrum of an optical fiber. Transmission loss measurements in the spectral range from 0.5 to 1.1 um wavelength are made by a two-point method. The optical power received at the end of a long fiber is measured in sequence at various wavelengths; the fiber is then cut and the received power from the shorter waveguide is measured at the same wavelengths. The ratio of the output to input power in decibels at the various wavelengths is used in plotting the transmission loss spectrum of an optical fiber. Figure 6 is a typical loss spectrum for a high silica low loss optical fiber. The spectral regions of primary interest for optical communication are 0.8 - 0.9 um and the region of the spectrum about 1.06 um. These are the regions of the spectrum where optical sources exist and the fiber loss is the lowest. Fibers are routinely made at BTL and CGW with losses less than 10 dB/km at 0.8 um and 1.06 um. Fibers with losses as low as 1.2 dB/km have been made.

Pulse Dispersion

A measure of pulse dispersion in an optical fiber can be obtained by observing how an optical pulse is broadened as it propagates down the guide. The dispersion of a dielectric waveguide mode is a function both of the material and of the waveguide characteristic. In multimode guides, the waveguide introduces delay between the various modes. The basic causes of pulse dispersion in an optical fiber are explained below.

1. Material Dispersion - The index of refraction of the glass is wavelength dependent. Many light sources considered for optical communication cover a fairly wide optical frequency band. Light emitting diodes have a relative band (bandwidth devided by the center frequency) of about 4%, GaAs lasers have up to 0.1%, and Nd: YAlG lasers about 0.01%. The temporal spread of a pulsed input signal depends on the bandwidth of this signal. For practical fiber materials, it is of the order of 1 nsec/km for every percent of relative bandwidth.[6]

2. Multimode Group Delay - For a single wavelength the power in each mode of a multimode fiber travels at a different velocity. The rays corresponding to each mode travel at different angles, and the higher the order of the mode, the longer the overall path becomes. For a high silica fiber with a 1% difference between the core and cladding refractive indexes, multimode delay distortion can be as high as 48 nsec/km.

3. Other Factors Affecting Pulse Dispersion - A reduction in multimode group delay can be obtained by shaping the refractive index profile of the core of a multimode fiber. Fibers with index profiles approximating that of a parabola have had measured pulse dispersion as low as 3 nsec/km. Mode coupling is another factor that will reduce multimode group delay. Propagation in a fiber can be viewed in terms of packets of energy traveling first in one mode, then in another, followed by still another - with specific delays characteristic of the uncoupled modes while the packet is in a particular mode. The result is that the energy arrives at the end of the fiber with a delay that is a weighted average of the delays of all of the modes.[5]

Measurement of Pulse Dispersion

Figure 7 is a diagram of a measuring set used to determine pulse dispersion in an optical fiber. A GaAs laser operating at 0.9 um wavelength is triggered to produce a train of short duration optical pulses. The train of pulses is injected into a fiber and the input and output light pulses are observed on a sampling oscilloscope. Figure 8 is an oscillogram showing the temporal delay of a 1 km low loss flat index profile high silica fiber (see Figure 6 for loss characteristics) with a numerical aperture of .133. The deconvolved output pulse width for this fiber was 8.1 ns/km. If we had assumed that the fiber had a flat index profile and that no mode mixing occurred, the calculated multimode group delay would have been 20 nsec/km.

Microbending Loss Due to Packaging

It has been known that small amplitude random bends in a fiber's axis in the order of 1 micrometer rms amplitude with a bend period of 1 millimeter can cause substantial optical loss.[7,8]

Figure 9 shows a 455 meter length of fiber wound under controlled tension onto a 10" diameter cast acrylic drum having a surface that is not perfectly smooth. The tension forced the fiber to partially conform to the surface roughness. The left half of the fiber was wound under 0.7 kg/mm^2 tensile stress, and the right half under 7 kg/mm^2. It can be seen from the scattering of the He-Ne laser light injected into the fiber that the light is decaying much more rapidly in the right half. In fact, the microbending loss is 15 dB/km in the left half and 145 dB/km in the right half. Random bends created by packaging can add hundreds of dB/km to the loss of the fiber, although several dB/km are more typical.[9] This loss can be decreased by increasing (N_1-N_2), increasing the cladding diameter, decreasing the core diameter, or applying a thick uniform coating to the fiber. The packaging should be designed to mechanically decouple the fiber from its environment as much as possible.

References

1. D. B. Keck and A. R. Tynes, "The Spectral Response of Low Loss Optical Waveguides," Applied Optics, Vol. 7, 1972.

2. A. H. Cherin, L. G. Cohen, C. A. Burrus and P. Kaiser, "Transmission Characteristics of Three Corning Multimode Fibers," Applied Optics, October, 1974.

3. A. H. Cherin, "Fiber Optics: An Over-View of a Future Alternative Transmission Medium," Proc. of 21st Internation Wire and Cable Symposium, December, 1972.

4. T. Li, E. A. J. Marcatili, "Research on Optical Fiber Transmission," Bell Laboratories Record, December, 1971.

5. S. E. Miller, E. A. J. Marcatili and T. Li, "Research Toward Optical Fiber Transmission Systems," Proc. of I.E.E.E., Vol. 61, December, 1973.

6. D. Gloge, "Dispersion in Weakly Guiding Fibers," Applied Optics, Vol. 10, November, 1971.

7. D. Gloge, "Bending Loss in Multimode Fibers with Graded and Ungraded Core Index," Applied Optics, Vol. 11, November, 1972.

8. D. Marcuse, "Losses and Impulse Response of a Parabolic Index Fiber with Random Bends," BSTJ, Vol. 52, October, 1973.

9. W. B. Gardner, "Microbending Loss in Optical Fibers," BSTJ (to be published).

ALLEN H. CHERIN

Allen H. Cherin received his Ph.D. Degree in Electrical Engineering from the University of Pennsylvania in 1971. He earned his MSEE Degree at the University of Vermont in 1965 and his BEE Degree in 1961 from the City College of New York.

Dr. Cherin joined Bell Laboratories in 1965 as a Member of Technical Staff. In the Transmission Media Laboratory he has worked on various projects related to the characterization of transmission lines. Since June, 1971, he has been working on problems related to the development and characterization of a fiber optic communications cable.

Dr. Cherin is a member of the I.E.E.E. and the Optical Society of America.

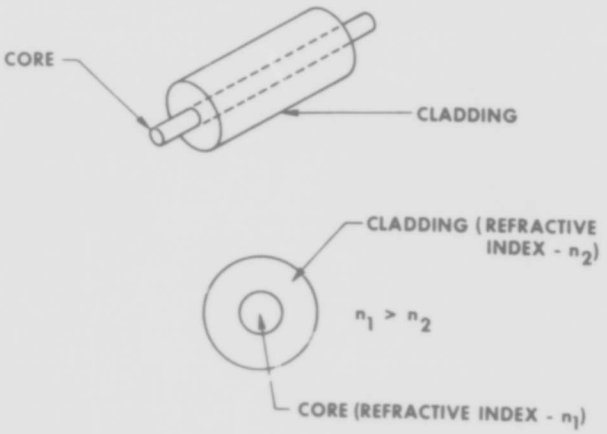

FIGURE 1
THE GEOMETRY OF A TYPICAL FIBER

$$N = \frac{k D_1^2}{\lambda^2} \left[n_1^2 - n_2^2 \right]$$

N= NUMBER OF PROPAGATING MODES

D_1 = CORE DIAMETER

λ = WAVELENGTH OF PROPAGATING ENERGY

n_1 = CORE REFRACTIVE INDEX

n_2 = CLADDING REFRACTIVE INDEX

k = PROPORTIONALITY CONSTANT

FIGURE 2

- MATERIAL ABSORPTION LOSS
- MATERIAL SCATTERING LOSS
- WAVEGUIDE SCATTERING LOSS
- OTHER LOSS MECHANISMS
  - Crosstalk
  - Lossy Coatings
  - Curvature Loss

FIGURE 3

TRANSMISSION LOSS MECHANISMS

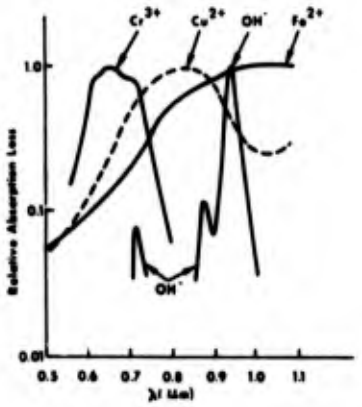

Ion	Concentration for 1-dB/km Peak Loss in Glass (fractions by weight)
OH^-	1.25 parts in 10^6
Cu^{2+}	2.5 parts in 10^9
Fe^{2+}	1 part in 10^9
Cr^{3+}	1 part in 10^9

FIGURE 4
RELATIVE ABSORPTION LOSS VERSUS WAVELENGTH FOR CERTAIN IONS IN GLASS

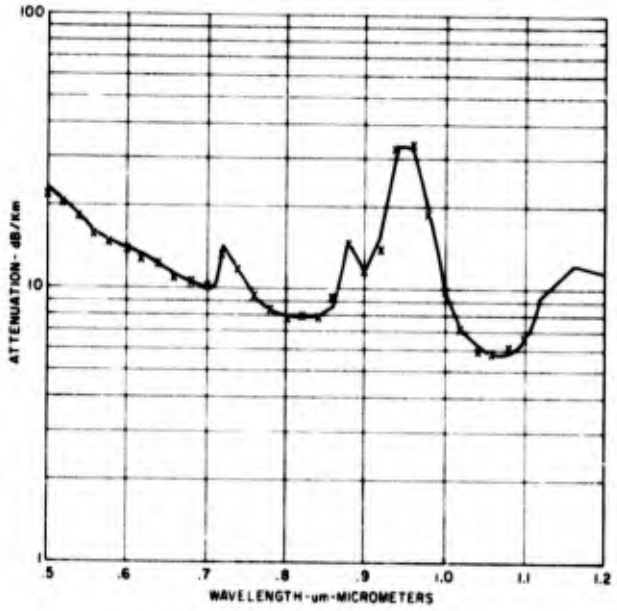

FIGURE 6
TYPICAL LOSS SPECTRUM OF LOW LOSS OPTICAL FIBER

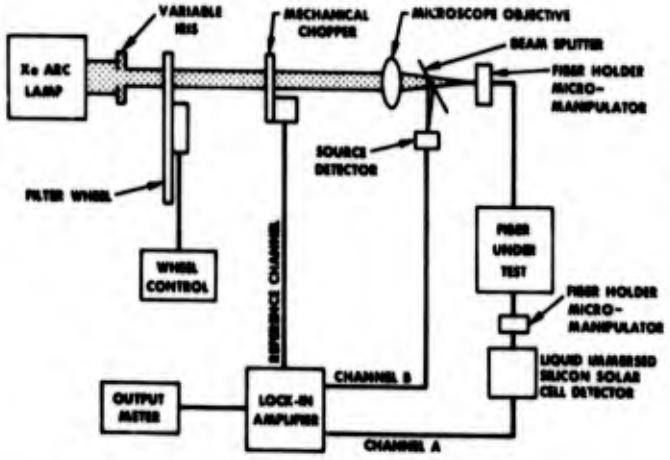

FIGURE 5
LOSS MEASURING SET FOR OPTICAL FIBERS

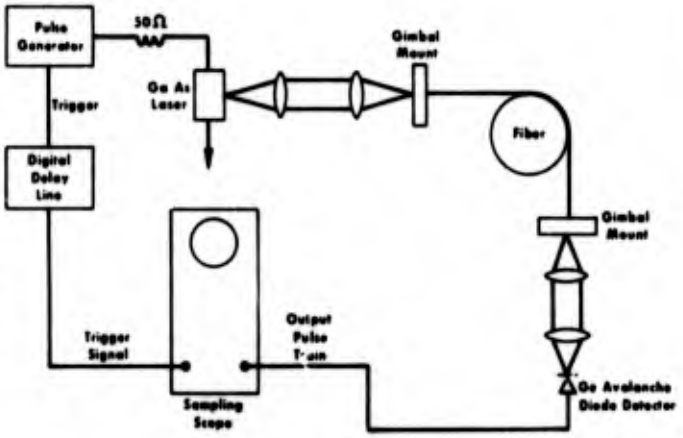

FIGURE 7
PULSE DISPERSION MEASURING SET

(a) Input Pulse Width = 2.4 ns

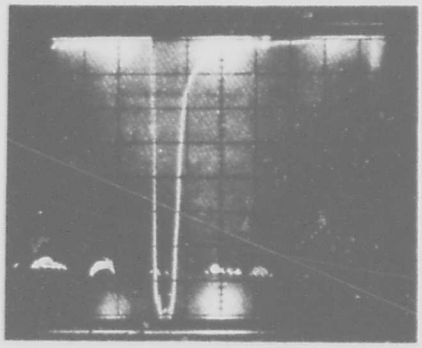

(b) Output Pulse Width = 8.4 ns

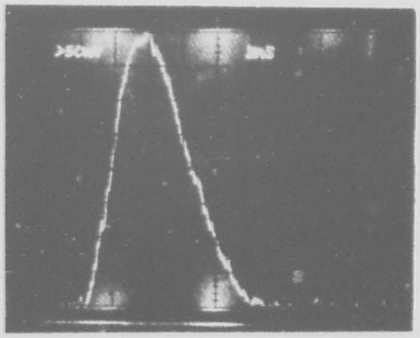

FIGURE 8

TYPICAL PULSE DISPERSION IN LOW LOSS OPTICAL FIBER

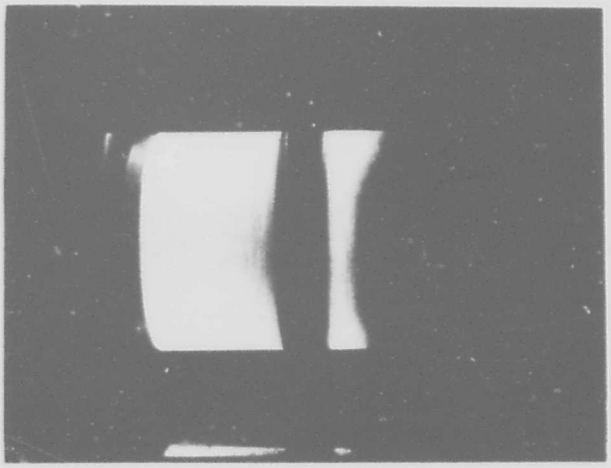

Figure 9

TACTICAL LOW LOSS OPTICAL FIBER CABLE FOR ARMY APPLICATIONS

By

Dr. Roger A. Miller
Corning Glass Works
Corning, New York 14830

And

Mr. Morton Pomerantz
United States Army Electronics Command
Fort Monmouth, New Jersey 07703

Summary. This paper describes the initial effort to develop low-loss optical cables for tactical army communications applications. Advantages of fiber optic versus metallic conductor cables are discussed as well as inherent problem areas associated with fiber optics. Design and processing approaches to resolution of problems and evaluation of fiber optic cable units are included.

INTRODUCTION

In July 1973, the US army Electronic Command (ECOM) initiated a program under contract with Corning Glass Works (Corning) for the development of low loss fiber optic communications cables for use in tactical Army applications. The stimulus for this program was the major breakthrough achieved by Corning toward the end of 1970 in producing glass fibers with attenuation at discrete near infrared wavelengths of 20dB/km. In the relatively short time since then both Corning and Bell Telephone Labs have achieved attenuation of 5dB/km and under. Since the 1970 breakthrough various studies conducted by the Services confirmed the feasibility of employing fiber optic cables in communications systems. This new low-loss medium offered the potential of many significant advantages compared with metallic conductors, including:

Long distance transmission (8 kilometers) without repeaters

EMP, EMI, Crosstalk immunity

Bandwidth capabilities
10^8 bits/sec/km for multimode fibers
10^{11} bits/sec/km for single mode fibers

Light weight

Difficult to tap

Long term cost reduction of communication systems

While the foregoing desirable features of low loss optical fibers were generally recognized, there were significant problem areas which had to be addressed in order to utilize them in cable constructions suitable for military communications systems. Prior to the start of the ECOM program, Corning was providing, in various lengths, bundles of 61 fibers loosely packaged within an extruded PVC jacket, and terminated with epoxy-filled brass ferrules. These served quite well for the military feasibility studies in sheltered environments, but were in no sense advertised as cables suitable for field use. The basic problem was the inherent fragility of the glass fibers themselves. This then was the thrust of the ECOM program with Corning; to develop low loss fiber optic communications cables which are lightweight, rugged, and flexible to withstand tactical field Army conditions. These included bending, twisting, impact, vibration, compression, abrasion, temperature extremes (-55°C to +85°C), humidity, water immersion, fungus environment, EMI, EMP, and nuclear radiation. Moreover, the optical fibers were expected to remain continuous with only minimal loss of their excellent transmission properties when subjected to these conditions.

Army Requirements for Tactical Fiber Optic Cables

Before proceeding with the discussion of the contractual development effort, it will be useful to present an overview of the Army's requirements for tactical fiber optic cables. Table 1 shows a summary of the Army requirements and applications. Although three distinct applications areas are shown, the great majority of applications are for moderate and long distance ground-based communications links. Accordingly, the bulk of the Army's activities will be directed toward developing cables for these applications. Tables 2 and 3 are essentially breakouts of the moderate and long distance applications, showing in more detail the short-term (1980 time frame) planning for application of fiber optic cables in communication systems. Some of the more serious problems with current conventional cables are shown together with planned fiber optics programs in the systems, cable technology, source, detector, and connector areas, and the major development barriers which must be overcome in each of these programs. For the long distance applications, cables with attenuation of 5 dB/km or better are required. Major barriers are fiber ruggedization and cabling to achieve continuous kilometer lengths of low loss cables, reduced pulse dispersions for high bit rate applications, and cost. For the moderate distance applications, attenuation up to 50 dB/km is satisfactory, thus providing possibilities for effecting greater cost reduction in this area.

FIBER OPTIC CABLE DEVELOPMENT

Fiber Strength Preservation

The basic approach in the development program was to try to provide strengthening and/or buffering of individual fibers such that subsequent bundling, cabling, and field use would not cause fiber breakage or adverse effect on the optical properties. Unlike metals, glass fails abruptly without previous yield or permanent deformation, and failure always results from a tensile component of stress even when the load is applied in compression. It is now generally acknowledged that failures in glass ultimately originate from surface flaws or imperfections. The stress concentration at such flaws can be many times greater than the nominal stress at the same point, and since there is no yielding, this stress can not be relieved. Thus, if a high enough tensile stress is applied, the result is flaw growth, propagation, and eventual failure. Glass, then, does not have a specific strength; its strength is a statistical phenomenon dependent on the size and frequency distributions of the surface flaws.

Although the as-drawn strength of glass fibers can

be quite high, fiber from any practical drawing unit is inevitably flawed to some extent during the drawing process and to an even greater degree during any subsequent handling. One approach for maximizing fiber strength is to preserve as much of the as-drawn strength as possible by applying an abrasion-resistant covering to the fibers on the fiber draw as soon as possible after the fiber-forming operation. In Corning's present fiber drawing process, this covering is a 0.1 to 0.2 mil-thick coating of KYNAR® 7201, a polyvinylidene fluoride material manufactured by the Pennwalt Corporation. Although this may not be the optimum coating for optical fibers, it does provide some degree of surface protection for the fibers and it has no effect on their optical attenuation. Since the construction of any cable structure containing glass fibers will depend upon their initial strength and their ability to withstand abrasions during the processing operations, some such protective coating must be considered a prerequisite.

Cable Unit Concept

The approach to cable construction, throughout this program, has been based on a unit concept. The unit was originally visualized as a sub-assembly made up of several waveguide fibers incorporated in an organic matrix. Such units would possess sufficient tensile strength to allow them to be handled on conventional cable-making equipment and thus could serve as the basic building blocks for cable construction. By bringing together a number of cable units and adding the appropriate strength members and external protective coating, cable assemblies of any design could be attained. Since cable unit construction involved the handling of individual fibers and the defining of strength and coating requirements, it proved difficult to separate this phase of cable construction from fiber manufacture in the initial work.

The optical waveguide cable unit (OWCU) as initially conceived is shown in Figure 1. This sectional view represents six KYNAR®-coated, low-loss fibers (B) stranded around a central member (A) of the same diameter. Based on the standard 5 mil-diameter fiber dimensions, the maximum stress produced in the fibers as a result of stranding at a lay of one turn per inch is 4500 psi. This was not considered detrimental from either a mechanical or optical standpoint. Though such stranding offers little in the way of increasing fiber length to accommodate for cable expansion and loading, it is a way of equalizing fiber length, improving flexibility and providing a known geometric array for fiber identification. Furthermore, the central member could impart some tensile strength to the unit if it were made from a high-strength, high-modulus material. Two materials which meet the central member requirements are glass and KEVLAR®-49, a product of the DuPont Company. The research identification for this latter material was PRD-49. The final stages of the cable unit assembly (C) and (D) were an encapsulation performed in conjunction with the stranding and a subsequent jacketing operation. The material considered for encapsulation was polyurethane and the jacketing material, although shown as KYNAR® 200 in Figure 1, could have been any material compatible with subsequent cabling operations.

Fiber Distortions

The first cable units based on this design had the six KYNAR®-coated fibers stranded around a KEVLAR® central member at one turn per foot. The urethane encapsulant was applied from solution or by an electrostatic powder coating process. In every case, the individual low-loss fibers in these assemblies showed quite sizeable increases in optical attenuation as a result of being included in the cable unit structure.

The cause of these attenuation increases is now known to be small axial distortions produced in the thin waveguide fibers during the encapsulation.(1) The force exerted by the encapsulant, either during its application or as it shrunk while curing, was sufficient to cause the fibers to bend or distort around the imperfections in the rough surfaced KEVLAR® central member. The attenuation increases due to such small axial distortions are perhaps most easily visualized with the aid of the ray diagram shown in Figure 2. Any ray inside the waveguide which is which is incident on the core-clad interface at an angle equal to or greater than the Snell's law critical angle θ will undergo total internal reflection and will propagate down the waveguide. This determines the waveguide acceptance angle γ. The effect of the distortion is to cause rays near the critical angle to be incident on the core-clad interface at some angle less than θ. These rays are no longer totally internally reflected and are soon lost.

Considerable improvement was noted when smooth steel wires were substituted for the KEVLAR® central member, but even then, three-fold increases in fiber attenuation were not uncommon. In these cases, the fiber perturbations were believed to arise from irregularities in the KYNAR® fiber coatings themselves. It was concluded from these early experiments that more had to be done to isolate the low-loss fibers from their environment in the cable unit structure. One solution appeared to be a smooth, thick, low-modulus coating capable of taking up some of the stress exerted by the encapsulant. Such a coating will be referred to as a buffer coating to distinguish it from the strength preserving coating applied at the time of fiber manufacture, although it is conceivable that the proper coating, properly applied might serve both functions.

Fiber Buffering

Buffer coatings have been applied to individual waveguide fibers from solution, by an electrostatic powder process and by extrusion. The materials available for solution coating cover a wide range of material properties and, in general, solution coatings do not significantly affect the optical attenuation of the fibers. However, for the 3 - 5 mil coating thickness range of interest, the coating process was slow, it was difficult to consistently obtain a smooth and uniform coating, and complete drying or curing was always a problem. The only materials applied by the electrostatic powder process, which did not drastically affect fiber attenuation, were low-modulus thermoplastics. Unfortunately, it is difficult to produce powders of the small particle size required for this particular electrostatic coating application from low-modulus materials, and it proved impossible to make smooth 3 - 5 mil-thick coatings from the 2 - 5 mil particle size powders which were available. The most successful buffer coatings have been those applied by extrusion. This method has the advantages that coatings can be applied from a variety of materials, they can be applied either tightly or loosely over a large range of thickness, and they can be made smooth and uniform.

The two families of materials which have been the most fully examined for extrusion buffering are the fluorocarbons and the urethanes. As shown in Table 4, neither TEFLON®, PFA or FEP applied as a loose coating nor urethane applied either as a loose or a tight coating degraded the optical properties of the

waveguide fibers. Although TEFLON®, PFA and FEP are not particularly low-modulus materials, they are capable of being extruded at high draw down ratios to give smooth, uniform coating at high production rates. Both TEFLON®, PFA and FEP and urethane extrusion-buffered fibers have been successfully incorporated in cable units.

Cable Unit Design

A sectional view of the first type of cable unit constructed around buffered fibers is shown in Figure 3. In this construction, the central member is also thickly coated as an added safeguard against fiber distortions. Various combinations of PVC and polyether-based urethanes were investigated for use as the encapsulating and jacketing material. The original solution or electrostatic encapsulating process had been abandoned in favor of a tubing-type extrusion. The outer jacket was also applied by extrusion. The culmination of work with this design was a cable unit 1100 feet long. The individual fibers were buffered with a 3 mil TEFLON® FEP-extruded coating and the central member was a 5 mil steel wire with a 3 mil TEFLON® PFA jacket. The fibers were stranded around the central member at one turn per foot. The encapsulant was urethane extruded to a diameter of 62 mils and the jacket was PVC extruded to give a final cable unit 125 mils in diameter. All six fibers were continuous in the 1100 foot length and none showed any significant increase in attenuation arising from the processing operations. The deficiency of cable units based on this design was tensile strength. Except for the limited tensile capability of the central member, the only tensile capability such units had was that provided by the optical members themselves.

The cable unit design shown in Figure 4 was an attempt to remedy the tensile deficiency of the previous design. It provided six parallel KEVLAR® strength members symmetrically positioned around the encapsulated unit at the encapsulant-jacket interface. Six, 380-denier KEVLAR® strands could be expected to add approximately 90 pounds to the tensile strength of the unit. Unfortunately, cable units based on this design were not successful. Regardless of the encapsulant-jacket combination used, the individual KEVLAR® strands buckled during the extrusion and reeling operations, and this resulted in a two to three-fold increase in fiber attenuation. Neither the 3 mil-thick TEFLON® FEP buffer coating on the fibers nor the intervening encapsulant was capable of shielding the fibers from distortions arising as the KEVLAR® buckled.

It may have been possible to have minimized the KEVLAR® buckling or the effects resulting from the buckling with additional process work, but this was not extensively pursued. Since a cable unit based on this design would possess far more tensile capability than was actually required in any subsequent cabling operations, the more expedient approach of simply removing some of the KEVLAR® seemed adequate. The configuration adopted is shown in Figure 5. This structure has only two parallel KEVLAR® strands positioned along the cable axis, but with 380 denier KEVLAR®, the strength of such a unit approaches 30 pounds. Buckling has not been a problem with this design and fibers packaged in this structure have shown little, if any, increases in attenuation. A recent modification of this design, shown in Figure 6, is a further attempt to prevent any possible strength member-fiber interaction. The thicknesses of the fiber buffer coatings and the encapsulant have both been increased to provide more isolation for the fibers. In this case, the jacket serves only as a covering for the KEVLAR® strength members. The performance of cable units based on this latter design will be discussed in a later section.

Materials

Once the feasibility of packaging waveguide fibers in a cable unit structure without degrading their optical properties had been established, the question of materials became critical. The central member used in all the experiments described above had been a coated steel wire. This had been used to expedite the evaluation of the basic units, but it was not acceptable for any final cable assembly. Urethane and PVC had been used interchangeably and in all possible combinations as the encapsulating and jacketing materials, and although both worked equally well at room temperature, it was impossible to obtain a PVC capable of satisfying both -55°C and +85°C temperature requirements. Consequently, all subsequent cable units have been constructed with a buffered waveguide fiber as the central member, and only polyether-based urethanes have been used for encapsulating and jacketing. The urethane presently in use is ROYLAR® E-9, a product of the Uniroyal Chemical Company. This material is reported to be capable of satisfying the abrasion, temperature, and weathering requirement of military cable jackets.

Cable Units for Final Evaluation

Cable units based on the design shown in Figure 6 have been constructed with black TEFLON® PFA and ROYLAR® E-9 urethane-buffered fibers and evaluated optically for their attenuation, optical isolation, and temperature coefficient of attenuation, and mechanically for their tensile, flexure, twist, and impact capabilities. These units consisted of six buffered fibers stranded around a seventh, similar fiber at one turn per foot. The stranded assemblies were encased in a 28 mil-thick extrusion of ROYLAR® E-9 and then jacketed with a 12 mil-thick layer of ROYLAR® E-9 in a subsequent extrusion. The two strength members were parallel strands of 380 denier KEVLAR® positioned 180° apart at the encapsulant-jacket interface. In all cases, the buffered fibers used in these assemblies were 15 mils in diameter. The PFA coatings were 3 mils thick and were applied to provide a 2 mil clearance between the fiber and the coating. The urethane was applied both as tight and loose-fitting coatings. The tight-fitting coatings were 5 mils thick; the loose-fitting coatings were 3.75 mils thick and applied to provide a clearance of 1.25 mils between the fibers and the coatings. In this latter case, the void between the fiber and the coating was filled with a Dow-Corning 200 Fluid which would remain fluid at -55°C.

Optical Evaluation - Attenuation

Cable unit evaluations have been based on the 820 nm attenuation of the individual fibers in the units. The basic measurement techniques for waveguide fibers have been well documented.[2,3] The total attenuation coefficient, B (λ), in dB/unit length is given by

$$B(\lambda) = \frac{10 \log I(L_2)/I(L_1)}{L_1 - L_2} \qquad (2)$$

where $I(L_1)$ and $I(L_2)$ are the transmitted light intensities, at wavelength λ, through lengths L_1 and L_2 of waveguide, respectively. First, the transmitted light intensity is measured through the total sample length L_1. Then, without altering the launching end configuration, a short length L_2 is cut from the sample and the transmitted intensity is measured through the

short length.

The measurement system used for the attenuation determinations is shown in Figure 7. The radiation source is a 150-watt xenon arc lamp. The light from this lamp is filtered by an 820 nm narrow band interference filter mounted directly in front of the lamp. The half-power bandwidth for this filter is ±5 nm. The filtered light next passes through a light chopper, for phase-sensitive detection, to a beam splitter where a portion of it is extracted and directed to a power meter which monitors the source output. The beam splitter also allows the launching end of the fiber to be viewed through a telescope for alignment purposes. The major portion of the light passes through the beam splitter and is incident on a 10X, .25 NA microscope objective which focuses it on the fiber end. The light transmitted through the fiber is detected by a PIN-10 photodiode. The PIN-10 and power meter outputs are fed into separate lock-in amplifiers, and the lock-in outputs go to an electronic ratioing device. This device normalizes the signal output to the reference input. The resulting signal is displayed on a strip chart recorder. The precision of the measurements made with this system is believed to be on the order of ±2 dB/km for cabled fibers. Using this system, the results of the attenuation measurements are presented in Table 5.

Optical Evaluation - Optical Isolation

A lower limit for the optical isolation of the fibers in the cable units was determined at 633 nm. For each cable unit, one fiber was physically isolated from the remaining six fibers at the input end of a 600-foot long sample and overfilled with light from a Ne-He laser. By attenuating the input beam, the detection limit of the measuring apparatus was found to be -60 dB. Then attempts were made to measure the total output of all combinations of any three of the remaining six fibers when the input beam attenuation was removed. In no case, for any of the cable units examined, could a detectable signal be observed. Since the detection limit of the apparatus had been established to be -60 dB, this implied that the optical isolation in the test samples was ≥ 60 dB.

Optical Evaluation - Temperature Coefficient of Attenuation

The effect of temperature on the attenuation of the cabled fibers was determined on 100-foot long cable unit specimens. These were loosely wrapped on a cardboard drum and then placed in a STATHAM® temperature test chamber. Both the input and output ends were maintained at room temperature. All data were taken at a wavelength of 633 nm. Differences in transmission upon temperature change were used to compute the temperature coefficients of attenuation. About 15 minutes were required for the transmitted light output to stabilize after each temperature change. No hysteresis effects were observed when the cable units were brought back to room temperature. The results are shown in Table 6. The values given are the dB/km/°C change in attenuation for a temperature change from 20°C to the indicated temperature. Because of the extremely large temperature coefficient for the cable unit containing fibers tightly buffered with urethane, no further characterization of this unit was performed.

Mechanical Evaluation - Tensile Test

Tensile tests were performed on cable unit samples as illustrated in Figure 8. Terminated specimens were brought around 3-inch diameter sheaves and clamped at one side of each sheave. The distance between the center of the sheaves was 25 inches. A force gage was attached to the top sheave and the load was applied at the lower sheave. The loading rate was 0.1 pounds/sec. The excess cable extending from the two clamps allowed the fibers to be continually monitored during the test in order to determine when failure occurred. Three samples were tested for each cable unit. The test results are given in Table 7.

Mechanical Evaluation - Flexure Test

Flexure testing was conducted on the fixture shown in Figure 9. The test consisted of flexing terminated cable unit samples over 5/8-inch diameter mandrels (5 times the cable unit diameter) 90° from their original vertical position, returning them 180° in one plane and then back again to their original position 10,000 times at a rate of 30 cycles per minute. The samples tested were 12 inches long and each was loaded with one pound. Six samples were tested for each cable unit. Only one fiber of the total of 84 fibers was broken after 10,000 flex cycles.

Mechanical Evaluation - Twist Test

Twist tests were conducted on the fixture shown in Figure 10. This test was accomplished by clamping one end of a cable unit sample, then passing it over a sheave and attaching a one-pound weight to the free end. The equilibrium distance between the center of the sheave and the free end of the sample was 22 inches. The weight was driven up and down and simultaneously twisted 30 times a minute to inflict a 180° twist (±90° from center) in the specimen between the sheave and the weight and a 180° bend in an 8-inch long segment of the sample as it passed over the top of the sheave. A 5/8-inch diameter sheave was used in this test. Three samples were tested for each cable unit. A test consisted of 2000 cycles. One TEFLON® PFA buffered fiber was broken after 1000 cycles. The remaining fibers were continuous after 2000 cycles.

Mechanical Evaluation - Impact Test

Impact testing was conducted on the fixture shown in Figure 11. Sixteen-inch long, terminated cable unit samples were centered under the drop hammer, fixed in position and subjected to 30 impacts per minute. The drop hammer radius was ½ inch. Six samples were tested at each drop height. Fiber transmissions were continually monitored during the tests. A test was terminated after 200 impacts or after a fiber was broken. The results of these tests are given in Table 8.

Cabling

The purpose of the cable unit approach was to provide a structure capable of being handled by conventional cable-making processes and equipment. The mechanical evaluation of the cable unit samples indicates that this has been accomplished. The ultimate test, however, will be the ruggedization of these units to provide the tensile strength, impact, etc., required for a tactical communication cable. Several cable manufacturers have proposed cable constructions structured around waveguide cable units to meet these specifications. This work is now in progress.

REFERENCES

1) R. Olshansky, "A Model of Distortion Losses in Cabled Optical Fibers," submitted for publication in Applied Optics

2) D. B. Keck and A. R. Tynes, "Spectral Response of Low-Loss Optical Waveguides," App. Opt. 11, 1502-1506 (1972)

3) J. F. Frazier and R. A. Miller, "Research and Development on Ultra-Lightweight Low-Loss Optical Fiber Communication Cable," Interim Report prepared for U. S. Army Electronics Command, Fort Monmouth, New Jersey, by Corning Glass Works under Contract DAAB07-73-C-0348, September 1974.

BIBLIOGRAPHY

Dr. Roger A. Miller

Dr. Roger A. Miller received his BS degree in Physics from Ohio University in 1956 and his PhD from Case Institute of Technology in 1963. He was a member of the Case Staff from 1963 to 1964. He joined Corning Glass Works in 1964 where he has worked for the past ten years on a variety of materials problems. He is now a Senior Research Physicist at Corning and is currently engaged in research and development activities on optical fiber waveguides and cables.

Dr. Miller is a member of the American Physical Society, the Optical Society of America, Association of Physics Teachers, Phi Beta Kappa, Phi Kappa Phi, and Sigma Xi.

Mr. Morton Pomerantz

Mr. Morton Pomerantz served in the Army in World War II from 1943 to 1946. He received his BEE degree from New York University in 1955. He has been employed at the U. S. Army Electronics Command since 1952 as an Electronics Engineer. In that time he has been engaged in R & R activities principally in the areas of RF cables and connectors and tactical communications cables.

Mr. Pomerantz is a Member of IEEE and the IEEE Electromagnetic Compatibility Group. He serves as a Working Group Leader of the ANSI committee on RF cables, and is a Department of Army advisor to the IEC National Technical Committee No. 46 on Cables, Wires, and Waveguides for Telecommunications Equipment.

He is currently engaged in development of fiber optic communication cable for tactical field army use.

TABLE 1

SUMMARY OF ARMY NEEDS AND APPLICATIONS

APPLICATIONS		
SHORT DISTANCE 1 m	MODERATE DISTANCE 1 m - 1 km	LONG DISTANCE 1 km +
1) INTRA-SHELTER WIRING. 2) AVIONICS DATA BUS. 3) ANTENNA CONNECTION	1) COMBAT POST DISTRIBUTION. 2) SPECIAL WEAPONS SYSTEM (OR SAM-D). 3) FIELD COMPUTER INTERCONNECT.	1) DOWN HILL FOV CABLE (NO REPEATERS). 2) 6 km PCM CABLE RUNS (WITH REPEATERS).

TABLE 2

MODERATE DISTANCE(100M - KM) CABLE CASE

APPLICATION	PROBLEMS	PROGRAM SEGMENT	BARRIER
REPLACE CURRENT 26 PAIR CABLE (CX-4366) WITH FIBER CABLE WITHIN COMMAND POST	CROSSTALK AT 30 KM s IN CURRENT CABLES IS INTOLERABLE	(1) SYSTEM INTEGRATION INTERFACE PROBLEMS	POWERING
	CABLE VOLUME REQUIRES SPECIAL TRUCK JUST TO TRANSPORT	(2) CABLE TECHNOLOGY: USE PLASTIC COATED [illegible] FIBERS	ACHIEVE CABLE STRENGTH. LOW COST (i.e. FEW CENTS/FT. PER FIBER)
	INSTALIATION TIME PROHIBITIVE	(3) SOURCE: HYBRID LOW COST LED AND DRIVER	SEMICONDUCTOR PACKAGING
		(4) DETECTOR: HYBRID PIN DIODE AND AMPLIFIER	INTEGRATION INTO SMALL PACKAGE
		(5) CONNECTORS: MULTIPAIR FIBER CONNECTOR	RUGGEDNESS RELIABILITY ALIGNMENT TOLERANCES, COUPLING LOSSES

TABLE 3

LONG DISTANCE(1KM +) FIBER CABLE CASE

APPLICATION	PROBLEMS	PROGRAM SEGMENTS	BARRIER
PROVIDING 6 KM 20 Mb/s DOWN-THE-HILL CABLE	LARGE CABLE VOLUME	(1) PROVIDE NECESSARY SYSTEM INTERFACE WITH EXISTING TERMINAL EQUIPMENT. PROVIDE LOCALLY POWERED REPEATER	
REPLACE CURRENT CX-11230 WITH FIBER CABLE	LARGE QUANTITY OF REPEATERS NEEDED. SERIOUS EMP PROBLEM FACED IN CURRENT SYSTEM	(2) CABLE TECHNOLOGY USE VERY LOW LOSS FIBER 5 dB/km	CABLE RUGGEDIZATION. CABLE LOSSES COST PULSE DISPERSION
		(3) SOURCE: USE HIGH PEAK POWER LASER (GaAlAs) SOURCE 20 Mb/s	LIFE TIME OF LASER
		(4) DETECTOR MODULE APD	
		(5) COUPLING: EMPLOY SPECIAL LENS COUPLERS	MOUNTING TOLERANCE
		(6) CONNECTORS	ALIGNMENT TOLERANCES RUGGEDIZATION COUPLING LOSSES

Table 4

Effect of Extrusion Coatings on Fiber Attenuation

All Coatings Extruded Over KYNAR®-Coated Fiber

Coating Material	Coated Fiber Diameter (mils)	Coating Condition	Fiber Attenuation @ 820 nm in dB/km ± 1 dB/km: Initial	After Coating
TEFLON® FEP	13	Loose	6.6	7
TEFLON® PFA	15	Loose	6.2	5.7
ESTANE® 58300 Urethane	14 - 20	Loose	5.4	5.2
ROYLAR® E-9 Urethane	15	Loose	6.8	6.1
ROYLAR® E-9 Urethane	15	Tight	6.5	8.0

Table 5

Optical Attenuation of Fibers in Cable Units(1)

Waveguide Buffer Coating	Cable Unit Length (feet)	Optical Attenuation of Cabled Fibers at 820 nm in dB/km ± 2 dB/km
TEFLON® PFA Loose-Fitting 0.003" Thick	1600	8, 10, 10, 10, 14, 17, 34
ROYLAR® E-9 Urethane Tight-Fitting 0.005" Thick	475	8, 9, 10, 10, 12 Two Fibers Broken
ROYLAR® E-9 Urethan Loose-Fitting 0.00375" Thick	1220	5, 7, 8, 8, 9, 9, 10

(1) Cable Unit Design Shown in Figure 6:

Total Buffered Fiber Diameter - 0.015 inches
ROYLAR® E-9 Encapsulant Diameter - 0.100 inches
ROYLAR® E-9 Jacket Diameter - 0.125 inches
Two 380-Denier KEVLAR® 49 Strength Members at Encapsulant-Jacket Interface

Table 6

Temperature Coefficient of Attenuation

The Values Shown are the dB/km/°C Change in Attenuation For a Temperature Change from 20°C to the Indicated Temperature

Temperature °C	OMCU Containing Fibers Loosely Buffered with TEFLON® PFA	OMCU Containing Fibers Tightly Buffered With ROYLAR® E-9 Urethane	OMCU Containing Fibers Loosely Buffered With ROYLAR® E-9 Urethane
85	-0.1		-0.05
80	-	-0.2	-
-20	+0.3	+2.2	-
-40	+0.4	+3.5	+0.3
-50	-	-	+1.3
-60	+0.65	+5.1	+1.4

Table 7

Tensile Test Data

1. OMCU Containing Fibers Loosely Buffered with TEFLON® PFA

Sample Number	Order of Fiber Failure	Load at Failure (Pounds) ± 0.2 Fiber	Cable Unit
1	1st 2nd-7th	15	28.8
2	1st 2nd 3rd-7th	15 19	30.0
3	1st 2nd 3rd-7th	25 33	36.0

2. OMCU Containing Fibers Loosely Buffered with ROYLAR® E-9 Uretha

Sample Number	Order of Fiber Failure	Load at Failure (Pounds) ± 0.2 Fiber	Cable Unit
1	1st-7th		27.6
2	1st 2nd-7th	34.5	35.0
3	1st-7th		32.0

Table 8

Impact Test Data

1. OMCU Containing Fibers Loosely Buffered with TEFLON® PFA

Sample Number	Impact Ft-Lbs	Number of Impacts	Number of Fibers Broken
1	0.19	200	0
2	0.19	200	0
3	0.19	200	0
4	0.19	200	0
5	0.19	200	0
6	0.19	146	1

2. OMCU Containing Fibers Loosely Buffered with ROYLAR® E-9 Urethane

Sample Number	Impact Ft-Lbs	Number of Impacts	Number of Fibers Broken
1	0.56	200	0
2	0.56	200	0
3	0.56	143	1
4	0.56	200	0
5	0.56	200	0
6	0.56	200	0

Figure 1 - Basic Cable Unit Design

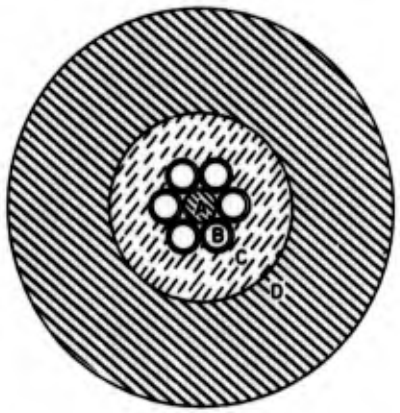

MATERIALS
A - DU PONT PRD-49
B - KYNAR # 7201 COATED WAVEGUIDES (6)
C - URETHANE
D - KYNAR # 200

Figure 2 - Ray Diagram

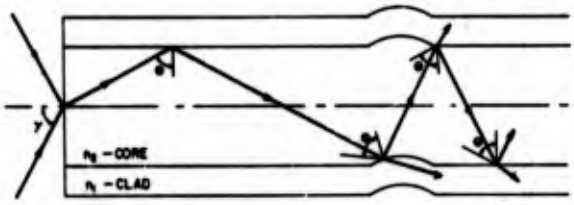

WHERE $\sin\gamma = \sqrt{n_2^2 - n_1^2}$
$\sin\theta = n_1/n_2$

Figure 3 - Experimental Cable Unit - Design #1

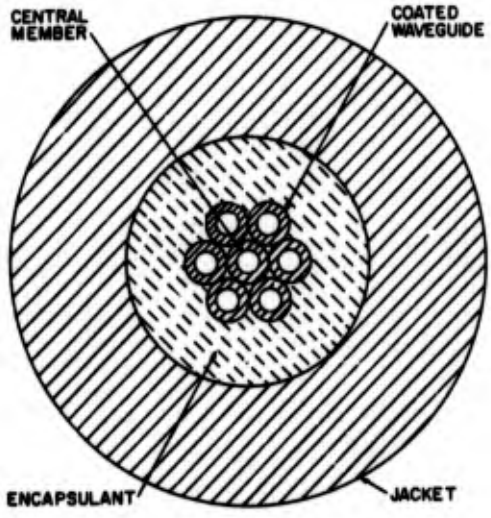

Figure 4 - Experimental Cable Unit - Design #2

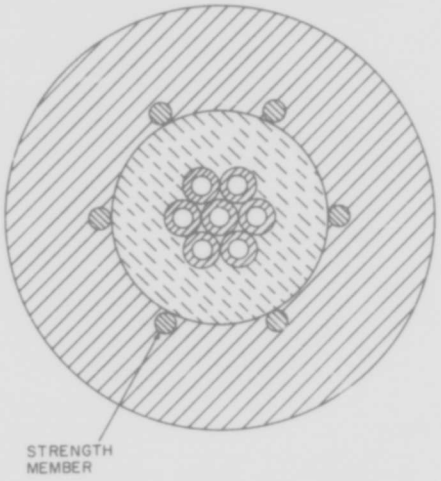

Figure 5 - Experimental Cable Unit - Design #2a

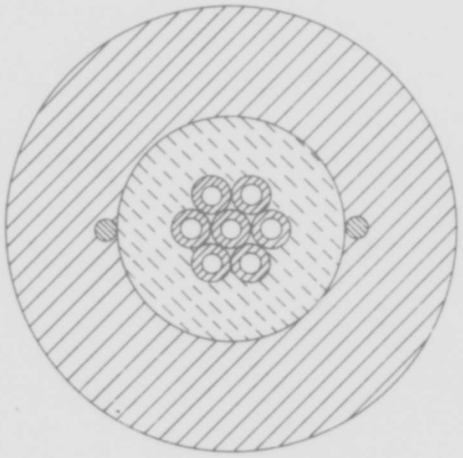

Figure 6 - Experimental Cable Unit - Design #3

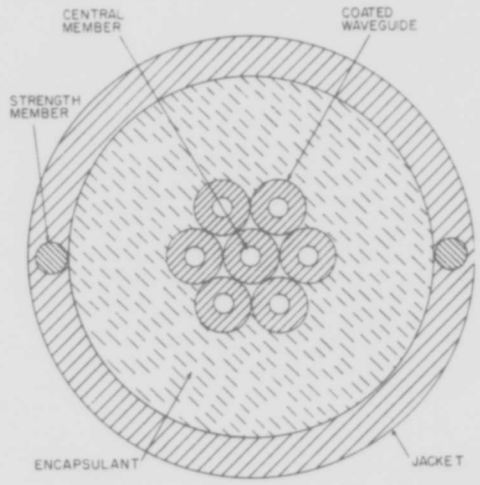

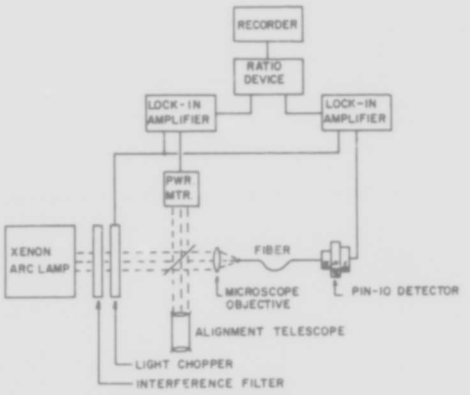

Figure 7 - Schematic of System for Measuring Attenuation

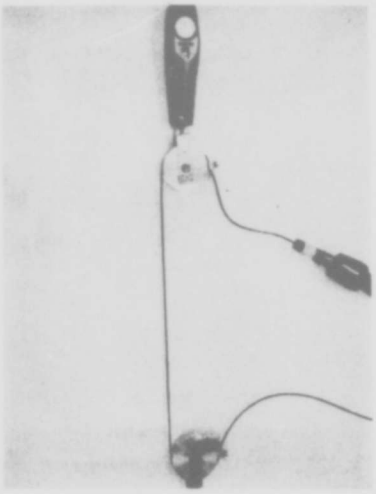

Figure 8 - Tensile Test Method

Figure 9 - Flexure (Bend) Test Fixture

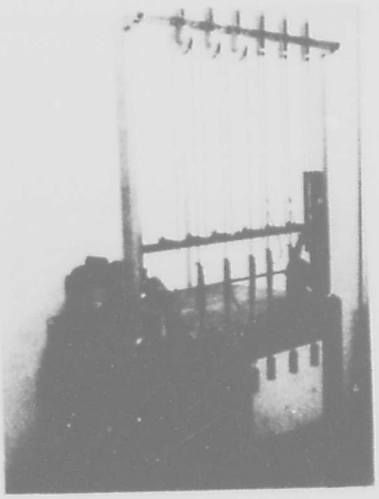

Figure 10- Twist Test Fixture

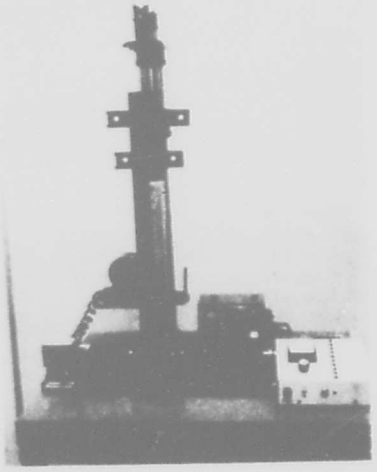

Figure 11- Impact Test Fixture

SOME DESIGN PRINCIPLES FOR FIBRE OPTICAL CABLES

S.G. Foord
W.E. Simpson
A. Cook
Standard Telecommunication Laboratories Limited,
London Road, Harlow, Essex, England.

Abstract

Basic design principles for practical fibre optical cables are discussed, with particular reference to mechanical aspects appropriate to manufacture, installation and service, and to some possible effects on optical performance. Problems relating to jointing of such cables are briefly reviewed.

Introduction

The prospect of using optical waveguides for the transmission of information at very high signalling rates has fired the imagination of communications engineers for a number of years. Principles for the assembly of complete systems have been well established but a great deal of work has had to be put in to provide the key components necessary to assemble a practical operating system. Such systems have been devised for a large number of applications ranging from comparatively short links of 100 metres or less to long-haul links in the order of kilometres. Most of the individual components required are associated with the terminal equipments which convert signals into modulated light beams and vice versa, but perhaps the most critical requirement is the optical waveguide itself. The accelerating interest in optical systems during the past few years can be ascribed largely to the striking reduction in optical attenuation which has been achieved in this component, and which makes possible transmission over long distances, e.g. in excess of 10km, without the use of repeating amplifiers.

Much has been published on the basic transmission properties of optical fibres, but comparatively little on the design and construction of practical cables. It is a main purpose of this paper to consider some of the problems associated with the latter aspect.

Basic optical fibre

The nature and mode of operation of an optical fibre was briefly described by Cherin at the 21st Wire and Cable Symposium in 1972. However, to assist in appreciating the problems of conversion into practical cables it is considered helpful to include a short description in this article.

The fibre comprises a central cylindrical core of high optical clarity surrounded by a cladding having a marginally lower refraction index. Two types of fibre are employed, depending upon the information rate and the length of the link, as shown in the following Table, which also gives typical dimensions of the core and cladding.

Fibre type	Information Rate	Link Length	Typical diameter (μ) Core	Cladding
Monomode	high	long	2	70
Multimode	high low/medium	short long	60	70

Successful operation has been demonstrated with both types of fibre, but although monomode fibre has the higher transmission capacity, and lower attenuation has been achieved with it, there are certain practical difficulties in its use which have resulted in more extensive employment of multimode fibre. From the point of view of cable making however, there is little fundamental difference in processing of both types when similar materials are used in their construction.

It is of interest to consider at this point what materials are employed in optical waveguides. The most commonly used materials are silica, borosilicate glasses, and soda lime silicate glasses, all in a very high state of chemical purity to minimise optical losses. For each system it is necessary to vary the composition as between core and cladding to achieve the required refractive index difference, which must be small and well controlled. This usually results in differences in softening temperature and melt viscosity, and thermal expansion coefficient. As a result the final product is likely to have built-in stresses, and it is desirable that these should be reduced to a minimum to achieve optimum optical and mechanical properties. A great deal of art as well as science is involved in achieving this result.

For completeness it should be mentioned that fibres have been produced with a cladding of silica or glass over a liquid core, and that by suitable choice of the liquid fibres of very low attenuation were obtained. Interest in this type several years ago was intense, but there are considerable practical difficulties in producing and using them, and they will not be further considered in this article.

Overall diameter of fibres has evolved in part from the optical requirements, but a limitation has been set by the brittle nature of glass and the need to retain sufficient flexibility for incorporation in cables. When subjected to tensile tests they break at about 1 - 2% elongation, but behave elastically over most of the range of extension; this means that considerable tensile stress can be applied without permanent deformation, since the elastic moduli of glasses are high. However, as a result of the small cross-sectional area the breaking tension of fibres is usually only of the order of a few hundred grams.

Freshly drawn glass fibres are extremely strong, but quickly lose their strength, particularly when exposed to moist air or other hostile environment, and touching the surface by hand has a particularly bad effect. This deterioration can be delayed considerably by the application of thin protective coatings immediately after drawing but eventually the tensile strength of the fibres approaches the relatively low value quoted above. There are opportunities for improvement in this respect, and work is proceeding to this end.

Fibre reinforcement and protection

Bare fibre waveguides obviously require modification to protect them from damage, and this is conveniently effected by application of a plastic coating.

The principal functions of such a coating are:

(a) Protection from chemical attack of the glass surface, e.g. by moisture or perspiration.

(b) Protection from effects of abrasion during winding and cabling operations.

(c) Retention of an adequate degree of flexibility of the fibre while preventing the formation of kinks of small radius (unprotected fibres fracture at bends of less than a few mm radius).

(d) Cushioning and spreading of radially applied forces so as to limit resultant stresses in the fibre.

(e) Provision of tensile reinforcement.

The first two functions and to a certain extent the third can be provided by a relatively thin coating. The last two require more substantial coatings, and in general the thicker the coating the better, limited only by the requirements to retain flexibility and to minimise the space occupied in a completely fabricated cable. In view of the need for adequate tensile strength in cabling operations, special attention has been given to the problem of tensile reinforcement, and this will be discussed in some detail.

When a system of parallel elements of uniform cross-section and equal length is extended, the tension T developed is related to the strain S by the relationship:-

$$T = S \Sigma EA \qquad (1)$$

where: E = Young's modulus of elasticity
A = cross sectional area of element
and the strain is less than that at the elastic limit.

Taking the clad fibre as a single element, the corresponding relation for a plastic coated fibre is:-

$$T = S (E_1 A_1 + E_2 A_2) \qquad (2)$$

where the subscripts 1 and 2 refer to fibre and coating respectively. Note that it is immaterial whether the coating is bonded to the fibre or not provided that both are subjected to the same strain.

As a general rule the elastic moduli of plastics are considerably lower than those of glasses, so that in order to make a significant contribution to the tension A_2 must substantially exceed A_1. However, since the flexibility of a cylindrical rod is inversely proportional to EA^2 it is obviously advantageous to keep A_2 as small as possible by using a plastic with a high value of E_2.

During cabling operations (e.g. bunching, stranding, braiding, sheathing, armouring, etc.) it is a common requirement in the manufacture of all types of cable to control the tension so that none of the constituents become permanently deformed. This is of paramount importance in dealing with glass fibres, which break at a low value of strain, but fortunately deform elastically up to about 1% elongation. It is therefore convenient as a design principle to calculate maximum operating tensions on the basis of this maximum value of the strain. Applying this principle to plastic coated fibre by inserting some practical values in equation (2) we obtain by way of example the curves in Figure 1, which relate to a glass fibre of 70 microns diameter and E_1 = 5000 kg/mm^2, coated with two types of high modulus plastic with E_2 values of 150 and 300 kg/mm^2.

It is shown that the permissible tension can be increased to above 1 kgf by the application of a plastic coating to an overall diameter of 0.6 - 0.8mm. A significantly higher tension is possible by a further increase to 1.0 mm, and this size has generally been used in the design of experimental multicore cables. A fortuitous further margin of safety has been provided by the observation that elongation at break of the glass fibre tends to be significantly higher in the plastic coated form.

Coating of fibres

Thin primary coatings intended to provide temporary environmental protection for the fibre surface immediately after drawing, or to act as a primer for thicker secondary coats, or which may be intended to serve an optical purpose can be applied by a variety of methods usable for the coating of thin wires, of which enamelling or dip-coating are common examples. If the fibres are thick and strong, and if space is particularly at a premium in the ultimate product, it may be possible to use them directly for cable construction, but in general it is preferred to apply a secondary coating to provide additional mechanical integrity, on the lines discussed above. The most practical way of doing this is by thermoplastic extrusion.

A range of coated fibres has been prepared in this way, with various combinations of fibre type and high modulus plastics, using extrusion lines based on $\frac{3}{4}$ inch and $1\frac{1}{2}$ inch extruders. Although the smaller extruder has an adequate throughput, it has been found more satisfactory to use the $1\frac{1}{2}$ inch machine with its better melting and mixing facilities and closer control of temperatures, all of which have proved to be important in obtaining a satisfactory product. Line tension is also critical in view of the relatively low strength of the fibre, and special pay-off and take-up arrangements have been devised which maintain the tension constant under normal running conditions while avoiding snatch during short periods of acceleration or following deceleration. A small telephone cable type of diehead has been employed, with die and point designed for minimum drag on the fibre. The extrudate was cooled first in air and then in a water trough, the cooling schedules being tailored to the type of plastics employed. For experimental purposes we have not employed high extrusion speeds, which were generally limited to about 10 m/minute.

The success of the extrusion coating process is very much dependent upon the mechanical quality of the input fibre. Diameter must be closely controlled, and above all small over-size lumps must be avoided since they may lodge in the point of the core tube and are almost impossible to remove. Screening through a die placed in front of the diehead entry is a useful precaution to minimise trouble due to this cause. The fibre must of course have been carefully handled following the original melt drawing process, and to this end special procedures have been devised for winding on to supply bobbins, transporting to the extrusion site, and protecting from sources of contamination at all stages. A particular problem which has been encountered is the attraction of dust particles to the fibre, which can accumulate in the point and lead to frequent breakages. When suitable precautions are taken it has proved possible to extrusion-coat optical fibres in continuous lengths of several kilometres, usually limited only by the original fibre length.

A number of plastics have been successfully employed for fibre coating, notably high density polyethylene, polypropylene, nylon 6, nylon 66 and polyethyleneterephthalate (abbreviations: HDPE, PP, nylon 6 or 66, PETP). All of these combine a fairly high elastic modulus at small extensions (< 1%) with adequate ductility to permit reasonably small radius bending. They also have high abrasion resistance and low coefficients of friction, which are favourable to cable construction and performance. Under completely dry conditions nylon 6 and 6/6 have a significantly higher Young's modulus (300 kg/mm^2) than the others, but when exposed to normally moist atmosphere, e.g. 50% RH, they absorb water and the modulus falls by at least half. All of the above polymers then have a Young's modulus of the same order, but with PP and PETP leading the field at about 150 and 180 - 200 kg/mm^2 respectively. For this reason, most of our work has been carried out with these two materials, more especially PETP supplied by Akzo Plastics under the trade name Arnite.

The tensile properties of extruded coatings are strongly dependent upon the extrusion conditions, which influence the degree of molecular orientation and the extent to which mechanical stresses are left in the extrudate. Orientation in the line direction can be used to impart increased mechanical strength and elastic modulus, and we have used this method to make strong coated optical fibres. There are however still some process difficulties to be overcome to allow long continuous lengths to be regularly obtained in this way. In general it is preferred that coatings should be free from stresses which if relaxed (e.g. by heating in a subsequent process such as sheathing) may lead to a change in length or even of shape. Such changes cannot be resisted by the fibre, which may break or become distorted, with consequent deterioration in the optical properties. These effects can be avoided by close control of the extrusion process.

Cable design

For many purposes, particularly for short links, the information capacity of a single fibre is adequate and the basic coated fibre can be used without further processing. For very large channel capacity, or where a number of separate information groups are required without multiplexing, multiple fibre cables are required. Multicore cables are also likely to be in demand for trunk telecommunications links, where they will be expected to compete successfully with coaxial cables on a cost per channel basis. It is apparent that the range of designs will be as large as the range of applications, but certain design principles will apply, as in the case of single cores. Consideration is simplified by assuming that all cabling operations applied to insulated conductors should be applicable to coated fibres, provided that due attention is paid to the mechanical forces which will be applied to the cable components during manufacture, and that similar attention is paid to the rigours of installation. The principal design requirements at all stages are to build-in adequate tensile strength and flexibility, and provide for protection of the finished cable from external damaging influences.

With regard to tensile strength we may use equation (1) to calculate the tension which can be applied to a composite system such as a complete cable, when a limited strain is imposed. This can be illustrated by taking as an example a cable comprising the following elements:-

(a) A number of plastic coated optical fibres enclosed within (b).
(b) A tubular plastic sheath or jacket.
(c) An additional member whose principal purpose is to increase the tensile strength of the composite, here referred to as the strength member.
(d) Binding tapes, heat barriers, etc.

Ideally the strength member will take most of the tension, with some assistance from the sheath, although the coated fibres will also normally elongate and can make a significant contribution to the tensile strength. The other components can generally be neglected. If all the elements are parallel the strain in the cable must be limited to 1% to avoid damage to the fibres. Some advantage can be gained by arranging the coated fibres in a helix, which reduces the strain in the fibres relatively to the other components, but the pitch of the helix must be kept long to avoid excessive deterioration of the optical attenuation. The helix can conveniently be generated by stranding.

Considerable importance attaches to the design of the strength member, which for maximum effect must be placed parallel to the cable axis, or in a long-pitched helix around it. In the former case it is preferred to place it coaxially, i.e. at the neutral axis of the cable, where it has a minimum effect on flexibility. However a helical strength member while reducing flexibility can double as an armour and protect the coated fibres from abrasion and radial forces. Incidentally, flexibility is enhanced by a helical configuration of the coated fibres when the frictional coefficient of the plastic coating (against itself) is low enough to allow relative motion longitudinally. Thus it has been found that cables can readily be bent around radii of ten diameters without damage to the fibres.

Steel wire has been extensively employed for strengthening conventional electric cables, and can also be employed for fibre optical cables. Irrespective of the ultimate tensile strength it has the high Young's modulus of about 20,000 kg/mm^2, but since the yield strain is little more than 0.1% it can only be stressed to about 20 kg/mm^2 within the elastic limit. This is however a usefully high value for employment in fibre cables.

For some purposes it is preferred to use non-metallic constructions, either to avoid the effects of electromagnetic induction or to reduce the cable weight. For this reason attention has been given to the use of plastic strength members. Unorientated plastic materials which have been used for glass fibre reinforcement are inadequate for this purpose, but their elastic moduli can be increased by 1 - 2 orders of magnitude by molecular orientation. Also, new high tensile organic fibres such as Kevlar 49 have become available recently and may be made the basis of strength members with a considerably higher elastic modulus than has so far been achieved with other materials. The potentialities of some of these materials are illustrated in Figure 2 which shows in bar chart form the elastic moduli of HDPE, nylon 66 and PETP, with various degrees of molecular orientation. As a matter of interest the bars marked Max give theoretical maximum values calculated for straight molecular chains and indicate a limit of about 10-fold for additional increase over the high tensile values obtained at present.

For further comparison bars are included in Figure 2 for glass and steel. The apparently higher value for steel is offset by the limited strain at the elastic

limit, here taken to be 0.15%, so that in practice glass may be the more effective at least for tensile reinforcement. For equivalent cross-section both of these materials offer about 3 times the reinforcement at present available from the other materials illustrated. However this gap has recently been bridged by Du Pont with the introduction of Kevlar 49 fibres in several forms having a Young's modulus in the order of 10,000 kg/mm^2, which is likely to revolutionise the design of high strength non-metallic cables. Furthermore, considered on a strength to weight basis Kevlar 49 stands out from glass, which is itself superior to steel.

The above considerations have been taken into account in the construction of cables for links exceeding 0.5 km, including a requirement for their installation in buried ducts. The force required to pull a cable into a simple straight duct is the product of the cable weight and the effective coefficient of friction between cable and duct. In practice the required force appreciably exceeds this value due to the existence of bends and surface irregularities in the duct. It is however clear that for a given duct the length which can be installed is directly related to the cable strength to weight ratio, where strength is interpreted as the tension which will produce a standard strain, e.g. 1% for a fibre optic cable. On this basis cables have been designed with strength members placed either within or around the coated optical fibres, which in principle can be pulled into suitable ducts up to several kilometres in length. Special techniques are of course necessary to instal such cables without risk of damage to the fibres. Important aspects are transmission of tension into the strength members of the cable, and limitation of the pulling-in tension to avoid even transiently exceeding the safe limit.

Connectors

Suitable connectors are an inseparable adjunct to any new design of cable, and present a considerable technical problem in the case of fibre optical cables. This arises from the circumstances that light must emerge from one fibre end and enter another with very little change in the beam angle, and a low order of attenuation, e.g. of the order of less than 1dB. The attenuation requirement involves in particular securing a very good alignment of the two waveguides. The difficulty of achieving this, not only with a single core but with a number simultaneously in a multicore cable, and in view of the very small optical core diameter, will be appreciated. However, practical solutions to the problem have been devised, at least for multimode fibres.

Acknowledgements

We thank the directors of Standard Telecommunication Laboratories for encouragement and permission to present this paper, and colleagues who have contributed to the progress of our work in this new field.

This work has been carried out with the support of Procurement Executive, Ministry of Defence UK, sponsored by CVD.

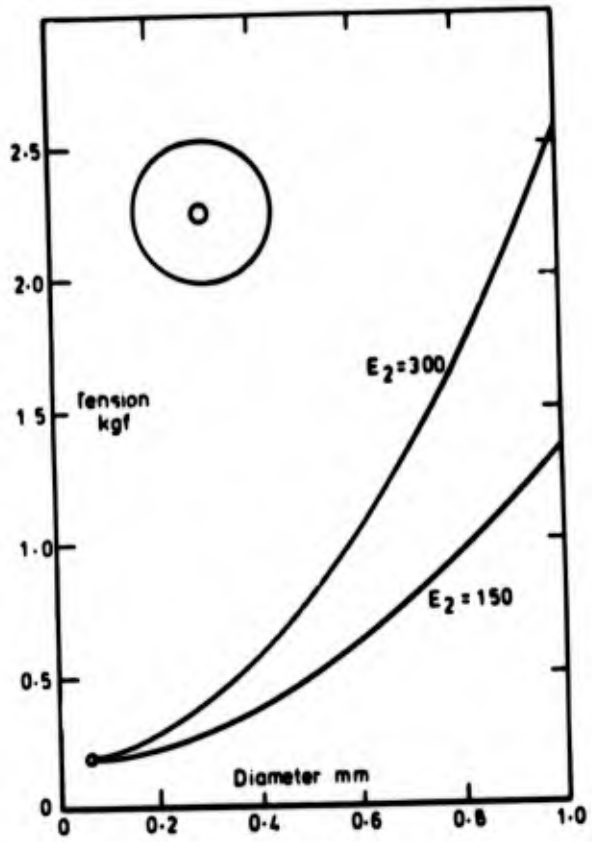

Fig.1 Tension in plastic-coated fibres at 1% elongation

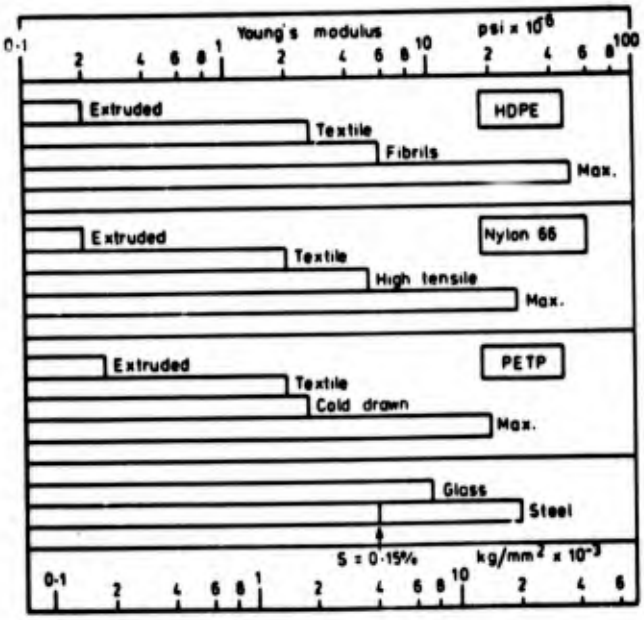

Fig. 2

Stanley G. Foord was born in 1910 at London, England. He received a BSc (Hons) degree in chemistry 1930, and PhD in 1933, both from London University. After 3 years postgraduate research at Cambridge, he joined Standard Telephones and Cables Limited at North Woolwich, where he worked in the materials laboratory. In 1946 he transferred to Standard Telecommunication Laboratories, where he is now head of the dielectrics and conductors department of the materials division. He has worked on a wide variety of projects in materials and electronic components, and has specialized in plastics and cable materials.

Eric Simpson was born in Cheshire, England in 1917. He obtained a first-class honours degree in chemistry from London University in 1940.

After working on plastics materials development, first with Fairey Aviation Company and then with Micanite and Insulators, he joined Standard Telecommunication Laboratories in 1949. Here, he is now head of the Plastics Laboratory which is principally concerned with new developments in the applications of polymers in cables and components.

Mr. Simpson is an Associate of the Royal Institute of Chemistry and a Member of the Plastics Institute.

Alan Cook was born in 1947, and received HNC in Chemistry in 1970. Since joining Standard Telecommunication Laboratories in 1969 he has worked on various aspects of the application of plastics materials for wire and cables, with recent specialisation in the development of practical fibre optical cables.

A PVC JACKET COMPOUND WITH IMPROVED FLAME RETARDANCY AND SUPERIOR PHYSICAL PROPERTIES

by

S. Kaufman
Bell Laboratories
Norcross, Georgia 30071

R. S. Dedier
Emery Industries
Cincinnati, Ohio 45232

ABSTRACT

Unplasticized poly(vinyl chloride) is a highly flame retardant polymer (oxygen index ~ 45%). However, the inherent flame retardancy of the polymer is greatly compromised in practical cable jacket formulations by the addition of flammable plasticizers. The oxygen index of a typical jacket compound is approximately 27%.

A new jacket compound with improved flame retardancy has been developed. An oxygen index of 32% has been achieved by utilizing reduced plasticizer levels. A brittleness temperature of -28°C was attained in the new formulation by the use of dioctyl azelate, a high efficiency plasticizer. The remaining physical properties of the compound are improved compared to conventional jacket compounds and are comparable to the properties of semirigid wire insulation.

INTRODUCTION

Poly(vinyl chloride), PVC, compounds are widely used throughout the wire and cable industry for flame retardant wire insulation and cable jackets. Unplasticized PVC is an excellent flame retardant material, but it is too rigid and brittle to be useful for insulation or jacketing. Compounding of plasticizer into PVC yields materials which generally have a desirable balance of properties, including flexibility and good low temperature impact properties. Unfortunately, most plasticizers are flammable and the resulting PVC compounds have greatly reduced flame retardancy. This paper reports on efforts to formulate a cable jacket with improved flame retardancy but without compromising low temperature impact properties. Our objective was to maintain a brittleness temperature of -25°C.

PROPERTIES OF PVC PLASTICIZED WITH DIOCTYL AZELATE

The basic approach to improve flame retardancy was to reduce plasticizer content from current levels. (The properties and formulation of two typical PVC compounds, a flexible jacket and a semirigid wire insulation, are given in Appendix A.) In order to reduce plasticizer content without compromising low temperature properties, it is necessary to use a high efficiency plasticizer - one of the so-called "low temperature plasticizers."[1] The volatility of three low temperature plasticizers and dioctyl phthalate (DOP) are shown in Table I as reported by Darby and Sears,[2] for 24 hours at 87°C in 67 phr formulations

Dioctyl adipate was eliminated from consideration because of its high volatility and dioctyl sebacate because of its high price, thus leaving dioctyl azelate.

TABLE I

PLASTICIZER VOLATILITY

Plasticizer		Volatility [Plasticizer Loss%]
Di-2-ethylhexyl adipate (DOA)	$R\text{-}O\text{-}\overset{O}{\overset{\|}{C}}\text{-}(CH_2)_4\text{-}\overset{O}{\overset{\|}{C}}\text{-}O\text{-}R$	13.9
Di-2-ethylhexyl azelate (DOZ)	$R\text{-}O\text{-}\overset{O}{\overset{\|}{C}}\text{-}(CH_2)_7\text{-}\overset{O}{\overset{\|}{C}}\text{-}O\text{-}R$	5.7
Di-2-ethylhexyl sebacate (DOS)	$R\text{-}O\text{-}\overset{O}{\overset{\|}{C}}\text{-}(CH_2)_8\text{-}\overset{O}{\overset{\|}{C}}\text{-}O\text{-}R$	4.2
Di-2-ethylhexyl phthalate (DOP)	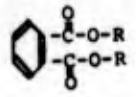	4.5

where $R=CH_2CH(C_2H_5)C_4H_9$

Effect of Plasticizer Level on Compound Properties

Test compounds were prepared with various levels of DOZ. Figures 1-8 show the variation in physical properties of these compounds with plasticizer concentration. In order to provide a frame of reference, the typical properties of a flexible jacket compound and a semirigid wire insulation are also shown in the figures. All compounds were stabilized with 5 phr of lubricated lead stabilizer, Dythal XL. See Appendix B for a discussion of test methods.

The variation of brittleness temperature with DOZ concentration is shown in Figure 1. It shows that a brittleness temperature of -25°C can be achieved with only 22 phr of plasticizer. A 25 phr DOZ compound (brittleness temperature -29°C) comfortably meets the -25°C objective and leaves room for the degradation of low temperature properties that occur when fillers are added to the compound. It also allows a margin for error in compounding and testing.

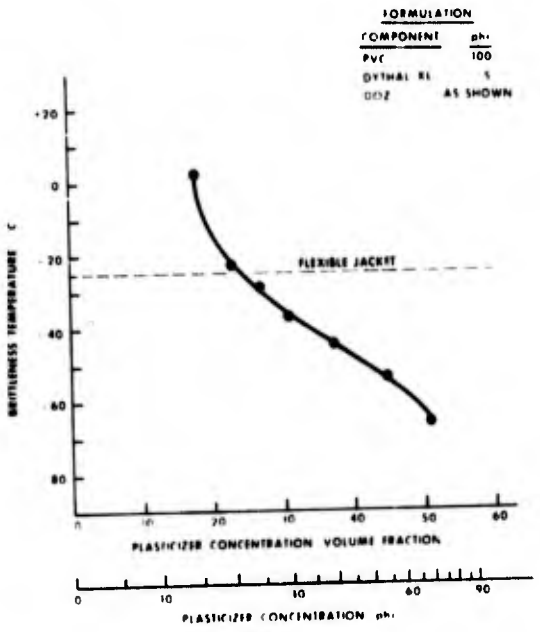

Figure 1

Figure 2 shows the variation of oxygen index with DOZ concentration. The flammability of the compounds increases (oxygen index decreases) dramatically with increasing plasticizer concentration. This phenomena is well known[3] and is the impetus to minimize plasticizer concentration. The typical value of the oxygen index of the flexible jacket compound, which contains 3 phr antimony trioxide and 45 phr phthalate plasticizer, can be matched by a 25 phr DOZ compound without any added fire retardant.

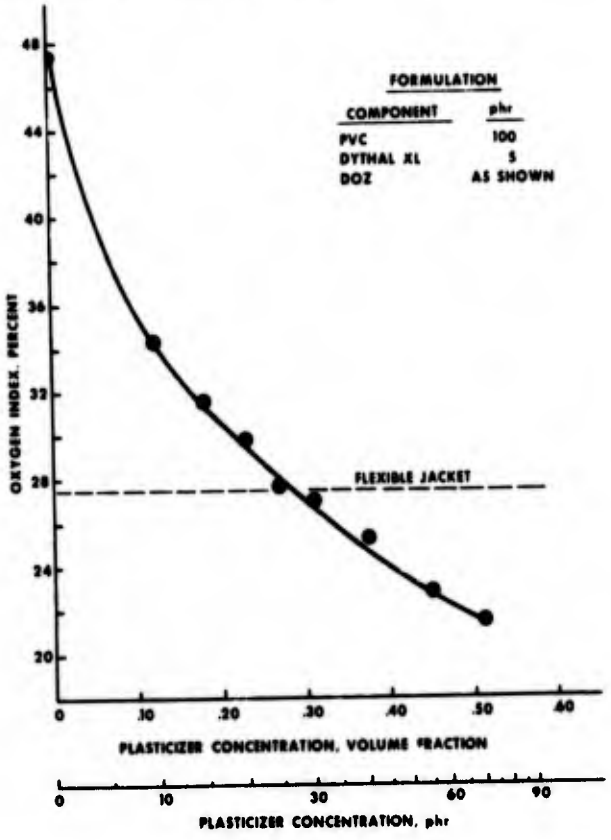

Figure 2

Low temperature performance and flammability are important properties of a PVC jacket compound. The relationship of oxygen index to brittleness temperature for a DOZ compound is shown in Figure 3. Cable designers should be aware of the trade-off between flammability and low temperature properties when specifying brittleness temperature for a cable jacket.

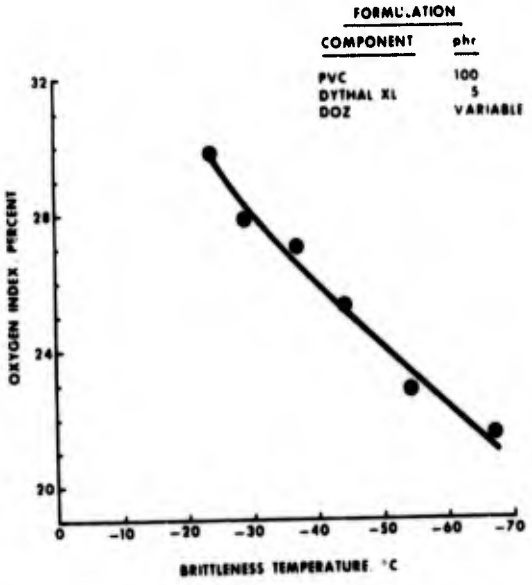

Figure 3

Figures 4 and 5 show the variations of shear and tear strengths with DOZ concentration. The shear and tear strengths of a 25 phr DOZ compound are approximately 50% greater than the typical values for the flexible jacket compound and approach the typical values for semirigid wire insulation. DOZ is efficient in lowering the brittleness temperature but less efficient in softening the compound at room temperature. This is a highly desirable property, since end uses require good low temperature impact properties, while high shear and tear strengths will permit a reduction in jacket thickness.

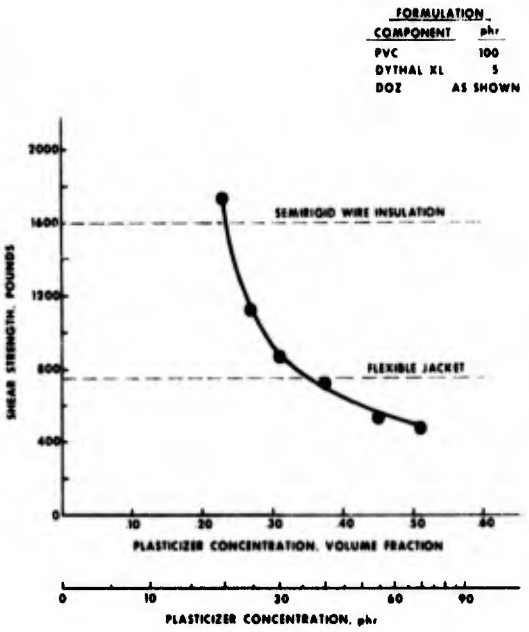

Figure 4

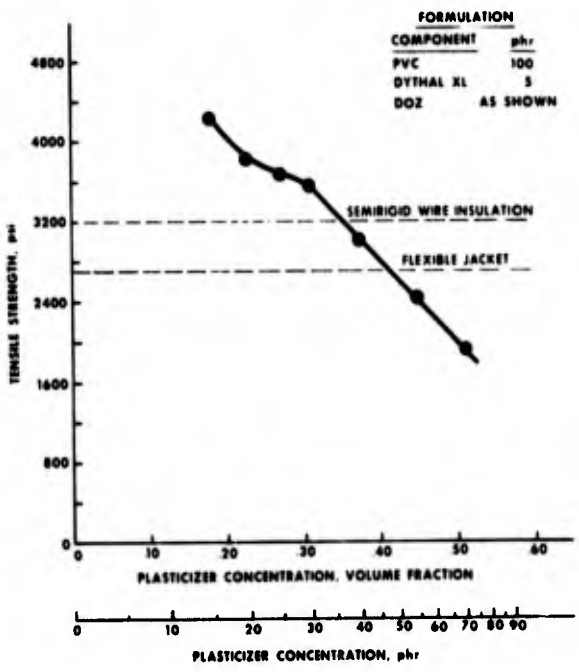

Figure 6

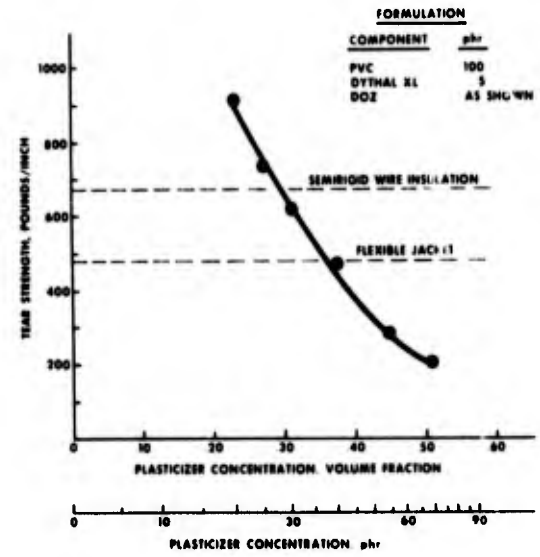

Figure 5

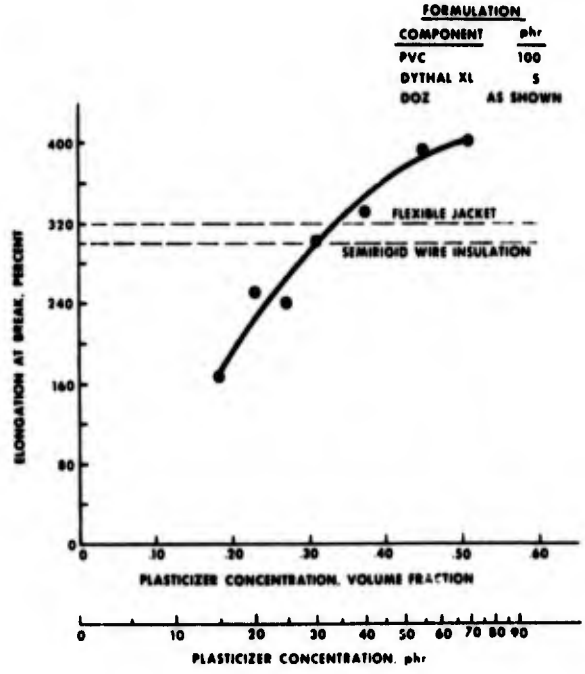

Figure 7

The variations of tensile strength and elongation at break with DOZ concentration are shown in Figures 6 and 7. The tensile strength of a 25 phr DOZ compound is greater than the typical value for the semirigid wire insulation, and approximately 1/3 greater than the typical value for flexible jacket compound. This again demonstrates that DOZ is more efficient in lowering brittleness temperature than plasticizing at room temperature. Elongation at break of the 25 phr DOZ compound is lower than typical values for flexible jacket and semirigid wire insulation compounds but is adequate for jacket and insulation applications.

The changes in the static and sliding coefficients of friction with plasticizer concentration are shown in Figure 8. The typical value of the static coefficient for the flexible jacket compound is approximately 0.6 compared to 0.9 for the 25 phr DOZ compound. It should be noted that the flexible compound contains a petroleum wax lubricant, which blooms to the surface and lowers the coefficient of friction. This mechanism may be used to reduce the coefficient of friction of the new compound, if necessary.

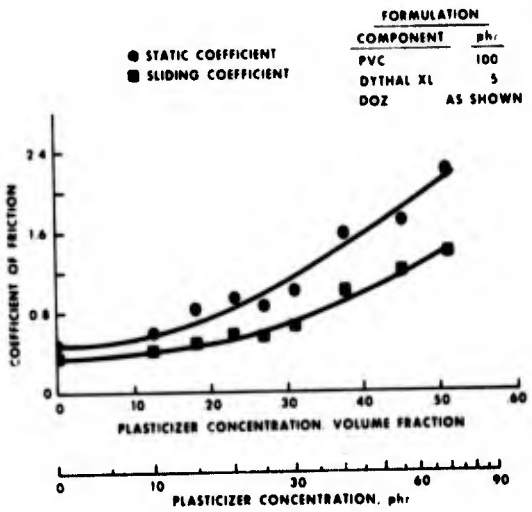

Figure 8

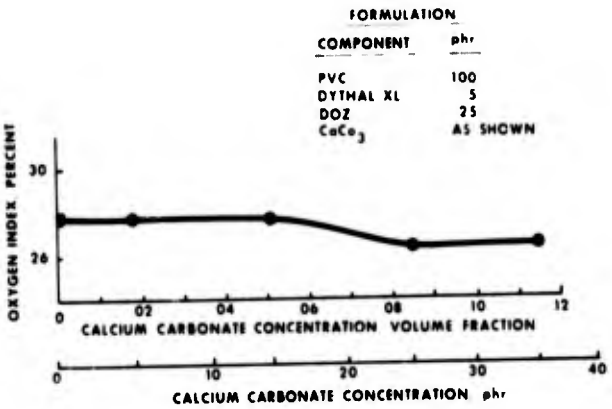

Figure 10

Effect of Fillers on Compound Properties

In order to determine the effect of filler, calcium carbonate and antimony trioxide compounds were prepared with 25 phr DOZ and various levels of the fillers. The addition of the first phr of antimony trioxide is extremely efficient, Figure 9, raising the oxygen index approximately 3 units (percent). The addition of the second phr is less efficient but still worthwhile, raising the oxygen approximately an additional 1 unit (percent). Additional antimony beyond 2 phr is wasted. The addition of greater than 15 phr of calcium carbonate causes a decrease in flame retardancy, as measured by oxygen index, Figure 10. A very low level of calcium carbonate, 5 phr, can be tolerated since it affects the brittleness temperature only slightly, Figure 11. Slightly higher levels, 15 phr, adversely affect the brittleness temperature. Very low levels, 5 phr, of calcium carbonate increase shear strength, Figure 12. In view of the adverse effects of higher levels of calcium carbonate on brittleness temperature, 5 phr appears optimal. Tear and tensile strengths are degraded by the addition of filler, Figures 13 and 14.

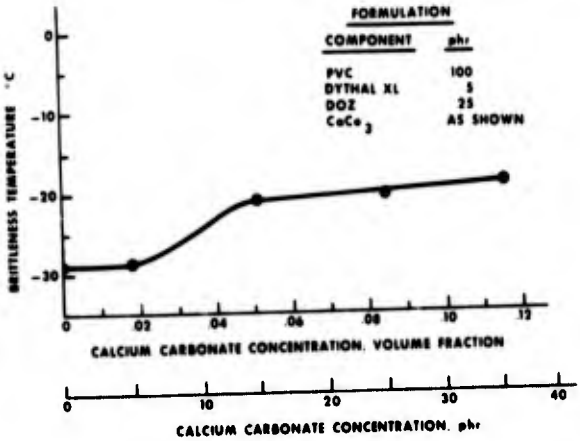

Figure 11

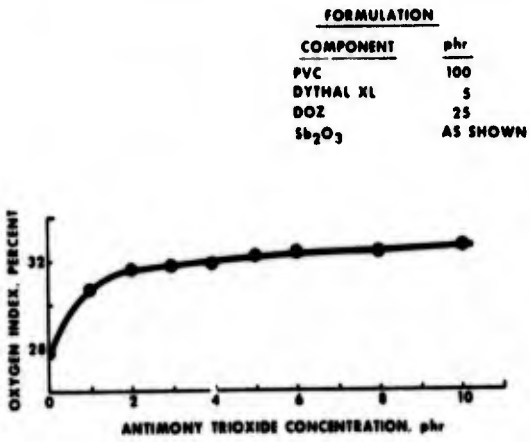

Figure 9

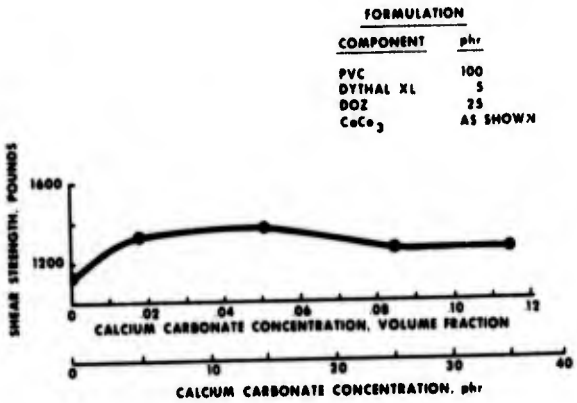

Figure 12

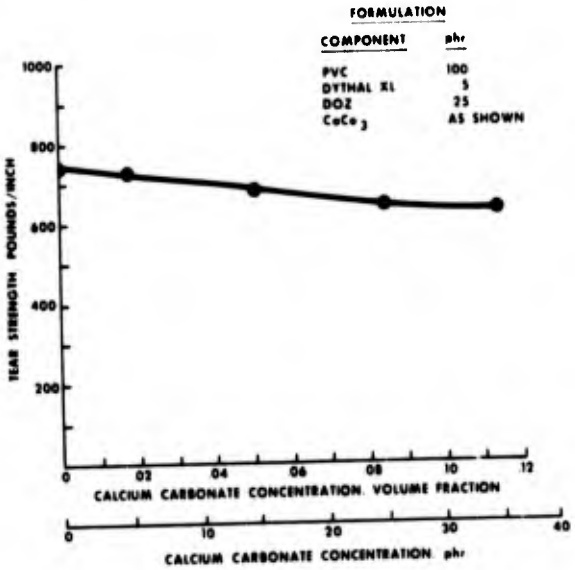

Figure 13

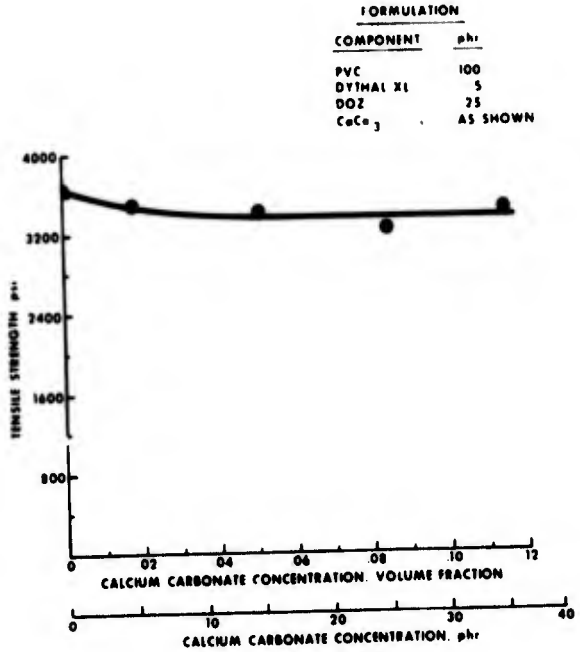

Figure 14

Effect of Phthalate Plasticizers on Compound Properties

Dioctyl azelate is often used in blends with phthalate plasticizers. In order to determine the effect of the addition of phthalate plasticizers, compounds were prepared with 25 phr plasticizer and varying ratios of DOZ to alkyl phthalate plasticizer. A mixed alkyl phthalate ester was chosen because it is a high efficiency phthalate plasticizer.

The brittleness temperature changes from -29°C for all DOZ to +2°C for all phthalate which demonstrates the greater efficiency of DOZ, Figure 15. Oxygen index was found to remain unchanged, within the accuracy of the measurement, as the DOZ/phthalate ratio was varied.

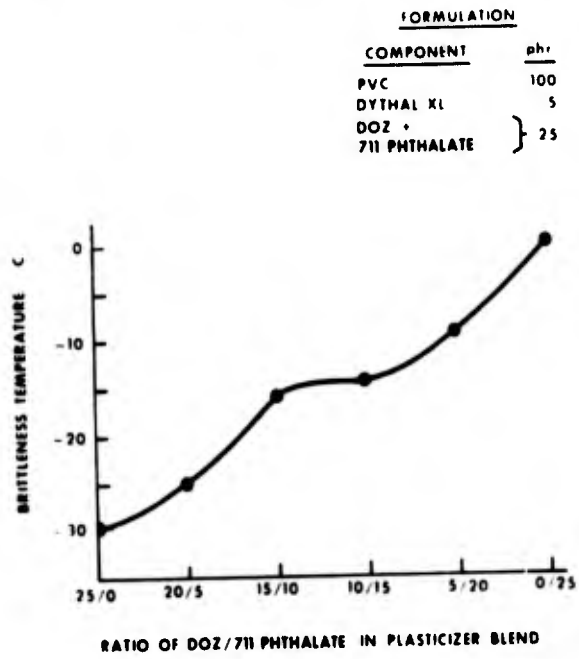

Figure 15

Figures 16, 17 and 18, respectively, show the variation of shear, tear and tensile strengths with DOZ/phthalate ratio. Shear strength doubles as the transition is made from all DOZ to all phthalate, but tear strength is only slightly affected. Tensile strength appears to be insensitive to the addition of phthalate plasticizer until the DOZ/phthalate ratio is below 10/15.

Phthalate plasticizers are often blended with DOZ in order to lower the fusion temperature of the compound. The minimum fusion temperature of a DOZ plasticized compound is 118°C versus 84°C for DOP.[2] The phthalate behaves similarly to DOP.[4]

Fusion tests carried out with the Brabender Plasticorder are shown in Figure 19. Unfused blends (55 grams) of PVC and plasticizer with varying DOZ/phthalate ratios were fed to the mixing chamber and the resulting torque versus time curves recorded. The jacket temperature was maintained at 138°C and a number 5 roller was used at 60 rpm. The peak in the torque versus time curve indicates fusion. The fusion temperature was read at this peak and in all cases occurred at approximately 165°C. Compounds containing more than half phthalate fused relatively quickly, in 4 to 5 minutes, while compound containing more than half DOZ required 11 to 14 minutes. Due to the longer times needed to fuse a DOZ compound, compounding costs may be higher.

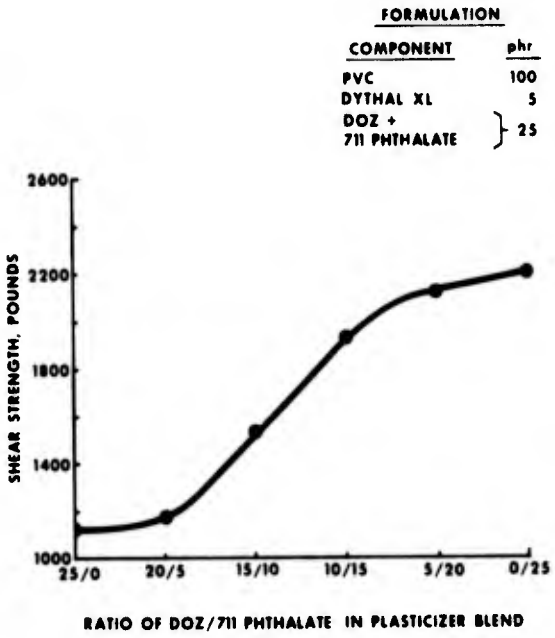

Figure 16

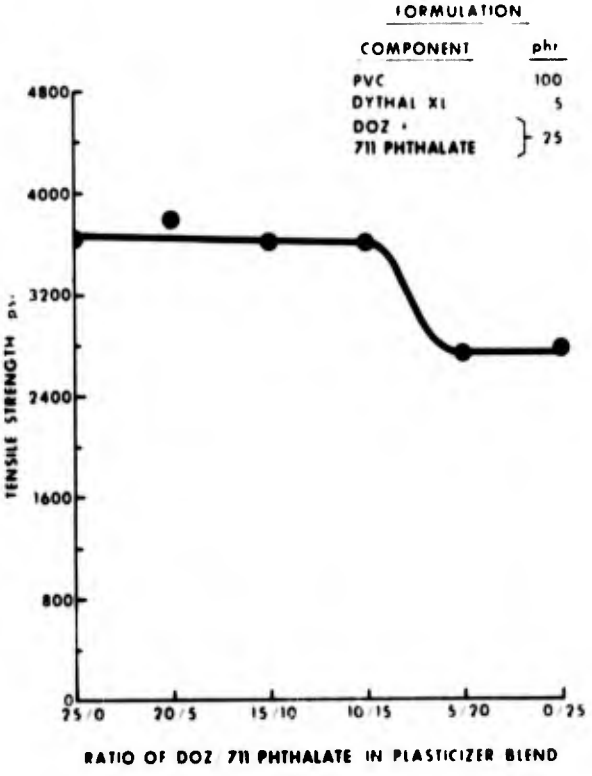

Figure 18

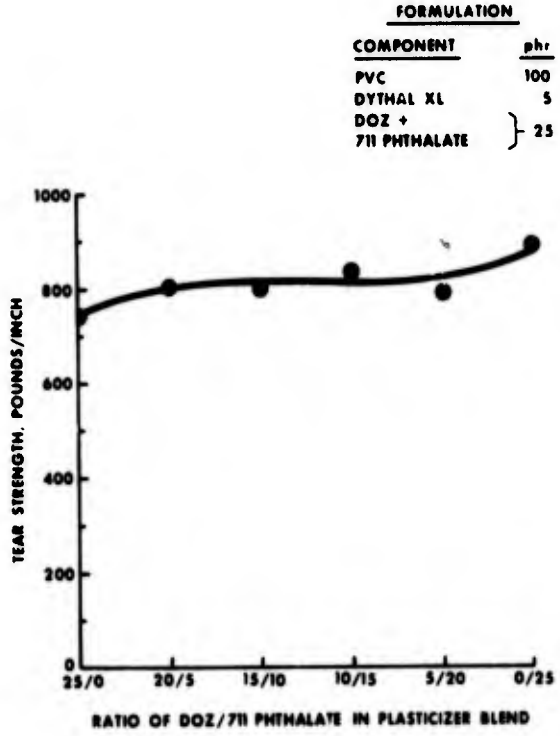

Figure 17

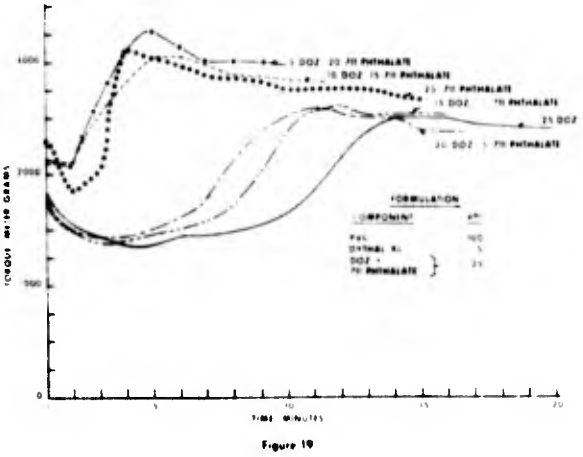

Figure 19

A equilibrium torque value is reached after fusion. The compounds containing more DOZ attain a lower equilibrium torque (∿2300 meter-grams versus 2900 meter-grams) and slightly lower melt temperature (∿170°C versus 175°C) than the compounds containing more phthalate plasticizer. This is a manifestation of the fact that DOZ is a more efficient internal lubricant than a phthalate.

Fusion tests[5] were also carried out on two compounds which were in the form of previously fused pellets. One compound contained 25 phr DOZ. Its formulation is given in Table III. The other compound had an identical formulation except that it contained 15 phr DOZ and 10 phr phthalate. The fusion test was carried out at a typical extrusion temperature, 180°C. The all DOZ compound fused in 1-1/4 minute while the DOZ/phthalate compound fused in 1 minute. Thus, it is concluded that the addition of phthalate plasticizer would not significantly improve the extrusion properties of the compound.

Stabilization and Lubrication

Initial work in this area was directed toward determining the need for any additional lubricant over the amount present in the lubricated stabilizer. A formulation was tested which contained 20 phr DOZ, 5 phr phthalate, 3 phr antimony trioxide and 5 phr Dythal XL. This formulation was tested with and without 0.2 phr of Plastiflow POP, a modified oxidized polyethylene lubricant. Stabilization time in the Brabender Plasticorder (see Appendix C) was 11 minutes without the Plastiflow POP and 16.5 minutes with it, a marked improvement.

Four lead stabilizers were tested at the 7 phr level in the above formulation with Plastiflow POP at 0.2 phr level. The results are shown in Table II. Tribase XL was the most effective.

TABLE II

PERFORMANCE OF LEAD STABILIZERS (7 phr)

Stabilizer	Stabilization Time Minutes
Lectro 78	15.5
Dyphos XL	16.5
Dythal XL	18.5
Tribase XL	23.5

Figure 20 shows the variation of stabilization time with Tribase XL concentration. A level of 7 phr Tribase XL has been chosen. Additional stabilizer can be added if necessary. One final stabilization experiment was carried out where 0.2 phr lead stearate was substituted for the 0.2 phr Plastiflow POP. Plastiflow POP was found to be more effective than lead stearate and both were more effective than using no additional lubricant at all.

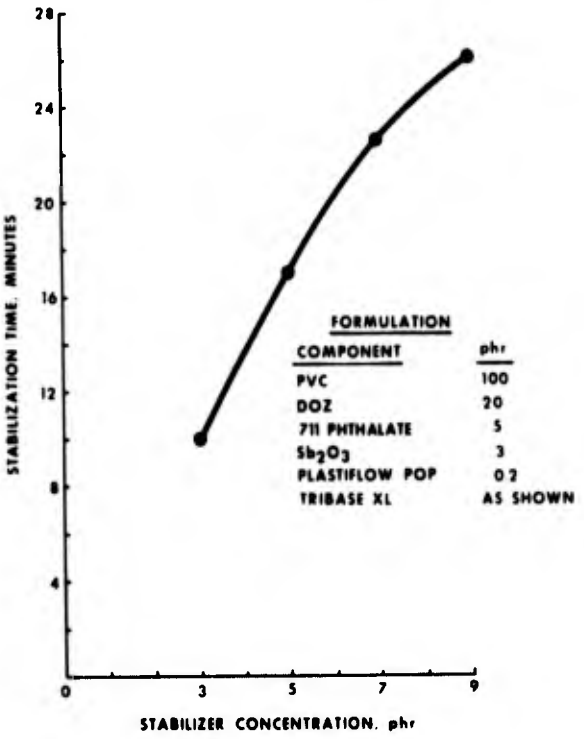

Figure 20

CHARACTERIZATION OF A FINAL FORMULATION

The data of the preceding sections were used to arrive at the final formulation shown in Table III.

TABLE III

FINAL FORMULATION

Component	Phr	Volume Fraction	Weight Percent
PVC	100	.696	71.8
DOZ	25	.265	18.0
$CaCO_3$	5	.018	3.6
Sb_2O_3	2	.004	1.4
Tribase XL	7	.015	5.0
Plastiflow POP	0.2	0.002	0.1

The physical properties of the compound are shown in Table IV.

TABLE IV

PHYSICAL PROPERTIES OF EXPERIMENTAL JACKET COMPOUND

Oxygen Index, Percent	32
Brittleness Temperature, °C	-28
Shear Strength, pounds	1140
Tear Strength, pounds/inch	
Die B	860
Die C	760
Tensile Strength, psi	3650
Elongation at Break, percent	300
Coefficient of Friction	
Static	0.8
Sliding	0.4

REFERENCES

1. W. H. Bauer and R. L. Cox, "What Should You Look for in Low-Temperature Plasticizers?" Plastics Technology, p. 35, July, 1963.

2. J. R. Darby and J. K. Sears, "Plasticizers," in Encyclopedia of Polymer Science and Technology, 10, pp. 288-306, (1969).

3. J. P. Hamilton, "Reducing Flammability in PVC Plastisols with Triarly Phosphate Plasticizer," Modern Plastics, p. 89, October, 1972.

4. M. F. Marx, "A Torque-Rheometer Fusion-Point Test for Evaluating Polyvinyl Chloride Extrudability," The Western Electric Engineer, XII, No. 3, p. 17, October, 1968.

APPENDIX A

PROPERTIES OF PVC JACKET AND INSULATION COMPOUNDS

The formulations and typical properties of a flexible jacket compound and a semirigid wire insulation are shown in Tables A1 and A2.

TABLE A1

FORMULATIONS

Component	Flexible Jacket		Semirigid Wire Insulation	
	Phr	Wt.%	Phr.	Wt.%
Resin				
PVC	100	52.9	100	70.0
Phthalate Plasticizer				
Di-2-ethylehexyl Phthalate (DOP)			35	24.5
Mixed Alkyl Phthalate Ester	45	23.8		
Flame Retardant				
Antimony Trioxide	3	1.6	--	--
Lead Stabilizer				
Dibasic Lead Phthalate	5	2.6		
Filler				
Calcium Carbonate	35	18.5	--	--
Lubricant				
Dibasic Lead Stearate	0.5	0.3	0.4	0.3
Petroleum Wax	0.5	0.3		
Amide Wax			0.4	0.3

TABLE A2

TYPICAL PROPERTIES OF PVC COMPOUNDS

	Flexible Jacket	Semirigid Wire Insulation
Brittleness Temperature, °C	-25	-10
Oxygen Index, percent	27	27
Tensile Strength (psi)	2700	3200
Tear Strength (pounds/inch)	550	800
Shear Strength (pounds)	750	1600

APPENDIX B

SAMPLE PREPARATION AND TEST METHODS

All compounds were prepared by dry blending in a small kitchen blender and then milled for 4 minutes at 335°F. Test plagues were molded at 350°F.

Property	Method of Test
Tensile Strength Ultimate Elongation	ASTM D412 using Specimen Die C and a speed of 20 inches/minute.
Tear Strength	ASTM D624 using Specimen Die C and a speed of 20 inches/minute.
Shear Strength	Bell System Wedge Test
Low Temperature Brittleness	ASTM D746
Oxygen Index	ASTM D2863 with a specimen 0.075 inch thick
Coefficient of Friction	Bell System Tripod Sled Test
Brabender Heat Stability	A number 5 head at 205°C was used at 100 rpm with 60 grams of compound. Stabilization time is the time between 30° slopes.

ACKNOWLEDGEMENTS

The authors gratefully acknowledge the technical assistance of Mr. Raymond Walker at Bell Laboratories, Miss Terry Kohls and Mr. Robert Braun at Emery Industries.

Stanley Kaufman

Stanley Kaufman is a Member of Technical Staff at Bell Telephone Laboratories. He received a B.S. in Physics from the City College of the City University of the City of New York, and a Ph.D. in Chemistry from Brown University. Before joining Bell Laboratories in 1970, he was a research scientist at the Uniroyal Research Center.

Robert S. Dedier

Robert S. Dedier earned a B.S. in Chemistry from the University of Cincinnati.

At Emery Industries, Inc., he has been actively involved in PVC synthesis and evaluation for the past eleven years. Currently, he is supervisor of the evaluation labs.

HIGH ENERGY CONDUCTOR SPLICING IN CABLE MANUFACTURE

B. H. Cranston
Western Electric Engineering Research Center
Princeton, New Jersey

D. A. Machusak
Western Electric Engineering Research Center
Princeton, New Jersey

C. A. Wiechard
Western Electric Atlanta Product Engineering
Control Center
Atlanta, Georgia

Abstract

Typically, conductors are joined by brazing, a high temperature fusion process that uses an intermediary alloy for the juncture. However, in addition to requiring skilled operators for the technique, brazing can be the source of defects resulting from reduced tensile strength in the conductor adjacent to the splice.

A high energy joining method, which uses the controlled deposition and detonation of an explosive mixture to produce metallurgical bonds, has been developed to splice conductors. This method of joining, is a safe, reliable method of producing bonds between metals on a microscale. In contrast to typical fusion joining methods, this solid phase bonding system does not produce enough heat to deteriorate the conductor insulation or weaken the wire adjacent to the splice. Initial feasibility studies, have shown that splices produced by this method have tensile strengths exceeding those of the parent conductors and that the joining does not increase the electrical resistance of the conductors. Both copper and aluminum splices were examined metallographically to verify solid phase bonding.

Explosive bonding mechanisms as related to conductor splicing will be briefly reviewed and data presented to confirm the integrity of the bond. Also, prototype equipment designed and constructed to meet all OSHA requirements, will be discussed. Advantages and disadvantages are cited which could influence potential users.

Introduction

Although explosive energy has been used for a number of years to produce large scale, solid phase bonds, its small scale use entails unique problems. Current studies have dealt with these problems and produced a bonding method scaled to the needs of the electronics industry.[1]

Explosive mixtures have been developed by the Western Electric Engineering Research Center to produce microscale bonds in a safe, reliable manner. (See Figure 1). The joining method, capable of forming bonds between materials usually considered difficult or impossible to join, contrasts sharply with more familiar joining processes. Costly bonding tools and equipment usually used in solid phase bonding are eliminated, the need for ultra-clean conditions and precious metal coatings to facilitate bonding are minimized by a unique contamination removal system inherent in the process, and fewer limitations are imposed on the process by the plastic properties of the materials being joined. This approach to bonding has produced solid phase bonds of greater strength than either parent material. The method is particularly attractive because materials can be kept well below their melting points, minimizing the changes in material properties common in fusion bonding.

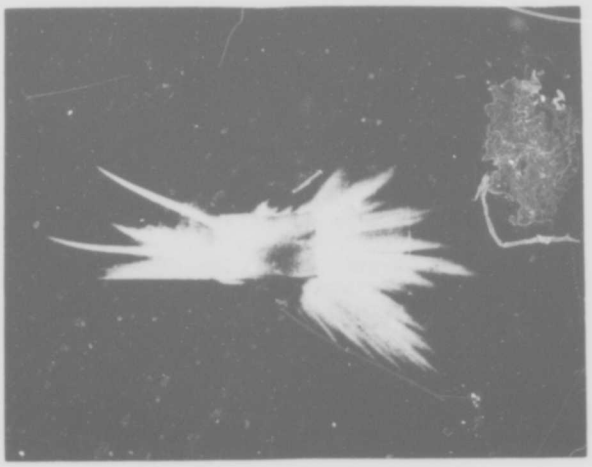

Figure 1. Explosive bonding, top view: glowing tungsten filament at left initiates detonation producing explosive reaction; resulting impact bonds an 0.005-in-thick copper strip to a piece of nickel.

Bonding Mechanism

In a typical explosive bonding system the materials to be bonded are positioned parallel with a space between them and a layer of explosive charge placed on the upper plate. Upon initiation of the explosive reaction, a pressure disturbance propagates outward through the explosive from the point of detonation. The energy released by the detonating explosive accelerates the upper plate, progressively deflecting it toward the base plate to produce a collision. As the explosive reaction proceeds, large transient pressures at the collision point produce severe surface strains inducing intimate contact between the materials. The combination of upper plate mass, the magnitude of its velocity on impact and surface flow characteristics must exert a pressure at the metal surfaces exceeding the dynamic yield point of the materials.

Two conditions are required to produce strong bonds: (1) the velocity of the induced pressure wave in the

bond material (i.e., the sonic velocity) must exceed the detonation velocity of the explosive and (2) the pressure generated by the explosive ahead of the collision point must exceed a critical value, related to the mechanical properties of the material. During bonding, extreme pressure exceeding the dynamic elastic limit in both plates causes the surfaces to deform plastically and behave like non-viscous fluids for a short interval forcing them to spurt out between the plates.[3,6] (See Figure 2). This "jetting"

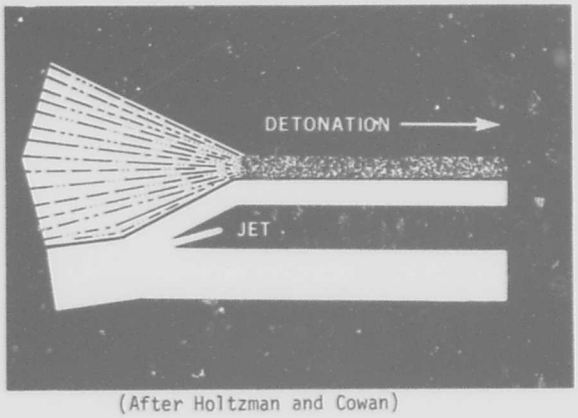

(After Holtzman and Cowan)

Figure 2. High velocity jet emanating from collision point.

phenomenon removes surface contaminants such as oxides, nitrides or absorbed gasses, bringing the underlying metals into direct contact.

The dynamics of the explosive bonding process can be described by three separate velocities of the overall system: (1) the detonation velocity (V_d), a property of the explosive material; (2) the collision point velocity (V_{cp}), the velocity with which the juncture of the plates moves in the direction of the detonation wave; and (3) the plated velocity (V_p), a function of the detonation velocity and the ratio of the explosive mass to the upper plate mass. Figure 3 is a representation of these velocities and β, the dynamic bend angle on impact. The β value, velocity components and mass ratio can be varied to produce different types of bond interface characteristics.

There are basically three types of metallurgical bonds that can result from high velocity collisions[6]: (1) a straight solid phase metal-to-metal bond, (2) a molten and resolidified layer between the metals, and (3) a wave or ripple pattern which is basically a solid phase bond that under certain conditions can exhibit small resolidified zones. The ripple interface is preferred in most commercial cladding applications for physical strength. The amplitude and period of this wavy interface, unique to explosive joining, is a function of the material being joined and the velocity of the impinging metals.

A correlation between bond interface structures and the system dynamics is illustrated in Figure 4. The parameters are cited in the figure captions. Mass ratios as referred in the captions defines the mass of explosive divided by the mass of the plate being accelerated.

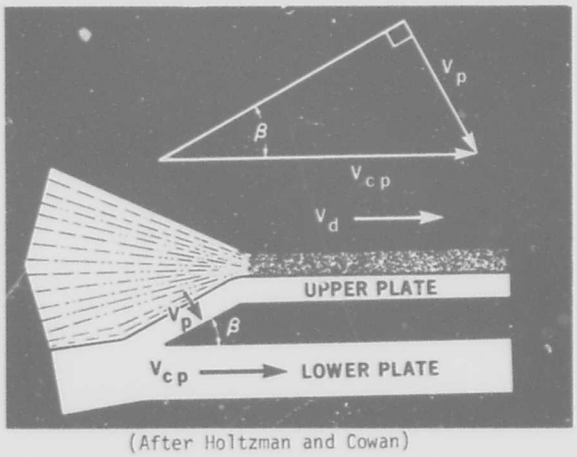

(After Holtzman and Cowan)

Figure 3. Parallel plate velocity components.
V_d - explosive detonation velocity
V_{cp} - collision point velocity
V_p - upper plate velocity
β - dynamic bend angle

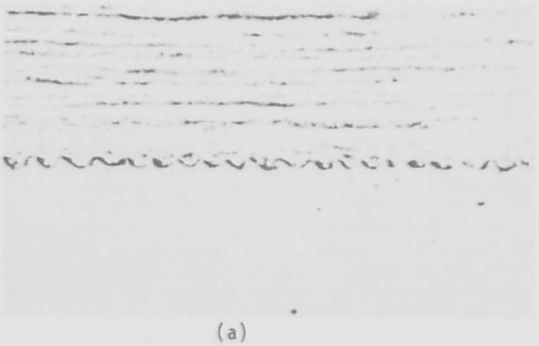

(a)

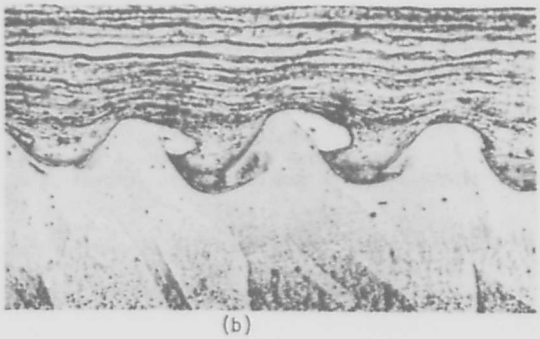

(b)

Figure 4 (a). Copper (0.005-in-thick) to nickel (0.030-in-thick) at 500X magnification. V_p = 985 ft/s; V_d = 10,800 ft/s; mass ratio c/m = 0.3503.
(b). Copper (0.005-in-thick) to nickel (0.030-in-thick) at 500X magnification. V_p = 3037 ft/s; V_d = 13,000 ft/s; mass ratio c/m = 1.2351.

The theory of the bond mechanism as discussed above has been published in references 2, 3, 4, 5, and 6.

Microscale Bonding

Applying the explosive bonding technique to micro-geometries requires a method to accurately deposit a specified quantity and configuration of explosive. Because of the very small workpieces involved, the usual procedure of initiating a secondary explosive by a primary explosive detonator is impractical. The method developed uses a directly detonated primary explosive as the energy source. Commercially available as powders, primary explosives cannot be accurately patterned in this form. Hence, the explosive was suspended in a medium and a screening technique was developed to generate accurate patterns on the workpiece.[7] The explosive media formulated met the standards of screenability but did not produce detrimental changes in the detonation velocity of the explosive material. In addition to its patterning advantages, the explosive medium keeps the normally sensitive explosive material temporarily inactive in a "wet" state.

In some cases, buffer materials, such as polyimides, were used between the explosive and the parts to be joined to protect the surface from explosive by-products and dampen pressure transfer. Buffers are also an advantage when their flatness can be used to facilitate screening. Reliable bonds have been formed through buffers with no welding to the buffer.

The Wire Splicing Method

It has been found that the principles discussed above can be applied to a different geometry in the splicing of conductors. Now a circular geometry is considered as opposed to the flat piecepart operations. The metal part now accelerated takes the form of a section of tubing which has been coated with explosive. (see Figure 5). A protective covering of either tape or lacquer is normally applied over the primary explosive mixture. The coated sleeves are presently being commercially fabricated by E. I. DuPont according to Western Electric specifications.

The two conductor ends to be spliced are inserted into the sleeve (Figure 5). The wire insulation is stripped from the conductor prior to insertion only to the length of insertion into the sleeve because the heat generated is not sufficient to degrade the adjacent insulation. No force is required to hold the wires in place during splicing and any clamping fixture which will adequately locate the conductors is sufficient. A resistance heated filament or transformer generated spark can be used to detonate the explosive.

To provide space for the surface "jetting" that occurs during explosive bonding, the inner diameter of the sleeve is typically .002-.006 inches larger than the diameter of the conductors. The outer diameter of the sleeve is calculated to provide a cross section equal to or exceeding the cross section of the conductor so that no additional electrical resistance is introduced into the conductor and the tensile strength will be maintained. A typical sleeve length of 1/2 inch provides a sufficient bond interface area for 22 gauge splicing applications. The technique as described above is referred to as High Energy Splicing.

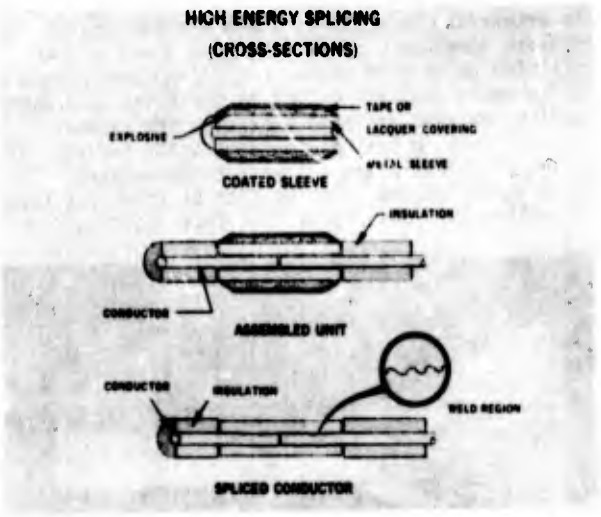

Figure 5. High Energy Splicing Assembly Sequence.

Testing Results

Copper and aluminum wires, .010 inches to .057 inches in diameter, were pull tested to failure after High Energy Splicing, and their breaking load was compared to the tensile strength of the original wires. Data from these tests, as illustrated in Appendix I, showed the splice to be stronger than the wire in all cases. When tested, the wires failed at random points along their length but not within or adjacent to the splice. The minimum explosive thickness to insure metallurgical bonding is equal to the sleeve-wall thickness for copper and .6 times the sleeve-wall thickness for aluminum.

To determine the electrical characteristics of the splice, resistance was measured across a unit length of conductors of various diameters before and after splicing. There was no measurable change in electrical characteristics due to the bond interface.

Metallographic Examination

Both copper and aluminum systems were examined metallographically to study the nature of the bond. A spliced 22 gauge copper wire is shown in Figure 6. Although it is difficult to discern the interface wave formations at a magnification of 50X, the interface structure is clearly visible at 500X. (See Figure 6). The wave formation is typical of that observed when two flat pieces of copper are explosively bonded. The darker lines at the interface are typical of accelerated, localized etching rather than the results of voids.

Prototype Splicing Equipment

A prototype splicing unit using a spark gap detonation has been designed and constructed. The splicer was designed for the twisting operation because the twisters have limited operating space. Hence, a splicing unit designed to operate on these machines can be easily accommodated in any of the other stages of cable manufacture.

At the twister-mounted splicing unit, the leads are inserted into an explosively coated sleeve, which is held in one of the indexed slots of the plastic disk at the side of the unit. The sleeve, together with the conductors, is lifted from the disk and positioned in clips between the electrodes. When the door is closed, the rubber gasket material forms around the

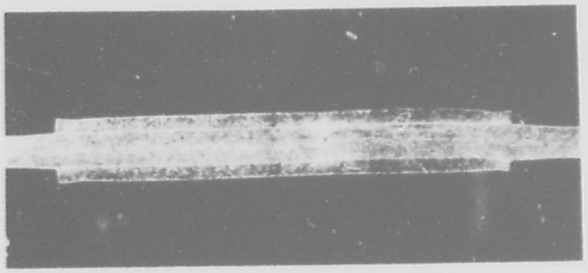

(a)

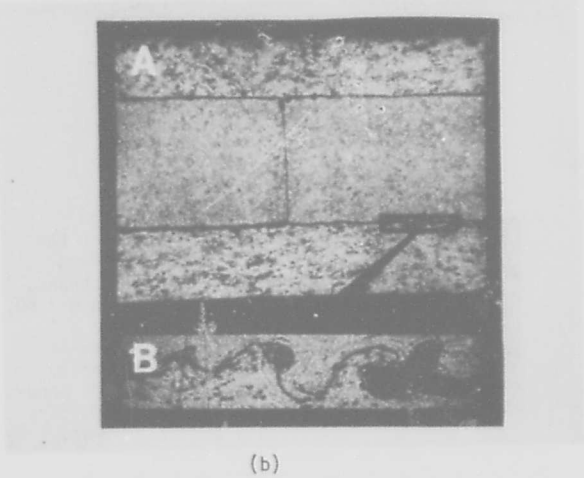

(b)

Figure 6 (a). A high energy spliced 22 gauge copper wire cross section at 10X.
(b). (Upper) cross section of conductor ends and bonded sleeve; (lower) interface structure is visible in the magnified section.

conductors extending from each side sealing the detonation chamber from the atmosphere. A spark is generated between the electrodes to detonate the explosive. Simultaneously a small vacuum motor in the lower section of the box begins a 2-second evacuation cycle of the chamber. The air is recycled through a filter, removing any particulate matter or other contamination dispersed as by-products of the detonation. To ascertain this, extensive environmental tests were designed to determine the amount of air-borne lead resulting from detonation of the lead azide explosive mixture.[8] The general procedure, test results and NIOSH standards are reported in Appendix II.

A cut away drawing of the unit is shown in Figure 7 which illustrates the filtration and detonation system.

The shell of the box is lined with a sound absorbing medium. Sound measurements were recorded at a position comparable to that of a machine operator. The sound level did not add to the ambient noise level and is safely below the requirements specified by OSHA. A safety interlock prevents detonation unless the door is closed. The basic design, which is intended for installation on a wire twister, can be modified for a specific installation or made portable.

Summary

A basic understanding of primary explosives has been developed which allows these materials to be used as a

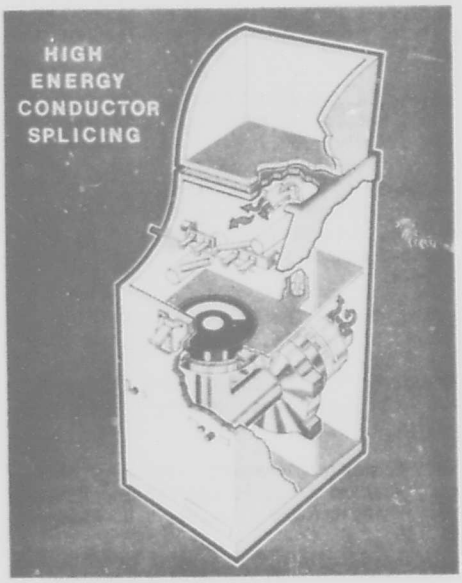

Figure 7. A cut away illustration of the high energy splicing unit designed for cable manufacture.

reliable energy source to bond metals on a miniature scale. These principles have been applied to join conductors as required in the manufacture of cable. The advantages of using a high energy splice are listed below:

- The highly localized energy application does not degrade either the insulation or the mechanical strength of the adjacent conductor.
- The bonding cycle is much shorter than the fusion processes.
- The strength of the union always exceeds the parent conductor strength, which should reduce "down-line" repair.
- The capital equipment cost is comparatively low.
- High Energy Splicing is equally effective with either aluminum or copper conductors.

Disadvantages of the process are summarized as follows:

- Caution is required when using explosive materials.
- Contamination of the work pieces could possibly result from by-products of the reaction.
- New techniques such as this will require training of the users, related to procedures and safety.

The disadvantages as listed above, have been minimized by the prototype equipment described in this paper. Further, sleeve packaging schemes are being developed with the cooperation of E. I. DuPont to insure that the product will be safe.

References

1. Cranston, B. H., Explosive Bonding of Electrical Interconnections, IEEE Transactions Vol. PHP 8 No. 3, September 1972.

2. Chadwick, M. D., Some Aspects of Explosive Welding in Different Geometries, The Explosive Welding Institute, Proceedings of the Select Conference, Hove, 1968.

3. Crossland, B., and Williams, J. D., Explosive Welding, Metals and Materials Mag., Vol. 4, Number 7, July 1970.

4. J. L. Edwards, B. H. Cranston, and G. Krauss, Miniature Explosive Bonding With a Primary Explosive, Metallurgical Effects of High Strain Rates Conference, Albuquerque, N. M., February 5-7, 1973.

5. Tylecote, R. F., The Solid Phase Welding of Metals, New York, St. Martins Press, 1968.

6. Holtzman, H. H., and Cowan, G. R., Bonding of Metals With Explosives, Welding Research Council Bulletin, #104, April 1965.

7. Private Communications and Assistance of T. G. Steele, Western Electric Engineering Research Center, Princeton, New Jersey; U.S. Patent 3,704,186.

8. Private Communication and Assistance of D. R. Lawson, Western Electric Engineering Research Center, Princeton, New Jersey.

Benjamin A. Cranston is a member of the research staff in the Integrated Cicuit Bonding Studies Group. His work at ERC has included continouous vacuum studies, thermal electron beam studies, and investigations of solid-state bonding techniques. Mr. Cranston has a B.S.M.E. degree from Drexel Institute of Technology, where he has also done graduate studies. A member of the Society of Manufacturing Engineers, he holds 13 patents related to bonding studies.

Donald A. Machusak is an engineering associate in the Integrated Circuit Bonding Studies Group. Mr. Machusak, who has been at ERC since 1960, has assisted in studies of thermocompression, ultrasonic, hot-work ultrasonic, compliant, and explosive bonding. He has attended Rutgers University and is currently enrolled in the associate's degree program in Mechanical Engineering Technology at Mercer County Community College.

Charles A. Wiechard, an engineering associate with the Wire and Cable PECC in Atlanta, has worked on the research, development, and implementation of conductor splicing systems. He holds certificates as a tool and die maker, mold maker, and tool designer. Mr. Wiechard has been working with members of the ERC staff on high energy splicing development since 1972. He has recently presented on this topic at an Interworks Twister Conference and the Assistant Managers' Cable Conference.

APPENDIX I

MECHANICAL TEST RESULTS OF HIGH ENERGY SPLICED ALUMINUM, COPPER BERYLLIUM COPPER, AND STEEL WIRES

TYPE WIRE	WIRE DIA. (MILS)	SLEEVE I.D. (MILS)	SLEEVE O.D. BEFORE (MILS)	SLEEVE O.D. AFTER (MILS)	AVG. WIRE TENSILE STG. (LBS)	SPLICE PULL STG. (LBS)	MODE OF FAILURE
Cu	39	41	74	73	44.4	44.8	WF
Cu	39	41	74	72	44.4	44.6	WF
Cu	39	41	74	72	44.4	44.8	WF
Cu	39	41	74	72	44.4	44.6	WF
Cu	39	41	74	73	44.4	44.6	WF
Cu	39	41	74	72	44.4	44.8	WF
Cu	30	32	62	60	29.7	29.4	WF
Cu	30	32	62	60	29.7	30.1	WF
Cu	30	32	62	60	29.7	30.1	WF
Cu	30	32	62	60	29.7	30.1	WF
Cu	30	32	62	60	29.7	30.1	WF
Cu	30	32	62	60	29.7	29.9	WF
BeCu	25	29	54	51	34.7	34.9	WF
BeCu	25	29	54	51	34.7	34.7	WF
BeCu	25	29	54	51	34.7	34.5	WF
BeCu	25	29	54	51	34.7	34.5	WF
BeCu	25	29	54	52	34.7	34.7	WF
BeCu	25	29	54	51	34.7	34.5	WF
Cu	10	15	35	31	4.8	3.3	WF
Cu	10	15	35	31	4.8	3.5	WF
Al	30	32	64	--	7.3	7.1	WF
Al	30	32	64	--	7.3	7.0	WF
Steel	39	52	85	77-78	238	>237	WF
Steel	39	52	85	--	238	>237	WF
Steel	39	52	85	75-78	238	>237	WF
Steel	39	47	85	80	238	>237	WF
Steel	39	47	85	--	238	>237	SF
Cu	57	61	100	97-99	85.8	82.5	WF
Cu	57	61	100	98	85.8	84.7	WF
Cu	57	61	100	--	85.8	86.9	WF
Cu	57	61	119	116-118	85.8	80.3	WF
Cu	57	61	119	115-116	85.8	77	WF
Cu	57	63	100	94-95	85.8	85.8	WF
Cu	57	63	100	94-96	85.8	84.7	WF
Cu	57	63	119	115-116	85.8	88	WF
Cu	57	63	119	117	85.8	77	WF

Instron Model - TM tensile testing machine used for strength measurements.
WF - wire failure, a separation of the wire away from the splice.
SF - sleeve failure, a separation of the splicing sleeve at the point the wires butt together.
The sleeve material for Cu and BeCu wire was Cu, for al. wire was al., and for steel wire was brass.

APPENDIX II

RESULTS OF MONITORING AIR-BORNE LEAD DURING HIGH ENERGY SPLICING

SAMPLER NO.	TYPE FILTER	SPLICE NO.	AIR FLOW RATE ($FT.^3/MIN$)	TOTAL AIR FLOW (M^3)	TOTAL LEAD COLLECTED (MG)	LEAD/M^3 AIR (MG/M^3)
1	Fiberglass	1-20	63	70.24	< 0.010	< 0.00014
2	Fiberglass	1-20	48	52.40	0.046	0.00088
1	Paper	21-40	63	69.60	0.050	0.00072
2	Paper	21-40	48	52.40	0.090	0.00172
1	Fiberglass	41-60	63	70.40	0.090	0.00128
2	Fiberglass	41-60	48	53.20	< 0.010	0.00019
1	Paper	61-80	63	68.80	0.154	0.00223
2	Paper	61-80	48	53.20	0.078	0.00147
1	Fiberglass	81-100	63	70.40	< 0.010	0.00014
2	Fiberglass	81-100	48	53.20	< 0.020	0.00038
1	Paper	101-120	63	68.40	0.098	0.00143
2	Paper	101-120	48	52.40	0.120	0.00229
1	Fiberglass	121-140	63	70.40	< 0.010	0.00014
2	Fiberglass	121-140	48	53.20	0.182	0.00342
1	Paper	141-160	48	52.72	0.102	0.00193
2	Paper	141-160	63	70.35	0.240	0.00341
1	Fiberglass	161-180	48	52.72	0.080	0.00152
2	Fiberglass	161-180	63	70.76	0.372	0.00526
1	Paper	181-200	48	53.6	0.100	0.00187
2	Paper	181-200	63	70.17	0.700	0.00998
1	Fiberglass	201-220	48	54.14	< 0.010	< 0.00018
2	Fiberglass	201-220	63	70.56	0.020	0.00028
1	Paper	221-240	48	53.88	0.125	0.00231
2	Paper	221-240	63	69.94	1.140	0.01630

Two high volume air samplers were located adjacent to each other in the operator breathing zone. The splices were made at 2 minute intervals. The filters in the air samplers were changed every 20 splices for a sampling time of 40 minutes per filter. The data from each sampler is presented above. Fiberglass and paper filters were alternated to prevent the filter type from influencing the results. The filter in the splicing unit was not changed during the test and after 240 splices was still effectively collecting the explosive by-products.

The NIOSH recommended TLV is 0.15 mg/m^3.

The filters were analyzed for lead content by Schwarzkopf Microanalytical Laboratory, Woodside, N. Y.

THE EFFECTS OF FATIGUE DAMAGE ON THE PROPERTIES OF COPPER-CLAD STEEL CONDUCTORS

Carl A. Shumaker, Jr.
Superior Continental Corporation
Hickory, North Carolina

Summary

Data presented herein indicate that fatigue fracture and fatigue-induced degradation of copper-clad steels occur at stress levels that are low with respect to composite wire tensile strength and substrate steel fatigue limit. The fatigue properties of these composite wires can be interpreted in terms of the damage which can occur at the edge of a propagating fatigue crack in copper and the microstructure of the cladding/base metal interface. Of significance here is the measured instability of conductivity, tensile strength, and resistance to brittle fracture of these types of wires at low stresses in a fatigue environment.

Introduction

Copper-clad steel wires used as transmission media may sustain severe damage in fatigue loading. In addition to fracture, degradation of some of the more significant properties of these conductors - electrical conductivity, tensile strength, and resistance to brittle fracture - can occur.

While some progress has been made[1,2] in defining specific fatigue endurance limits of the various types of copper-clad steel conductors, there still remains considerable lack of understanding of the general effects of copper claddings on the properties of the substrate steels used in the composite metal wires. In particular, data are required which explain the relatively low values of fatigue limit of these conductors with respect to the extremely high tensile strengths which can be developed in these wires.

This paper will present data showing that fatigue fracture and concomitant fatigue-induced degradation of the properties of these types of composite wires can be best understood on the basis of complex interactions between the various types of claddings and steel substrates.

Experimental Procedure

Microstructure and Mechanical Properties

The microstructures and mechanical properties of the various copper-clad steel wires and predrawn, unclad steel wire used in these studies were determined using metallographic techniques and tensile testing. The densities of these wires were determined by weighing in air and in bromo-benzene. The significant data obtained from these measurements are shown in Table 1.

In addition to the metallographic studies, electron-probe microanalysis was used to characterize the microchemistry of the copper cladding/steel base metal interfaces. Both line scans and stepwise quantitative measurements[3] were made to determine the extent of iron and copper diffusion between the cladding and substrate in the various types of conductors. These data and a description of the clad wires are summarized in Figure 1.

Elastic Modulii Determination

The Young's Modulii of the aforementioned wires were measured using an ultrasonic pulse-echo technique[4] developed for this purpose. A magnetostrictive transducer was used to generate 100 kHz broad-band longitudinal waves through a nickel-base alloy transmission wire. Subsequently, samples of experimental wire were cemented to this transmission line, producing conditions which caused reflection of characteristic echos from the joint and sample ends. These echos were separated by a time t, which is the round-trip travel time of the longitudinal waves in the sample of length ℓ. The velocity, V_E, was expressed as:

$$V_E = 2\ell/t \qquad (1)$$

Young's modulus E_y of the conductors is directly related to the sample density and the longitudinal wave velocity, and was calculated by the following expression:

$$E_y = \rho V_E^2 = \rho(2\ell/t)^2 = 4\rho\left(\frac{\ell^2}{t^2}\right) \qquad (2)$$

In these studies, a Tektronix - Type 556 dual-beam oscilloscope with delay-time multiplication was used to measure pulse-echo separation time - Typical reflections are given in Figure 2. Elastic modulii obtained from the samples of interest in this study are shown in Table 2.

Fatigue Test and Data Reduction

The reversed-bending fatigue studies were carried out on a Haigh-Robertson fatigue testing machine designed specifically for wire. The samples were supported at one end by a mechanical chuck and at the other end by a matched ball bearing assembly. The wires were deflected in the horizontal plane by application of a small thrust load at the bearing end, resulting in a curve of flexure which was very nearly harmonic. The maximum bending stresses in the wires occurred at mid-length and were calculated according to the classical Euler equation:

$$\sigma_f = \frac{\pi^2}{360}(\theta \text{ in degrees})\frac{d}{\ell}E_y \qquad (3)$$

This relationship becomes directly applicable when the angle of flexure, as measured with a vernier built into the tester, is small. Lengths of samples tested in these experiments were chosen such that fatigue stresses of interest could be obtained at $\theta \gtrsim 9°$.

The fatigue data were obtained in such a manner as to estimate the fatigue limits of the various conductors using the well-defined staircase method[5]. This technique, as used in this work, involved initially testing a sample at a stress level near the estimated value of the fatigue limit. Failure of this specimen required testing of a sample at a defined, incrementally lower value, until eventually definitive survival was obtained. The next sample was tested at the same incrementally increased stress, observing either failure or survival. The procedure was continued further, the stress being decreased until a specimen survived, and increased until it failed. Sufficient data were generated to estimate the fatigue limit of the sample at the predefined survival level. Normally, for steels, the knee of the conventional σ-n curve occurs between 10^6 and 10^7 cycles; therefore, survival in these experiments was defined at 1×10^7 cycles of reversed bending stress.

Analysis of Fatigue Failure and Degradation

Various metallographic and mechanical testing techniques were used to study the fatigue fracture processes and accompanying degradation of the composite wires. In addition to conventional metallographic techniques, scanning electron microscopy was used to characterize fracture processes. Degradation of conductivity of the samples in fatigue loading was determined using an ESI Model 300 Potentiometric Voltmeter-Bridge in the resistance mode. Tensile testing and a qualitative slow-bend test were used to determine loss of tensile strength and susceptibility to brittle fracture, respectively.

Cladding-Induced Degradation

Fatigue Limits of Copper-Clad Steels

The fatigue data, as determined by staircase testing, of the continuously plated steel, the composite conductor manufactured by molten-welding processes, and the continuously plated and drawn clad steel, are shown respectively in Figures 3-5. At the previously defined survival level of $n = 1 \times 10^7$, the continuously plated conductor exhibits a significantly higher fatigue limit than the corresponding molten-welded and continuously plated and drawn wires. The magnitude of this difference is ~21% in the case of the molten-welded samples, and ~27% in the case of the continuously plated and drawn wires. These data, which are not related in a systematic way to the corresponding tensile strengths of the composite wires, suggest that, at comparable tensile strength levels, fatigue processes, particularly at the various cladding/base metal interfaces, must be taken into account.

Effect of Copper Claddings on Fatigue Limits of Substrate Steels

In at least one sample (continuously plated steel), the effects of cladding can be measured directly with respect to quantitative data obtained from the predrawn steel substrate (Figure 6). In the case of the molten-welded and continuously plated and drawn samples, these data are not directly obtainable; however, with appropriate assumptions, some important estimates of this effect can be made.

The extent to which direct cladding of copper on steel wire can degrade the fatigue limit of the underlying steel substrate is summarized in Figures 3 and 6. As shown, the fatigue limit of the continuously plated composite wire is on the order of 50,700 psi, while the fatigue limit of the predrawn steel substrate is approximately 76,000 psi. This represents a nominal reduction of about 33% in terms of the fatigue limit of the steel substrate. More detailed examination of these data serves to further emphasize the magnitude of this difference - the probability of survival of the clad sample is fairly low at stresses greater than about 55,000 psi, while failure of the steel substrate wire is unlikely at stresses less than about 70,000 psi.

The particular manufacturing methods used do not permit a direct comparison of the effects of cladding on the fatigue limits of substrate steels in the case of the molten-welded and continuously plated and drawn wires. However, some conclusions can be drawn by examination of the fatigue limits of these conductors and some related properties of the corresponding steel substrates of these and continuously plated wires.

The staircase data obtained from molten-welded and continuously plated and drawn samples (Figures 4 and 5) indicate that the fatigue limits of these conductors are lower, but comparable in magnitude to the continuously plated sample. If it could be assumed that the fatigue limits of the steel substrates of the molten-welded and continuously plated and drawn samples are *no less* than the fatigue limit of the predrawn steel wire underlying the continuously plated cladding, then degradation of the fatigue limits of these steels due nominally to their respective types of claddings can be estimated. To a first approximation, it would appear that this assumption is justifiable on the basis of steel substrate microstructure and hardness. All of the steel substrates exhibit very heavily cold-worked and textured microstructures of pearlite and ferrite. The hardness of the various substrates is comparable, with the exception being the molten-welded sample, which is somewhat higher. Thus, it is reasonable to expect that both claddings of the molten-welded type and continuously plated and drawn type have the same strong effect on the fatigue limits of the corresponding steel substrates. These data are summarized below:

Effect of Copper Claddings on Fatigue Limits of Substrate Steels

Sample	$\bar{\sigma}_f$ fatigue limit ($X10^3$ psi)	KHN_{500}* (Steel)	% Reduction in $\bar{\sigma}_f$
Predrawn steel substrate wire	76.0	403	-
Continuously plated wire	50.7	403	~33
Molten welded wire	39.9	426	~48
Continuously plated and drawn wire	37.0	407	~51

*Knoop Hardness Number, 500-gram load

Fatigue-Induced Degradation of Conductivity

It has been shown previously[1] that reversed bending fatigue can induce degradation of the electrical conductivity of continuously plated composite wire at stresses below the fatigue limit, although similar degradation was not detected in typical molten-welded and continuously plated and drawn wires. Since degradation of conductivity of "survival" samples of all conductor types were noted during the course of staircase testing, some more systematic studies of this phenomenon were carried out.

Using stress levels near the lowest levels defined in the staircase fatigue testing (Figures 3-5), data were obtained which show that, at these stress levels, the conductivity of the various copper-clad steels does systematically decrease with increasing cycles of stress. These data are summarized in Figures 7-9. From these curves, it can be seen that the degradation of conductivity with the number of cycles of reversed bending fatigue stress is initially quite rapid in the continuously plated sample. In the case of the molten-welded and continuously plated and drawn samples, degradation is sluggish until about the $n = 10^6$ cycle level, at which more rapid decreases in conductivity occur. The limiting conductivity of all conductors, at high-cycle levels, is less than 20% IACS, with the lowest measured conductivity occurring in the continuously plated sample (~15% IACS at $n = \sim 2 \times 10^7$).

The differences in the slopes of the curves with respect to the continuously plated sample and the molten-welded and continuously plated and drawn samples is related in part to the higher stress level used in the tests conducted on the continuously plated wire. Data

available, but not shown here, indicate that at about 36,000 psi, the conductivity-cycle curve for this conductor is similar in shape to the curves shown for the molten-welded and continuously plated and drawn samples. In addition, the conductivity at $n = 1 \times 10^7$ is of the same order of magnitude.

Interestingly enough, some degradation of conductivity was measured in all samples at stresses as low as 16,000 psi at cycle levels of 1×10^7. This value of stress is close to the fatigue limit of copper measured in a recent study by Opie[6] at the same cycle level.

Fatigue-Induced Degradation of Tensile Strength

Since fatigue fracture can occur in copper-clad steels at stress levels that are low with respect to relative tensile strength, some tests were conducted to determine the effects of fatigue damage on the initial tensile strengths of these types of conductors. Samples of continuously plated, molten-welded, and continuously plated and drawn wires were tested at the lowest stress levels of the staircase plots at which no failures were observed. The corresponding reductions in tensile strength in samples surviving 1×10^7 cycles, expressed as a ratio of UTS (fatigue damaged)/UTS (as-received wires), is .87 for the continuously plated wire, .97 for the molten-welded wire, and .94 for the continuously plated and drawn wire.

The maximum reduction in tensile strength occurred in the continuously plated wire; however, this wire was subjected to fatigue damage at a nominally higher stress level than the molten-welded and continuously plated and drawn wires.

Metallography of Fatigue Damage

The metallographic data indicate that both fracture at stress levels in the vicinity of the fatigue limit and degradation of conductivity and tensile strength at lower stress levels are related to the development of fatigue-induced microstructural damage in the various copper-clad steels. Examples of this damage are shown in Figures 10-12, which are photomicrographs of continuously plated, molten-welded, and continuously plated and drawn wires failed in fatigue at stress levels corresponding to the highest stresses at which no survival occurred during the staircase testing. Extensive fatigue cracking of all of the claddings has occurred; however, both the molten-welded and continuously plated and drawn samples have sustained additional complex microcracking in a narrow zone on the copper side of the Cu/Fe interface. Associated with this severely cracked zone in these samples are hardness levels which are high with respect to the outer layers of softer cladding. In the case of the continuously plated and drawn sample, the hardness of the damaged zone is about $KHN_{(25)}$ 132 with respect to an outer cladding hardness of $KHN_{(25)}$ 79. The hardness of the thin zone adjacent to the steel substrate in the molten-welded wire is on the order of $KHN_{(25)}$ 147 with respect to the outer cladding hardness of $KHN_{(25)}$ 105.

There is a general absence of complex microcracking and hardening (of the type observed in the molten-welded and continuously plated and drawn samples) in the continuously plated wire. Instead, there is a general tendency for the fatigue cracks formed at the surface of this type of wire to propagate through the cladding and along the original Cu/Fe interface. This results in quite extensive rupture of the cladding. This can be seen in Figure 13, a scanning electron micrograph of a continuously plated wire damaged in fatigue and tested to failure in tension.

Brittle Fracture of Clad Wires

The metallographic data presented above suggest that fracture processes in the vicinity of the cladding/base metal interface are important in limiting fatigue strength and contributing to secondary degradation. Further evidence to support these data has been obtained through examination of both fracture surfaces produced during the course of the fatigue testing and slow bend testing.

The micrograph shown in Figure 14 is representative of the types of fatigue fractures produced in all continuously plated wires and most of the molten-welding and continuously plated and drawn wires. Several fatigue cracks have initiated in the copper cladding and have propagated into the steel through the cladding/base metal interface. The propagation of the cracks has resulted in the formation of characteristic striations (Figures 15 and 16) through the cladding and the bulk of the steel cross section and, finally, ductile rupture (Figure 17) of the remaining cross section.

Fractures produced in several fatigue tests, and in slow bend tests of fatigue-damaged molten-welded and continuously plated and drawn wires are of the type shown in Figures 18 and 19. These are scanning electron micrographs of a fracture surface of a continuously plated and drawn wire failed in fatigue. As in the case of the continuously plated sample, fatigue cracks have propagated into the steel substrate; however, there is evidence of cleavage fracture which has been initiated in the vicinity of the cladding/base metal interface. The cleavage fracture appears to have moved rapidly to link up with the tip of the main fatigue crack front, resulting in final fracture via a mixed cleavage/ductile mode.

Fractures of the type shown in Figures 18 and 19 were produced in many slow bend tests of molten-welded and continuously plated and drawn wires which had survived the staircase testing. It is significant that no fractures of this type were observed in fatigue or slow bend testing of the continuously plated wires which had survived fatigue over a much higher range of stresses. These data, while not quantitative, do suggest a *tendency* for cleavage to occur, probably as a result of the severe notch effects created at the microcracked substrate of these types of wires as a consequence of fatigue.

Fatigue Processes and Degradation

Fatigue fracture in all of these clad wires is resultant from the propagation of fatigue cracks initiated at the cladding surface through the Cu/Fe interface and steel substrate. At stresses lower than the composite wire fatigue limit, the steel wire surface can effectively act as a barrier to crack propagation. At stresses near the composite wire fatigue limit, the microstructure of the Cu/Fe interface becomes extremely significant. The fatigue-induced microstructural damage near the cladding/base metal interface of the molten-welded and continuously plated and drawn wires apparently contributes to the lower stresses required to initiate and propagate fatigue cracks into the respective steel substrates. This is due, in part, to the interfacial alloying that occurs during manufacturing of the wires and the tendency for localized cleavage fracture to occur in conjunction with fatigue crack propagation at the respective Cu/Fe interfaces. The lack of alloying and absence of cleavage fracture tendencies in the continuously plated wires is apparently responsible for the higher observed fatigue

limit in this composite conductor.

Purcell, in a recent paper[7], draws attention to the nature of the damage which can be produced at the edge of a propagating fatigue crack in copper. At applied fatigue stresses which are low with respect to the yield strength of copper, hardnesses and dislocation densities near these fatigue crack tips are much higher than those found in the vicinity of the edges of corresponding tensile fractures in copper. Thus, it is not surprising that, in the copper clad steels, extremely high local stresses can be created near the copper/steel interface due to propagating fatigue cracks. These stresses, in effect, reduce the amount of applied stress which would be required to initiate cracks into the unclad substrate. This, coupled with the observed microcracking and cleavage fracture in two of the composite wires, would tend to explain both the general effects of copper claddings on steels and the specific differences between types of copper claddings with respect to fatigue resistance.

General Conclusions

Copper claddings of the type studied herein are, in general, detrimental to the fatigue strengths which can be developed in the underlying steels. This observation, coupled with the data regarding fatigue-induced degradation of conductivity, tensile strength, and resistance to brittle fracture which can occur in the clad wires, would suggest caution in the application of these conductors in fatigue-sensitive environments.

References

1. Fox, Alfred, *Reversed Bending Fatigue Characteristics of Copper-Clad Steel Conductors*, Journal of Materials, JMLSA, Vol. 3, No. 1, March 1968, pp. 32-42.

2. Houghton, J. R., *Fatigue Tests of Aerial Telephone Conductors*, NBS Lab Reports 8104 and 8515, October 1963, and June 1964.

3. Colby, J. W., Advanced X-Ray Analysis, Vol. 11, pp. 287-305, 1968.

4. Lynnworth, L. C., *Ultrasonic Measurement of Elastic Modulii in Slender Specimens Using Extensional and Torsional Wave Pulses*, Journal of Testing and Evaluation, JTEVA, Vol. 1, No. 2, March 1973, pp. 119-125.

5. Dixon, W. J., and Mood, A. M., Journal of American Statistical Association, Vol. 43, p. 109, 1948.

6. Opie, W. R., et al., *A Fundamental Comparison of the Mechanical Properties of OFHC and ETP Coppers*, Copper and Its Alloys, The Institute of Metals, 1970, pp. 106-110.

7. Purcell, A. H., and Weertman, J., *Crack Tip Area in Fatigued Copper Single Crystals*, Metallurgical Transactions, Vol. 5, pp. 1805-1809, 1974.

Table I

Properties of Copper-Clad Steel Conductors and Steel Substrate used in these experiments.

Sample	UTS ($X10^3$ psi)	YS ($X10^3$ psi)	ρ (gm/cc)	t cladding (mils)	d wires (mils)	Conductivity (%IACS)
Continuously Plated Wire	244	231	8.11	2.6	40.5	30.4
Predrawn Steel Wire	278	253	7.86	——	35.5	——
Molten – Welded Wire	257	234	8.10	2.8*	40.5	32.3
Continuously Plated & Drawn Wire	246	233	8.11	2.7*	40.2	31.9

(1) Steel drawn and plated to final size
(2) Steel drawn to size and unplated – substrate of continuously plated wire
(3) Manufactured by molten–welding process
(4) Continuously plated and drawn to finished size
* Average cladding thickness of inhomogeneous claddings

Figure 1 - Electron - Probe Microanalysis of Copper-Clad Steels at Cladding/Base Metal Interface

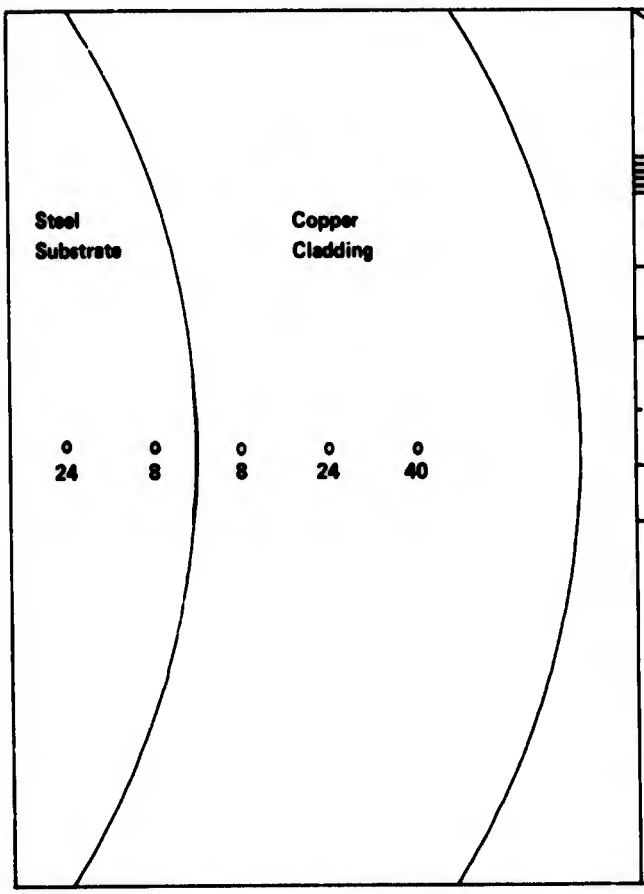

Distance (Microns) \ Sample	Continuously Plated Wire		Molten – Welded Wire		Continuously Plated and Drawn Wire	
	(1) Cu	(1) Fe	Cu	Fe	Cu	Fe
40	99.79	0.21	99.67	0.33	99.61	0.39
24	99.70	0.30	99.42	0.58	99.28	0.72
8 (2)	99.02	0.98	98.20	1.80	97.92	2.08
8	0.41	99.59	1.13	98.87	1.62	98.38
24	0.34	99.66	1.02	98.98	0.98	99.02

(1) All concentrations in atomic percent normalized from corrected weight percent data
(2) Cu/Fe interface (metallographic)

Figure 2 - Pulse-Echo Reflections from typical wire sample

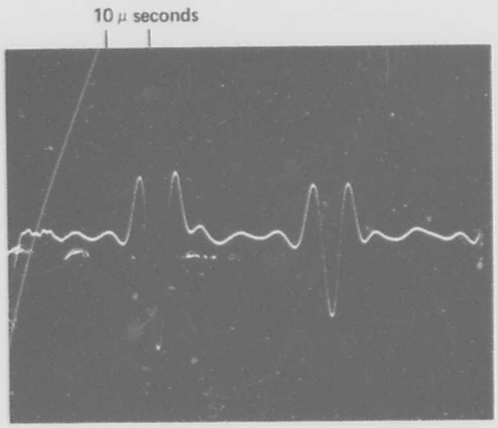

Table 2
Modulii of Experimental Wires

Sample	ρ gm/cc	E ($X10^6$ psi)
Continuously Plated Wire	8.12	26.458
Molten-Welded Wire	8.10	26.877
Continuously Plated and Drawn Wire	8.11	27.382
Predrawn Steel* Substrate Wire	7.86	28.966

*Unplated Substrate of Continuously Plated Wire

Figure 3 - Staircase data for wire continuously plated to final size from predrawn steel

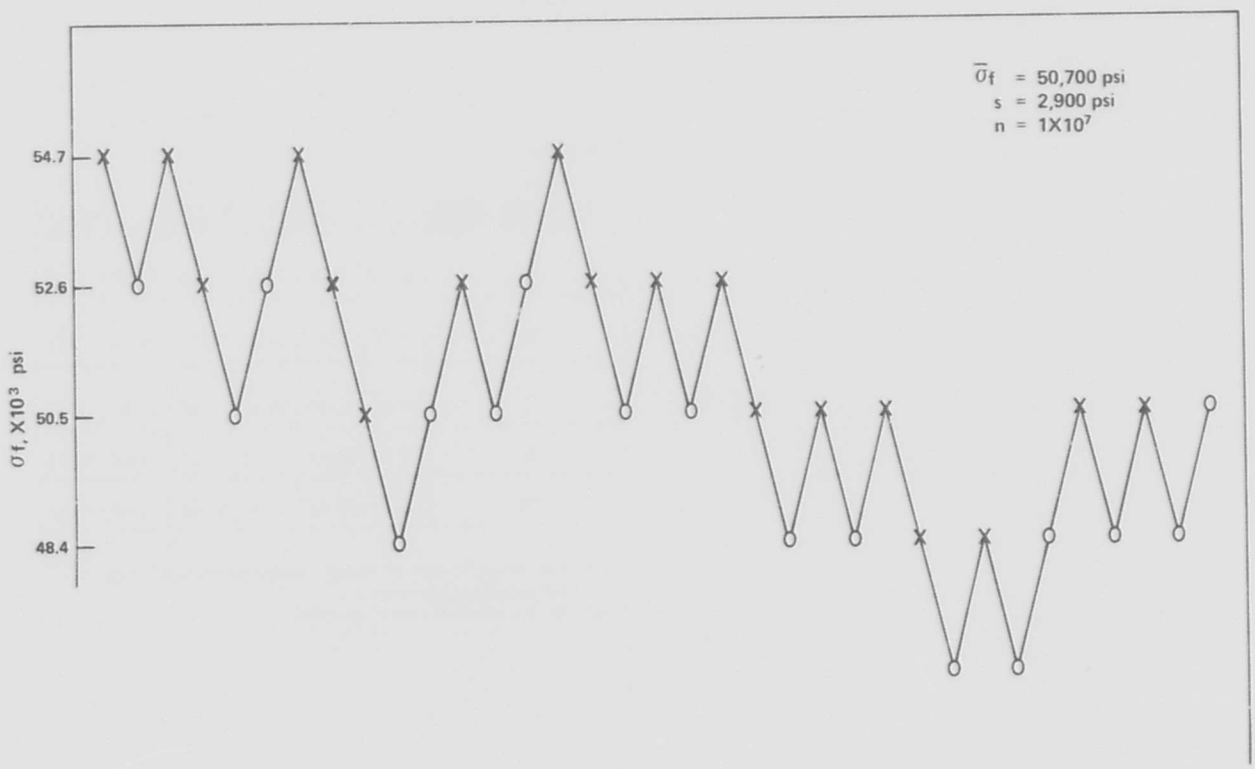

Figure 4 - Staircase data for wire made by molten welding processes

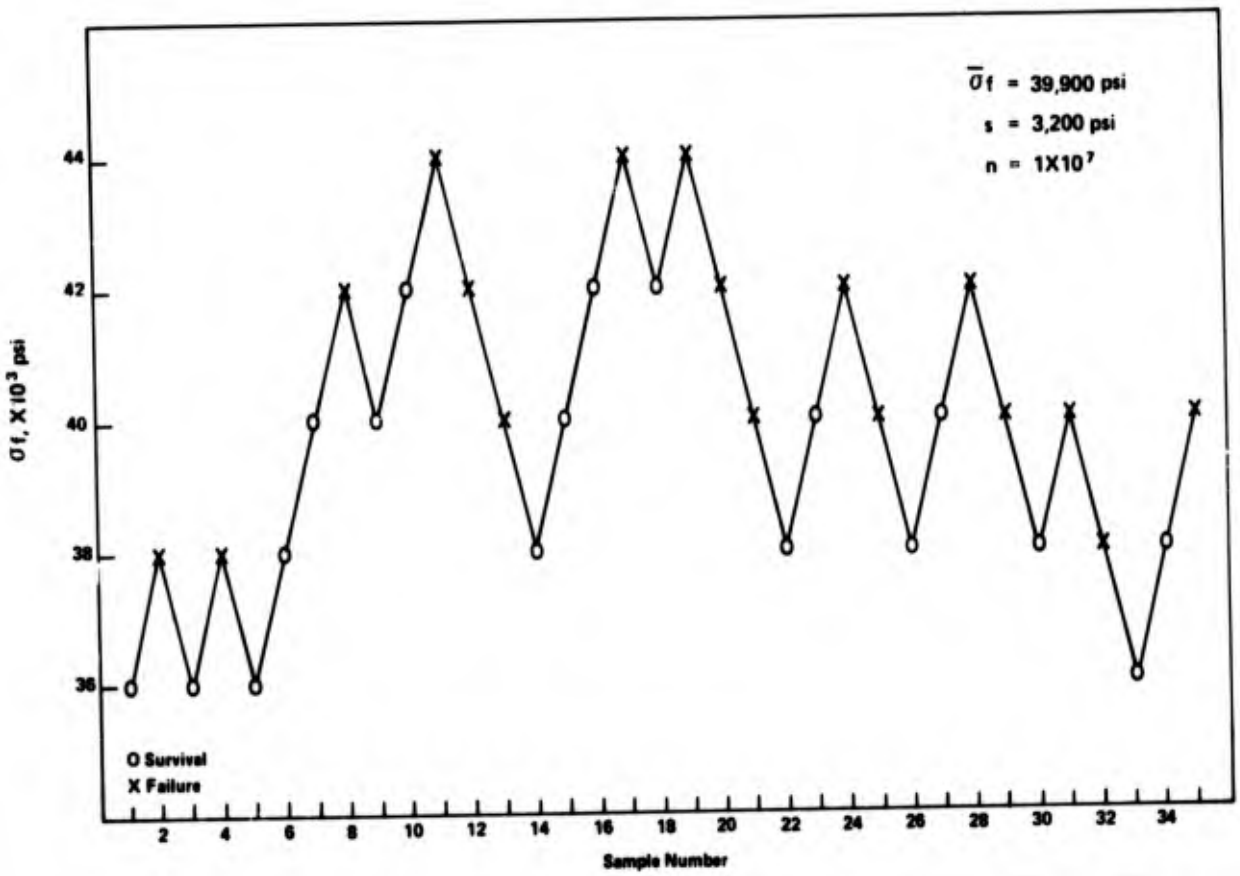

Figure 5 - Staircase data for continuously plated and drawn wire

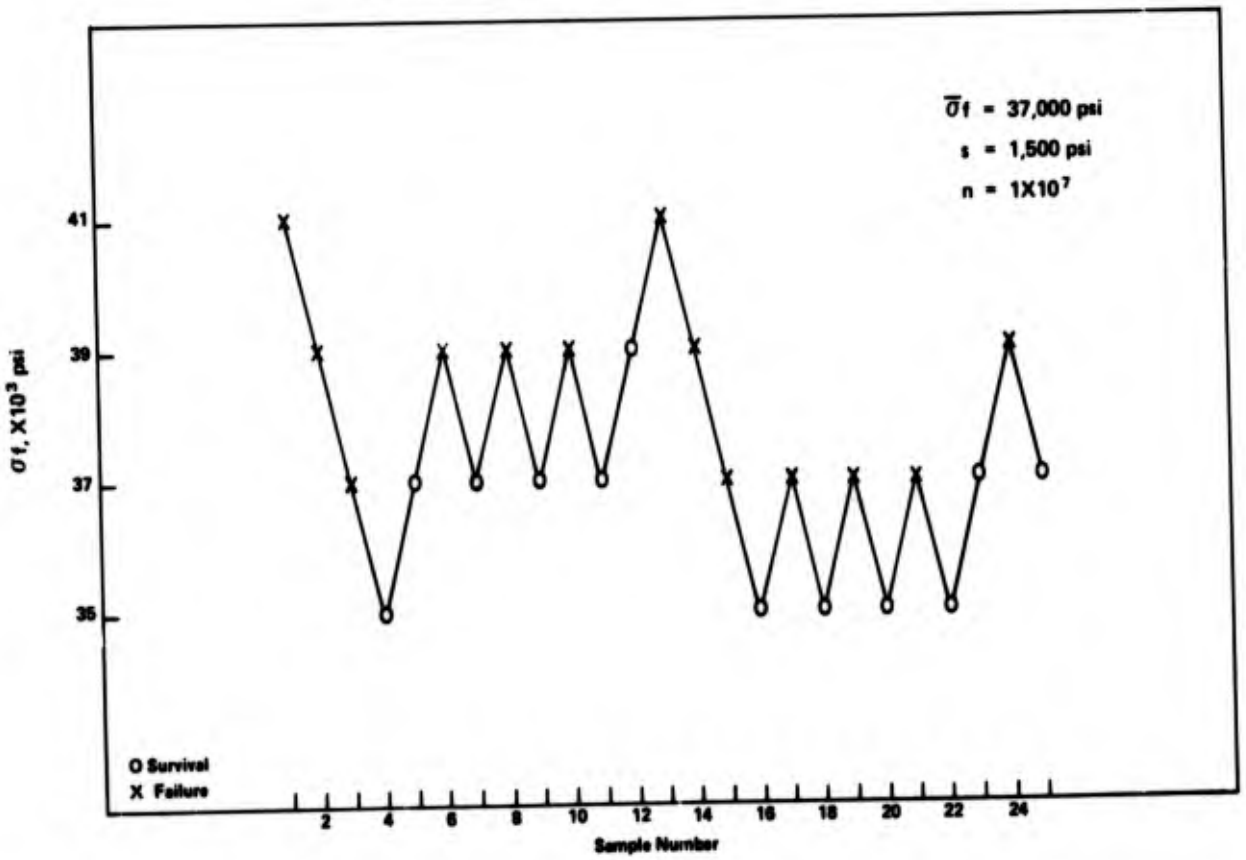

Figure 6 - Staircase data for steel substrate wire underlying continuously plated wire

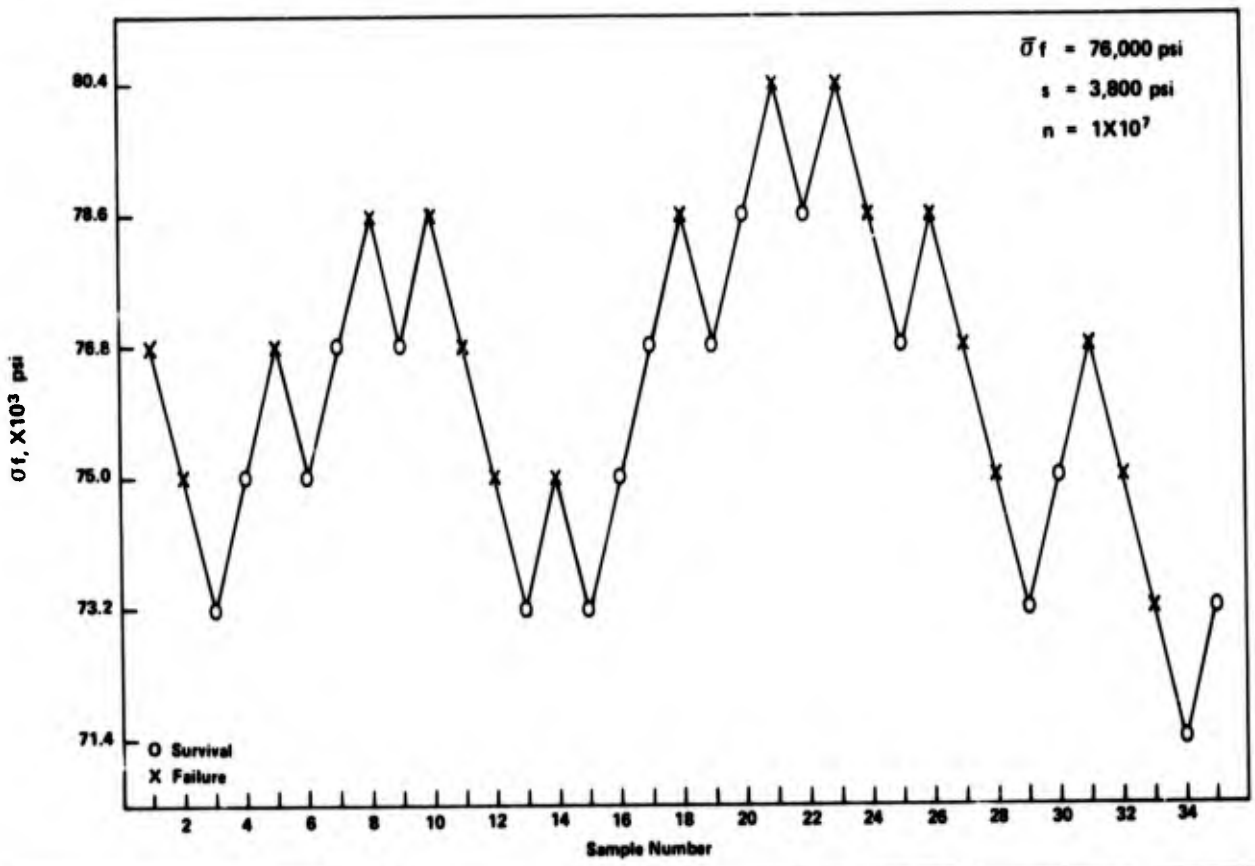

Figure 7 - Conductivity degradation at constant stress in continuously plated wire

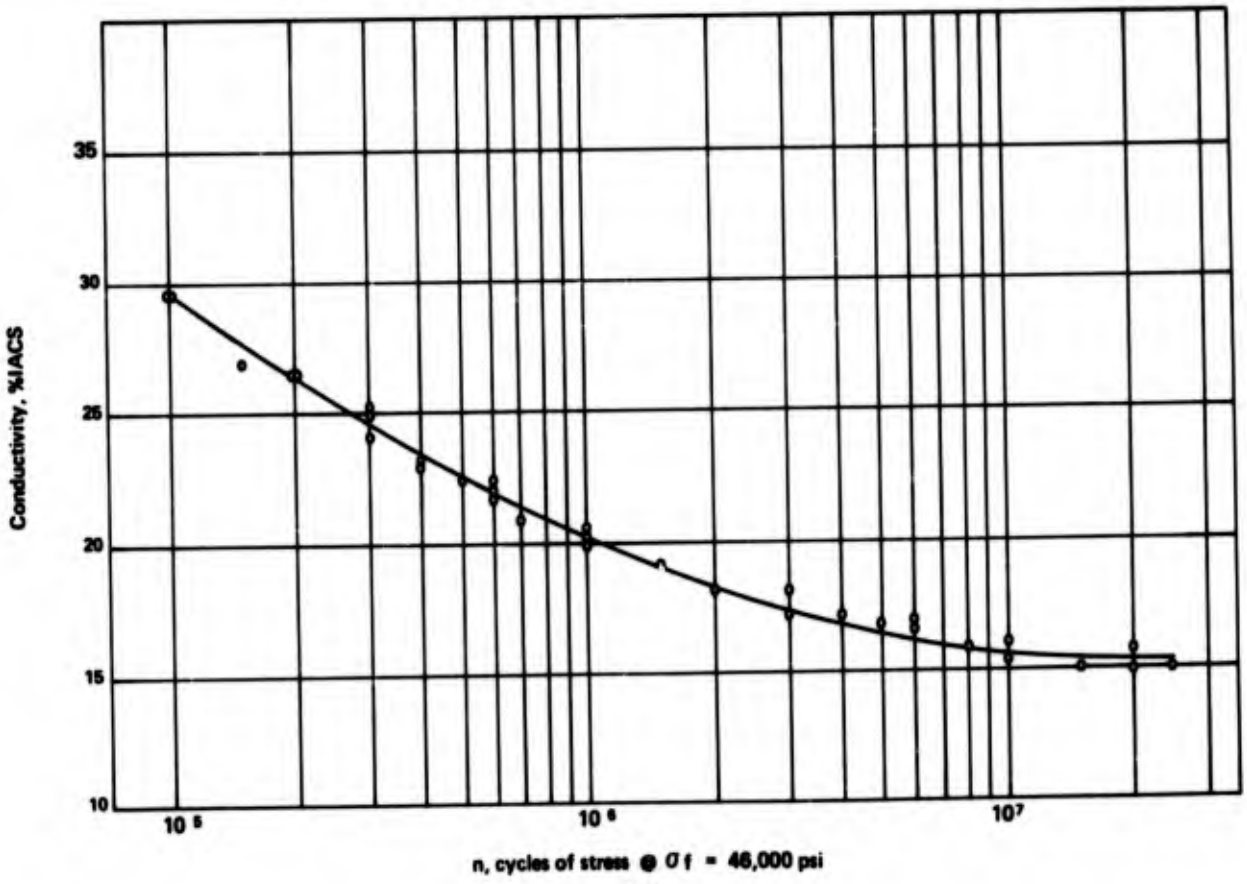

Figure 8 - Conductivity degradation at constant stress in wire produced by molten-welding process

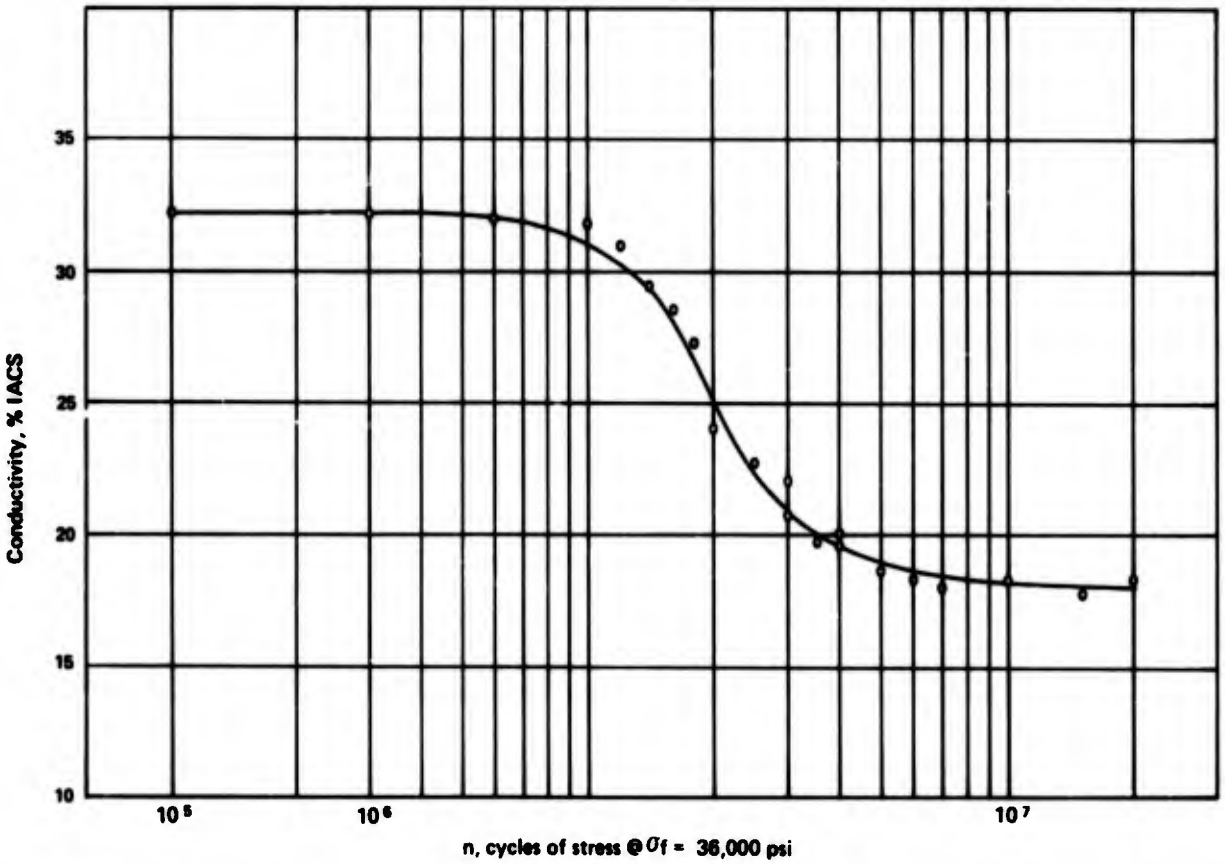

Figure 9 - Conductivity degradation at constant stress in continuously plated & drawn wire

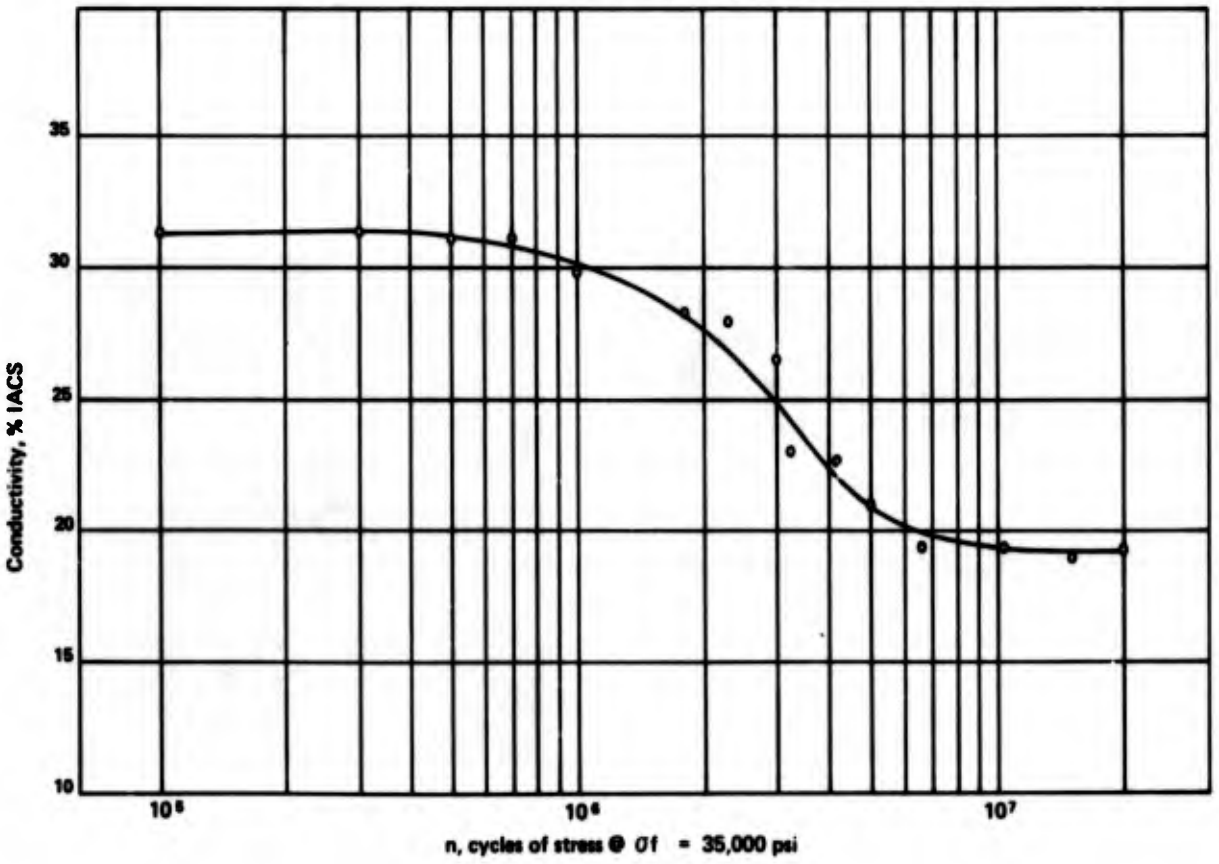

Figure 10 - Fatigue Damage in Continuously Plated Wire

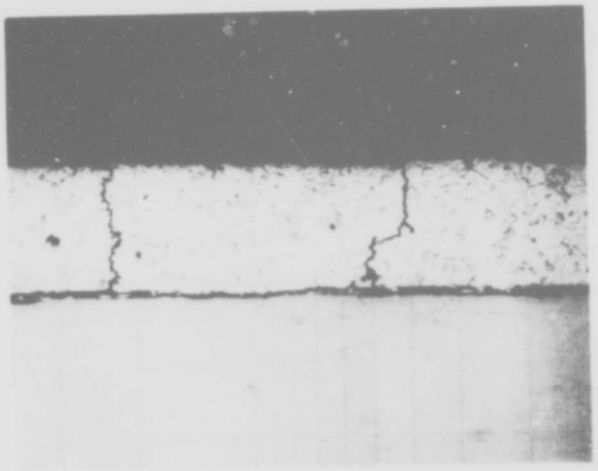

Figure 11 - Fatigue Damage in Molten-Welded Wire

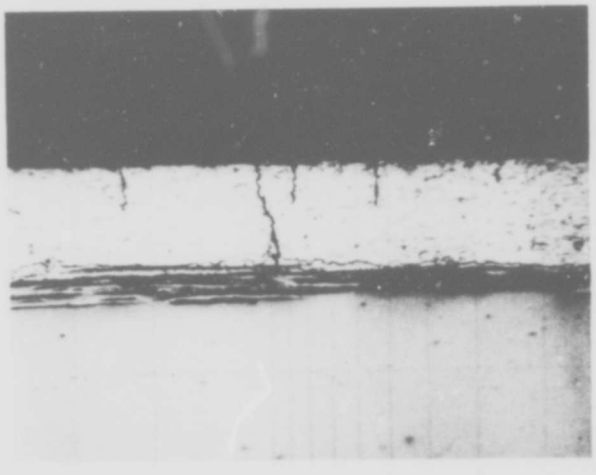

Figure 12 - Fatigue Damage in Continuously Plated & Drawn Wire

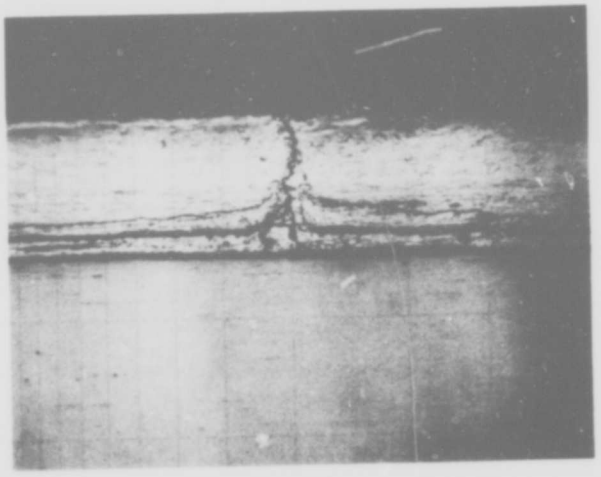

Figure 13 - Tensile failure of fatigue-damaged Continuously Plated Wire

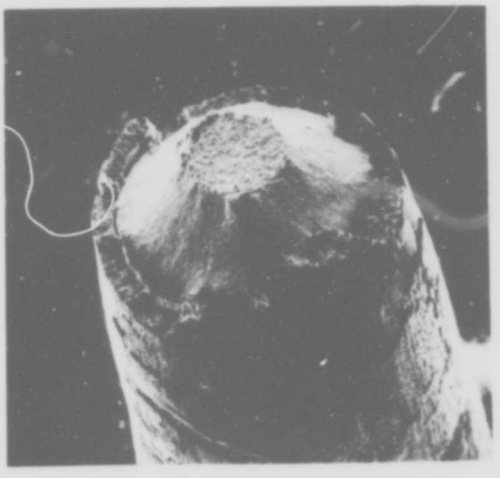

Figure 14 - Fatigue fracture in Continuously Plated Wire

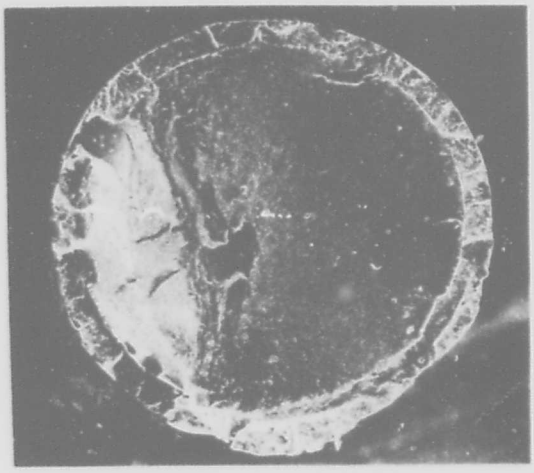

Figure 15 - Striations formed by fatigue crack propagation

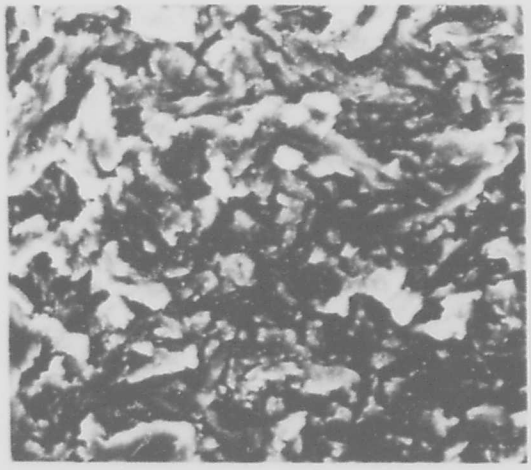

Figure 16 - Fatigue at Cladding/Base Metal Interface

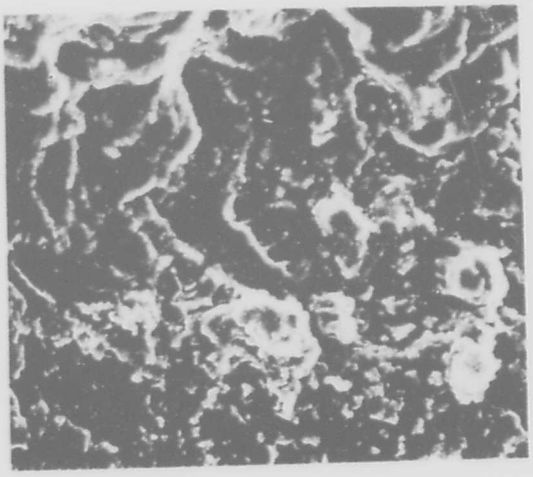

Figure 17 - Terminating ductile fracture of steel

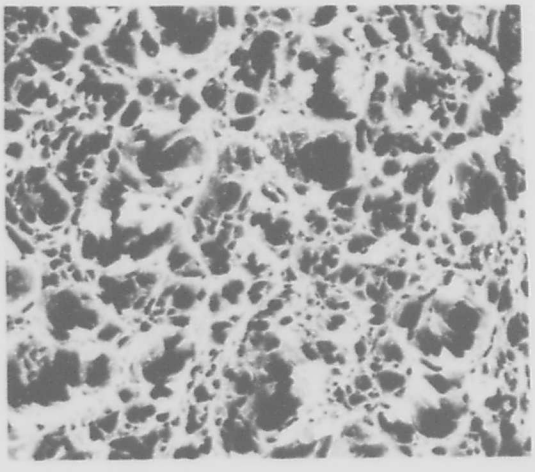

Figure 18 - Fatigue and cleavage in Continuously Plated & Drawn Wire

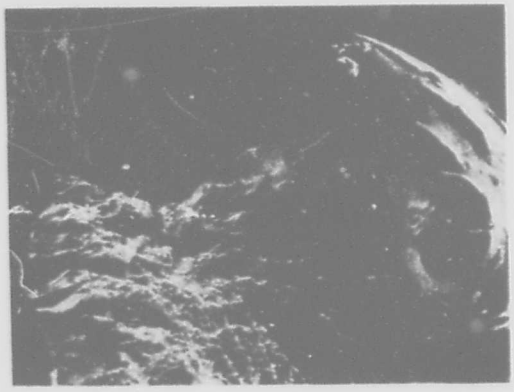

Carl Shumaker

Carl Shumaker is a member of the Wire & Cable Engineering Group at Superior Continental Corporation. He received a B.S. and M.S. in Metallurgical Engineering from North Carolina State University. Prior to joining Superior Continental in 1971 he was with ESSO Research & Engineering Company in Florham Park, N.J.

Figure 19 - Cleavage and ductile fracture modes in above micrograph

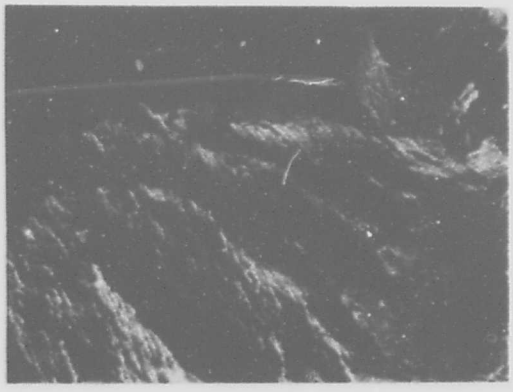

MUTUAL CAPACITANCE CORRECTION FACTORS FOR SERIES MODE BRIDGES

T. Lamar Moore
Rural Electrification Administration
Washington, D. C.

Kenneth W. Brownell, Jr.
Brand-Rex Company
Willimantic, Connecticut

Abstract

This paper presents capacitance correction factors for series mode bridges as a function of cable length and as a function of measured dissipation factor. Errors due to variations in the primary constants are discussed.

The calculation of meaningful mutual conductance data is discussed along with error analysis due to bridge inaccuracies.

Measured data is utilized to substantiate the claims of the paper.

Introduction

Telephone cables are designed for specific primary and secondary parameters. Cable specifications generally state limits on three of the four primary parameters (resistance, capacitance and conductance) which in turn control the secondary parameters. This control ensures the cable end user that the line impedance and attenuation will be within acceptable design limits.

Cables are checked for compliance to specifications by measuring the dc loop resistance of pairs and the 1000 hertz effective mutual capacitance and conductance. There are only incremental differences between dc resistance and 1000 hertz resistance of telephone cables. Advances in manufacturing capabilities, cable design and customer handling capabilities have prompted the move toward longer lengths of telephone cables being shipped to operating telephone companies from cable suppliers. This, coupled with movements toward finer gauge telephone plant design, make it increasingly more difficult to measure cable capacitance and conductance without significant errors due to propagation effects.

There are a number of good books and engineering papers that discuss paired cable, propagation effects, apparent errors, and related subjects.[1] The cable parameters are calculated and measured as open circuit admittance (Y_{oc}) and short circuit impedance (Z_{sc}). This classic technique of cable measurements in the laboratory on short cable lengths has provided very accurate information for many decades.

The world outside the laboratory must be dealt with in a practical manner. The measurement of cable mutual capacitance on shipping reel lengths to verify specification requirements might be done in the classic manner of measuring Y_{oc} and Z_{sc} and then calculating the primary parameters, but generally the verification will consist of open circuit measurements and some simplified method of determining the true capacitance and conductance. Paper presented at the International Wire and Cable Symposium by J. V. Buscemi and A. E. Widmer in 1964[2] and by R. A. Frisch, I. Kolodny, and J. A. Olszewski in 1967[3] provided practical techniques and nomographs for converting measured capacitance to true capacitance at 1 kHz. These correction techniques were based on the traditional measurement of capacitance and conductance in the parallel mode (admittance).

Many of the commonly used portable capacitance bridges measure capacitance and dissipation in the series mode (impedance). Using parallel mode correction factors on data obtained with series mode bridges has resulted in some confusion on long cable lengths. Valid data can be obtained with either bridge type if properly corrected. Examination of the correction factors show that propagation affects the series measurements less than the parallel measurements at longer measurement lengths. This can result in more accurate and less complex corrections as the cable parameters vary from nominal values. The major reason for this is that the dissipation arm tends to balance out the cable series resistance without regard to the exact value of the resistance.

The body of this paper further presents mutual capacitance series mode bridge correction factors for a wide variety of primary constant permutations. In addition mutual conductance determination from series mode dissipation factor is derived and error limits are stated.

All theoretical developments have been verified by measured data. A small portion of this data is presented in Appendix 1.

Development of Series Mode Correction Factors

Capacitance bridges that are used to measure telephone cable pairs generally yield data in one of three ways:

1. Capacitance and Conductance in Parallel (C_p and G_p).

2. Capacitance and Dissipation in Series (C_s and D)

3. Capacitance and Dissipation in Parallel (C_p and D)

These values can be converted into "true" mutual capacitance or effective distributed mutual capacitance by using correction factors.

Capacitance correction factors may be applied in several ways. In this paper they shall be developed as a function of cable length and as a function of measured dissipation factor. All discussions refer to

1000 hertz measurements and calculations.

It can be shown that a transmission line of length ℓ can be represented by an equivalent T circuit as is illustrated in Figure 1.[4] This representation is equivalent for any load impedance (Z_L). If Z_L is infinite (open circuit) it follows that the impedance seen looking into terminals A - B (Z_{AB}) can be readily calculated as follows:

$$Z_{AB} = Z_o \tanh \frac{\rho \ell}{2} + \frac{Z_o}{\sinh \rho \ell} , \quad (1)$$

where

$$Z_o = \sqrt{\frac{R + j\omega L}{G + j\omega C}} , \quad (2)$$

$$\rho = \sqrt{R + j\omega L} \cdot \sqrt{G + j\omega C} , \quad (3)$$

C, G, R, L are the cable primary constants and ℓ is the cable length in consistent units. There exists a classical identity:

$$\tanh \frac{m}{2} = \frac{\cosh m - 1}{\sinh m} , \quad (4)$$

where m is any complex variable.

Applying Eq. (4) to Eq. (1)

yields

$$Z_{AB} = Z_o \frac{\cosh \rho \ell - 1}{\sinh \rho \ell} + \frac{1}{\sinh \rho \ell} \quad (5)$$

or

$$Z_{AB} = Z_o \coth \rho \ell \quad (6)$$

Eq. 6 is consistant with classical transmission line theory and represents the impedance seen by the series mode bridge when the open circuit measurement is being made. Therefore, from Figure 1:

$$Z_{AB} = R_s + \frac{1}{j\omega C_s} ,$$

or

$$R_s + \frac{1}{j\omega C_s} = Z_o \coth \rho \ell , \quad (7)$$

where

R_s = measuring arm resistance (8)

C_s = measuring arm capacitance (9)

$= 2\pi f$ (10)

Equating the real and imaginary parts of Eq. 7 allows the calculation of C_s and R_s as a function of C, G, R, L, and ℓ. In addition, the definition of dissipation factor,

$$D = \frac{\text{Power Dissipated}}{\text{Power Stored}} = \frac{I^2 R_s}{I^2 \, 1/\omega C_s}$$

or

$$D = R_s \omega C_s , \quad (11)$$

allows for the conversion between R_s and D.

These equations were utilized in a computer program for 47 permutations of C, G, R and L and for ℓ in 1,000 foot steps from 1 kilofoot through 30 kilofoot with $\omega = 6.28 \times 10^3$ per second.

Standard primary constants utilized were as follows:

R = 15 (19 AWG), 171 (22 AWG), 274 (24 AWG) or

431 (26 AWG) ohms/mile,

L = 1.09 millihenry/mile,

G = 0.0001 micromho/mile,

C = 0.083 microfarad/mile.

Data and error analysis are presented in the next section of this paper. Cable lengths are sometimes presented as fractions of a wavelength (λ) to lend consistency between the data for differing gauge sizes. A summary of 1000 hertz wavelength are given in Table 1.

Capacitance Correction Factors

Correction factors (CF) were developed which can be multiplied times the bridge reading (C_s) to yield the true mutual capacitance of the cable (C) within the required accuracy limitations. This is accomplished by applying the following formula to the proper computer output:

$$CF = 1 + \frac{C - C_s}{C_s} \quad (12)$$

Correction Factors as a Function of Cable Length

Series mode and parallel mode capacitance correction factors as a function of cable length are presented in Figure 2 for standard primary constants. It is obvious from Figure 2 that the two types of correction factors can not be used interchangeably. It is also obvious that the series mode factors are of lesser magnitude than the parallel mode factors for long cable lengths.

Detailed curves for series mode capacitance correction factors as a function of length are presented in Figure 3 for the four common gauges and ± 10% variations in loop resistance, with all other primary constants standard. In cases which require extreme accuracy and where cable length is also greater than 0.1 wavelength, loop resistance can be measured and the

curves interpolated.

Error analysis of the standard value series mode capacitance correction factors as a function of cable length is presented in Figure 4 for 24 gauge cable. Other gauges have similar error curves when length in wavelength is compared, and a summary of these errors is presented as Table 2.

It is apparent from Table 2 that the length correction factors presented in Figure 3 yield an error of less than 1.0% for cable lengths up to 0.1 wavelength - which is consistent with the accuracy of most portable capacitance bridges. Length correction accuracy can be extended to 0.15 wavelength by measuring loop resistance and interpolating curves.

Correction Factors as a Function of Dissipation

To improve the accuracy of parallel mode correction factors, cable engineers devised an improved method of correction.[3] This consisted of calculating the ratio of measured capacitance to conductance and applying a correction factor as a function of that ratio. Since dissipation represents a ratio of capacitance to conductance, C_s capacitance correction factors for standard primary constants were developed as a function of dissipation and are presented in Figure 5. Correction factors to correct C_p as a function of dissipation can be developed in like manner for bridges that measure C_p and D.

This method is not prone to significant errors from 10% variations in R, L, and C or G in the range of 10 micromho/mile. These errors are illustrated in Figure 6. However, it is limited by the bridge accuracy in determining D. Therefore, the correction factors as a function of dissipation would generally be utilized as a data verification tool.

Head to Tail Correction Factors

Long reels of cable can be measured with good accuracy using a technique called "head-to-tail."[2] This consists of accessing the top end of the cable pair (head) and the bottom end of the cable pair (tail) for measurement simultaneously. This technique effectively reduces the measurement length to one-half. This has the same effect of measuring two cable pairs in parallel, each being one-half the reel length. Therefore, the capacitance correction factors as a function of length presented in Figure 3 can be utilized by entering the graph at one-half the true reel length. Capacitance correction factors as a function of dissipation remain unchanged.

This is a very effective tool in accurately determining cable capacitance on the reel. The effective measuring length is now doubled to 0.2 wavelength, or longer, with excellent accuracy. Head-to-tail measurements cannot be applied to installed cable since both ends cannot be accessed simultaneously.

Mutual Conductance

The determination of cable conductance from an open circuit measurement is difficult for long lengths of cable due to the masking of the leakage by the loop resistance. It is extremely difficult to obtain accurate conductance readings when true conductance is in the 0.001 micromho/mile range, but, at the same time, accurate field results are not generally required when conductance is in this range.

Utilizing the series expansion for $Z_o \coth \rho\ell$, taking the dominant terms of the real part, and equating this to D through Eq. 11 results in Eq. 13 below.

Cable conductance can be calculated by the following formula on a limited basis:

$$G \cong \ell \omega^2 C^2 \left[\frac{D}{\omega C_s} - \frac{R\ell}{3}\right] , \qquad (13)$$

where

G is in units mho/mile

ℓ is cable length in miles

ω is $2\pi f$

C is corrected mutual capacitance in farad/mile

D is measured dissipation factor

C_s is the uncorrected bridge capacitance in farads

$R\ell$ is the measured loop resistance in ohms.

The authors make no claim as to the accuracy of the above formula for very low G. However, G in the range of 3.3 micromho/mile is the area of practical field interest. The limitations and accuracy of Eq. 13 in this area of interest are presented below:

If it is assumed that D, C, C_s, ω, and $R\ell$ are known precisely, Eq. 13 is accurate to within $\pm$ 10% for all permutations of the primary parameters and cable lengths up to 0.05 wavelength.

C, C_s, ω, and $R\ell$ are not ever known precisely, of course. Worst case errors are summarized in Table 3. It is imperative that D, ω, C_s, and $R\ell$ are known with the highest practical precision.

If it is assumed that the accuracy of D cannot be controlled tighter than $\pm$ 5% and that the combined accuracy of ω and C_s cannot be controlled tighter than $\pm$ 2%, it is obvious from Table 3 that measurements of lengths greater than 0.05 wavelength are unrealistic. Beyond this point, or whenever it becomes absolutely necessary to insure that accuracy of G, complete open circuit/short circuit measurements must be taken unless D can be determined accurately. It has been assumed that Wheatstone bridge measurements would yield accurate $R\ell$ data.

When head-to-tail measurements are employed, conductance can be calculated by:

$$G \cong \ell \omega^2 C^2 \left[\frac{D}{\omega C_s} - \frac{R\ell}{12}\right] \qquad (14)$$

Therefore, measurement lengths could be safely doubled with the same degree of accuracy in calculated G.

Conclusions

The series mode capacitance measurement technique can yield accurate mutual capacitance values by utilizing either correction factors as a function of cable length (Figure 3) or correction factors as a function of dissipation factor (Figure 5). Corrections up to

0.15 wavelength can be made with an accuracy comparable to the accuracy of most portable bridges.

Mutual conductance values can be calculated utilizing Eq. 13 with reasonable accuracy in the 3.3 micromho/mile range and measurement length up to 0.05 wavelength.

Measured data is presented in Appendix 1.

Acknowledgements

The authors gratefully acknowledge the assistance of Mr. John Micol of Superior Continental Corporation in data gathering, Mr. Ken Bedard of Brand-Rex Company in data reduction, and the Communications Engineering Product Center of Anaconda Wire and Cable Company and Mr. H. D. Hoiberg and Mr. R. J. Peterson of the Rural Electrification Administration in Computer Programming.

References

1. H. H. Skilling, Electric Transmission Lines, New York: McGraw-Hill Book Company, Inc., 1951.

2. J. V. Buscemi and A. E. Widmer, "Apparent Errors in the Measurement of Mutual Capacitance on Longer Lengths of Cable Pair at 1000 CPS." Prepared for Thirteenth Annual Wire & Cable Symposium, December 2, 1964.

3. R. A. Frisch, I. Kolodny and J. A. Olszewski, "Simplified Determination of Low Frequency Mutual Capacitance of Long Lengths of Telephone Cables." Presented at Sixteenth International Wire and Cable Symposium, November 29, 30 and December 1, 1967.

4. M. P. Weinbach, Principles of Transmission in Telephony, New York: The MacMillan Company, 1924.

Biography

T. Lamar Moore received the Associate in Science Degree in electronics and communications technology from Southern Technical Institute, Marietta, Georgia, in 1958. He joined the Transmission Branch of the Rural Electrification Administration in 1958. He is a Communications Specialist and since 1965 has been responsible for trunk and subscriber carrier requirements and specifications.

Kenneth W. Brownell, Jr. joined the Telecommunications Cable Division of Brand-Rex Company earlier this year as Manager of Engineering and Development. He holds B.S.E.E. (1971) and M.S.E.E. (1972) degrees from the University of Tennessee. Prior to his present position he served as an electronics technician in the U.S. Navy, as an instrument technician at Oak Ridge National Laboratories and as a research and development engineer at Superior Continental Corporation.

FIGURE 1

Equivalent T Circuit With Series Mode Equivalent Balancing Circuit

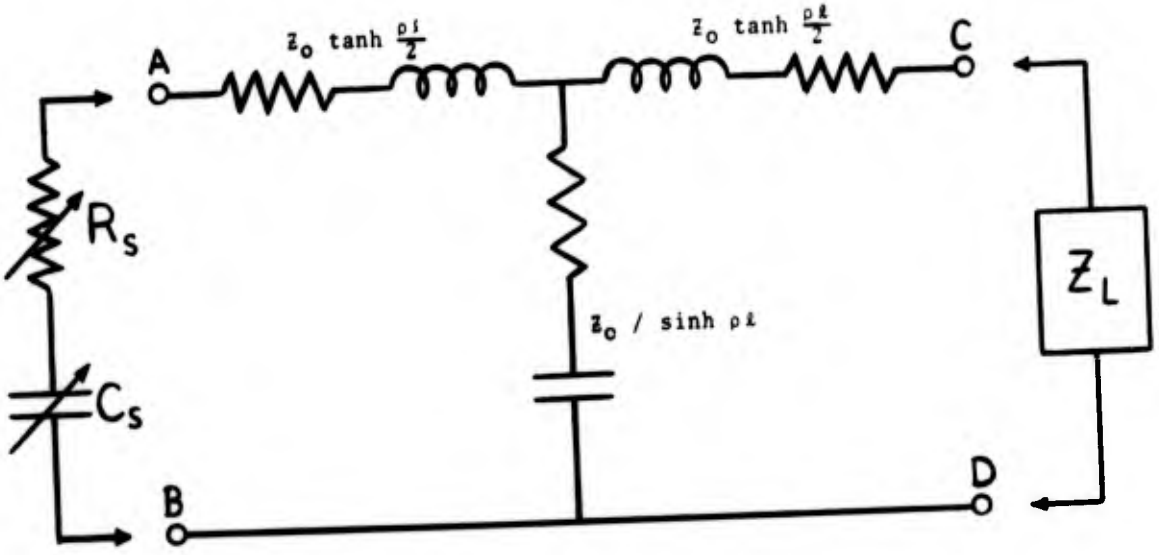

FIGURE 2

COMPARISON BETWEEN SERIES MODE AND PARALLEL MODE CAPACITANCE CORRECTION FACTORS WITH STANDARD PRIMARY CONSTANTS.

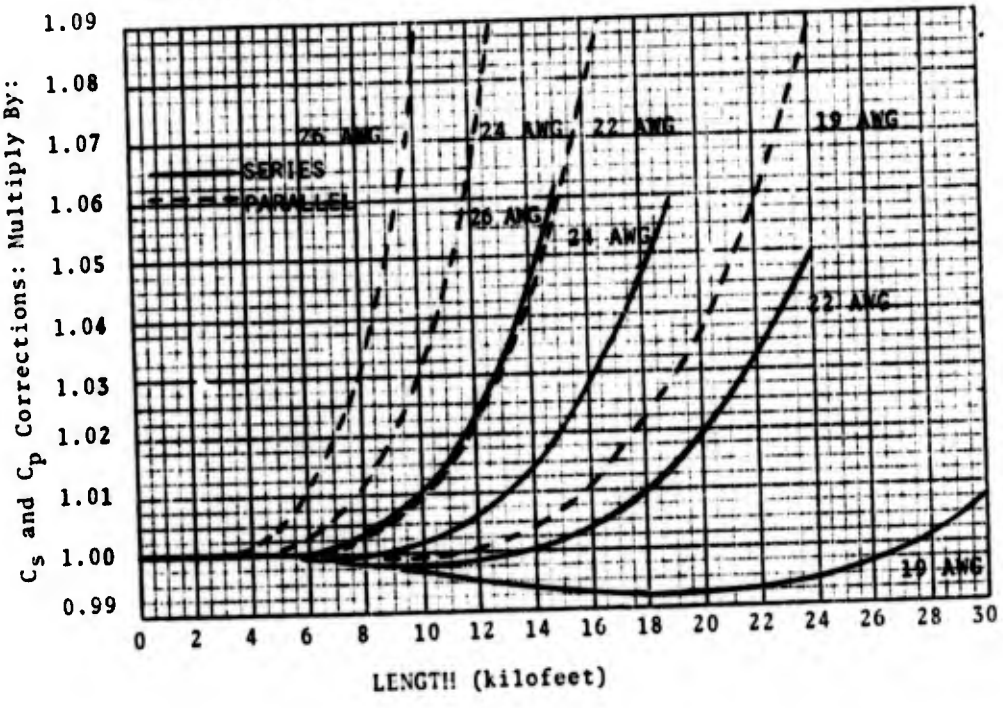

FIGURE 3

SERIES MODE CAPACITANCE CORRECTION FACTORS
AS A FUNCTION OF CABLE LENGTH

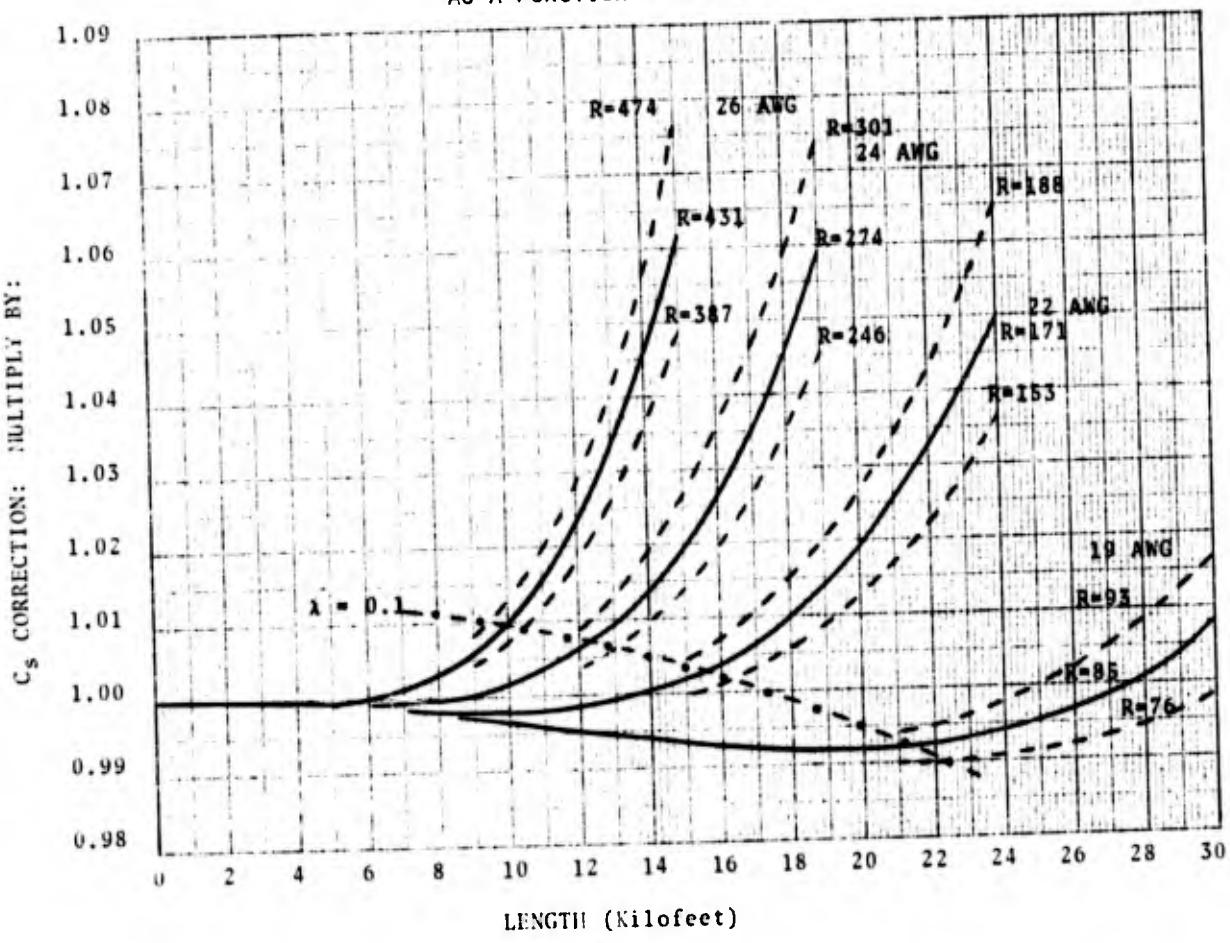

FIGURE 4

PERCENT ERROR IN 24 AWG CAPACITANCE LENGTH CORRECTION FACTOR
DUE TO VARIATIONS OF PRIMARY PARAMETERS.

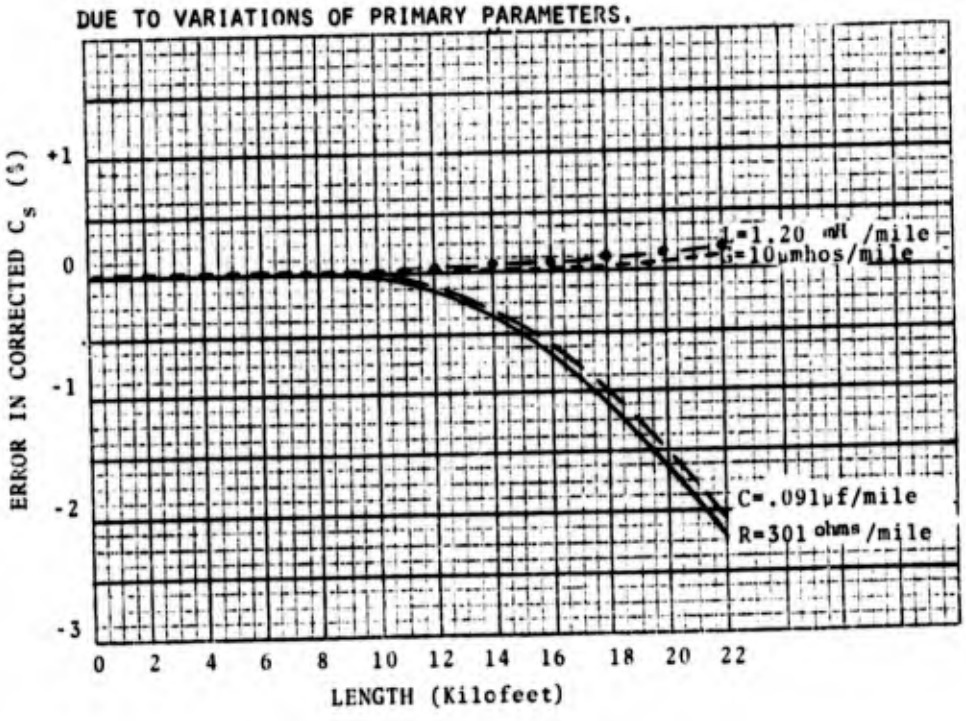

FIGURE 5

SERIES MODE CAPACITANCE CORRECTION FACTORS AS A FUNCTION OF DISSIPATION FACTOR

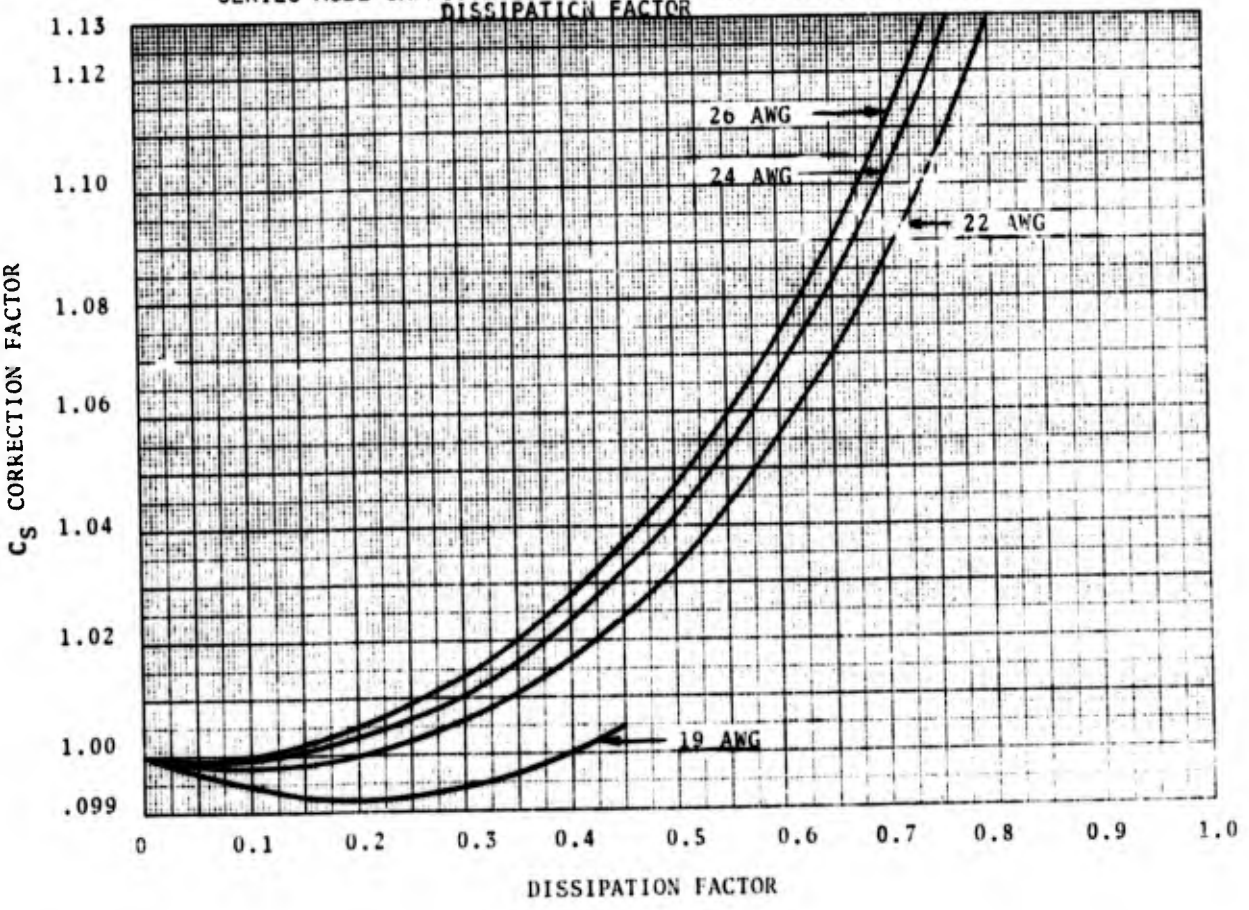

FIGURE 6

PERCENT ERROR IN 24 AWG CAPACITANCE DISSIPATION CORRECTION FACTOR DUE TO VARIATIONS OF PRIMARY PARAMETERS

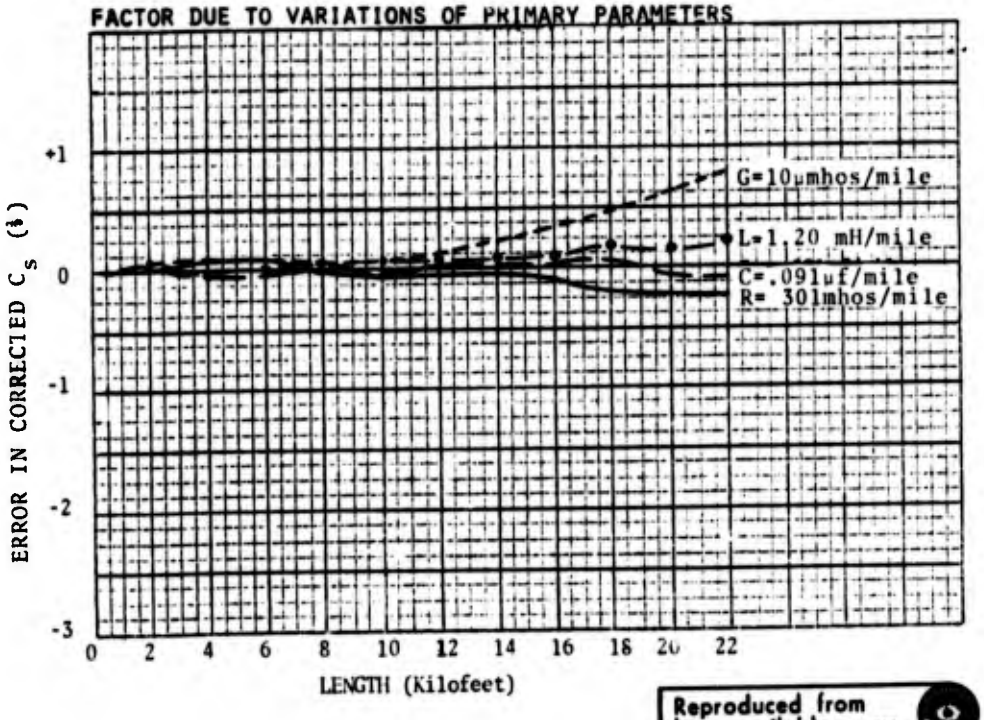

Table 1

Cable Length in Kilofeet Versus
Cable Length in 1000 Hertz Wavelength

AWG	0.05λ	0.10λ	0.15λ
19	10.75	21.50	32.25
22	7.70	15.40	23.10
24	6.15	12.30	18.45
26	4.90	9.80	14.70

Table 2

Percentage Error in Series Mode Capacitance Length Correction
Factors Due to Variation of Primary Constants from Standard Values

AWG	λ	R x 1.1	C x 1.1	G = 10μ mhos	L x 1.1	Worst* Combination
19	0.10	-0.2	0	0	0.2	-0.5
	0.14**	-1.0	-0.6	0	0.3	-2.0
22	0.10	-0.3	-0.2	0	0.1	-0.6
	0.15	-1.3	-1.1	0	0.2	-2.7
24	0.10	-0.3	-0.2	0	0.1	-0.6
	0.15	-1.3	-1.1	0.1	0.2	-2.6
26	0.10	-0.3	-0.3	0	0	-0.6
	0.15	-1.3	-1.2	0.1	0.1	-2.6

*Worst combination used is: R x 1.1, L x 0.9, G = 10μ mhos, C x 1.1
**30 Kilofeet was longest calculated length.

Table 3

Calculated Values for Cable Conductance Versus True Cable
Conductance as a Function of Bridge Error and Cable Length

AWG	λ	TRUE G=0.0001 μ mhos/mile					TRUE G=3.3 μ mhos/mile					TRUE G=10.0 μ mhos/mile				
		No Error	D=+5%	D=-5%	D=+5% & ω=-2%	D=-5% & ω=+2%	No Error	D=+5%	D=-5%	D=+5% & ω=-2%	D=-5% & ω=+2%	No Error	D=+5%	D=-5%	D=+5% & ω=-2%	D=-5% & ω=+2%
19	.025	.072	.478	-.335	.627	-.506	3.40	3.97	2.83	4.05	2.72	11.19	12.16	10.23	12.07	10.27
	.05	.105	1.69	-1.48	2.28	-2.16	3.44	5.19	1.69	5.71	1.07	11.77	13.94	9.60	14.28	9.14
	.10	.513	6.87	-5.84	9.21	-8.54	3.80	10.32	-2.71	12.60	-5.35	10.39	17.24	3.54	19.37	1.03
- -	- -	- - - - - - - - - - - - - - - -					- - - - - - - - - - - - - - - -					- - - - - - - - - - - - - - - -				
22	.025	-.194	.219	-.607	.381	-.792	3.38	3.97	2.79	4.06	2.67	11.35	12.34	10.36	12.27	10.39
	.05	.933	2.62	-.762	3.22	-1.43	3.48	5.30	1.66	5.85	1.02	10.13	12.28	7.97	12.68	7.46
	.10	.116	6.72	-6.48	9.17	-9.30	3.40	10.16	-1.68	12.54	-6.12	9.98	17.07	3.10	19.31	.253
- -	- -	- - - - - - - - - - - - - - - -					- - - - - - - - - - - - - - - -					- - - - - - - - - - - - - - - -				
24	.025	.082	.515	-.350	.672	-.531	3.42	4.02	2.82	4.11	2.70	10.08	11.01	9.15	10.96	9.16
	.05	.152	1.87	-1.57	2.51	-2.30	3.48	5.37	1.60	5.94	.931	10.14	12.36	7.92	12.79	7.38
	.10	-.033	6.71	-6.77	9.21	-9.66	3.25	10.16	-3.65	12.60	-6.47	9.82	17.06	2.59	19.36	-.105
- -	- -	- - - - - - - - - - - - - - - -					- - - - - - - - - - - - - - - -					- - - - - - - - - - - - - - - -				
26	.025	.359	.809	-.102	.965	-.282	3.69	4.31	3.06	4.39	2.95	10.35	11.30	9.39	11.25	9.40
	.05	.0060	1.76	-1.75	2.41	-2.50	3.34	5.26	1.42	5.84	.733	9.99	12.24	7.74	12.68	7.18
	.10	-.361	6.63	-7.35	9.24	-10.38	2.92	10.07	-4.24	12.62	-7.18	9.49	16.97	2.01	19.38	-.109

Appendix 1

This appendix contains some examples of measurement data corrected in the manner recommended in this paper. The cables measured are as follow. Selected pairs from four reels of 25 and 50 pair 22 gauge filled cable were measured individually for series capacitance (C_s), dissipation (D), dc loop resistance ($R\ell$) and occasional other parameters. Pairs of reel one were then connected in series with pairs of reel two and remeasured. This process was continued until pairs of four reels was connected in series to extend the effective measurement length of the pairs.

The measurement data and corrected results are presented in Tables A and B. Measured capacitance (C_s) of individual pairs was corrected to true capacitance (C) by:

$$C = C_s \times CF$$

where CF is the standard length correction factor. The true conductance (G) of individual pairs was determined by:

$$G = \left[\frac{D}{\omega C} - \frac{R\ell}{3}\right] \omega^2 C^2$$

The sum of these individual corrected values of C and G (referred to as $C\Sigma$ and $G\Sigma$) was used as the reference for comparing the measurements of pairs when reels were connected in series. The error in corrected capacitance is shown as a percent of C. Conductance error is shown as the difference of G and $G\Sigma$ in micromhos (Table B).

As a further check, C was also corrected using dissipation correction factors. There were only slight differences between the dissipation and length correction factors to 0.15 wavelength.

Table A

Capacitance Measurement Data on Individual Pairs of Four Reels of 22 Gauge Cable

Pair	Reel	Length (Feet)	Measured Data C_s (μF)	D	$R\ell$ (Ω)	CF	C (μF)	G ($\mu \upsilon$)
1	1	5,290	0.08268	0.0300	173.3	0.999	0.08260	-0.01
1	2	5,030	0.07556	0.0264	163.6	0.999	0.07548	0.23
1	3	5,076	0.08041	0.0281	163.1	0.999	0.08033	0.32
1	4	5,058	0.08030	0.0272	160.4	0.999	0.08022	0.11
2	1	5,290	0.08190	0.0295	171.0	0.999	0.08182	0.08
2	2	5,030	0.07533	0.0259	161.2	0.999	0.07525	0.23
2	3	5,076	0.08033	0.0279	161.8	0.999	0.08025	0.34
2	4	5,058	0.07826	0.0272	163.5	0.999	0.07818	0.19

Table B

Capacitance Measurement Data on Cable Pairs With Reels Connected in Series

Pair	Reels	Length (Feet)	Wave-length	Measured Data C_s (μF)	D	$R\ell$ (Ω)	CF	C (μF)	$\frac{(C - C\Sigma) \times 100}{C}$ Error (%)	G ($\mu \upsilon$)	G - $G\Sigma$ Error ($\mu \upsilon$)
1	1--2	10,120	0.07	0.1586	0.112	0.112	0.998	0.15828	0.13	0.09	-0.13
1	1--3	15,196	0.10	0.2385	0.252	500.0	1.002	0.23898	0.24	3.33	2.74
1	1--4	20,254	0.13	0.3128	0.438	660.4	1.021	0.31937	0.23	10.91	10.26
2	1--2	10,120	0.07	0.1576	0.110	332.2	0.998	0.15728	0.13	0.34	0.03
2	1--3	15,196	0.10	0.2372	0.249	494.0	1.002	0.23767	0.15	5.35	4.70
2	1--4	20,254	0.13	0.3100	0.427	657.5	1.021	0.31651	0.32	0.15	-0.69

Additional measurements were made where pairs within the same reel were connected in series to extend the measurement length. This technique was discussed by Buscemi and Widmer in 1964.[2] Although it is possible for couplings within a cable core to alter the measurement paramenters slightly, it was not enough to affect the results of measured capacitance up to 0.15 wavelength. Tables C and D show examples of measurement data and error. Table D shows the error in true capacitance (C) when corrected with standard length correction factors. Error in corrected capacitance of head-to-tail measurements are shown in Table D. Note that only 0.4 percent correction is necessary for 22.8 kilofeet of 24 gauge cable when measured head-to-tail; for normal measurements, 12.8 percent is needed.

Table C

Capacitance Measurement Data With Pairs Connected in Series Within a Reel

Pairs	Length (Feet)	Wave-Length	Measured C_s (μF)	CF	C (μF)	CΣ (μF)	$\frac{(C - C) \times 100}{C}$ Error (%)
2	3,800	0.03	0.05812	1.000	0.05812	0.05811	0.02
3	5,700	0.05	0.08915	0.999	0.08906	0.08911	-0.06
4	7,600	0.06	0.1188	1.000	0.11880	0.11871	0.08
5	9,500	0.08	0.1480	1.001	0.14815	0.14815	0
6	11,400	0.09	0.1774	1.004	0.17811	0.17821	-0.06
7	13,300	0.11	0.2046	1.011	0.20685	0.20710	-0.12
8	15,200	0.12	0.2319	1.021	0.23677	0.23679	-0.01
9	17,100	0.14	0.2562	1.037	0.26568	0.26574	-0.02
10	19,000	0.15	0.2783	1.059	0.29472	0.29447	0.08
11	20,900	0.17	0.2977	1.089	0.32420	0.32438	-0.06
12	22,800	0.19	0.3173	1.128	0.35385	0.35381	0.01

Table D

Head-To-Tail Capacitance Measurement Data With Pairs Connected in Series Within a Reel

Pairs	Length (Feet)	Wave-Length	Measured C_s (μF)	CF	C (μF)	CΣ (μF)	$\frac{(C - C) \times 100}{C}$ Error (%)
1	1,900	0.02	0.02884	1.000	0.02884	0.02884	0
2	3,800	0.03	0.05811	1.000	0.05811	0.05811	0
3	5,700	0.05	0.08913	1.000	0.08913	0.08911	0.02
4	7,600	0.06	0.1188	1.000	0.11880	0.11871	0.08
5	9,500	0.08	0.1483	1.000	0.14830	0.14815	0.10
6	11,400	0.09	0.1784	0.999	0.17822	0.17821	0.01
7	13,300	0.11	0.2073	0.999	0.20709	0.20710	0
8	15,200	0.12	0.2368	1.000	0.23680	0.23679	0
9	17,100	0.14	0.2657	1.000	0.26570	0.26574	-0.02
10	19,000	0.15	0.2941	1.001	0.29439	0.29447	-0.03
11	20,900	0.17	0.3236	1.003	0.32457	0.32438	0.06
12	22,800	0.19	0.3523	1.004	0.35371	0.35381	-0.03

Capacitance measurements and corrections were made on the following reels of cable where length was extended by connecting pairs in series. The worst errors up to 0.15 wavelength are shown when measured capacitance was corrected by standard length correction factors and by dissipation correction factors. Except for the 50 pair 26 gauge cable the largest error in corrected capacitance was 0.55 percent for both length and dissipation corrections. The 50 pair 26 gauge showed 1.48 percent when length corrections were applied. This error was reduced to 0.45 percent when dissipation corrections were applied. Loop resistance measurements were not made, but capacitance measurements made with other instruments on this same length of cable indicate that the error is due to a combination of capacitance measurement error and to the loop resistance being greater than 431 ohms per mile. Up to one-tenth wavelength, no corrected measurement exceeded 0.5 percent error.

Table E

Capacitance Measurement Data - Worst Error

Cable Reels Measured	Worst Error (%) Length	Dissipation
Reels in Series 5290 feet, 50 x 22 filled 5030 feet, 50 x 22 filled 5076 feet, 25 x 22 filled 5058 feet, 25 x 22 filled	0.32	0.43
Pairs in Series (In a Reel)		
3028 feet, 100 x 19	0.15	0.15
5290 feet, 50 x 22 filled	0.34	0.44
5034 feet, 12 x 22 filled	0.34	0.44
5038 feet, 25 x 22	0.33	0.23
3014 feet, 20 x 24 filled	0.55	0.55
5038 feet, 12 x 24	0.32	0.32
1900 feet, 12 x 24	0.12	0.17
3012 feet, 25 x 26 filled	0.44	0.20
5028 feet, 50 x 26	1.48	0.45

A COMPUTARIZED TESTING SYSTEM FOR SYMMETRICAL CABLES AND ITS POSSIBILITIES FOR STATISTICAL TESTING.

D.J. Dekker
PTT Administration
of The Netherlands

S. Dijkhuizen, H.L. Gorissen and J.P. Hartwijk
NKF KABEL B.V.
DELFT HOLLAND

SUMMARY

In this paper a recently developed cable testing system for symmetrical cable is discussed.
This system contains two important elements namely connecting tables for connecting up to 60 starquads to the system and a process computer for controlling the system. Both elements are known in present systems, but it is the combination that makes this system very advantageous.
The use of connecting tables is time saving because connecting and testing are performed separately.
Because of the computarization of the system it has a high flexibility and it contains some intelligence.
Judgements about the cable can be made during and after testing.
With this new testing system, we can test on a statistical base, by taking samples of the starquads in a cable and taking cables as samples. This possibility can limit the number of measurements and a discussion is given on the aim of statistical tests and the number of tests to be performed.
Accordingly the cable specification must then be written in a statistical way. An example of such a statistical specification is given.

PRESENT CABLE TESTING SYSTEMS

In former days the testing of symmetrical cables was done by manually operated capacitance, capacitance unbalance and resistance bridges. Every starquad to be tested was connected to the bridges separately and thereafter the measurement was carried out and the measured values were written down on forms.
This needed, in most cases, two persons; one for connecting and one for measuring. Such a system of cable testing is of course very costly because it takes much time and man power.
The first time saving step was made with the development of automatic capacitance, capacitance unbalance and resistance bridges. These bridges can be remote controlled and have the possibility of connecting a printer to it.
These features offer the possibility of testing the cable by only one person who connects the cable to the measuring leads of the test sets. After connecting the starquad, measuring and printing out the results are performed automatically.

A next step was to combine these automatic bridges to a complete testing system, which includes a capacitance bridge, a bridge for measuring capacitance unbalances and a resistance bridge.
An additional control unit offers the possibility of measuring the different properties of the connected starquad sequently. This control unit was hardware programmed.
For different types of cable the programming can be altered by changing connections in this unit. This enables us to use the control unit for a range of cables.
A big advantage of this system is the possibility of measuring all properties within one starquad by connecting it only once. However for measurements between two starquads new connections have to be made.

A further improvement is the use of a connecting table to which at first all elements of the cable to be measured are connected.
This method is easy and time saving because no stripping of the wire insulation has to be done. By means of a relay system two independent starquads can be chosen and connected to the measuring system. For all types of measurements the connections have to be made only once.
Whilst one cable being connected the measuring system can measure another cable which was connected to a table before. Therefore in the same time this system can handle more cables than former systems.
The control unit for the relay system of the connecting table can be combined with the control unit of the measuring system. The programming of the total system is in hardware or with a paper tape which is stepped through during the measuring procedure.
In general the output of this kind of systems is a paper tape. This makes further analysis of the results easier to handle.
This kind of systems still have a number of disadvantages e.g.:

- Because of the hardware programming the system is not very flexible.
- These systems do not have much intelligence because there are hardly any possibilities of controlling the system on faults during operation.
- The judgement about the cable has to be done after the completion of the testing. If there have occured any faults during measuring, sometimes the complete testing has to be done again.
- On line calculations are impossible.

THE COMPUTERIZED TESTING SYSTEM

In order to overcome the problems mentioned before, we replaced the control unit by a process computer.
Figure 1 shows the lay out of the complete system.
The system consists of the following parts:

1. Connecting tables manufactured by Sieverts for connecting up to 60 starquads simultaneously. In this connecting table any two starquads can be connected to the exit of the table by remote control.
   The two starquads chosen are connected to the matrix, which arranges the proper connection to the test sets. The arrangement depends on the type of measurement to be carried out. Both the control unit for the relays and the matrix are directly controlled by the process computer.
2. Resistance test set, developed by NKF.
   The working principle of this set is based on measuring the voltage over the unknown resistance which is connected to a current source.

In order to get a high accuracy the current is 100 mA per Ohm.
The accuracy of the test is better than 0.1 % of the measured value. The measuring range is 1 Ohm to 1000 Ohms. The measuring time is about 0.1 sec.

3. Capacitance unbalance and mutual capacitance test set, developed by NKF.
This instrument does not work with the usual bridge principle but measures directly the current through the unknown impedance. Figure 2 shows the diagram. Both the generator part and the detector part are fully floating and have very small stray capacitances to earth. The latter is obtained by means of guards.
The accuracy is 0.1 % of the measured value.
The range is 0.1 pF to 2 nF in 5 steps.

4. Process computer.
This is a standard type process computer (Hewlett-Packard). It contains a memory of 8K words of 16 bits.
The computer is programmable with every normal language.
Eight I/O channels are available for connection of the instruments and the peripheral devices.

5. A standard teletype for operators control, input of the specific cable data (such as, type, length, cable number) and output of a summary of the test results.

6. Paper tape reader for loading the program and paper tape punch for storing all individual data.

SOFTWARE

System software can be devided in two parts.

- Basic control system which contains all drivers for the devices connected to the I/O interfaces, system tables, I/O handling etc. This part is written in assembler language and mainly delivered by the computer manufacturer.
- User program which comprises all tasks to be performed by the system during operation.
This program is a combination of subroutines which have specific tasks and can be devided in three groups:
  1. control of the measuring instruments and connecting the starquads to be tested to these instruments.
  2. handling the results e.g.
     - calculation of the results to standard length and temperature
     - comparing these values with the requirements of the cable specification
     - calculation of several statistical characteristics such as mean, standard deviation and extreme values.
  3. input of the specific cable data and output of results.

  This users program is written in Fortran, which does not result in the smallest program in core but has the advantage that it can be written faster, which is needed as for testing any new type of cable a new program has to be written.

  Only the routines for chosing the different measurements, for chosing the desired combinations of starquads and for comparison with the specification have to be changed.

Figure 3 shows a typical flow chart of a cable test program.

WORKING PROCEDURE

The computer, the measuring instruments and the input/output devices are not located on the testfloor. Only the connecting tables are situated on this floor close to the cables.

On the testfloor the starquads of the cables that have to be tested are connected to the tables. One of them - about 10 tables belong to one system - can be connected to the test system.
There are two types of programs. One for the measurements of mutual capacitance and capacitance unbalances - in that case one end of the cable must be open - and one for the resistance measurements - in that case the same end must be short circuited.

After initialisation of a program the computer asks for the specific cable data, which must be typed in on the teleprinters keyboard. These specific cable data are tested by the computer.
After acceptance the measuring instruments are tested on proper working by taking measurements of standard capacitances or resistances. If the results do not agree with the values mentioned in the program the system types out a message on the teleprinter and halts. Only after repairing, the program can be continued.

Then actual testing is started. Each value is processed and everytime a value is detected that does not agree with the requirements the system types out a message and halts. Proper connection of the cable can be checked and the program restarted by the operator. The latest measurements are repeated. If the results are accepted they are punched out. Otherwise the message is printed again. Then the operator can decide to repeat or to skip certain measurements.
After completion of all measurements a test report is printed out on the teletype.
A new cable can be connected and the program reinitialised.

ADVANTAGES OF THE SYSTEM

1. Control of the whole system by the computer. Changing software programs is relatively easy, which makes the system very flexible.
2. Cables have to be connected only once.
3. During operation the computer can handle different fault conditions and take actions.
4. Corrections for cable length and temperature are performed automatically.
The results can be compared with the cable requirements.
If they do not agree, the system halts and asks for a check.
The measurements can be repeated before punching occurs.
5. Because a computer is available, on line judgements on a statistical basis are possible.
After testing a cable, mean, standard deviation and extreme values are printed out. Hereafter the system gives a judgement about the cable.
6. The punched output may be used for further analysis by means of other computers.

ECONOMICS OF THE COMPUTARIZED TESTING SYSTEM

The costs of acceptance tests with this system are at present about the same as the costs of former systems. Compared with the former systems less people are needed but the system costs are higher. Because the costs of labour increase more than the cost of electronics we expect that the system will be economically advantageous within a few years time.

ARE ACCEPTANCE TESTS NECESSARY?

The discribed testing system is very advanced, but still costly and therefore one could ask oneself if acceptance tests are really necessary or merely a custom.
In discussing this question we shall limit ourselves to those properties of symmetric cables which have an influence on the transmission performance of the network in which these cables are used.
In the past the quality of the machines in a cable factory and of the applied materials was such, that the electrical properties of all stranded elements could differ much. Therefore all these properties, such as conductor resistance, insulation resistance, mutual capacitance and capacitance unbalance, had to be measured. At that time these measurements were absolutely necessary in order to protect the cable user against inferior or even defective products.
Nowadays cable manufacturing is perfected in such a way that :

1. defects (short circuits, broken wires) hardly occur any more
2. the chance of unacceptable deviations of the quality is relatively small.

Therefore the acceptance tests are no longer strictly necessary.
One could perhaps even drop the acceptance tests and be content with the fact that a cable manufacturer guarantees the quality of his products.
If after applying the cable in a network any defects are observed the manufacturer can be hold responsible for them.
However, the quality of a cable is not a workable criterion for the network where it is used in.
A cable with inferior electrical properties is functioning most of the times and the laying of such cables tends only in the long run to a noticable degradation of the quality of the network.
If it is to be ascertained afterwards whether a particular length of cable meets the manufacturer's guarantee this is only possible if the relevant electrical properties are measured during or after installation of the cable. As a rule these measurements are only carried out in network parts where relatively few cables are used, i.e. in trunk and toll networks (carrier or loaded cables). Figure 4 for instance shows the structure of the Dutch telecommunication cable network.

When installing local cables they are tested on broken wires and insulation resistance only, these tests however do not give any information on the transmission performance of the cable. Therefore acceptance tests are a necessity if we want to prevent the transmission performance of the local or urban networks from degradation.

During and after installing toll cables the relevant electrical properties are measured. The total length of cable pairs, yearly put into service in urban networks, is a multiple of the total length of cable pairs put into service in the toll connections.
Dropping the acceptance tests of the toll cables will therefore give only a relatively small benefit.
On the other hand the cable manufacturer wants to test the cables too in order to monitor his quality and to assure that he meets gis given guarantees.
The benefits of both parties by dropping the acceptance tests but still requiring guarantees, will be negligible. Moreover, when the acceptance tests are dropped and the possible defects are noticed during or after installing the cable, the costs of replacement of such a cable are, specially in the Dutch situation where all cables are directly burried, very high.
The acceptance test thus remains necessary to avoid:

1. a gradual decline of the transmission performance of a cable network
2. high replacement costs.

VOLUME OF ACCEPTANCE TESTS

The necessity of acceptance tests being obvious, we still can discuss the volume of these tests in reference to:

1. the number of properties of the cable which has to be tested
2. the frequency in which each property has to be measured.

In principle every item mentioned in the specification must be checked. It should be borne in mind, however, that every check takes equipment and labour time and therefore costs money. It is true these costs constitute only a small portion of the total cost but this should not tempt us to do more checking than is strictly necessary. Considering the enormous amounts that have to be invested in cables, every percent that can be saved on the total cost is of great importance. So for each type of cable it must be considered what items of the specification require checking.
The item uninterrupted conductors, for example, is in itself of prime importance but it is pointless to check it where cables with thick conductors (diameters over and including 0,8 mm) are concerned.
The same applies to short circuits and insulation resistance and to a certain extend to mutual capacitance when testing plastic insulated cables.
The number of tests carried out on each item to be checked strongly depends on the way in which:

1. the measurements are performed (manually operated or with automatic testing systems)
2. the specification is written.

With manually controlled measurements, the measuring time is long in comparison with the connecting time. However when automatic testing systems as described above are used, testing times are very short and after connecting a cable to the connecting table the number of measurements does not matter any more.
So far it nearly always has been standard practice, when specifying cable requirements, to lay down limits for the items concerning electrical properties. Sometimes two limits per item are given, one for 90 % and one for 100 % of the elements to be checked, but in any case such a specification implies that all the items to be checked must be measured on all elements. So the volume of an acceptance test can only be reduced by decreasing the number of items to be measured.

If one desires to reduce also the number of measurements per item it will be necessary to waive the stipulation that certain limits are not to be exceeded and to formulate requirements in statistical terms. Only then it is possible to reduce furthermore the volume of the acceptance test by taking samples.

REQUIREMENTS FORMULATED IN A STATISTICAL WAY

The electrical properties: capacitance unbalance, mutual capacitance and resistance lend themselves well to statistical circumscription of the relevant requirements since they are in general normally distributed and therefore can be characterized by means of the statistical conceptions mean ($\bar{x}$) and standard deviation (σ)
However fixing $\bar{x}$ and σ for the various electrical properties is rather a problem.
Only the mean of the capacitance unbalance is well defined, since this value must of course be nominally zero.
As an example we give a method to obtain the values of $\bar{x}$ and σ of the capacitance unbalance.
The present requirement for the capacitance unbalance is, that its value must not exceed a certain limit. In practice this upper limit is only seldom exceeded. This implies that this upper limit corresponds with the 4 to 6σ-value, if we suppose a normal distribution of the capacitance unbalances.
If the number of exceedings is 1 on 10^6, the allowed maximum is the same as the 5σ-value (figure 5).
We might conclude from this that the value σ must be 1/5 of the maximum value allowed. However this is not a very exact method for determining the value of σ.

The next method is a better one:

1. Measure the capacitance unbalances with sign of a large number of cables and determine the frequency distribution.
2. Examine wether this frequency distribution is sufficiently normal and after that calculate the standard deviation (σ).
3. Consider the collection of capacitance unbalances mentioned above as the population and the number of the capacitance unbalances per cable as a sample out of this population.
4. The standard deviation of the distribution per sample (s) must have a value of:

$$s = \sigma \pm \frac{2\sigma}{\sqrt{2n}}$$

   In this formulae n is the number of capacitance unbalances per sample.
   This value of s lies, according to the probability theory, within the 95 % confidence limits (fig. 5)
5. The mean ($\bar{x}_s$) of the in point 4 mentioned sample must be:

$$\bar{x}_s = \bar{x} \pm \frac{2\sigma}{\sqrt{n}}$$

   For the capacitance unbalances we can state: $\bar{x} = 0$.

   When we apply this method to the other properties then of course $\bar{x} \neq 0$.

Defining the requirements in this way gives the user a more extended knowledge about the quality of the cables and therefore the following possibilities:

1. A better opportunity to search for new applications of the cables.
2. Comparing the cables of different manufacturers.
3. Monitoring the quality as a function of time.

The advantages for the manufacturer are:

1. Monitoring of production is made easier.
2. By continuous knowing the exact quality level the tolerances in production can be kept within closer ranges.
3. By taking samples it is only necessary to measure a fixed number of the elements of a cable. This makes the use of one type of connecting table possible for all cables used.
4. Less testing time is needed. Consequently testfloor space can be used more efficiently.

CONCLUSION

The computarized measuring system described gives certainly in future a saving of costs because the costs of labour are increasing faster than the costs of electronics. This system gives the opportunity of testing in a statistical way.
Although the manufacturing methods have been improved, acceptance tests are still necessary. By defining the requirements in statistical terms the number of measurements can be decreased.
Getting the results per cable in a statistical way is advantageous for the user as well as the manufacturer.

Daniël J. Dekker was born in Rotterdam in 1923 and joined the PTT-Administration of the Netherlands in 1939.
He has been active in the field of telecommunication cables for about ten years and is now leader of the cable development group.
Mr Dekker is a graduate of the Higher Technical School in Rotterdam and a member of CCITT and IEC.

H.L. Gorissen received his electrical engineering degree in 1971 from Delft Technical University.
He joined NKF in 1960 and worked in the Telecommunication Cable Development.
Since 1971 he is head of the Telecommunication Cable Lab, responsible for the development of telecommunication cables and electronic test and measuring equipment.

S. Dijkhuizen received his electrical engineering degree in 1963 from Delft Technological University.
He joined the NKF Delft and engaged in research and development of telecommunication cables and automatic telephone cable test instruments.
Since 1970 he is chief of the Telecommunication Cable Design Department.

J.P. Hartwijk joined NKF in 1966 and worked in the pilot plant. In 1969 he is transfered to the Telecommunication Cable Laboratory and is working on the development of automatic measuring equipment and test systems for symmetrical telecommunication cables.
He is a graduate of the Higher Technical School in Rotterdam since 1971.

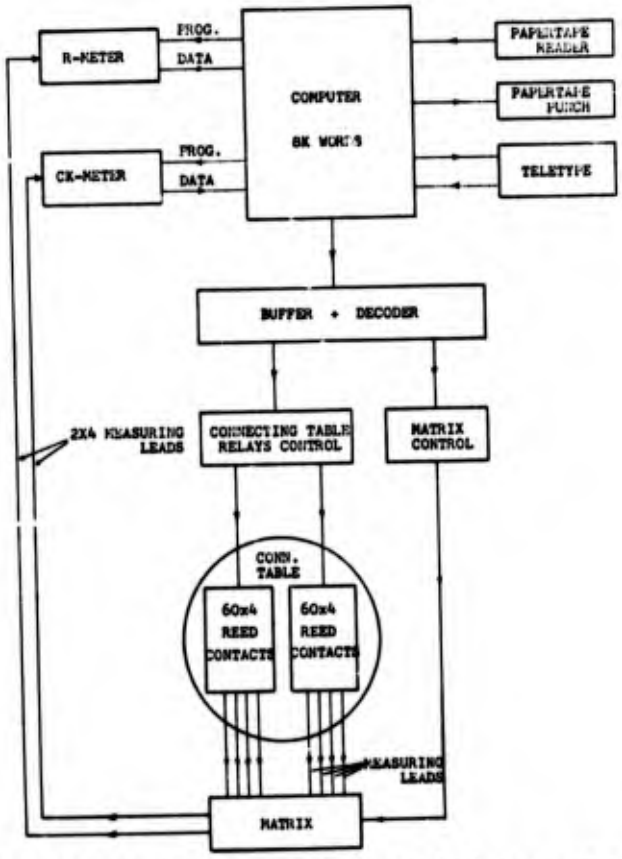

Figure 1 - Block diagram of computarized test system

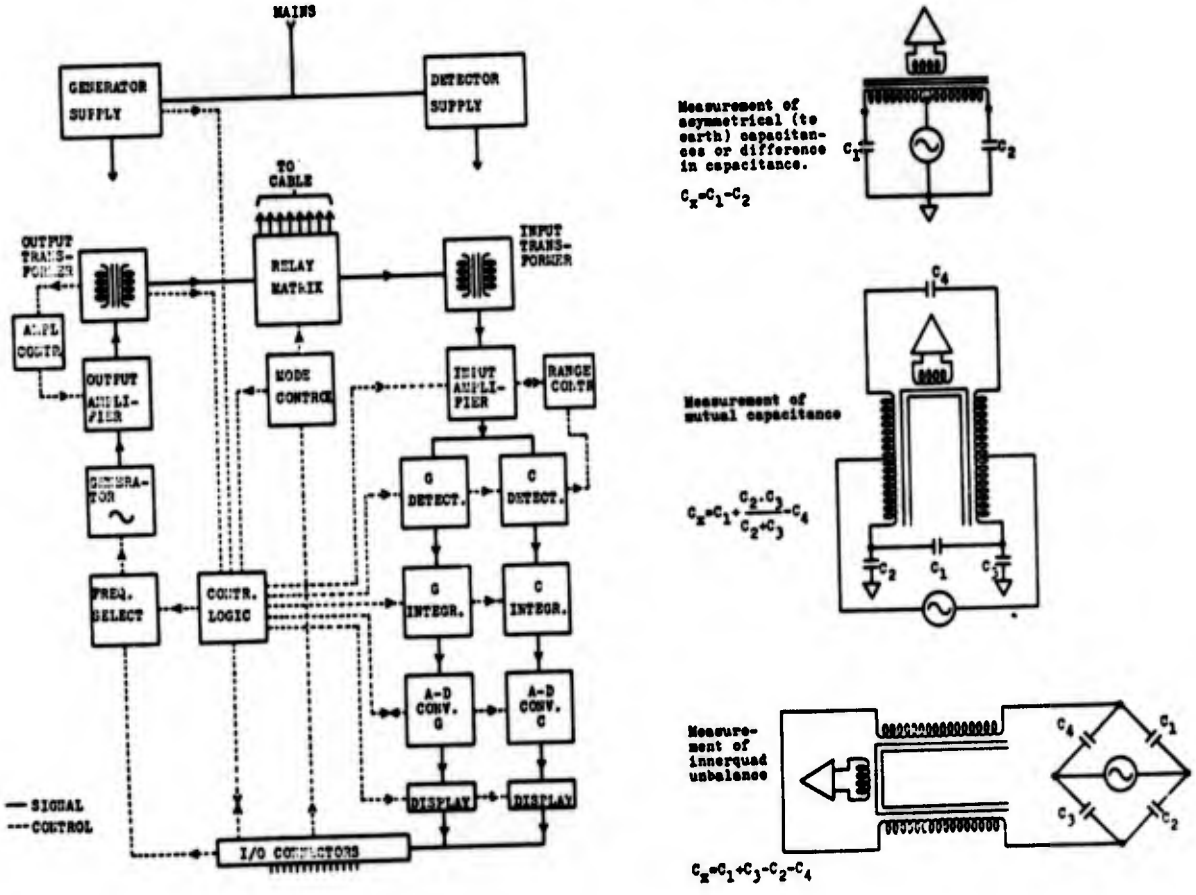

Figure 2 - Block diagram of capacitance test set

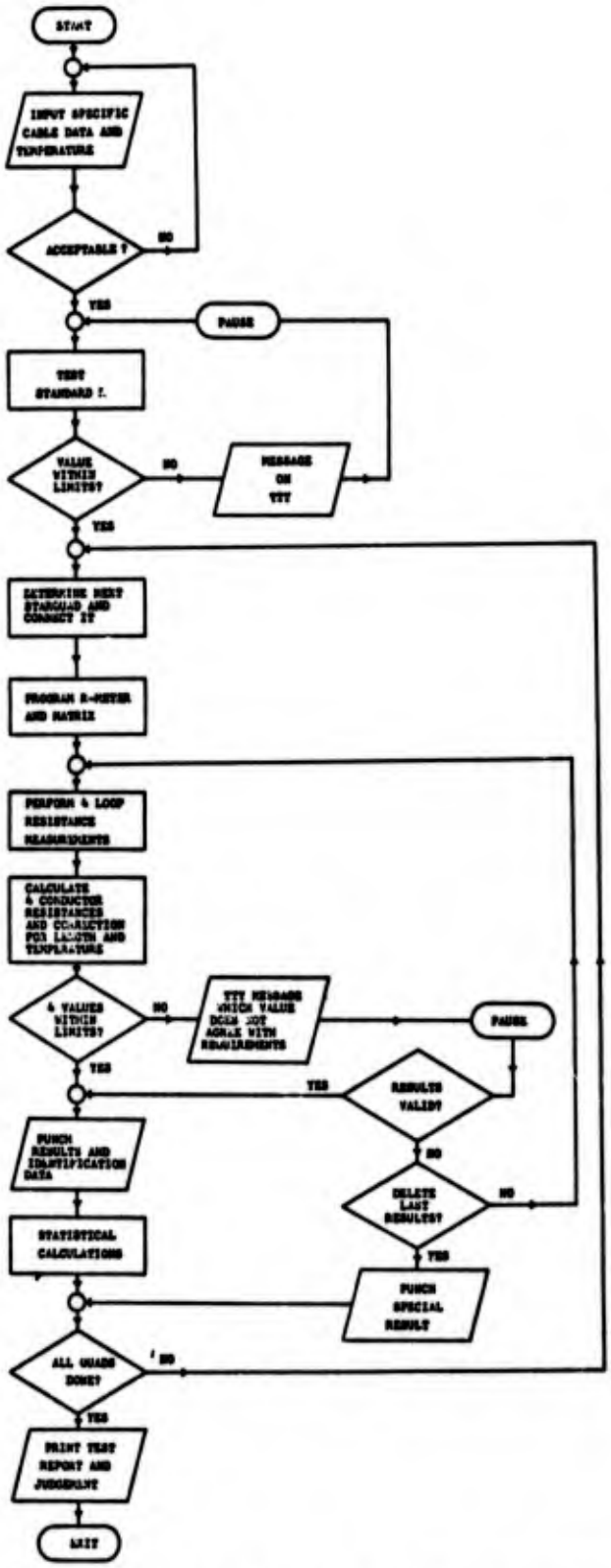

Figure 3 - Typical Flow Chart of a cable test program

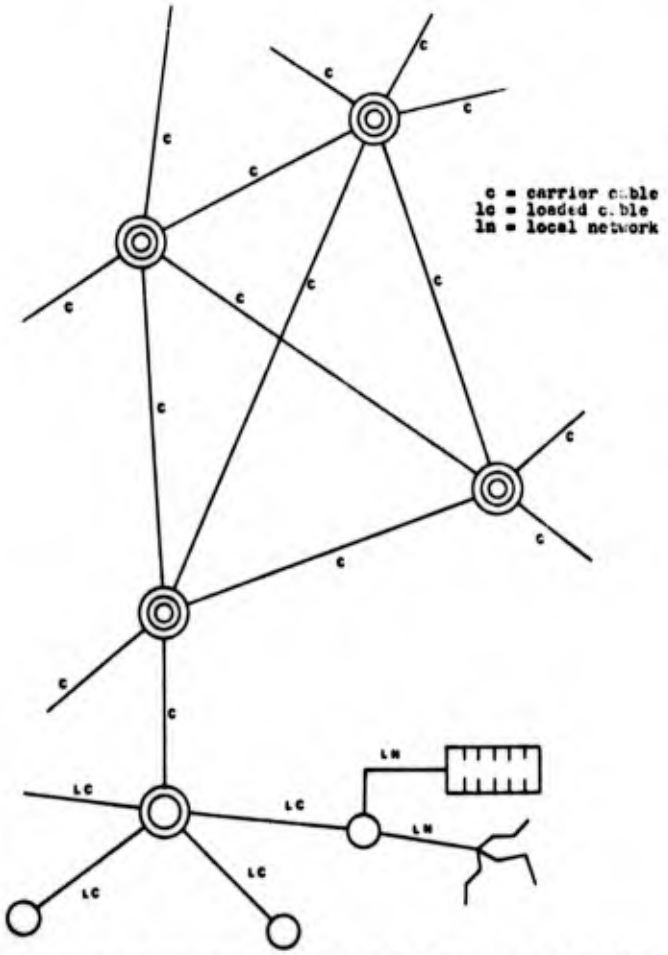

Figure 4 - Structure of the Dutch telephone cable network

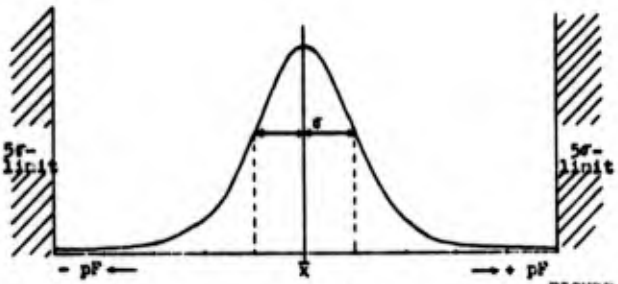

FIGURE 5a

FIGURE 5b

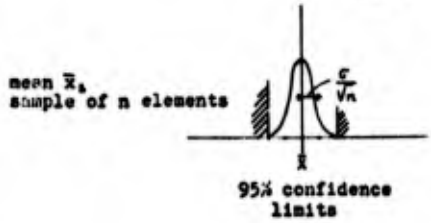

FIGURE 5c

Figure 5 - Relations between population and samples out of this population.

USING A LASER MICROMETER FOR PRECISION CONTROL OF WIRE DIAMETER AND POSITION ON A CV LINE

by
F. M. Taylor
Autometrix Division
Dayton, Ohio

Laser Micrometer - Operating Principles

A laser micrometer performs a function similar to that of vernier calipers. But instead of precision mechanical jaws, a precisely aligned parallel beam of laser light is used. This parallel beam is rapidly scanned over the measurement aperture and any object in the measurement region will interrupt the beam as illustrated in Figure 1. Because the beam is perfectly parallel and because the sweep rate is constant, the time duration of the shadow cast by the object is directly proportional to the dimension casting the shadow. The rising and falling edges of this signal are used to gate a high frequency oscillator whose digital pulses are counted, converted to BCD (Binary-Coded Decimal) and displayed on the front of the readout head. Any of the segments of the shadow can be measured by this method. Thus, the position of object can be measured as well as its diameter. Figure 2 illustrates the block diagram of the instrument. A precise and stable drive frequency for the scanner motor is obtained by subdividing the pulses from the oscillator and shaping them into a sine wave. This technique "locks" the scan velocity and phase of the motor to the bit count rate used to determine distance. This technique provides excellent repeatability.

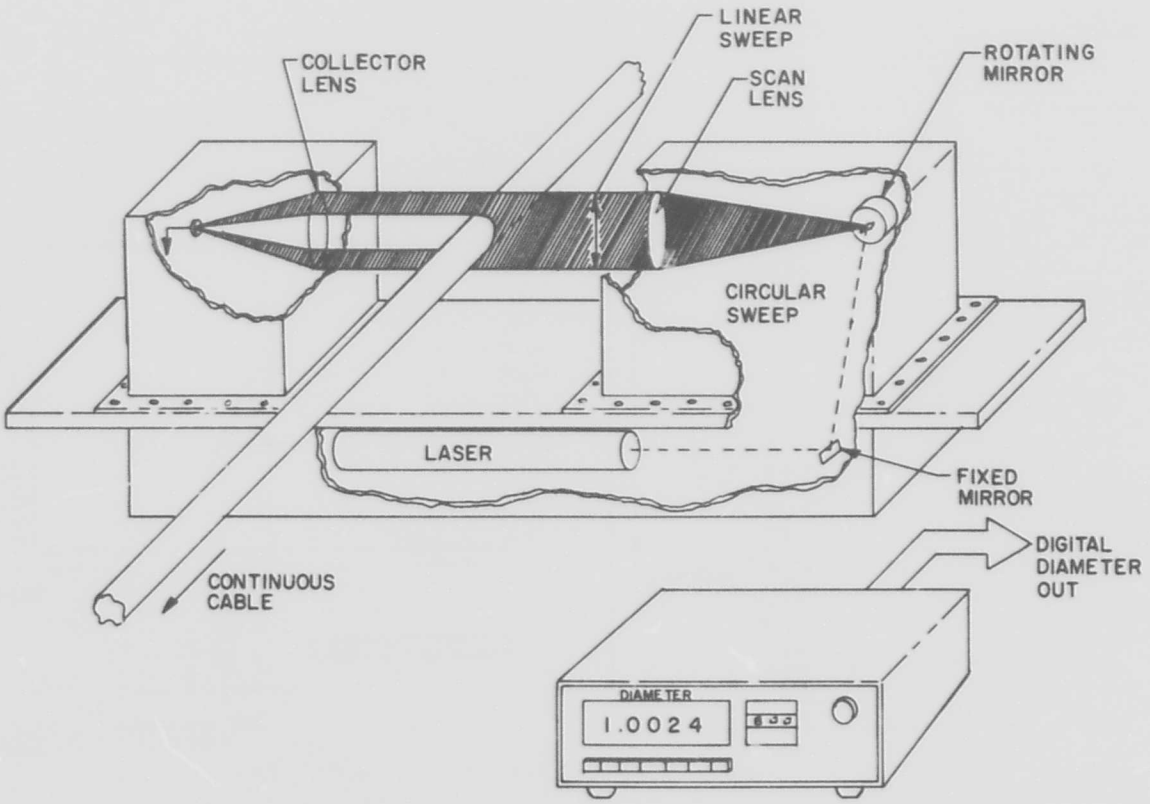

Figure 1. Laser Micrometer System.

Other Applications

The laser micrometer can be adapted to measure both average diameter and/or ovality of wire or cable. Figure 4 illustrates the scan mechanism for a two diameter scan system. The two diameter measurements are then averaged in the readout head. For ovality, a 3-scan unit is used to obtain 3 diameter inputs (D_1, D_2, D_3) which are used to solve the following set of equations for A_0, B_0 and C_0

$$A_0 D_3^2 - 1 = 0$$

$$\frac{1}{4} A_0 D_1^2 + \frac{\sqrt{3}}{4} B_0 D_1^2 + \frac{3}{4} C_0 D_1^2 - 1 = 0$$

$$\frac{1}{4} A_0 D_2^2 - \frac{\sqrt{3}}{4} B_0 D_2^2 + \frac{3}{4} C_0 D_2^2 - 1 = 0$$

A_0, B_0 and C_0 are then substituted in the general equation for an ellipse of arbitrary rotational orientation.

$$A_0 X^2 + B_0 X Y + C_0 Y^2 - 1 = 0$$

The equation is then reduced to normal form

$$\frac{X'^2}{a^2} + \frac{Y'^2}{b^2} = 1$$

where b-a = (Max. Diam.) - (Min. Diam.)

The process does assume that the out-of-roundness is oval-shaped (an elipse); an assumption which is normally justified. The calculations are performed on-line by a micro-computer interfaced directly to the laser micrometer readout.

For applications involving multiple lines which run only one product and do not need sophisticated active control loops, the laser micrometer can be used with a large number of laser heads feeding one central readout which automatically monitors each line, as illustrated in Figure 5. In automatic sequence, the diameter of the wire is measured on each line in turn, compared to Hi and Low limits previously set by the operator for that line and a local and remote alarm occurs if either condition is exceeded. The system is expandable in modular form and offers a significant cost savings over having individual systems for each line.

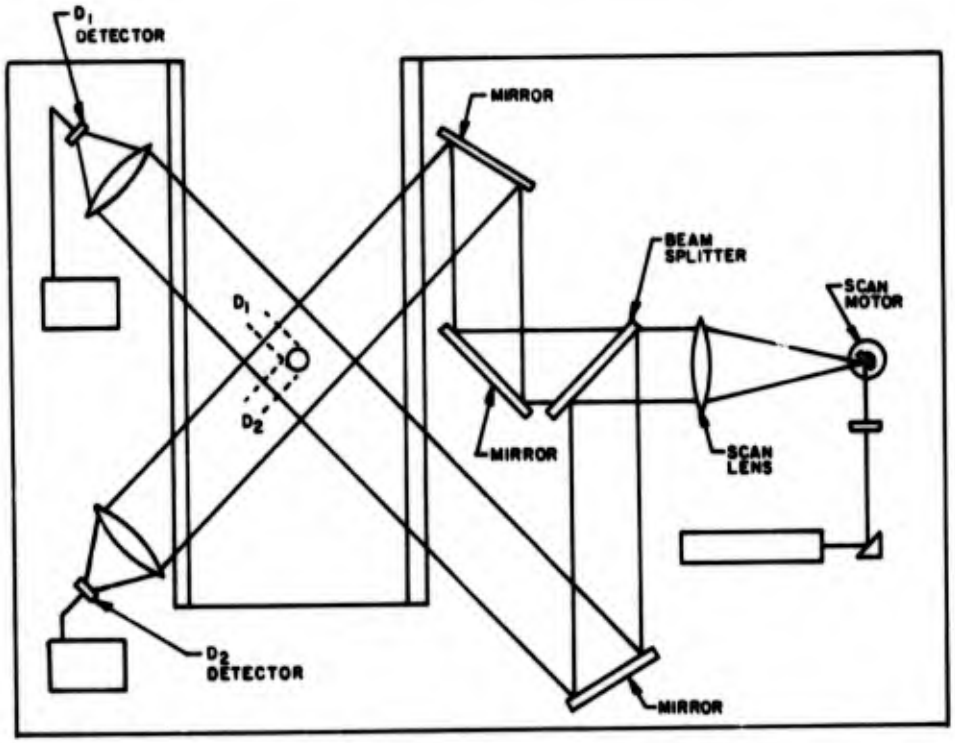

Figure 4. Double-beam laser micrometer.

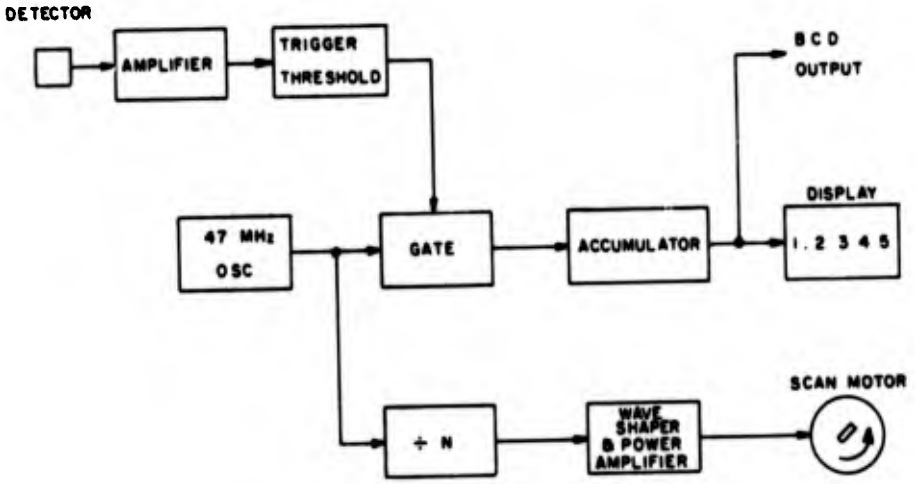

Figure 2. Laser micrometer block diagram.

On a CV Line

Figure 3 illustrates the use of a laser micrometer to control both the position and diameter of a catenary CV line. A 4" sight glass in the chamber allows the laser beam to enter the chamber and perform the measurements without disrupting the vulcanizing seal. Two digital controllers, one for position and one for diameter then processes the information from the laser micrometer and provides independent control outputs. The controllers are digital proportioning with reset and line speed correction. Control point is set digitally either locally or remote. Diameter is controlled within ±.001 inches and position is controlled within ±.010 inches.

All inputs and outputs of the control loop are digital, providing excellent repeatability and stability. The digital characteristic also allows direct interface with a computer for control and/or monitoring. The remotely programmable set points in the controllers permit direct computer control of the start-up process, which, in terms of time and material, is the most wasteful part of the process.

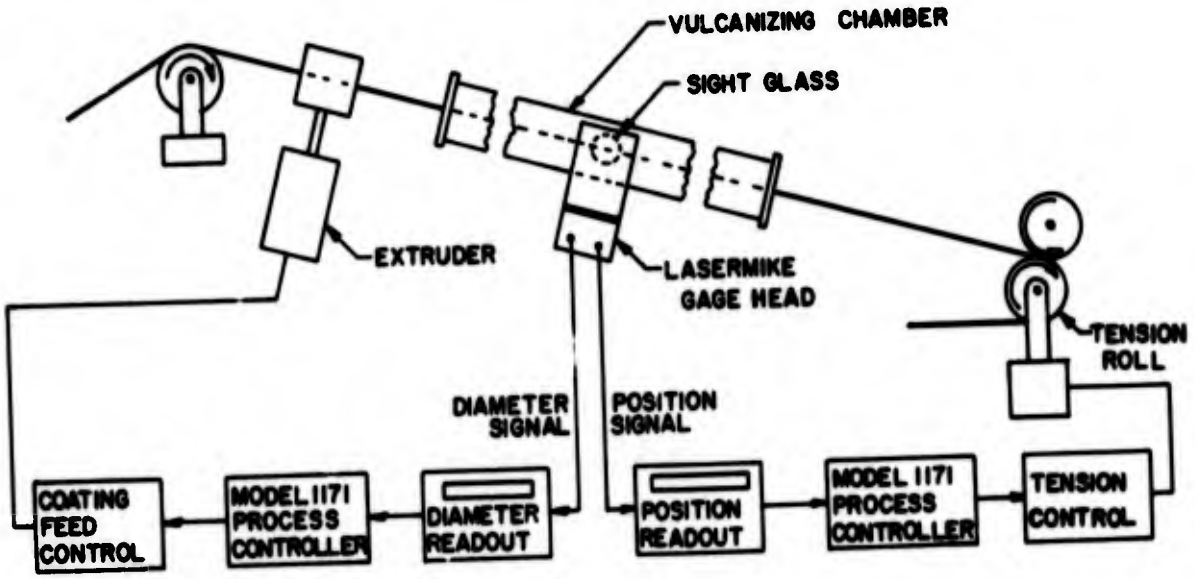

Figure 3. Control of diameter and position on a CV line.

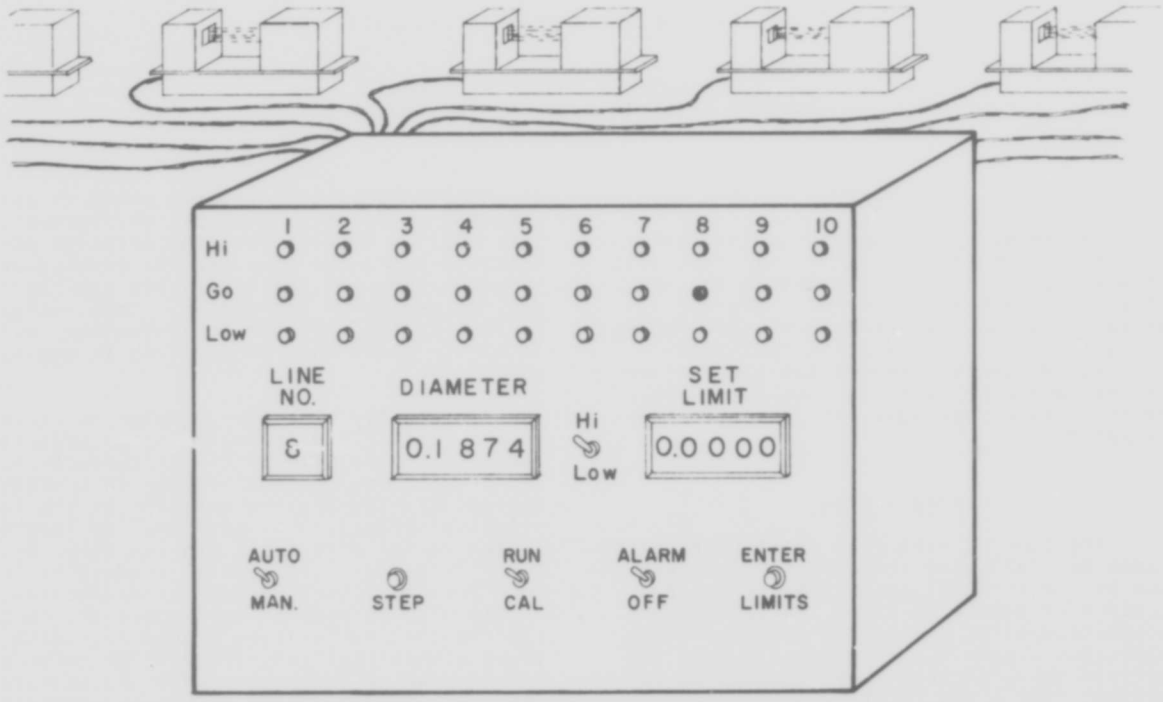

Figure 5. Multi-line diameter monitoring system.

Instrumenting for the Future

In this day of shortages and ever-increasing costs, every effort must be made to run an efficient, lean operation. Shipping excess product out the door in the way of oversize wire and cable doesn't really buy you any friends. Of course, it's preferable to running undersize and making enemies. But the point is that you should avoid both these extremes. Manufacture a product which does meet minimum specs, but without a layer of fat to be "safe". To do this will often mean that the sensors, controls, and/or monitoring systems on wire lines must be upgraded to modern standards. Many, if not most, continuous manufacturing processes in the United States are already totally automated, operating under computer control. This is true in the paper industry, sheet plastic, refineries, etc. The wire and cable industry is behind the times in this respect. In the past, we've been able to afford the wastage. Not so today. The instruments described in this paper were specifically designed for integration into a fully computerized line. It is time to start moving in that direction.

F. M. Taylor

Biographical Sketch

Mr. Taylor graduated from Ohio State University with a B. S. in 1963, receiving his M. S. in Physics from Ohio State University in 1966. He has had extensive experience in lasers, electro-optics and their application to the problems of industrial control processes. His most recent efforts have been directed towards combining modern electro-optic sensors with computer-compatible instrumentation for closed-loop control of continuous industrial processes. Mr. Taylor is presently Technical Director of Autometrix, Dayton, Ohio.

THE COOLING PROCESS IN PLASTIC INSULATED WIRE

J. C. Calhoun and W. M. Flegal
Western Electric Company, Incorporated
Norcross, Georgia

Summary

Two methods of determining the temperature distribution in plastic insulated wire at any instant immediately following the extrusion process are reported. The first method predicts the temperature distribution for a given set of operating conditions. The second method measures the temperature of the conductor as it is insulated. Results of each technique are presented and compared.

Introduction

The cooling rate of a plastic insulated conductor following the extrusion process is one of the controlling factors in the production of insulated wire. In an existing production line, the length of the cooling apparatus determines to a great extent the maximum speed at which the line may be operated. For a new facility, the optimum design of the cooling apparatus is dependent on a knowledge of the cooling rate for the type of insulated wire to be produced and the insulating materials to be used.

In the past, trial-and-error techniques have been used in the design of various cooling devices and the methods for evaluating their performance were more qualitative than quantitative. In other words, if the quality of the final product was good, or if the bulk temperature of the finished reel was low, then the device was a "good" one. Theoretical methods[1, 2] for predicting the insulation temperature at any time after the extrusion process have been developed, but these methods required approximations of the convective heat transfer coefficient in the gas and liquid coolant environments.

The purpose of this paper is to present a new analytical model which is applicable to a wide range of cooling conditions for solid, foam, and multi-layer insulations. The validity of the model has been verified by an experimental method of measuring the temperature of the conductor during the insulating process. The experimental results are compared to analytically predicted values for several insulation materials, line speeds and insulation thicknesses.

Theoretical Analysis

Consider a small segment of bare wire that has just entered an extruder die. At the instant that the hot plastic contacts the conductor, the conductor temperature is approximately constant across its cross section and the plastic is similarly at a uniform melt temperature. The cooling process which follows lowers the temperature of the insulated wire segment until it approaches equilibrium with the environment. This cooling results from the exchange of energy between the wire and the insulation by conduction and the insulation and the cooling medium by convection. Some energy is lost by the wire through radiation, but it can be shown that this effect is negligible.

Internally, the energy which is stored in the plastic and the metal is transferred radially and longitudinally by conduction. The longitudinal conduction may be neglected because the temperature gradient in the longitudinal direction is much smaller than that in the radial direction, and the cross sectional area for longitudinal conduction is much less than that for radial conduction. It may also be assumed that there are no circumferential temperature gradients. With the above simplifications, the problem reduces to solving the radial heat conduction equation for a cylinder composed of two or more different materials. If the temperature dependence of thermal conductivity and density are considered, the heat conduction equation may be written

$$\frac{\partial}{\partial r}\left(k\,\frac{\partial T}{\partial r}\right)+\frac{k}{r}\,\frac{\partial T}{\partial r}=\frac{\partial(\rho u)}{\partial t} \qquad (1)$$

where k is the thermal conductivity, ρ is the density and u is the specific internal energy. For the plastic, Equation (1) must be solved subject to the following boundary conditions:

1. The initial temperature of the plastic is uniform and at a known value.
2. The energy lost to the environment by convection from the outer surface is equal to the energy conducted to the surface from within.
3. The temperature of the plastic and the wire are equal at the interface.

To find the temperature distribution in the conductor, either of two approaches may be used. The first approach requires the solution of Equation (1) subject to appropriate boundary conditions. In the second approach, the conductor is considered as a body at a uniform temperature. A heat balance is then made on the conductor with the additional assumption of constant physical properties. For this method to be applicable, there must be a very small temperature variation between the conductor-insulation interface and the center of the wire. This temperature variation will be small if the thermal resistance of the wire is much smaller than the thermal resistance of the insulation. The thermal resistance is given by $R = \Delta x/k$. The thermal conductivity of most

plastics is approximately 2000 times smaller than that of metal conductors. Therefore, this simplification is incorporated into the solution.

In the cooling of plastic insulation, the heat of fusion released as the plastic changes from the molten to the solid state must be considered. In most heat transfer problems where a change of phase is involved, it is necessary to consider that the heat of fusion is released at a solid-liquid interface which moves through the material. The moving interface enters the solution as a boundary condition coupling the equations for the liquid and solid regions. If the actual functional relationship between the specific heat and temperature is used, however, the heat of fusion is taken into account without introducing a moving solid-liquid interface. Equation (1) now becomes

$$\frac{\partial}{\partial r}\left(k\,\frac{\partial T}{\partial r}\right)+\frac{k}{r}\,\frac{\partial T}{\partial r}=\frac{\partial}{\partial t}\left(\rho CT\right) \qquad (2)$$

where C is the specific heat of the material. In the following discussion, the heat conduction equation as given by Equation (2) will be used.

Solution of Differential Equation

At this point, it is necessary to decide what type of solution to seek. An exact solution to Equation (2) can be found if the surface temperature is assumed equal to the cooling medium temperature (infinite convective heat transfer coefficient) and the properties are considered constant. Guenther and Biggs[1] obtained such a closed form solution under the above conditions. While mathematically sound, this approach has limitations. The assumption that the surface temperature is instantaneously that of the cooling medium is approximate for a liquid cooling medium. However, for the passage of the wire through an air gap, this assumption cannot be justified. In addition, special constructions like dual insulation would complicate the solution immensely. In order to solve a greater variety of problems, a finite heat transfer coefficient must be used at the outer surface. It is also desirable to consider temperature-dependent properties. To find a closed-form solution under these conditions would be extremely difficult, if not impossible, and a different approach is necessary.

The method of finite differences is a flexible approach which can be used in this situation. In this method, a network of nodal points is superimposed on the region under study. Given the temperature at all nodes at one instant of time, the temperature at a time Δt later can be calculated from an energy balance on each node. If the thermal conductivity is taken to be linear with temperature ($k = k_0 + aT$), then such an energy balance yields

$$T'_s = T_s + \frac{k_0\,\Delta t}{\rho_s C_s(\Delta r)^2}\left[T_{s+1}\left(1+\frac{\Delta r}{2r}\right)-2T_s+T_{s-1}\left(1-\frac{\Delta r}{2r}\right)\right]$$

$$+\frac{a\,\Delta t}{2\,\rho_s C_s(\Delta r)^2}\left[\left(1+\frac{\Delta r}{2r}\right)T^2_{s+1}+\left(1-\frac{\Delta r}{2r}\right)T^2_{s-1}-2T^2_s\right] \qquad (3)$$

where T'_s is the temperature at nodal point s at time $t + \Delta t$, Δr is the radial distance between nodal points, and ρ_s and C_s are the density and specific heat of node s at temperature T_s. The temperature at time $t + \Delta t$ depends on the temperature at nodes s, s - 1 and s + 1 at time t and on the thermal properties of the material at node s.

Equation (3) is valid at all points except those located on the boundaries. Special consideration must be given to these points. The appropriate boundary condition must be incorporated into the equation for the temperature at a boundary node. At the surface of the insulating material, the energy lost to the cooling medium by convection must equal the energy conducted to the surface from within. Incorporating this boundary condition into the finite difference equation for the temperature at the surface node n yields

$$T'_n = T_n\left[1-\frac{4k_0\,\Delta t}{\rho_n C_n(\Delta r)^2}+\frac{2k_0\,\Delta t}{DOD\,\Delta r\,\rho_n C_n}-\frac{4h\,\Delta t}{\rho_n C_n\,\Delta r}\right]$$

$$+T_{n-1}\left(\frac{4k_0\,\Delta t}{\rho_n C_n(\Delta r)^2}\right)\left(1-\frac{\Delta r}{2DOD}\right)+\frac{4h\,\Delta t}{\rho_n C_n\,\Delta r}\,T_e$$

$$+\frac{2a\,\Delta t}{\rho_n C_n(\Delta r)^2}\left(T^2_{n-1}-T^2_n\right)\left(1-\frac{\Delta r}{2DOD}\right) \qquad (4)$$

where h is the convective heat transfer coefficient and DOD is the outer diameter (diameter over dielectric). As before, the "new" temperature depends on the "old" temperature at adjacent nodes and on the material's thermal properties. In addition, the outer surface temperature T_n is also a function of the convective heat transfer coefficient h and of the environment temperature T_e. The convective heat transfer coefficient can be approximated using turbulent flow over a flat plate theory[3] or extrapolated using data obtained by Mueller[4] for flow parallel to a very fine wire. In either case, the heat transfer coefficient is on the order of 10 to 50 BTU/min-ft^2 ^{0}F for water and 0.1 BTU/min-ft^2 ^{0}F for air.

The temperature of the nodal point located at the interface of two dissimilar materials (the surface of the conductor, for

example) is found from an energy balance which reflects the different thermal properties of the two materials. By application of the appropriate boundary condition, the temperature at the interface node at time $t + \Delta t$ can be expressed in terms of the temperatures at adjacent nodes at time t and the thermal properties of the interface node.

By calculating all temperatures at time $t + \Delta t$ and using these values as the initial temperatures in the equations, the temperature at any later time is found. To maintain accuracy and stability of the solution, the size of the time step is limited to very small values which makes it necessary to perform many calculations in order to study the temperature distribution during the desired time interval of several seconds. These calculations are handled easily by a high-speed digital computer. Equations for the temperatures at the various nodal points have been programmed in Fortran IV, and the resulting program has been run extensively on a Xerox Sigma 9 computer system. This program permits the analytical study of the effect on the cooling process of such variables as wire gauge; insulated diameter (DOD); insulation material and construction; line speed; heat transfer coefficient; and melt, conductor preheat, and cooling medium temperatures.

Figure 1 demonstrates that the results from this analysis agree with those obtained from the closed form solution of reference 1 for a very large heat transfer coefficient and constant physical properties. It also demonstrates the effect that a realistic heat transfer coefficient has on the cooling rate.

Experimental Procedure

The work presented so far has been totally theoretical. Like all theoretical work, the level of confidence given to this analysis can be increased greatly if the results are verified experimentally. The problem then became the discovery of a method to measure the magnitude of the important variables.

The curves of Figure 1 show that after a period of time the conductor temperature has the highest value in the radial direction. Since the length of time necessary for the insulated wire to reach a given temperature is of considerable interest, a measurement of the conductor temperature would be an excellent method to determine the magnitude of this time interval.

One of the most common temperature measurement devices is the thermocouple. To use a thermocouple to measure the conductor temperature after the insulating process requires that a method be devised to hold the junction in thermal communication with the conductor. Another approach would be to use the thermocouple itself as the conductor whose temperature it is desired to measure. The major advantage in this approach is that the temperature of the junction is identically that of the conductor, and the response of the junction to temperature changes is instantaneous. If a high impedance potentiometric device is used to measure the small voltage generated, then the length of the wire is not significant since the current which will flow in the thermocouple circuit is extremely small, and the resultant voltage drop in the leads is negligible. This is important because long lengths of wire (10,000 to 20,000 feet) are necessary to use this method in conjunction with an insulating line.

A copper/constantan thermocouple (Type T) was used because copper was the desired conductor metal and constantan was the most suitable thermoelement material. Lengths of constantan and copper approximately 300 feet long were butt-welded together in an alternating pattern to produce a series of thermocouples in the same circuit. The thermocouples were wound onto a reel, and a long copper lead (approximately 10,000 to 20,000 feet) was welded to the outermost piece of constantan. The length of this lead was determined by the speed at which the line was run and the time required for it to reach equilibrium after start-up. The lead wire was passed through all the machines in the insulating line and connected to one terminal of a millivolt recorder as shown in Figure 2. A mercury slip ring was used to make rolling contact with the bare wire, and was connected to the other terminal of the recorder.

The line was started and brought up to speed with the desired insulation diameter. As hot plastic covered each thermocouple junction in the circuit, an emf was generated and recorded. The polarity of each response alternated as each successive junction passed over the slip ring. The slip ring sheave was made of copper and acted as the reference junction while the constantan was in contact with it, and the previous junction acted as the reference junction when the copper was in contact with the sheave. Only one segment of constantan was required to obtain two response curves.[5] However, three segments of constantan were used in each experiment to obtain six response curves. If any erroneous signals were recorded, the other curves were still usable. The repeatability of the measurements could also be verified.

The melt temperature was measured with a hand held thermocouple probe after the thermocouple cooling rate experiment had been run. A special valve was installed in the extruder head. The extruder was started and brought up to the same screw speed, head pressure, and output as during the original experiment. The thermocouple probe was immersed in the plastic flowing from the die and the measured temperature was used as the melt temperature.

Any type cooling apparatus can be used. The temperature of the cooling medium and the distance over which it was in contact with the insulated wire were measured and recorded. This information used in conjunction with the computer program permits the

cooling rate to be predicted for the entire cooling length.

Discussion of Results

Experiments were conducted using low and high density polyethylene (LDPE and HDPE), polypropylene (PP), polyvinyl chloride (PVC), expanded high density polyethylene (EXHD), and expanded polypropylene (EXPP) as the insulating material. Insulation constructions which have been evaluated are solid, foam, and dual (solid skin over expanded core).

Experimental and analytical cooling curves of the various insulating materials are shown in Figures 3 through 8 and the applicable extrusion conditions are given in Table 1. These curves show good agreement between the analytical and experimental results. The accuracy of the analytical results is greatly dependent on the physical property data of the insulating material. An attempt has been made to obtain the best property data available for incorporation into the computer program.

The thermal conductivity is especially significant in determining the shape of the cooling curve for a given material. Since the thermal conductivity of insulating plastics is low, it follows that any increase in the DOD would increase the required residence time in the coolant to reach a given temperature. This effect is clearly exhibited in Figure 9 which shows the experimental cooling curves for HDPE with DOD's of .043, .049 and .055 inches. Extrusion conditions for these curves are given in Table I.

Experiments were conducted at various line speeds from 1000 to 5000 feet per minute. The agreement between the experimental and analytical results exhibited no appreciable dependence on the line speed. The thermal conductivity of the plastic is the most significant parameter in the heat transfer process and tends to obscure the effects of changes in other variables.

Although developed primarily to predict the cooling rate of plastic insulated wire for telecommunication applications, the model is correspondingly applicable for larger size wires and thicker insulations. On several occasions it has been used to predict cooling rates of thick walled insulations on large wires. In Figure 10, the predicted cooling rate of a coaxial ocean cable core is compared with some experimental results obtained at Western Electric's Baltimore Works. The agreement between the experimental and analytical values is seen to be excellent.

Conclusions

For the first time, the cooling rate of dual insulation can be predicted accurately. The cooling rates of solid and foam insulations can now be predicted using a model which has been verified experimentally by the unique method of measuring the conductor temperature which was developed. Used separately or together, the analytical and experimental methods are valuable tools for the insulating engineer. Applying the results of the techniques presented here, the design of the optimum cooling apparatus for any wire insulating application becomes feasible.

Acknowledgments

The authors wish to thank Messrs. H. T. Folger, Jr., J. C. Clark and E. C. Akins for their assistance in conducting the many experiments involved in this work. The preparation of the illustrations in this paper by Mr. G. F. Bramlett is appreciated. The technical advice of Mr. C. B. Heard is gratefully acknowledged.

Bibliography

1. Biggs, R. D. and Guenther, R. P., "The Cooling Rate of Polyethylene Insulated Wire During the Extrusion Process", Eleventh Annual Wire and Cable Symposium, 1962.

2. Boysen, R. L., "An Analysis of Cooling Problems in Communications Cable Insulation", Proceedings of the 19th International Wire and Cable Symposium, pp. 294-301, 1970.

3. Kreith, F., Principles of Heat Transfer, International Textbook Company, Scranton, Pennsylvania, pp. 312-315, 1964.

4. Mueller, A. C., "Heat Transfer from Wires to Air in Parallel Flow", AICHE Transactions, Volume 38, pp. 613-627, 1942.

5. U. S. Patent No. 3,737,982, "Method of and Apparatus for Measuring the Temperature of a Moveable Elongated Conductor", J. C. Calhoun and W. M. Flegal, June 12, 1973.

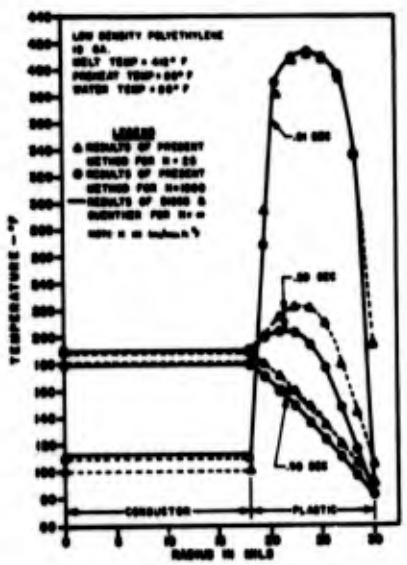

FIGURE 1
COMPARISON OF RESULTS
FOR TWO ANALYTICAL METHODS

FIGURE 2: EXPERIMENTAL APPARATUS

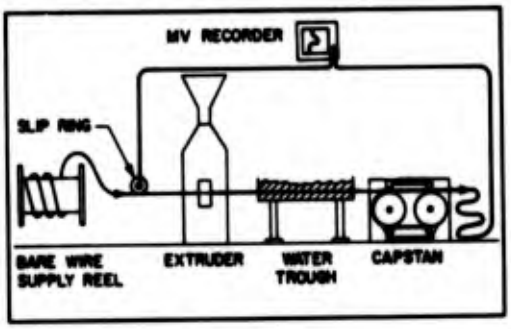

FIGURE 5: COOLING RATE OF CONDUCTOR INSULATED WITH PP

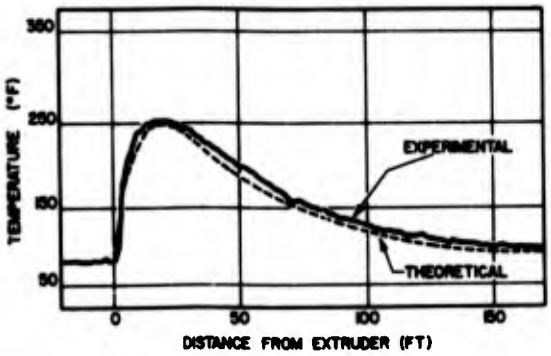

FIGURE 3: COOLING RATE OF CONDUCTOR INSULATED WITH LDPE

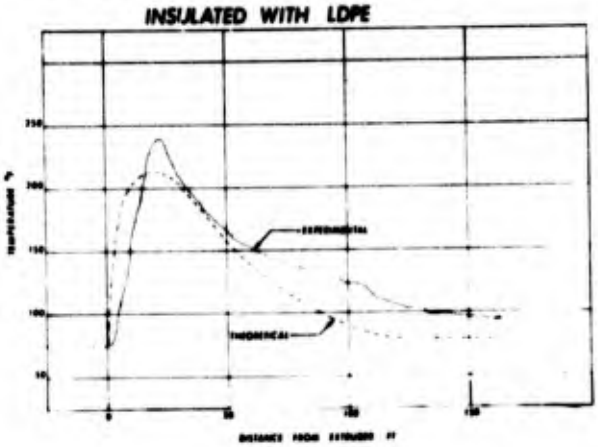

FIGURE 6: COOLING RATE OF CONDUCTOR INSULATED WITH PVC

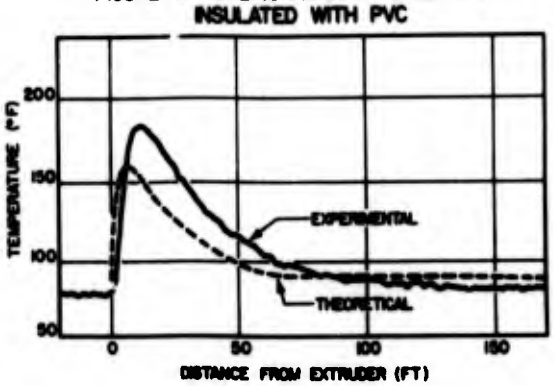

FIGURE 4: COOLING RATE OF CONDUCTOR INSULATED WITH HDPE

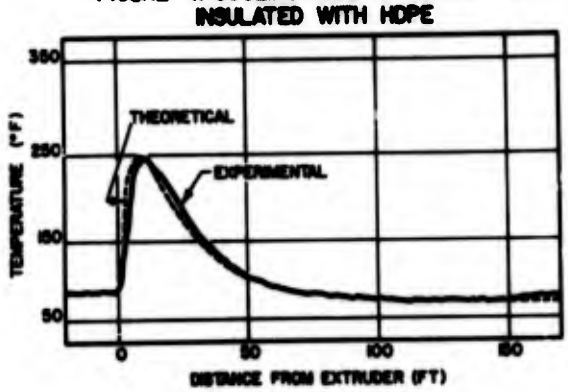

FIGURE 7: COOLING RATE OF CONDUCTOR INSULATED WITH EXPANDED POLYPROPYLENE

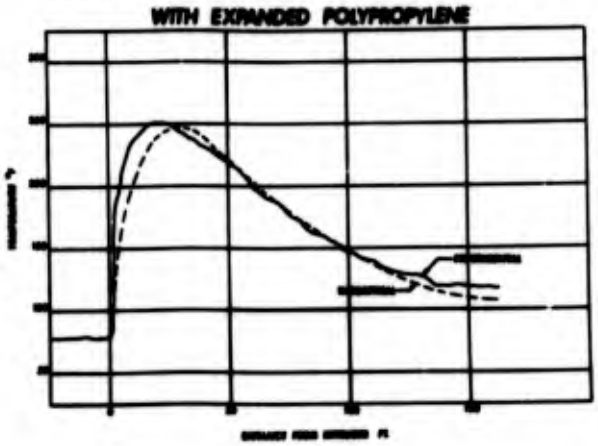

FIGURE 8: COOLING RATE OF CONDUCTOR INSULATED WITH DUAL EXPANDED INSULATION

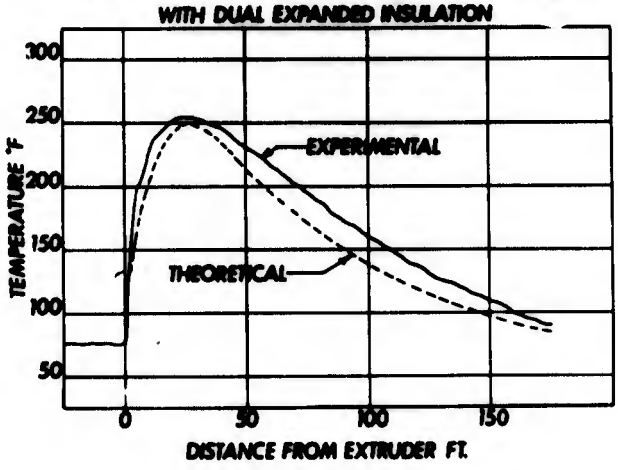

FIGURE 9: EFFECT OF DOD ON COOLING RATE OF CONDUCTOR INSULATED WITH HDPE

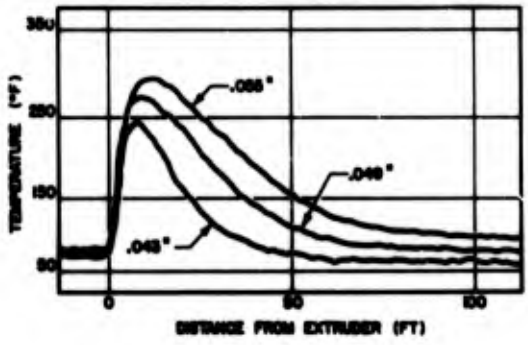

TABLE I

EXTRUSION CONDITIONS

Figure No.	Compound	Wire Gauge	DOD (in.)	Line Speed (FPM)	Bare Wire Temp. (°F)	Melt Temp. (°F)	Air Gap (in.)	Dist. In Water (ft.)
3	LDPE	22	.043	5000	76	472	18	104
4	HDPE	22	.043	3000	82	515	18	120
5	PP	22	.052	3000	80	452	18	120
6	PVC	22	.043	3000	78	370	18	50
7	EXPP (52%)	22	.079	1000	77	404	18	104
8	HDPE (Skin) EXPP (50%) (Core)	22	.0825	1313	72	540 (HDPE) 437 (EXPP)	6	170
9	HDPE	22	.043	2000	82	500	18	120
9	HDPE	22	.049	2000	73	525	18	50
9	HDPE	22	.055	2000	83	540	18	50
10	LDPE	5/16"	1.00	33	100	465	18	510

FIGURE 10: COOLING RATE OF OCEAN CABLE CORE

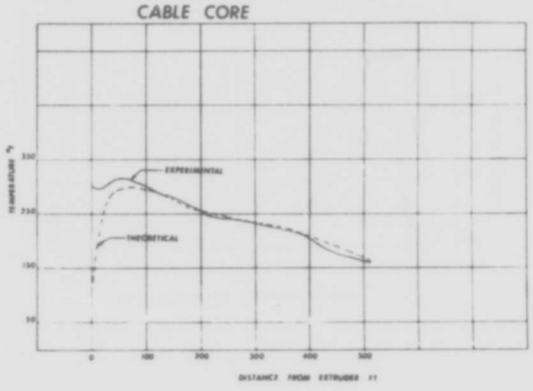

John C. Calhoun

John C. Calhoun received a Bachelor of Science degree in Mechanical Engineering from the University of Texas, Arlington, Texas in January, 1968. After serving two years in the Army, he joined the Western Electric Atlanta Works in July, 1970. He worked as a Development Engineer in the Product Engineering Control Center for three years and has worked in Product Engineering for the last year.

William M. Flegal

William M. Flegal received the Bachelor of Mechanical Engineering (1966), Master of Science in Mechanical Engineering (1968), and Doctor of Philosophy (1970) degrees from the Georgia Institute of Technology. He joined Western Electric's Cable and Wire Product Engineering Control Center in 1970 as a Senior Development Engineer in the Plastic Insulating Department. For three years he was on active duty with the U. S. Navy as an Engineering Duty Officer, returning to Western Electric in March, 1974.

GAS INJECTION EXTRUSION PROCESS FOR A FOAMED PLASTICS INSULATION, SUPPLYING A FIXED QUANTITY OF GAS

M. Azuma K. Orimo K. Toyoda T. Shimano S. Yamamoto
The Furukawa Elec. Co., Ltd., Tokyo, Japan

1. Summary

We developed a wire coating line for foamed plastics insulated wires by nitrogen gas injection. It was completed by development of a gas injection apparatus which is capable of injecting a fixed amount of gas into molten polymer in the extruder barrel even when the pressure of the molten polymer varies at the gas inlet. This line makes it possible to extrude various kinds of plastics on various sizes of conductor at various line speeds by the use of one and the same screw, producing foamed plastics insulated wires of highly unifoam quality.

2. Introduction

Development of mechanical foaming method has been carried on in many countries since about twenty years ago. In the previous meeting of IWCS we reported a wire coating process by making gas sorbed into solid polymer pellets in the extruder hopper. This time we report on a wire coating process by making gas injected into molten polymer in the extruder barrel that we have been developing along with the gas sorbing process, which is simpler and easier to operate than most of the conventional mechanical foaming methods.

In the extrusion of foamed plastics insulation, one of the requirements that must be met to ensure uniform properties of insulated wire is to keep the amount of gas dissolved in molten polymer uniform until the polymer reaches the die. Attempts have long been made to fulfil this requirement by injecting gas into the extruder barrel, and they all involve gas supply under a constant pressure. In such methods, however, the pressure of molten polymer must be kept constant at the gas inlet. For this reason, the pressure at the inlet must usually be kept "zero" or close to "zero" and the use of the extruder is limited to a narrow range (in respect to output and kind of plastics used). Therefore we developed a process in which a fixed amount of gas is supplied irrespective of the pressure of molten polymer in the extruder and completed a new wire coating line in which gas is fed into the barrel.

3. Flow of gas through a nozzle

The gas flow through the convergent nozzle (Fig. 1) is expressed by Formula (1) below if the gas used is in an ideal condition, that is, it is a perfect gas, expands adiabatically, is friction-free, and so on,

$$G = a\sqrt{2g\,\frac{\gamma}{\gamma-1}\,\frac{P_1}{\rho_1}\left\{(1+x)\left(\frac{P_2}{P_1}\right)^{\frac{2}{\gamma}} - \left(\frac{P_2}{P_1}\right)^{\frac{\gamma+1}{\gamma}}\right\}} \quad \cdots\cdots (1)$$

$$\left[\, x = \frac{\gamma-1}{\gamma}\,\frac{v_1^2}{2gRT_1} \,\right]$$

where G : Mass flow of gas
P_1: Upstream pressure
P_2: Downstream pressure
T_1: Upstream temperature
ρ_1 : Upstream specific volume
v_1 : Velocity of gas at the inlet-side of a nozzle
γ : Ratio of specific heats
R : Gas constant
a : Cross-sectional area of the outlet-side of the nozzle
g : Acceleration of gravity

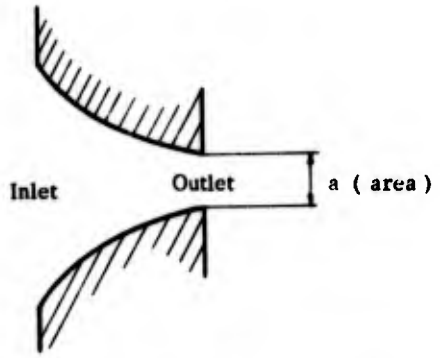

Fig. 1. Cross Section of Convergent Nozzle

In Formula (1), "x" represents the effect of the velocity of gas at the inlet of the nozzle and is usually negligible because the velocity of gas is smaller at the inlet than at the outlet.

Therefore,

$$G \sim F\left(\gamma, \frac{P_2}{P_1}\right) a \frac{P_1}{\sqrt{RT_1}} \quad \cdots\cdots\cdots (2)$$

$$\left[\, F\left(\gamma, \frac{P_2}{P_1}\right) = \sqrt{2g\,\frac{\gamma}{\gamma-1}\left\{\left(\frac{P_2}{P_1}\right)^{\frac{2}{\gamma}} - \left(\frac{P_2}{P_1}\right)^{\frac{\gamma+1}{\gamma}}\right\}} \,\right]$$

$F\left(\gamma, \frac{P_2}{P_1}\right)\sqrt{\frac{\gamma-1}{2g\gamma}}$, plotted in relation to P_2/P_1, is shown by the dotted line in Fig. 2 in the case of $\gamma = 1.4$ (N2 gas). This curve takes unrealistic values in the range in which P_2 is lower than P_c (which is the value of P_2 when

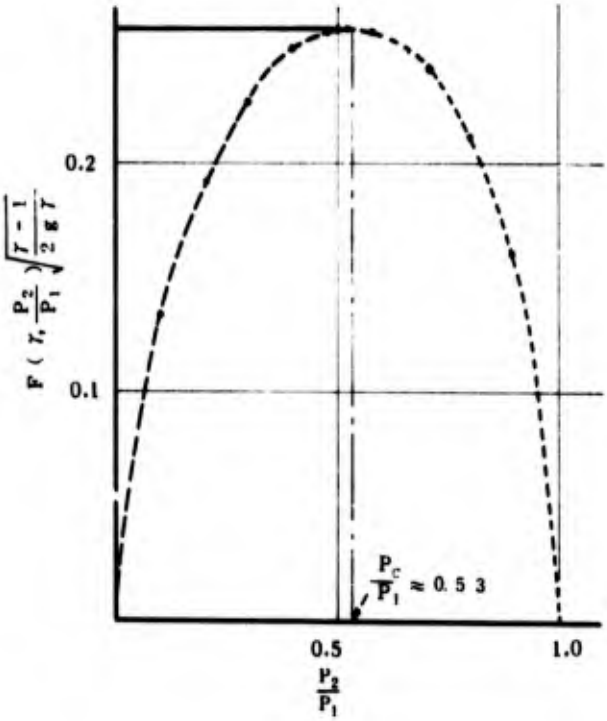

Fig. 2

$F(\gamma, \frac{P_2}{P_1})\sqrt{\frac{\gamma-1}{2g\gamma}}$ is maximum). But this is based on the assumption that the gas pressure at the cross section of the outlet of the nozzle is always equal to P_2. In reality, however, when the pressure ratio is P_c/P_1 or less, P_2 is constant P_c regardless of the downstream pressure.

Therefore, the curve of $F(\gamma, \frac{P_2}{P_1})\sqrt{\frac{\gamma-1}{2g\gamma}}$ versus P_2/P_1 becomes as shown by the solid line in the range in which P_2 is lower than P_c.

Because of the condition

$$\frac{d}{d(\frac{P_2}{P_1})}\left\{F(\gamma, \frac{P_2}{P_1})\right\} = 0 \quad , \quad \cdots\cdots\cdots (3)$$

the value of P_c is as follows:

$$P_0 = P_1 \left\{\frac{2}{\gamma+1}\right\}^{\frac{\gamma}{\gamma-1}} \quad \cdots\cdots\cdots (4)$$

(in the case of N_2 gas, $P_c \approx 0.53\ P_1$)
Therefore, when the downstream pressure is not more than P_c obtainable from Formula (4), the gas flow has no relation with the pressure.

4. Foamed plastics insulated wire manufacturing process

An outline of the equipment of our process is shown in Fig. 3.

It differs from the equipment of ordinary chemical blowing process in that it has a venting type screw, that a gas inlet is provided on the middle of the extruder barrel, above the venting zone, and that it includes a new apparatus that supplies a fixed amount of gas.

4-1. Apparatus for injecting a fixed amount of gas.

On the basis of the above-mentioned discussion, we devised an apparatus shown in Fig. 4.

It compresses N_2 gas into a high pressure by means of a compressor and keeps the upstream pressure (P_1) of the metering valve at a constant level by the use of a pressure reducing regulator. The value of P_1 is so fixed as to make the downstream pressure (P_2) not more than P_c obtainable from Formula (4). The pressure P_2 is somewhat higher than the pressure of molten polymer at the gas inlet and varies with the fluctuation of the polymer pressure. But, by fixing P_1 as above mentioned, the amount of gas passing through the metering valve and flowing toward the gas inlet is made constant irrespective of P_2.

In this way, according to insulating conditions, for example, the kind of material used, conductor diameter insulation thickness, capacitance of wire, line speed, etc., the amount of injecting gas is fixed, then the on-off valve is opened and the desired gas flow is preset on the gas flow meter by the metering valve. Then the extruding conditions are set and the on-off valve is closed. With these done, insulated wires having desired properties can be produced.

4.-2. Extruder and screw.

The extruder used in our manufacturing line has a barrel, 65 mm in inner diameter and 30 in length-diameter ratio (L/D), and a screw of venting type which is so designed that its venting zone is located just at the gas inlet. The screw is

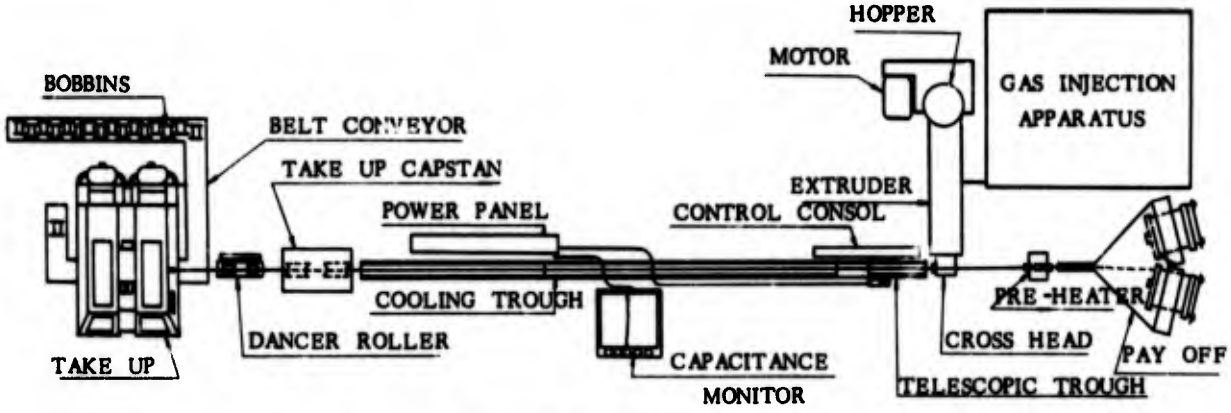

Fig. 3 Wire Coating Line

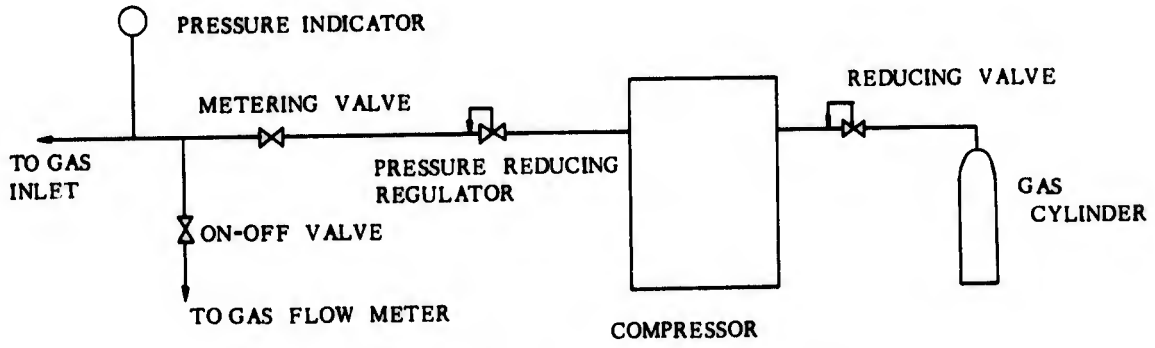

Fig. 4 Apparatus for Injecting A Fixed Amount of Gas.

also designe specially to reduce the fluctuation of pressure of molten polyer at the venting zone. The pressure in the venting zone need not be "zero" or close to "zero" as mentioned in the foregoing. Rather, consideration was given to prevent the pressure in the venting zone from changing substantially according to the output or the pressure in the extruder cross-head. It is known to be difficult to reduce change in the pressure in the venting zone which is determined by various extruding conditions (for example, line speed, conductor diameter, materilas used.) Such difficulty, however, can be overcome by the use of our apparatus for injecting a fixed amount of gas described above. The apparatus makes it possivle to inject a fixed amount gas into molten polymer in the extruder barrel irrespective of change in the pressure in the venting zone.

4-3. Control of capacitance of foamed plastics insulated wire

The foamed plastics insulation line generally has a telescopic trough at the first section of the cooling trough. The telescopic trough automatically controls the capacitance of foamed plastics insulated wire by signal from a capacitance monitor. Our process also uses this control system.

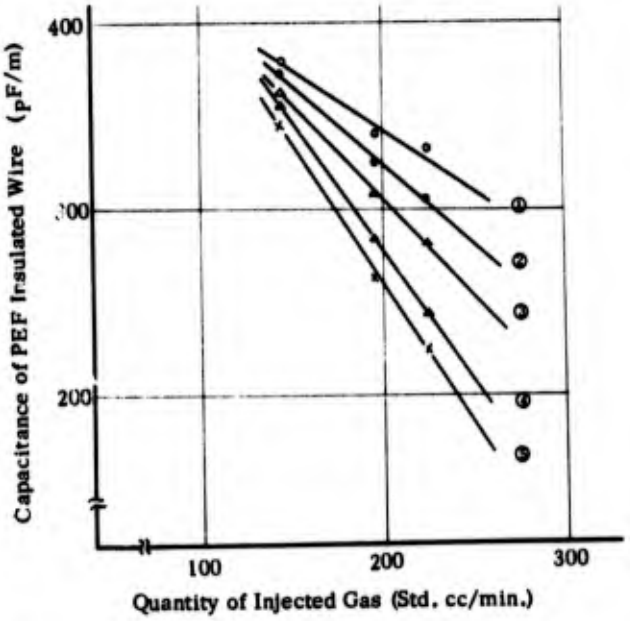

Fig. 5 Capacitance of PEF Insulated Wire vs. Quantity of Injected Gas.

Conditions:
1) Material of insulation - High density polyethylene (density - 0.942, M.I. - 0.4 g/10 min.)
2) Injected gas - N_2
3) Conductor diameter - 0.65 mm (22 AWG)
4) Insulation thickness without injecting gas - 0.125 mm
5) Line speed - 750 m/min.
6) Air gap between die and trough
   (1) - 10 cm (2) - 20 cm (3) - 30 cm (4) - 50 cm
   (5) - 70 cm

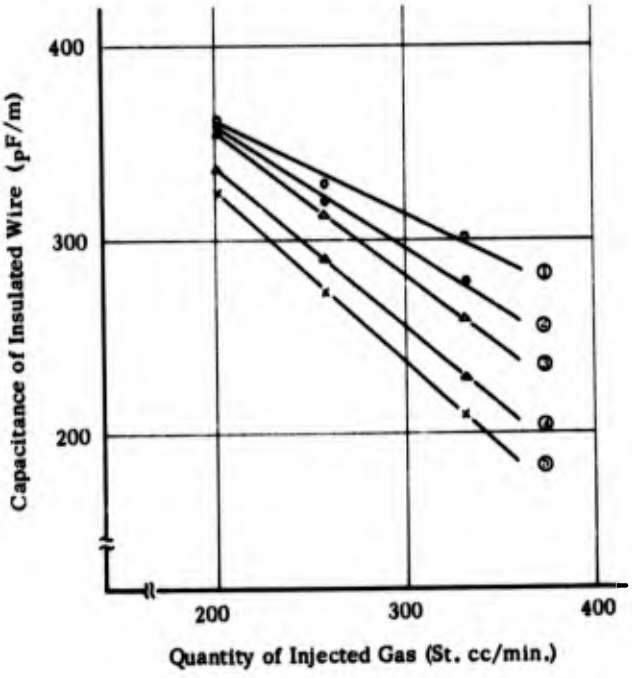

Fig. 6 Capacitance of PEF Insulated Wire vs. Quantity of Injected Gas.

Conditions:
1) Line speed - 1000 m/min.
2) Others are same as Fig. 5.

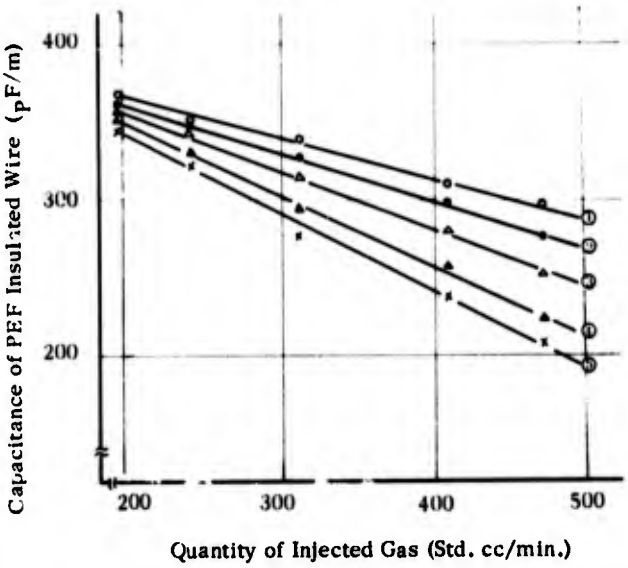

Fig. 7 Capacitance of PEF Insulated Wire vs. Quantity of Injected Gas.

Conditions:
1) Line speed - 1500 m/min.
2) Others are same as Fig. 5.

In Figs. 5 to 7 are plotted the relations between the capacitance of insulated wire and the amount of injected gas at different line speeds and for different air gaps between the die and the trough. In these tests, the diameter of insulated wire in a state were gas in not injected is kept constant (0.90 mm). The figures show that the capacitance fluctuation of wire caused by the fluctuation of the amount of injected gas can be considerably made up for by movement of the telescopic trough.

For example, in Fig. 6, when the line speed is 1,000 m/min. even if the amount of injected gas changes from 220 Std. cc/min. to 350 Std. cc/min. a foamed plastics insulted wire having the same capacitance (290 $_p$F/m) can be produced, theoritically speaking, by changing the die-trough air gap (air gap between die and telescopic trough) from 70 cm to 10 cm. But, if the die-trough air gap is too wide or too narrow, it will causes irregularity in the electrical properties of the insulated wire produced. This is known from Fig. 8 and 9. For instance, when in Fig. 9 a foamed plastics insulated wire having a capacitance of 290 pF/m is produced at a line speed of 1,500 m/min. the dietrough air gap is 13 cm in the case of 470 Std. cc/min. gas injection and the "trough control sensitivity" (change in capacitance per centimeter of movement of the telescopic trough -$_p$F/m/cm.) is about 2.7 $_p$F/m/cm. In the case of 310 Std. cc/min. gas injection, the die-trough air gap is 55 cm and the trough control sensitivity, about 0.9 $_p$F/m/cm. For the same degree of change in capacitance, therefore, the trough is moved about three times as much in the latter case as in the former case. Consequently if the die-trough air gap is made too narrow in the capacitance controlling, a slight movement of the trough causes a substantial chang in capacitance and if the gap is too wide, the movement of the trough cannot follow major change in capacitance.

To prevent these, the amount of injected gas must be so controlled as to allow a proper gap between the die and the trough for a specific line speed. In our trial production of foamed plastics insulated wire by the newly developed process, we preset the amount of injecting gas most suitable for a specific line speed, insulation thickness, etc., and the moved distance of the trough was within 7 cm. Fig. 10 shows the capacitance chart of the insulated wire produced in this way (conductor diameter - 0.65 mm (22 AWG), line speed - 1,500 m/min.) recorded on the capacitance monitor.

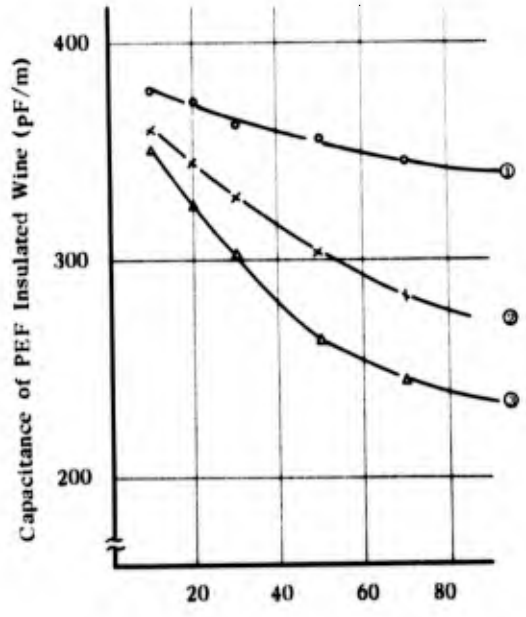

Fig. 8 Capacitance of PEF Insulated Wire vs. Air Gap Between Die and Trough.

Conditions:
1) Material of insulation - High density polyethylene (density - 0.942 g/cm^3, M.I. - 0.4 g/10 min.)
2) Injected gas - N_2
3) Conductor diameter - 0.65 mm (22 AWG)
4) Insulation thickness without injecting gas - 0.125 mm
5) Line speed - 750 m/min.
6) Quantity of injected gas
(1) - 144 Std.cc/min., (2) - 195 Std.cc/min.,
(3) - 224 Std.cc/min.

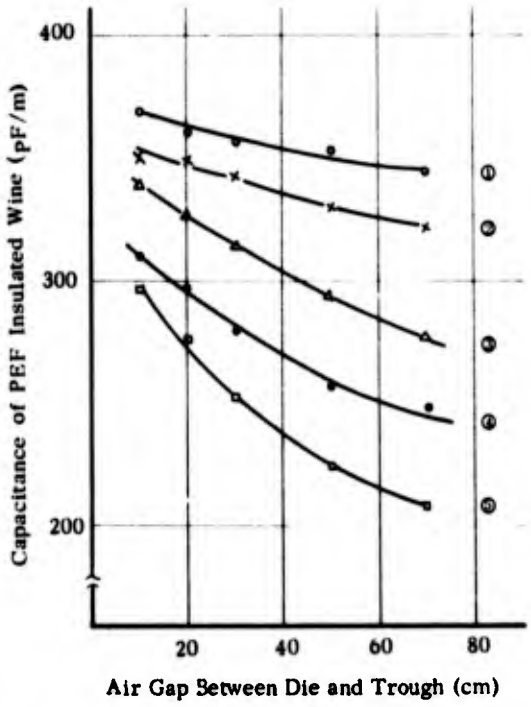

Fig. 9 Capacitance of PEF Insulated Wire vs. Air Gap between Die and Trough.

Conditions:
1) Line speed - 1500 m/min.
2) Quantity of injected gas
   (1) - 192 Std.cc/min., (2) - 240 Std.cc/min.,
   (3) - 311 Std.cc/min., (4) - 408 Std.cc/min.,
   (5) - 470 Std.cc/min.
3) Others are same as Fig. 9.

4-4. Range of application

In most of the conventional methods in which gas is injected into the barrel, the pressure of the gas at the gas inlet is kept at a constant level by a pressure reducing regulator. Therefore the amount of gas dissolved in plastics is changed by the pressure of molten polymer at the inlet, because the amount of gas dissolved in plastics is determined by difference between the gas pressure and the molten polymer pressure at the inlet. Consequently, most of the conventional methods require accurate control of the pressure of molten polymer at the inlet. But this is very difficult to perform under a high level of the pressure. In experimental foamed plastics insulation extrusion, we obtained the result that uniform wires can be produced when the pressure of molten polymer at the gas inlet is kept at "zero" or close to "zero". From this we have come to know that in such converntional methods the range of material, line speed, insulation thickness and so on for the same screw are limited.

On the other hand, our method offers a fairly extensive choice of material, line speed, insulation thickness, etc.,

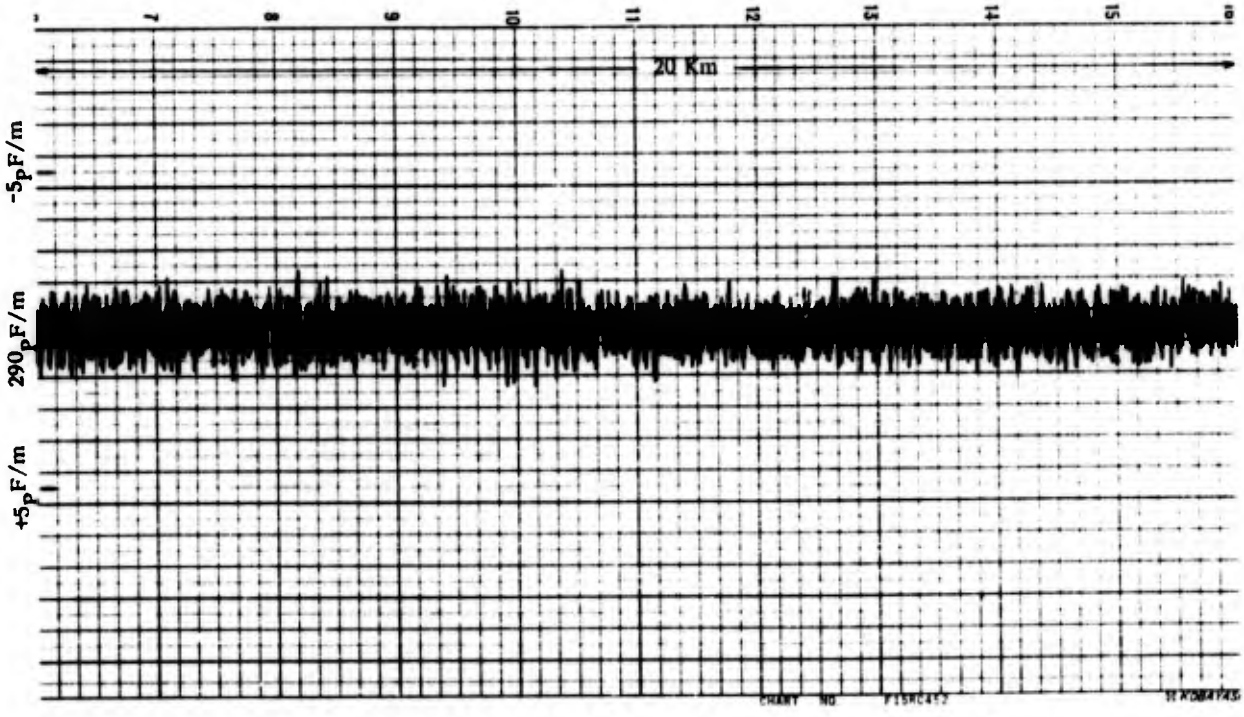

Fig. 10 Capacitance Chart of PEF Insulated Wire.

Conditions:
1) Material of insulation - High density polyethylene (density - 0.942 g/cm^3, M.I. - 0.4 g/10 min.)
2) Injected gas - N_2
3) Quantity of injected gas - 390 Std.cc/min.
4) Line speed - 1500 m/min.
5) Conductor diameter - 0.65 mm (22 AWG)

Table 1. Properties of PEF Insulations Produced by Our New Technique

Conductor Dia. (mm) (AWG)	Insulation Thickness (mm)	Expansion Rate (%)	Tensile Strength (g)	Elongation (%)	*1 Thermal Shrinkage (%)	*2 Thermal Stress Crack	*3 Environmental Stress Crack	*4 Abrasion Test (Times)	*5 Surface Roughness (μ)
0.4 (26)	0.1	14	510	370	0.0	No Crack	No Crack	9	1 >
0.5 (24)	0.125	17	670	410	0.1	No Crack	No Crack	25	1 >
0.65 (22)	0.15	21	840	450	0.0	No Crack	No Crack	65	1 >

Notes:

*1 24 hours in 80°C air with conductor.

*2 The insulated conductor were wound on its own diameter in 20 contiguous turns, and kept in 80°C air for 1000 hours.

3 The insulated conductor were wound on its own diameter in 20 contiguous turns, and kept in 50°C solution of Igepal CO 630 (20% volume) for 100 hours.

*4 Nema type abrasion tester was used. The diameter of the abrasion-bar was 4mm and a 500 g dead weight was applied.

*5 Values are shown by root mean square.

Table 2. Pair-To-Pair Capacitance Unbalance Within A Quad (pF/m)

Cable Size	Paper Insulated Cable		PEF (Chemically Blown) Insulated Cable		PEF (Gas Injection method) Insulated Cable	
	Average	Individual Maximum	Average	Individual Maximum	Average	Individual Maximum
0.4 mmφ (26 AWG) 2400 pairs	59.0	201.3	17.6	85.0	17.3	84.5
0.5 mmφ (24 AWG) 1800 pairs	56.5	187.6	15.9	61.5	15.7	61.3
0.65 mmφ (22 AWG) 1000 pairs	55.4	176.4	14.4	49.6	14.6	49.7

because the amount of injected gas is not affected so much by the pressure of plastics. The applicable range of this method is determined by the upstream pressure of the metering valve and the pressure of molten polymer at the gas inlet, that is, venting zone of the screw. As is evident from Fig. 2, the smaller the ratio of the upstream pressure to the downstream pressure of the valve, the smaller the amount of injected gas as compared with the preset level measured under the condition that the downstream pressure of the metering valve is the atmospheric pressure, and the grater the change in the amount of injected gas due to fluctuation of the pressure at the venting zone. Therefore, the upstream and downstream pressure must be so maintained that their ratio will not become too small.

Since the upstream pressure is limited by the maximum operating pressure of the valve, the maximum pressure at the venting zone is also limited accordingly from the viewpoint of the above discussion. A broader allowable range of the pressure at the venting zone means a broader choice of material, line speed, insulation thickness, and, as just mentioned, this depends on the maximum operating pressure of the metering valve.

As a result of an experimental wire coating made in our coating line, using only one screw specially designed by us, it was found possible to use both high-density and low-density polyethylene as insulation materials and to produce insulated wires having satisfactory properties at a line speed of 1,700 m/min. for 0.4 mm-and 0.5-diameter conductors and 1,500 m/min. for 0.65 mm conductor.

5. Properties of insulated wire and cable

By this new process we insulated copper conductors, 0.4 mm (26 AWG), 0.5 mm (24 AWG) and 0.65 mm (22 AWG) in diameter, using high density polyethylene (density - 0.942 g/cm^3, M.I. - 0.4 g/10 min.) and nitrogen gas, at the line speeds of 1,700 m/min. for 0.4 mm and 0.5 mm conductors and 1,500 m/min. for 0.65 mm conductor. The properties of the insulated wires produced are shown in Table 1. The wires were made into PEF-LAP city junction cables and their capacitance unbalance was measured, with the result shown in Table 2, and Photo. 1 shows cable samples and the cross sections of the insulated wires used for the cables.

Only one screw was used for coating these wires.

6. Conclusion

As has been described above, we completed a foamed plastics insulated wires by gas injection into the extruder barrel, which has a fairly extensive range of application. This process is more simple in equipment than most of the conventional processes and produces insulated wires of high quality by simple operation. As we have no auxiliary equipment for insulated wires of larger diameter, we have not as yet experimented production of wires. But, the application of this process to such field is very attractive and we are planning to test it in the near future.

7. Acknowledgements

We gratefully acknowledge the guidance of the people of N.T.T., Kazuo Tsunoda, Masao Matsumoto and Toshio Saito in The Furukawa Electric Co., Ltd., and the contributions of co-workers of our laboratory, particularly Mikio Kanda and Mitsuru Sakai.

8. References

1. R. H. Reinhard, C. L. Lonely and G. W. Daues
The Extrusion of Cellular Polyethylene Insulation.
16th IWCS, November, 1967.

2. B. H. Maddock
Extrusion of Cellular Polyethylene.
18th IWCS, December, 1969.

3. S. Verne, B. G. Howell and G. A. Layzell Ward
A New process for Manufacture of Telephone Cores with Cellular Insulation.
18th IWCS, December, 1969.

4. S. L. Soo
Thermodynamics of Engineering Science (Book)
Maruzen Co., Ltd., 1958.

Photo. 1 Cable Samples and Cross Section of Cores of PEF-LAP City Junction Cables Insulated by New Technique.

(a) 0.4 mm (26 AWG)
2400 pairs.

Conditions:
1) Line speed-1700 m/min.
2) Injected gas-N_2
3) Quantity of injected gas 175 Std.cc/min.

(b) 0.5 mm (24 AWG)
1800 pairs

Conditions:
1) Line speed-1700 m/min,
2) Injected gas-N_2
3) Quantity of injected gas 250 Std.cc/min.

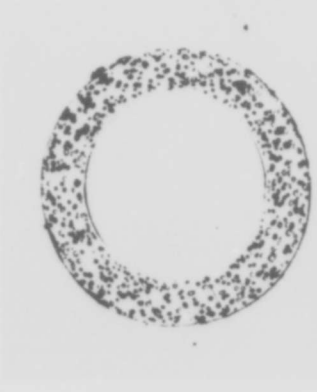

(c) 0.65 mm (22 AWG)
1000 pairs

Conditions:
1) Line speed-1500 m/min.
2) Injected gas-N_2
3) Quantity of injected gas 390 Std.cc/min.

MASAO AZUMA
The Furukawa Electric
Co., Ltd.
6-1 Marunouchi 2-Chome,
Chiyoda-ku, Tokyo,
Japan

Mr. Azuma graduated from the Tokyo Institute of Technology with a B. Sc. in chemical engineering in 1959. Then he joined The Furukawa Electric Co., Ltd., and has been engaged in research and development of plastic materials and manufacturing methods for telephone cables. Mr. Azuma is now Manager of the Production Engineering Department of Telecommunication Division of The Furukawa Electric Co., Ltd., and a member of the Society of Polymer Science of Japan.

KATSUMI ORIMO
The Furukawa Electric
Co., Ltd.
6-1 Marunouchi 2-Chome,
Chiyoda-ku, Tokyo,
Japan

Mr. Orimo graduated from Kyoto University in 1966 with a B. Sc. in Applied Chemistry.

Then he joined the Furukawa Electric Co., Ltd. and has been engaged in research and development of plastic materials and manufacturing methods for telephone cables.

Mr. Orimo is now a member of the Material Research Department of the Telecommunication Laboratory of The Furukawa Electric Co., Ltd., and a member of the Society of Materials Science of Japan.

KUNIHIKO TOYODA
The Furukawa Electric
Co., Ltd.
6-1 Marunouchi 2-Chome,
Chiyoda-ku, Tokyo,
Japan

Mr. Toyoda graduated from Waseda University with B.Sc. degree in 1965 and M.Sc. degree in 1967 in mechanical engineering.

Then he joined The Furukawa Electric Co., Ltd. and has been engaged in the designing of machines for telephone cable production.

Mr. Toyoda is now a member of the Plant Engineering Division of The Furukawa Electric Co., Ltd.

TAKASHI SHIMANO
The Furukawa Electric
Co., Ltd.
6-1 Marunouchi 2-Chome,
Chiyoda-ku, Tokyo,
Japan

Mr. Shimano graduated from Tokyo Kyoiku University with a B. Sc. in Physics in 1969.

Then he jointed The Furukawa Electric Co., Ltd. and has been engaged in research and development of plastic materials and manufacturing methods for telephone cables.

Mr. Shimano is now a member of the Material Research Department of the Telecommunication Laboratory of The Furukawa Electric Co., Ltd.

SHOJI YAMAMOTO
The Furukawa Electric
Co., Ltd.
6-1 Marunouchi 2-Chome,
Chiyoda-ku, Tokyo,
Japan

Mr. Yamamoto graduated from Hakodate Technical College in 1972, where he majored in Industrial Chemistry. Then he joined The Furukawa Electric Co., Ltd., and he now is a member of the Material Research Department of the Telecommunication Laboratory.

AUTOMATIC PROCESS CONTROL IN THE INSULATING OF TELEPHONE CABLES

BY

E. Kertscher

Maillefer, S. A.
Ecublens-Lausanne
Switzerland

1. Introduction

High performance extrusion lines for the production of plastic insulated telephone wires have reached a relatively high degree of reliability . This was achieved on the one hand by process oriented thinking of certain equipment manufacturers together with a better understanding of the total process, and on the other hand by the availability of raw materials with repeatable characteristics. However, it must be mentioned that in comparison to other industries such as the synthetic fibre industry, the cable industry has not made equivalent progress.

The purpose and goal of this development is to provide the telephone cable manufacturer with equipment for the economical production of telephone wires. It is, however, impossible to describe all the details involved in these automatic controls. Therefore, only the more important features of this system will be described in detail. An outline will be presented showing the way toward automatic monitoring and control of groups of machines by a central computer. Besides, this kind of system can reduce the problems caused by personnel shortages and lack of qualified personnel. With this system it is desired to achieve a balanced optimum utilization of machines, materials and personnel. Specific emphasis is not necessarily on the top speed of various machine components but on the following:

- Continuous production of machines without downtime
- Best material usage with high quality output
- Minimum scrap

This goal can be achieved with meaningful automation and suitable inline process control.

A new generation of high capacity telephone wire insulating lines will be introduced. These lines are so conceived that during operation no adjustments on the part of the machine operator are necessary. The operating data for the production of a particular telephone wire are programmed into a data carrier which controls the operation of the process.

The following parameters are monitored and when necessary automatically corrected:

- Capacitance of insulation for foamed polyethylene
- Capacitance of insulation for solid insulation
- Insulation wall thickness
- Wire elongation
- Spark test failures

The above controls are part of the automatic system.

An accurate length measuring device insures constant lengths of wire on each reel.

Color changes can be accomplished at full line speed in a few seconds with a minimum of scrap.

2. The State of the Art

2.1. Classical Composition of the Extrusion Line

The production of plastic insulated telephone wires is accomplished either by means of tandem lines which besides the extrusion equipment also include a wire drawing machine and an annealer, or by simple extrusin lines whic are fed the annealed wire from a flyer type pay-off.

The following is an outline of the personnel requirements for a six line telephone wire extrusion department which more or less corresponds to what is being currently done in the field by modern manufacturers.

Each line has its own operator and a helper is available for the supply of raw materials and another for the removal of the finished wire.

A group of six lines also requires the services of a set-up man and a foreman. Besides there is usually an inspector to check the quality of the production by measuring conductor diameter , insulation thickness and centering. Further tests on the product are later performed in the laboratory.

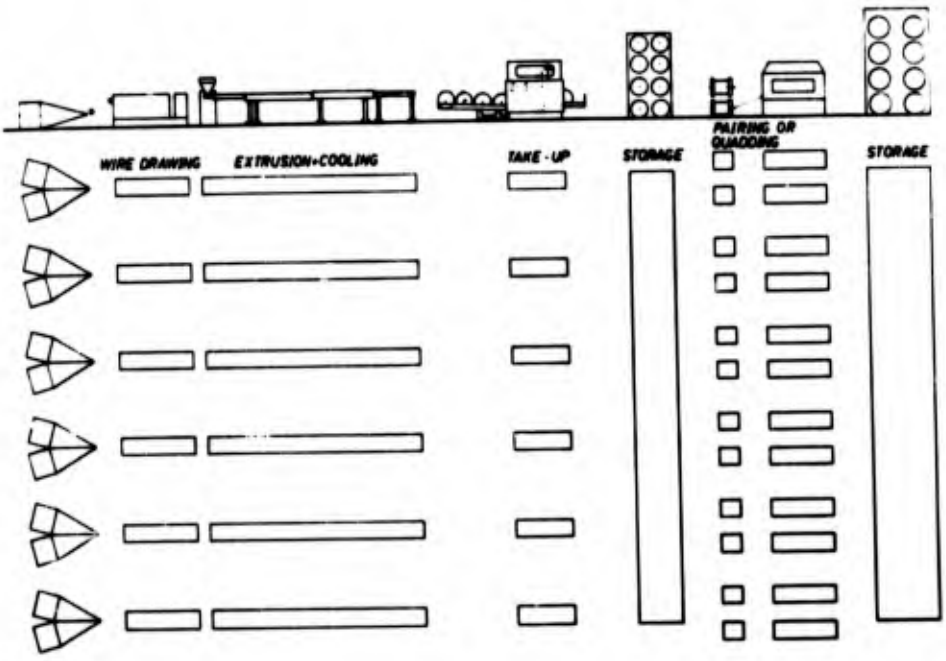

1. Classical Layout for Telephone Wire Insulating Department

What advantages or disadvantages result from this kind of organization?

- The machine is set up by a specialist who is mostly overworked.
- Corrections in the operation of the machine are made by the operator or the setup man who do not always achieve the desired results.
- Supervision of the operating personnel is relatively difficult.
- High personnel requirements, i. e. 11 persons for 6 machines.
- Uneconomical use of personnel since such machines operating at over 6,000 ft./min., operate at 90% of the time or better.
- Each reel is checked for insulation thickness to avoid waste of materials.
- Much of the work is still donne manually.
- In spite of the fact that wire capacitance, insulation faults and wire elongation are usually measured and controlled, usually no records are provided to record these parameters. This results in possible bad conductors going into further production, resulting in faulty cables which are only detected at final testing.
- There exist no possibility to analyze faults or variations in quality of the product. Therefore, the optimization of the production process is impossible.
- Valuable data and individual experiences are lost with each change of personnel.
- Raw materials are often not checked at all. With critical materials this can lead to unpleasant surprises and a great amount of scrap.
- All the above problems will sooner or later have to be solved. This is accomplished by minimizing or if possible eliminating the various shortcomings.

In the future it may become easier to find a good engineer than a good operator. The restructuring of manufacturing enterprises is not too far off if it has not already started. In general, it is doubtful that the quality of the available machine operators will improve.

2.2. How Far to Automate?

Automation of certain machines or processes must take into account, at the same time, the work flow before and after the automated process. The positioning of machines should be such as to minimize the movement of products and raw materials.

One has to consider both the quantity and the quality of the required personnel. How such an installation is maintained and when necessary repaired must also be taken into consideration.

How far to automate depends to a large extent upon the production program and the limitations of the process. In any case, one must be able to sow savings through automation. Automation for its own sake serves no purpose. Extrusion lines and especially lines for telephone wires offer many possibilities to automate.

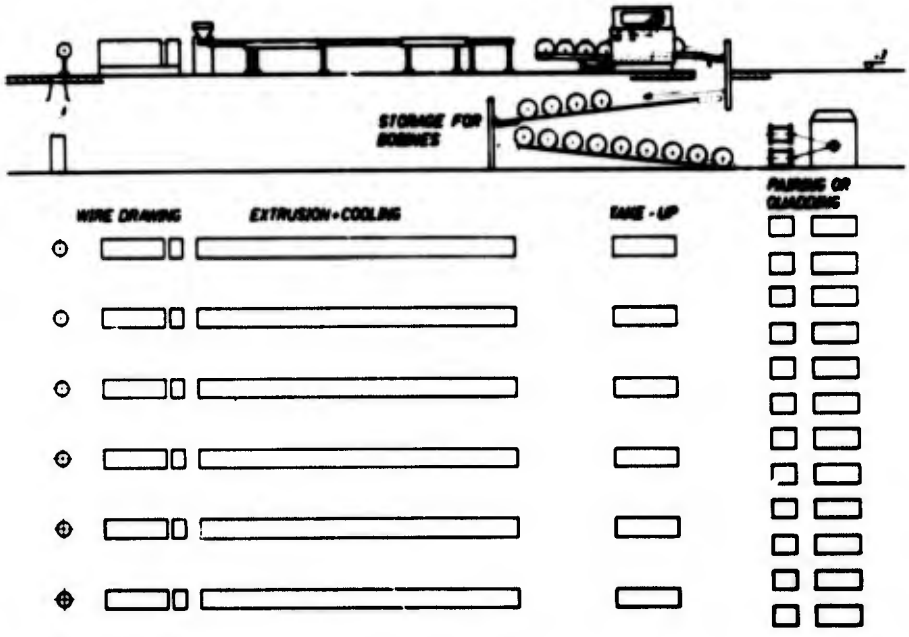

2. Improved Extrusion Line Layout with Automatic Matrials Handling System

A production layout as shown in Fig. No. 2. above, does no longer require individual operators for each line. The layout is so designed that the intermediate annealed wire is transported to the machine at one end and the reels of insulated wire are automatically fed into the twinning machines at the other end. The insulating compound is automatically fed through a pneumatic conveying system. The operation of the idividual lines is automatically monitored and controlled through a punch card system. This allows fast product changes on the lines when necessary.

Each line can be controlled:

a) Automatically by means of punch cards

b) Manually

c) Automatically with manual override

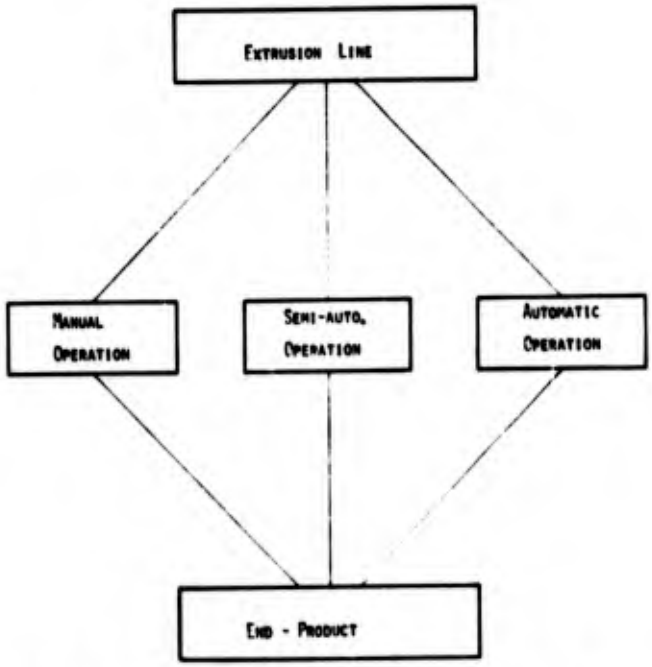

3. Control Possibilities of SECAP Line

Since all materials handling problems have been minimized and the istallation operates automatically, the required personnel can also be reduced. A installation of this kind can be operated with six people, two operators for the drawing machines, two operators for the extruders, a set-up man and a foreman or process engineer.

3. Elements of an Automated Insulating Process

Several prerequisites must be fulfilled to obtain maximum line efficiency:

3.1 Raw materials with reproducible characteristics

3.2 willingness to properly organize personnel

3.3 Employment of the necessary machines and devices to insure reliable operation

3.1 Raw Materials

The quality of raw materials is not always uniform. This can lead in certain cases to considerable difficulties. Problems can be encountered with the copper, the plastic insulation or the color additives. These problems can be eliminated through an incoming inspection procedure.

Allowable tolerances must be adhered to by the raw material suppliers. Test procedures must be agreed to between the suppliers and the user.

3.2 Willingness to Properly Organize

A number of organizational problems have previously been outlined.

It is necessary, first of all, to understand that a general solution to the problem of higher productivity is not achieved only through improvements in machinery and processing methods. Raw material problems, lack of training of personnel, prejudices and work rule problems can have considerable influence over the profitability of an operation.

Equipment manufacturers are often criticized because they are equipment oriented and they do not consider how tneir machinery fits into the complete picture of the cable manufacturing process.

This criticism may be justified in many cases, however, one should not generalize.

We shall return to the problem of organization later in order to present a well rounded picture of the total problem.

3.3 Application of Machines and Auxiliary Equipment for Maximum Reliability

It is no longer sufficient, on the basis of present day relatively labor intensive methods, to run extrusion lines automatically. Automatically operating extrusion lines exist already. The extrusion process must be improved by the application of the systems approach to the problem. In this manner, weak points in the process can be identified and eliminated to obtain a more reliable production system.

It was only possible to assemble a programmed extrusion line after sufficiently reliable components were developed and became available to the system supplier. Drift free instrumentation was one of the most critical requirements. The requirement for daily calibration of capacitance gauges and diameter measuring devices etc. had to be eliminated.

As a result of this requirement, suitable instruments were eventually developed which resulted in higher line reliability and the elimination of the need for many final inspection procedures.

4. Why a Punch Card?

The punch card is an information carrier of standard size used in many data

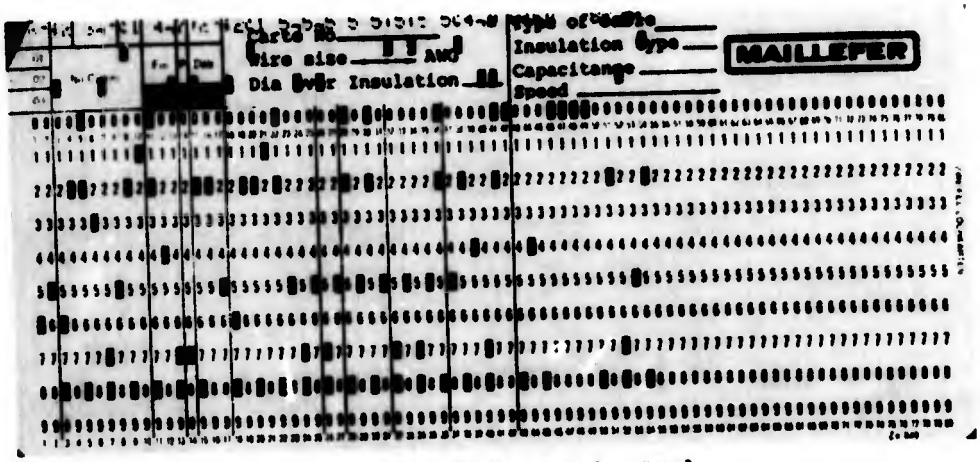

4. The SECAP Punch Card

processing applications.

The dimensions are as follows:

Length	7.375"
Width	3.25"
Thickness	.0067"

Generally printed information on one or both sides of the card explain the contents of the card. In comparison to perforated tapes or magnetic tapes the punch card is a compact unit which can easily be filed and sorted.

The standard punch card (Fig. No. 4) consists of 80 rows with 12 holes each. In contrast to other data storage devices a card is relatively inexpensive and can easily be reproduced in case of damage.

The main disadvantage of a punch card is its limited storage capacity. For example in comparison to perforated tapes which can be any length, the punch card holds only 80 characters.

However, this limited information carrying capacity is sufficient for programming an extrusion line and therefore this method was selected. Each different product to be made requires a separate card. The number of cards required depends therefore on the number of products to be manufactured.

A static card reader was selected for this application for the following reasons:

1. As information carrier the punch card is inexpensive.

2. The puch cards and the card reader are not affected by electrical noise which is usually found in factories.

3. The use of magnetic tapes would require programmable storage devices.

4. Compared to machine tools, for example, the operation of an extrusion line is quite different. In programming a machine tool successive operations are performed. In the operation of an extrusion line a certain number of parameters are constantly monitored and some are constantly automatically corrected.

5. All operations are controlled by relays, counter etc. This facilitates the maintainance of the equipment by generally available factory maintainance personnel.

5. The Assembly of the Installation

The necessary data for a production run are introduced into the system by means of the punch card which is inserted into the card reader. In this manner certain conditions can always be reproduced, extraneous information deleted and it is always possible to make certain manual adjustments.

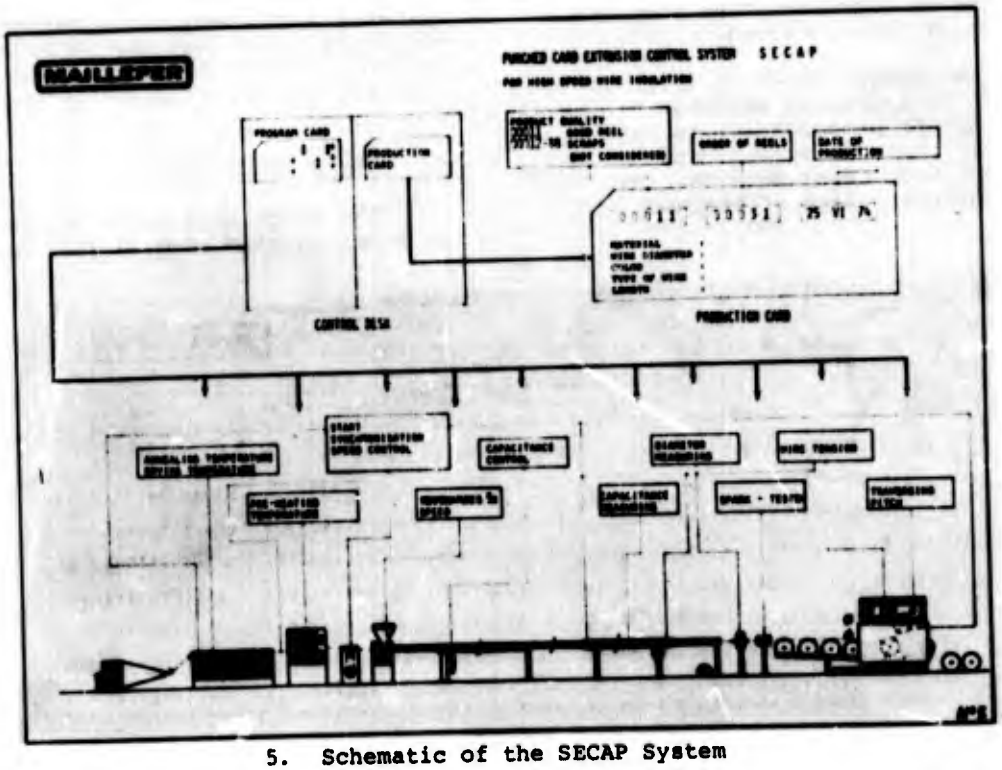

5. Schematic of the SECAP System

5.1 Description of Operation

The layout of the installation can be seen in Fig. No. 5 and can be divided into three parts.

5.1.1 The programmmable controller to control the installation.

5.1.2 The production control section

5.1.3 Equipment Monitoring

The installation can also be operated semi-automatically or manually. The selection of the mode of operation is made by means of a key operated selector switch to prevent tampering with the equipment by unauthorized persons.

5.1.1 Programmable Controller

In this part the following parameters are stored:

- Temperatures of the extruder
- Temperature of the head
- Temperature alarms for the extruder and the head
- Take-up speed
- Drawing machine speed
- Screw RPM
- Pay-off speed
- Take-up reel wire length
- Nominal wire diameter
- Nominal capacitance
- Diameter tolerance
- Capacitance tolerance
- Number of allowable spark failures per reel
- Take-up cutover instructions
- Annealing current
- Pre-heater temperature
- Take-up wire tension
- Regulation of the installation

5.1.1.1 Process Control

In order to make the installation as versatile as possible the use of various materials and combination of materials has been forseen. The necessary control functions to allow this equipment to operate with different plastic compounds have been incorporated into the equipment.

The following controls are incorporated:

A) Diameter control

B) Capacitance control

C) Capacitance control for cellular polyethylene

A) Diameter Control

Diameter control is used when materials are being extruded which do not have stable dielectric constants such as PVC. With PVC capacitance control is not possible. With this type of control either the line speed or the screw speed can be varied.

B) Capacitance Control

Capacitance control can be used with materials such as most types of polyethylene which exhibit stable dielectric characteristics. The actual control is as in A) above.

C) Capacitance control for cellular polyethylene

To control the capacitance of a cellular polyethylene insulated wire a special sytem is employed as shown in Fig. No. 6. Both the quench point of the wire and the temperature of the fourth zone of the extruder are varied.

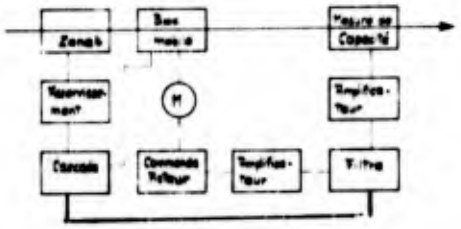

6. Capacitance Control, Block Diagram

Beyond the above the following are also monitored:

D) Insulation faults

E) Wire elongation

D) Insulation testing

A high rate of spark failures can have many causes, among them the following:

- dirty conductor or poor tinning
- moist conductor
- high insulation eccentricity
- too much color concentrate
- poorly mixed color concentrate
- moisture in the compound and color concentrate
- damaged insulation

and many others!

Under normal conditions can the eccentricity of the insulation be easily connected with frequent insulation faults.

As can be seen in Fig. No. 7 the capacitance changes little with a slight amount of

eccentricity. Further increases in the eccentricity increase the wire capacity considerably.

In the same sense, as the eccentricity of a conductor increases so will eventually the spark faults.

For this reason a spark tester is, even if not directly, a very important part of an extrusion system.

E) Wire elongation

The elongation of the conductor is also an important factor to consider in the operation of an extrusion line. A reduction in the conductor diameter strongly influences the capacitance value of the insulated wire. Therefore the elongation or rather the reduction in diameter of the wire should be always monitored. How this is done is shown in Fig. No. 8.

The high investment in control and monitoring equipment can be justified by the resulting savings in material, both copper and insulation. It must be considered that about 80% of the cable costs can be materials, possibly three quarters copper costs and one quarter insulation costs.

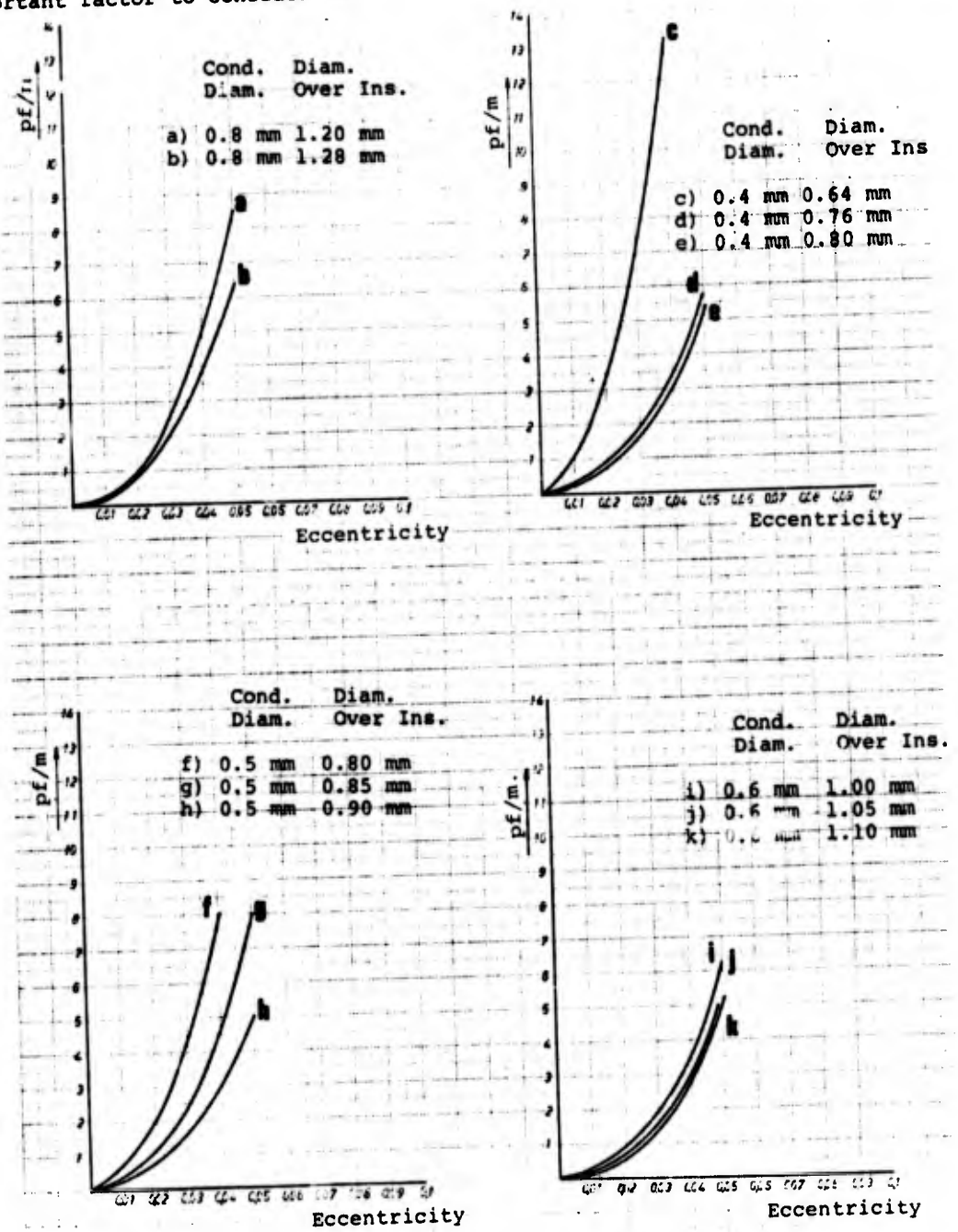

7. Effect of Eccentricity on Capacitance

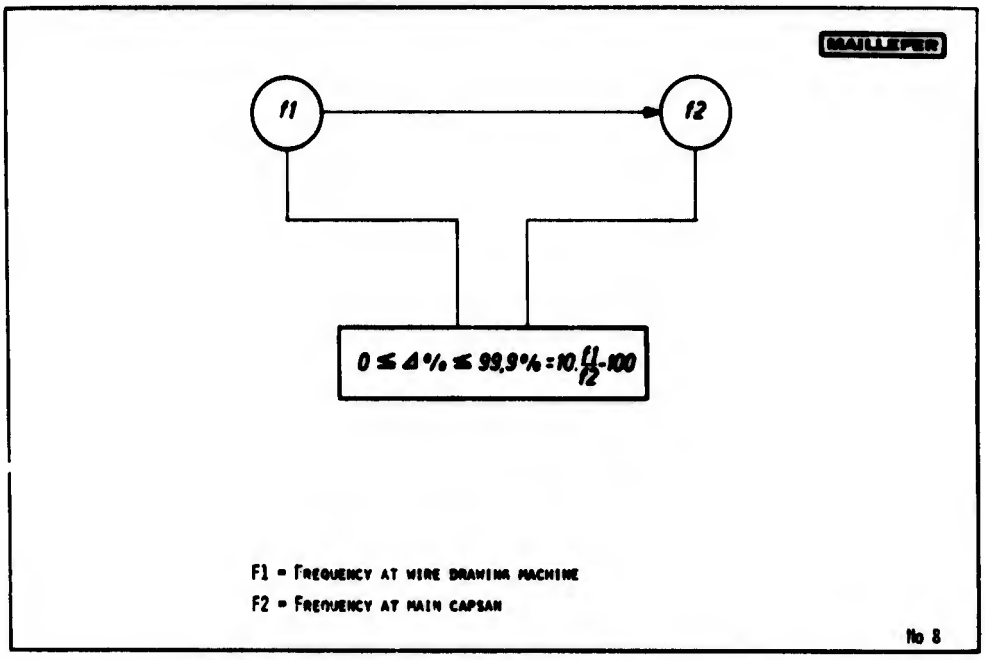

8. Elongation Measuring System, Schematic

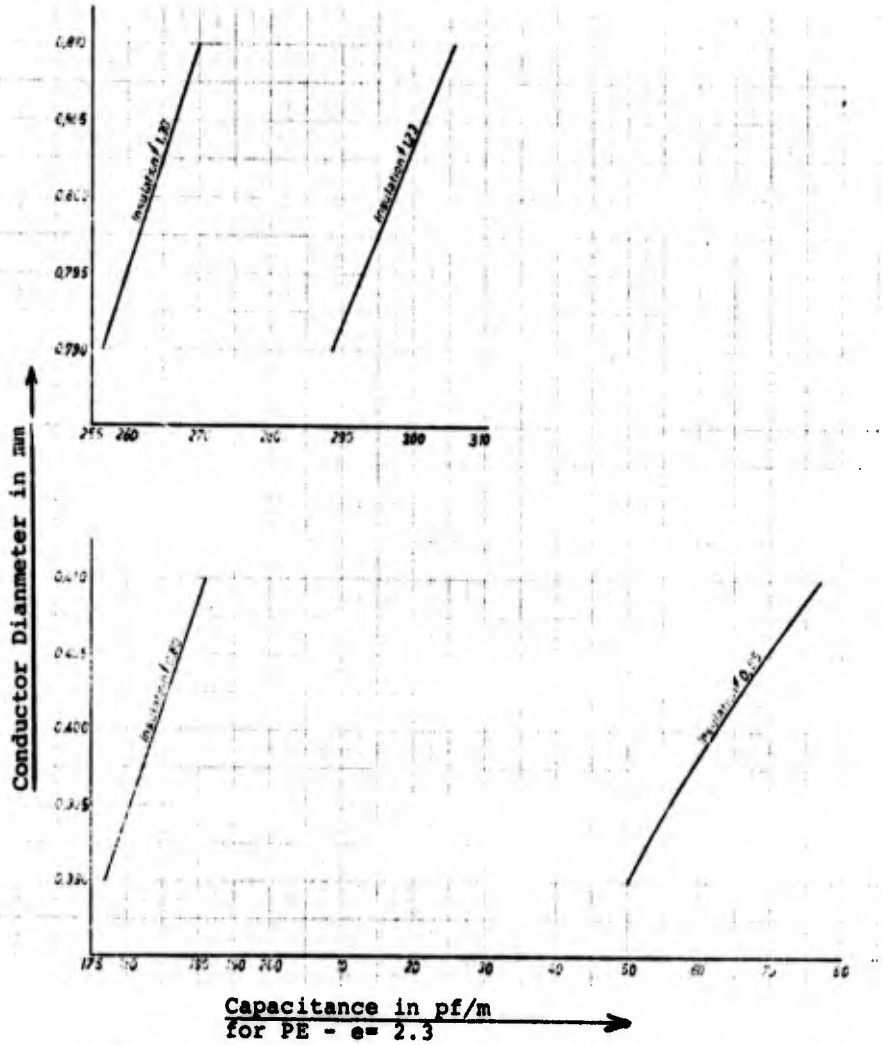

9. Capacitance Variations Caused by Conductor Diameter Reduction

5.1.2 Production Control

The following parameters are included:

- Capacitance
- Diameter over insulation
- Insulation faults
- Wire elongation
- Wire length on each reel

The tolerances of the various production control parameters are programmed. However, in order to limit the number of inputs into the control system, only the values falling outside those tolerances are registered. If one of the controlled values is outside its tolerance limit a light will blink which must be acknowledged by the operator by pushing a button. at the same time a card is printed which indicates the following:

- Deviating parameter
- Reel number
- Date
- Machine number

The production efficiency of each machine can be determined at the end of each production order.

$$\frac{\text{fault free reels x length/reel}}{\text{total length}}$$

Color changes can be made with the aid of a color change counter in a few seconds without stopping the operation. Since the volume of the granules in the extruder remains constant, the color change can be programmed depending upon the crossection of the extrudate by the use of the table in Fig. No. 10. This can be done because of the self cleaning feature of the MAILLEFER BM extrusion screw.

An automatic color change system is provided. When a color change is desired the feeding of the compound and the color concentrate is stopped at a precise moment. The new compound and color concentrate is then fed to the machine some time later. This time depends upon the extruder screw RPM. After the last reel is filled with the old color the reel is changed and the color change follows a few seconds later. As soon as the new color is established the reel is changed again and the short length of wire with the mixed color is scrapped.

Half full reels and reels with defects are sorted at the exit conveyor of the take-up. They are separated from the good reels and a printer prints a ticket indicating the fault on the reel.

5.1.3 Equipment Monitoring

Besides the previously mentioned controls of the line there are also monitoring functions which serve to monitor various aspects of the functioning of the machine as follows:

- Extruder temperature tolerances
- Extruder heaters
- Thermocouples
- Heater controllers
- Punch card reader
- Air pressure
- Reel position in take-up
- Compound in the hopper
- Programming error in punch card
- GO or NO-GO for production after machine start up

The individually programmed values can also be recorded on a separate punch card. The values of all the parameters can thus be recorded at one time

A recorder for the wire diameter and the wire capacitance completes the installation.

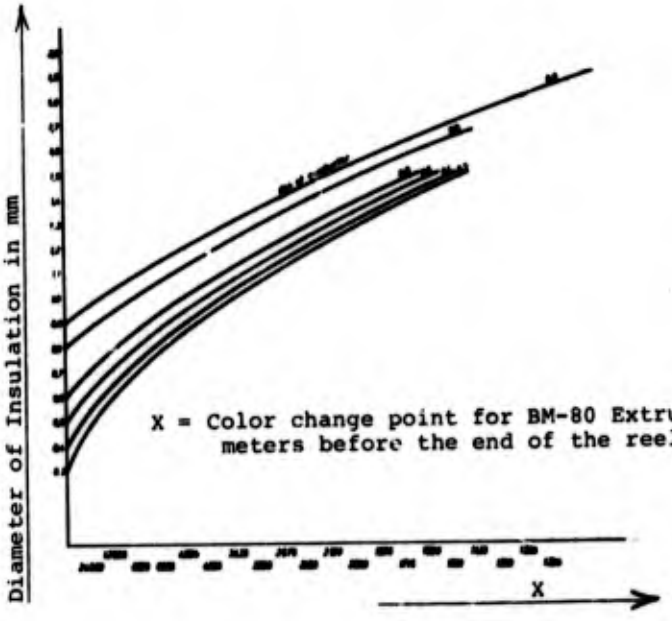

10. Color Change Table

PROGRAMM

MAILLEFER

Wire Cu/Al * ø mm
Quality
Over isulation ø mm
Capacity pF/m
Length of wire/reel m

Tolerance ± mm
of elongation max. %
Tolerance ± mm
Tolerance ± pF/m
Total length to be produced

Max. elongation % min. %
Material Type
Colour concentrate Type
m

Colour No.	reels to be produced	Colour No.	reels to be produced
Colour No.	" " " "	Colour No.	" " " "
Colour No.	" " " "	Colour No.	" " " "
Colour No.	" " " "	Colour No.	" " " "
Colour No.	" " " "	Colour No.	" " " "
Colour No.	" " " "	Colour No.	" " " "
Colour No.	" " " "	Colour No.	" " " "

Temperature		Alarm Temp.	
Zone 1	°C	±	°C
Zone 2	°C	±	°C
Zone 3	°C	±	°C
Zone 4	°C	±	°C
Head	°C	±	°C

Start operation level	%
Line stabilisation at	%
Stabilisation time	seconds
Time before control on	sec.
Pre-heater temperature	°C

Quality control*
Type of control
Capacity
Diameter
Insulation
Elongation

Production speed	m/min.
Entry capstan speed	%
Screw speed	r.p.m
Traverse (average)	mm

Servo-control system*
Cap./telescopic trough
Cap./screw speed
ø /screw speed

Tension on dancer*
1,4 Kp/cm2
1,8 Kp/cm2
2,5 Kp/cm2
3,2 Kp/cm2

* Mark where applicable

11. SECAP - Production Data Sheet

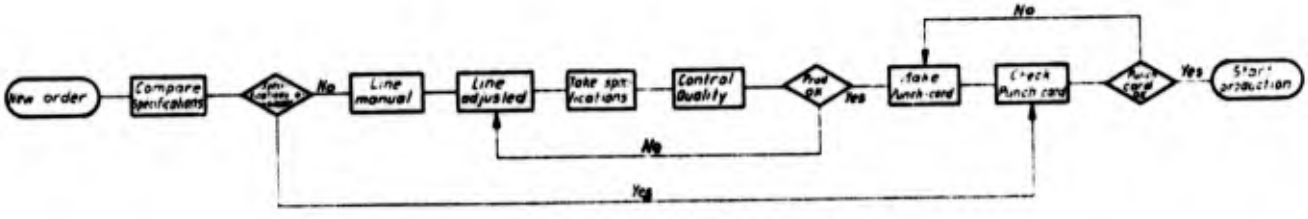

12. Order Processing and Punch Card Generation

6. Determination of Production Data

The production parameters for a particular wire are detemined by means of a one time experimantal run. The data is then recorded on a puch card which later serves to repeat the production run. The values as indicated in Fig. No. 11 are determined and recorded.

Obviously in order to determine this data a knowledge of and considerable experience with extrusion operations is required.

The data is then analyzed and processed as shown in Fig. No. 12.

When a new order is received it is necessary to find out whether this operation has already been performed. If this job has already been run then a punch card with the required data is sent to the supervision of the production department who use this card to set up the machine to run it.

With the aid of the punch card reader which is incorporated in the extrusion line control cabinet it is possible to check the value of various parameters of the wire which is being produced against the desired value as indicated on the control punch card. See Fig. No. 12.

A Start point of the line

B Start point of the Extruder (DBA)

C Stabilisation at speed V1

D Point of synchronised acceleration (DEC)

E Production level V1 + V2

F Start of production

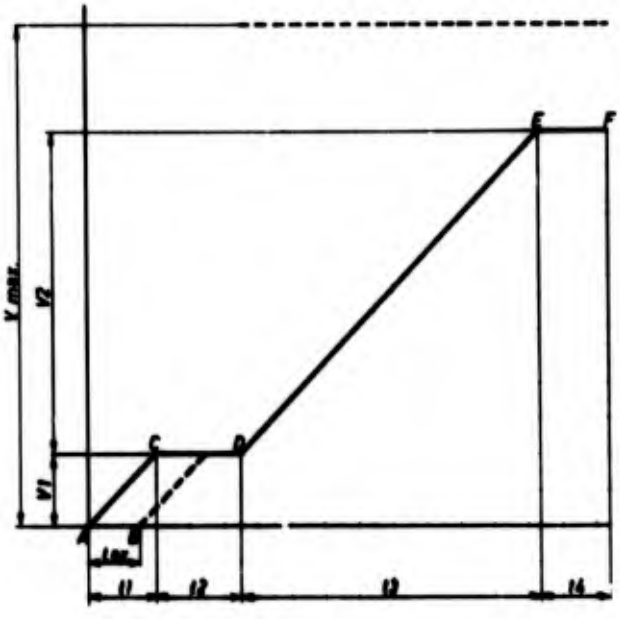

13. Line Start-Up Program

The machine operator receives together with his production order a punch card which is used to control the process. He mearly inserts this card into the machine selects the number of reels to be run and then performs certain manual functions such as loading the reels, the compound, the conductor and inserting the proper tooling into the extrusion head. The machine will then do nothing until the proper extruder temperatures have been reached. At that time a signal lamp lights and the operator can push the ON button to start the operation.

There exist a number of ways to bring the line up to production speed one of these methods is shown in Fig. No. 13. This process can be optimized to eliminate as much as possible the production of scrap.

The points B, C, D, E, and F can be located to suit the particular process depending upon the conductor and the insulating compound used.

As outlined above the control system incorporates enough flexibility to allow the production to be varied and to make it possible to accept a practically infinite variety of production programs.

Because of the number of inline cotrols in the system which constantly monitor the quality of the wire it is possible to limit the final quality control of the wire to statistical checks. This of course is based on the assumption that the raw materials entering into the process meet all required specifications.

7. Maintainance

All the major components of the system are plug in type units for ease in maintainance as shown in Fig. No. 15.

Therefor in case of a malfunction of the system it is easy to interchange the units. Beyon this there exists a logic diagram for the complete installation which allows the operator or the maintainance man to quickly determine in which unit the problem lies.

Some of the modules are also equipped with trouble lights which indicate when there is a malfunction in the module or when the program is not correct.

8. Expansion Possibilities

This whole system is computer compatible and isofar as the SECAP system is not used as a closed loop system the information can be fed into a computer which can supervise a number of extrusion lines.

It is also possible to cetralize the critical components in an air-conditioned room for supervision of the whole manufacturing program.

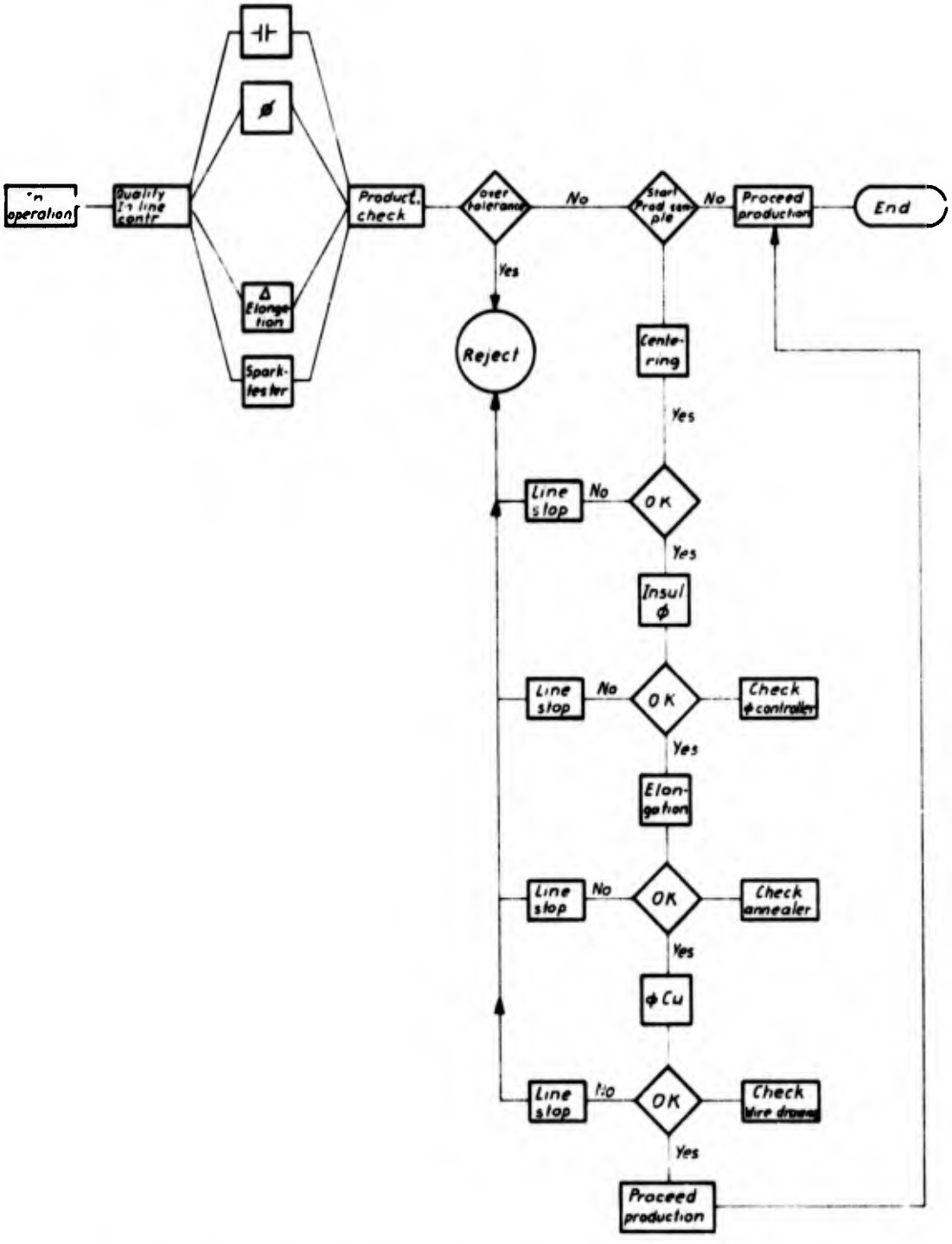

14. Process Control and Statistical Quality Control, Logic Diagram

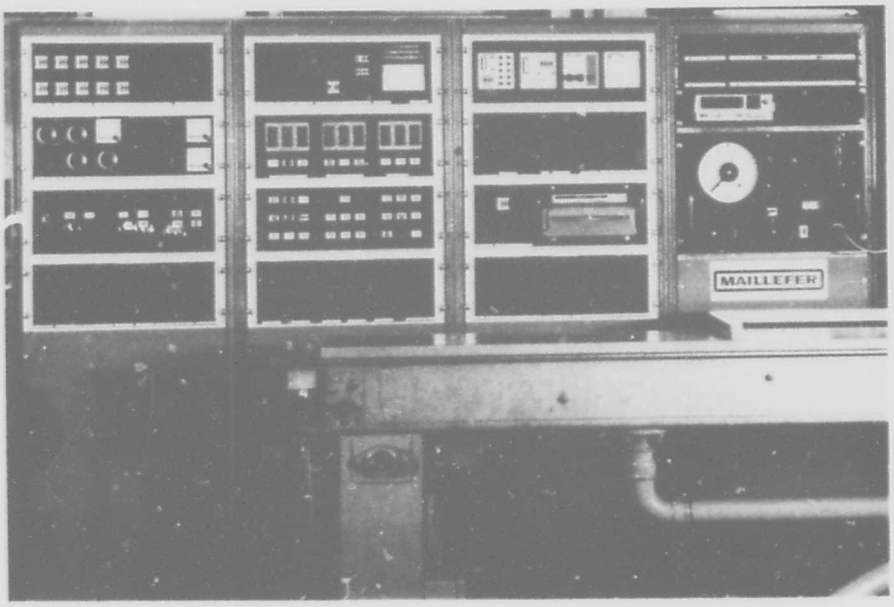

15. SECAP Control Panel

REFERENCES:

1. Beschicken von Kunststoffverarbeitungs-maschinen, O. Brandaner VDI Berichte No. 169, 1971.

2. Equipment Suppliers, Do Thev Know Their Products, R. R. Yeoman, Wire Journal, February 1974.

3. Betriebliche Ausbildung in der Kunststoffindustrie, Probleme und Losungsmoglichkiten u. Porath Berichte zum 7. Kunststofftechnischen Kolloquium 20.- 21.3.1974, Aachen.

4. Aufdecken von Rationalisierungs-reserven durch gezielte Schwachstellenanalyse, 7. Kunststofftechnischen Kolloquium, 20. - 21.3.74 Aachen.

5. Recent Developments in High Speed Insulation of Quality Telephone Wires, by E. Kertscher 22nd I W C Symposium, 1973.

6. Wire Manufacturing Testing and Control by A. E. Hartmann, Wire Journal, March 1974, pp. 65-72.

E. Kertscher
MAILLEFER, S. A.
Route du Bois
CH-1024
Ecublens-Lausanne
Switzerland

Eberhard Kertscher was born in 1939 and in 1962 was graduated from the Staatlische Fachschule fur Betriebstechnik in Stuttgart, Germany.

He was active at Lanza, S. A. in Basel, Switzerland as a Process Engineer and later as Plant Engineer.

In 1968 he was invited to join MAILLEFER, S. A. where he worked in their process development department. He has been responsible for the development of the MAILLEFER high speed extrusion system for telephone wires.

At the present time he is engaged in the marketing of advanced extrusion systems.

ULTRASONIC JACKET THICKNESS AND ECCENTRICITY MONITOR AND CONTROL SYSTEMS

BY

L. M. Boggs
Western Electric Co.
Norcross, Georgia

A. M. Isley
Western Electric Co.
Phoenix, Arizona

J. W. Levengood
Western Electric Co.
Norcross, Georgia

INTRODUCTION

Background

Most designs of multipair communication cable contain at least one jacket of polyethylene. In some cases, more than one polyethylene jacket is required. Providing a process to apply these jackets uniformly has long been a goal of the Western Electric Company.

The jacketing process involves passing a multipair conductor core through an extruder where a cylindrical tube of polyethylene is applied. It is desirable to maintain uniform thickness of the polyethylene jacket around the cable and along the cable length. Accomplishing this involves both the extrusion process and techniques for monitoring and controlling the cable jacket thickness.

Difference in opposite wall thicknesses is referred to as eccentricity and is stated as a percent of desired nominal thickness. Major adjustment of eccentricity is accomplished by lateral and vertical positioning of a movable die about a fixed core tube in the extruder. Smaller variations in eccentricity occur because of out-of-round core and the position of the core in the core tube.

Jacket thickness uniformity along the cable is determined by the ratio of line and extruder speeds. Conventional control systems maintain this ratio once it is set by the operator. Pertubations of either the line or screw speeds separately cause jacket thickness variations.

Potential Jacketing Improvements

The most desirable cable jacket is one that has zero eccentricity and sufficient thickness to protect the cable core. Such a jacket would have minimum cost (material usage) and the cable would be easy to handle and splice. We have previously applied excessive jacket material in some areas to assure adequate thickness of the overall jacket because of difficulty in achieving low eccentricity. Poor response of the eccentricity measurement has been a primary cause of difficulty. Measurement equipment was located near the take-up reel, typically about 90 feet from the extruder. Precise adjustment of eccentricity was precluded by the 1 1/2 to 3 minute delay between crosshead adjustment and measurement of the effect.

Systems that were used to measure jacket thickness and eccentricity mechanically "scanned" around the cable. One scan cycle would require more than one minute of additional waiting time. Furthermore, most cables twist in the cooling trough so that orientation of the cable changes between the point of adjustment and the measurement location.

A separate difficulty in achieving good eccentricity has been in positioning the die at the extruder. A large wrench and much muscle has been required with poor incremental control. These factors combined to make a 35 percent eccentricity seem good.

Developments Needed

In order to improve eccentricity, the first step was to develop a sensor that could be located near the extruder to measure jacket thickness at four locations simultaneously around the cable. Several techniques were investigated and success was achieved with a pulse echo ultrasonic approach. With non-contacting probes located within 18" of where the cable enters the cooling trough, the Ultrasonic Jacket Thickness and Eccentricity Test Set senses a change in eccentricity a few seconds after an adjustment is made at the crosshead.

A second development was required to facilitate easy adjustment of eccentricity. Western Electric's Phoenix Works developed an electrically positioned adjustable core tube and Eccentricity Controller. The controller automatically changes the eccentricity of the extrudate to make opposite wall thickness equal based on eccentricity signals from the test set.

After the jacket thickness sensor and eccentricity controllers were operational, we were in a position to achieve further savings in jacket materials by automatically controlling thickness. A Jacket Thickness Controller was developed to adjust the ratio of line and extruder speeds to maintain the desired average jacket thickness.

Figure 1 shows the Ultrasonic Jacket Thickness and Eccentricity Test Set, Eccentricity Controller, and Jacket Thickness Controller as they exist on a jacketing line. All three systems work together to improve jacket quality and to conserve jacket material.

JACKET THICKNESS TEST SET

Desired operating characteristics of a jacket thickness sensor are: operation near the extruder, noncontacting on the cable surface, measure both inner and outer polyethylene jackets, and produce outputs of thickness and eccentricity suitable for automatic control. After considering several different sensing techniques, ultrasonics was chosen for intensive investigation.

Ultrasonic Principle

Figure 2 shows the functional arrangement for the ultrasonic pulse-echo measurement approach. Only one of four measurement channels is shown. Water of the cooling trough serves as the coupling medium for

transmitting the ultrasonic energy to the cable jacket. Operation consists of pulsing an ultrasonic crystal, which transmits a "ringing" signal through water to the cable jacket. Part of the signal reflects off the outer surface of the jacket and returns to the crystal, which then operates as a detector. A second reflection, or echo, occurs off the inner surface of the jacket and arrives back at the crystal after the outer surface reflection by a time difference that relates to thickness of the cable jacket. These echo signals are then processed to produce a measure of jacket thickness.

The amount of processing to obtain thickness depends on the uniformity and stability of sound velocity in polyethylene for different extrudate temperatures and jacketing line conditions. Empirical data based on a large assortment of cable samples indicated a sufficiently constant sound velocity to scale echo separation time directly into jacket thickness for all cable sizes.

Test Set Operation

Referring to Figure 2, the Receiver Amplifier provides 40 to 60 db of gain with a bandwidth of over 30 megahertz. This provides echoes in the volt range for the Receiver Logic circuit which then produces a pulse width corresponding to echo separation time. The Interval Counter quantizes the echo separation with a resolution of $\pm$ 10 ns (about $\pm$ .2 mil). The counter output is a 10 bit binary number to indicate thickness and the number is stored in a Buffer between successive measurements. A Digital-to-Analog Converter then produces an analog thickness output.

Achieving an operational jacket thickness measurement system was made through progress in areas such as ultrasonic crystals, electronics, and polyethylene sound properties.

Ultrasonic Crystals

The crystals are excited by a voltage impulse, which causes cyclical mechanical stresses in the crystal material. These stresses generate high frequency pressure gradients or waves in the water coupling medium. The pressure waves, varying in intensity as a damped sinusoid, propagage to the cable jacket surface where a reflection occurs due to acoustical impedance mismatch. This generates the outer surface echo. Part of the wave travels into the cable jacket, and a second reflection occurs at the inner surface of the jacket. This determines the second, or inner surface, echo.

There are two essential points to consider when selecting a crystal for cable jacket measurement -- one is electrical and the other is physical. The electrical constraint is the impulse response "ringing" time of the crystal which determines the minimum thickness that can be measured. Since the crystals tend to ring for a fixed number of cycles, crystal frequency must be 5 to 10 megahertz in order to have a first echo of about .5us or less duration. This corresponds to about 10 mils of polyethylene jacket thickness.

The primary physical constraint is that the crystal must tolerate normal cable motion without loss of signal. After experimentation with different crystal designs, a 1 1/2 inch wide unit was used across the cable to tolerate up to $\pm$ .75" lateral and vertical cable motion. To maintain signal quality, uniformity in crystal sensitivity over this 1 1/2" width must be achieved.

Electronics

Early electronics development concentrated on the Pulser and Receiver Amplifier circuits. High voltage pulsers were used to evaluate insensitive crystals. Also, a wide band width, high gain, low noise receiver amplifier was required. Later improvements in crystal sensitivity reduced these requirements somewhat.

The novel electronic developments were incorporated in the Receiver Logic function. This circuit receives the echo signals as input and produces a pulse whose width corresponds to echo separation. The leading edge of the first echo signal, through threshold detection, determines the beginning of a pulse whose width is determined by the leading edge of the second echo. This circuit also examines characteristics of the first and second echoes and produces an Active Signal pulse for each valid measurement. Because of occasional noise pick-up or poor crystal/cable alignment, excessive errors were made until this "intelligence" was added. In case an Active Signal pulse is not generated during a measurement cycle, the last previous good measurement is retained in the Buffer. The Active Signal is also an enable for both the eccentricity and thickness controllers.

It should be noted that the echo characteristics tested by the Receiver Logic are presently calibrated for hot polyethylene jackets and the crystals that Western Electric uses. Cold polyethylene, other jacketing materials, or different crystals yield considerable different echo patterns.

Polyethylene Sound Properties

Two sound properties of polyethylene, acoustical impedance and propagation velocity, are particularly important. Both depend on temperature and had not been previously investigated for extrudate temperatures. Also, both could be calculated from more fundamental material properties, but these properties are also unknown for extrudate temperatures.

Acoustical impedance is important because it affects the strength of the echoes and the penetration of the ultrasonic energy into the polyethylene. The first echo reflection depends on the difference in acoustical impedance between water and the extrudate. The ultrasonic energy not reflected propagates toward the inner surface of the extrudate. There a second reflection occurs. This second echo is sufficiently strong when polyethylene interfaces with either air, metal, flooding material or core wrap. Since the acoustical impedance mismatch between polyethylene and water is low, the second reflection easily escapes the jacket and propagates to the crystal.

Propagation velocity of sound in polyethylene affects directly the echo separation time and recorded thickness. Extensive on-line tests were conducted to determine the effects of jacket cooling on the propagation velocity and the most desirable location for the probes. Echo separation times were recorded at one- and two-foot intervals along the cooling troughs of several different jacketing lines. Increases in propagation velocity of 100 percent from hot to cold conditions were generally prevalent. By measuring samples of jacket thickness and comparing the data to corresponding chart recordings, the most stable propagation velocity was found to occur near the extruder. We could not detect a difference in propagation velocity for different cable types at

the entrance of the cooling trough over the normal extrudate temperature range. However, if line speed were reduced below 20 feet per minute, a significant increase in propagation velocity would occur due to jacket cooling and cause the test set to indicate a thinner than actual jacket. This could be corrected in the test set by recalibrating for the lower speed if desired.

Performance

The ultrasonic test set meets all of the desired operating characteristics mentioned previously. Measurements of jacket thickness are made at a 500 Hz rate on each ultrasonic probe in a top, right, bottom, left sequence. Orthogonal pairs of thickness measurements are subtracted to yield top/bottom and left/right eccentricity signals for automatic eccentricity control. The four thickness and two eccentricity outputs are displayed continuously on the front of the test set. Also, thickness and eccentricity data are on a linear chart paper so that interpretation is direct. This allows operating and quality assurance personnel to readily monitor the jacket quality. Furthermore, the quick response of the test set has permitted analysis of the jacketing lines to locate the causes of jacket thickness fluctuations.

ECCENTRICITY CONTROLLER

While the ultrasonic test set was being designed, development work was also concentrated on a method to automatically control the eccentricity of the plastic jacket. A device was developed that physically moves the tip of a guider tube within the extruder die. In this way, the flow of plastic material being extruded onto the cable core is controlled. Through the operation of an Eccentricity Controller, stepping motors position the guider tube in the lateral and vertical directions. Signals from the ultrasonic test set are used by the controller to determine when and in which direction the guider tube should be moved to correct the eccentric jacket.

Controller Design

The Eccentricity Controller was designed around the premise that trying to control to perfect concentricity was unrealistic. Acceptable levels of eccentricity were determined and limits were set. If the controller detects an out of limit condition, for example in the vertical plane, the motor which moves the guider tube in that plane in gated on with the direction of rotation determined by the controller. The motor is allowed to run for a maximum predetermined amount of time and then gated off. The results of the guider tube movement do not show an immediate change of eccentricity on the ultrasonic test set. There are two reasons for this delay: (1) the plastic takes time to readjust to the new flow pattern, and (2) there is a physical separation between the sensing devices (ultrasonic crystals) and the tip of the guider tube. After the motor is gated off, the controller waits for another predetermined amount of time before an additional change can be made. If the eccentricity of the plastic being extruded onto the cable after this off-time is still out of limit, the above mentioned cycle repeats. The same adjusting procedure as stated in the vertical plane is also used in the horizontal plane.

Controller Operation

The front panel of the controller is shown in Figure 1. Two modes of operation are manual and automatic. In manual mode, the controller responds to direction from the joy stick to change eccentricity without feedback. In automatic mode the joy stick is disabled from eccentricity control and signals from the ultrasonic test set are in command.

The controller uses six signals from the ultrasonic test set. Two are percent eccentricity signals and the remaining four are the active Signal verification pulses. Top/bottom percent eccentricity is given by the following equation:

$$\% \text{ Ecc.} = \frac{(T - B)}{NOM} 100$$

where T = top plastic thickness in mils,

B = bottom plastic thickness in mils,

and NOM = desired thickness in mils.

In a similar manner, left/right percent eccentricity is developed. With these two eccentricity signals, the controller determines if an out-of-limit eccentricity condition exists and in which direction the guider tube should move to bring the eccentricity back within limits. The limits are adjustable so that different operating conditions of a particular jacketing line can be taken into account. For example, if the core is very irregular due to small diameter variations in a particular plane, the most optimum limits are ± 10 percent. If the core is regular, as in a small diameter cable, the limits can be set for automatic operation of ± 5 percent. If the limits are too low, the controller will oscillate the eccentricity between the limits.

The four verification signals originating in the ultrasonic test set are indicators that the thickness data coming from a particular test set channel is correct. The eccentricity controller monitors these four signals and if any one of the two for a particular plane is missing, either vertical or horizontal, the appropriate eccentricity adjustment motor is kept off. As an example, if the bottom Active Signal is missing, the eccentricity controller detects this and gates off the motor which drives the guider tube in the vertical plane. The vertical drive motor is kept off as long as the Active Signal from the bottom is missing. Since only the bottom verification signal is missing, the eccentricity controller still controls in the horizontal plane.

Status

The Eccentricity Controller is in operation at six Western Electric Wire and Cable locations. Expected savings have been obtained in achieving uniform jacket thickness around the cable. Furthermore, start-up time and operator attention to the jacketing line have been significantly reduced.

JACKET THICKNESS CONTROLLER

The thickness of a polyethylene sheath placed on a cable depends upon the speed of the cable moving through the jacketing line and the rate at which the polyethylene is supplied from the extruder. Thickness may be controlled by changing either the line speed or extruder speed. A Jacket Thickness Controller has been designed to accept the measure of thickness produced by the ultrasonic test set and adjust the ratio of line speed to extruder speed to effect the desired thickness control.

Figure 1 presents a photograph of the controller front panel. Presently this controller is being installed on all applicable Western Electric jacketing lines.

SUMMARY

New cable jacketing equipment which monitors and controls jacket thickness and eccentricity has been developed. Improved quality of the jacket has been achieved while reducing the jacket material used. Furthermore, the better process control has permitted the specified cable jacket thickness to be reduced thus allowing additional material savings. Automatic operation of the quipment has reduced operator attention to the jacketing process, and eliminated difficult start-up procedures.

ACKNOWLEDGEMENTS

The authors wish to acknowledge the assistance and support of all Western Electric Wire and Cable locations. Numerous individuals have contributed to the accomplishments that were identified. Particular recognition is given to Messrs. J. A. Hudson and H. J. Flichman of the Atlanta Works for major design and development contributions.

Arthur M. Isley, Jr., a Development Engineer with Western Electric Company at the Phoenix Works, was graduated from North Dakota State University in 1971 with a Bachelor of Science degree in Electrical Engineering. In 1971 he joined Western Electric Company and is presently engaged in the design and development of process control systems related to cable manufacturing.

L. M. Boggs is a Senior Development Engineer with the Western Electric Product Engineering Control Center at Norcross, Georgia. He received a B.S. in EE from Clemson University in 1963 and an M.S. in EE from Georgia Tech in 1965. He joined Western Electric in 1971 after 8 years with the Lockheed Georgia Research Laboratory. Current responsibilities include project direction for developing new instrumentation and control systems for manufacturing and testing wire and cable products.

J. W. Levengood is a Senior Development Engineer with the Western Electric Product Engineering Control Center at Norcross, Georgia. He received a B.S. in Electrical Engineering from the University of Florida in 1959 and an M.S. in Electrical Engineering from New York University in 1961. He joined Western Electric in 1970 after eleven years with the Bell Telephone Laboratories. Current responsibilities include project direction for development of new instrumentation and control systems for manufacturing and testing wire and cable products.

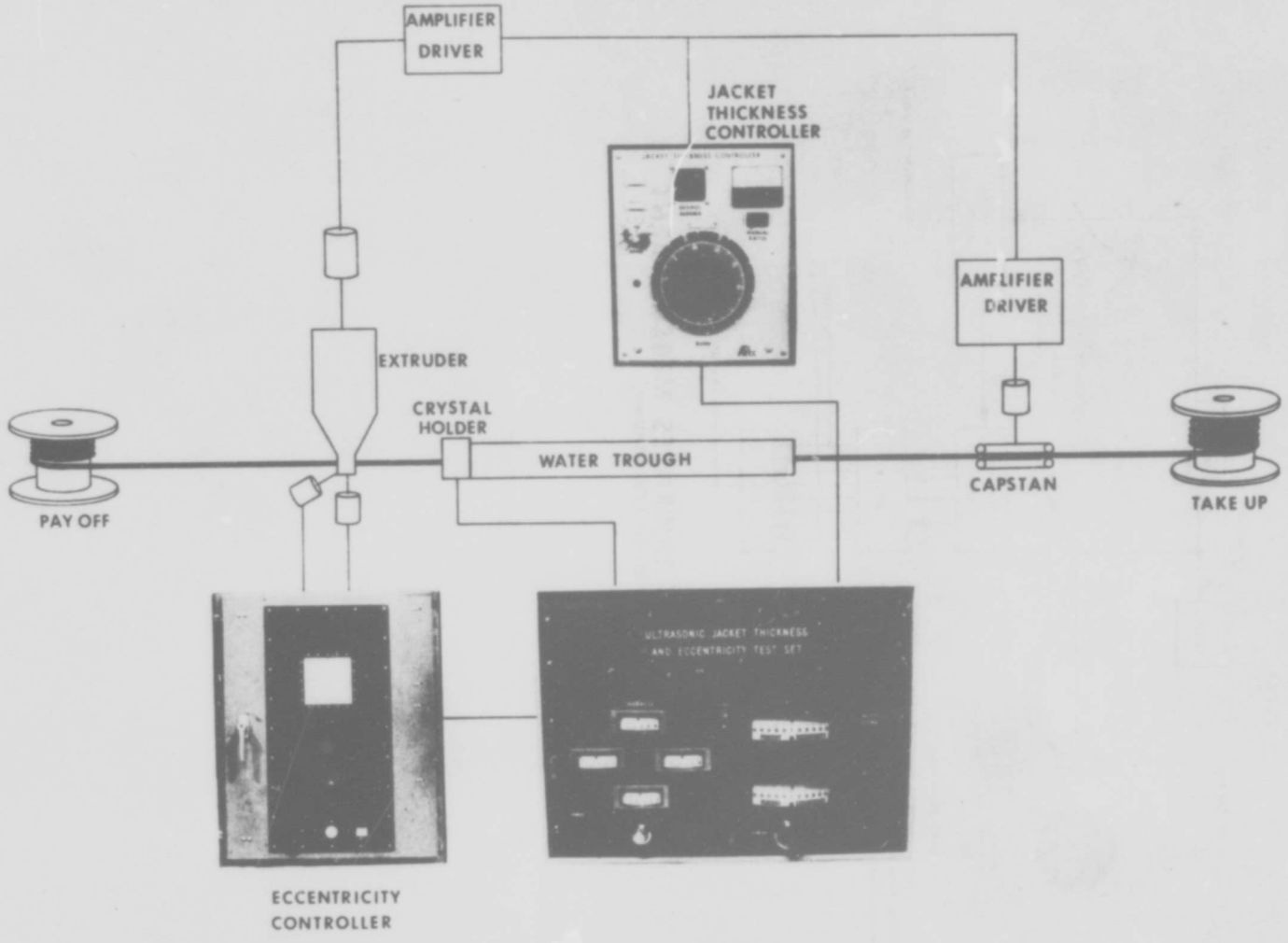

FIGURE 1 JACKET THICKNESS MONITOR AND CONTROL SYSTEMS

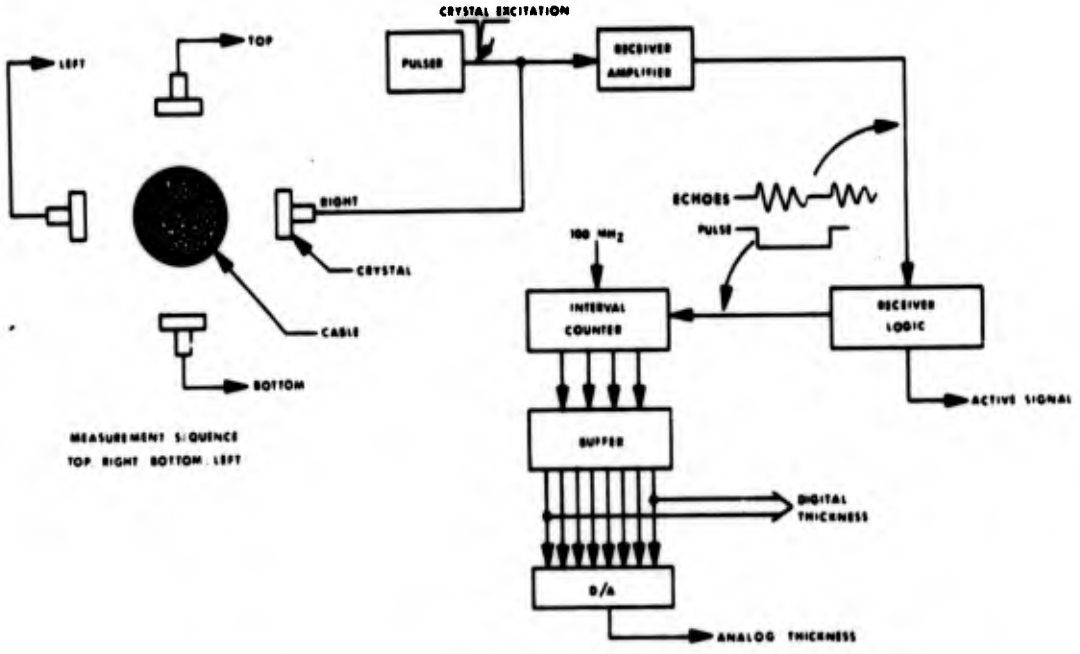

FIGURE 2 JACKET THICKNESS MEASUREMENT
(ONE CHANNEL OF FOUR SHOWN)

TECHNIQUES IN MANAGING A TELEPHONE TRUNK CABLE NETWORK TO PROVIDE ECONOMICAL, DEPENDABLE SERVICE

by

J. M. Robertson
Rochester Telephone Corporation
109 South Union Street
Rochester, New York 14607

SUMMARY

The objective of this paper is to demonstrate the importance of the management and administration of a typical telephone cable network, in completing the mission of the design, engineering, manufacturing and installation personnel by furnishing superior telephone service to the public. The industry should be commended for the technical advances and accomplishments achieved in the telecommunications field over the years. In local line plant, for instance, the advent of PIC (polyethylene insulated conductor) cables, color coded, laid up in binder groups and designed for ready access terminals could be regarded as the most notable advance of the 1960s and has enabled very effective utilization of distribution cables compared to the old fixed count terminal method.

TRUNK NETWORK

It is proposed however, not to dwell on the many complexities of outside plant local distribution, but to describe in some detail the telephone trunk cable plant of the Metropolitan and Suburban areas of the Rochester (N.Y.) Telephone Corporation. The present cable network comprises cables placed in 1899, having textile insulated conductors and with lead sheath up to the latest 1974 products of pulp insulated, Stalpeth sheathed unit type cables with interstitial pairs. During the years between, many different types of cable have been installed, fortunately all working together compatibly - by design.

In the network to be described, there are 92 physical routes of all gauges up to 19, or 20 lb/mile loaded and non-loaded complements with many cable carrier installations ranging from N toll grade and short haul analog to PCM types. Excluding three microwave systems, this trunk network presently supports the following statistics shown in Figure 1.

	Physical Conductors	Carrier Channels
Total Facilities	38,324	4,528
Traffic Circuits Working	16,647	3,452
Special Services Working	14,518	575
Defectives	2,565	-
Spares	4,594	501

These trunks serve a base of 310,000 Main Stations in a 2500 square mile area, to give a frame of reference of the ratio of lines to trunks.

The actual administration and assignment of the available facilities in the trunk network is performed by a supervisory clerk operating a Computer Consoles machine employing disk storage devices and video terminals. Print-out facilities are available for work operations or study purposes and statistical data may be readily extracted from the record.

CONTINUITY OF SERVICE

It is in the selection of routing patterns, judicious assignment of facilities and application of protective measures that the trunk network is rendered more reliable than if routine assignment procedures were practiced.

Continuity of service is the primary consideration in any telephone network and a very high standard has come to be expected by the public in the North American continent. None can predict the moment, however, when emergency or catastrophe might render the availability of a telephone as a service of the utmost importance. In the Direct Distance Dialling trunk hierarchy many alternate routes have been provided but it is in the local Toll areas that more can be done in utilizing existing plant to attain a greater degree of security and reliability.

Telephone service interruptions in urban areas, other than those involving individual subscribers, invariably may be attributed to cable damage by domestic services contractors, highway reconstruction operations, corrosion, electrolysis, lightning strokes, power contacts or other hazards. While damage to subscriber distribution cables can result in considerable inconvenience to customers in a specific area, the interruption of service in a trunk cable affects all of the subscribers calling beyond the local switching machine. Consequently our main concern must be for those cable sheaths in which are routed the interoffice, toll connecting and other high grade circuits linking the particular Central Offices and the outside world.

TYPICAL ROUTING

In the typical urban area shown in Figure 2, the main Toll Center is surrounded by switching centers contained within a single exchange area. The trunk network will comprise

a variety of Traffic circuits; large groups of direct inter-office or high usage trunks between adjacent Central Offices having high community of interest; smaller groups of inter-office trunks between distant Central Offices may route via intermediate Main Distribution Frames; various types of Toll Connecting trunks with which we are particularly concerned, will usually occupy separate sheaths from the high usage inter-office trunks. Included in the Toll Connect category of trunks are two directions of inter-local overflow trunks switched at a local tandem machine to serve as a secondary route to the directly connected inter-office trunks in normal circumstances and as primary service in the event of disruption of the high-usage trunk routes. See Diagram No. 3.

PROTECTIVE MEASURES

It is proposed now to describe the procedures and practices which have been developed in an effort to prevent cable damage or at least minimize the effect on telephone service in the event of interruption of a trunk cable.

STAKE OUT

The first precautionary measure is directed at the hazard of dig-up by contractors, by making available a common reporting center operated by the "Utilities Coordinating Committee" which serves all utilities, city and county agencies. This center, manned 24 hours, receives calls from contractors proposing to excavate on highway or private property and by means of teletype all participating agencies in the scheme are alerted. Each utility arranges for stake-out at the appropriate time and place if their plant is involved or in the vicinity of the contractors' operations. The prompt attention given by the utilities to these requests for location and stake out of services since inception of the program, has encouraged contractors to rely upon the system and has facilitated their construction activity with the assurance of the presence or absence of power, telephone, gas, water etc. services. The Tele number for "Dig-up Alert", as the service is entitled, is well publicized in all Media and is contained in the preface to the telephone directory. Emphasis on this joint effort, which has already reduced incidence of cable interruptions, will impart a greater security to the underground plant of all services.

AIR PRESSURIZATION

A second scheme for the protection of the trunk cable network utilizes a system of continuous flow dry air equipment available in every Central Office cable vault since 1957. Each machine applies dry air at 40°F and 10 lbs./square inch pressure to all cables, subscriber feeder or trunk, to prevent the ingress of moisture in the event of a sheath break. In trunk cables, pressure contactors set to operate at one pound less than the pressure measured at the location, are installed in convenient manholes at approximately 12,000 feet intervals and connected to dedicated alarm pairs within a trunk complement. These alarm pairs are connected in series with alarm pairs in other trunk cables in such a manner that loops are formed from a centralized test center where the loops terminate on "in" and "out" jacks as shown in the Sketch No. 4. A contactor, reacting to a loss in air pressure because of a sheath puncture or break, places a short on the alarm pair to display the operated condition at the maintenance center. Precise testing of the loop resistance by means of a Wheatstone Bridge to the activated contactor, both from the "in" and the "out" jack, if necessary, will define the manhole or splice location of the fault by reference to pre-recorded values of loop resistance measured at the time of installation of the contactor. If a resistance measurement is obtained on one jack and an open circuit reading on the other, it can be assumed that loss in pressure has been caused by a cable disruption in one leg of the loop.

The system of looping alarm pairs up to the 10,000 ohms supervision limit of the equipment is most economical in alarm circuitry and has enabled the whole Metropolitan Trunk Network to be monitored from one location at the downtown main emergency center with a single 30 jack installation test board. Alarm pairs are invariably jumpered straight at intermediate Central Office MDFs, but these points are, of course, readily available and accessible for confirmation of test resistance measurements if the bothway loop around test proves to be suspect for some reason.

The Plant Operating Practice specifies that the contactor trouble report be investigated and cleared in four hours by cable repair personnel. The practice also provides for alarm loop continuity tests on a weekly routine basis and it will be readily seen that a shorting plug in jack number one will activate the alarm for loop number one if alarm pair continuity exists.

METROPOLITAN DIVERSE ROUTING

The third method of protecting the trunk network and at least assuring a measure of continuity of service, with an accepted degradation of grade of service, is entitled "Diverse Trunk Routing". The procedure really consists of good bookkeeping practices and judicious assignment of facilities and equipment.

The development of an interoffice trunk network in most urban areas will be found to follow a growth pattern whose incremental nature of provision at engineering economic intervals lends itself to diverse routing. The nature of the growth and the gradual expansion of the cable plant may obscure this fact and unless an overall fundamental plan is evolved, many opportunities for providing diverse routing and obtaining the consequential security of service may be overlooked.

The first step in arranging, or perhaps "re-arranging" is more appropriate, the trunk

facilities is to classify those Toll Connecting Type trunks and inter-local overflow trunks to which diversity should be accorded. These are the trunks which provide access to and from the outside world, either directly dialed or operator assisted, via the DDD Network together with the overflow trunks which serve as back-up to all of the local high usage trunk groups.

The next step requires examination of the various trunk complements with particular reference to geographic routing, separate cable sheaths, transmission loss if physical and if carrier, system availability to the home Toll Center. These trunk complements should then be graded for each Central Office as first choice, second and so on, preferably in order of reliability.

The procedure to be followed next is to ensure that each type of traffic circuit group is equitably assigned to the primary, secondary or other route up to the limits of facility availability. It is most desirable that the separate facility transmission losses should be closely matched, although adherence to standard design limits should ensure that no more than two db disparity occurs in circuits of similar category i.e. toll connecting trunks design conforms to Via Net Loss + 2.5 db maximum 4 db and direct interoffice trunks VNL + 5 db maximum 8 db.

The form shown in Figure 5, is representative of the record used to effectively control the assignment and display the distribution of the various circuits among the available transmission media. In the event of disruption of a route, the circuits remaining intact will be readily discernible.

What has been expected, and so far has been achieved, of the foregoing measures is that the loss of a trunk cable in the Metropolitan Network will neither result in dislocation of traffic flow nor complete isolation of a Central Office from the outside world. It is not intended that the Busy Hour grade of service - usually .01 probability - will obtain in these emergent circumstances but this is a small price to pay for continuity of service.

Constant surveillance must be exercised in maintaining diversity, once established, as rearrangements and changes in the trunk plant could very well undo a well thought out plan.

The principle of diversity need not be costly to implement but should be superimposed on the plan for provision of growth in trunking facilities.

SUBURBAN TRUNK NETWORK

The suburban trunk network poses a different problem, for the multiplicity of cable routes of the Metropolitan area does not prevail. The routes depicted in this Sketch No. 6, mostly carrier routes, mainly utilize cables 100 pair or less and because the growth rate is small there are seldom requirements for parallel cables. In these circumstances, the position is taken that a damaged color coded cable can be quickly restored by cable repair forces. Despite this approach, an opportunity to provide diversity will occasionally be presented and it is proposed to conclude this talk by describing a means of exploiting an existing network configuration by closing a ring at small cost, as shown in Sketch No. 7.

The various community dial offices are served by N analog carrier routes from the Toll Center in a clockwise pattern. The first cable route in a clockwise direction carries 18 carrier systems and with two more to be added in 1975, the carrier complement approaches exhaust.

Expansion of cable plant for subscriber service between the Toll Center and the first office in the counterclockwise direction, offered the means of establishing a ring main of trunk cable pairs as shown.

The next Diagram No. 8 demonstrates the proposed plan for the addition of carrier systems which will, in the ultimate, serve each CDO with cable carrier systems routing to the Toll Center over clockwise and counterclockwise routes.

The protection derived from this arrangement and the economy of plant and equipment achieved will be readily apparent from the sketch. The slow growth rate of toll circuits characteristic of these Community Dial Offices should ensure that this plan will provide for the development of the area for many years.

In conclusion, it is hoped that this description of Management of a large Independent Telephone Company's Trunk Network will serve as a guide to others in the industry seeking to provide the most reliable telephone service possible.

John M. Robertson
109 South Union Street
Rochester, New York 14607

Born in Ayrshire, Scotland in 1915, John M. Robertson attended Glasgow Royal Technical and Nottingham University Colleges. He received telecommunications training in the British Post Office and was employed in Engineering and Traffic Divisions in Glasgow and London from 1938 to 1953. He served in the Royal Corps of Signals during World War 2. Employed since 1955 with Rochester Telephone in various capacities, he is presently Engineering Manager-Trunk Facilities.

TRUNK FACILITIES DATA 1974

	Physical Conductors	Carrier Channels
Total Facilities	38,324	4,528
Traffic Circuits Working	16,647	3,452
Special Services Working	14,518	575
Defectives	2,565	-
Spares	4,594	501

$\frac{\text{Workers}}{\text{Total}} = \frac{31165}{38324} = 81.3\%$

$\frac{\text{Defectives}}{\text{Total}} = \frac{2565}{38324} = 6.7\%$

$\frac{\text{Spares}}{\text{Total}} = \frac{4594}{38324} = 12\%$

Figure 1

TANDEM SWITCHING

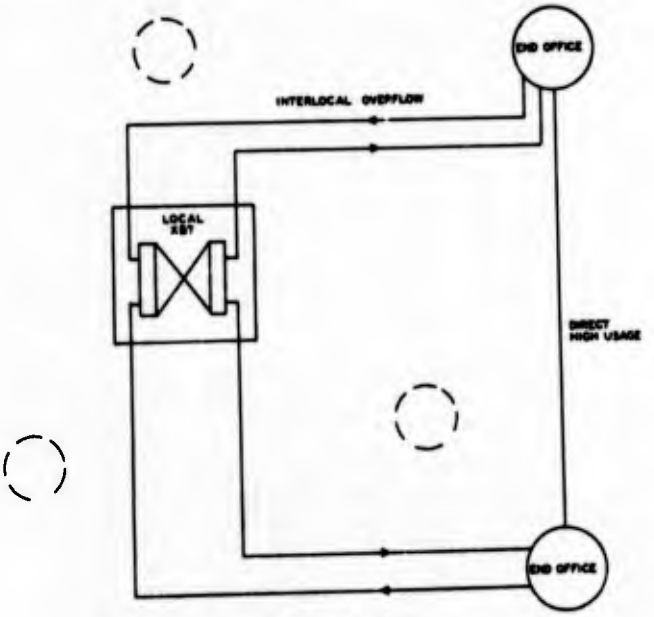

Figure 3

METROPOLITAN AREA
INTER OFFICE TRUNK ROUTES

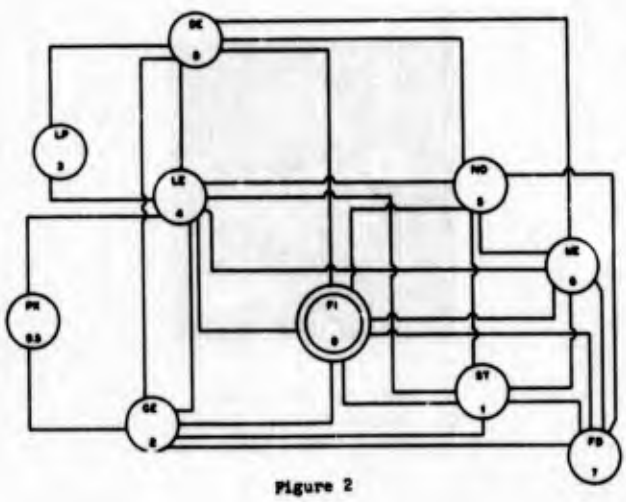

Figure 2

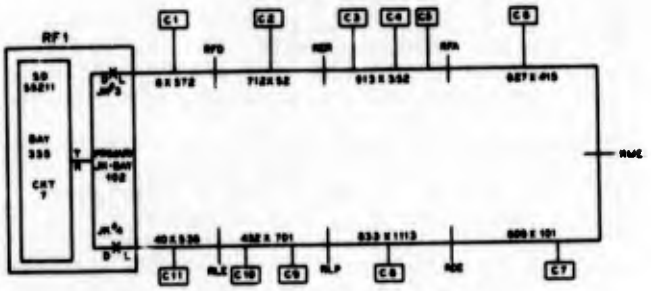

CON-TACTOR	RESIST. JACK#3	RESIST. JACK#4	CABLE-PSI	ALARM-PSI	CON-TACTOR	RESIST. JACK#3	RESIST. JACK#4	CABLE-PSI	ALARM-PSI
1	340	9250	5.15	4.1	7	5970	3660	7.5	6.5
2	947	8660	4.2	3.2	8	6640	2990	5.2	4.2
3	2400	7280	2.5	1.5	9	7800	1980		
4	3034	6556			10	8680	980	2.7	1.7
5	3581	6006	4.8	3.8	11	9380	199	3.7	2.7
6	4310	5303	3.85	2.8	12				

FOR # 2130-99 LOOP NO 2

CKT _____ OPERATION _____ CLASS _____
FOREIGN EXCH. TEL. NO. _____ PRIORITY _____
CUST. _____ CONTROL OFFICE _____
ADDRESS _____ TYPE SERVICE _____
SERVICE HOURS _____ CODE _____

Figure 4

ROCHESTER TELEPHONE - ENGINEERING DEPARTMENT

REPORT OF DIVERSE TRUNK ROUTING STATUS

TOLL CTR Rochester

ISSUE DATE 1-31-76

C.O.	DIVERSE CABLE ROUTES	CATEGORIES OF CIRCUITS TO & FROM TOLL CENTER: TOLL SWITCH	DDT SWITCHED: OUT	DDT SWITCHED: IN	"D": COIN	"D": MINCOM	"DX": MINCOM	"D" and "DX": COIN	"D" and "DX": MINCOM	DISTRIBUTION OF CCTS. PRIMARY, SECONDARY & OTHER	REMARKS
	50	36	37	39	3	5	7	5	20	150	
Avon	10				2	1	4	1	11	43	
	20	27	29	32						88	
	8	26	10		4					18	
Field	47	36	6	19		4	12	15	13	105	
	752	1	9	8			6		21	44	
	765	16	7		5	5	7	12	15	67	
	12	46	16	13	3	4	15	8	18	140	
Ingrams	42	31	13	16	2	4	9		20	105	
	283	42	28	20	1	8	5	8	10	122	
	49	15	11	27	1	7	12	1	18	156	
Varsbank	8	12		21				5	23	81	
	15	20	16		2	4	8		7	57	

Figure 5

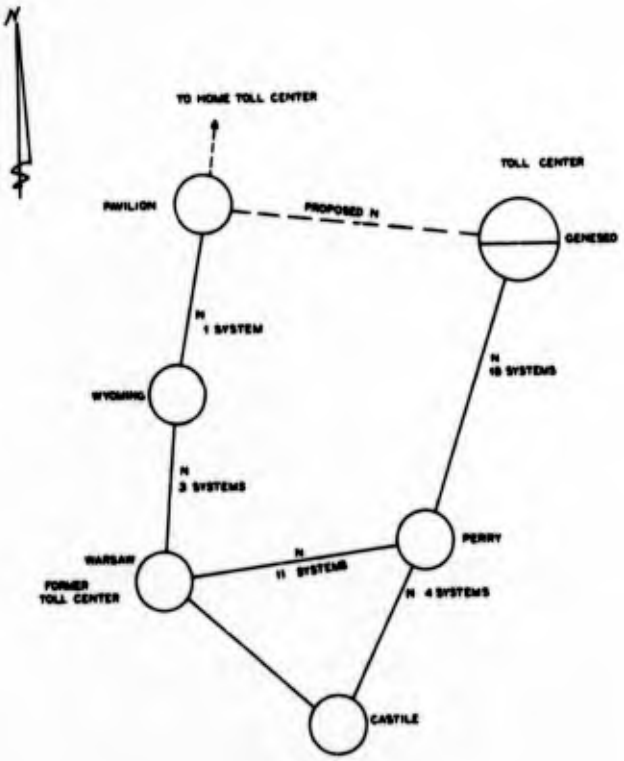

Figure 7

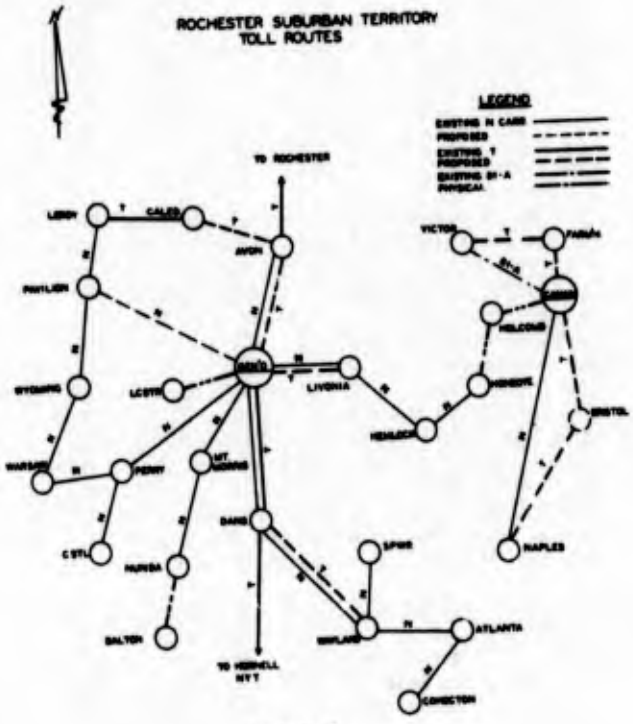

Figure 6

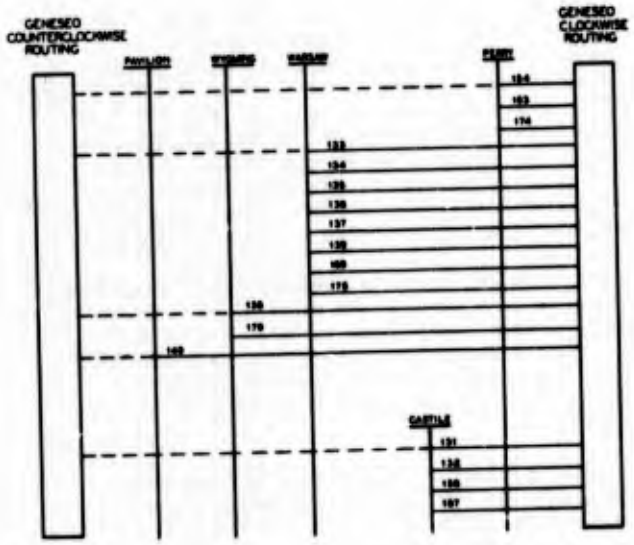

Figure 8

SIMULTANEOUS FIELD SPLICING AND TESTING

By Gary H. Knippelmier
Automation Products Company
Austin, Texas

ABSTRACT

Recent improvements in wire joining techniques have greatly increased efficiency. Concurrently, pressure has increased for quality with respect to cost and service. These factors have been the stimulus for improving the fault detection and correction techniques utilized in cable splicing. This paper will define the most common cable irregularities, determine a measuring parameter and its limitations, describe the physical measurement methods and detail an optimum technique for obtaining quality without sacrificing efficiency.

I. COMMON SPLICING AND CABLE FAULTS

The most common types of construction cable irregularities for new cable are opens, crosses, splits, shorts and grounds.

An open is obviously a non-continuous pair or wire in a pair. The majority of opens are located at the splice points and are due to craft error when splicing, although some opens are created during cable installation and others are caused by manufacturing process problems. Opens can be detected by measuring the mutual capacitance (Cm) and comparing it with a good pair or measuring wire to sheath capacitance and comparing it with a good reference.

A cross is defined as the metallic connection of one wire of a pair to another wire in a different pair. A schematic representation is shown in figure 1. Crosses are caused by cable damage or by excessive pair handling causing wire insulation to be removed. Comparison of the wire to sheath capacitance will detect a cross as well as measuring the Cm and comparing it to a reference.

Splits are defined as the metallic connection of one wire of a continuous pair to a wire of another continuous pair as shown in figure 2. Although this appears to be a rather difficult configuration to obtain, it is a common occurrence when enough wire is exposed during splicing to allow the pairs to become untwisted. Splits can only be detected by comparing the mutual capacitance with a reference. The only places where splits can occur are at connection points.

A short is defined as a metallic connection from one side of a pair to the other side. Shorts, like crosses, are caused by cable damage or insulation removal resulting from excessive pair handling. Shorts can be detected either by measuring continuity or by comparing Cm to a reference.

A metallic contact between one or both sides of a pair and the sheath is known as a ground. The primary cause of grounds are the same as for a short or cross. Detection is possible by measuring conductivity between the pair and sheath or again by comparing Cm.

A change in the mutual capacitance of the affected pair is common to all the irregularities that have been previously mentioned.

II. LIMITATION OF USING MUTUAL CAPACITANCE FOR THE MEASURING PARAMETER.

A three port artificial line was constructed in order to measure the effect of each type of irregularity with length. One section of the artificial line is shown in figure 3. Some cable on-reel specifications limit the mutual capacitance to 0.083 $\pm$ 0.006 uf/mile, which is a range of $\pm$ 7.2%. If this range is used to set the maximum acceptable Cm variation, the ability of a Cm measurement to detect each type of fault can be determined. Figure 4 shows the amount of faulted cable required to give a 7.2% change in the mutual capacitance for the irregularities that are length dependent. Figure 4 also points out that splits are essentially undetectable if they occur in the last 20% of a cable run.

Let us consider methods for making the actual physical measurement.

III. TESTING METHODS ON NEW CABLE

A. Testing from the mainframe out, as cable is being spliced, is probably the most common system in use today. The MDF is the only place where the pairs are easily accessible, and a number of test sets are available which can access the pairs via MDF shoes. The biggest disadvantage from the mainframe is that splits in the last 20% of the cable can not be detected consistently. Since the measurement point is fixed throughout the splicing operation, there is no way to design out the cable tolerance limitation. Also, since the testing is usually done after the splice is complete, re-entering the splice to make corrections is normally required.

B. A second method involves testing the cable at the splice point after the splice is complete. This method has the advantage that the 20% limitation can be planned out by selecting the splice lengths that are greater than 20% of the total as shown in figure 5. Also, most faults can be corrected before the splice is closed. Craft confidence can be increased because each man is testing his own work. The main disadvantage of splice point testing is that accessing pairs at the splice is a very time consuming procedure, since each pair must be manually attached and the working environment in most instances is far from ideal. Also, both ends of the cable must be cleared before meaningful results can be obtained.

C. The third method of new cable testing is simultaneous splicing and testing of each pair. This method requires a connector presser with automatic means of making metallic contact to the pair being spliced and a PASS-FAIL indication.

Although this method would still require both ends to be cleared, this is a small amount of

time in relation to re-entering even one splice and appears to be the optimum method both in terms of time and accuracy.

IV. ANALYSIS OF A PASS-FAIL FAULT DETECTOR FOR SIMULTANEOUS SPLICING AND TESTING.

In order to detect the cable irregularities discussed previously with a PASS-FAIL system, a measurement method must be used that will measure Cm for cable lengths from 300 to 40,000 feet and the test needs to be fast enough to avoid slowing down the splicing operation. The steady state solution of the general transmission line equations defines the propagation constant of a pair as

$$\gamma = \sqrt{(R + jwL)(G + jwC)} = \alpha + jB \qquad (1)$$

where: R = series resistance
L = series inductance
G = Parallel conductance
C = mutual capacitance
α = attenuation constant
B = phase constant

The characteristic impedance of a pair is defined as

$$Zo = \sqrt{R + jwL/G + jwC} \qquad (2)$$

The line impedance can be represented as a function of cable length as

$$Z = Zo \left[\frac{1 + \Gamma_R \left(e^{-2\alpha\ell} \cdot e^{-2jB\ell} \right)}{1 - \Gamma_R \left(e^{-2\alpha\ell} \cdot e^{-2jB\ell} \right)} \right] \qquad (3)$$

where: Γ_R = reflection coefficient
ℓ = cable length

As a pair approaches its characteristic impedance, it can be observed that faults such as splits, opens, grounds and crosses, which are capacity dependent will not give a uniform percent capacitance variation with respect to length. See Fig. 6. One method of reducing the propagation effect is to operate at a frequency where the maximum cable length is less than 20% of the wavelength. The wavelength is defined as

$$\lambda = 2\pi/B = VP/f \qquad (4)$$

Vp = velocity of propagation
f = frequency

If the maximum operating length is set at 40,000 feet for 26 AWG, using H88 loading, Fig. 7 demonstrates that the maximum frequency should not be greater than 200 Hz.

If the measuring frequency is decreased to 200 Hz or less, we need to consider the effects of interfacial polarization on the measured results. Interfacial polarization will exist in most dielectrics that are made up of two or more substances having different dielectric constants and conductivities. In most multi-pair cable the dielectrics would be represented by either paper-air or polyethylene-air. In composite dielectric systems, the capacity is dependent upon the charging time due to the accumulation of charge at the interface between two layers and whose resistance may be high enough so that the interface does not become completely charged during the time allowed for charging.

If absolute capacity magnitudes had to be measured such effects would need to be considered in more detail. However, if the measurement system worked on the ratio of pair capacity, interfacial polarization could be minimized.

The PASS-FAIL system described in the next section uses a very low frequency charge integration technique to measure the pair capacity. A system block diagram is shown in Fig. 8. The measured value is compared against a digitally stored reference value to determine if the pair is defective. The total splice and test operation requires less than 250 milliseconds. System linearity is better than 1% over the range from 300 feet to 40,000 feet.

V. OPERATION OF A SIMULTANEOUS SPLICING AND TESTING SYSTEM.

There are a couple of systems available today which are capable of testing some of the modular type of splices, but the system I am going to describe operates with the Taped B-Wire Connector. The splicing machine is a pneumatic operated presser as shown in Fig. 9 which is equipped with 2 probes for metallic contact to the B-Wire Connector. The taped connectors are fed into the machine and precisely aligned.

After the wires are inserted into the connectors and the presser button depressed, the probes enter the small holes in the back of the connectors as the presser completes the crimping cycle. At the end of the cycle, the probes are withdrawn and the connector tape cut allowing the crimped pair to be ejected. The presser also has a sensory switch which activates the PASS-FAIL tester when the probes have engaged the connectors. The system has been in field operation for over four years.

Gary H. Knippelmier has been employed by Automation Products Company for the past four years as a Design Engineer for outside plant test equipment. Prior to joining APC he was involved in the design of automatic fault isolation equipment for Collins Radio Company. He received his B.S. of Electrical Engineering degree from the University of Houston in 1966 and is a member of the IEEE and Eta Kappa Nu.

The PASS-FAIL unit shown in Fig. 10 is activated by connecting to the presser unit. The START switch is depressed and the LED on the presser lights. The first pair to be spliced is inserted into the presser and the presser button held down, within 2 seconds the LED will extinguish or an alarm will sound. If the LED goes out, the unit was able to range up to the proper cable length, measure the pair's capacitance and digitally store a normalized value for the pair. If the alarm sounded, the pair was either shorter than 300', longer than 40,000' or had a resistance fault less than 1 meg ohm. Assuming the pair was good and within the range of the unit, the splicer would begin splicing without any additional adjustments. The unit would then compare each newly spliced pair with the initial pair and if the spliced pair had a capacitance value of $\pm$ 7.2% different from the stored value, the alarm would sound for approximately 1 second and the LED on the CS-10 would blink indicating a bad pair. Because of Murphy's Law, the first pair selected for setting the unit may not fall in the center of the cable's normal capacitance distribution. An added feature of the unit is that it performs a limited range "tweaking" of the stored reference value. After approximately 20 pairs have been spliced the reference value will have changed to a value that closely represents the average pair. If the alarm sounds, the pair can be tested manually to determine if the internal probes in the presser made good contact or if the pair is definitely out of tolerance. The direction to the fault can be determined by cutting the pair and resplicing each side with another pair. The pair that remained faulted would determine the direction.

A 25 pair automatic scanner is available which functionally works the same as above except that the bad pair number is digitally displayed when a fault is encountered. The scanner is equipped with interface cables to adapt the unit to the different types of modular splicing systems.

REFERENCES

1. "Interaxial Spacing and Dielectric Constant of Pairs in Multipaired Cables", J. T. Mauplin. Bell System Technical Journal, New York, New York, Vol. 30, July 1951, pp. 652-67.

2. "Direct Capacity Measurements", G. A. Campbell Ibid., Vol. 1, Nov. 1922, pp. 18-38.

3. "The Dielectric Properties of Insulating Materials", E. J. Murphy and S. O. Morgan, Ibid., Vol. 16, 1937.

4. "Primary and Secondary Parameters of Non-loaded Cable Pairs and Inductively Loaded Systems", H.P. Price, Engineering Bulletin EB 40-1, July 1970, Anaconda Wire and Cable Company, Sycamore, Illinois.

5. "Primary and Secondary Parameters of Telephone Cable at Carrier Frequencies", E. W. Riley, Engineering Bulletin EB49-0, December 1973, Anaconda Wire and Cable Company, Sycamore, Illinois.

6. "Apparent Errors in the Measurement of Mutual Capacitance on Longer Lengths of Cable Pair at 1000 CPS", J. V. Buscemi and A. E. Widmer Wire and Cable Symposium, Atlantic City, 1964.

7. "Transmission Properties of Polyethylene Insulated Telephone Cables at Voice and Carrier Frequencies", G. S. Eager Jr., L. Jachimonwicz, I. Kolodny, D. E. Robinson. AIEE Transactions (Communication and Electronics) November 1959.

8. Traveling-wave Engineering, R.K. Moore. Mc Graw-Hill, Inc., 1960.

9. "Definitions and Measurement of Electrical Parameters of Paired Telephone Cables", U. S. Dept. of Agriculture - REA, June 1962.

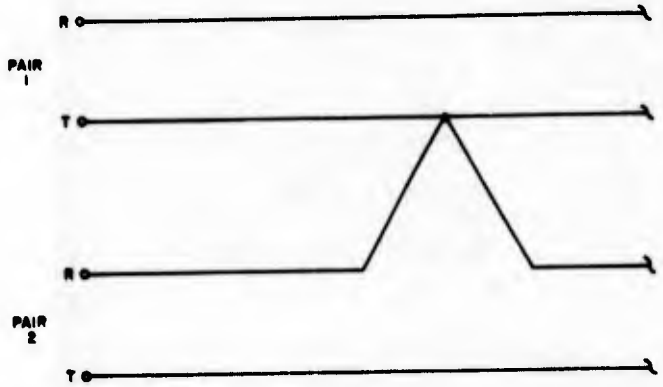

FIGURE 1
SCHEMATIC OF A CROSS

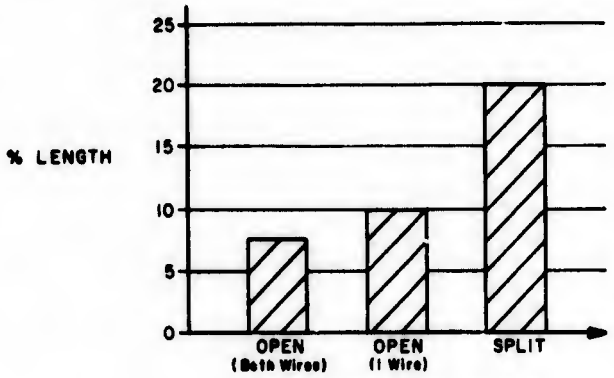

FIGURE 4
PERCENT LENGTH TO CAUSE 7.2% ERROR

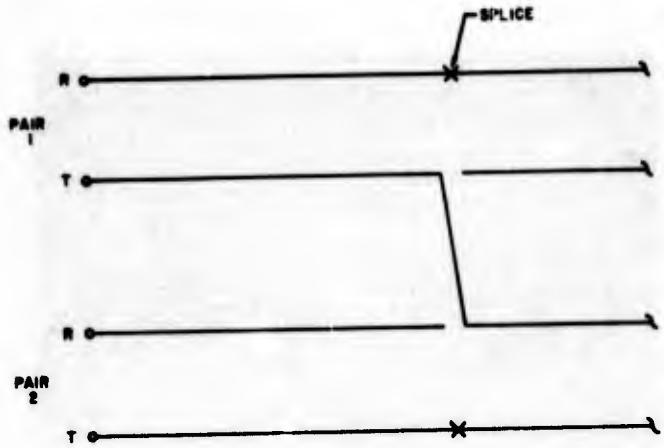

FIGURE 2
SCHEMATIC OF A SPLIT

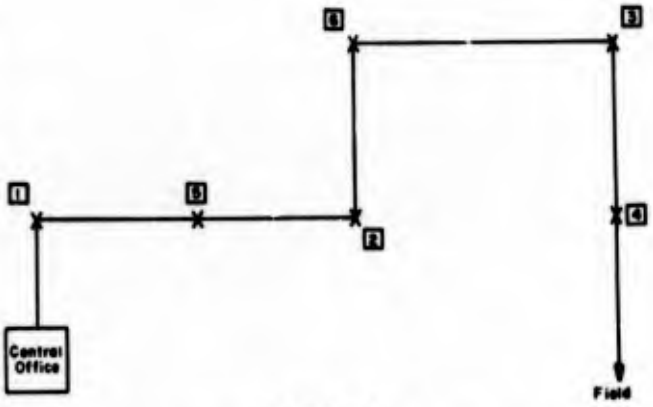

FIGURE 5
SPLICING SEQUENCE TO ELIMINATE SPLIT LIMITATION

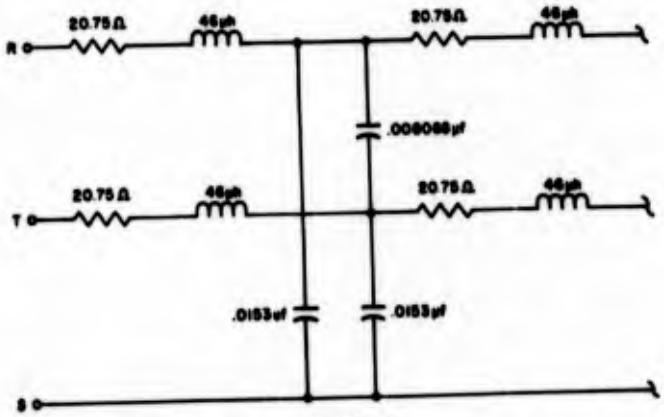

FIGURE 3
ONE SECTION OF 26 AWG ARTIFICIAL LINE

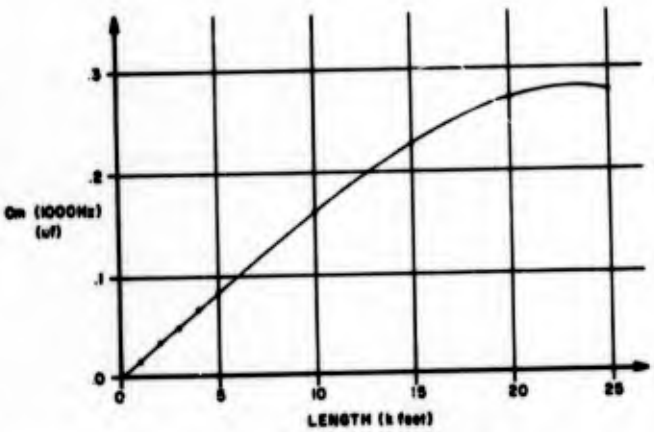

FIGURE 6
NON-LINEAR EFFECT OF Cm VS LENGTH

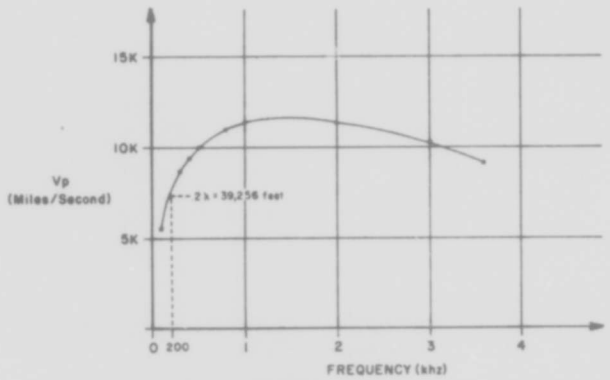

FIGURE 7
PROPAGATION FOR 26 AWG WITH H-88 LOADING

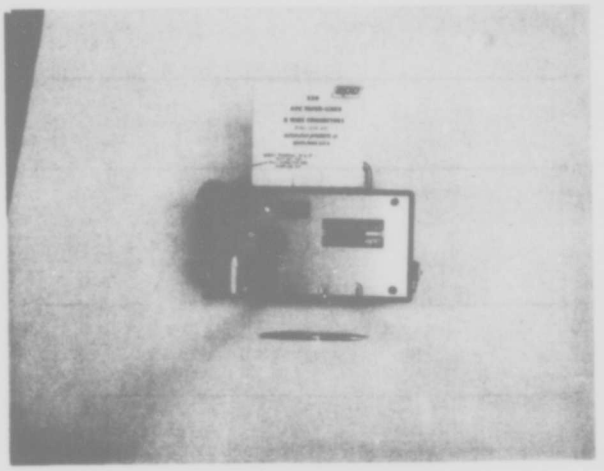

Figure 9 - Pneumatic Presser for Taped B-Wire Connectors

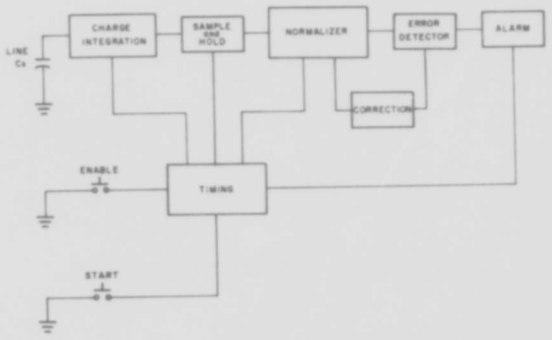

FIGURE 8
BLOCK DIAGRAM OF PASS-FAIL MEASUREMENT UNIT

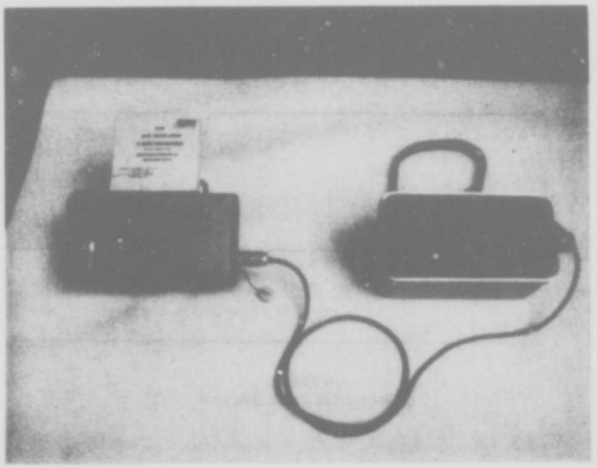

Figure 10 - Simutaneous Splicing and Testing System

AN ALL POLYETHYLENE CABLE SPLICE EMPLOYING HEAT FUSION TECHNIQUES FOR POLYETHYLENE JACKETED CABLES

by J.G. Nevison and D.T. Parr

Telephone Cables Division
British Insulated Callender's Cables Limited
Prescot, Merseyside, England.

Summary

The jacket closure designs generally available for plastics jacketed cables are briefly reviewed and it is concluded that a fusion method is likely to offer the best security. The development of such a system over the past decade is described and the relevant features of the technique, the splicing equipment and components are discussed, together with the results of laboratory tests and field experience.

Introduction

The traditional paper insulated lead jacketed telephone cable is rapidly being superseded by plastics jacketed cable in the toll and trunk network and plastics insulated and jacketed cable in the distribution network with a clear trend towards the latter for all networks. Consequently the need arises for a plastics jacket closure design which is comparable or superior in performance to the plumbed lead sleeve commonly used for lead jacketed cables. This paper describes the development of a jacket closure design for polyethylene jacketed cables which comprises essentially a polyethylene sleeve with ends fused to the cable jacket by an injection moulding process such that a true weld is obtained between the sleeve and jacket. The integrity of the closure so formed makes this design particularly suitable for toll and trunk cables of high circuit capacity where maximum security is of prime importance.

Design Requirements

When considering the development of any new splice closure design the parameters of importance must be established. In general the requirements are as follows:

(a) Splice Closure Materials

1) Simple component design.
2) Minimum number of components for a given closure size.
3) Minimum range of component sizes to cater for all possible splice and cable configurations.
4) Low cost components.

(b) Splicing Tools

1) Robust simple design with high reliability.
2) Minimum number of tools for a given closure size.
3) Minimum number of tools to cater for all cable diameters and combinations of cable sizes.
4) Low cost.
5) Portability.

(c) Technique

1) Simple; to reduce operator training to a minimum.
2) Quick; to reduce operator cost and increase efficiency.
3) Manual skills should be reduced to a minimum.

(d) Design Considerations

1) Integrity and strength of jacket closure equal to that of the cable jacket.
2) Ability to accommodate all cable diameters.
3) Facilities for multiple cable entry.
4) Ease of reopening and reclosure.
5) Ability to test the jacket closure immediately after completion.
6) Capable of use in all climates.

It is considered that the closure design to be described fulfils the above requirements although provision for multiple cable entry is restricted to four cables which may be inadequate in exceptional circumstances and thus require the introduction of an additional splice for flexibility. This means that the splicing system is entirely adequate for the toll and trunk cable network and also for the normal requirements of the local distribution network.

Choice of Fusion Technique

The success of polyethylene as a cable jacketing material has been due in part to the fact that it is largely chemically inert and therefore not subject to corrosion in the same way as the earlier metal jacketed cables using lead, aluminium or steel. Unfortunately this very property makes it difficult to achieve a satisfactory bond to polyethylene with the result that the splicing of polyethylene jacketed cables is still the subject of much development work in which no single technique has yet received universal acceptance. Resins, particularly of the epoxy type, have been used extensively. They attempt to obtain a satisfactory key to polyethylene by mechanical means relying on the contraction which takes place when the resin cures. Unfortunately differential expansion between the resin and polyethylene which occurs on temperature cycling reduces their effectiveness and usually it has been found necessary to roughen the polyethylene jacket or flame treat it, prior to the application of the resin, to improve the adhesion.

Similarly due to the high temperature coefficient of expansion of polyethylene coupled with its cold flow properties, designs of the pot and bung type which attempt to obtain a seal to the polyethylene by mechanical compression have achieved only limited success and usually a secondary closure such as a compound filled box has been found necessary to achieve adequate performance.

In the light of the above experience it was considered that systems which merely attempted to stick polyethylene splicing components to the polyethylene cable jacket would be inferior to a true fusion technique as a means of achieving a high integrity closure, particularly against the probable advent of high capacity coaxial cables jacketed in polyethylene. Accordingly it was decided to proceed with the development of a fusion type splice involving the forming of a mould cavity around the cable jacket/splicing sleeve interface and injecting molten polyethylene into this mould so as to weld the jacket to the sleeve.

Initial Design of Fusion Closure

The initial arrangement comprised an injection gun, splicing jig, transparent acrylic thermoplastics mould boxes and splicing components consisting of a cylindrical polyethylene sleeve and two sleeve to jacket adaptors. The foregoing items are shown in Figures 1-4. The jacket adaptors are necessary to avoid the need for massive moulds to bridge the relatively large diameter step between the cable and splice sleeve respectively.

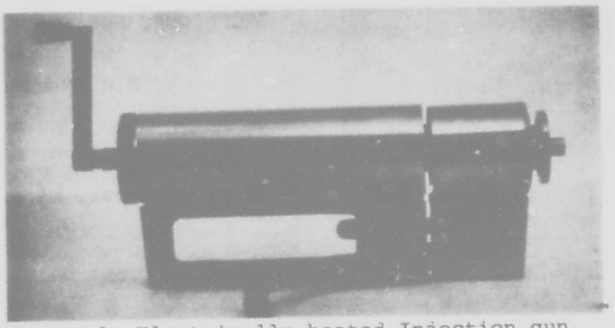

Figure 1 Electrically heated Injection gun

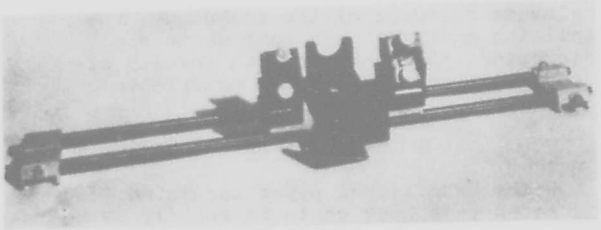

Figure 2 Splicing Jig

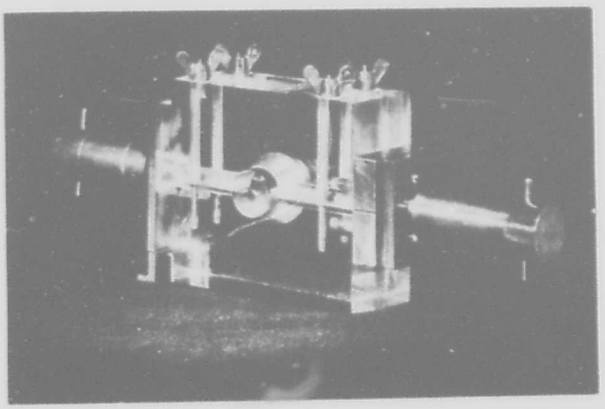

Figure 3 Transparent acrylic thermoplastics mould box

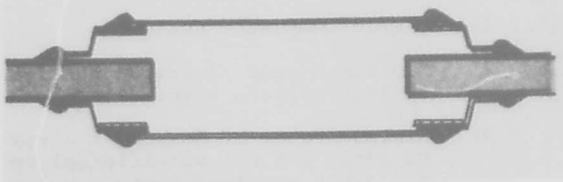

Figure 4 Polyethylene sleeve and two sleeve to jacket adaptors

The method of operation consisted essentially of injecting molten polyethylene at a temperature of 330°C into a transparent acrylic thermoplastics mould box surrounding the cable jacket and the end of the sleeve to jacket adaptor. With the transfer of heat from the injectant, the surfaces of these components are melted thereby purging them of any oxidised surface film. This permits fusion in the molten state between the surfaces of the injectant, the cable jacket and the adaptor, this fusion remaining to the solid state.

The transparent acrylic thermoplastics mould box is formed from two mating halves which are clamped together; one half containing an entry port and the other an egress port for the polyethylene injectant. The advantages of transparent acrylic thermoplastics as a mould box material are that it enables the whole operation to be seen and controlled; also it does not stick to the injectant, jacket or adaptor and being an insulating material it prevents rapid loss of heat from the injectant, which is required for melting the components to be fused. Its disadvantages as a mould material are lack of mechanical strength and vulnerability to damage coupled with a tendency to warping under the influence of the relatively high injectant temperature.

In practice the molten polyethylene is at first injected rapidly into the mould until this is filled and polyethylene is seen to exude from the egress port. This is possible because at the aforementioned temperature the polyethylene is of low viscosity and by rapid injection the cable jacket and adaptor can be surrounded with molten polyethylene before melting of these components takes place. Heat transfer to the inside of the cable jacket is also minimized.

When the mould box has been filled with injectant, the remainder of the molten polyethylene in the injection gun is forced more slowly through the mould so that a good rate of heat transfer from the molten polyethylene to the cable jacket and adaptor takes place, and any oxide films are washed away. If the colour of the injectant is different from that of the components to be fused, melting of the latter will be indicated by the colour traces in the material issuing from the outlet port. Melting of natural polyethylene components can also be observed as they become transparent.

In order to ensure adequate heat transfer occurs and to reduce the element of operator judgement necessary for the operation, both the injection gun and mould volumes were designed on the basis of extruding a full charge through each mould.

When the contents of the injection gun are exhausted it is disconnected from the mould box and rams are fitted to seal both the inlet and outlet ports. The purpose of these is to prevent the formation of contraction voids in the polyethylene injectant which would otherwise take place on cooling, due to the high temperature coefficient of expansion of polyethylene. When the incipient formation of voids is observed through the transparent walls of the mould box, the two rams are screwed equally into the mould box until the voids are observed to disappear. This action is continued until the contents of the mould have cooled and solidified, when the mould box, which is designed to split about an axis of symmetry through the port areas, may be removed and the sprues cut off.

The remaining welds may then be made in a similar manner. Usually four such welds are required for the complete jacket closure, namely two adaptor to jacket welds and two adaptor to sleeve welds. Alternatively the latter two welds may be made as a separate operation in advance of splicing in which case the adaptor sleeve arrangement so formed may be divided as convenient on location when only three welds are required to complete the closure as shown in Figure 5.

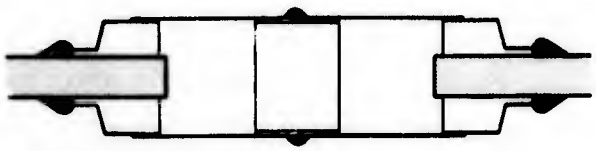

Figure 5 Polyethylene sleeve and prewelded adaptors with brass liner.

It will be apparent that in order to weld together the two halves of a divided sleeve some form of internal support is required both to prevent the sleeve collapsing when melted by the injectant and to avoid molten polyethylene being forced into the conductor splicing area. These difficulties are overcome by using a brass liner located inside the splicing sleeve and supporting the interface between the two half sleeves.

Similarly to prevent molten polyethylene gaining access to the inside of the adaptors and to ensure a tight fit between the transparent acrylic thermoplastics mould box and the adaptor and cable jacket, it is necessary to seal the diameter steps between these components, since pressure of 200 - 300 kN/m^2 are developed in the mould box during the injection process and subsequent tightening of the rams. Furthermore air must not be permitted to enter the mould during the cooling period. Sealing is usually done by applying paper tape wraps to the components until a push fit is obtained.

Injection Gun and Injectant

The electrically heated injection gun used is shown in perspective cutaway in

Figure 6a and 6b. It is essentially a miniature hand extruding machine and comprises a cylindrical brass heat exchanger and extrusion nozzle by means of which heat supplied from an electrical element surrounding a portion of the heat exchanger may be evenly transferred to a polyethylene charge inserted from one end of the gun. A suitably encased platinum resistance thermometer is in contact with the gun wall, thus enabling the temperature of the injectant to be monitored and controlled. The polyethylene charges consist of natural material in specially moulded cylindrical rods 130 mm long and 25 mm diameter and with Melt Flow Index (MFI) of 2. Two charges are present in the loaded gun at any one time, the first charge being melted in the heat exchanger and the rear charge remaining unmelted in the barrel until extrusion takes place. The molten polyethylene is forced from the gun by a plunger assembly consisting of a heat resisting piston operated by a screwed shaft connected to a crank handle which pushes the rear charge into the heat exchanger area. This equipment requires a 230 volt ac 50 Hz 300 watt supply and is suitable for use with a small portable generator.

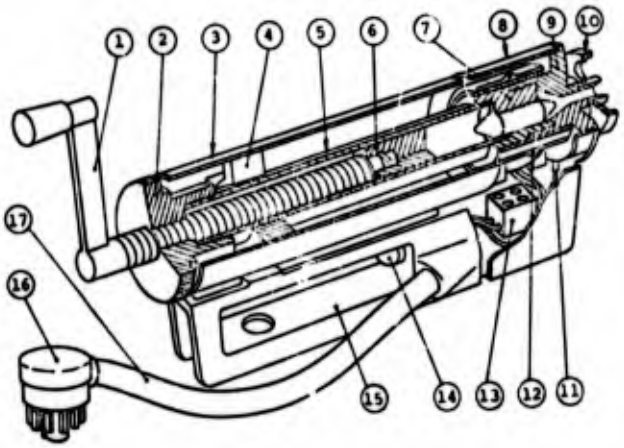

Ref. No.	PARTS DESCRIPTION
1	Crank Handle and Spindle Assembly
2	Feed Nut
3	Tubular Shield
4	Barrel Clamp
5	Barrel
6	Spindle Head
7	Heat Exchanger Body
8	Heat Exchanger Shield
9	Nozzle
10	Latch Plate
11	Temperature Sensing Element
12	Heating Band
13	Terminal Block
14	Indicator Lamp
15	Handle
16	Plug
17	Cable

Figure 6a Perspective cutaway diagram of injection gun.

Figure 6b Cross section diagram of injection gun.

As mentioned earlier the polyethylene charge in the injection gun is raised to about 330°C prior to injection. This ensures that adequate heat is available from the injectant to enable subsequent washing away of any oxide films present on the cable jacket or polyethylene splicing components to be carried out effectively. In addition the viscosity of the material must also be satisfactory at the extrusion temperature in order that adequate control of the injection process may be exercised by means of the crank handle of the gun. In this respect the use of copolymers as injectant materials is limited due to their rapidly changing and low viscosity over the extrusion temperature range.

At temperatures above 290°C a limited extent of pyrolysis occurs in polyethylene, resulting in a gradual increase in MFI. The pyrolysis becomes more rapid and its extent greater at higher temperatures, above 330°C. A much more rapid breakdown at these temperatures is brought about by the presence of traces of oxygen. The extent of degradation is confined to within acceptable limits, by the addition of appropriate antioxidant and by ensuring that the injectant is used as soon as the injection temperature has been attained.

It has been found that a residual antioxidant concentration of 0.2% Nonox WSP (or similar) is normally sufficient at 330°C to maintain the MFI at a constant level for several minutes.

From tests conducted to determine the requirements, Figure 7 shows the resultant MFI of the extrudate of three grades of polymer (as determined by BS 2782 105C Procedure A) after heating to various temperatures. The increased value of MFI with increasing temperature indicates a permanent change in structure due to loss of antioxidant.

The graph in Figure 8 shows the further change in MFI for similar polymers at 330°C over a period of time.

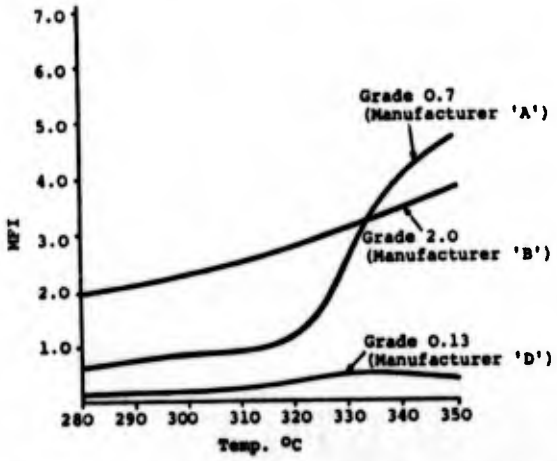

Figure 7 Graph showing change in MFI of 3 homopolymers (measured to BS 2782 105C) after heating in a closed container to various temperatures and allowing to stand for 1 minute.

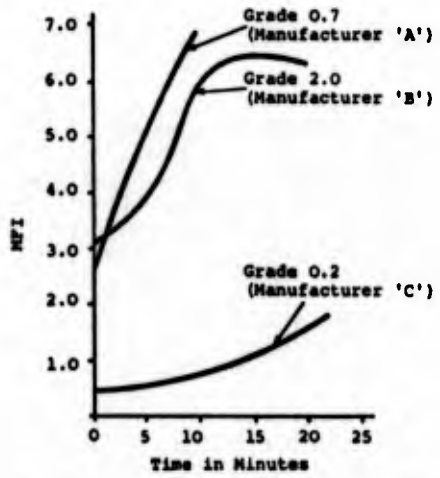

Figure 8 Graph showing variation of MFI with time for 3 homopolymers after heating to 330°C in a closed container. (MFI measured to BS2782 105C).

Lower MFI number polymers require greater pressures during extrusion; consequently, for hand operated injection systems and the range of flow path lengths required, homopolymers lower than approx 0.7 MFI are unsuitable due to the viscosity being excessive at the relevant temperature and flow rate (the ratio of shear stress to shear rate is strongly dependent on the rate of shear). The effect of applying high pressures to low MFI materials is to increase their effective MFI. Similarly although homopolymers of low MFI have been tried at higher temperatures, as can be seen from Figure 7 the antioxidant is used up more quickly, because of the higher temperatures involved.

These effects cause a rise in MFI (In extreme cases, discolouration, decomposition and a fall in MFI) the final result being inferior to a higher MFI material used at a lower temperature.

To limit the extent of cross linking of the injectant, the gun should be heated at a rate equal to the thermal conductivity of the material, i.e. about 34 x 10^{-6} J/m s deg K, giving an overall heating time from ambient temperature to 330°C for the 129 x 10^{-6} m^3 injector, of approx 9 minutes and a reheat time from 32°C, of 4.3 minutes. This can be related to between 1.0 and 1.2 seconds at the ideal heating rate, per 100 μm of film thickness/unit area.

If excessive heat is applied, the antioxidant in the material nearest the source of heat is lost prematurely, allowing the outer layers to degrade. On the other hand if too little heat is applied, there is the risk of losing all the antioxidant before the operating temperature is attained, because of the time taken.

The conditions necessary for fusion to occur require a suitable combination of temperature and viscosity. These conditions can be achieved by a range of polymers over a range of temperatures, but the ideal situation is one which allows the use of the lowest MFI for the greatest flowpath length required, at the lowest temperature possible to ensure fusion at the extremity of the flowpath, with the least residual stress. With the simple moulds employed, polyethylene compounds with an MFI in the range 0.8 - 2.0 have been found to be the most suitable.

Figure 9 shows the curve of temperature gradient against path length of a typical polymer injected into a mould.

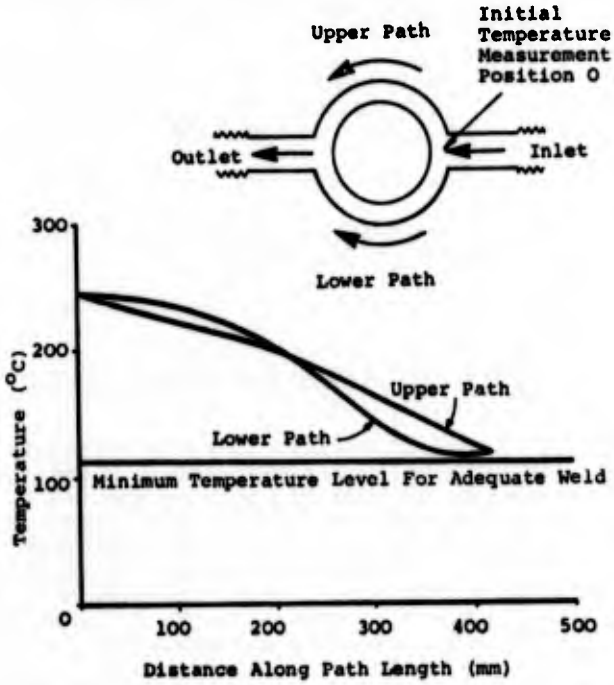

Figure 9 Graph showing curve of temperature gradient against path length of a typical polymer injected into a mould.

Testing Jacket Closure

A significant advantage of this method over those involving the use of resin, where appreciable cure times are usually involved, is that the completed closure may be immediately air pressure tested through a Schrader valve fitted in the splicing sleeve. A transparent plastic sheet water bath formed round the welds enables the presence of any leaks to be detected.

Reopening and Reclosing

In the event of the completed welds proving faulty they may be removed by rasping off the formed mouldings which restores the components to their original form and enables reclosure to be carried out by the procedure already described.

Further Developments

Whilst the above method served to establish the technical feasibility of this fusion technique and was used for a decade up to 1967 nevertheless it became apparent that in its existing form it possessed several weaknesses which would need to be overcome if the technique was to gain general acceptance. The features requiring further examination are listed below.

a) The need for a 230V ac 50 Hz supply to heat the injection gun detracted from its flexibility.

b) Twenty transparent acrylic thermoplastics moulds were required to cover the range combination of cable diameters and splicing sleeves.

c) A correspondingly large range of cable jacket/splicing sleeve adaptors were required.

d) Possible reduction of closure time.

e) Possibility of dispensing with the jointing jig.

The above points were resolved in the following manner.

a) Alternative heating arrangements for the injection gun

It was realized that the necessity to provide an electricity supply and a control unit for the gun represented a complication and cost penalty. Furthermore with the existing heating element design, at least an hour was required to heat the initial charge, and even this was subject to ambient weather conditions e.g. wind shielding was essential.

An alternative approach was adopted. This consisted of placing the gun in a special muffle and heating it with a gas torch as in Figure 10. Using this method the need for an electricity supply and control unit would be eliminated and the time required to heat a polyethylene stick charge reduced. By carefully observing the temperature of the thermometer embedded in the injection gun satisfactory performance has been obtained using this method and the heating time per charge reduced to 10-15 minutes with associated cost reductions in time and equipment.

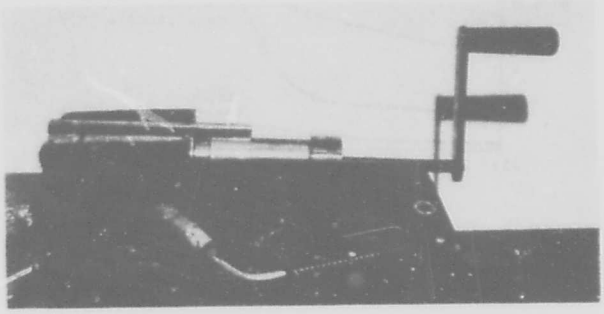

Figure 10 Injection gun heated by gas torch

b) Reduction in the number of moulds required

The capital cost of providing a range of transparent acrylic thermoplastics moulds which required individual machining was appreciable and contributed significantly to the high capital cost of the equipment. It was realized that the provision of a more flexible mould arrangement was required which would enable the range of necessary moulds to be substantially reduced. Although in the early development it was believed that visual inspection of the operation was essential for a satisfactory weld, it was soon realized that operators in fact were rapidly becoming experienced in the technique and only rarely inspected the weld for voids during the cooling period.

Consequently design effort was concentrated on the introduction of metal strip moulds (See Figure 11), incorporating tubular metal stems to permit connection of the injection gun or insertion of metal rams as previously described.

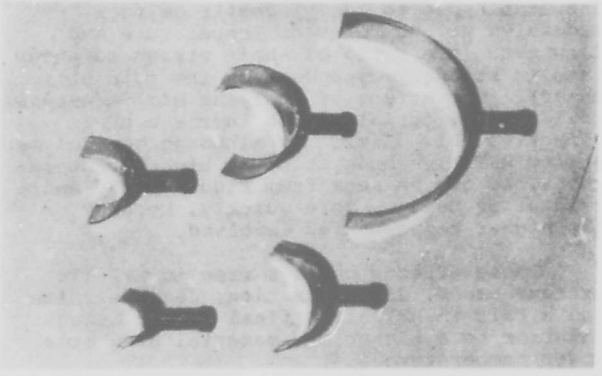

Figure 11 Strip moulds

By increasing the use of paper or aluminium tape build ups in conjunction with these strip moulds, which were held in position with worm drive clips, a satisfactory mould box was formed (See Figure 12) and only five sizes of mould strip were necessary to meet all requirements. This new arrangement effected a substantial reduction in both the cost and the bulkiness of the splicing equipment.

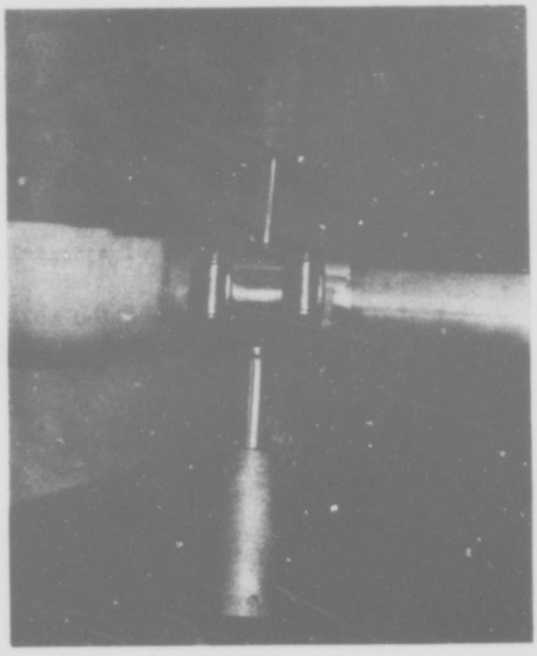

Figure 12 Strip moulds (assembled)

c) Reduction in required range of adaptors

In order to accomodate the required range of cable diameters and splicing sleeves the technique requires the provision of appropriate polyethylene adaptors with single and multiple entry facilities. A reduction in the number of designs to a minimum was clearly desirable to reduce tooling and thus component costs. With this purpose in mind multiple concentric ring adaptors were developed.

Figure 13 shows how a number of combinations of cable and splicing sleeve diameters could be provided by one size of adaptor. By suitable machining of a given size of adaptor unwanted rings of material could be removed leaving only the required combination of diameters. Such adaptors have been in general use over the past seven years.

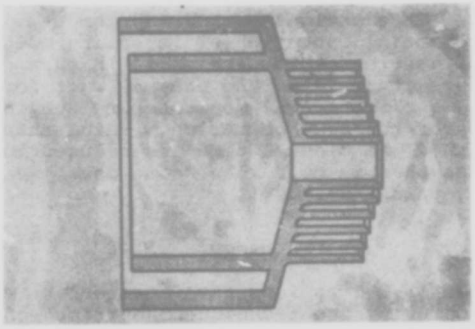

Figure 13 Multiple concentric ring adaptor

d&e) Reduction in time to effect sheath closure and elimination of splicing jig

The original equipment involved the use of a splicing jig to support the jacket closure and mould box during the welding process, and each weld was a separate operation. In congested manholes the splicing jig proved inflexible and difficult to set up and was clearly undesirable.

The introduction of the relatively cheap metal mould strips also enabled the splicing jig to be eliminated. Sufficient mould strips could now be available without cost penalty to enable all the required moulds to be fitted prior to commencing the first polyethylene injection. The moulds themselves serve to align and secure the complete closure in position. (See Figure 14).

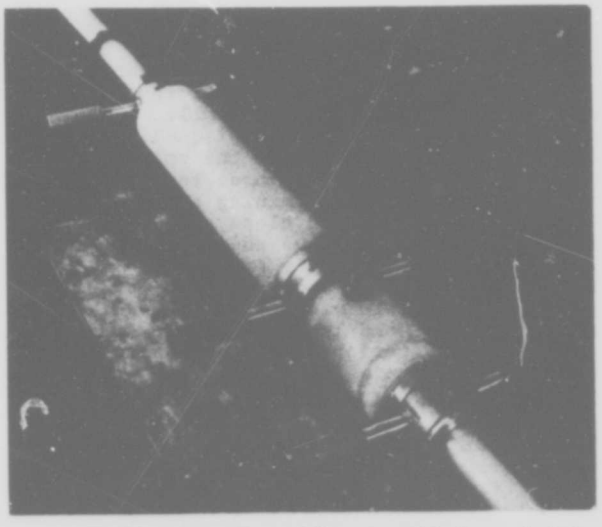

Figure 14 Set of moulds assembled on joint

This obviously assisted the sequential operation of injecting molten polyethylene into each mould in turn, since it obviated the need to wait for the cooling of the mould before setting up for the next operation. Using this method the closure time was reduced to less than an hour when using one injection gun.

Performance

Some 33,000 splices have now been installed using the techniques described and a very low fault rate has been experienced. The significant faults which have occurred have been associated with mechanical stresses and environmental pollutants and in this context the materials used in the splicing process together with environmental stress crack resistance (ESCR) need to be considered.

Materials

Considerable development work has been expended on polyethylene polymers for cable jackets over the past few years and low density high molecular weight polyethylene with an MFI of 0.13 and possessing good tensile properties, resistance to cracking and low brittleness temperature is now available. Similar polymers with an MFI less than 0.3 and otherwise complying with the same specification as the cable jacketing materials are used for the manufacture of both the splicing sleeves and the adaptors. The polyethylene stick charges used for the injectant are however made from a Grade 2.0 MFI homopolymer since as indicated earlier a material with an MFI less than 0.8 cannot be extruded with a hand operated injection gun without the use of excessive pressure and unusually high temperatures. The optimum injectant, jacket and splicing sleeve material to give the best overall system performance is considered later.

Weld and Closure Performance

It is clear that a means of establishing jacket closure performance other than by long term field assessment is desirable. In addition to the application of quality assurance specifications to the splicing materials and components three tests have been developed for determining the quality of the welds and completed closure. One test is used to confirm that true fusion of the cable jacket and adaptor to the injectant has occurred (Weld Test) the second to establish that the ESCR performance of the weld is adequate (ESCR Weld Test) and the third to prove the ESCR performance of the complete closure is adequate (ESCR Closure Test).

(a) Weld Test

Weld strength is assessed by means of a peel test. On completion of a jacket closure several longitudinal sections of the adaptor to jacket weld are taken from around the cable weld circumference as Figure 15a.

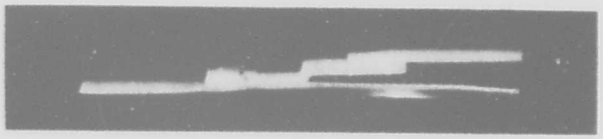

Figure 15a Peel strength sample - before test

The adjacent jacket and adaptor ends of the sample are gripped between jaws and tension applied until the sample breaks. (As shown in Figure 15b).

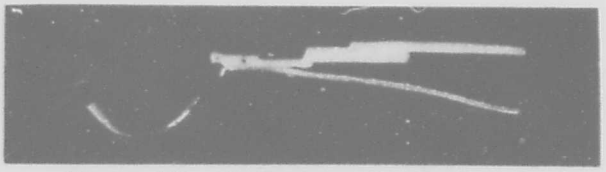

Figure 15b Peel strength sample - broken

Failure should occur in the cable jacket or adaptor material, not in the weld area and should not be of a brittle nature.

A similar test can be applied to the adaptor to sleeve weld or the sleeve weld on a divided sleeve.

(b) ESCR Weld Test

The sample is prepared as previously described and bent into a 'U' shape of radius approximately 6 mm, the ends of the 'U' being tied together. The sample is immersed in Shell Teepol GD53 containing 40% solids, at a temperature of 50°C for a period of 5 days as Figure 16. No failure of the weld should be observed.

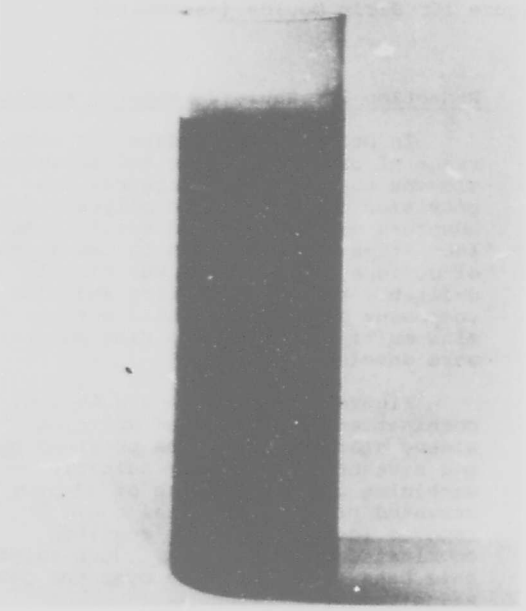

Figure 16 Tied 'U' sample in beaker of Teepol

(c) ESCR Closure Test

The cable ends should be bent to a diameter of 12D, (where D is the overall diameter of the cable jacket) and tied together. The complete sample should then be immersed in Teepol GD53 as previously specified at 50°C for a period of 5 days during which period no fracture of the closure or jacket should occur, (see Figure 17). This test is considered extremely severe and much more onerous than the stress likely to be experienced by the cable or closure during its normal life expectancy.

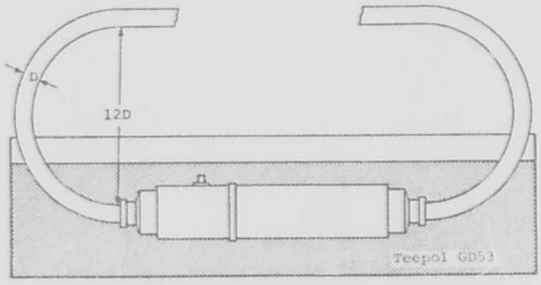

Figure 17 Bent splice immersed in Teepol

The latest form of ESCR test provides a quicker method of determining the performance of materials used for the splice than the closure test described above.

Figure 18 shows the test rig which provides a combination peel and tensile test in a stress cracking environment, simulating the compound stress produced by a closure test. It consists of a number of tanks containing Teepol GD53 at a temperature of 50°C, which are indirectly heated by water, each tank accommodating up to 8 strain jigs holding one sample each. These strain jigs consist of a frame which houses two pairs of jaws, one fixed and one adjustable, into which one of the 6 equal segments of a weld section is placed and tensioned. A micro switch is used to sense failure of a specimen, which is recorded in terms of minutes on an impulse recorder.

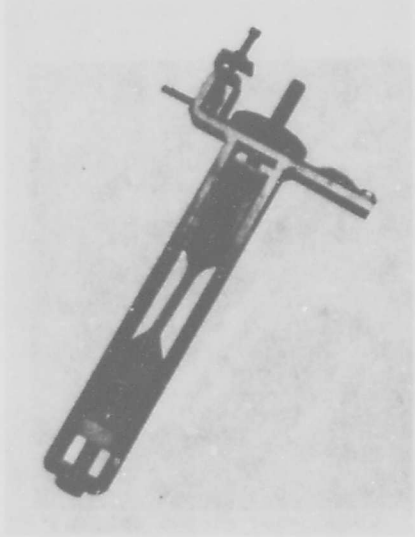

Figure 18 ESCR test rig

Many tests have been conducted using this method and table I indicates the improvements in performance which can be expected using EVA co-polymer jacketing materials compared with homopolymers.

Discussion of Test Results

It will be appreciated that the tests enumerated are extremely severe and hence should give a reliable indication of any inherent weaknesses of the system together with a performance rating. In fact the injection welding technique described enables these tests to be met using a preferred combination of injectant, splice and jacket materials whereas it has been found that techniques which merely depend on melting of the components to be spliced, without any displacement of the component materials, are unable to pass even the peel test. Similarly an unsuitable combination of materials for the system components will result in failure to meet these tests.

A further indication of the severity of the ESCR closure test is indicated by the fact that although the field performance of the sleeve adaptor system has been very satisfactory the time to failure in relation to the table is shown to be the lowest.

As might have been expected, step diameter changes in the splice profile give rise to points of appreciable stress and some failures were experienced in the early stages. Vulnerable points are the adaptor jacket weld edges, the wall thickness of the adaptor and diameter step on the adaptor. By increasing thickness margins and adjusting profiles improved performance has been obtained. However further development work has been carried out with a view to increasing safety margins and reducing the cost of the technique even further and these are outlined below.

Modification to Weld Profile

When a completed closure is subject to the ESCR test already described, the point of maximum stress is the outer edge of the adaptor jacket weld as shown on Figure 19a. Unfortunately this tends to be a weak point because the polyethylene in this area has become more highly crystalline and more brittle, due to the fact that the injectant is allowed to cool naturally as opposed to quench cooled. The area so affected is within 3-4 mm of the weld itself. When the weld is made a naturally formed integral collar is produced at each side of the weld over a distance of approximately 0.75 mm. It was apparent that by increasing the length of this collar the applied stress could be removed from the crystalline area. This is achieved

by applying a heat resisting tape such as mylar, over the cable jacket in this region and extending this natural collar in the weld over it (See Figure 19b). No weld occurs to that portion of the jacket covered by the tape but in effect it provides a close fitting supporting polyethylene collar which transfers the point of maximum stress away from the immediate weld area.

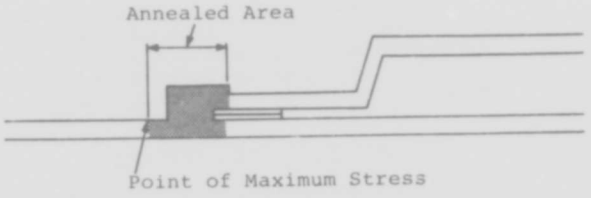

Figure 19a Weld profile showing maximum stress point within annealed area of weld

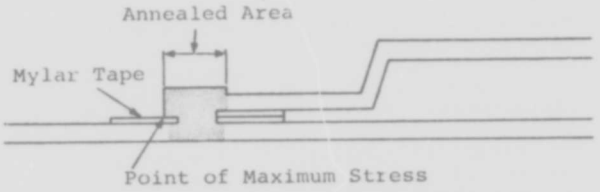

Figure 19b Weld profile showing maximum stress point outside annealed area of weld

This procedure effectively increased the time to failure on the ESCR closure test as far as splices on small diameter cables were concerned but was only marginally effective on the larger cable diameters.

Development of Cone Ended Sleeve

Although the sleeve adaptor system has proved very successful, the need to achieve the best possible ESCR performance together with further cost reductions, has led to the consideration of those aspects of the technique where these parameters might be improved.

Some consideration was given to the reduction of inherent stress in the splicing components, and to see whether changes in the splicing sleeve or adaptor profile would be beneficial. It was further noted that in the current adaptor design the diameter steps preclude minimizing the weld volume, where the cable does not exactly fit the nearest adaptor diameter. Similarly the use of a sleeve and adaptors implies a four weld system, whereas if the adaptor facility could be combined with the main splicing sleeve a three weld system would result with an inherently increased reliability.

These considerations have led to the development of a cone ended splicing sleeve, manufactured by a rotational moulding process, which results in an essentially stress free sleeve using Grade 2 MFI compound. Although the use of a rotational moulding process necessitates the use of Grade 2.0 or higher MFI materials with consequent reduction in ESCR performance this is offset by the nature of the manufacturing process and by using compounded materials (See Figure 20). This splicing sleeve has no sharp diameter steps, eliminates the need for adaptors and can be trimmed to fit the cable diameter precisely thus avoiding the need for internal jacket to sleeve tape barriers and resulting in a weld of consistent size and optimized dimensions. The improved ESCR performance obtained with these splicing sleeves is shown in Table I.

Figure 20 Cone ended splicing sleeves

Cone ended splicing sleeves have been in general use since 1972 and a full range of single and multiple entry splicing sleeves up to 174 mm diameter is available. To date some 8,000 splices have been installed with very satisfactory results. Figure 21 shows a typical jointing installation using these sleeves.

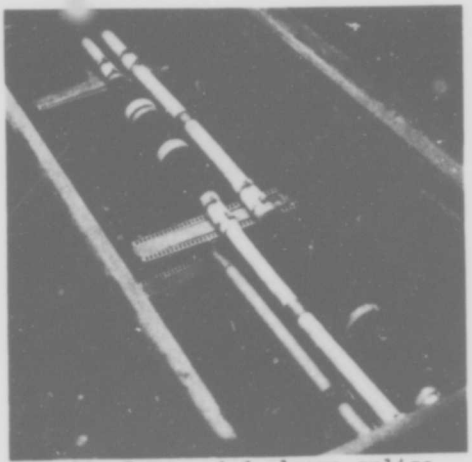

Figure 21 Cone ended sleeve splice installation

Figure 22 shows the manner in which a gas pressure contactor is accommodated in a breeches sleeve for pressurised cable systems.

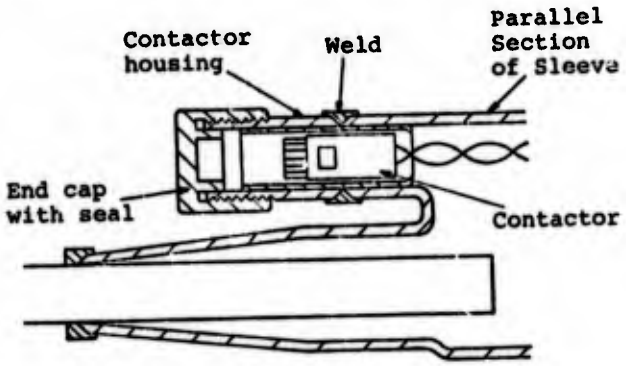

Figure 22 Breeches sleeve with contactor

Choice of Injectant Material

Reference has already been made to the importance of correct heating rate, choice of MFI and antioxidant level for the injectant. These aspects of the technique were further examined following the introduction of the cone ended sleeves to secure optimum overall system performance. Figure 23 shows the results of a linear programming approach to the evaluation of the system parameters and constraints. It will be seen from the feasibility area for an injectant consistent with adequate ESCR performance, that a material with MFI 0.8 and an operating temperature of about 345°C should be optimum and trials using material conforming to these requirements have confirmed this prediction.

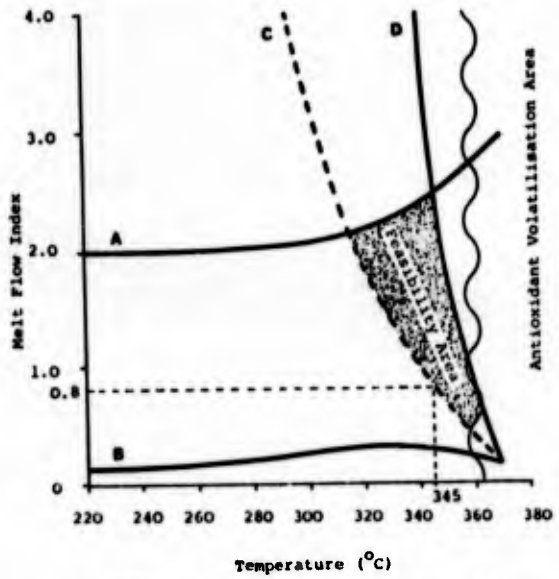

A - Stability curve of a 2.0 MFI Homopolymer, (the highest MFI material to give adequate ESCR).

B - 0.13 MFI Homopolymer stability curve.

C - Lowest temperature/melt flow index combination for a 150 mm diameter flow path length.

D - Upper temperature limit for satisfactory melt viscosity.

Figure 23 Linear programme for injection welding constraints.

As the use of compounded materials for the splicing sleeve gave an improved closure performance the same materials were also tried as an injectant. Although these gave further slight improvements in ESCR closure performance the welds obtained failed to pass the peel test.

The optimum overall performance is thus obtained on suitable copolymer jackets using cone ended sleeves manufactured by a rotational moulding process from Grade 2 MFI compounded material and a homopolymer injectant Grade 0.8 MFI 0.2% antioxidant.

Table 1 Results of ESCR tests on various sleeve, injection and jacketing materials

Jacket Material	Sleeve Material	Injectant	Average Time To Failure (mins)	Position of Failure(s)	Figure of Merit
EVA Co-Polymer	B	X	>20,000	-	1
"	A	Y	>20,000	-	1a
"	D	Y	>20,000	-	1b
"	C	X	18,300	Jacket to Weld	2
"	B	Y	17,000	Sleeve to Weld	3
"	C	Y	14,000	Sleeve to Weld	4
Homopolymer	B	X	3,000	Jacket to Weld and Sleeve to Weld	5
"	C	Y	2,018	Jacket to Weld	6
"	D	Y	753	Adaptor to Weld and Jacket to Weld	7

SLEEVE

A - Conical, Rotationally moulded grade 2.0 MFI Polyethylene + 10% Polyisobutylene.

B - Conical, Rotationally moulded Grade 2.0 MFI Polyethylene + 5% Polyisobutylene.

C - Conical, Rotationally moulded Grade 2.0 MFI.

D - Adaptor/extruded sleeve, Injection moulded Grade 0.3 MFI Polyethylene.

INJECTANT

X - Grade 2.0 MFI Polyethylene + 5% Polyisobutylene.

Y - Grade 2.0 MFI Polyethylene.

Conclusions

With the realization of this new range of splicing components and simplified tools it is considered that an economic and high security closure is now available for polyethylene jacketed cables which meets the design criteria enumerated at the beginning of this paper. The rotationally moulded cone ended splicing sleeves are virtually stress free, their profile enables jacket to sleeve adaptors and sharp diameter changes to be eliminated and tape wraps minimized. The special splicing tools comprise one injection gun and muffle and a small range of cheap metal strip moulds and rams, these tools being reliable, portable, and robust. The ability to apply a simple air pressure test immediately a closure is completed is of prime importance in enabling the operator to check his work quickly. This also allows operator standards to be established by an administration. The ease with which faulty closures may be repaired or reopened and closed following pair reallocation can also be considered a significant advantage of this method. Finally it is confidently anticipated that the ease and speed with which operators can be trained in the efficient use of this technique will lead to its increasing acceptance in many parts of the world.

Acknowledgement

The authors are grateful for the assistance of a number of colleagues who have been associated with the development of this technique. They also wish to thank the Directors of British Insulated Callender's Cables Limited for permission to publish this work.

References

1. Post Office Electrical Engineering Journal Volume 59 No.3 pp 206-210 October 1966 "Sheath Jointing of Plastic Sheathed Cables" E.D. Latimer and H.E. Robinson.

2. Transactions and Journal of the Plastics Institute December, 1967 pp 8,23-8,30 "Plastics in Telecommunication Cables: Jointing" W.C. Ward.

3. Siemens Review Volume 33 No.1 January 1966 pp 25-28 "Welding for Bonding of Polyethylene Materials for Communication Cables" Wolfgang Buckholz.

J.Graham Nevison,
Telephone Cables Division,
BICC Ltd.,
Prescot,
Merseyside,
England.

J.Graham Nevison graduated in Physics at Liverpool University, England in 1945 and has spent the whole of his professional career with BICC Ltd., in the area of Telecommunication Cables. As Construction Manager (General Home and Overseas Contracting) he has responsibility for the installation of telephone cable systems. He is a Member of the Institute of Physics.

David T. Parr,
Telephone Cables Division,
BICC Ltd.,
Prescot,
Merseyside,
England.

David T. Parr is Head of the Telephone Cables Accessories Development Laboratory of BICC Ltd., where he has been involved with the cable splicing development for the past seven years. As a mechanical engineering student he worked at Hawker Siddley Dynamics on guided weapon development and later spent three years at Lockheed Hydraulics followed by two years at Carborundum Company developing high temperature resistant materials. He is a Member of the Plastics Institute and is in the Institution of Mechanical Engineers.

POLYBUTYLENE-JACKETED AIR-CORE PIC CABLES FOR USE IN STEAM EXPOSED DUCTS

J. D. Dykes and G. F. DeVeau
Bell Telephone Laboratories, Inc.
Norcross, Georgia

Summary

A cable with polypropylene insulated conductors and a polybutylene jacketed sheath has been developed to reduce high temperature steam related cable failures. The sheath is known as STEAMPETH and will increase the maximum operating temperature for plastic sheaths from 170°F to 230°F. Polypropylene insulated conductors will prevent low insulation resistance failures that sometimes occur in pulp cable when it is exposed to steam conditions.

Water sensors and improved water removal techniques that restore wet PIC cable to its original condition have been developed for this introduction of PIC cable in the underground.

The combination of air core PIC cable and these new maintenance techniques promises to do more than just solve steam related failures. Color-coded plastic insulated cables with the maintainability of pulp thereby become available, and in the future expanded plastics can be introduced to increase duct efficiency.

The Steam Problem

In New York, Boston, and other cities steam is used as an energy source to heat and air-condition buildings. The steam, often 400°F or hotter, is pumped through an underground distribution system, and frequently the steam lines either cross or run parallel to telephone cables. Poorly insulated steam lines or actual steam leaks cause high temperature conditions that have resulted in many cable failures. In 1973 New York Telephone experienced over 100 steam related cable failures in Manhattan; New England Telephone had over 50 failures in Boston.

Three Types of Cable Failures

With pulp insulated stalpeth sheath cables, three types of steam induced failures have been experienced. The most frequent problem is cracking of the stalpeth jacket. A second failure mode occurs even without sheath cracking; low insulation resistance failures are caused by moisture drying from the pulp and condensing at a "cold spot" downstream from the heated section. The third failure mode is pulp insulation degradation; high temperature degrades the pulp to the point where handling of the conductors causes it to fall off the wire.

To avoid polyethylene sheath damage, stalpeth cables should not be installed where temperatures exceed 170°F. Above this temperature, pressurized sheaths, will expand and slits will soon occur in the jacket. For example, in laboratory tests cable samples held at 185°F and under 9 psi ruptured within 3 days. Both pressurized and nonpressurized stalpeth cables are subject to thermal stress cracking. Nonpressurized test samples bent to a 9" radius and placed in a 212°F environment cracked in less than a week.

Laboratory experiments demonstrated that high temperature conditions can cause low insulation resistance failures without sheath cracking.[1] If a length of dry (3% relative humidity) pulp insulated cable is exposed to a temperature of 180°F or so moisture is released as water vapor from the "dry" pulp. This moist air is then transported down the cable by normal air flow supplied by the gas pressurization system. At a cooler spot downstream from the heated section of cable, condensation may occur resulting in low insulation resistance failures. However, if a gradual cooling of the cable occurs, the released moisture will be redeposited over a long length of cable; this will prevent circuit failures. Thus, these failures are a function of the temperature profile and air flow rates.

Pulp insulation exposed to high temperature for long periods of time becomes brittle and turns to a natural tan color; telephone splicers have dubbed it "tobacco cable". If handled, it will fall off the wire so that as repair is attempted, shiners develop faster than repairs can be made. Laboratory aging for two months at 248°F converted pulp insulation into tobacco cable. Lower temperatures also cause degradation, but naturally the exposure times are longer.

Operating Companies indicate that stalpeth sheath cracking is the major problem, but a significant number of low insulation resistance failures occur and that pulp degradation is least common. Steam-exposed duct temperatures are generally between 150°F and 200°F, but there have been a few cases of temperatures exceeding 212°F.

Cable Design Alternatives to Reduce Steam Related Failures

General

A number of sheath and insulating materials have better high temperature properties than pulp and polyethylene, but high temperature performance is not the only significant factor in developing a steam resistant cable. Other points to be considered include (1) material cost and availability, (2) compatibility of designs with existing manufacturing equipment, (3) efficient use of duct space, and (4) compatibility with installation and maintenance procedures.

Sheath Materials

One solution to the high temperature polyethylene sheath cracking problem is to return to a lead sheath. But compared with stalpeth, lead sheath increases the cable cost about 20% and nearly doubles the cable weight. Lead's bend and friction characteristics also serve to increase the force needed to pull the cable into ducts; this sometimes necessitates smaller diameter cables (reduced pair counts) and/or shorter reel lengths (more splices). However, the main disadvantage to the lead sheath is its susceptibility to corrosion. Thus in cities with both steam and corrosion problems, the lead sheath alternative only gives the Outside Plant Engineer an option of how sheath failures will occur, it will not solve his problem.

Polybutylene, a plastic which has exceptional resistance to environmental stress-cracking and superior high temperature performance, has also been suggested to replace the polyethylene jacket. Polybutylene can be processed on existing equipment, and its long term hoop stress resistance at 150°F is compared with that of low density polyethylene in Figure 1.[2]

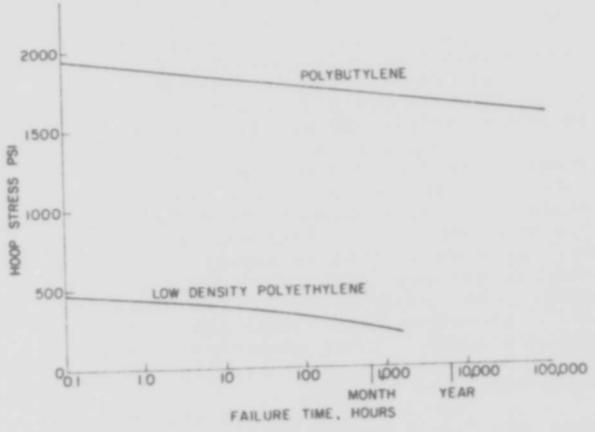

FIGURE 1

LONG TERM HOOP STRESS RESISTANCE 150°F

Samples of polybutylene-jacketed and polyethylene-jacketed cables have been tested under various conditions and typical results are shown in Table 1.

TABLE 1

High Temperature Sheath Tests
Straight, Pressurized Sections -
10-20 psi

	Failed within 2 days	Surviving After a Year
Polybutylene Jacket	248°F	230°F
Polyethylene Jacket	185°F	170°F

The polybutylene jacket is still withstanding 230°F under 20 psi after 12 months. As mentioned earlier, polyethylene jacketed cables at 185°F and 9 psi failed in 3 days; this is in line with polyethylene's accepted temperature limit of 170°F. Thus 45°F to 60°F improvement in jacket protection is indicated. It is estimated that the polybutylene jacket will withstand 212°F for 20 years.

The handling characteristics of polybutylene and polyethylene jacketed cables differ at low temperatures. Samples 7' long and 2.8" in diameter were bent at temperatures ranging from 0°F to 75°F. The efforts required to bend the cables were similar, but both materials stiffened at low temperatures to the extent that at 0°F it took twice as much force to bend the samples around a wheel with a 13" radius as it took at 75°F. However, the polybutylene cracked when sharply bent at low temperatures. As shown in Figure 2, a "free" bend at 20°F to about a 4" radius of curvature caused some polybutylene samples to crack; at 0°F a free bend to about a 10" radius caused samples to fail. No polyethylene jacketed cables cracked during these tests.

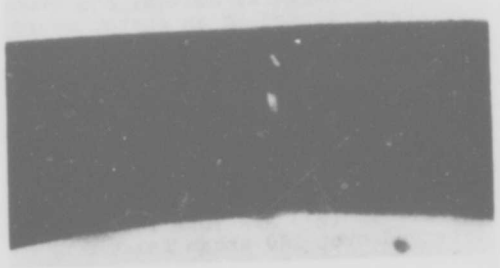

FIGURE 2

STEAMPETH SHEATH SAMPLE THAT CRACKED DURING A 4" RADIUS BEND

Polybutylene jacket will not crack if the bending operation is performed above 32°F and then subjected to cold temperatures. However, an investigation is underway to find a grade of polybutylene having better low temperature bending properties and with good high temperature performance.

Insulating Materials

To prevent cable failures related to pulp insulation, a different material is required. It should not absorb or give off moisture, and it should withstand high temperatures for a long period of time. The material's cost and dielectric constant are also of prime importance.

Dupont's Teflon[R] FEP-Fluorocarbon Resin is nonhydroscopic and will withstand high temperatures for extended periods. It has an attractively low dielectric constant of 2 but the material and insulating costs would be prohibitive.

Fortunately, other less expensive plastics, polypropylene, low and high density polyethylene, are available which will solve the low insulation resistance problems. Of these plastics, polypropylene has the best high temperature properties, and oxygen uptake tests indicate that it can be made to withstand 212°F for 5 years. Because of its high-temperature longevity, low price, low dielectric constant, and processability, well stabilized polypropylene is the current choice of insulating materials for steam exposed cables.

Recommendation for a Steam Resistant Cable

A cable with well stabilized polypropylene insulated conductors and polybutylene-jacketed sheath is recommended to reduce high temperature steam related cable failures. This design is referred to as PIC STEAMPETH cable.

PIC STEAMPETH Cable

Cable Construction

Figure 3 summarizes the PIC STEAMPETH cable design:

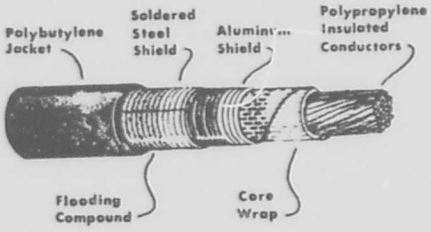

FIGURE 3

PIC STEAMPETH CABLE

The STEAMPETH sheath is similar to stalpeth; it has a corrugated aluminum shield, a soldered steel barrier, and a plastic jacket. Of course, the plastic jacket for STEAMPETH is polybutylene and not low density polyethylene. The steel is coated with a flooding compound to prevent corrosion and water flow in case of sheath cracking. "STEAMPETH" is printed on the jacket to distinguish it from other plastic sheaths.

PIC STEAMPETH cables follow the standard PIC color-code except the multiunit binder colors follow a scheme like Bell System pulp cables to prevent crossover splices. The cable consists of 100 pair multiunits and 25 pair primary units. For identification within a multiunit, each of the 4 primary units has a different binder; these binders are blue-white, orange-white, green-white, and brown-white as shown below. Pairs within each 25 pair primary unit follow the standard PIC color code.

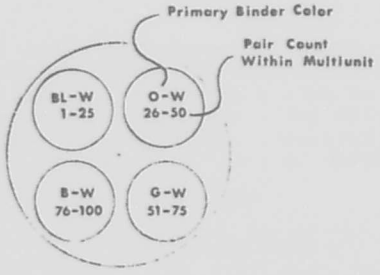

FIGURE 4

Each multiunit has a two color binder. One color, alternately yellow and black, is used to identify all the multiunits in a layer; the sequence starts with yellow on the outside layer. One multiunit in each layer has green as the second binder color, and this is the marker unit for the layer. These green units are placed over each other, and each one is flanked alternately by red and blue bound multiunits until each desired layer component is reached. The 1800 and 2700 pair cores are shown below:

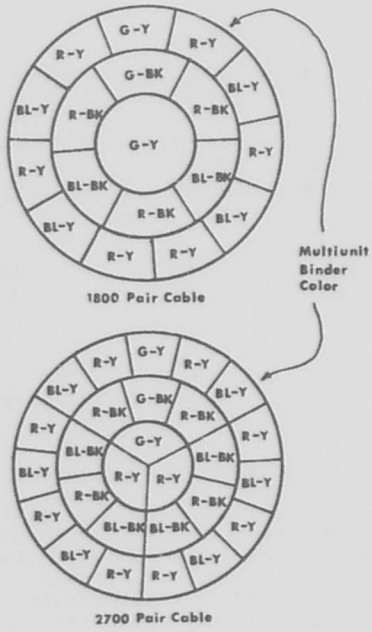

FIGURE 5

As in pulp cables, the unit count starts with the green center unit and proceeds through other center multiunits in a clockwise direction when the cable cross section is viewed looking away from the central office. The count continues with the same rules through the first layer, and then through any subsequent layers. Within a multiunit, pairs can be identified by color and binder group.

Table 2 compares the cable diameter of 1800 and 2400 PIC STEAMPETH cables with that of pulp stalpeth (other sizes of PIC STEAMPETH cable are available; these are just two examples). In large size cables the PIC design is about 0.1" larger.

TABLE 2

CABLE DIAMETERS

	26 AWG		24 AWG	
Pair Count	PIC STEAMPETH	Pulp Stalpeth	PIC STEAMPETH	Pulp Stalpeth
1800	2.50"	2.46"	3.14"	3.00
2400	2.87"	2.80"	-	-

Transmission Characteristics

The mutual capacitance of PIC STEAMPETH cable pairs is the standard 83 nF/mile. As shown in Table 3 the d.c. resistance and voice frequency loss (1 kHz) of the pairs are the same as pulp. However, at higher frequencies such as 772 kHz (center frequency for T1), PIC pairs have lower shunt conductance losses than pulp pairs.

TABLE 3

TRANSMISSION CHARACTERISTICS
(55°F)

	D.C. Resistance Ohms/mile	Voice Frequency Loss (1 kHz) dB/mile	T1 Engineering Loss (772 kHz) dB/mile
24 AWG			
PIC	274	2.31	29.5
Pulp	274	2.31	35.9
26 AWG			
PIC	440	2.85	39.5
Pulp	440	2.85	43.1

Advantages of PIC Cable

In addition to better high temperature properties, PIC STEAMPETH cables offer other advantages relative to paper or pulp insulated cables. Plastic insulation is more durable and is readily color-coded. It has higher dielectric strength than pulp and, as seen above, has lower high frequency loss (20% lower at 772 kHz) than equivalent gauge pulp pairs. Expanded plastic air core cables can also be employed to increase duct efficiency.

Since PIC cables do not fail immediately when wet, they are inherently more realiable than pulp. However, the overall maintenance package for combatting water in PIC cable left something to be desired.

Cable Maintenance

General

Compared to plastic one of the few advantages of pulp insulation is its maintainability with respect to water problems. Pulp, when wet, loses all working circuits giving an immediate alarm while the core swells limiting water travel. The point of water entry can then easily be determined since it is adjacent to the low resistance faults caused by the wet pulp. These low resistance faults can easily be located by welding the pair together with a breakdown set and tracking down the weld with resistance/length measurements or a tone and pickup coil. The cable is restored by localized drying of the core, clearing the welded pair, and restoring the sheath.

Air core PIC is not so easily maintained.[3] Water may enter the cable and due to the high insulation resistance of plastic go undetected for days or weeks before causing problems such as noisy circuits or open conductors. The ease with which water may travel longitudinally in PIC cable creates yet another problem. The point of water entry and the electrical fault may be hundreds of feet apart or, if water travels far enough, there may be two or more separate locations with electrical faults. Even locating an electrical fault in PIC cable is difficult since the fault is usually of a high and variable resistance. Because of this high resistance, and without paper pulp to carbonize and thereby catalyze a weld, the breakdown set is useless on PIC cable. Once the water has been located it sometimes has been more economical to replace the cable since many pairs may have corroded open and because water removal has been so difficult.

Before PIC STEAMPETH cables could be introduced as an attractive alternative to pulp cables in the underground, new maintenance techniques were needed that would:

1. Immediately detect water,
2. Help in locating the water,
3. Find the cause of water entry,
4. Facilitate restoral.

A maintenance system that includes these functions has been developed. It consists of gas pressurization, water alarms, and when needed, water removal techniques. These techniques are discussed below.

Gas Pressurization

A continuous pressure maintenance system will, in most cases, prevent water from entering PIC STEAMPETH cables. Continuous monitoring with pressure transducers will warn of slow pressure leaks as well as major sheath breaks. In case of a major sheath break, pressure gradients can be

drawn to estimate its location.

Since PIC STEAMPETH cables have one-fifth the pneumatic resistance of pulp the pressure feed points can be spaced farther apart; this reduction of feed points will simplify gas supply, and monitoring gas pressure to detect leaks.

Water Detection and Location

A simple means to immediately detect water entry and aid in the location of the water was sought. Placing a standard pulp pair in the PIC core may appear to be the obvious way. However, this is impractical since the insulation resistance of pulp at relatively high humidities (greater than 50%) would mask the resistance change in the pair caused by a wet spot. In order to desensitize the effect of humidity while preserving the desirable effect of pulp and paper when wet, a special water sensing element was devised. The sensor consists of paper insulated wire and a PIC wire with the insulation removed at the tip. The two are twisted together and the bare copper at the end of the PIC wire is tightly twisted around the paper insulated wire. The probe is shown in the following diagram.

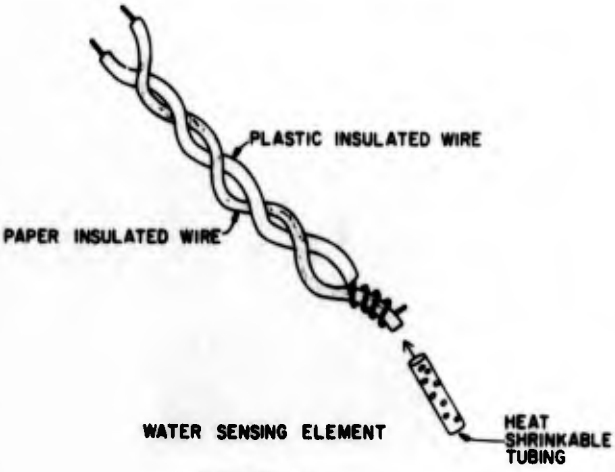

FIGURE 6

The water sensing end of the probe is covered with perforated heat shrinkable tubing to prevent inadvertent shorts while at the same time allowing water to reach the tip. The design of this probe is such that the two conductors are separated by plastic except at the very tip. This allows operation in high humidity (greater than 90%).

The sensor can be bridged onto either a dedicated pair or on working pairs. When wet, the sensor's resistance drops from many megohms to about 20 kΩ. Monitoring equipment senses this change, and an alarm is given. In order to pinpoint the trouble location, a breakdown test set may be used to weld the wet sensing element. By making a resistance measurement or by using a tone and exploring coil, the wet splice can be located.

For convenience water sensing elements are placed only in splices because (1) over three-fourths of wet cable problems occur in manholes and (2) it would be difficult to clear a welded pair if it were not in a splice. Besides if water does enter the cable between manholes, it will likely flow to a splice. Given an adjacent manhole location and noting air flow readings, sheath damage between manholes should be easy to detect and locate.

Cable Restoration

With a pressurization system and water alarm sensors, the occurrences of water in the cable should be minimal. In most cases when water does enter the cable, the amount to be removed should be small. However, there still may be some failures that require a method of quickly restoring a very wet PIC cable.

Existing methods of drying wet PIC cables include the use of acetone and dry nitrogen. Since acetone has a low flash point and will dissolve connectors using polycarbonate parts, its use is discouraged. Forcing dry nitrogen into the cable core will absorb some water, but long lengths of waterlogged cable may require months of drying and hundreds of nitrogen cylinders.

Although B Reclamation Compound[4] is a very effective technique used to reclaim waterlogged buried PIC cable, its extensive use in underground PIC is not attractive. B Reclamation Compound has maximum applicability in unpressurized, buried plant where numerous small sheath defects exist and where more are likely to occur. In the underground cables sheath defects in the conduit should be minimal. If leaks occur they will most likely be at manhole locations either in the sheath or closures. If B Reclamation Compound is used in underground PIC, pressure bypasses around the blocked section would be necessary. The compound also increases capacitance 30-40 percent which could cause transmission problems with high frequency carrier systems.

An improved cable restoration technique[5] has been developed for cases where the cause of water entry can be determined and repaired. The method uses a high output air compressor (10,000-20,000 cubic feet per day) which feeds into an air-dryer. By developing pressures up to 35 psi at the input, dry air equal to 50-100 tanks of nitrogen per day is pushed through the cable. In order to speed moisture removal, air in the cable core can be heated so that it will hold more moisture. This is done by forcing a high current through parallel and/or series combinations of spare pairs connected to a low voltage power supply. As the spare pairs are heated, air in the cable core becomes warmer, and its moisture carrying capacity increases.

The time needed to dry a wet cable can also be reduced by increasing the amount of air flowing into the cable. The flow of air, however, is limited by pressures which the cable sheath or splice closures can withstand. The STEAMPETH sheath can withstand 50 psi, but if air is forced through a splice closure, only 25-35 psi can be allowed.

Four field tests of the new water removal technique have been tried, all successfully. In the first three tests

the amount of water in the cable did not require the heating of spare pairs. However, in the fourth due to large amounts of water and to low temperatures during the restoration process, raising the cable core temperature by heating several pairs was necessary.

Although the water removal technique is capable in restoring completely waterlogged cables, it is believed that cables completely filled with water will not be typical; gas pressurization and water sensors should keep the amount of water entering a cable to a minimum.

ACKNOWLEDGEMENTS

Many have contributed to developing the PIC STEAMPETH cable system, but special thanks are due to Bruce Gesner, Nathan Hardwick, Jess Jackson, Wendell Nutt, Ralph Sabia and Fred Wight.

REFERENCES

1. J. M. Jackson, Internal Bell Laboratories memorandum.

2. Mobile Chemical Technical Bulletin and H. G. Scott and J. F. Humphries, Modern Plastic, March 1973.

3. M. C. Biskeborn and D. P. Dobbins "Waterproof Plastic Insulated Multipair Telephone Cable," Seventeenth Annual Wire and Cable Symposium, December 1968.

4. S. Kaufman and R. Sabia, "Reclamation of Water-Logged Buried PIC Telephone Cable," Twenty-first International Wire and Cable Symposium, December 1972.

5. N. E. Hardwick, "Restoration of Wet PIC Cable Using Vaporization Drying," Twenty-third International Wire and Cable Symposium, December 1974.

James D. Dykes

Mr. Dykes is a member of the Technical Staff at Bell Labs and has worked in the Multipair cable and Wire Department since joining the company in 1970. Mr. Dykes received a B.E.E. degree from Georgia Tech in 1970 and an M.S.E.E. degree from Stanford University in 1971. He is also a member of IEEE, Eta Kappa Nu, and Tau Beta Pi.

George F. DeVeau

Mr. DeVeau is an Associate Member of Technical Staff at Bell Laboratories, Norcross, Georgia. Since joining in 1967 his work has been concerned with multipair cable design and development. More recently he has developed several new techniques for maintaining PIC cables in the underground plant.

RESTORATION OF WET PIC CABLE USING VAPORIZATION DRYING (ANALYSIS AND APPLICATION)

Nathan E. Hardwick III
Bell Telephone Laboratories
Greensboro, North Carolina

SUMMARY

A viable scheme of water removal was needed before air core PIC telephone cable could become attractive for use in the underground plant. Although the basic concepts of vaporization drying are not new, this paper presents analytical studies that resolve questions related to vaporization drying schemes as well as steps for optimum restoration procedures.

NOMENCLATURE

B	Driving force for mass transfer.
c_p	Specific heat at constant pressure.
g	Reynolds flux (lb/ft^2 hr).
h	Surface heat transfer coefficient ($Btu/hr \cdot ft^2 \cdot °F$).
m_{H_2O}	Water concentration, mass of H_2O in a small volume divided by the mass of all the material in that volume element.
$\dot{m}''$	Mass transfer flux ($lb/ft^2 \cdot hr$).
M	Quantity of moisture removed from cable (lb/hr).
P	Pressure (psi).
$\dot{q}''$	Heat flux ($Btu/hr \cdot ft^2$ °F)
t	Temperature (°F)
V	Air velocity in cable.
W	Amount of air entering or leaving cable section.
X	Quality of water vapor (mass of vapor divided by total mass of air-water mixture).

Subscripts

G	G-state (i.e., bulk gas).
L	L-state on control volume surface.
S	S-state on control volume-surface.

INTRODUCTION

Necessity for Restoration

There are functional as well as cost advantages in using polyethylene insulated conductor (PIC) cable in the underground duct system. However, a problem that must be resolved before air core PIC cable can be introduced as an attractive alternative to pulp insulated cable in the underground plant is the development of an effective method of water removal from the core.

Besides this future application there is also a present-day need for a water removal technique, i.e., this technique is also adaptable to buried PIC cable in cases where the B-Reclamation Compound is not suitable.

Restoration Complementary to Reclamation

The process discussed in this paper is viewed by the author as complementary to the Reclamation Process[1] in buried plant. (Reclamation involves pumping a gelatin-like substance, B-Reclamation Compound, into the cable core to remove water and preclude future water entry.)

Cable conditions that would favor restoration by water removal versus reclamation for wet PIC cable are listed in Table I.

TABLE I

RESTORATION - RECLAMATION ALTERNATIVE (BURIED PLANT)

I. CONDITIONS FAVORING RESTORATION BY AIR DRYING

1. Pressurized double-sheath cable (e.g., buried toll and trunk cables, feeder cables).
2. Water entry probably a singular occurrence.
3. Increase in capacitance by 35% not tolerable (e.g., special service circuits).

II. CONDITIONS FAVORING B-RECLAMATION COMPOUND

1. Single-sheath buried cable (e.g., Alpeth cable with lightning holes).
2. Cable likely to get wet again and again.
3. Nonpressurized cable.
4. Increase in capacitance by 35% is tolerable.

Briefly, restoration using techniques discussed in this paper is preferred in buried plant for pressurized double-sheath cable. Also, water removal is preferred in cases of one-time water entry problems such as construction equipment damage, open splice cases, and entry prior to installation. However, the method can be extended to other cases where the 35% capacitance increase resulting from B-Reclamation Compound would be detrimental to service.

On the other hand, B-Reclamation Compound is the ideal solution to water-logged non-pressurized or single-sheath cable in buried plant. (For example, a condition where lightning has caused multiple holes in an Alpeth sheath.)

New "In-Depth" Investigation

Although a number of schemes for water removal have been proposed in the past, no in-depth investigations have been found. In sifting through these proposals as well as some newer ideas, a number of questions related to these various schemes became evident. Most of these questions could be resolved using thermodynamic and heat transfer analyses without costly and time-consuming experimentation. Furthermore, this study would eliminate, once and for all, consideration of proposed schemes that are impracticable or not theoretically feasible.

However, the key objective sought was to use the results of the analyses to determine a method that optimizes the process of water removal from both a time and cost standpoint.

METHODS PROPOSED AND QUESTIONS TO BE ANSWERED

Basic Mechanism of Water Removal

The basic water removal process is a two-step procedure. In the first step the bulk of the water in the cable is removed by forcing high pressure air into the cable core. The air acts like a piston and forces the water out of the cable at selected vent point. After this initial step, less than 15% of the air space in the cable is left with water.

The second step in the restoration process is to vaporize the residual water and transport the vapor out of the cable. The air is forced through the cable causing the water surface or moist regions on the solid surfaces to be scrubbed and usual vaporization to occur. A crude model of the basic mechanism is shown in Figure 1. W is the amount of air entering the cable. Since the water content, X, of the air must increase, $M = W (X_2 - X_1)$ is the amount of water accumulated. The air can only produce drying while it remains unsaturated (i.e., as long as it remains in a state above its dew point temperature).

Forced Convection of Dry Unheated Air at High and Low Pressures

There are two approaches that can be used to vaporize the remaining water. First, the high pressure procedure can be continued as shown in Figure 2. In this case a compressor

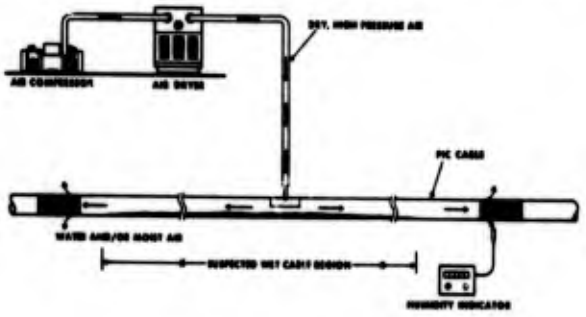

Fig. 2 Schematic of Water Removal Arrangement for Wet Cable

and air dryer are used to force massive amounts of dry air through the cable core until the moisture level of the exiting air is reduced below an acceptable level. A second approach is to use the available air pressurization source to force air through the cable section at a lower velocity.

Although the high pressure procedure will dry the cable in a shorter time period, it has the disadvantage that additional equipment (sometimes manned) will be required. Thus, one aspect of this problem that can be resolved theoretically is a comparison of the vaporization rates for the two processes. This analysis will also answer the question regarding the efficiency of exiting from the cable with fully saturated air at the lower velocity versus the possibility of exiting with a lower vapor quality at the higher velocities.

THERMODYNAMIC ANALYSES OF WATER VAPORIZATION RATES FOR COMPETING DRYING SCHEMES

A thermodynamic analysis is required to determine the water vaporization rates for

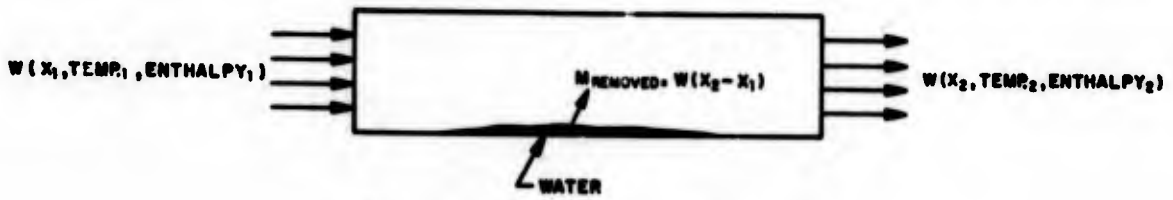

Fig. 1 Mathematical Model for Basic Mechanism of Vaporization Drying

the competing high and low pressure schemes. For readers who are primarily interested in the nonanalytical aspects of this work, sections marked by asterisks (*) may be omitted without loss of continuity.

*Model for Phenomena Adjacent to Interface When a Water Surface is Exposed to Dry Air

In order to develop an analysis of convective mass transfer for the drying process, details of the happenings close to the air-water interface are important. When water vaporizes into air, the air has a greater moisture content in the neighborhood of the interface than at a distance further out from the fluid. Thus, there is a steady transport of water vapor through the air along this gradient.

The rate at which material will be transferred from one phase to another across the interface is to be calculated. To accomplish this, a small element of the interface between the two regions (each containing a different phase) is considered. The phase which attracts the major part of the attention (air in this case) can be defined as the considered phase, to distinguish it from the other which is designated the neighboring phase.[2]

Now consider this element for an idealized model of a water film within the cable being scrubbed by dry air (see Figure 3a). A control volume is assumed that has two surfaces,

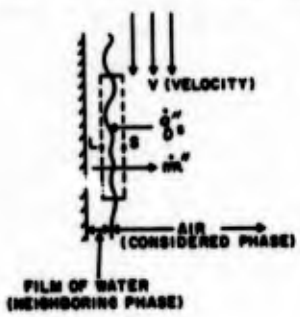

(a)

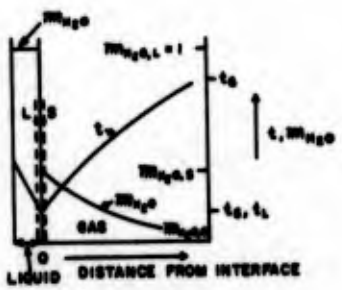

(b)

Fig. 3 Phenomena adjacent to the Interface when a Water Surface is Exposed to Dry Air

designated S and L (see temperature and mass profile in Figure 3b), which are parallel to the interface element but separated from it by a distance of a few mean free paths of the molecules. The mass-transfer flux, $\dot{m}''$(lb/ft^{2}hr) is defined as the net rate at which material crosses unit area of the interface from the neighboring phase and into the considered phase per unit time. Similarly $\dot{q}''$ (Btu/ft^{2}hr°F) denotes the rate of heat transfer per unit area.

An exploration of the composition of the air using Figure 3b reveals that the concentration of steam (i.e., water vapor) in the mixture varies steadily along a normal to the interface, having its highest value $m_{H_2O,S}$ adjacent to the interface and its lowest value within the bulk of the air stream. Note that m_{H_2O}, unlike the temperature (t), exhibits a discontinuity at the interface because the water film is in the liquid phase ($m_{H_2O,L} = 1$), while the adjacent gaseous mixture may only contain a small proportion of steam ($m_{H_2O,S} << 1$).[2]

*The Reynolds Flow Solution

The processes contributing to mass transfer are numerous. However, the Reynolds Flow Hypothesis[2] can be used to express the complex heat-and mass-transfer relations in an Ohms' law type relation,

$$\dot{m}'' = g \cdot B \qquad (1)$$

where g is the conductance and B is the driving force. The Reynolds Flux, g, can be regarded as a quantitative measure of the rate of "scrubbing action" of the fluid stream on the interface (i.e., g represents the amount of stream material which is brought to the S-condition by contact with the surface). This conductance g can be deduced from the surface heat-transfer coefficient, h, of convective heat transfer theory by means of the relation,

$$g = h/c_p, \qquad (2)$$

where c_p is the specific heat of the mixture at constant pressure.[2]

The driving force B in Equation (1) is related to the thermodynamic properties of the various states in the idealized model. In the present case, the driving force is related to the water concentrations by the equation[2]

$$B = \frac{m_{H_2O,G} - m_{H_2O,S}}{m_{H_2O,S} - 1}. \qquad (3)$$

When a stream of air flows through a duct, the G-state is chosen as an average of the states of the fluid flowing past the section in question. Normally, the "mixing cup" average is used. (This is the state which would prevail in the steady state in an adiabatic well-stirred vessel with its only entrance at the cross-section in question.) In the case of interest the G-state is fully specified as to composition and temperature.

Usually $m_{H_2O,S}$ is found to take a value which depends only on the temperature t_S and the local pressure, (i.e., the phase change can take place so easily that thermodynamic equilibrium prevails between the L- and the S-states). However, the interface temperature and the S-state composition are not known. In order to determine the S-state characteristics for a particular case, information from three sources can be brought to bear on the problem, namely from mass transfer theory, from thermodynamics, and heat-transfer theory. This involves either a laborious trial and error method or a graphical scheme that requires enthalpy-composition diagrams be constructed for each pressure condition.[2]

WATER ACCUMULATION COMPARISON

Using the Reynolds Flow model, vaporization rates were calculated for conditions encountered in the proposed drying schemes. These results were used to compute how a specific volume of air accumulates water as it traverses a cable section under the various conditions. (As the air accumulates additional water vapor, the driving force diminishes and the rate of vaporization for a particular volume of air decreases.) The water accumulation results provide the quantitative basis for obtaining the total drying rate throughout a cable section under the conditions of the proposed drying methods.

Figure 4 gives the total mass of water accumulated by air at 70°F throughout a uniformly wet cable section plotted against the time after the first dry air enters the cable section. Each new mass of air entering the cable will have a similar vaporization pattern as long as the entire cable section is wet. Hence, the curves provide a snapshot of the ongoing vaporization process prior to the time that the initial section of the cable becomes dry.

These curves reveal that during the time that it takes a slug of low pressure air to traverse a 500-foot cable section, four times as much water is accumulated by air at the higher pressure and velocity. Although each high pressure slug of air accumulates less water at each point, the high pressure slug of air moves much more rapidly through the section. Hence, more air moves through each section in a given time. The additional water accumulation by the higher pressure flows would be even more pronounced with either hotter air or longer cable sections.

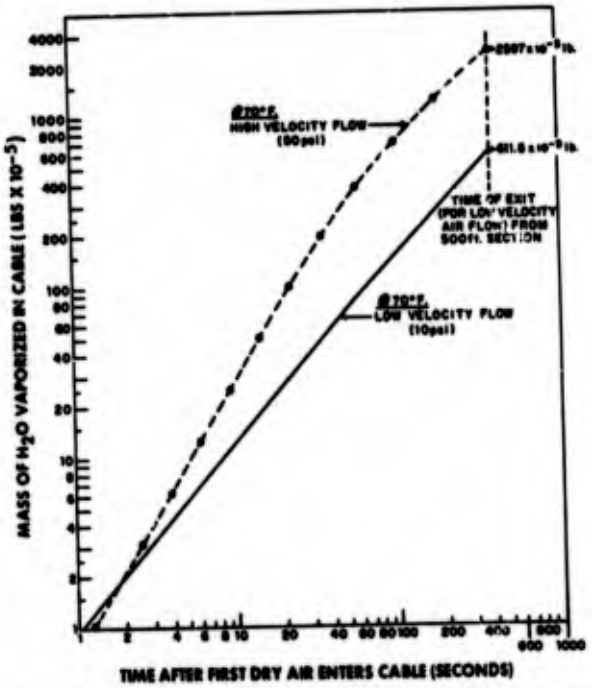

Fig. 4 Total Mass of Water Accumulation by Air at 70°F Throughout a Uniformly Wet Cable (500 feet long)

Therefore, intuitive reasoning that the ideal drying conditions exist when air exits from the cable at 100 percent relative humidity is incorrect. Ideally one wants to have air with the largest possible capacity and highest flow velocity.

ACCELERATED DRYING

The next echelon of sophistication is accelerated drying. Since 50 psi is the maximum temporary pressure that Bell System standards will allow in a cable core, the flow velocity cannot be increased further. Thus, referring to Equation (1), the capacity of the air must be increased in order to increase the vaporization driving force.

Benefits of Higher Temperature

Increasing the temperature of the air will achieve this end. Figure 5 is a plot showing the water capacity of a cubic foot of saturated air at various temperatures. For temperatures below 100°F the amount of water that a volume of air will hold almost doubles with each 20°F rise in the air temperature. Figure 6 repeats the curves for the total mass of water accumulated by air at 70°F throughout a uniformly wet cable section. In addition, similar curves are included for the high and low pressure cases when the air temperature is elevated to 90°F. Note that the total water accumulation throughout a cable increases with air temperature at the same rate as the water-holding capacity of the air (i.e., approximately doubles for 20°F increase).

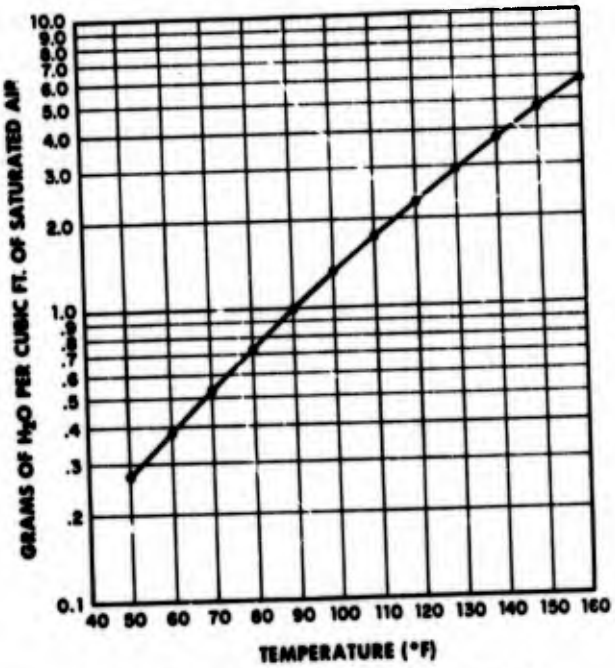

Fig. 5 Water-holding Capacity of a Cubic Foot of Saturated Air at Various Temperatures

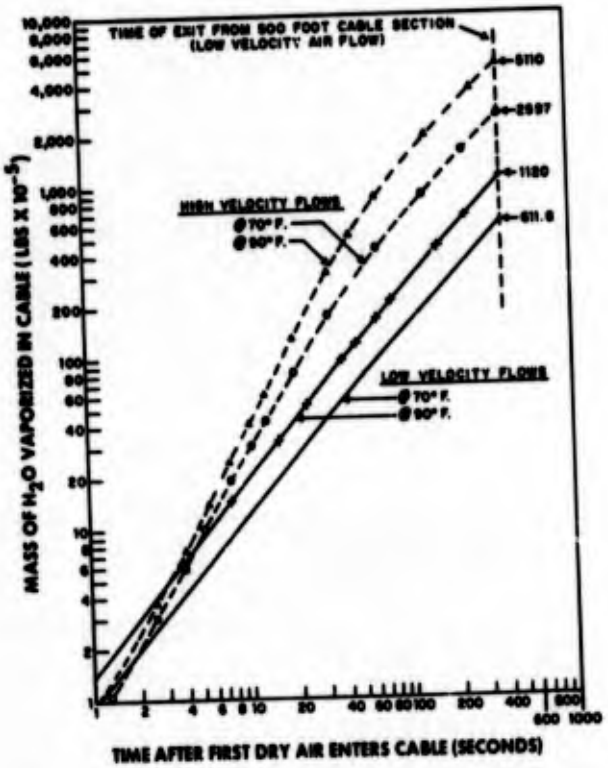

Fig. 6 Total Mass of Water Accumulation by Heated Air in a 500 Foot Cable Section that is Uniformly Wet

Drying Time for a Typical PIC Cable Section

Using information from the thermodynamic analysis, the drying time for a typical PIC cable section can be estimated. Assuming a 500-foot cable section (600-pair, 22-gauge ARPAP) with 10% of the available air core filled with water, the drying times are given in Table II.

TABLE II

DRYING TIME FOR PIC CABLE*

TYPE FLOW	DRYING TIME	
	T_{air} = 70°F	T_{air} = 90°F
HIGH PRESSURE	5.7 days (5.0)	2.9 days (2.8)
LOW PRESSURE	24.3 days	13.3 days

* 500' SECTION OF 600 PAIR-22 GAUGE ARPAP

Experiments were performed using a similar cable in a 500-foot dry test duct in order to verify the calculated results. The experimental results (shown in parenthesis in Table II) corroborated the theoretical findings within the accuracy allowed by the mathematical modeling.

Heating Schemes

Technique of Preheating Air. One often proposed scheme for increasing air temperature is to use a preheater to heat the air prior to entering the cable. There is no heat supplied within the cable, therefore, a heat transfer analysis is important to determine how sharply the air temperature drops along the length of cable.

*The method of solution is to first obtain the thermal resistance to heat loss from the inner core through the sheath and its environment. Then using this as a boundary condition, an extension to the separation of variable solution of the heat transfer equation is made using a special form of a series of eigenfunctions.[3]

Assuming the inlet air to be preheated to 150°F the resulting temperature distributions are plotted in Figure 7 for buried and underground cables with both high and low pressure (i.e., velocity) conditions. The calculated temperature distributions indicate that the air core temperature cannot be maintained significantly higher than the temperature of the surroundings for more than a few hundred feet under the best conditions. Thus, this recurring proposal does not appear feasible since the advantage of having heated air would be negated.

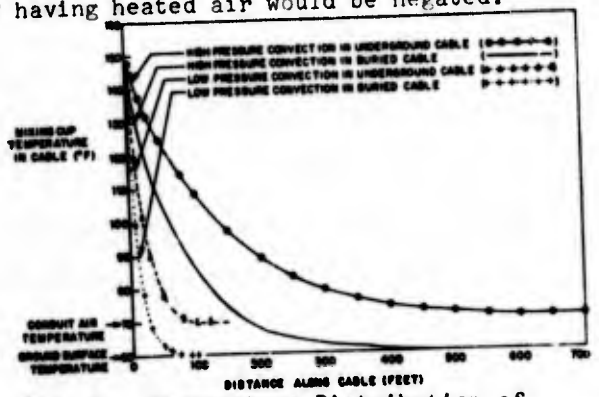

Fig. 7 Temperature Distribution of Heated Air being Convected along the Section of Cable

Technique of I^2R Heating. Another method of heating the cable is to employ I^2R (or Joulian) heating. As illustrated with Figure 8, the air within the cable is heated by applying current to some of the spare conductors within the cable core with the far ends shorted together. The single

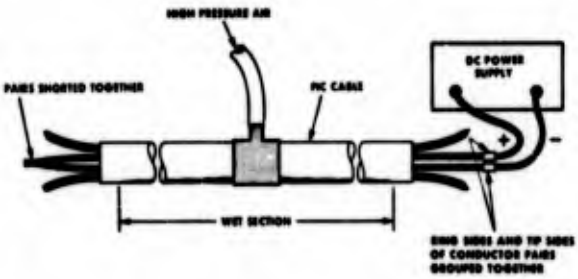

Fig 8 Schematic of I^2R Heating Setup for Accelerated Drying

most important question to be answered here is how much energy is necessary to provide a sufficient temperature rise in the traversing air.

*The heat transfer solution for this case is obtained from a superposition of fundamental solutions of the differential equation for the temperature field in laminar pipe flow. Lundberg, et. al.,[4] obtained the eigenvalues, eigenfunctions, and expansion coefficients (arising in the resulting Sturm-Lioville equation) through a direct numerical integration facilitated by a convergent iteration method for obtaining the eigenvalues.

In the analysis for buried cable the ground temperature is assumed to be 60°F and the inlet air from the compressor is assumed to be 70°F. The resulting temperature curves showing the mean temperature within the cable versus distance from the air inlet are plotted in Figure 9 for buried cable. The lower curve represents the case where no current is introduced to the conductors. (All solid curves are for a low pressure driving force of ΔP = 10 psi). Note that the air temperature approaches that of the ground a short distance downstream from the cable inlet.

The middle solid curve represents the air temperature distribution when one watt/foot of I^2R energy is introduced. This energy output can be attained when seven conductor pairs (22 gauge) of 500-foot lengths are subjected to a potential of 50 volts. This magnitude of heat energy is sufficient to maintain the convected air at 9°F above the ground temperature. However, if 100 volts are applied across these same conductors the energy output is increased fourfold to 4 watts/foot. This case is indicated by the upper solid curve. A significant increase in the temperature of the air within the cable occurs (96°F terminal temperature) under these conditions.

The dashed line represents the 4 watts/foot power output case when the high pressure air (ΔP = 50 psi) is forced through the cable. In this case the same terminal temperature is reached. However, this temperature is attained at a position of about 60 feet from the cable inlet. The terminal temperature is reached when the heat loss from the cable air core to the environment equals the heat flux from the Joule energy at this temperature. Thus, Joule heating can be used to increase the air temperature for either the low pressure or high pressure convection methods.

For underground plant the cables are in conduits and resistance for heat loss by convection to the air is much larger (providing the ducts are not flooded). Assuming no flooding, the resulting curves for mean temperature in underground cables are given in Figure 10. The magnitudes of

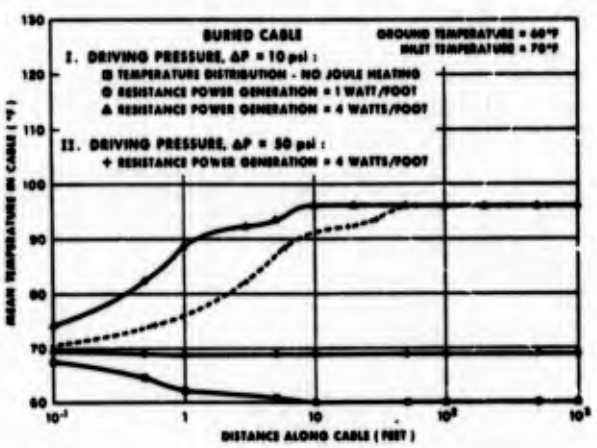

Fig. 9 Temperature Distribution in Buried Cables due to Joule (I^2R) Heating

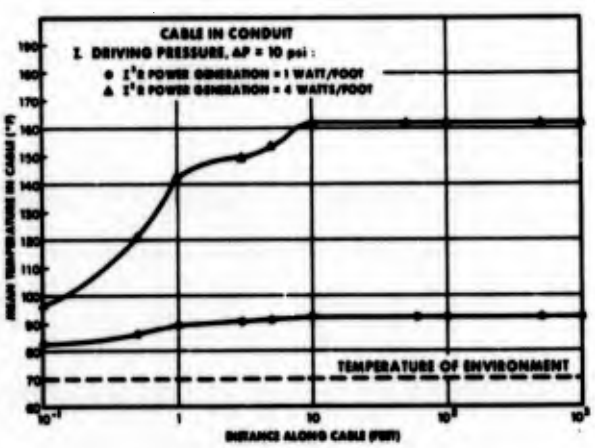

Fig. 10 Temperature Distribution in Underground Cables due to Joule (I^2R) Heating

the terminal temperatures are much higher than the corresponding buried cable values because of the higher resistance to heat loss to the environment.

APPLICATION OF RESTORATION PROCEDURES

As in the reclamation process the following factors should be taken into account in selecting the optimum length of cable section for restoration: (1) the length of cable suspected of containing water; (2) the slope of the terrain; (3) location of splice cases in section: (4) pneumatic resistance of the section. The preferred arrangement is to open existing splice cases or, in their absence, remove the cable sheath outside the extremities of the wet cable section and introduce high pressure dry air at a centrally located point (see Figure 2).

A wet section of underground PIC cable is different from buried PIC in that the section length for restoration is fixed by the manhole-to-manhole spacing. In all other respects, the procedure is the same.

Restoration Equipment

The equipment arrangement for restoration by vaporization using high pressure dry air is shown in Figure 11. It is important

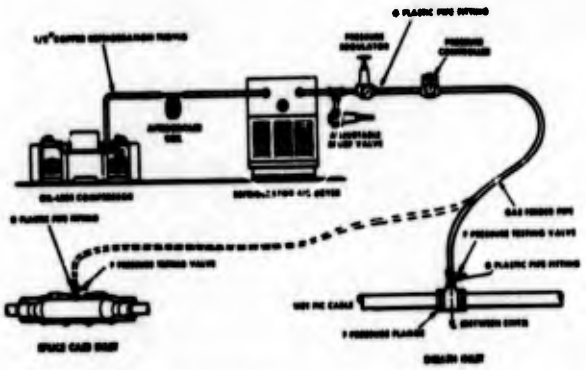

Fig. 11 Equipment Arrangement for Vaporization of Residual Water from PIC Cable

to recall that the drying time is directly related to the rate at which the dry air is forced through the cable. This is why the pressure should always be maintained as high as the cable (50 psi) or splice case (35 psi) can safely withstand (i.e., the greater the pressure at the inlet, the greater the flowrate will be for a certain cable length). The flowrate is greater for a shorter cable section (i.e., having a lower total pneumatic resistance). Thus, the compressor and air dryer are sized to have a large flow capacity in order to permit operation at the optimum conditions of maximum allowable inlet pressure. Figure 12 shows a plot of approximate flow rates for various pneumatic resistance units of PIC cables. By manifolding, a second compressor can be used to accelerate the completion of a particular project. Details of the functional requirements of the equipment components as well as generic specifications are discussed in the equipment supplement to this paper in Appendix A.

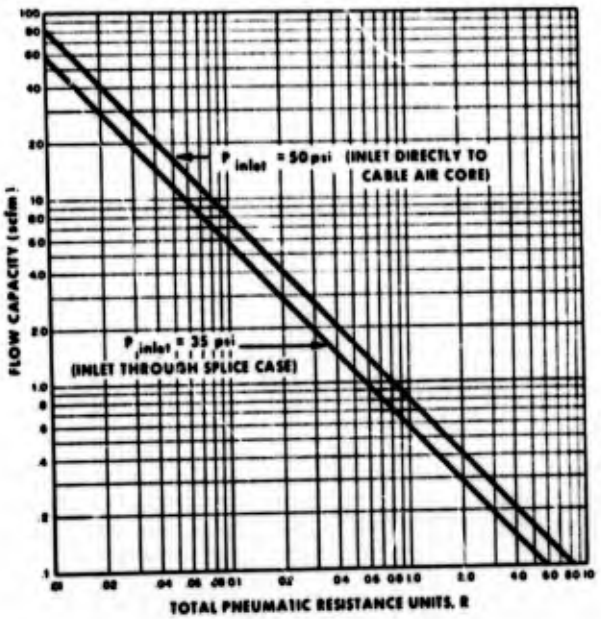

Fig. 12 Air Flow Rates as a Function of Pneumatic Resistance Units for Given Inlet Pressures

Cable Moisture Level Check

Periodically the moisture level of the air exiting from the cable should be checked with a humidity indicator to see if acceptable moisture levels have been reached. When the relative humidity of the outlet air (with a 10 psi inlet pressure) drops to less than 35% rh the cable is considered technically dry.

Electrical Testing to Confirm Restoration

When acceptable moisture levels have been reached all the known problem pairs are to be rechecked. If no pairs are found to have insulation resistance less than 10 megohms (conductor-to-ground), the restoration is completed.

RESTORATION EXPERIENCES

A series of six field experiments in restoring actual wet cable sections have been completed using these restoration techniques. In all but one of the cases the high leakage pairs were restored within two days using only high pressure dry (unheated) air. In the other case extremely cold conditions as well as the necessity of pumping uphill dictated that I^2R heating be employed to restore this 1510' section. Despite these conditions,

the restoration costs were only 25% of the estimated cost of replacement (the only alternative possible because the section was too long for reclamation). In most cases the water-related faults cleared after the bulk purge.

DISCUSSION OF RESULTS AND CONCLUSIONS

The principal conclusion from the study is that vaporization drying using high pressure unsaturated air is a viable means for restoring wet PIC cable in both underground and buried plant provided the cause of water entry is corrected. This water removal process is considered a complete restoration process. That is, application of this technique to a cable very soon after water has entered will essentially restore the cable to its previous condition. In addition, it avoids the necessity of bypassing a filled reclaimed section with air pipe.

The thermodynamic analysis determined that ideal vaporization conditions result from having air with the largest possible water-holding capacity and highest flow velocity. Also quantitative values result that allow prediction of reduced drying times so economic tradeoffs are possible between the optimum restoration equipment and overall drying costs. In conjunction with the thermodynamic analysis the heat transfer analyses provided the magnitude of energy required for accelerated drying using I^2R heating as well as revealing that preheating the air is not feasible.

The use of forced air drying (without heating) has been approved for Bell System use. It is considered that this technique will accommodate most wet cable problems. The feasibility of accelerated drying with I^2R heating has been demonstrated, and this technique is under evaluation for application in cold weather conditions and for cable sections containing large amounts of water.

REFERENCES

1. S. Kaufman and R. Sabia, "Reclamation of Water-Logged Buried PIC Telephone Cable," (21st International Wire and Cable Symposium, December, 1972).

2. D. B. Spalding, Convective Mass Transfer, (New York: McGraw-Hill, 1963).

3. S. Sideman, D. Luss, and R. E. Peck, "Heat Transfer in Laminar Flow in Circular and Flat Conduits with (Constant) Surface Resistance," Applied Science Research, Section A, Volume 14, 1964-65, pp. 157-171.

4. R. E. Lundberg, W. C. Reynolds, and W. M. Kays, "Heat Transfer with Laminar Flow in Concentric Annuli with Constant and Variable Wall Temperature and Heat Flux," (Washington, D. C.: NASA Technical Note D-1972, August, 1963).

APPENDIX A

EQUIPMENT SUPPLEMENT

This equipment supplement is included to provide generic equipment specifications as well as to explain the functional requirements of the equipment components which are not readily apparent.

Mounting of the equipment is left to the discretion of the users. Positions for "quick-disconnects" are indicated to simplify on-site assembly. When the equipment is placed inside a van during restoration, adequate ventilation must be assured to prevent the heat dissipated by the equipment from causing excessive ambient temperature (e.g., leave windows and doors open).

CONFIGURATION: CONTINUOUS DUAL-COMPRESSOR SYSTEM

The restoration system is shown schematically in Figure A1. Instructions and settings

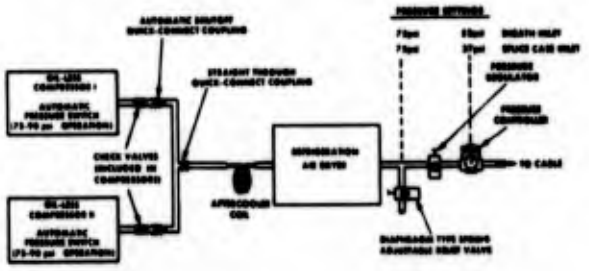

Fig. A1 Schematic of Continuous Dual-Compressor System Utilizing "Manifolding" to Provide Maximum Flow through Cable Section

of equipment components for different types of cable sections are given below.

(i) High Pneumatic Resistance Section

The functional requirements imposed upon the regulators and relief valves depend upon whether the wet sections has a high or low total pneumatic resistance. A High Pneumatic Resistance Section is defined as a section in which the compressor capacity is sufficient to create an inlet pressure greater than the allowable inlet pressure for restoration (e.g., greater than 35 psi for splice case entry).

For this case the pressure controller should be set to provide the allowable pressure at the inlet to the cable air core. The bleed relief valve should be set at a 60 psi pressure or higher if continuous compressor operation can be maintained (i.e., slightly below the upper pressure cutoff). This setup maintains higher pressure at the inlet of the air dryer as well as continuous operation of compressors having automatic pressure switches. (Higher inlet pressure results in more efficient dryer operation.) Without the relief valve the compressors would cycle rapidly because of the low volume in the air lines.

In a High Pneumatic Resistance Section the intermediate regulator does not come into play and should be set wide open.

(ii) Low Pneumatic Resistance Section

A Low Pneumatic Resistance Section is defined as a section having such a low total pneumatic resistance that the available compressor capacity is not capable of creating the objective pressure at the air core inlet. For this case, the pressure controller is set to the inlet pressure merely to prevent unsafe pressures during the initial bulk water purge.

The intermediate pressure regulator is closed until at least a 60 psi pressure is created at the inlet to the air dryer. The flow will be choked somewhat under these conditions but the higher pressure results in more efficient drying. This is particularly important under cold environmental conditions because the dew point temperature is lowered following expansion through the regulator.

The bleed relief valve does not come into play with a Low Pneumatic Resistance Section because the compressors are not capable of flow rates necessary to cause pressure cutoff conditions.

(iii) General

The aftercooler is necessary to dissipate thermal energy generated during compression so that the temperature of the air entering the dryer does not exceed the specified level.

Manifolding compressors in the manner shown has two advantages. First, the flow capacity of the system is increased above 15 scfm which will provide optimum drying conditions for essentially all cases. Second, drying will continue if one compressor malfunctions. For cases where one compressor will provide the optimum capacity (e.g., flowrate less than 8.2 scfm) the other unit may be unplugged when the equipment is attended. (These compressors have automatic check valves to prevent air backing into them.) Additional flexibility is gained by using self-closing quick disconnects at the compressor outlet. This allows one unit to be easily removed for maintenance or to be included only when conditions require the added capacity.

Generic Specifications

(1) Compressor

The oil-less compressors should be capable of delivering at least 7.5 scfm at 75 psi with an output temperature less than 200°F.

(2) Air Dryer

The refrigerator air dryer should be capable of delivering at least 15 scfm of 75 psi air at a dew point not greater than 0°F at 14.7 psi when the inlet temperature is 150°F. The air dryer should also have an automatic temperature bypass so the cooling chamber will not freeze at very low flow rates.

(3) Aftercooler

The aftercooler must be capable of dissipating enough energy to reduce the outlet temperature of the air from the compressor to the specified inlet temperature of the air dryer (preferably less than 130°F). A suitable aftercooler can be constructed locally by forming several turns of 1/2-inch OD copper tubing into a helix approximately one foot in diameter. Experience has shown that at least six turns should be used to provide adequate cooling.

(4) Adjustable Relief Valve

The adjustable relief valve should be capable of bleed flows up to 15 scfm at 5 to 125 psi. A pressure gauge having the same range is also required.

(5) Dial Air Pressure Controller

The Dial Air Pressure Controller should have an associated gauge and be capable of operating at 150 psi (up to 200°F) and 15 scfm.

(6) Pressure Regulator

The regulator should be of industrial quality having a compatible pressure gauge. The operating range should be 5-125 psi at a flow rate of 15 scfm.

COST

The following listing gives approximate costs of the equipment recommended for the restoration process.

COMPONENTS	COST
Oil-less Compressors (2)	$1000
Refrigeration Air Dryer	500
Aftercooler	15
Dial Regulator (with gauge)	20
Regulator (with gauge)	15
Relief Valve (with gauge)	20
Quick Disconnects	10
TOTAL	$1580

Nathan E. Hardwick
Bell Laboratories
Mt. Hope Church Road
Greensboro, North Carolina 27420
Phone (919) 697-4906

Nathan E. Hardwick has received B.S. and M.S. degrees in Mechanical Engineering from the University of South Carolina and a Ph.D. in Mechanical Engineering from Lehigh University. He joined Bell Laboratories at Allentown, Pennsylvania in 1965 and was initially engaged in eutectic chip bonding. He later became responsible for coordinating the initial design of the ceramic package for beam lead integrated circuit chips for the Bell System. Then he worked on the temperature characterization of the packages and free convection studies applied to multi-chip substrates. More recently he has formulated analyses for air pressurization source locations in toll and trunk cables as a member of Transmission Surveillance Department at Greensboro, North Carolina.

ECONOMICS AND PERFORMANCE CONSIDERATIONS OF TELEPHONE CABLE PLUGGING

FRANCIS M. FARRELL, III, MANUEL FILREIS, JAMES D. GROVES, and HENRY K. KAPPELL
3M COMPANY, ST. PAUL, MINN.

SUMMARY

Due to several significant trends in the use of pressurization in the outside plant the subject of cable plugging deserves a re-examination.

The use of centrally read transducers, along with air-pipe systems, allow better than ever sheath condition monitoring. The development of a cable plugging system that compliments these advances is discussed.

Economic considerations point to several interesting conclusions.

INTRODUCTION

The entire history of improved telephone service has been marked with milestones representing advances in the quality of the transmission path. Probably the largest single advance was the replacement of open wire by cable. This in turn required the development of pressurization techniques. Pressurized cable equates to a dry and therefore relatively steady state transmission path which has allowed practitioners of electronics to multiplex many signals onto one pair and bring incredible economies to information transmission. Pressurization, especially the control of it through gas tight dams is the topic of this paper.

Pressurized cable plant has been evolving for half a century. Advances have come steadily and now it is a well developed tool that offers high utility. Most of the overall benefits it can afford us are already being realized, however, significant improvements continue to be made in various components of the overall pressure system. It is important to recognize the interaction of these various components and what net effect a change in any one component will have on the entire system. Only those component improvements increasing the overall system value are acceptable. It is in this light then that we should evaluate the present effort in cable plugging.

HISTORICAL PERSPECTIVE

Before plunging into specifics, let's take a look at what has led us to the present state-of-the-art.

The first field use of cable pressurization was in lead sheathed toll cables during the 1920's. These cables lent themselves to gas pressure because they were long runs with few branches. Since they produced high revenue, there was ample economic justification for the higher initial cost of pressurization. The benefits sought were twofold, namely; protection of the core from moisture entry and a method of monitoring sheath condition. Some controversy exists as to which one was the primary motivation but that's a concern for historians.

A pressure "system" then was a discrete section of cable, typically seven to eleven miles long, maintained under a static pressure (Fig. 1). Static pressure in the section was maintained by periodic charges of dry gas, usually nitrogen, from a high pressure cylinder. Leak location was a matter of reading pressures at valves spaced along the cable, either in manholes for underground cable or at poles for aerial cable, and then making a graphical analog of the findings. The intersection of the plotted gradients approximated the leak's location (Fig. 2). A soap solution was then painted on the suspected area to find the actual leak.

In the early 30's, pressure contactors gained wide acceptance. They were placed along the cable, three or four to a section, and could be set to any desired pressure level. If pressure dropped, an alarm would sound in the central office to indicate a change in sheath condition. This was a quantum jump in the monitoring function of pressurization.

The condition of remotely placed nitrogen cylinders was also monitored when they were used to feed discrete sections that required a constant pressure source. Central office alarms would indicate when cylinders needed replacement. Thus another link in the system had been added. Not only could sheath condition be monitored but also the provision of the pressure medium itself.

Through all these developments, the discrete pneumatic sections were isolated with only one type of gas dam or cable plug as it is commonly called. As shown in Fig. 3, this plug was made by removing a section of sheath and replacing it with a lead sleeve. The sleeve was first filled with liquid paraffin to saturate the conductor insulation, the paraffin was then "boiled" out and replaced with hot asphalt which solidified to a reliable gas tight dam. This was a notable achievement but the plug construction was very time consuming and relatively dangerous.

The benefits of pressurization to toll cable in reduced maintenance cost and improved reliability were so substantial that by the late 40's attempts were underway to pressurize portions of exchange area cable.

Exchange cable presented a new set of difficulties, as is illustrated in Fig. 4. Whereas in toll cable there were large cables, few branches and long runs, exactly the opposite was true in the exchange cable plant. Frequent entries into the sheath were necessary for small branch cables and circuit rearrangement and most of the early terminals were not pressure tight.

These fundamental differences required two basic changes in pressure systems. First, a better source of pressurizing gas other than a nitrogen cylinder was needed because high activity in the exchange cable plant produced large leaks reducing its overall pneumatic integrity compared to toll cable. Secondly, a more economical and rapid plugging system was required because of the vast increase in number of plugs per unit length over toll cable.

The mid 50's provided solutions to both problems. Continuous feed air dehydrators were developed which provided large quantities of dry air which was fed directly into cables as they left the central office vault. A "cold resin" method of plugging was a corresponding development which reduced the cost, complexity and danger of the old hot asphalt plugs.

The newly developed system was primarily an advance in materials since a thermosetting epoxy was substituted for two troublesome thermoplastics. The advantage offered by the epoxy resin was that a chemical reaction occurring at ambient temperature caused it to go from an injectable liquid to a gas-tight solid, rather than the heating and cooling cycle needed for wax and asphalt.

Along with the development of epoxy as an improved material, came the introduction of a new method of application -- sheath injection. This method was developed primarily to accelerate and simplify plugging the large number of small diameter cables found in the distribution network. Using this method, a craftsman would simply drill a hole through the lead sheath and inject the epoxy resin directly into the core.

The sheath injection method never gained widespread use on larger cables because their layered core construction prevented thorougn resin penetration and therefore, reliable plug formation. Instead the new epoxy compound was poured or injected into lead sleeves. This method, nonetheless, was a vast improvement over the wax/asphalt method.

Plastic insulated conductor (PIC) cable was the next significant development that had an effect on pressurization. For the exchange cable plant, it was a mixed blessing; since service was less immediately affected by moisture entry, sheath breaks remained unnoticed and open longer allowing large amounts of water to collect far from the point of entry. As PIC cable matured as a product, a more realistic approach to its use developed. It became generally accepted that high humidity in the core was tolerable but bulk water was not. Ways of keeping it out were needed.

Pressurization, of course, was one of the options selected to supply the answer. Double sheath PIC cable was designed specifically for use on pressurized trunk and toll routes, as well as for feeder cable to cross connect terminals in the exchange plant. Single sheath cable was also pressurized to a limited extent.

A need now arose for a method of plugging PIC cable with several solutions emerging. Epoxy resins, as used in pulp cable, were unacceptable because their high exotherm during cure would degrade, or even melt, polyethylene conductor insulation. Specially formulated epoxies were developed which had smaller temperature rises but this was done at the expense of rapid cure. Namely, the large heat of reaction inherent with epoxy had to be dissipated over a longer cure time. A further disadvantage was the tendency of epoxy to dramatically reduce in viscosity just prior to gelling. This behavior was especially troublesome in PIC cable because the conductor insulation was completely non-absorbent; thus allowing the thinned plugging compound to flow down the core leaving voids.

Polyurethanes began to arouse interest at this time. This class of resins is a chemically reacting thermoset similar to epoxy but offers some essential advantages over epoxy. These are:

- --- lower cost.
- --- lower exotherm during cure preventing thermal damage to the plastic insulation.
- --- uniform viscosity increase to gellation thus not flowing down the core away from the plug location.
- --- less offensive odor.
- --- less skin irritation.
- --- better insulation resistance.
- --- improved compliance with conductors and sheath during thermal cycling.
- --- greater resistance to thermal and mechanical shock.
- --- shorter wait until pressurization.

(Fig. 5) illustrates a polyurethane plug. It is somewhat analogous to the earlier lead sleeve plug, filled with epoxy, with several exceptions. Unlike lead, the plastic sleeve method required internal strain relief and shield bonding. This development was a doubly significant advance since it introduced polyurethanes to the outside plant, not only as a plugging compound but also as a splice encapsulant. It is still dominant in both roles.

The early 70's saw another change in plugging methods gain widespread popularity. It was a modification of the earlier sheath injection method, this time using a polyurethane compound where the sheath itself contains the compound rather than an applied sleeve. The new method required that an opening, or a "window", be cut into the sheath, the core prepared, a fitting attached and the compound injected (Fig. 6). Since the need for a plastic sleeve and additional mechanical and electrical continuity was eliminated it resulted in a sizable time savings. It could be used with all types of cable and therefore appeared to offer a universal advantage.

To place this sheath injected urethane plugging method in perspective as one component in the overall system it is necessary to consider the other components which constitute a modern cable pressure system. As mentioned earlier, a single component's worth is determined by its effect on total system performance.

PRESENT STATE-OF-THE-ART

Without placing them in chronological order, several recently available components in a modern pressure system are:

Air Pipe - the high pneumatic resistance in cable limits the distance pressure can be maintained at a useful level when it is fed only from central office dryers. "Air pipe" systems overcome this by paralleling cable runs with low pneumatic resistance air lines (Fig. 7). Dry air can then be manifolded into cables at proper intervals to keep cable pressures at any selected level. This does for the air pressure in a cable, what a repeater does for the signal being transmitted.

Pole Mount Air Dryers - allows either cables or air pipe systems to be fed at locations distant from the central office. They are disproportionately expensive to operate compared to a central office dryer, but excessively long runs and/or leaky systems require them.

Pressure Transducer - a pressure measuring device which produces an output proportional to the pressure it senses. It gives a quantitative reading. It allows for a much more sophisticated, remote monitoring system.

Automated Monitoring Systems - a mechanized approach to cable plant monitoring where remote devices are periodically accessed and interrogated. When a device gives a reading outside pre-set limits an alarm is given alerting maintenance forces to the

location and nature of the problem. Devices which are typically monitored include air dryers, contactors, transducers and air flow rate indicators. These automated systems vary in sophistication from simply monitoring a few contactors on a priority cable, to elaborate computer controlled networks monitoring entire geographical areas. Such a system is described below.

Cable Pressure Monitoring System - briefly stated is the latest advance in the state of the art. It is both a monitoring and management tool (Fig. 8). It was designed by Bell Laboratories to upgrade and unify the pressurization efforts that had become very extensive and complex since the introduction of pressurization to the exchange plant. CPMS, as it is commonly called, will monitor up to 15,000 miles of pressurized cable, reporting changing conditions to the responsible repair forces and also provide management with current information on the status of the maintenance of pressure systems.

The system is extremely flexible since changes can be made by simply altering the controlling computer program. The overall effect of CPMS is to maximize the benefit of the large investment already made in pressurization and minimize the incremental cost of further additions.

From this perspective we can now look at the specific topic of modern cable plugging.

Air dryers, pipe systems, transducers and CPMS are all acknowledgments that leaks are expected in cable pressure systems. These leaks occur at splice cases, repeater housings, manifolds, cable plugs and in air pipes, to name a few. In fact any computer assisted pressure system design program allows for a fixed leakage in a given amount of plant.

It is critical, however, that tolerated leak rate be small compared to leaks the system is designed to protect against. Anything else is poor design and poor economy since it decreases the system's capacity to protect and its sensitivity to monitor.

A USER'S NEED

A large user of cable pressure plugs recently began an evaluation of the state-of-the-art in plugging, considering both methods and materials. A specification was written stating their performance and economic requirements. The specification placed a high premium on a universal system, one in which a common method and material would perform up to required levels for both pulp and PIC cable. To comply with this requirement, all our development efforts, except as noted, treated pulp and PIC cable in a similar manner.

The economics of plugging are inextricably tied to the overall economics of pressurization. A low first-cost plug that requires subsequent maintenance and reduces long term pneumatic integrity of the system is a very false economy. Therefore, the plugging system that meets design criteria is the only economical choice. Why set performance criteria otherwise?

Performance then, was the controlling factor. The specification addressed this by stating required levels of performance and how attainment of those levels was to be proven.

The most stringent requirement set a maximum allowable leakage rate for sample plugs after they had been aged through thermal cycling. There is good justification for this method of accelerating age because the failure mode of most plugs in the field is thermally induced dimensional changes. It is simply speeded up in the laboratory to reduce development and evaluation intervals.

The actual test is:

24 plugs are made in both pulp and PIC insulated cable. (eight each at 20, 70 and 95° F.)

All 48 plugs are cycled for 50 cycles.
(0 to 100° F. for pulp, −40 to 140° F. for PIC)
under a constant 10 psig pressure.

At the conclusion of the cycling, leakage rates past the plugs are measured at 0, 40 and 95° F.

In order to meet the specification, pulp samples must have an average leakage rate not exceeding 10 cc/min and PIC samples must not exceed 1 cc/min (both corrected to standard conditions; 0° C and 760 mm Hg). The difference in allowable rates is based on intended use of the different cable types and their different pneumatic resistances.

There were other requirements but this one appeared dominant. Our first attempt therefore, was to try to qualify the sheath injected urethane method which had gained wide popularity. Groups of samples, including both PIC and pulp cables, were prepared and tested using several different commercial urethane formulations.

TABLE 1

PNEUMATIC TEST DATA FOR SHEATH INJECTED

CABLE PLUGS

CABLE		PLUGGING CONDITIONS		# CYCLES PASSED
SIZE	TYPE	TEMPERATURE	COMPOUND	
600/24	PAP FPA - PIC	70	A	33
300/24	PAP FPA - PIC	70	A	3
600/24	PAP FPA - PIC	32	A	12
600/24	PAP FPA - PIC	70	B	12
300/24	PAP FPA - PIC	70	D	3
600/24	PAP FPA - PIC	32	C	12
2700/26	STALPETH - PULP	32	A	FAIL INITIAL
2700/26	STALPETH - PULP	32	C	FAIL INITIAL
2700/26	STALPETH - PULP	70	A	12
2700/26	STALPETH - PULP	70	B	FAIL INITIAL
2700/26	STALPETH - PULP	70	C	FAIL INITIAL
200/24	STALPETH - PULP	70	B	FAIL INITIAL
200/24	STALPETH - PULP	70	A	12

Table 1 illustrates the limited success of the sheath injection technique. Typically a sheath injected plug will provide a good initial plug on PIC cable, but will begin to leak after a few cycles due to the severe stress of the temperature cycles of this type of specification. Performance is more mixed on pulp cables. Present sheath injection plug compounds and techniques do not measure up to these new severe specifications.

At this point, one might ask how applicable this type of specification is to the typical user of pressure plugs. Obviously, existing systems will make plugs and under many use conditions these may perform indefinitely. However, just as obviously these plugs may also break down and leak under many conditions. It would seem desirable, in view of the economic penalties of maintenance or failure of plant, to use systems which assure long term performance.

Examining the failed samples of sheath injected plugs by staining the leak paths with a dye solution, it was very evident that the sources of difficulty were the many interfaces between the plugging compound and the various layers of the sheath that remained in place. A look at a double sheath cable construction, Fig. 9, will illustrate the many interfaces that may cause continuous leak paths through the length of the plug. Since the sheath seemed to be the problem, consideration was given to the earlier methods where the sheath was removed. A modification of the classical sleeve method was developed (Fig. 10). It simplified core preparation, shield bonding and sleeve placement. A urethane was formulated to meet the material requirements in the user's specification and perform satisfactorily in both types of cables. Its wetting action was improved over earlier urethanes so it would penetrate and saturate the core of pulp cable yet not run down the core in PIC cable. Compound introduction into the sleeve was simplified and economized by the use of a standard two part plastic bag which can be injected with a regular caulking gun. In addition, the method is more universal than sheath injection since the rate of compound introduction is independent of cable type unlike sheath injection where it must be metered into PIC cable to prevent excessively long plugs.

TABLE 2

PNEUMATIC TEST DATA FOR SLEEVE INJECTION

CABLE PLUGS

CABLE		PLUGGING CONDITIONS		# CYCLES PASSED
SIZE	TYPE	TEMPERATURE	COMPOUND	
200/24	STALPETH - PULP	70	A	51
200/24	STALPETH - PULP	70	A	51
200/24	STALPETH - PULP	70	A	51
1200/24	STALPETH - PULP	70	A	54
2700/26	STALPETH - PULP	70	A	54
2700/26	STALPETH - PULP	70	A	51
200/26	STALPETH - PULP	70	A	54
2700/26	STALPETH - PULP	70	A	56
2700/26	STALPETH - PULP	70	A	56
900/24	STALPETH - PULP	70	A	63
600/22	STALPETH - PULP	70	A	53
2700/26	STALPETH - PULP	70	A	53
900/24	STALPETH - PULP	70	A	55
200/24	STALPETH - PULP	20	A	51
200/24	STALPETH - PULP	20	A	51
200/24	STALPETH - PULP	20	A	51
200/24	STALPETH - PULP	20	A	51
2700/26	STALPETH - PULP	20	A	51
2700/26	STALPETH - PULP	20	A	51
2700/26	STALPETH - PULP	32	A	54
2700/26	STALPETH - PULP	32	A	69
2700/26	STALPETH - PULP	95	A	51
2700/26	STALPETH - PULP	95	A	51
200/24	STALPETH - PULP	95	A	51
200/24	STALPETH - PULP	95	A	51
200/24	STALPETH - PULP	95	A	51
200/24	STALPETH - PULP	95	A	51
2700/26	STALPETH - PULP	95	A	51
2700/26	STALPETH - PULP	95	A	51

Table 2 shows the revised sleeve method did meet the leakage rate requirements of the specification. Furthermore, an average craftsman can apply the modified sleeve plug in the same time required to inject a plug into the sheath on equivalent cables. This latter consideration was an added help in bringing the first cost of a modified sleeve plug in line with the first cost of a sheath injected plug.

TABLE 2 (con't.)

PNEUMATIC TEST DATA FOR SLEEVE INJECTION

CABLE PLUGS

CABLE		PLUGGING CONDITIONS		CYCLES	
SIZE	TYPE	TEMP ° F	COMPOUND	PASSED	COMMENTS
900/24	STALPETH - PULP	70	A	6	CONTINUED 1/2 SHIELD
2700/26	STALPETH - PULP	70	A	FAIL	CONTINUED 1/2 SHIELD
100/24	PCP	20	A	54	NO SEALING COLLAR
600/24	PCP	32	A	56	NO SEALING COLLAR
600/24	PCP	32	A	56	NO SEALING COLLAR
900/24	PAP FPA - PIC	70	A	53	SEALING COLLAR
900/24	PAP FPA - PIC	70	A	53	SEALING COLLAR
900/24	PAP FPA - PIC	70	A	53	SEALING COLLAR
100/24	PCP	95	A	54	NO SEALING COLLAR
600/24	PCP	95	A	58	NO SEALING COLLAR
600/24	PCP	95	A	58	NO SEALING COLLAR
600/24	PCP	95	A	55	NO SEALING COLLAR
600/24	PCP	95	A	55	NO SEALING COLLAR
900/24	PAP FPA - PIC	70	A	6	NO SEALING COLLAR
100/22	PAP FPA - PIC	70	A	51	NO SEALING COLLAR
100/22	PAP FPA - PIC	70	A	6	NO SEALING COLLAR
900/24	PAP FPA - PIC	20	A	1	NO SEALING COLLAR
900/24	PAP FPA - PIC	20	A	3	NO SEALING COLLAR
100/22	PAP FPA - PIC	20	A	3	NO SEALING COLLAR
100/22	PAP FPA - PIC	20	A	3	NO SEALING COLLAR
100/22	PAP FPA - PIC	95	A	3	NO SEALING COLLAR
100/22	PAP FPA - PIC	95	A	3	NO SEALING COLLAR
900/24	PAP FPA - PIC	95	A	1	NO SEALING COLLAR
900/24	PAP FPA - PIC	95	A	51	NO SEALING COLLAR
900/24	PAP FPA - PIC	95	A	1	
600/24	PCP	70	A	FAIL	CONTINUED 1/2 SHIELD

TABLE 3

SLEEVE INJECTION PLUGGING COMPOUND

I. UNCURED PROPERTIES	METHOD	VALUE
-- Free TDI (%)		None
-- Volatile Isocyanate (%)	ASTM 2615	2.3
-- Viscosity (Cps- 25° C)	Brookfield Viscometer	
Prepolymer		3,500-4,000
Polyol		1,000-1,500
Mixed (1 Minute)		1,500-2,000
-- Gel Time (min., 25° C)	Sunshine Gel Meter 100 g. Mass	20-25
-- Maximum Exotherm (°C)	100 g. Mass	75-80
II. CURED PROPERTIES		
A. PHYSICAL		
-- Tensile Strength (psi)	ASTM D-412-68	1,500-2,000
-- Elongation (%)	ASTM-D-412-68	150-200
-- Hardness (Shore A)		85-90
-- Density (gm/cc)	3M*	1.10
-- Volume Shrinkage (%)	3M*	1.5
-- Copper Corrosion	3M*	None
-- Fungus Resistance	ASTM D-1924-63	"O" Growth
-- Hydrolytic Stability (7 days, H_2O, 100° C.)	3M*	
a) Weight Increase (%)		2.5-3.5
b) Shore A Loss		15-20
-- Heat Stability (21 days, 135° C)	3M*	
a) Weight Loss (%)		3.0-3.5
b) Shore A Increase		10-15
-- Thermal Shock	3M* 10 Cycles 1/4" Insert −55° C to 130° C	No Cracking
B. ELECTRICAL		
-- Dielectric Strength (Volts/mil) (1/8" Sample)	ASTM D149-64	450-500
-- Dielectric Constant 10^2Hz	ASTM D150-70	25° C 5.3 60° C 6.2 90° C 7.3
-- Dissipation Factor 10^2Hz	ASTM D150-70	25° C 0.065 60° C 0.073 90° C 0.077
-- Insulation Resistance (ohms) (28 days, 40° C, 96% R. H.)	3M*	1×10^{10}

The material properties of the polyurethane adapted for the modified sleeve method are given in Table 3. The properties listed are those called for by the customer's specification and are appropriate to a plugging compound.

Two properties deserve some in-depth consideration; dry heat aging and dielectric constant.

Dry heat aging is particularly significant to a plugging compound because it simulates long term aging in the presence of dry air. Two hazards to an improperly formulated urethane come from dry aging; weight loss from plasticizer volatility or migration which causes shrinkage and, thereby, opens leak paths and hardness increase due to oxidation. Hardness increase reduces the urethane's ability to follow thermally caused dimensional changes in the plug, also a major cause of leak paths.

TABLE 4

EFFECT OF DRY HEAT AGING

ON A SHEATH INJECTED CABLE PLUG

(Temperature 135° F.)

Days	Leakage Rate (cc per min.)			
	Stable Compound (Scotchcast 4407)		Non-Stable Compound X	
	Stalpeth	PAP	Stalpeth	PAP
0	0	0	0	0
17	0	0	0	0
48	0	0	9	2
88	13	1	48	25

To verify this theory four sheath injected plugs were made, two with a urethane resistant to weight loss and hardness increase, the other susceptible to both. The plugs were aged at 135°F for 88 days. Table 4 shows the progressive change caused by the degradation in the thermally unstable compound.

A cable plug is viewed by the signal being transmitted in a cable as a lumped capacitance. In other words it appears as a capacitor in series in the transmission path. Capacitance is a function of plate spacing, plate area, and dielectric constant of the intervening material. In a section of cable containing a plug the capacitive effect depends on: the spacing between the individual conductors, which is essentially the same in all plugging methods; the area of conductors (plates) exposed to the dielectric medium, which is proportional to plug lengths for a given cable; and the dielectric constant of the compound. Since spacing is constant for all methods, only area (length) and dielectric constant matter. Thus, it can be seen that the capacitive influence of a plug in any given cable is proportional to the length of the plug times the dielectric constant of the material.

This is good news for a sleeve type plug which incorporates a relatively low dielectric compound. Furthermore, a sleeve plug is typically 10-12" long while an injected plug averages 36", and some compounds used for sheath injection have dielectric constants above 9. Thus a sheath injected high dielectric plug can have a capacitive influence 4 or 5 times that of the system described herein.

Improved Test Facility

The large number of plugs that were tested in the foregoing program has lead to an improved testing facility. The latest facility as shown in Figure 10 is centered around a mass flow meter which constantly monitors the pressurized samples in a temperature cycling chamber.

The system is designed to include a strip chart recorder giving us a hard copy record of leakage rates during the temperature cycling. This will enable better identification of failure modes which will allow further improvement and simplification in cable plugging.

Conclusion

Pressurization has evolved from primitive beginnings to today's highly automated servant. Plugging has always been part of it and continues to be as fundamental as ever. More options are available for today's plugging requirements, yet quality and reliability is now more important than ever.

The options must be carefully evaluated and their true costs assessed. Plugs that don't maintain long term pneumatic integrity as specified in the design of modern pressure systems reduce the value of those systems.

In what we see as a definitive study, where performance was quantified, the data strongly indicates that "new" sheath injection method of plugging does not fill the bill. The classical sleeve method modified and combined with a new polyurethane and delivery system does meet the need and, furthermore, does it for a lower first cost.

REFERENCES:

1. Allen, Richard - "Cable Pressurization Proves In" Telephone Engineer and Management, April, 1964.

2. Bell Telephone Laboratories - Transmission Systems for Communications, Revised Fourth Edition.

3. Jackson, J. M. - "Dry Air Pressure System for Exchange Cable" Bell Laboratories Record, October, 1956.

4. Jackson, J. M. - "New Air Dryer for Pressurizing Cables" Bell Laboratories Record, January, 1961.

5. Masterson, J. B. - "Pressure Dams in Communication Cables" Proceedings of the International Wire and Cable Symposium, October, 1969.

6. Piccolo, F. P. - "Automatic Detection of Low Gas Pressure in Exchange Cables", Bell Laboratories Record, January, 1964.

7. Ratta, J. A. - "Cold-Resin Gas Dams for Telephone Cables" Bell Laboratories Record, July, 1954.

8. "R E A Specifications for Encapsulations, Splice Closures and Pressure Blocks", PE 70, March 1971, Revised.

9. Theriot, E. J. - "An Automated Cable Pressure Monitoring System" Int'l. Symposium Subscriber Loops and Services, May, 1974.

10. Western Electric Specification for G, H and J Plug Compound AT 8649, March, 1974, Issue I.

11. Williams, J. L. - "Polyurethane Goes Underground" Bell Laboratories Record, October, 1968.

FRANCIS M. FARRELL, III

Francis M. Farrell, III received a B.S. in Chemical Engineering from the University of Dayton in 1968. He worked for Western Electric for four years as a product engineer concentrating on splice encapsulants and cable plugging compounds.

In 1972 he joined Devcon Corporation to develop and market a proprietary line of products for the telephone industry.

He has been a Product Development Manager in 3M's TelComm Department since January. His area of responsibility includes Cable Accessories and Materials R & D.

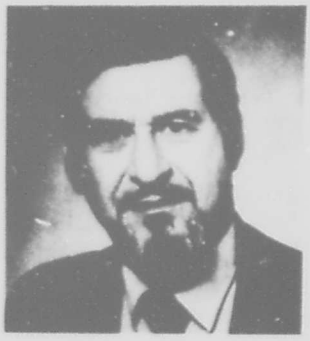

MANUEL FILREIS

Manuel Filreis holds a B.S. Degree from North Carolina State University in Textile Engineering in 1949. Since then he worked for Burlington Industries, Inc. and B. F. Goodrich Chem. Company prior to joining 3M Company in 1960 as a Product Development Engineer. Currently, he is employed as a Senior Development Engineer in the TelComm Department, Cable Accessories Group.

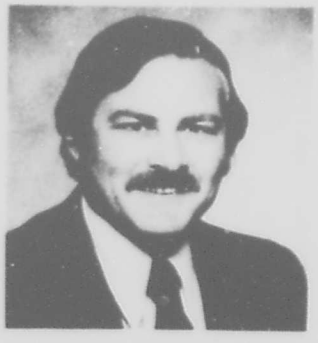

JAMES D. GROVES

James Groves received a B.S. in Chemistry from Washington State University, an M.S. from the University of Minnesota and a Ph.D. in Physical Organic Chemistry from the University of Colorado in 1958. He joined the 3M Company in 1959 as an Organic Research Chemist. Since 1967 he has worked exclusively in the area of Materials Research and Development for the power and communications industries. Currently, he is the Materials Research and Development Supervisor in the TelComm Department Laboratory.

HENRY K. KAPELL

Henry Kapell graduated in February, 1959 from the University of Illinois with a B.S. Degree in Chemical Engineering and joined 3M Company at that time. His career at 3M has been in Product Development and he has been associated in that capacity with TelComm Department since 1969. He has been Product Development Supervisor for the Closures and Cable Accessories Group since 1972.

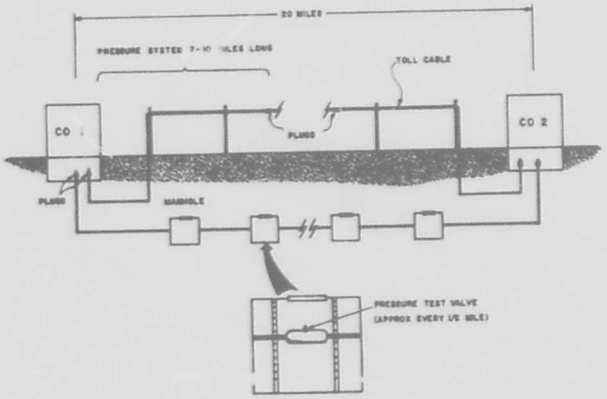

FIGURE 1. EARLY DISCRETE PRESSURE SYSTEM

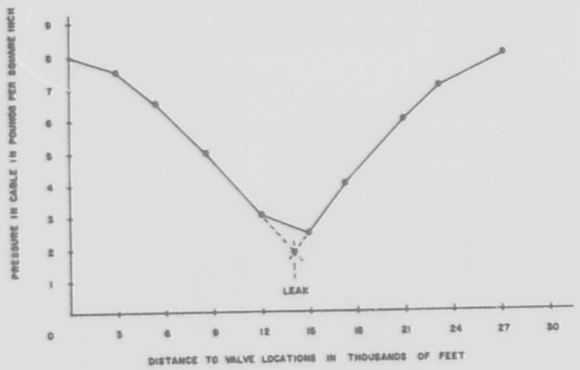

FIGURE 2. LEAK LOCATION, GRAPHICAL METHOD

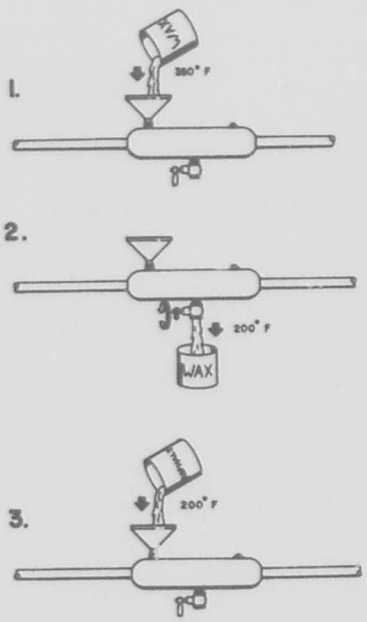

FIGURE 3. ASPHALT PLUG PREPARATION

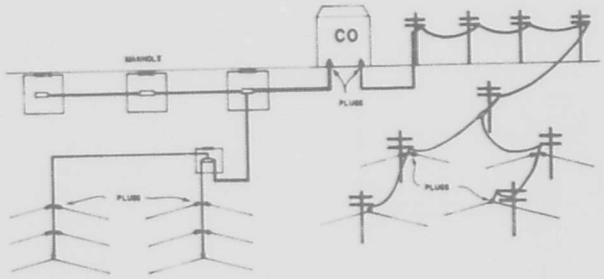

FIGURE 4. TYPICAL EXCHANGE AREA CABLE PLANT

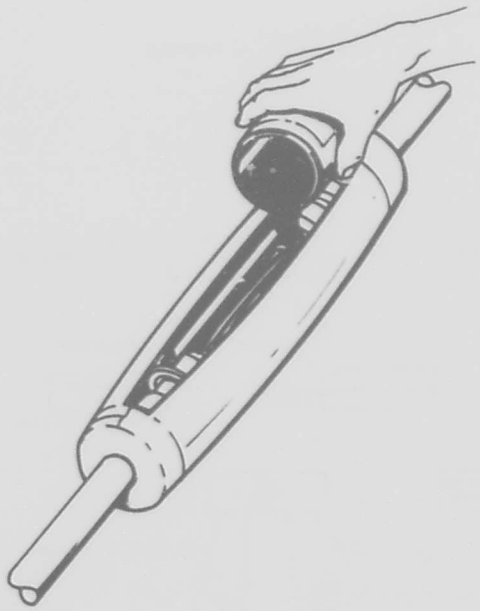

FIGURE 5. "SLEEVE POURED" PIC CABLE PLUG

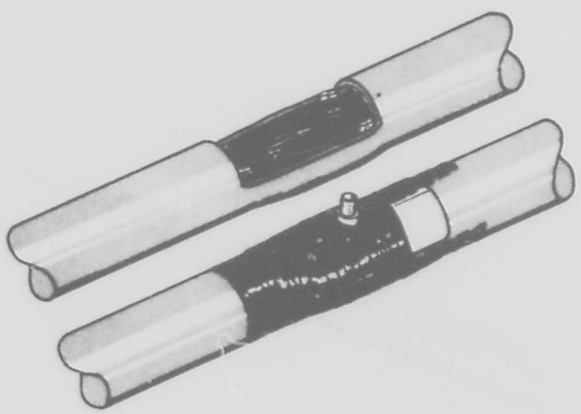

FIGURE 6. SHEATH INJECTED UNIVERSAL CABLE PLUG

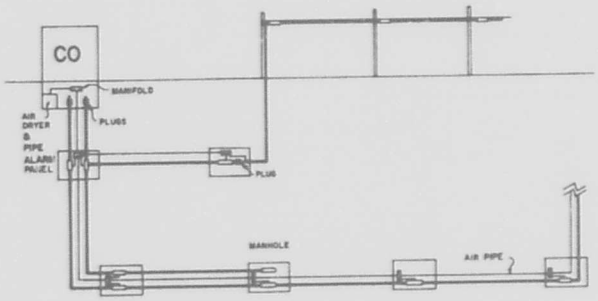

FIGURE 7 TYPICAL AIR PIPE SYSTEM

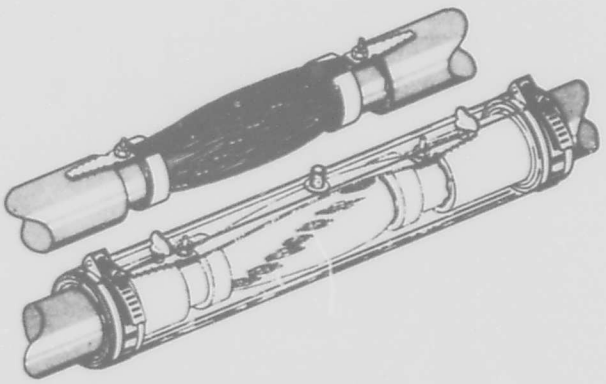

FIGURE 10 MODIFIED SLEEVE INJECTED UNIVERSAL CABLE PLUG

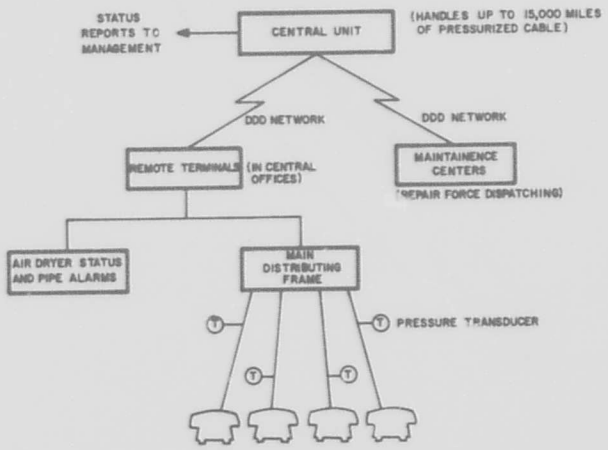

FIGURE 8. TYPICAL CPMS INSTALATION

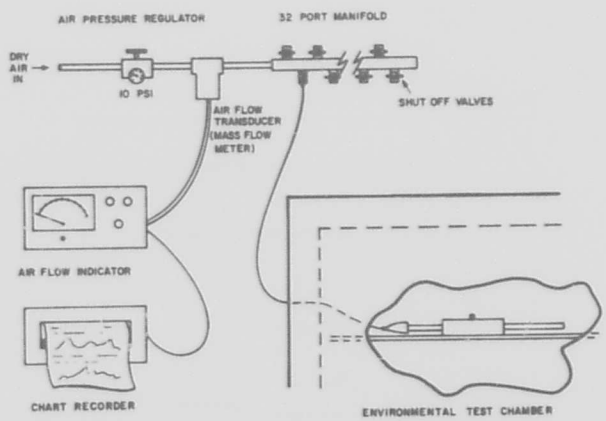

FIGURE 11 CABLE PLUG TEST FACILITY

FIGURE 9 SECTIONED DOUBLE SHEATH PIC CABLE

AUTHOR INDEX

Ance, L. ... 82
Azuma, M. ... 337
Baboian, R. ... 239
Boggs, L. M. ... 359
Bostwick, R. ... 68
Bradshaw, R. A. ... 252
Bragg, L. ... 59
Brownell, K. W., Jr. ... 309
Calhoun, J. C. ... 330
Calzolari, P. ... 169
Campbell, H. D. ... 226
Chan, M. G. ... 34
Cherin, A. H. ... 261
Chiba, H. ... 205
Cook, A. ... 276
Cranston, B. H. ... 290
Dedier, R. S. ... 281
Dekker, D. J. ... 319
DeVeau, G. F. ... 387
Dijkhuizen, S. ... 319
Di Leonardo, R. ... 19
Doty, D. J. ... 127
Dykes, J. D. ... 387
Farrell, F. M. III ... 403
Filreis, M. ... 403
Flegal, W. M. ... 330
Foord, S. G. ... 276
Fukutomi, H. ... 205
Galperin, I. ... 59
Gilroy, H. M. ... 42, 46
Godwin, E. F. ... 252
Gorissen, H. L. ... 319
Groves, J. D. ... 403
Hardwick, N. E. ... 393
Hartley, R. ... 239
Hartwijk, J. P. ... 319
Higashimoto, T. ... 205
Hyman, D. ... 239
Isley, A. M. ... 359
Ito, A. ... 182
Kaibuchi, S. ... 205
Kamaguchi, K. ... 97
Kapell, H. K. ... 403
Kato, T. ... 143
Kaufman, J. J. ... 76
Kaufman, S. ... 281
Kertscher, E. ... 346
Knippelmier, H. ... 370
Kishi, H. ... 97
Kishimoto, T. ... 135
Kitani, H. ... 135
Kokta, E. ... 46
Lannan, P. ... 105
Levengood, J. W. ... 359
Lilly, J. C. ... 1
Longoni, S. ... 161
Luisi, T. E. ... 76
Luzadis, D. A. ... 116
Machusak, D. A. ... 290
Manfre, Dr. ... 26
Manilii, A. ... 161, 169
Marshall, D. I. ... 63
Masaki, M. ... 97
McCann, P. ... 82
McLaughlin, J. F. ... 13
Metcalf, E. D. ... 53
Miller, R. A. ... 266
Minematsu, S. ... 182
Mitchell, D. M. ... 216
Miyamoto, Y. ... 135
Moore, T. L. ... 309
Nagai, Y. ... 135
Naruse, T. ... 143
Nevison, J. G. ... 375
Orimo, K. ... 337
Osterfield, J. R. ... 161
Paladin, G. ... 169
Parr, D. T. ... 375
Patton, G. A. ... 127
Pomerantz, M. ... 266
Rigling, W. ... 112
Robertson, J. M. ... 365
Sakamoto, N. ... 97
Sako, T. ... 143
Sawada, R. ... 91
Schumacher, W. ... 123
Scrofani, F. ... 169
Servi, G. ... 26
Shimano, T. ... 337
Shumaker, C. A., Jr. ... 297
Sibbald, D. ... 194
Silcock, H. W. ... 194
Simons, K. A. ... 152
Simpson, W. E. ... 276
Smith, G. C. ... 116
Suzuki, K. ... ⅔ ⅓
Taylor, F. M. ... 326
Toyoda, K. ... 337
Toyokawa, A. ... 205
Turnipseed, J. M. ... 63
Vogelsberg, D. ... 7
Webster, G. H. ... 216
Wiechard, C. A. ... 290
Wight, F. R. ... 63
Yamamoto, S. ... 337
Yasuhara, H. ... 143
Yoshikawa, T. ... 97
Yotsuya, M. ... 182